UNIVERSITY OF NAIROBI

PHYTOCHEMICAL STUDY OF SELECTED *DRACAENA* SPECIES FOR ANTI-INFLAMMATORY AND ANTICANCER PRINCIPLES

BY

NCHIOZEM-NGNITEDEM VADERAMENT-ALEXE

(I80/52552/2018)

A THESIS SUBMITTED FOR EXAMINATION IN FULFILLMENT OF THE REQUIREMENTS FOR AWARD OF THE DEGREE OF DOCTOR OF PHILOSOPHY IN CHEMISTRY OF THE UNIVERSITY OF NAIROBI

2021

DECLARATION

I declare that this thesis is my original work and has not been submitted elsewhere for examination, award of a degree or publication. Where other people's work, or my own work has been used, this has properly been acknowledged and referenced in accordance with the University of Nairobi's requirements.

Signature..... Date 21/04/2021

Nchiozem-Ngnitedem Vaderament-Alexe

(I80/52552/2018)

This PhD thesis has been submitted for examination with our approval as research supervisors

	Signature	Date
Prof. Leonidah Kerubo Omosa Department of Chemistry University of Nairobi lkerubo@uonbi.ac.ke	.....	21/04/2021
Dr. Solomon Derese Department of Chemistry University of Nairobi sderese@uonbi.ac.ke	.....	21/04/2021
Prof. Dr. Dr. h.c Michael Spiteller Department of Chemistry Technical University of Dortmund michael.spiteller@tu-dortmund.de	Michael Spiteller	19 April 2021

DEDICATION

This thesis is dedicated to my mother Ngnintedem Bernadette, my grandmother Dongmo Suzanne and my late father Ngnintedem Bernard, for their sacrifice towards my education.

ACKNOWLEDGEMENTS

The academic journey has been long but fruitful. As a matter of utmost importance, I begin by giving my profound gratitude to the Almighty God for granting me good health since the inception of my research work to the end. It is with lofty pleasure, I extend my unwavering gratefulness to my supervisors Prof. Leonidah Kerubo Omosa, Dr. Solomon Derese and Prof. Dr. Dr. h. c. Michael Spiteller for their mentorship, patience and encouragement throughout my research. Prof. Leonidah K. Omosa, I sincerely appreciate for your constant guidance, motherly love you accorded to me and for being always available for consultation when things seemed to hit a deadlock, you always came in handy. Words may not sufficiently express my gratitude but you remain to be my solid academic pillar that has earned me this PhD. I am indebted to Prof. Abiy Yenesew, Prof. John Onyari and Dr. Albert Ndakala, all from chemistry department for their motivation, friendship and valuable discussion on areas that seemed a challenge to me. Without forgetting the late Prof. Tane Pierre from the University of Dschang who was one of my supervisors.

I am extremely grateful to my sponsor, the German Academic Exchange Service (DAAD) for a PhD scholarship which was awarded through the Natural Products Research Network for Eastern and Central Africa (NAPRECA) and for supporting my stay at INFU, TU Dortmund, Germany. I am cognizant of the financial support from the International Science Programme (ISP) through the KEN-02 project. I am thankful to Dr. Wolf Hiller (Technical University of Dortmund), Dr. Matthias Heydenreich (University of Potsdam) for NMR analysis and Prof. Dr. Thomas Efferth's team for anticancer assay.

I'm so grateful to my family and friends who assisted in one way or the other especially with prayers, motivation and material support during my study. The late Mr. Lucas Ombongi can't go unmentioned for his assistance in collection and grinding of plant materials. Last but not least, special thanks to Mr Obegi Jackson Matundura, for his valuable input in the achievement of this thesis. Lastly, my heartfelt appreciation goes to my colleagues and labmates in the department of chemistry for their support and encouragement during my low moments.

ABSTRACT

Chronic inflammation is associated with the onset of chronic disorders such as cancer. The currently available anti-inflammatory and anticancer drugs are associated with diverse undesirable side effects. Hence, search for new drugs with better efficacy and less toxicity against these associated inflictions is necessary. In this study, three *Dracaena* species from Kenya namely: *Dracaena usambarensis*, *Dracaena aletriformis* and *Dracaena steudneri* were phytochemically investigated and tested for their anti-inflammatory and anticancer potencies. The different parts of the plants were extracted ($MeOH/CH_2Cl_2$ (1:1)) and chromatographically separated using silica gel and Sephadex LH-20 as solid matrix followed by purification on chromatotron and semi-preparative HPLC). Structure elucidation of isolates were deduced using a panel of spectroscopic (NMR, UV, IR, optical rotation, CD and X-ray analysis) and spectrometric ($HRESIMS^n$) methods. The isolated compounds and the standard drug ibuprofen were evaluated for their anti-inflammatory potency against four inflammatory biomarkers (IL-1β, IL-2, GM-CSF and TNF-α). In addition, the cytotoxicity of the crude extracts and isolates were determined by resazurin reduction assay in comparison with the standard drug doxorubicin. Phytochemical analysis of the stems of *Dracaena usambarensis* afforded eleven secondary metabolites out of which five are novel (**176** – **180**). The roots of the same plant yielded seven secondary metabolites of which two were new (**186** and **189**). Phytochemical investigation of the whole plant of *Dracaena aletriformis* afforded three previously reported phenolic amides (**193** – **195**). The seeds and leaves of *Dracaena steudneri* afforded twenty eight secondary metabolites including six novel flavonoids (**203** – **208**). A total of fifty (50) secondary metabolites including thirteen (13) novel ones were reported from these plants. Among the tested compounds, at a concentration of 100 µM, compounds **180** (1.61 to 27.53% of LPS control), **182** (14.48 to 58.04% of LPS control), **184** (0.06 to 11.61% of LPS control) and **216** (0.35 to 27.53% of LPS control), showed a clear decrease of all the cytokines compared to the standard drug, ibuprofen. At a concentration of 10 µM, compound **200** displayed strong cytotoxicity against both leukemia cell lines: CCRF-CEM (IC_{50} of 7.88 ± 0.74 µM) and CEM/ADR5000 (IC_{50} of 5.28 ± 0.85 µM), while compound **213** had an IC_{50} values of 8.80 ± 0.74 µM and 3.31 ± 0.36 µM µM, respectively. Moderate cytotoxicity was observed for compound **186** against CCRF-CEM (IC_{50} of 40.43 ± 10.26 µM). This study showed that, compounds from

Dracaena exhibited strong to moderate anti-inflammatory and cytotoxic potencies and can be considered as lead compounds for drug discovery.

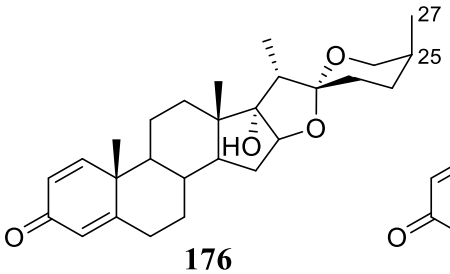

176

177 $\Delta^{25(27)}$

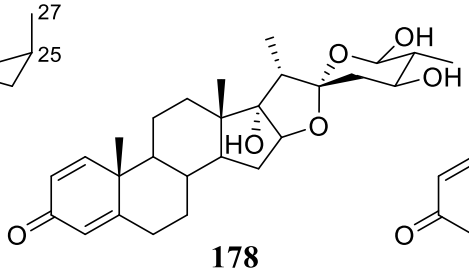

178

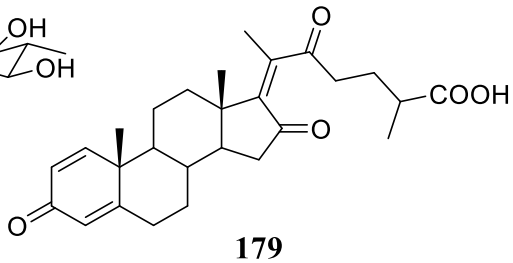

179

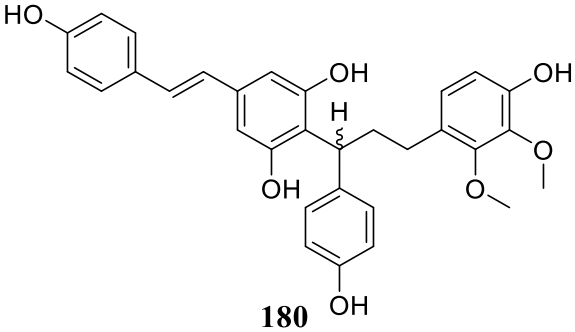

180

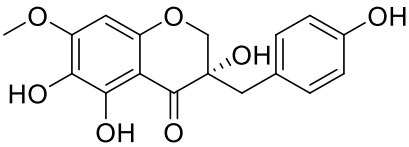

186

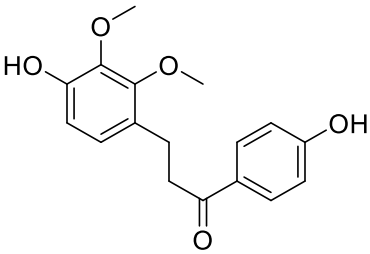

189

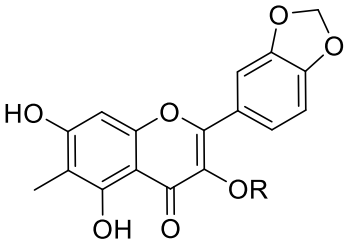

	R
200	H
204	CH_3

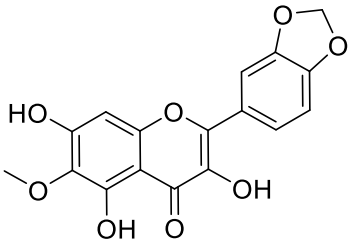

205

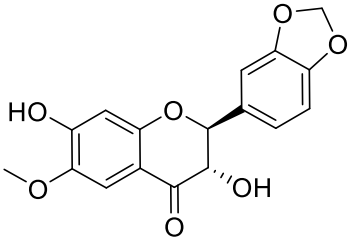

206

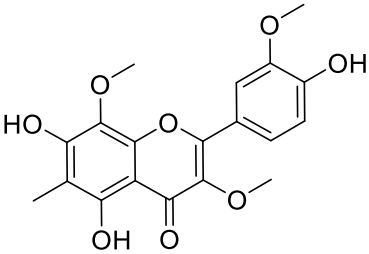

207

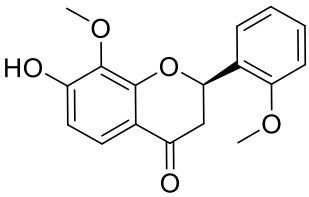

208

TABLE OF CONTENTS

LIST OF TABLES

LIST OF FIGURES

LIST OF SCHEMES

LIST OF APPENDICES

LIST OF ABBREVIATIONS/ACRONYMS AND SYMBOLS

A-431	Human Epidermoid Cells
A549	Human Lung Adenocarcinoma Cells
APG	Angiosperm Phylogeny Group
Arap	Arabinopyranose
B16	Mice Melanoma Cells
BT-549	Human Breast Carcinoma cells
CaCo2	Human Epithelial Colorectal Adenocarcinoma Cells
CC	Column Chromatography
CD	Circular Dichroism
CD_3OD	Deuterated Methanol
CD4	Cluster of Differentiation 4
$CDCl_3$	Deuterated Chloroform
CH_2Cl_2	Dichloromethane
$CHCl_3$	Chloroform
CID	Collision-Induced Dissociation
COSY	Correlation Spectroscopy
COX	Cyclooxygenase
d	Doublet
D	*Dracaena*
DAAD	German Academic Exchange Service
dd	Double Doublets
DEPT	Distortionless Enhancement by Polarization Transfer
DLD-1	Human Colorectal Adenocarcinoma Cells
DMSO-d_6	Deuterated Dimethylsulfoxide
EtOAc	Ethyl Acetate
EtOH	Ethanol
FDA	Food and Drug Administration
HMBC	Heteronuclear Multiple Bond Correlation
HPLC	High-Performance Liquid Chromatography
HRESIMS	High-Resolution Electrospray Ionization Mass Spectrometry
HSQC	Heteronuclear Single Quantum Correlation
HT-1080	Human Fibrosarcoma Cells
Hz	Hertz
IC_{50}	Inhibitor Concentration 50%
ILs	Interleukins
IR	Infra-Red
Jurkat	Human T-Cell Leukemia Cells
K562	Human Myeloid Leukemia Cells
KB	Human Epidermal Carcinoma Cells
LC-MS	Liquid Chromatography–Mass Spectrometry
LC-UV	Liquid Chromatography–Ultra-Violet
LLC-PK1	Mammalian Kidney Cells
LPS	Lipopolysaccharide
m	Multiplet
m/*z*	Mass to Charge Ratio
MCF-7	Human Breast Carcinoma Cells
MDA-MB-435	Human Melanoma Cells
MeOH	Methanol
MHz	Mega Hertz
MS	Mass Spectrometry
NAPRECA	Natural Products Research Network for Eastern and Central Africa
NMR	Nuclear Magnetic Resonance
NO	Nitric Oxide
NOESY	Nuclear Overhauser and Exchange Spectroscopy

Fuc	Fucose	NSAIDs	Nonsteroidal Anti-Inflammatory Drugs
GM-CSF	Granulocyte-Macrophage Colony-Stimulating Factor	SAR	Structure-Activity Relationship
GPS	Global Positioning System	SGC-7901	Human Gastric Cells
H_2O	Water	SK-MEL	Human Melanoma Cells
H_2SO_4	Sulfuric Acid	Skov-3	Human Ovarian Carcinoma Cells
HeLa	Human Cervical Adenocarcinoma Cells	SMMC-721	Human Liver Cells
Hep3B	Human Hepatocar-Cinoma Cells	SMMC-7221	Human Hepatocellular Carcinoma Cells
HIV	Human Immunodeficiency Virus	*t*	Triplet
HL-60	Human Leukemia Cells	TGF_β	Transforming Growth Factor beta
p	Quintet	TLC	Thin Layer Chromatography
PBMCs	Peripheral Blood Mononuclear Cells	TNF-α	Tumor Necrosis Factor - Alpha
PLA2	Phospholipase A2	UV	Ultra Violet
q	Quartet	VERO	Mammalian Kidney Cells
RAW 264.7	Murine Macrophage Cells	WHO	World Health Organization
Rhap	rhamnopyranose	Xyl	Xylose
Rhm	rhamnose	δ	Chemical Shift
s	Singlet	µg/mL	Microgram Per Milliliter

LIST OF PUBLICATIONS

1. **Vaderament-A Nchiozem-Ngnitedem**, Leonidah Kerubo Omosa, Solomon Derese, Pierre Tane, Matthias Heydenreich, Michael Spiteller, Ean-Jeong Seo, Thomas Efferth (2020). Two New Flavonoids from *Dracaena usambarensis* Engl. *Phytochemistry Letters*. **36**: 80–85.

2. **Vaderament-A Nchiozem-Ngnitedem**, Leonidah Kerubo Omosa, Kibrom Gebreheiwot Bedane, Solomon Derese, Lukas Brieger, Carsten Strohmann, Michael Spiteller (2020). Anti-inflammatory Steroidal Sapogenins and a Conjugated Chalcone-stilbene from *Dracaena usambarensis* Engl. *Fitoterapia*. **146**: 104717, https://doi.org/10.1016/j.fitote.2020.104717

3. **Vaderament-A Nchiozem-Ngnitedem**, Leonidah Kerubo Omosa, Kibrom Gebreheiwot Bedane, Solomon Derese, Michael Spiteller (2020). Inhibition of Proinflammatory Cytokine Release by Flavones and Flavanones from the Leaves of *Dracaena steudneri* Engl. *Planta Medica*. https://doi: 10.1055/a-1306-1368

4. **Vaderament-A Nchiozem-Ngnitedem**, Leonidah Kerubo Omosa, Solomon Derese, Thomas Efferth, Michael Spiteller (2021). Cytotoxic Flavonoids from the seeds of *Dracaena steudneri* Engl. *Manuscript***,** *xxxxxxxxxx*

CHAPTER 1: INTRODUCTION

1.1: Background

Since millennia medicinal plants keep on playing a primordial role in the treatment and management of innumerable infections that confront mankind (Arif *et al.*, 2009; Handral *et al.*, 2012). It has been documented that, 75% of the population worldwide still relies on traditional medicine because of their efficacy, less toxicity, availability and affordability compared to synthetic drugs (Gidey *et al.*, 2015; Shaikh *et al.*, 2016; Zhang, 2004). Unlike the western medicine which relies on a unique active component that act in one specific pathway, herbal medicine which is a decoction or concoction work in way that depends on an orchestral approach (Vikrant and Arya, 2011). Herbal drugs contain active components that act synergistically on target elements of a complex cellular pathway (Durmowicz and Stenmark, 1999).

Natural products derived from plants, classified as primary or secondary metabolites, are diverse classes of compounds and have been documented as a major source of compounds for drug discovery (Dias *et al.*, 2012; Mishra and Tiwari, 2011; Rey-Ladino *et al.*, 2011). Primary metabolites (amino acids, lipids and phytosterols) are biosynthesized in all plants species and participate directly in their growth and development (Croteau *et al.*, 2000; Schäfer and Wink, 2009). Whereas, secondary metabolites (terpenoids, alkaloids and phenolic compounds) are organic compounds particularly found and distributed among limited taxonomic groups within the plant kingdom and they appeared not to participate in growth and development. They are biosynthesized by plants for their protection, defense against microorganisms, protection against UV radiation among others (Croteau *et al.*, 2000; Schäfer and Wink, 2009). Secondary metabolites which plants synthesize for their ecological interaction with their environment have also been

documented to have a wide spectrum of activities against diseases that affect other organisms including humans (Manthey *et al.*, 2001; Ragasa *et al.*, 2005; Wang *et al.*, 2016a).

For example, curcumin (**1**) and colchicine (**2**), two isolates reported from *Curcuma longa* and *Colchicum autumnale*, respectively, are used for management of inflammation (Fürst and Zündorf, 2014). Secondary metabolites from plants have also been used for treatment of cancer, examples include camptothecin (**3**), isolated from *Camptotheca acuminata* and its derivative topotecan (**4**) (Hostettmann *et al.*, 1998).

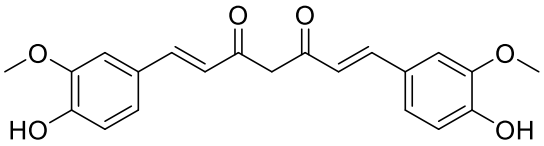

1

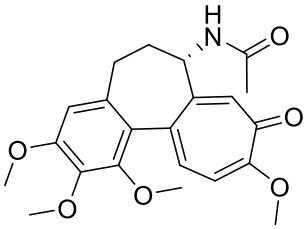

2

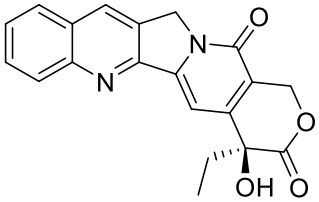

3

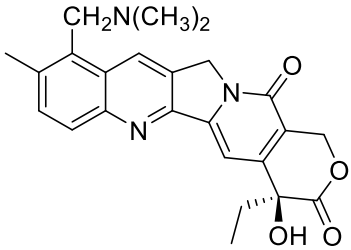

4

Several other plants which are used traditionally for management of inflammation and treatment of cancer can serve as sources of drugs against these diseases. Example of such plants are plants that belong to the genus *Dracaena*. These plants are deployed worldwide in the management of different inflammations and pains due to their potent anti-inflammatory, analgesic (Li *et al.*, 2012) and anticancer effects (Sun *et al.*, 2019). In this study, three Kenyan *Dracaena* species namely *Dracaena usambarensis* Engl, *Dracaena aletriformis* (Harv.) Bos and *Dracaena steudneri* Engl were investigated for their potential use in the management of inflammation and cancer.

1.2: Statement of the Problem

Inflammation is an innate immune response of the body to reestablish homeostasis after an infection, injury or exposure to harmful toxins (Antonelli and Kushner, 2017). However, when inflammation persist through over expression and imperfect regulations of inflammatory modulators it becomes chronic. It has been associated with disorders such as diabetes, obesity and cancer among other chronic disorders (Lawrence and Gilroy, 2007). Thus, it is essential to control inflammation using anti-inflammatory drugs. Anti-inflammatory drugs have also been used in controlling chronic ailments including cancer (Thun *et al.*, 2010). Cancer is recognized as a critical problem worldwide affecting both the developed and developing countries. In a period of three years from 2015 to 2018, more than half a million new cases were recorded worldwide increasing the number of deaths from 8.7 (Fitzmaurice *et al.*, 2017) to 9.6 million (Bray *et al.*, 2018) during this period. If nothing is made to address this disease, it is projected that cancer cases will rise to more than 25 million new cases with 17 million deaths in the next two decades (WHO, 2020). In a developing country like Kenya, more than 40,000 new cases with 28,000 deaths are reported yearly making it the 3rd leading causes of death after cardiovascular and infectious diseases (Topazian *et al.*, 2016).

Although many anti-inflammatory drugs are used to manage cancer (Thun *et al.*, 2002), the appearance of drug resistance and side effects to commercially available anti-inflammatory and anticancer drugs constitute the main obstacle in the treatment and management of inflammation and cancer (Sando *et al.*, 2015). Even though many pharmaceutical companies have shifted to combinatorial chemistry, plants still form an integral segment in medicine development. Thus, it is important to find new lead compounds which are effective and with less side effects from the genus *Dracaena* with anti-inflammatory and anticancer potencies. The stock of diverse

phytochemicals with different frameworks biosynthesized by the genus can be characterized and used as starting materials by the pharmaceutical industry to replace the drugs currently available in the market.

1.3: Objectives

1.3.1: Overall Objective

The principal objective of this work was to characterize secondary metabolites from selected *Dracaena* species with anti-inflammatory and anticancer properties.

1.3.2: Specific Objectives

Specifically, this study was designed:

i. To characterize compounds from *Dracaena usambarensis*, *Dracaena aletriformis* and *Dracaena steudneri*.
ii. To assess the anti-inflammatory potency of the isolated compounds.
iii. To evaluate the anticancer potency of the crude extracts and isolates.

1.4: Justification of the Study

Investigations into the anti-inflammatory activities of some *Dracaena* species showed that their crude extracts and isolated compounds have shown moderate to significant activities (Tang *et al.*, 2019; Tapondjou *et al.*, 2008). In an *in vivo* anti-inflammatory investigation, the crude extracts (ethanol and *n*-butanol) and isolated compounds of *D. manni* showed significant and moderate activities, respectively, (Tapondjou *et al.*, 2008). In another study, the extracts (ethanol and methanol) of the red resin of *D. cochinchinensis* showed excellent anti-inflammatory activity with IC_{50} = 11.5 – 20.44 µg/mL against nitric oxide (NO) production (Tang *et al.*, 2019). Whereas,

some of the compounds displayed strong anti-inflammatory activity with IC_{50} < 10 µM (Tang *et al.*, 2019).

In addition, extracts and isolates from this genus have been shown to have anticancer activities (Sun *et al.*, 2019; Teponno *et al.*, 2017). The methanolic extract of *D. viridiflora* showed cytotoxicity towards Skov-3 A549, CaCo2 and Jurkat with IC_{50} values 11.76 – 23.69 µg/mL (Teponno *et al.*, 2017). Some of the isolates obtained from the same plant had strong response towards the cell lines under study with IC_{50} < 4 µg/mL (Teponno *et al.*, 2017). In addition, the chloroform extract of *D. combodiana* showed strong cytotoxic activity against B16 and SMMC-721 cancer cell lines with IC_{50} values 4.5 and 6.0 µg/mL, respectively (Sun *et al.*, 2019).

Pro-inflammatory cytokines have been listed as important mediators linking inflammation and cancer (Karin, 2009; Taniguchi and Karin, 2014). Their effective inhibition constituted a main strategy in the treatment of chronic diseases. Based on this, three *Dracaena* species were investigated for their potential in inhibiting pro-inflammatory cytokines. Despite the wide biological activities of the different species reported from the genus *Dracaena* in the literature, there is barely no phytochemical and pharmacological study including anti-inflammatory and anticancer potencies on *D. usambarensis, D. aletriformis* and *D. steudneri*.

CHAPTER 2: LITERATURE REVIEW

2.1: Inflammation

Inflammation is a reaction of the immune system towards either an injury, wound, or infection by microorganisms (Jung *et al.*, 2019). It is usually characterized by pain and red swelling on the affected area (Ferrero-Miliani *et al.*, 2007). During inflammation, different inflammatory mediators/markers including prostaglandins, interleukins and nitric oxide (NO) among others are released by the damaged tissue as part of their immune response system (Vane *et al.*, 1994).

Excessive production of these inflammatory markers results in a disproportion between inflammatory and anti-inflammatory cytokines culminating in different illnesses, such as atherosclerosis, depression and cancer (Gori *et al.*, 2009; Vane *et al.*, 1994). Based on the duration and the persistence of the lesion, inflammation can be categorized into acute and chronic (Paramita and Kosala, 2017). Acute condition is an instantaneous response of the body's tissues to harmful stimuli lasting relatively for a short period. However, if the acute inflammation persist it will lead to chronic inflammation which results from self-replication of organisms, e.g. virus, bacteria and neoplasm or malignant growth (Kosala *et al.*, 2018). This form of inflammation has been linked to various chronic ailments such as heart attacks, Alzheimer's disease, rheumatoid arthritis, vascular diseases and cancer (Coussens and Werb, 2002; Jung *et al.*, 2019). To overcome these diseases associated with chronic inflammation, the development of inflammatory mediators inhibitors has been of great interest to researchers. There are a number of anti-inflammatory drugs currently being used for management of inflammation including those that are of natural origin.

2.1.1: Anti-inflammatory Drugs

Standard anti-inflammatory drug used to relieve inflammation and pain are mainly corticosteroids: dexamethasone (**5**), prednisolone (**6**) and triamcinolone (**7**) (Kawai and Akira, 2011). There are

also nonsteroidal anti-inflammatory drugs (NSAIDs) such as aspirin (**8**), diclofenac (**9**), ibuprofen (**10**), indomethacin (**11**), naproxen (**12**) and rofecoxib (**13**) in the market (Harris *et al.*, 2005). Corticosteroids (steroidal) and NSAIDs act by inhibiting the enzymes *phospholipase* A2 (PLA2) and *cyclooxygenase* (COX), respectively (Oyekachukwu *et al.*, 2017).

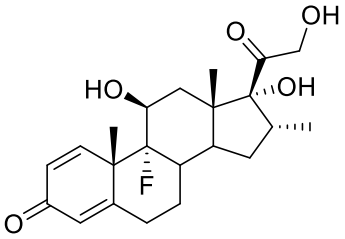

5

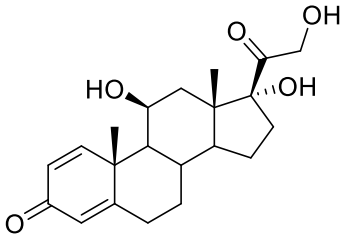

6

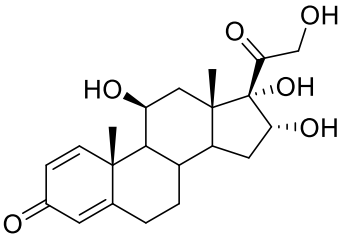

7

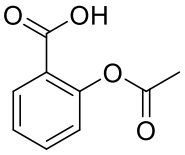

8

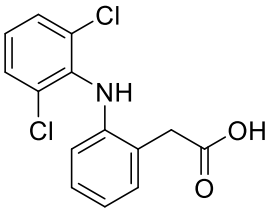

9

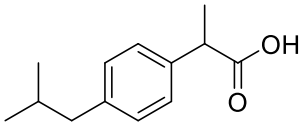

10

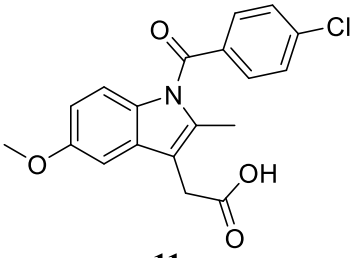

11

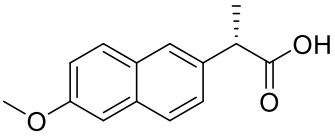

12

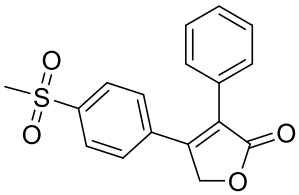

13

These drugs are less effective with a lot of side effects, despite their benefits to human beings. It has been reported that some non-selective COX inhibitors such as diclofenac (**9**) and ibuprofen (**10**), cause deposition of urate crystals in the kidneys, liver and heart. Moreover, they have been linked to gastrointestinal tract and coagulation system disorders (Modi *et al.*, 2012; Rocca *et al.*, 2005). The selective COX-2 inhibitors (example rofecoxib (**13**)) decreases this effect but have been documented to have cardiovascular disease complications (Cipollone *et al.*, 2008). The main

disadvantage of corticosteroids is the appearances of resistance by microorganisms to some of the commercially available anti-inflammatory drugs (Vazquez-Tello *et al.*, 2013).

Plant-based products have been reported to contain secondary metabolites with anti-inflammatory and anti-cancer effect and less toxicity (Zaynab *et al.*, 2018). This makes them together with their semisynthetic derivatives lead compounds as alternative source of new anti-inflammatory drugs.

2.1.2: Natural Products with Anti-Inflammatory Potencies

People living in the village have been in touch with effective anti-inflammatory plants belonging to different families since antiquity for their primary healthcare (Kaileh *et al.*, 2007; Shaikh *et al.*, 2014). These families of plants yield diverse substances mainly phenolic, terpenoids and alkaloids with anti-inflammatory properties (Panche *et al.*, 2016; Souto *et al.*, 2011).

A homoisoflavan, phenolic, isolated from the bulbs of *Ledebouria ovatifolia*, (3*R*)-3′,4′,7-trihydroxy-5-methoxyhomoisoflavane (**14**), was shown to display selective cyclo-oxygenase-2 (COX-2) inhibition with IC_{50} < 10 μM which are within the permissible range of non-selective inhibitors drugs (Waller *et al.*, 2013). Zhao and co-workers reported from the whole plant of *Angelica decursiva* the isolation of the phenolic umbelliferone-6-carboxylic acid (**15**) which displayed strong activity against nitric oxide production in RAW 264.7 (IC_{50} = 72.98 μg/mL) (Zhao *et al.*, 2012). Another phenolic secondary metabolite that has been shown to inhibit the production of NO with IC_{50} = 5.80 μM is [6]-shogaol (**16**), a compound isolated from *Zingiber officinale* (Li *et al.*, 2011).

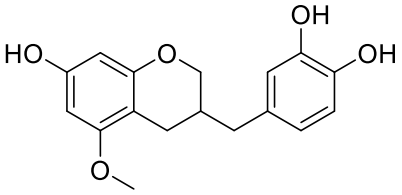

14

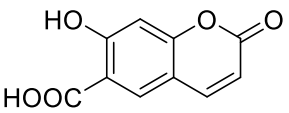

15

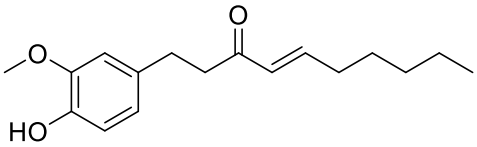

16

The terpenoids (12-*O*-benzoylphorbol 13-nonanoate (**17**), 12-*O*-benzoylphorbol 13-octanoate (**18**), yuanhuatin (**19**), genkwadaphnin (**20**) and gniditrin (**21**)) isolated from *Daphne aurantiaca* displayed strong anti-inflammatory effect with IC_{50} of 0.01 – 0.07 μM (Liang *et al.*, 2010).

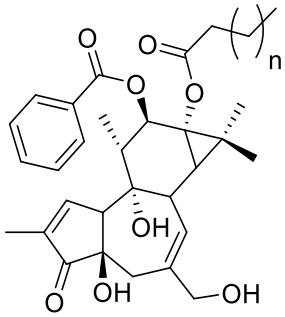

17 n = 6
18 n = 5

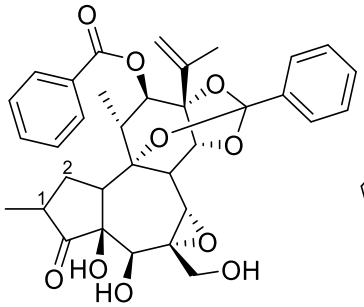

19
20 $\Delta^{1,2}$

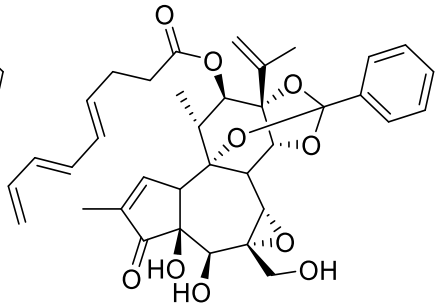

21

Alkaloids have also been reported as a prominent sources of anti-inflammatory agents that have been used in fighting inflammation. For instance, ailanthamide (**22**) a phenolic amide isolated from *Zanthoxylum ailanthoides* showed anti-inflammatory activity with IC_{50} of 3.71 – 4.23 μg/mL. While decarine (**23**), a benzophenanthridine alkaloid, isolated from the same plant had an IC_{50} of 1.29 – 1.94 μg/mL (Chen *et al.*, 2009). Liu et al from *Nauclea officinalis* isolated 17-*O*-methyl-19-(*Z*)-naucline (**24**), which showed significant inhibitory activity against NO (IC_{50} of 3.6 μM) (Liu *et al.*, 2017). Hence, plants can be explored as a pharmaceutical arsenal for the discovery and development of anti-inflammatory drugs.

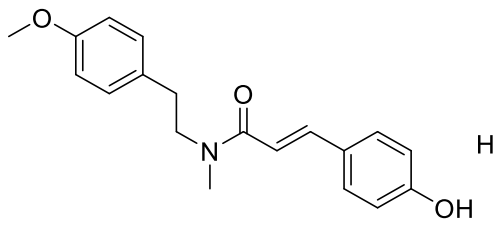

22

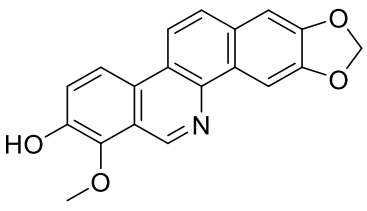

23

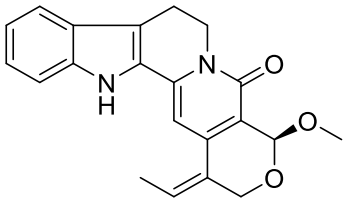

24

2.2: Cancer

Cancer is an assemblage of syndromes characterized by abnormal development and proliferation of cells (Armstrong *et al.*, 2018). This disease is recognized as a critical problem globally with about 18.0 and 9.6 million cases and deaths, respectively (Bray *et al.*, 2018). It has been reported that this malignant growth cause more death than malaria, HIV and tuberculosis combined (Vorobiof and Abratt, 2007). In Africa, in 2018 more than 258,500 cases of cancer recorded were due to infectious agents (Parkin *et al.*, 2020). The problem of cancer is expanding in the developing world (Africa) because of increase prevalence of risk aspects linked with lifestyle, overweightness, lack of physical exercise, smoking, UV radiation and procreative behaviors (Jemal *et al.*, 2012).

The main approaches in the management of cancer include immunotherapy, radiotherapy, chemotherapy, surgery, photodynamic therapy and endocrine therapy (Chilakamarthi and Giribabu, 2017; Liu and Yang, 2015). The extensive usage of these strategies is limited because they have been associated with many side effects (Pandey and Madhuri, 2009). Among the methods of treatment of cancer, cancer chemotherapy is highly advanced yet it's not 100% efficient against specific cancer cells (Gottesman, 2002). For example, paclitaxel (**25**) a chemo preventive agent used against breast cancer act by targeting only proliferating tumor cells but inactive in dormant malignant cells (Bu *et al.*, 2014; Volk-Draper *et al.*, 2014). The main

disadvantage of radiotherapy are undesirable side effects such as cardiac, renal and pulmonary toxicity (Roy and Bharadvaja, 2017).

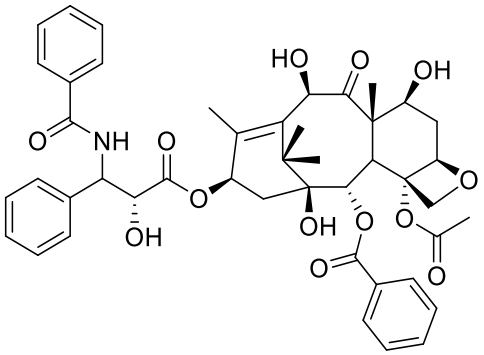

25

Furthermore, there is an emergence of resistance of cancerous cell lines to the current drugs of choice. With continued application, many cancerous cell lines have adapted to medicines used to kill them, making the drugs less effective (Bektas and Iscimen, 2005). This is because most cancer cells reproduce rapidly and develop resistance when they get exposed to anticancer drugs (Raguz and Yagüe, 2008). Based on all aforementioned, it is of utmost importance to find new drugs to fight drug-resistant cancer particularly from plants as they have been a very good source of anticancer drugs.

2.2.1: Anticancer Drugs of Natural Origin

The screening of herbal medicine as anticancer agent has provided allopathic medicine several effective cytotoxic pharmaceuticals (Kuete *et al.*, 2013a). In fact, about 60% of the drugs available in the market as anticancer agents were natural products or their synthetic derivatives (Newman and Cragg, 2007; Stevigny *et al.*, 2005). A typical enumeration of this is the anticancer drug daunorubicin (**26**) against leukemia cancer cells which was obtained from *Streptomyces coeruleorubidus* (Mortensen *et al.*, 1992). Another such example is the breast cancer drug vinblastine (**27**) which is an alkaloid isolated from *Vinca rosea* Linn (Beard, 2001; Keglevich *et*

al., 2012). More recently, the natural products omacetaxine mepesuccinate (**28**) and ingenol mebutate (**29**) isolated from *Cephalotaxus harringtoni* and *Euphorbia paralias*, respectively, have been approved by the FDA as anticancer drugs (Butler *et al.*, 2014).

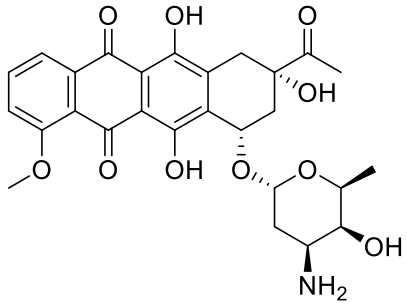

26

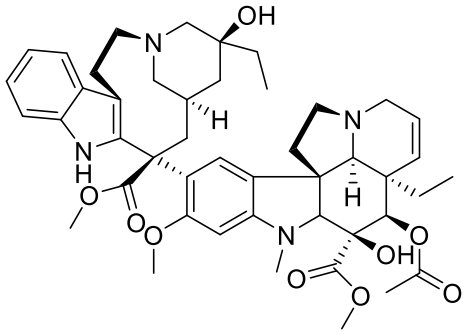

27

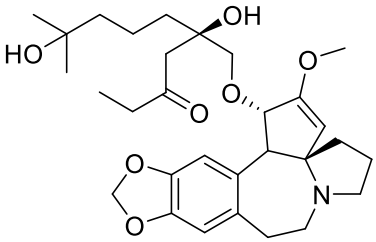

28

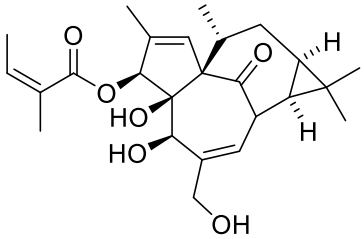

29

2.2.2: Natural Products with Anticancer Properties

Several classes of secondary metabolites have been shown to have anticancer activities, amongst these are flavonoids, homoisoflavonoids and saponins (Sun *et al.*, 2019). For example morusin (**30**), a prenylated flavonoid obtained from the leaves of *Morus alba* displayed cytotoxic activity against HeLa (IC_{50} of 0.64 μM), MCF-7 (IC_{50} of 7.88 μM) and Hep3B (IC_{50} of 9.21 μM) cancer cells lines (Dat *et al.*, 2010). Cyclomorusin (**31**), a flavonoid isolated from the same plant, had an IC_{50} values of 1.66, 7.85 and 7.55 μM, respectively, against the three cell lines (Dat *et al.*, 2010). Alali et al reported two homoisoflavonoids, 3′,5,7-trihydroxy-4′-methoxyhomoisoflavane (**32**,

IC_{50} of 1.0 μM) and 3′,5-dihydroxy-4′,7,8-trimethoxyhomoisoflavane (**33**, IC_{50} of 1.1 μM) from *Bellevalia* species active against MDA-MB-435 cell line (Alali *et al*., 2015).

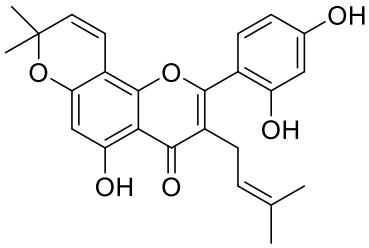

30

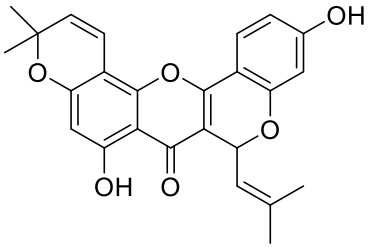

31

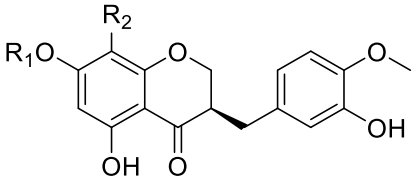

	R_1	R_2
32	H	H
33	CH_3	OCH_3

The cytotoxic activity of saponins (**34** – **37**) isolated from *Panicum turgidum* were evaluated against LLC-PK1, SKOV-3, VERO, KB, BT-549 and SK-MEL cell lines. All the saponins displayed strong cytotoxicity with IC_{50} values of 0.295 – 8.25 μM against these cancer cell lines (Zaki *et al.*, 2017). Another example of steroidal saponins with cytotoxic potency include janponicosides A (**38**) and B (**39**) isolated from *Smilacina japonica*. These compounds exhibited excellent properties towards human's cell lines (SMMC-7221 and DLD-1) with IC_{50} of 1.19 to 5.40 μM (Liu *et al.*, 2012).

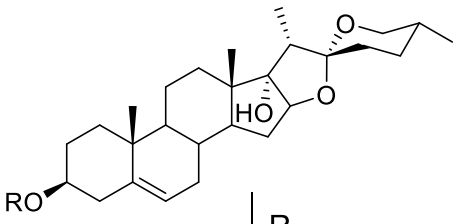

	R
34	Sugar 1
35	Sugar 2

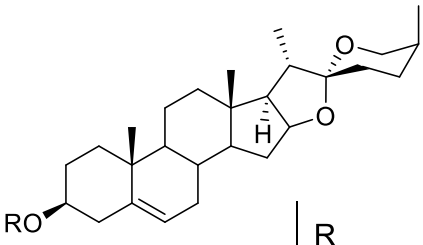

	R
36	Sugar 1
37	Sugar 2

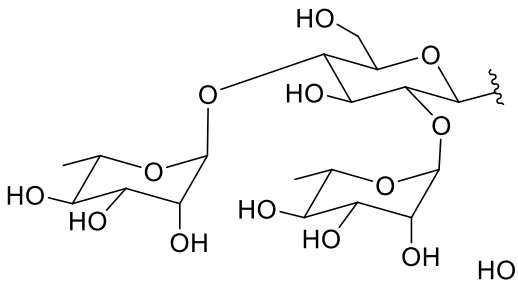

Sugar 1

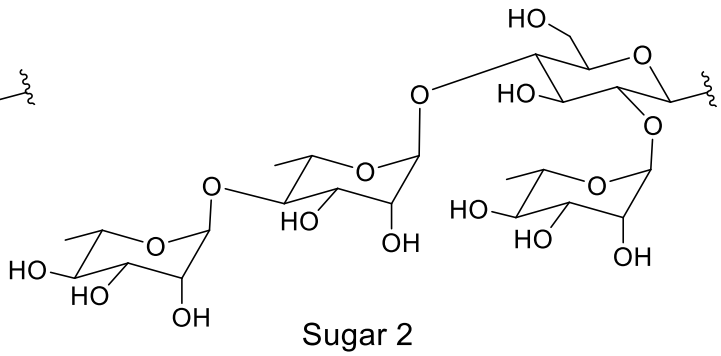

Sugar 2

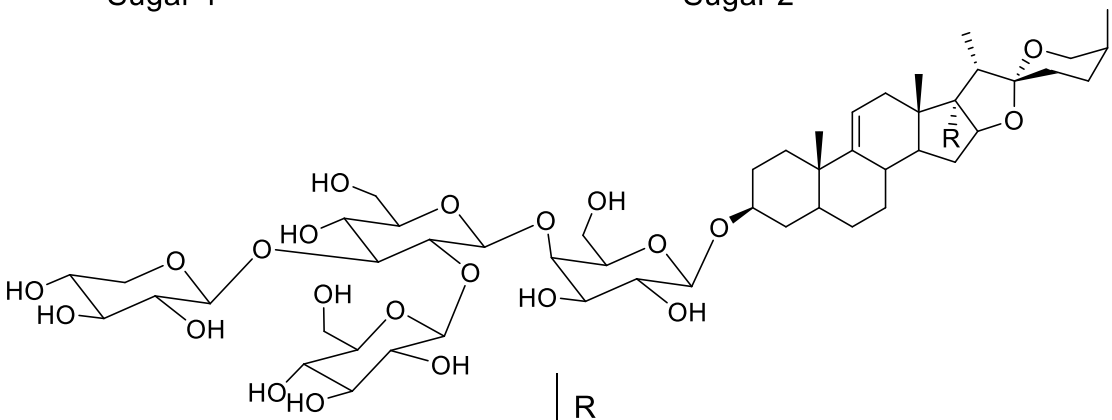

	R
38	H
39	OH

2.2.3: Inflammation and Cancer

The link between inflammation and cancer has always been a hot topic. In 1863, Rudolf Virchow was the first to identify the presence of leukocytes within tumors indicating a possible relationship between inflammation and cancer (Grivennikov *et al.*, 2010). Recent data highlighted that chronic infections and inflammation play a pivotal role in carcinogenesis including tumor initiation, promotion, progression, and metastasis (Karin, 2006). About 90% of cancers are associated with somatic mutations and environmental factors such as tobacco, alcohol, UV radiation, environmental pollutants and lifestyle (Aggarwal *et al.*, 2009). These factors increase the risk of developing cancer through inflammation. In addition to these, many anti-inflammatory drugs have been used in management of cancer (Rayburn *et al.*, 2009). A typical example is ibuprofen (**10**), a non-steroidal anti-inflammatory drug reported to decrease the risk of breast cancer (Harris *et al.*,

2003). Another anti-inflammatory drug dexamethasone (**5**) (corticosteroid) has been shown to be active against lung cancer in animals exposed to tobacco smoke (Witschi *et al.*, 2005).

2.3: The Family Asparagaceae

Plant species of the family Asparagaceae are generally trees, shrubs or herbaceous distributed worldwide with the highest abundance in the Southern Africa region (Mulholland *et al.*, 2013). This family is subdivided into seven subfamilies known as Nolinoideae, Brodiaeoideae, Agavoideae, Scilloideae, Asparagoideae, Aphyllanthoideae and Lomandroideae (Chase *et al.*, 2009). It has approximately 2,900 species occurring in about 114 genera, including the genus *Dracaena* which is in the subfamily Nolinoideae (Christenhusz and Byng, 2016).

2.3.1: The Genus Dracaena

The genus has its place to the large family of flowering plants Asparagaceae, subfamilly Nolinoideae (APG, 2016; Lu and Morden, 2014). This genus is composed of more than 100 species of succulent shrubs and trees distributed in tropical and subtropical regions (Lu and Morden, 2010; Thu *et al.*, 2020). Out of the 100 species reported in this genus, 8 of them are found in Kenya. The 8 *Dracaena* species that are found in Kenya are *D. usambarensis* Engl, *D. aletriformis* (Harv.) Bos, *D. steudneri* Engl, *D. afromontana* Mildbr, *D. deremensis* Engl, *D. ellenbeckiana* Engl, *D. fragrans* (L.) Ker-Gawl and *D. laxissima* Engl (Beentje, 1994).

2.3.1.1: Dracaena usambarensis

D. usambarensis, Figure 2.1, is a tree of 3-6 m in height (Beentje,1994). The flowers of this plant are white with orange to red fruits (Beentje,1994). It grows mostly in moist forests usually near streams and is distributed in the coastal regions of Kenya, Tanzania, DR Congo, Burundi, Zimbabwe and South Africa (Beentje, 1994; Damen *et al.*, 2018).

(Photo taken by Nchiozem, March 2018)

Figure 2.1: Stems (left) and leaves (right) of *Dracaena usambarensis*

2.3.1.2: Dracaena aletriformis

D. aletriformis, Figure 2.2, commonly known as large-leaved dragon tree, is a shrubby species and is native to East Africa and other neighboring islands of the Indian Ocean (Madagascar and Mauritius) (Nayak *et al.*, 2019).

(Photo taken by Nchiozem, March 2018)

Figure 2.2: Whole plant of *Dracaena aletriformis*

2.3.1.3: Dracaena steudneri

D. steudneri, Figure 2.3, it is an evergreen tree of more than 5 m in height (Kale *et al.*, 2019). The flowers are pale white-yellow-green and the fruits are green (Kale *et al.*, 2019). This plant is found in DR Congo, Ethiopia and East to Southern Africa (Damen *et al.*, 2018).

(Photo taken by Nchiozem, November 2018)

Figure 2.3: Seeds (left) and leaves (right) of *Dracaena steudneri*

2.4: Ethnobotanical Uses of Plants from the Genus *Dracaena*

Dracaena is also known as red resin, due to its red gum resin from injured fruit and bark of some *Dracaena* species. This red resin has been used since ancient times for the treatment of injury, fractures, diarrhea, stomach ulcers, diabetes and bleeding (Li *et al.*, 2014; Min *et al.*, 2010). Some plants of this genus are used as ornamentals while others have medicinal values (Yokosuka *et al.*, 2000). Among the *Dracaena* species, *D. cinnabari*, *D. ombet*, *D. draco*, *D. cambodiana*, *D. marginata* and *D. cochichinensis* have been documented as sources of dragon's blood (Edward *et al.*, 2001; Gupta *et al.*, 2008). Traditionally, the red resin of *D. cochinchinensis* is used in Chinese pharmacopeia to promote blood circulation (Ghaly *et al.*, 2014). In Cameroon, the extract from

root of *D. mannii* is used in the management of erectile dysfunction while the bark decoction is used against abdominal pains (Noumi *et al.*, 1998). In the same country, the leaves of *D. viridiflora* are used against infectious diseases, convulsions and epilepsy in childhood (Teponno *et al.*, 2017). The roots of *D. angustifolia* is used to treat diarrhea, inflammation and asthma (Huang *et al.*, 2013). *D. cambodiana* one of the species found in China is used in the treatment of ostealgia, congestion, ulcers and pimples (Chau *et al.*, 2009). The stem of *D. laureiri* are used to treat fever, cough and inflammation (Thiengsusuk *et al*., 2013). The decoction of the root of *D. fragrans* are taken to raise the CD4 counts in HIV patients (Moshi *et al*., 2012). In Uganda, the leaves and bark of *D. fragrans* are used traditionally in the treatment of ear pain and malnutrition, respectively (Lacroix *et al*., 2011). In Tanzania, the extract from the leaves of *D. steudneri* is used indigenously for the treatment of splenomegaly, hernia, asthma and chest problems (Moshi *et al.*, 2012) and in Rwanda this species is used to treat liver diseases (Mukazayire *et al.*, 2011). In Kenya, the extract from the stem is drunk for the management of hepatic liver ailments, treatment of measles and reducing pain during childbirth (Kokwaro, 2009).

2.5: Phytochemistry from the Genus *Dracaena*

Phytochemical investigation study on different parts of *Dracaena* species indicated the presence saponins, sapogenins, homoisoflavonoids, flavonoids, flavonoids dimers, lignans and phenolic amides among others (Sun *et al.*, 2019; Thu *et al.*, 2020).

2.5.1: Saponins from the Genus Dracaena

A literature survey on this genus showed that, saponins are the main constituents found in the genus *Dracaena*. Saponins are chemical compounds widespread in plant species and made up of thirty carbon precursor oxidosqualene to which sugar moieties are connected (Vincken *et al.*, 2007). The number of glycosyl chain connected to the genins vary, giving rise to another

dimension of nomenclature (mono-, bi-, and tridesmosidic saponins). A representative sample of saponins from the genus *Dracaena* are as shown in Table 2.1.

Table 2.1: Saponins of the genus *Dracaena*

***Dracaena* species (Plant part)**	**Name**	**Reference**
D. angustifolia (Stem)	Angudracanosides A – F (**40 – 45**)	Xu *et al.*, 2010
D. angustifolia (Whole plant)	Alliospiroside A (**46**)	Huang *et al.*, 2013
	Drangustosides A (**47**) and B (**48**)	
D. angustifolia (Roots and Rhizomes)	Namonins A – F (**49 – 54)**	Tran *et al.*, 2001
D. arborea (Bark)	Arboreasaponins A (**55**) and B (**56**)	Kougan *et al.*, 2010
D. concinna (Stem)	Concinnasteoside A (**57**)	Mimaki *et al.*, 1997
D. cambodiana (Dragon's blood)	Cambodianosides A – B (**58 – 63**)	Shen *et al.*, 2014
	Cambodianoside G (**64**)	Luo *et al.*, 2015
D. deisteliana (Stem)	Deistelianosides A (**65**) and B (**66**)	Kougan *et al.*, 2010
D. draco (Leaves)	Icodeside (**67**)	Hernández *et al.*, 2006
D. draco (Stem bark)	Draconins A – C (**68 – 70**)	González *et al.*, 2003
D. mannii (Stem bark)	Mannioside A (**71**)	Tapondjou *et al.*, 2008
D. surculosa (Whole plant)	Surculosides A – C (**72 – 74**)	Yokosuka *et al.*, 2000
D. viridiflora (Leaves)	Dioscin (**75**)	Teponno *et al.*, 2017
	Prosapogenin A of dioscin (**76**)	
	Trillin (**77**)	

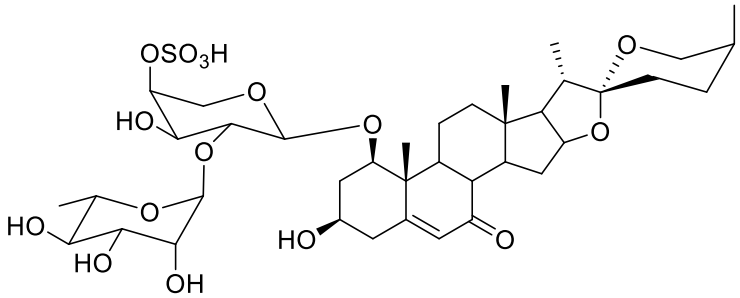

40

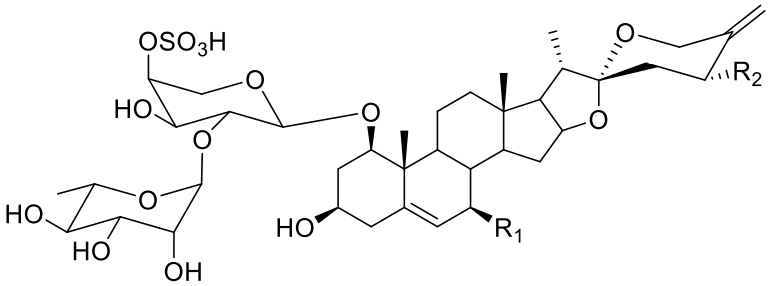

	R_1	R_2
41	H	H
42	OH	H
43	H	OH

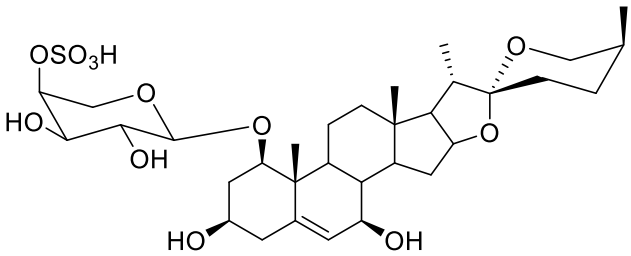

44

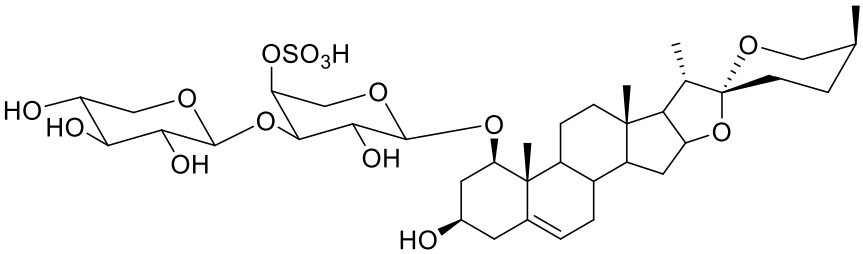

45

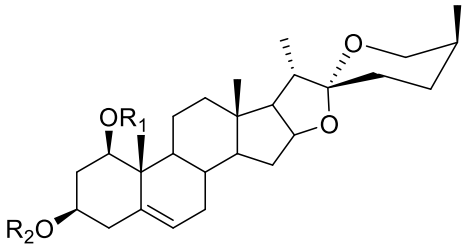

	R_1	R_2
46	H	Sugar 1
47	H	Sugar 2
48	Sugar 3	H

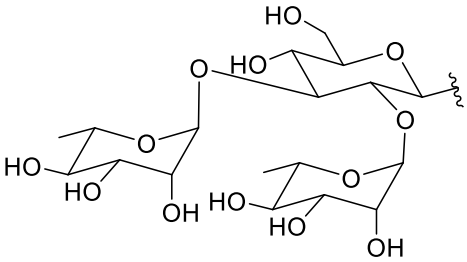

Sugar 1

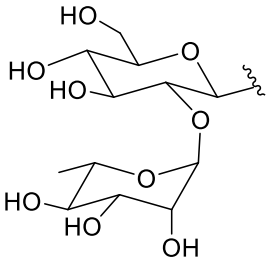

Sugar 2

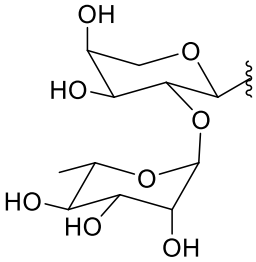

Sugar 3

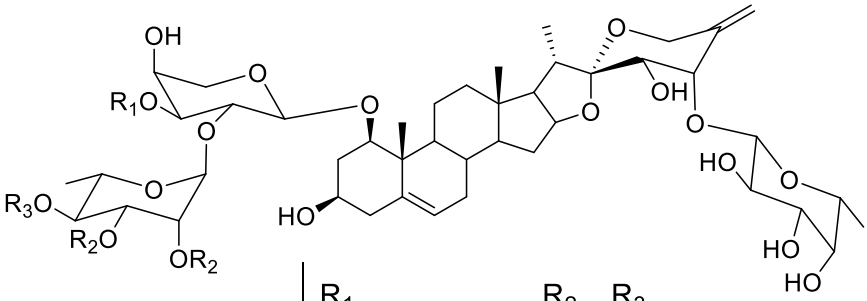

	R_1	R_2	R_3
49	3-*O*-AcetylXyl	Ac	Ac
50	4-*O*-AcetylXyl	Ac	Ac
51	H	H	H
52	H	H	Ac

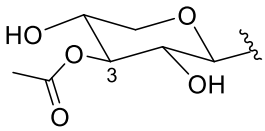

3-*O*-AcetylXyl

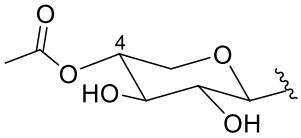

4-*O*-AcetylXyl

Ac

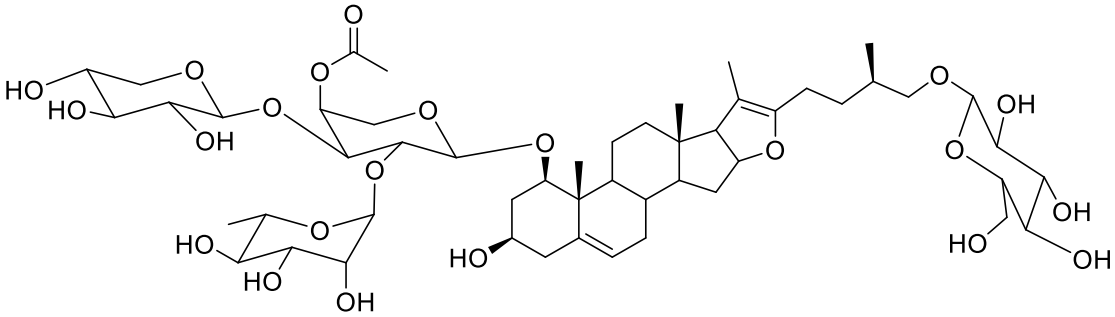

53

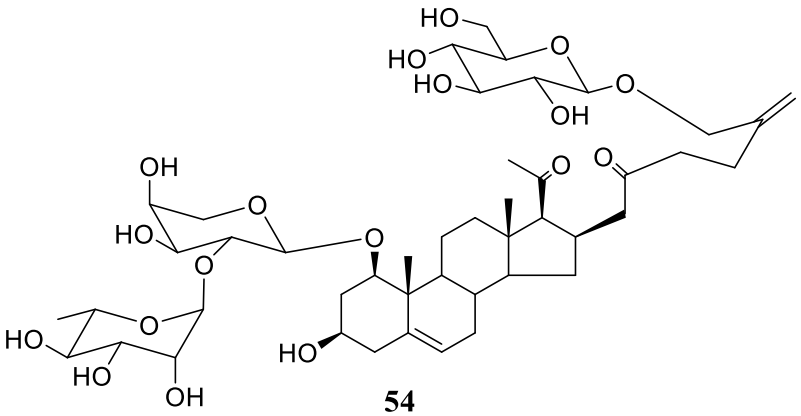

54

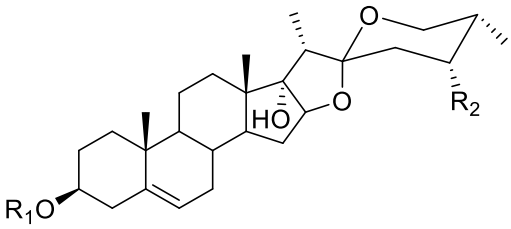

	R_1	R_2
55	Sugar 4	H
56	Sugar 5	OH

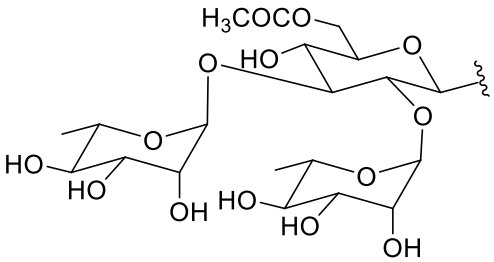

Sugar 4

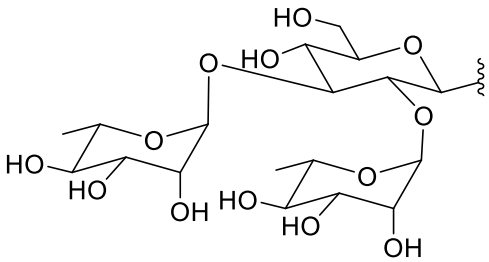

Sugar 5

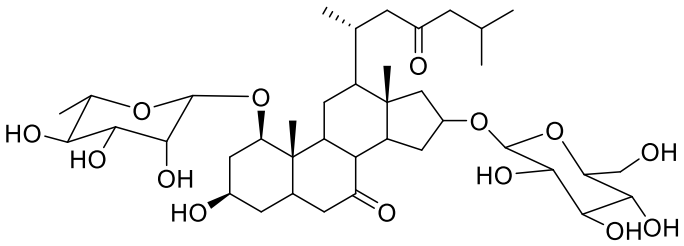

57

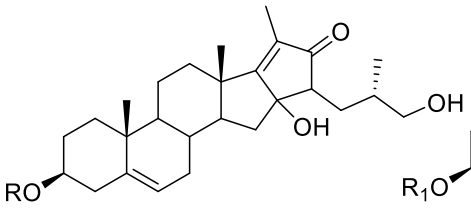

	R
58	Sugar 6

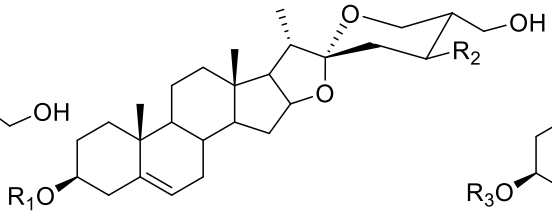

	R_1	R_2
59	Sugar 6	OH
60	Sugar 6	H

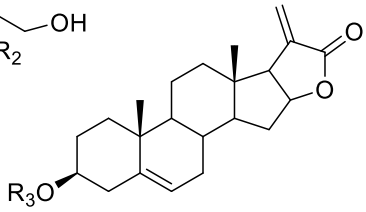

	R_3
61	Sugar 6

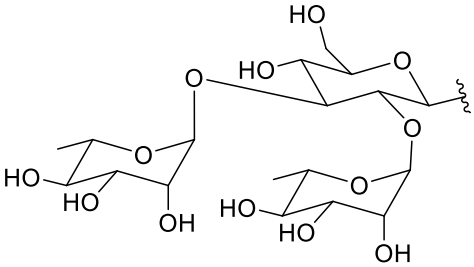

Sugar 6

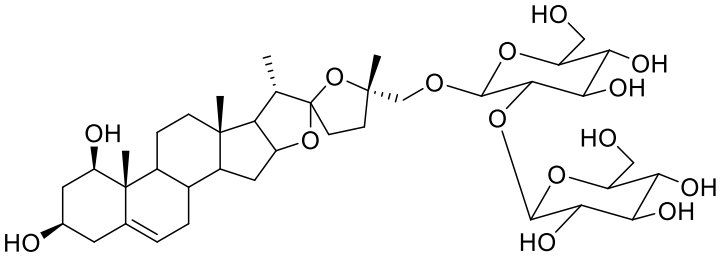

62

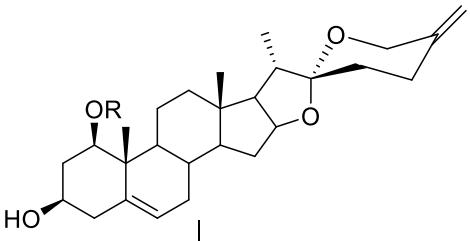

	R
63	Sugar 7

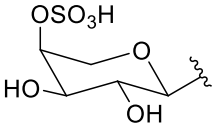

Sugar 7

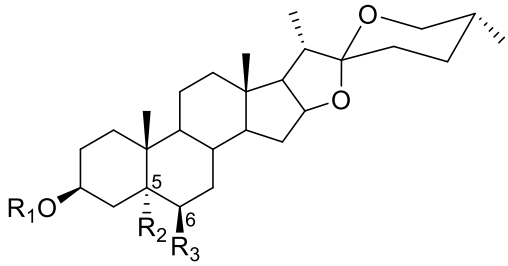

	R_1	R_2	R_3
64	Sugar 8	OH	OH
65$\Delta^{5(6)}$	Sugar 9	H	H

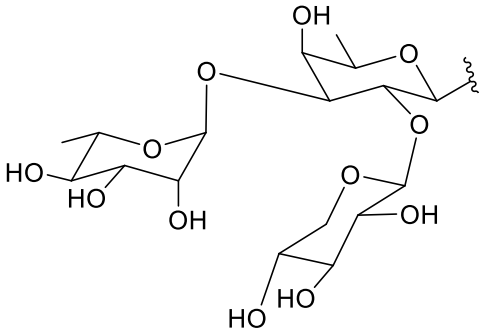

Sugar 8

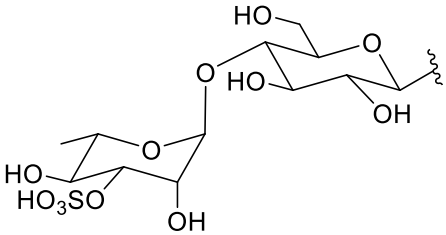

Sugar 9

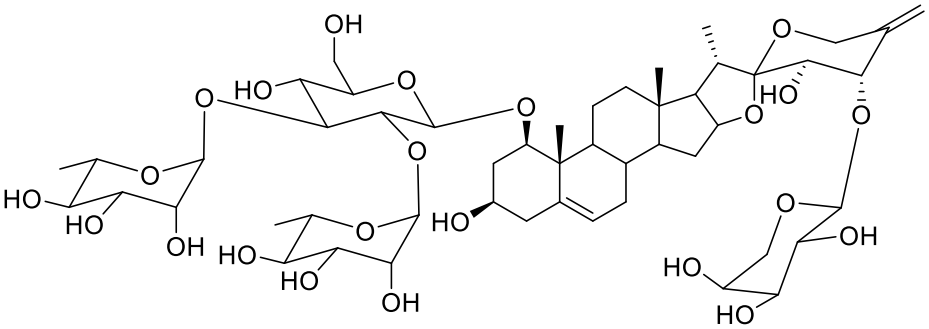

66

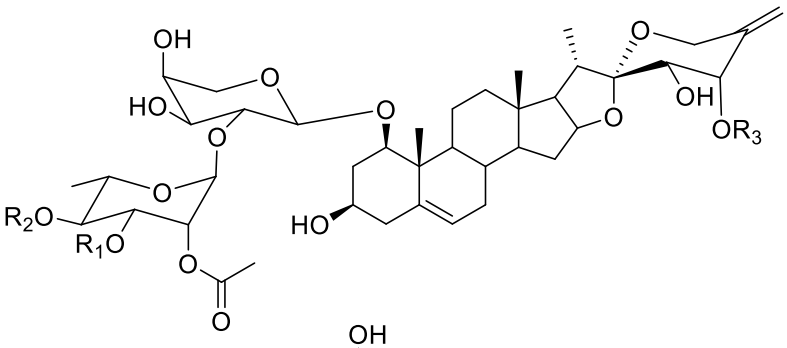

	R_1	R_2	R_3
67	Ac	Ac	α–L-Arap
68	Ac	Ac	H
69	Ac	H	H
70	H	H	H

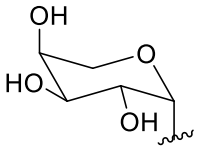

α–L-Arap

Ac

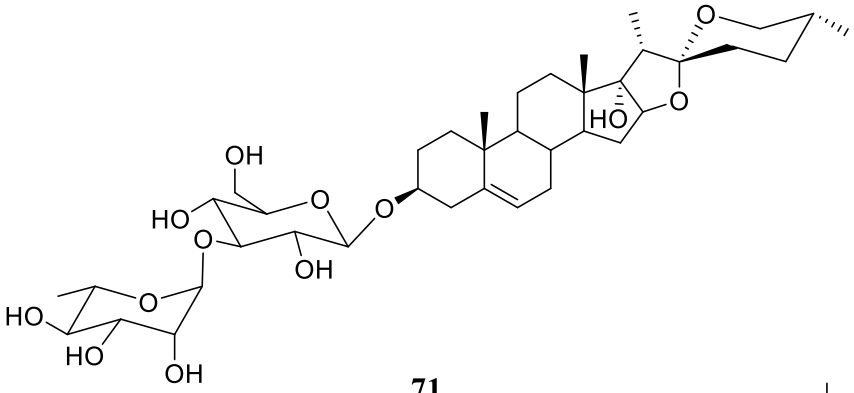

71

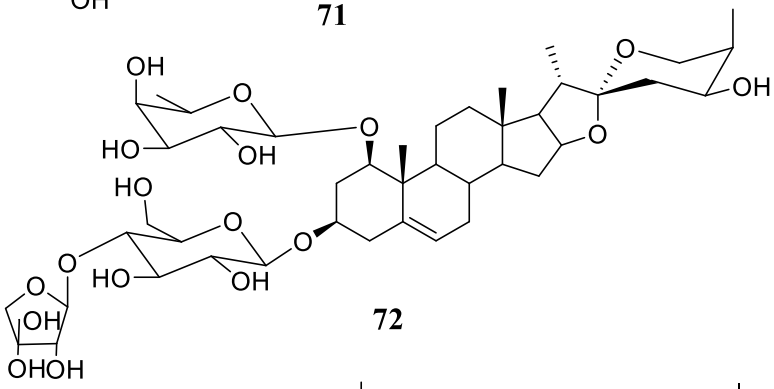

72

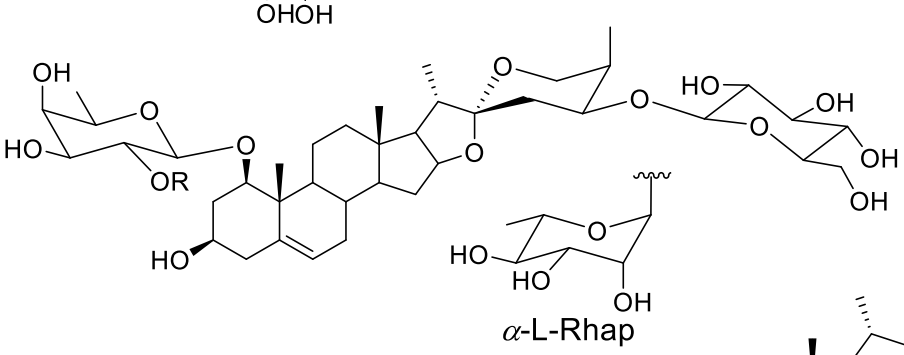

	R
73	H
74	α-L-Rhap

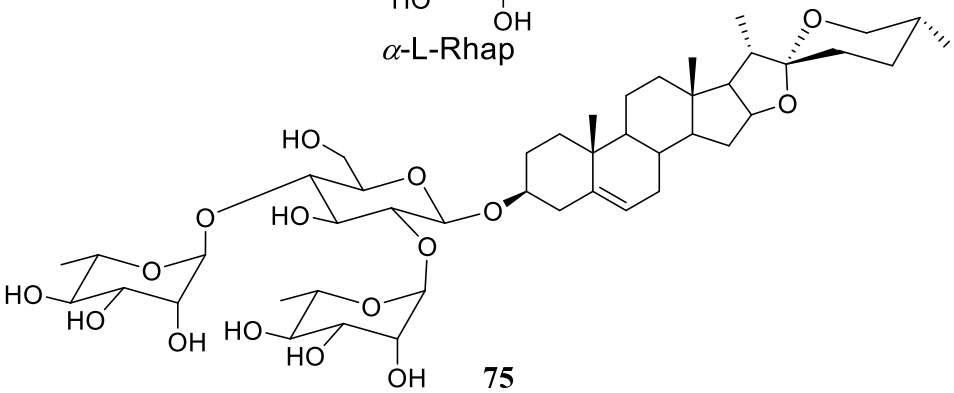

75

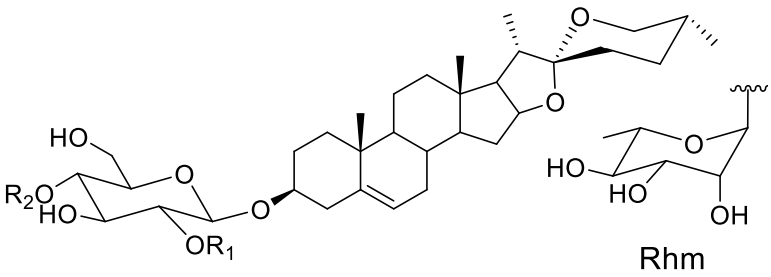

	R_1	R_2
76	H	H
77	Rhm	Rhm

2.5.2: Sapogenins from the Genus Dracaena

Sapogenins represent the aglycone (glycoside-free) of saponins with a triterpene (C_{30}) or a steroid (C_{27}) backbone. Only a few of them have been documented from the genus *Dracaena*. They are only reported from *D. angustifolia*, *D. draco* and *D. cochinchinsis* as depicted in Table 2.2.

Table 2.2: Sapogenins of the genus *Dracaena*

***Dracaena* species (Plant part)**	**Name**	**Reference**
D. angustifolia (Roots and Rhizomes)	Namogenins A – C (**78 – 80**)	Tran *et al.*, 2001
D. cochinchinsis (Red resin)	Dracaenogenins A (**81**) and B (**82**)	Zheng *et al.*, 2006a
D. draco (Root)	Diosgenone (**83**)	Hernandez *et al.*, 2004
	Diosgenin (**84**)	

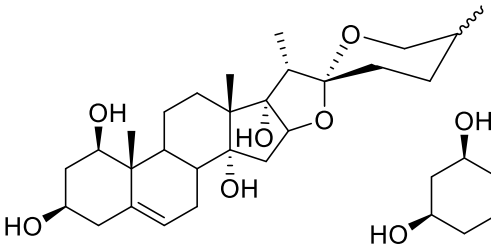

78

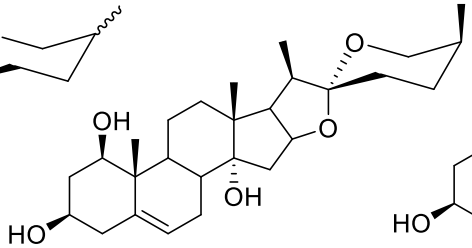

79

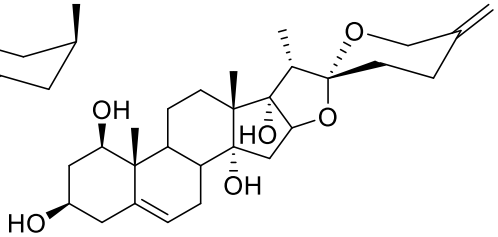

80

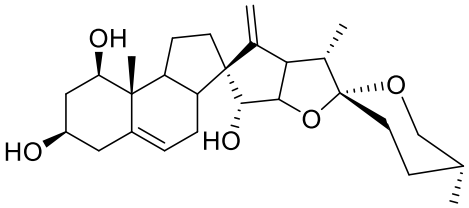

81

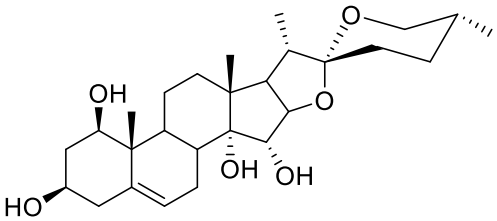

82

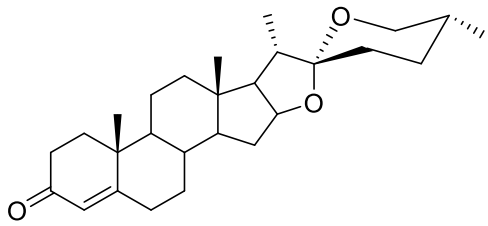

83

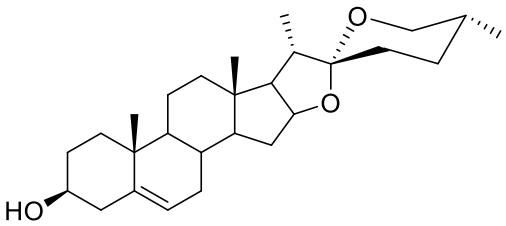

84

2.5.3: Homoisoflavonoids from the Genus Dracaena

Homoisoflavonoids are phenolic compounds whose structure differ from that of isoflavonoids by addition of a methylene group (CH_2) into the scaffold (Lin *et al.*, 2014). On the basis of their scaffold, this class of compounds can be classified into five sub-classes as scillascillin (**I**), brazilin (**II**), protosappanin (**III**), caelsalpin (**IV**) and sappanin (**V**) classes of homoisoflavonoids, Figure 2.4 (Lin *et al.*, 2014). Caelsalpin (**IV**) and sappanin (**V**) type homoisoflavonoids were reported from the genus *Dracaena*.

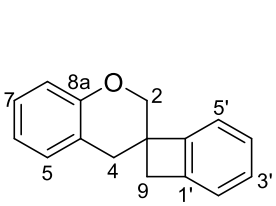

I

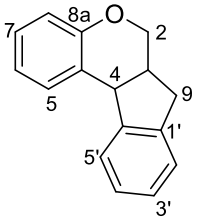

II

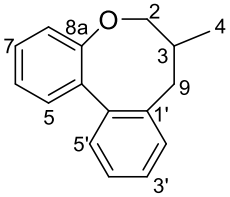

III

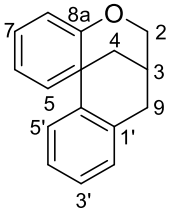

IV

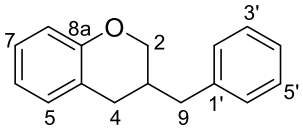

V

Figure 2.4: Skeleton of types of homoisoflavonoids

2.5.3.1: Sappanin-type Homoisoflavonoids from the Genus Dracaena

Skeleton **V** can be further subdivided based on the substitution pattern in ring C (Adinolfi *et al.*, 1986; Lin et al., 2014). Representative of the four sappanin-type homoisoflavonoids isolated from the genus *Dracaena* are presented herein.

2.5.3.1.1: 3-Benzylchroman type Homoisoflavonoids from the Genus Dracaena

3-Benzylchroman type homoisoflavonoids bears a chroman core in which the benzyl group is connected at C-3 position, their basic skeleton is shown in Figure 2.5. Previous studies showed

that, such compounds have been reported from the red resin of *D. cinnabari*, *D. cochinchinensis* and *D. draco* (Table 2.3).

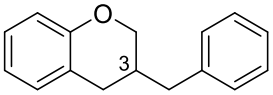

Figure 2.5: Basic skeleton of 3-benzylchroman type homoisoflavonoids

Table 2.3: 3-Benzylchroman type homoisoflavonoids of the genus *Dracaena*

***Dracaena* species (Plant part)**	**Name**	**Reference**
D. cinnabari (Dragon's blood)	7-Hydroxy-3-(3-hydroxy-4-methoxybenzyl)chroman (**85**)	Masaoud *et al.*, 1995a
	7-Hydroxy-3-(4-hydroxybenzyl)-8-methoxychroman (**86**)	
	3-(4-Hydroxybenzyl)-7,8-methylenedioxychroman (**87**)	
	7-Hydroxy-3-(4-hydroxybenzyl)chroman (**88**)	
D. cochinchinensis (Dragon's blood)	(3*R*)-4′,7-Dihydroxy-6-methoxyhomoisoflavane (**89**)	Pang *et al.*, 2018
	3′,7-Dihydroxy-4′,8-dimethoxyhomoisoflavane (**90**)	Su *et al.*, 2014
	4′-Hydroxy-7,8-dimethoxyhomoisoflavane (**91**)	
	3-(4-Hydroxybenzyl)-5,7-dimethoxychroman (**92**)	
	Dracaeconolide B (**93**)	Xu *et al.*, 2016
	(3*R*)-4′,7-Dihydroxy-8-methoxyhomoisoflavane (**94**)	
	(3*R*)-4′,7-Dihydroxy-5-methoxy-homoisoflavane (**95**)	
	(3*R*)-4′,6-Dihydroxy-8-methoxyhomoisoflavane (**96**)	
D. draco (Dragon's blood)	3-(4-Hydroxybenzyl)-5,7-dimethoxychroman (**97**)	González *et al.*, 2000

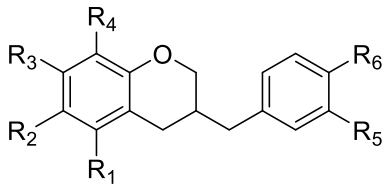

	R_1	R_2	R_3	R_4	R_5	R_6
85	H	H	OH	H	OH	OCH_3
86	H	H	OH	OCH_3	H	OH
87	H	H	$-OCH_2O-$		H	OH
88	H	H	OH	H	H	OH
89	H	OCH_3	OH	H	H	OH
90	H	H	OH	OCH_3	OH	OCH_3
91	H	H	OCH_3	OCH_3	H	OH
92	OCH_3	H	OCH_3	H	H	OH
93	OCH_3	H	OH	OCH_3	H	OH
94	H	H	OH	OCH_3	H	OH
95	OCH_3	H	OH	H	H	OH
96	H	OH	H	OCH_3	H	OH
97	OCH_3	H	OCH_3	H	H	OH

2.5.3.1.2: 3-Benzylchroman-4-one type Homoisoflavonoids from the Genus Dracaena

3-Benzylchroman-4-one type homoisoflavonoids differ from 3-benzylchroman type homoisoflavonoids by incorporation of a keto group at C-4 position, Figure 2.6.

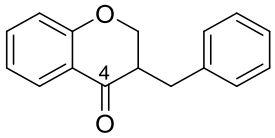

Figure 2.6: Basic skeleton of 3-benzylchroman-4-one type homoisoflavonoids

Their occurrence has been reported in some *Dracaena* species. The stem wood of *D. loureirin* provided 4′,5,7-trihydroxyhomoisoflavanone (**98**) and 4′,7-dihydroxy-5 methoxyhomoisoflavanone (**99**) (Ichikawa *et al.*, 1997). Two compounds, (3*R*)-4′,7-dihydrohomoisoflavanone (**100**) (Luo *et al.*, 2011a) and 7-hydroxy-4′-methoxyhomoisoflavanone (**101**) (Hu *et al.*, 2015) were reported from *D. cambodiana* and *D. cochinchinensis*, respectively.

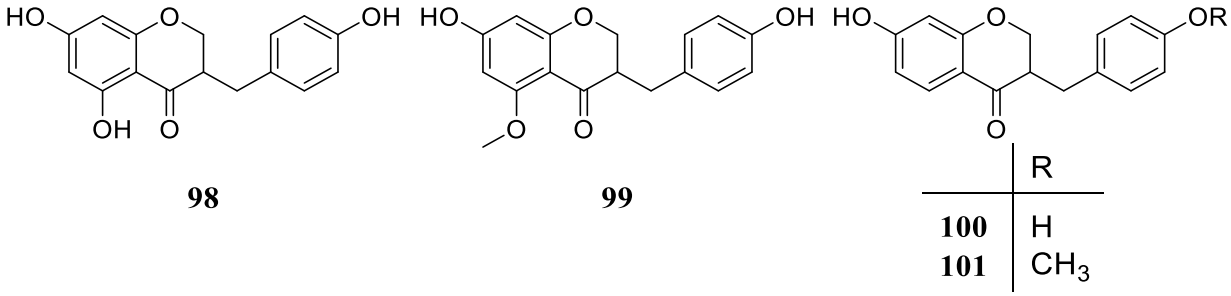

2.5.3.1.3: 3-Benzylchroman-3-ol-4-one type Homoisoflavonoids from the Genus Dracaena

3-Benzylchroman-3-ol-4-one type homoisoflavonoids are characterized by having a hydroxyl at C-3 position in a 3-benzylchroman-4-one skeleton, Figure 2.7.

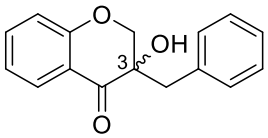

Figure 2.7: Basic skeleton of 3-benzylchroman-3-ol-4-one type homoisoflavonoids

A small number of 3-benzylchroman-3-ol-4-one type homoisoflavonoids have been reported from the genus. Secondary metabolites with such scaffold are reported in Table 2.4.

Table 2.4: 3-Benzylchroman-3-ol-4-one type homoisoflavonoids of the genus *Dracaena*

***Dracaena* species (Plant part)**	**Name**	**Reference**
D. cambodiana (Stem)	Cambodianol (**102**)	Liu *et al.*, 2009
D. cochinchinensis (Leaves)	(3*R*)-3,7-Dihydroxy-4′,8-dimethoxyhomoisoflavanone (**103**)	Hu *et al.*, 2015
D. cochinchinensis (Dragon's Blood)	Dracaeconolide A (**104**)	Su *et al.*, 2014
	(3*S*)-3,4′,7-Trihydroxy-5-methoxy homoisoflavanonol (**105)**	Pang *et al.*, 2018
D. draco (Leaves)	Dracol (**106**)	Hernández *et al.*, 2006
	Eucomol (**107**)	
D. loureiri (Stem wood)	Loureiriol (**108**)	Kittisak *et al.*, 2002

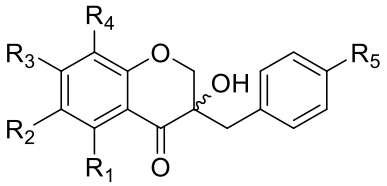

	R_1	R_2	R_3	R_4	R_5	
102	OH	CH_3	OH	H	OCH_3	3β
103	H	H	OH	OCH_3	OCH_3	3β
104	H	H	OH	H	OCH_3	3α
105	OCH_3	H	OH	H	OH	3α
106	OH	H	OCH_3	OCH_3	OCH_3	3β
107	OH	H	OH	H	OCH_3	3β
108	OH	H	OH	H	OH	3β

2.5.3.1.4: $\Delta^{2,3}$ 3-Benzylchroman-4-one type Homoisoflavonoids from the Genus Dracaena

$\Delta^{2,3}$ 3-Benzylchroman-4-one type homoisoflavonoids are 3-benzylchroman-4-one type homoisoflavonoids with an α,β-unsaturation, Figure 2.8. *Dracaena draco* and *D. cochinchinensis* yielded 4′,7-dihydroxyhomoisoflavone (**109**) (González *et al.*, 2000) and 4′,5-dihydroxy-7-methoxyhomoisoflavone (**110**) (Pang *et al.*, 2018), respectively. Homoisoflavonoids, 4′,5,7-trihydroxy-6-methylhomoisoflavone (**111**), 4′,5,7-trihydroxy-8-methylhomoisoflavone (**112**) and 4′,5,7-trihydroxyhomoisoflavone (**113**) were reported from *D. angustifolia* (Zhao *et al.*, 2020).

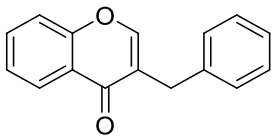

Figure 2.8: Basic skeleton of $\Delta^{2,3}$ 3-benzylchroman-4-one type homoisoflavonoids

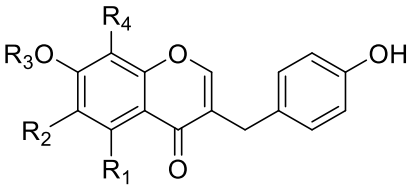

	R_1	R_2	R_3	R_4
109	H	H	H	H
110	OH	H	CH_3	H
111	OH	CH_3	H	H
112	OH	H	H	CH_3
113	OH	H	H	H

2.5.3.2: Caesalpin-type Homoisoflavonoids from the Genus Dracaena

The caesalpin-type homoisoflavonoids, isolated from *Dracaena* species include dracaenone (**114 – 118**) obtained from *Dracaena* cochinchinensis (Pang *et al.*, 2018, Zheng *et al.*, 2006b).

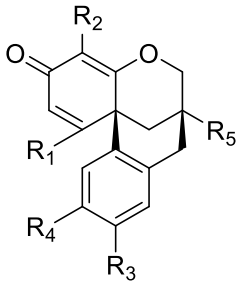

	R_1	R_2	R_3	R_4	R_5
114	H	OCH_3	OH	OCH_3	OH
115	OCH_3	H	OH	OH	H
116	OCH_3	H	OCH_3	OH	H
117	H	H	OH	OCH_3	H
118	H	H	OH	OH	H

2.5.4: Flavonoids from the Genus Dracaena

Flavonoids represents a wide range of natural compounds belonging to the family of polyphenols. These are colored substances that may be responsible for the yellow, orange and red colours of different plant organs (Havsteen, 2002; Medić-Šarić *et al.*, 2004). From a structural point of view, flavonoids have a common biosynthetic origin, therefore, have the same basic skeleton (Grotewold, 2006). From this genus, flavonoids that belong to the flavan, flavone, chalcone, dihydrochalcone and retrodihydrochalcone subsclasses were reported.

2.5.4.1: Flavans from the Genus Dracaena

Flavans belong to the subclass of flavonoids known as 2-phenylbenzopyrans. Flavans isolated from the genus *Dracaena* are reported in Table 2.5.

Table 2.5: Flavans of the genus *Dracaena*

***Dracaena* species (Plant part)**	**Name**	**Reference**
D. angustifolia (Stem)	2-(3-Hydroxy-5-methoxyphenyl)-5-methoxy-8-methylchroman-7-ol (**119**)	Zhao *et al.*, 2020
	2-(4-Hydroxy-3-methoxyphenyl)-5-methoxy-8-methylchroman-7-ol (**120**)	
D. cambodiana (Dragon's blood)	Cambodianin D (**121**)	Chen *et al.*, 2012
	2-(3-Hydroxy-4-methoxyphenyl)-8-methylchroman-7-ol (**122**)	
D. cambodiana (Stem)	(2*S*)-4′,7-Dihydroxyflavane (**123**)	Liu *et al.*, 2008
	2-(4-Hydroxyphenyl)-6,8-dimethylchroman-7-ol (**124**)	
	2-(4-Methoxyphenyl)-8-methylchroman-5,7-diol (**125**)	
D. cambodiana (Dragon's blood)	Dammaradienol (**126**)	Shen *et al.*, 2007
	(-)-5-Methoxyflavan-7-ol (**127**)	
D. cochinchinensis (Leaves)	2-(4-Hydroxy-3-methoxyphenyl)-8-methylchroman-7-ol (**128**)	Hu *et al.*, 2015
D. cochinchinensis	2-(4-Hydroxyphenyl)-8-methylchroman-7-ol (**129**)	Xu *et al.*, 2016
	2-(4-Hydroxyphenyl)-5-methoxy-8-methylchroman-7-ol (**130**)	
	2-(4-Hydroxy-3-methoxyphenyl) chroman-7-ol (**131**)	

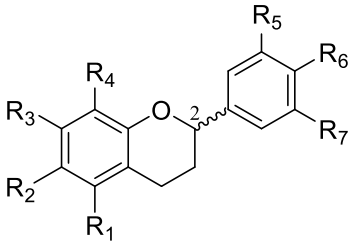

	R_1	R_2	R_3	R_4	R_5	R_6	R_7	
119	OCH_3	H	OH	CH_3	OH	H	OCH_3	2β
120	OCH_3	H	OH	CH_3	OCH_3	OH	H	2β
121	OH	CH_3	OCH_3	CH_3	H	OH	H	2α
122	H	H	OH	CH_3	OH	OCH_3	H	2α
123	H	H	OH	H	H	OH	H	2α
124	H	CH_3	OH	CH_3	H	OH	H	2α
125	OH	H	OH	CH_3	H	OCH_3	H	2α
126	OCH_3	H	OH	H	H	H	H	2β
127	OCH_3	CH_3	OH	H	H	H	H	2β
128	H	H	OH	CH_3	OCH_3	OH	H	2α
129	H	H	OH	CH_3	H	OH	H	2α
130	OCH_3	H	OH	CH_3	H	OH	H	2α
131	H	H	OH	H	OCH_3	OH	H	2α

2.5.4.2: Flavones from the Genus Dracaena

Flavones bear a chromanone core in which a phenyl group is attached at C-2. Examples of this class of secondary metabolites are 3′,7-dihydroxy-4′-methoxyflavone (**132**), 4′,7-dihydroxyflavone (**133**) and 7-hydroxyflavone (**134**) reported from *D. cochinchinensis* (Tang *et al.*, 2019)

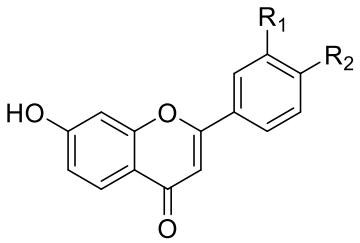

	R_1	R_2
132	OH	OCH_3
133	H	OH
134	H	H

2.5.4.3: Chalcones, Dihydrochacones and Retrodihydrochacones from the Genus Dracaena

Chalcones are the precursors of flavonoids and homoisoflavonoids (Abegaz *et al.*, 2007; Mirossay *et al.*, 2018). Representatives of the chalcones (**135** – **137**) (Wang *et al*., 2011), dihydrochacones (**138** and **139**) (Luo *et al*., 2011a) and retrodihydrochalcones (**140** – **144**) (Ichikawa *et al*., 1997) reported from *D. cambodiana* (stems), *D. cambodiana* (dragon's blood), *D. loureirin* (stem wood), respectively.

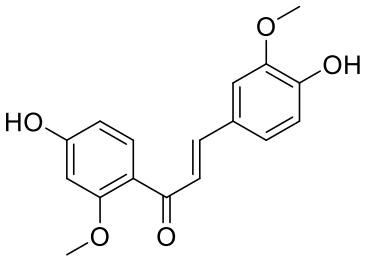

135

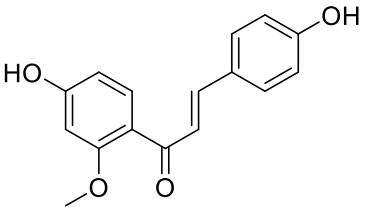

136

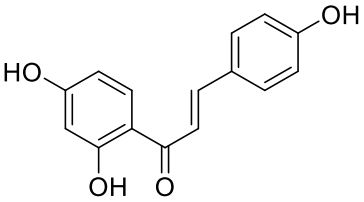

137

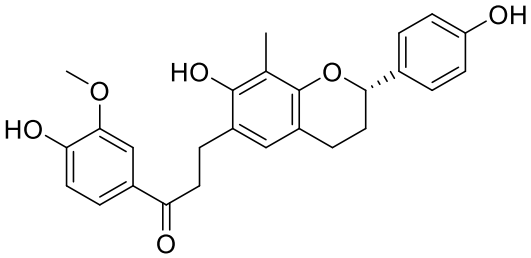

138

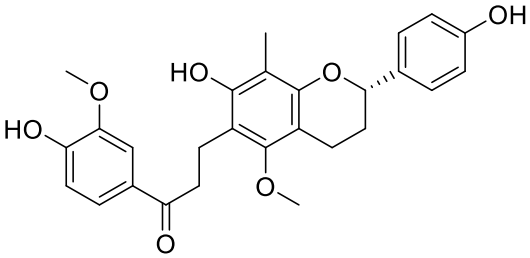

139

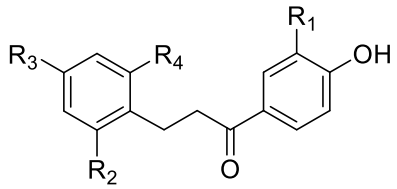

	R_1	R_2	R_3	R_4
140	OCH_3	OCH_3	OH	H
141	H	OCH_3	OH	OCH_3
142	H	OH	OCH_3	OCH_3
143	H	OCH_3	OCH_3	OCH_3
144	H	OCH_3	OH	OH

2.5.5: Conjugated Chalcone-stilbenes and Polymeric Flavonoids from the Genus Dracaena

Two dragon's blood species, *D. cochinchinensis* and *D. cambodiana*, have been reported so far as the main sources of conjugated chalcone-stilbene and flavonoid dimers. Cochinchinenenes A – D, G and H (**145** – **150**) are examples of conjugated chalcone-stilbenes which have been reported from different parts of *D. cochinchinensis* (Hao *et al.*, 2015; Zhu *et al.*, 2007).

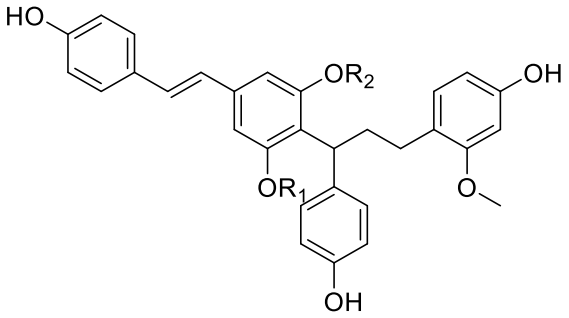

	R_1	R_2
145	CH_3	CH_3
150	H	H

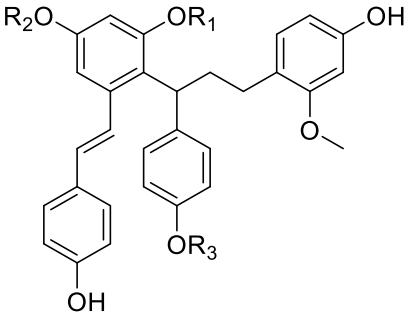

	R_1	R_2	R_3
146	H	CH_3	CH_3
147	CH_3	H	H
148	H	H	H
149	CH_3	CH_3	CH_3

Bisflavonoids reported in this genus include socotrin derivative (**150 – 152**) isolated from *D. cambodiana* (Dai *et al.*, 2012) and bisflavonoids (**153** and **154**) obtained from the red resin of *D. cinnabari* (Masaoud *et al.*, 1995b). The dragon's blood of *D. cochinchinensis* afforded another set of bioflavonoids, (-)-cochinchinenins I-M (**155** – **159**) (Pang *et al.*, 2016), cochinchinenene G (**160**) (Tang *et al.*, 2019), dracaenin A (**161**) (Tang *et al.*, 2019) and biflavocochins A – D (**162** – **165**) (Lang *et al.*, 2020).

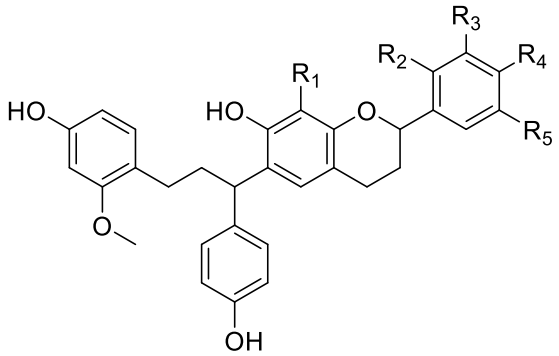

	R_1	R_2	R_3	R_4	R_5
150	CH_3	H	OCH_3	OH	H
151	CH_3	H	OH	OCH_3	H
152	CH_3	H	H	OH	H
153	H	OCH_3	H	H	OH

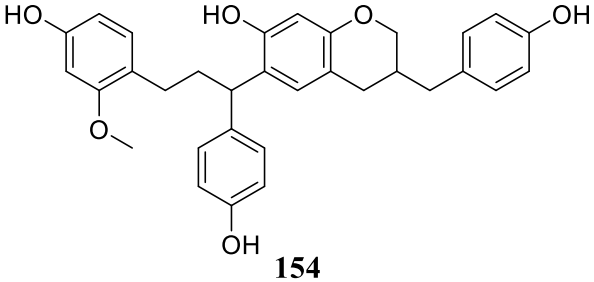

154

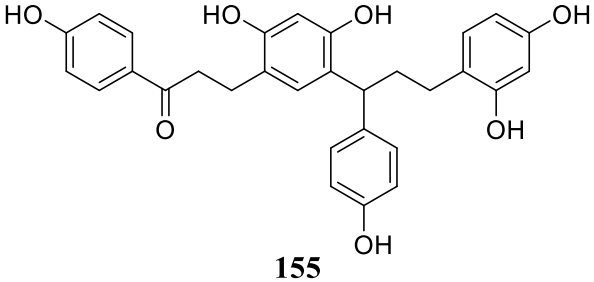

155

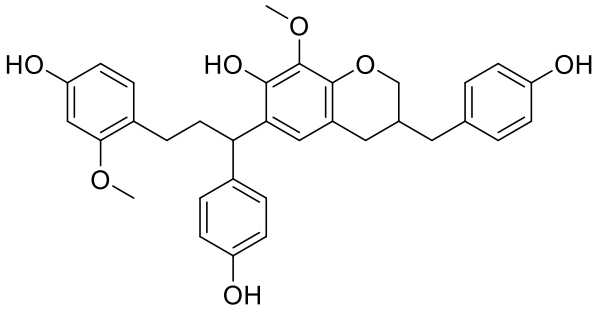

156

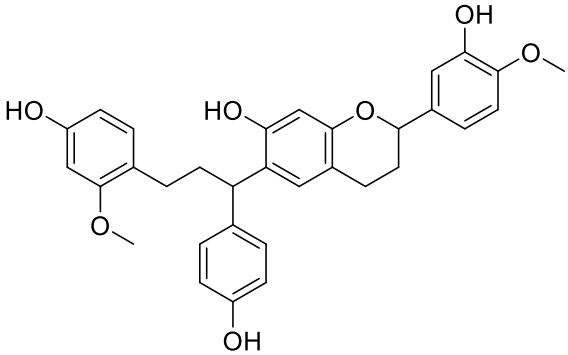

157

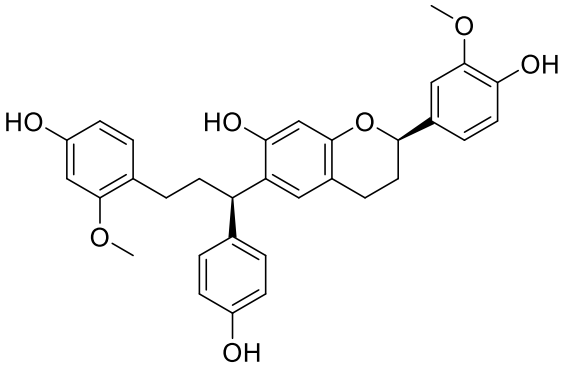

158

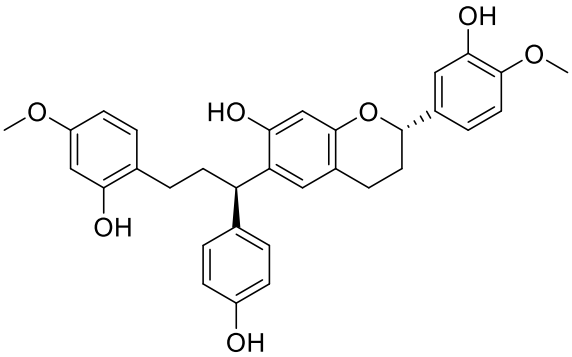

159

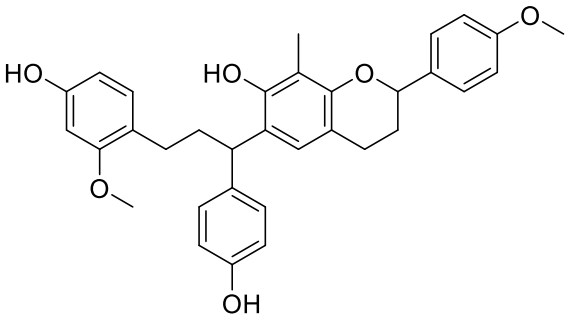

160

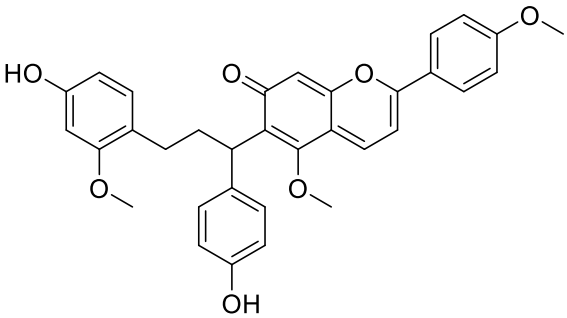

161

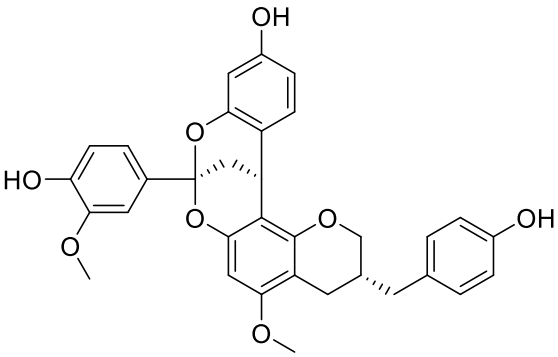

162

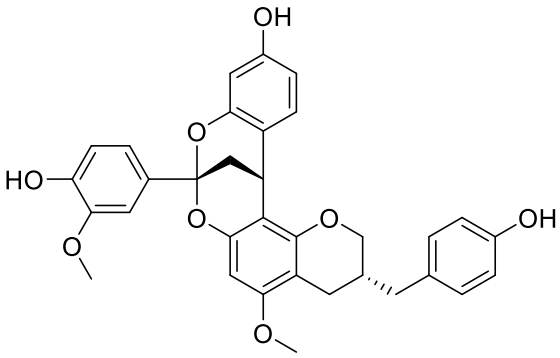

163

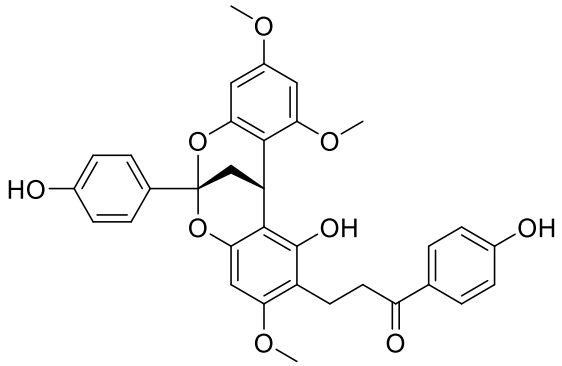

164

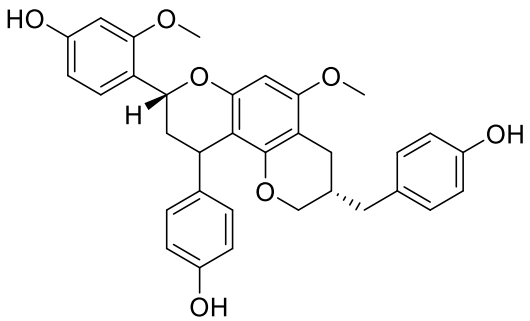

165

2.5.6: Lignans, Phenolic Amides and Stilbenoids from the Genus Dracaena

Few lignans including syringaresinol (**166**), pinoresinol (**167**) and balanophonin (**168**) were reported from the red resin of *D. cambodiana* (Luo *et al.*, 2011b).

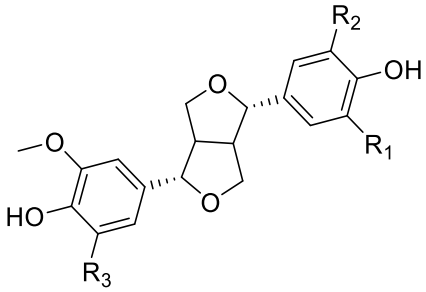

	R_1	R_2	R_3
166	OCH_3	OCH_3	OCH_3
167	H	OCH_3	H

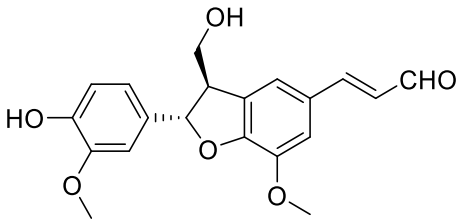

168

Some of the phenolic amides reported from the genus are compounds **169** – **172** (Hu *et al.*, 2015).

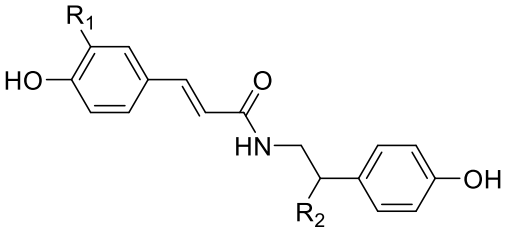

	R_1	R_2
169	OCH_3	H
170	H	H
171	OCH_3	OH

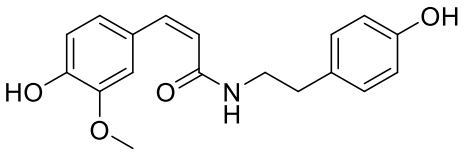

172

Stilbenoids isolated from the genus *Dracaena* include 3′,4,5′-trihydroxystilbene (**173**), 3′,4-dihydroxy-5′-methoxystilbene (**174**) and 4-hydroxy-3′,5′-dimethoxystilbene (**175**) reported from the stem wood of *D. loureirin* (Kittisak *et al.*, 2002).

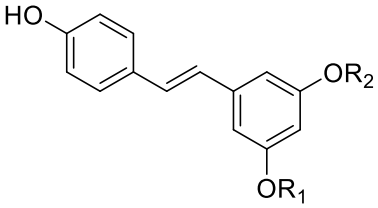

	R_1	R_2
173	H	H
174	CH_3	H
175	CH_3	CH_3

2.6: Biological Activities of the Phytochemicals from *Dracaena* Species

Biological activities of phytochemicals from the genus *Dracaena* include anti-inflammatory (Gupta *et al.*, 2014), cytotoxic (Tran *et al.*, 2001), antimicrobial (Zhu *et al.*, 2007) and antifungal (Xu *et al.*, 2010) among others. Majority of them being reported from *D. angustifolia, D. cochinchinensis, D. draco, D. arborea, D. viridifolia* and *D. angustifolia*. In the following sections, the anti-inflammatory and cytotoxic activities of secondary metabolites from the genus will be reviewed.

2.6.1: Anti-Inflammatory Activity of the Phytochemicals from Dracaena Species

A homoisoflavan, compound (**87**) obtained from *D. cinnabari* displayed anti-inflammatory effect against the production of NO and two biomarkers (IL-6 and TNF-α) in LPS stimulated mouse macrophage RAW 264.7 cells (Gupta *et al.*, 2014). Compounds 4′,7-dihydroxyhomoisoflavanone (**100**), (3*S*)-3,4′,7-trihydroxy-5-methoxyhomoisoflavanonol (**105**) and 10-hydroxy-11-

methoxydracaenone (**117**) isolated from dragon's blood *D. cochinchinensis* showed moderate inhibition of NO production with IC_{50} between 60.4 – 75.6 μM (Pang *et al.*, 2018). Similarly, the flavonoid dimers (-)- cochinchinenins L (**158**) and M (**159**) obtained from *D. cochinchinensis* displayed strong inhibition of NO production with IC_{50} values of 4.9 ± 0.4 and 5.4 ± 0.6 μM, respectively (Pang *et al.*, 2016). The stilbenoids (**173** – **175**) isolated from the stem wood of *D. loureirin* inhibited the enzymes COX-1 and COX-2 with IC_{50} ranging from 1.29 – 4.92 μM (Kittisak *et al.*, 2002).

2.6.2: Cytotoxic Activity of the Phytochemicals from Dracaena Species

Namonins A (**49**) and B (**50**) purified from *D. angustifolia* showed significant cytotoxicity towards HT-1080 with IC_{50} of 0.2 and 0.3 μM, respectively (Tran *et al.*, 2001). Icodeside (**67**), a bisdesmosidic steroidal saponin, obtained from the leaves of *D. draco* exhibited cytotoxicity towards HL-60 and A-431 after 72 h of exposure with IC_{50} values of 9.0 ± 4.0 and 16.1 ± 1.0 μM, respectively (Hernández *et al.*, 2006). Draconin A (**68**), purified from *D. draco* displayed cytotoxic effect towards HL-60 with IC_{50} value of 9.7 ± 2.7 μM (González *et al.*, 2003). Cambodianol (**102**) a homoisoflavonoid purified from the stem of *D. cambodiana*, showed significant cytotoxic potency towards K562 and SGC-7901 with IC_{50} of 1.4 and 2.9 μg/mL, respectively (Liu *et al.*, 2009).

CHAPTER 3: MATERIALS AND METHODS

3.1: Plants Materials

The plants under investigation in this study namely; *Dracaena usambarensis* (roots and stems), *Dracaena aletriformis* (whole plant) and *Dracaena steudneri* (seeds and leaves) were collected in March and November 2018. The plant materials were authenticated by a botanist in School of Biological Sciences, University of Nairobi, where a serialized voucher specimens were deposited, Table 3.1.

Table 3.1: Voucher number and place of collection of the three *Dracaena* species

Plant name	Voucher number	GPS	Place of collection
Dracaena usambarensis Engl.	NNA 2018/001	S 04°19′51.2″ E 039′31′05.7″ 68 m	Kaya Muhaka forest in the coastal region of Kenya
Dracaena aletriformis (Harv.) Bos	NNA 2018/002	S 04°24′53.1″ E 039′28′49.1″ 49 m	Gongoni forest in the coastal region of Kenya
Dracaena steudneri Engl.	NNA 2018/003	S 1°16′9.25″ E 36°47′52.6″ 900 m	Riverside Drive Garden in Nairobi

3.2: Chromatography

TLC was carried out on pre-coated kieselgel 60 plates 254 and 360 nm. For visualization of compounds, the spotted TLC plates were exposed to UV (λ_{max} 254 and 360 nm) light and further sprayed with a solution of H_2SO_4–EtOH (1:9, *v*/v). Different grades of silica gel (60-120 and 70-230 Mesh) and Sephadex LH-20 (25–100 μm) were used as stationary matrix for column chromatography (CC). For further purification, C_{18} semi-preparative HPLC was used. The HPLC separation was achieved using MeOH (B) in H_2O (A) (containing 0.1% methanoic acid) gradient program.

3.3: Spectroscopy and Spectrometry

NMR experiments were recorded on a Brucker advance I (500 MHz) and III (700 and 600 MHz). The NMR results were processed using MestReNova-9.0.1 software. The CD spectra and IR measurements were done using Jasco J-715 and Bruker Tensor 27 FT-IR Spectrometer, respectively. Specific rotations were measured using Kruss Optronic Polarimeter P8000-T. The mass spectra were generated on HRESIMS LTQ Orbitrap spectrometer. All tandem mass spectrometry (MS/MS) were measured using collision-induced dissociation (CID) with different energies of 15, 25 and 35 eV and the data was analyzed using Xcalibur software.

3.4: Extraction and Isolation of Compounds

3.4.1: Compounds Isolated from the Stems of Dracaena usambarensis

The stems of *D. usambarenis* were cut into small pieces, dried to constant weight under shade and ground. The ground plant material (2.1 Kg) was macerated in methanol/dichloromethane (1:1, 10 L, 24 h x 3). It was then filtered and evaporated yielding a red crude extract (72 g). About 2 g of this extract was reserved for bioassays. The remaining part was chromatographically separated on CC using silica gel (60-120 mesh) as solid matrix. The column was eluted with a mixture of cyclohexane/EtOAc (10:0, 9:1, 8:2, 7:3, 6:4, 1:1, 3:7 and 0:10) followed by EtOAc/MeOH (9:1, 8:2 and 0:10) in increasing polarity as mobile phases. This resulted into 160 fractions each of 500 mL which were pooled based on their LC-MS and TLC similarities into six sub-fractions $Fr_{A-F.}$

The fraction Fr_B obtained with 30% EtOAc in cyclohexane was loaded onto silica gel CC and eluted with a ternary system of cyclohexane/EtOAc/MeOH (6/3/1) to yield four sub-fractions Fr_{B1-4}. Using semi-preparative HPLC (MeOH/H_2O (6/4), flow rate 4 mL/min) sub-fraction Fr_{B3} was further purified to yield compound **176** (12.0 mg). Sub-fraction Fr_C (40% of EtOAc in cyclohexane) was purified with semi-preparative HPLC (MeOH/H_2O (1:1 upto 10:0), for 30 min

(flow rate 4 mL/min)) to give compounds **181** (3.5 mg) and **180** (4.7 mg). Similarly, sub-fraction Fr_D (70% of EtOAc in cyclohexane) gave compounds **177** (1.0 mg), **182** (0.5 mg) and **170** (0.7 mg). Sub-fraction Fr_E which eluted with 10% MeOH/EtOAc was passed through silica gel CC and eluted with an isocratic system of cyclohexane/EtOAc/MeOH (6.5:3:0.5) to afford five sub-fractions coded Fr_{E1-5}. Semi-preparative HPLC (MeOH/H_2O (6:4 upto 10:0), for 25 min (flow rate 4 mL/min)) of Fr_{E1} led to the isolation of compound **178** (0.6 mg), while Fr_{E2} afforded compounds **171** (3.6 mg) and **185** (3.0 mg). Similarly, compounds **184** (2.3 mg), **183** (7.4 mg) and **179** (1.2 mg) were isolated from sub-fractions $Fr_{E3,}$ Fr_{E4} and Fr_{E5}, respectively.

3.4.2: Compounds Isolated from the Roots of Dracaena usambarensis

The dried roots of *D. usambarensis* (2.4 Kg) were macerated with MeOH/CH_2Cl_2 (1:1, 10 L, 24 h x 3) yielding 120 g of a brownish residue. The crude extract (110 g) was subjected to CC on silica gel and run with gradients of *n*-hexane/EtOAc and EtOAc/MeOH to afford 330 fractions of 500 mL each which were pooled on the basis of their TLC profiles into nine sub-fractions Fr_{A-I}. Sub-fraction Fr_B that eluted with *n*-hexane/EtOAc (9:1 – 8.5:1.5) was purified on silica gel CC (gradients of *n*-hexane/EtOAc) to give compound **191** (35.1 mg). Sub-fraction Fr_C (*n*-hexane/EtOAc (8.5:1.5)) was loaded onto a silica gel column and eluted with a binary system of *n*-hexane/EtOAc (9:1) to afford compound **187** (8.0 mg). Purification of sub-fraction Fr_D (*n*-hexane/EtOAc (8:2 – 3.5:6.5)) using Sephadex LH-20 (MeOH/CH_2Cl_2, 1:1) yielded compound **188** (15.2 mg). The mother liquor was further purified in silica gel column (*n*-hexane/EtOAc/MeOH (7:2.5:0.5)) to provide compounds **189** (20.4 mg) and **190** (12.8 mg). Similarly, sub-fraction Fr_E (*n*-hexane/EtOAc (3.5:6.5)) afforded compound **186** (17.7 mg). Finally, repeated CC in Sephadex LH-20 (CH_2Cl_2/MeOH (1:1)) and chromatotron (CH_2Cl_2/MeOH (9.5:0.5)) gave compound **192** (28.5 mg).

3.4.3: Compounds Isolated from the Whole plant of Dracaena aletriformis

Following the same procedure as stated above, 170 g of the residue of *D. aletriformis* (whole plant) was obtained from 2.2 Kg of the air-dried material by maceration. A portion of 160 g was fractionated and eluted gradually with *n*-hexane/CH_2Cl_2 (1:1, 4:6, 3:7, 2:8 and 1:9) and CH_2Cl_2/MeOH (9.8:0.2, 9:1, 8:2 and 0:10) to give 179 fractions of 500 mL each which were pooled into eleven sub-fractions coded Fr_{A-K}. Sub-fractions Fr_I which was obtained with CH_2Cl_2/MeOH (9:1) was passed through Sephadex LH-20 (MeOH/CH_2Cl_2 (1:1)) to give compound **195** (1.0 mg). Sub-fractions Fr_K (CH_2Cl_2/MeOH (7:3)) was purfied on a silica gel column and eluted with cyclohexane/EtOAc/MeOH (6.5:3:0.5) to give two sub-fractions coded Fr_{K1} and Fr_{K2}. These two fractions were further purified with semi-preparative HPLC (MeOH/H_2O (1:1), flow rate 4 mL/min, for 13 min) to provide compounds **193** (5.0 mg) and **194** (3.0 mg), respectively.

3.4.4: Compounds Isolated from the Seeds of Dracaena steudneri

The dried powdered seeds (2.9 Kg) of *D. steudneri* were soaked in MeOH/CH_2Cl_2 (1:1, 3 L, 24 h x 3) affording 320 g of oily crude extract. Using flash column chromatography with silica gel as a solid matrix, 300 g of the crude extract was defatted with 100% cyclohexane (3 L) and sequentially extracted using a gradient system of cyclohexane/EtOAc (9:1, 1:1 and 0:10) followed by EtOAc/MeOH (9:1, 1:1 and 0:10). Based on their TLC and LC-MS similarities, the fractions were combined into four sub-fractions Fr_A (cyclohexane/EtOAc (10:0 – 9:1)), Fr_B (cyclohexane/EtOAc (1:1 – 0:10)), Fr_C (EtOAc/MeOH (9:1 – 1:1)) and Fr_D (MeOH). Sub-fraction Fr_C was subjected to semi-preparative HPLC set as follow: gradient elution started at 10% upto neat MeOH for 20.5 min, then the solvent system MeOH/H_2O (10:0) remained constant for 9.5 min, the solvent system reversed back with an interval of 1.0 min to the initial concentration of 10% (methanol) and was

constant for 9.0 min to afford seven isolates **196** (2.3 mg), **197** (0.7 mg), **198** (2.5 mg), **199** (1.5 mg), **200** (2.0 mg), **201**) (1.1 mg) and **202** (0.6 mg).

3.4.5: Compounds Isolated from the Leaves of Dracaena steudneri

The dried leaves of *D. steudneri* (3.3 Kg) were macerated using (MeOH/CH_2Cl_2 (1:1), 12 L, 24 h x3) to give 150 g of raw extract. About 120 g was then liquefied in water (250 mL) and sequentially partitioned successively with cyclohexane (2 L) and ethylacetate (3 L). The ethylacetate portion (35 g) was fractionated on silica gel column using a stepwise gradient of cyclohexane/EtOAc (9:1, 8:2, 7:3, 1:1 and 0:10) followed by MeOH (neat) to yield five sub-fractions labelled Fr_{A-E} which were pooled on their TLC and LC-MS similarities. Sub-fraction Fr_A was mainly fatty acids and was not investigated further. Sub-fraction Fr_B (cyclohexane/EtOAc (8:2)) was passed through Sephadex LH-20 (MeOH) to give two sub-fractions Fr_{B1} and Fr_{B2}. Fr_{B1} was further purified on semi-preparative HPLC (MeOH/H_2O (1:1), flow rate 4 mL/min, for 35 min) to give compounds **220** (1.8 mg), **208** (1.2 mg), **219** (2.5 mg), **216** (1.7 mg), **209** (1.4 mg) and **203** (0.5 mg). Following the same procedure, sub-fraction Fr_{B2} provided compounds **204** (0.9 mg), **217** (0.8 mg) and **218** (0.5 mg).

Size-exclusion chromatography (Sephadex LH-20, MeOH) of sub-fraction Fr_C (cyclohexane/EtOAc (7:3)) yielded four minor sub-fractions Fr_{C1-4}. Sub-fraction Fr_{C1} was further purified with semi-preparative HPLC (MeOH/H_2O (1:1), flow rate 4 mL/min, for 15 min) to afford compound **216** (1.0 mg). Similarly, sub-fraction Fr_{C4} yielded compounds **212** (1.4 mg) and **205** (0.5 mg). Silica gel CC (cychohexane/EtOAc/MeOH (7:2.5:0.5)) of the fourth sub-fraction Fr_D (cyclohexane/EtOAc (1:1)) provided three sub-fractions Fr_{D1-3}. Sub-fraction Fr_{D1} was subjected to semi-preparative HPLC (MeOH/H_2O (1:1), flow rate 4 mL/min, for 25 min) to yield compounds **221** (1.4 mg) and **211** (0.9 mg). Similarly, Fr_{D2} granted compounds **207** (1.4 mg), **222** (1.8 mg)

and **223** (2.0 mg). Lastly, sub-fraction Fr_{D3} yielded compounds **206** (0.9 mg), **215** (1.4 mg), **213** (1.6 mg) and **214** (0.6 mg) by purification with semi-preparative HPLC (MeOH/H_2O (1:1), flow rate 4 mL/min, for 35 min).

3.5: Biological Assays

3.5.1: In-vitro Anti-inflammatory Assay

The anti-inflammatory potency of isolates (100 µM) was assessed by quantifying the concentration of different mediators (IL-1β, IL-2, GM-CSF and TNF-α) in comparison to controls. The detailed experimental procedure is described herein.

3.5.1.1: PBMCs Isolation

The peripheral blood mononuclear cells (PBMCs) used in this study were obtained from blood isolated from four vials of cells obtained from four healthy donors with different origin, blood types and Rhesus: Caucasian (male, 41 years old, AB+), African-American (male, 31 years old, B+), African American-Hispanic (male, 29 years old, A+) and Caucasian (male, 32 years old, O+).

3.5.1.2: Anti-Inflammatory Assay

Dimethyl sulfoxide was used to dissolve the isolated compounds as well as the standard drug (Ibuprofen) in order to obtain 20 mM stock solution. Each of these solutions were further diluted to give 100 µM of test samples. The four vials of cells were combined and placed in 96 well plates and treated with the isolated compounds and standard (100 µM). The cells were treated with lipopolysaccharide (LPS) at 10 µg/mL to induce inflammation. In order to assess the anti-inflammatory potency of isolates, the inflamed cells were incubated with ibuprofen as well as the isolated compounds. The detailed experimental procedures have been published (Bedane *et al.*, 2020; Mukavi *et al.*, 2020; Owor *et al.*, 2020).

3.5.2: In-vitro Anticancer Assay

The anticancer activity of the crude extracts (10 µg/mL) and the isolated compounds (10 µM) was performed based on resazurin reduction assay. The detailed experimental procedure is described herein.

3.5.2.1: Cell cultures

Cell lines used for cytotoxicity are depicted in Table 3.2. To assess the selectivity of the compounds against cancer cells, they were tested also against two normal cells lines namely, HepG2 (Hepatocarcinoma) and AML12 (hepatocytes) (Doyle *et al.*, 1998; Efferth *et al.*, 2003; Kimmig *et al.*, 1990; Kuete *et al.*, 2013b).

Table 3.2: Cell lines tested

Solid tumor cell lines	Sensitive cancer cell lines	Resistant cancer cell lines
Leukemia	CCRF-CEM	CEM/ADR5000
Breast	MDA-MB231-pcDNA3	MDA-MB231/BCRP
Glioblastoma	U87.MG	U87MG.ΔEGFR
Hepatocarcinoma	HepG2	
Hepatocytes	AML12	

3.5.2.2: Cytotoxicity Assay

The cytotoxicity of the crude extracts, isolates and the reference drug (doxorubicin), were first screened against the most sensitive cell, leukemia cancer cell lines. The most active compounds and crude extracts with inhibition effects above 70% were selected and tested against the other cell lines (Omosa *et al.*, 2016) (Table 3.2). The cytotoxicity were evaluated by using the resazurin reduction assays (O'brien *et al.*, 2000). The test is based on the reduction of resazurin to resorufin which is highly fluorescent to viable cells. The non-viable cells, since they rapidly lose the capacity

to reduce resazurin through metabolism do not fluoresce. The detailed experimental procedure has been documented (Kuete *et al.*, 2017; Nyaboke *et al.*, 2018).

CHAPTER 4: RESULTS AND DISCUSSION

Phytochemical study of the selected *Dracaena* species yielded fifty isolates. Among these thirteen were novel. Moreover, this is the first report of the compounds from these plants (*D. usambarensis*, *D. aletriformis* and *D. steudneri*). Structure elucidation of isolates was achieved using spectral evidence. The anti-inflammatory property of the isolates (100 µM) was assessed by calculating the levels of LPS-induced inflammatory mediators in comparison to controls. The anticancer activity of the crude extracts (10 µg/mL) and the isolated compounds (10 µM) was determined using resazurin reduction assay. The results of this study will be discussed in the following sections.

4.1: Characterization of Compounds Isolated from the Stems of *Dracaena usambarensis*

Twelve compounds including five new ones were purified from the stems of *D. usambarensis*. In the following section the structure elucidation of these compounds is discussed.

4.1.1: Dracaenogenin C (176)

Compound **176** was obtained as a white solid with $[\alpha]_D^{21} = -35.2$ (*c* 0.230, $CHCl_3$) optical rotation. The HRESIMS exhibited a protonated molecular ion at *m/z* 427.2844 $[M+H]^+$ (calcd. 427.2804) matching the molecular formula $C_{27}H_{38}O_4$ accounting for nine sites of unsaturation. The UV (λ_{max} 221 nm) and signals observed in the IR spectrum at 3475 (O-H) and 1661 (C=O) cm^{-1} suggested **176** to be a spirosta-1,4-dien-3-one derivative (Zhang *et al.*, 2013). Further, signals characteristic of (25*S*)-spirostanol moiety at 980, 917 and 889 cm^{-1} were observed (Xu *et al.*, 2010). The NMR data (Table 4.1, Appendix 1) displayed signals for four methyl groups: two angular methyls (δ_H 0.89 (Me-18) and 1.26 (Me-19)) and two secondary methyls (δ_H 0.94 (Me-21) and 1.09 (Me-27)) which showed HSQC correlations with carbons at δ_C 17.2, 18.8, 7.9, 16.0, respectively. Further inspection indicated the presence of a 1,4-dien-3-one system in **176** based on signals detected in

the NMR at δ_H 7.07 (H-1), 6.24 (H-2) and 6.08 (H-4) together with signal of carbon ascribable to ring A (Table 4.1) which accounted for three double bonds equivalent. All these spectroscopic data together with signal observed for an acetal carbon at δ_C 110.6 (C-22), were relevant to conclude that **176** is a steroid with a spirostanol skeleton (Meng *et al.*, 2015; Wang *et al.*, 2016b). The ^{13}C NMR spectrum displayed a total of twenty seven carbon signals which was sorted with the aid of DEPT and HSQC spectra.

The position of the oxidized tertiary carbon at δ_C 89.7 (C-17) was confirmed with X-ray analysis and HMBC locus between signal at δ_H 2.09/1.33 (H-15) with δ_C 44.0 (C-13), 51.6 (C-14) and 89.7 (C-17); a correlation between the oxymethine proton at δ_H 3.96 (H-16) with δ_C 44.0 (C-13) and 89.7 (C-17); between the angular methyl proton at δ_H 0.89 (H-18) with δ_C 31.5, 44.0, 51.6 and 89.7 were attributable to C-12, C-13, C-14 and C-17 position, respectively. The remaining six degrees of unsaturation in **176** indicated that rings A-C and F share the chair conformation while rings D and E an envelope conformation. The A/B ring junction was established on the basis of the HMBC spectrum which showed correlations between signal at δ_H 1.26 (H-19) with δ_C 155.8 (C-1), 169.0 (C-5), 51.9 (C-9) and 43.6 (C-10). While for B/C/D ring junction, correlations between signal at δ_H 1.72 (H-14) with δ_C 33.6 (C-7), 35.2 (C-8), 44.0 (C-13) and 31.2 (C-15) were observed. To come out with the complete configuration of **176** around the stereogenic carbons, the sample was recrystallized from methanol:water mixture (9:1) and subjected to X-ray diffraction analysis (Figure 4.1). Consequently, **176** was newly characterized as (25*S*)-17*α*-hydroxyspirosta-1,4-dien-3-one (trivially named as dracaenogenin C).

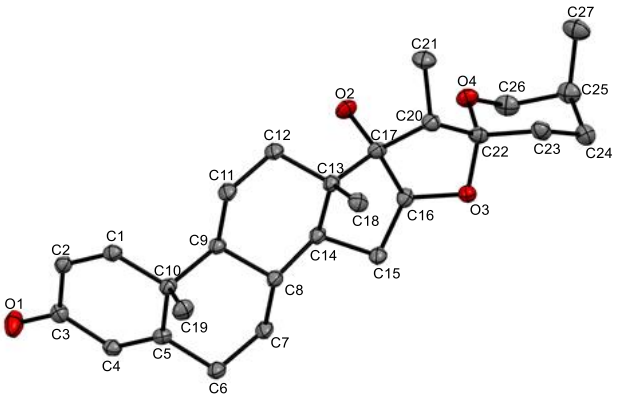

Figure 4.1: X-ray and absolute configuration of **176**

4.1.2: Dracaenogenin D (177)

Compound **177** was purified as a white solid with optical rotation $[\alpha]_D^{21} = -23.4$ (*c* 0.084, $CHCl_3$). The UV (λ_{max} 223 nm) and IR (3437, 2932, 1660, 1621, 1453, 1041, 918 and 754 cm^{-1}) data were characteristic of spirosta-1,4-dien-3-one moiety (Zhang *et al.*, 2013). The molecular formula $C_{27}H_{36}O_4$ was elucidated from its HRESIMS (*m/z* 425.2686 $[M+H]^+$ (calcd. 425.2647)). The spectroscopic data of **177** (Table 4.1, Appendix 2) was superimposable with **176** except that this compound has an exo-methylene moiety between the C-25 (δ_C 142.7) and C-27 (δ_H 4.82 *m*, δ_C 109.3 (C-27)). Furthermore, the position of the exo-olefinic group was established with the 2D NMR spectrum which displayed ^3J correlations between the exo-olefinic proton at δ_H 4.82 (H_2-27) with δ_C 27.8 (C-24) and 65.0 (C-26). Based on this, **177** was characterized as 17α-hydroxyspirosta-1,4,25(27)-trien-3-one (**177**) (trivially named as dracaenogenin D) which is a new compound.

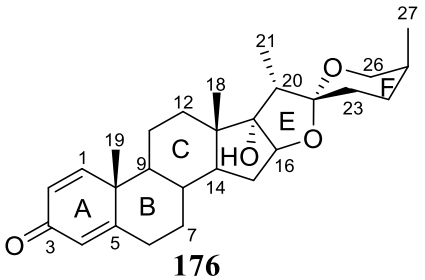

176

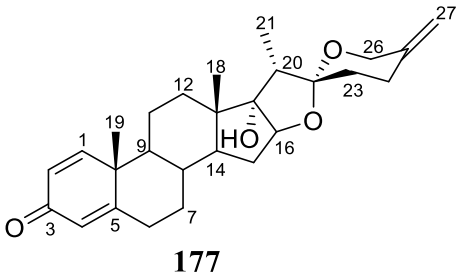

177

Table 4.1: NMR data for compounds **176** and **177** in $CDCl_3$

No	**176**[a]			**177**[a]		
	δ_C	δ_H (*m, Hz*)	HMBC	δ_C	δ_H (*m, Hz*)	HMBC
1	155.8	7.07 *d* (10.1)	C- 3, 5, 6, 9, 10, 19	155.7	7.08 *d* (10.1)	C- 3, 5, 6, 9, 10, 19
2	127.5	6.24 *dd* (10.1, 1.9)	C- 4, 10	127.6	6.26 *dd* (10.1, 1.9)	C- 4, 10
3	186.4	-	-	186.4	-	-
4	123.9	6.08 *br s*	C- 2, 6, 10	123.9	6.09 *br s*	C- 2, 6, 10
5	169.0	-	-	168.9	-	-
6	32.8	2.49 *m*, 2.37 *m*	C- 4, 5, 7, 8, 10	32.8	2.50 *m*, 2.38 *m*	C- 4, 5, 7, 10
7	33.6	1.97 *m*, 1.09 *m*	-	33.6	1.98 *m*, 1.10 *m*	-
8	35.2	1.79 *m*	-	35.3	1.81 *m*	-
9	51.9	1.12 *m*	C- 8, 9, 11. 19	51.9	1.12 *m*	-
10	43.6	-	-	43.5	-	-
11	22.6	1.78 *m*, 1.70 *m*	-	22.6	1.79 *m*, 1.71 *m*	C- 12
12	31.5	1.79 *m*, 1.41 *m*	-	31.5	2.11 *m*	C- 13, 17
13	44.0	-	-	44.1	-	-
14	51.6	1.72 *m*	C- 7, 8, 13, 15	51.6	1.75 *m*	-
15	31.2	2.09 *m*, 1.33 *m*	C- 13, 14, 17	31.2	2.12 *m*, 1.36 *m*	C- 14, 16
16	90.8	3.96 *m*	C- 13, 17	90.9	4.02 *t* (7.6)	C- 13, 17
17	89.7	-	-	89.8	-	-
CH_3-18	17.2	0.89 *s*	C- 12, 13, 14, 17	17.2	0.91 *s*	C- 12, 13, 14, 17
CH_3-19	18.8	1.26 *s*	C- 1, 5, 9, 10	18.8	1.27 *s*	C- 1, 5, 9, 10
20	45.1	1.99 *m*	-	44.6	2.08 *m*	C- 13, 17, 21, 22, 23
CH_3-21	7.9	0.94 *d* (7.1)	C- 17, 20, 22	8.0	0.92 *d* (6.0)	C- 17, 20, 22
22	110.6	-	-	110.3	-	-
23	25.3	1.90 *m*, 1.40 *m*	C- 22, 24	32.2	1.76 *m*	C- 24
24	25.1	2.06 *m*, 1.42 *m*	C- 23, 25, 27	27.8	2.61 *m*, 2.28 *m*	C- 23, 25, 26, 27
25	26.9	1.74 *m*	-	142.7	-	-
26	65.2	3.96 *m*	C- 22, 24, 25, 27	65.0	4.32 *d* (12.1)	C- 25, 27
		3.34 *d* (10.9)	C- 22, 24, 25, 27		3.91 *dd* (12.1, 1.6)	C- 24, 25, 27
CH_3-27	16.0	1.09 *d* (7.1)	C- 24, 25	109.3	4.82 *m*	C- 24, 26

[a] Recorded at 600 MHz

4.1.3: Dracaenogenin E (178)

Compound **178** was purified as a white solid. The molecular formula of **178** was deduced as $C_{27}H_{38}O_6$ by interpretation of its MS profile at *m/z* 459.2737 $[M+H]^+$ (calcd. 459.2702). It is an optically active compound with optical rotation of $[\alpha]_D^{21} = -18.8$ (*c* 0.038, MeOH). The spirostanol skeleton in **178** was evident based on UV (λ_{max} 244 nm) and IR (3410, 2971, 1658, 1598 and 1055 cm^{-1}) data (Zhang *et al.*, 2013). The spectrometric data of **178** was 32 Dalton higher than **176** implying the presence of an additional oxygen in this molecule. This is further reinforced by NMR spectra (Table 4.2, Appendix 3) which exhibited signals attributable to two downfield oxymethine carbons at δ_C 70.1 (C-24) and 95.6 (C-26). Further, HMBC correlations between the proton at δ_H 1.09 (Me-27) with δ_C 70.1 (C-24), 46.7 (C-25) and 95.6 (C-26) confirmed the loci of the two hydroxyl groups at their respective position. NOESY correlation between H-24 and H-26 as well as the large coupling constant (*J* = 8.8 Hz) between H-24 and H-25 allowed the placement of the two hydroxyl groups in ring F at equatorial orientation (Jin *et al.*, 2004). Therefore, **178** was established to be (24*S*,25*R*,26*R*)-17*α*,24,26-trihydroxyspirosta-1,4-dien-3-one (**178**) (trivially named as dracaenogenin E) which is a new compound.

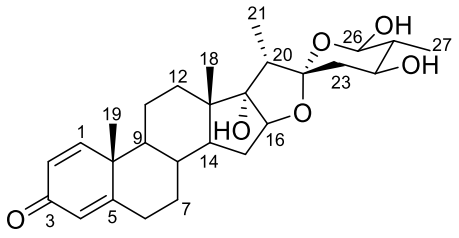

178

4.1.4: Dracaenogenin F (179)

Compound **179** was purified as a white solid. The MS profile of this compound (**179**) displayed a protonated molecular ion at *m/z* 439.2478 $[M+H]^+$ (calcd. 439.2440) consistent with $C_{27}H_{34}O_5$,

eleven degrees of unsaturation. Absorptions observed in the UV (λ_{max} 248 nm) and IR (3366, 2966, 2942, 1715, 1656, 1066, 800 and 669 cm^{-1}) spectra indicated a cholesta-1,4-dien-3-one moiety (Zhang *et al.*, 2013). It is an optically active compound with an optical rotation of $[\alpha]_D^{21} = -25.8$ (*c* 0.010, MeOH).

The NMR data of **179** (Table 4.2, Appendix 4) in rings A-C was homomorphous to the one observed in **176** – **178**, but different in rings D-F. The ^{13}C NMR data of **179** displayed signals of α,β-unsaturated diketone moiety together with a carbonyl of a carboxylic acid at δ_C 180.2 (C-26). These features indicated the possibility of rings E and F being open forming a cholesta-1,4-dien-3-one derivative. The α,β-unsaturated diketone moiety was confirmed with the aid of HMBC spectrum based on the correlations observed between protons of the methyl group at δ_H 1.96 (Me-21) to carbons at δ_C 143.7 (C-17), 146.5 (C-20) and 212.6 (C-22), with signal at δ_H 2.18 (H-15) to carbons at δ_C 45.0 (C-13), 50.9 (C-14) and 207.0 (C-16). With the proton at δ_H 1.22 (H-18) to carbons at δ_C 37.0 (C-12), 45.0 (C-13), 50.9 (C-14) and 143.7 (C-17). Furthermore, the position of carboxyl group was as evidence of ^2J and ^3J correlations between the proton at δ_H 1.18 (Me-27) with carbons at δ_C 28.3 (C-24), 39.7 (C-25) and 180.2 (C-26). Based on this, **179** was characterized as 3,16,22-trioxocholesta-1,4,17(20)-trien-26-carboxylic acid (**179**) (trivially named as dracaenogenin F) which is a new compound.

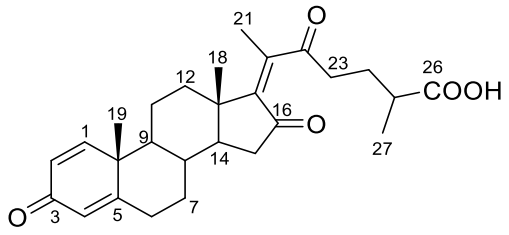

179

Table 4.2: NMR data for compounds **178** and **179** in CD_3OD

No	**178**[a]			**179**[a]		
	δ_C	δ_H (*m*, *Hz*)	HMBC	δ_C	δ_H (*m*, *Hz*)	HMBC
1	159.5	7.32 *d* (10.1)	C- 3, 5, 19	158.9	7.33 *d* (10.1)	C- 3, 5, 10, 19
2	127.6	6.24 *dd* (10.1, 1.9)	C- 10	127.8	6.26 *dd* (10.1, 1.9)	C- 10
3	188.7	-	-	188.6	-	-
4	124.0	6.09 *br s*	C- 2, 6, 10	124.2	6.11 *br s*	C- 2, 6, 10
5	173.5	-	-	172.9	-	-
6	33.9	2.60 *m*, 2.42 *m*	-	33.6	2.65 *m*, 2.46 *m*	C- 4, 5, 7
7	35.1	2.04 *m*, 1.08 *m*	-	34.7	2.00 *m*, 1.17 *m*	-
8	36.8	1.93 *m*	-	35.4	2.01 *m*	-
9	54.0	1.04 *m*	-	53.5	1.27 *m*	-
10	45.4	-	-	45.3	-	-
11	23.6	1.83 *m*, 1.76 *m*	-	23.8	1.98 *m*	-
12	32.7	1.74 *m*, 1.40 *m*	-	37.0	2.40 *m*, 1.79 *m*	-
13	46.2	-	-	45.0	-	-
14	52.8	1.75 *m*	-	50.9	1.64 *m*	C- 8, 13, 18
15	32.1	2.08 *m*, 1.34 *m*	C- 13, 17	38.6	2.18 *m*	C- 13, 14, 16
16	90.9	4.08 *t* (7.8)	C- 17	207.0	-	-
17	90.6	-	-	143.7	-	-
CH_3-18	17.6	0.94 *s*	C- 12, 13, 14, 17	17.3	1.22 *s*	C- 12, 13, 14, 17
CH_3-19	19.1	1.32 *s*	C- 1, 5, 9, 10	19.0	1.35 *s*	C- 1, 5, 9, 10
20	45.7	2.19 *q* (7.3)	-	146.5	-	-
CH_3-21	9.0	0.93 *d* (7.3)	C- 17, 20, 22	15.8	1.96 *s*	C- 17, 20, 22
22	112.0	-	-	212.6	-	-
23	41.2	1.88 *m*, 1.60 *m*	C- 22, 24, 25	39.3	2.57 *t* (7.5)	C- 22, 24, 25,
24	70.1	3.58 *td* (10.9, 4.9)	-	28.3	1.96 *m*, 1.77 *m*	C- 22, 23, 26, 27
25	46.7	1.29 *m*	-	39.7	2.50 *m*	C- 24, 26, 27
26	95.6	4.56 *d* (8.8)	-	180.2	-	-
CH_3-27	12.7	1.09 *d* (6.5)	C- 24, 25, 26	17.7	1.18 *d* (7.1)	C- 24, 25, 26

[a] Recorded at 600 MHz

4.1.5: 3″-Methoxycochinchinenene H (180)

Compound **180** was isolated as a brown solid. This compound (**180**) was elucidated as $C_{31}H_{30}O_7$ based on UV (λ_{max} 326 and 228 nm), IR (3373, 2941, 1605, 1510, 1424, 1233, 1072, 959 and 835 cm^{-1}) and NMR spectrums together with HRESIMS (*m/z* 515.2068 $[M+H]^+$ (calcd. 515.2025)). It is an optically active compound with an optical rotation of $[\alpha]_D^{21}$ = + 1.2 (*c* 0.043, MeOH). The ^1H NMR spectrum of **180** (Table 4.3, Appendix 5) exhibited signals of resveratrol moiety which accounts for nine rings double bond equivalent with resonances at δ_H 7.34 (H-2′/6′) and 6.77 (H-3′/5′) indicating the presence of 1,4-disubstituted benzene ring, together with a sharp singlet at δ_H 6.48 (H-2/6) (Lee *et al.*, 2009). In addition, signals of a *trans* olefinic bond based on the magnitude of their *J* = 16.2 Hz values were observed at δ_H 6.93 (H-β) and 6.77 (H-α). Further, the presence of a second set of *para*-disubstituted benzene ring was evident on the basis of signals observed at δ_H 7.30 (H-2‴/6‴) and 6.65 (H-3‴/5‴). Furthermore, the ^1H NMR spectrum displayed signal of AB spin system at δ_H 6.73 (H-6″) and 6.53 (H-5″) attributable to a 1,2,3,4-tetrasubstituted aromatic ring.

The NMR spectra of this compound is similar to cochinchinenene H, a conjugated chalcone-stilbene isolated from *D. cochinchinensis*, except that compound **180** has an additional methoxy substituent (Hao *et al.*, 2015). The ^{13}C NMR chemical shift of the additional methoxy was observed at δ_C 60.9, a downfield shifted signal indicating that it is di-*ortho* substituted hence placing it at C-3″. The connectivity of the two fragments of the molecule, the chalcone and the stilbene, was established based on the HMBC correlations between the methine proton at δ_H 4.54 (H-γ′) with carbons at δ_C 35.5 (C-β′), 118.9 (C-4), 130.3 (C-2‴/6‴), 138.2 (C-1‴) and 157.9 (C-3/5). Hence compound **180** was characterized as 3″-methoxycochinchinenene H, a new compound.

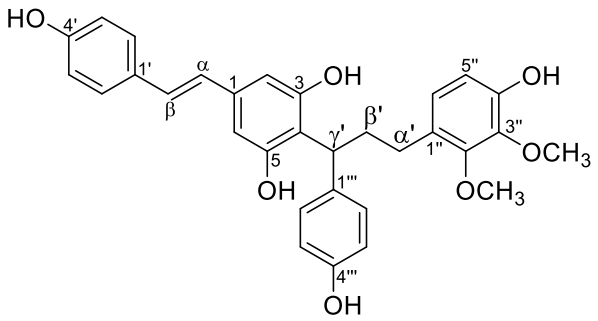

180

Table 4.3: NMR data for compound **180** in CD_3OD

No	**180**[a]		
	δ_C	δ_H (*m*, *Hz*)	HMBC
1	138.0	-	-
2/6	106.1	6.48 *s*	C- 4, α, 2/6, 3/5
3/5	157.9	-	-
4	118.9	-	-
α	127.0	6.77 *d* (16.2)	C- 1′, 2/6,
β	128.4	6.93 *d* (16.2)	C- 1, 2′/6′
1′	130.6	-	-
2′/6′	128.6	7.34 *d* (8.7)	C- 3′/5′, β, 4′
3′/5′	116.5	6.77 *d* (8.7)	C- 3′/5′, 4′
4′	158.2	-	-
1″	129.2	-	-
2″	152.8	-	-
3″	142.1	-	-
4″	149.8	-	-
5″	112.3	6.53 *d* (8.4)	C- 1″, 3″, 4″
6″	125.6	6.73 *d* (8.4)	C- α′, 2″, 4″
α′	29.9	2.45 *m*	C- β′, γ′, 1″, 2″, 6″,
β′	35.5	2.56 *m*, 2.32 *m*	C- α′, γ′, 1″, 1‴, 4
γ′	41.1	4.55 *m*	C- β′, 1‴, 3/5, 4, 2‴/6‴,
1‴	138.2	-	-
2‴/6‴	130.3	7.30 *d* (8.7)	C- γ′, 3‴/5‴, 2‴/6‴
3‴/5‴	115.3	6.65 *d* (8.7)	C- 1‴, 4‴, 3‴/5‴
4‴	155.7	-	-
CH_3O-2″	61.2	3.79 *s*	C- 2″
CH_3O-3″	60.9	3.83 *s*	C- 3″

[a] Recorded at 600 MHz

4.1.6: Trans-resveratrol (181)

Compound **181** was purified as a white solid. The MS profile exhibited a quasi- molecular ion at *m/z* 229.0860 $[M+H]^+$ (calcd. 229.0820) matching the chemical formula of $C_{14}H_{12}O_3$, and nine unsaturation sites. The UV profile displayed absorption bands at λ_{max} 305 and 228 nm. In the ^1H NMR, signals of a 1,4-disubstituted benzene ring with an AA′BB′ spin system (δ_H 7.37 (H-2′/6′) and 6.78 (H-3′/5′)), a *trans* alkene (δ_H 6.82 (H-α) and 6.97 (H-β)) and signal of a 1,3,5 trisubstituted benzene ring (δ_H 6.46 (H-2/6) and 6.18 (H-4)) were observed. These accounted for the nine degrees of unsaturation in compound **181**. The ^1H and ^{13}C NMR (14 signals) spectrums indicated that this compound is a resveratrol derivative (Table 4.4, Appendix 6) (Oleszek *et al.*, 2001). The HMBC correlations between the olefinic proton at δ_H 6.82 (H-α) with δ_C 105.7 (C-2/6), 130.4 (C-1) and 141.3 (C-1′) were relevant for the interconnectivity of the two benzene rings. Based on all aforementioned data, this compound was identified as *trans*-resveratrol, a compound previously isolated from the root of *Arachis hypogaea* (Lee *et al.*, 2009).

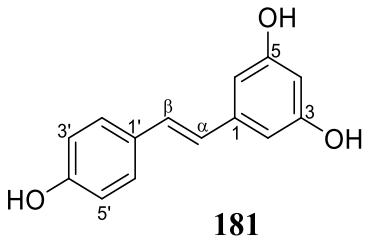

181

Table 4.4: NMR data for compound **181** in CD_3OD

No	**181**[a]		
	δ_C	δ_H (*m, Hz*)	HMBC
1	130.4	-	-
2/6	105.7	6.46 *d* (2.1)	C- 4, α, 2/6, 3/5
3/5	159.7	-	-
4	102.6	6.18 *t* (2.1)	C- 2/6, 3/5
α	127.0	6.82 *d* (16.2)	C- 1, 1′, 2/6
β	129.4	6.97 *d* (16.2)	C- 1′, 2′/6′
1′	141.3	-	-
2′/6′	128.8	7.37 *d* (8.5)	C- β, 4′, 3′/5′, 2′/6′
3′/5′	116.5	6.78 *d* (8.5)	C- 4′, 3′/5′
4′	158.4	-	-

[a] Recorded at 600 MHz

4.1.7: 4,4′-Dihydroxy-3′-methoxychalcone (182)

Compound **182** was purified as a yellow solid. The planar structure was elucidated based on spectral evidence. The MS profile exhibited a protonated molecular ion peak at *m/z* 271.0966 $[M + H]^+$ (calcd. 271.0926) for $C_{16}H_{14}O_4$. The UV (λ_{max} 350 nm) and NMR (δ_H 7.38 (H-α), 7.46 (H-β), δ_C 123.9 (C-α), 141.2 (C-β) and 188.6 (C=O) spectra indicated that **182** (Table 4.5, Appendix 7) is a chalcone derivative (Singh *et al.*, 2008). The non-aromatic proton observed at δ_H 3.84 was consistent with the presence of a methoxy (CH_3O-) group in **182**. The ^1H NMR profile exhibited seven signals among which four displayed an AA′BB′ spin system (δ_H 7.54 (H-2/6) and 6.81 (H-3/5)), the other three had an ABX spin system (δ_H 6.43 (H-6′), 7.51 (H-5′) and 6.49 (H-2′)). The methoxy substituent was placed at C-3′ due to the strong HMBC correlations observed between its protons and the carbon at δ_C 160.5 (C-3′) as well as the NOESY (CH_3O and H-2′). The ^{13}C NMR spectrum displayed a total of sixteen signals. Hence, compound **182** was elucidated as 4,4′-dihydroxy-3′-methoxychalcone, a compound which has been previously isolated from the roots of *Brassica rapa* ssp (Jeong *et al.*, 2013).

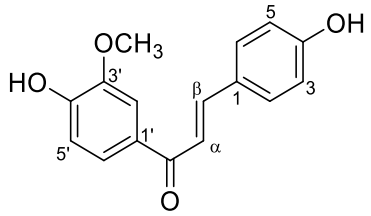

182

Table 4.5: NMR data for compound **182** in DMSO-d_6

No	**182**[a]		
	δ_C	δ_H (*m, Hz*)	HMBC
1	125.9	-	-
2/6	130.2	7.54 *d* (8.4)	C- β, 4, 2/6
3/5	115.9	6.81 *d* (8.4)	C- 1, 4, 3/5
4	159.9	-	-
α	123.9	7.38 *d* (15.7)	C- 1, β, C=O
β	141.2	7.46 *d* (15.7)	C- α, 1, 2/6, C=O
1′	119.8	-	-
2′	99.3	6.49 *d* (2.1)	C- 1′, 6′
3′	160.5	-	-
4′	165.1	-	-
5′	132.2	7.51 *d* (8.5)	C- 3′, C=O
6′	108.1	6.43 *d* (8.5, 2.1)	C- 1′, 2′
CH_3O-3′	55.6	3.84 *s*	C- 3′
C=O	188.6	-	-

[a] Recorded at 600 MHz

4.1.8: N-Trans-coumaroyltyramine (170)

Compound **170** (UV λ_{max} 308 and 234 nm) was purified as a white solid. The chemical formula $C_{17}H_{18}NO_3$ was deduced from the signal observed in the MS profile at *m/z* 284.1281 $[M + H]^+$ (calcd. 284.1242). The ^{1}H NMR spectrum (Table 4.6, Appendix 8) exhibited two sets of AA′BB′ coupling partner at δ_H 7.42 (H-2‴/6‴) and 6.80 (H-3‴/5‴); 7.07 (H- H-2″/6″) and 6.73 (H-3″/5″) ascribable to aromatic protons of cinnamic acid and phenylethylamine moieties. The ^{1}H NMR displayed signals for two olefinic protons (δ_H 6.40 (H-2) and 7.46 (H-3)) and the geometry of the double bond was assigned to be *trans* ($J_{2,3}$ = 15.7 Hz). Further, the signals depicted at δ_H 3.48 (H-1′) and 2.77 (H-2′) in the ^{1}H NMR for mutually coupled protons indicated the presence of *N*-ethyl

chain. The ^{13}C NMR spectrum displayed a total of seventeen carbon atoms which were assigned based on HSQC and HMBC spectra. This compound therefore, was identified as *N-trans*-coumaroyltyramine. The compound has been previously reported from *Tribulus terrestris* (Song *et al.*, 2016).

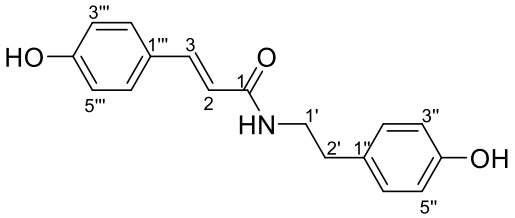

170

4.1.9: N-Trans-feruloyloctopamine (171)

Compound **171** (UV λ_{max} 322 and 240 nm) was obtained as a white solid. The chemical formula of compound **171** (Table 4.6, Appendix 9) was determined to be $C_{18}H_{19}O_5N$ as evidence of MS profile which displayed an *m/z* 330.1337 $[M + H]^+$ (calcd. 330.1297) indicating ten unsaturation sites. The skeleton of compound **170** and **171** are similar based on their NMR features. A signal observed in the HRESIMS of **171** at *m/z* 312.1231 $[M + H]^+$ consistent with a neutral loss of water (18 Dalton) indicated the existence of a hydroxyl substituent in this compound. The hydroxyl group was allocated to C-2′. The ^1H NMR of **171** displayed an AA′BB′ (δ_H 7.24 (H-2″/6″) and 6.79 (H-3″/5″)) and an ABX (δ_H 7.15 (H-2‴), 6.81 (H-5‴) and 7.05 (H-6‴)) spin systems. In addition, the presence of a *trans* olefinic double bond was observed at δ_H 6.48 (H-2) and 7.46 (H-3, J = 15.7 Hz). Further, the spectrum exhibited a signal of an oxymethine proton at δ_H 4.74 (H-2′); a methylene proton at δ_H 3.46-3.55 (H-1′), along with a proton of a methoxy group at δ_H 3.91. The ^{13}C NMR spectrum had a total number of 18 carbons composed of one unit of *p*-tyramine moiety derivative and one unit of *p*-hydroxycinnamic acid. The methoxy group was placed at C-

3′′′ (δ_C 149.3) based on the HMBC connectivity of its protons with C-3′′′. The placement of the methoxy group in the cinnamic moiety was further confirmed based on correlations observed between H-3 with the carbons at δ_C 169.5 (C-1), 128.3 (C-1′′′), 118.6 (C-2), 111.5 (C-2′′′) and 123.3 (C-6′′′). Hence, **171** was identified as *N-trans*-feruloyloctopamine, a phenolic amide previously isolated from *Tribulus terrestris* (Song *et al*., 2016).

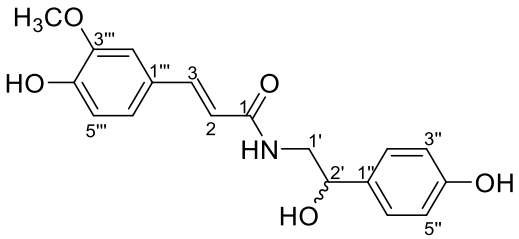

171

Table 4.6: NMR data for compounds **170** and **171** in CD_3OD

No	**170**[a]			**171**[a]		
	δ_C	δ_H (*m, Hz*)	HMBC	δ_C	δ_H (*m, Hz*)	HMBC
1	169.2	-	-	169.5	-	-
2	118.4	6.40 *d* (15.7)	C- 1, 1‴	118.6	6.48 *d* (15.7)	C- 1, 1‴
3	141.8	7.46 *d* (15.7)	C- 1, 2‴/6‴	142.2	7.46 *d* (15.7)	C- 1, 1‴, 2, 2‴,6‴
1′	42.6	3.48 *t* (7.4)	C- 1, 1″, 2′	48.3	3.55 *dd* (13.6, 4.9)	C- 1, 1″, 2′
	-	-	-	-	3.46 *dd* (13.6, 7.9)	C- 1, 1″, 2′
2′	35.8	2.77 *t* (7.4)	C- 1′, 2″/6″	73.4	4.74 *dd* (7.9, 4.9)	C- 1′, 1″, 2″/6″
1″	131.3	-	-	134.7	-	-
2″/6″	130.7	7.07 *d* (8.3)	C- 2′, 4″, 2″/6″	128.5	7.24 *d* (8.4)	C- 2′, 4″, 2″/6″
3″/5″	116.3	6.73 *d* (8.3)	C- 1″, 4″, 3″/5″	116.1	6.79 *d* (8.4)	C- 1″, 4″, 3″/5″
4″	156.9	-	-	158.1	-	-
1‴	127.7	-	-	128.3	-	-
2‴	130.5	7.42 *d* (8.5)	C- 3, 4‴, 2‴/6‴	111.5	7.15 *d* (1.9)	C- 3, 4‴, 6‴
3‴	116.7	6.80 *d* (8.5)	C- 1‴, 4‴, 3‴/5‴	149.3	-	-
4‴	160.6	-	-	149.9	-	-
5‴	116.7	6.80 *d* (8.5)	C- 1‴, 4‴, 3‴/5‴	116.5	6.81 *d* (8.2)	C- 1‴, 4‴
6‴	130.5	7.42 *d* (8.5)	C- 3, 4‴, 2‴/6‴	123.3	7.05 *dd* (8.2, 1.9)	C- 2‴, 3, 4‴
CH_3O-3‴	-	-	-	56.4	3.91 *s*	C- 3‴

[a]Recorded at 600 MHz

4.1.10: 7-Hydroxy-1-(4-hydroxy-3-methoxyphenyl)-N_2,N_3-bis(4-hydroxyphenethyl)-6-methoxy -1,2-dihydronaphthalene-2,3-dicarboxamide (183)

This compound (**183,** UV λ_{max} 310, 280 and 228 nm.) was purified as a brown solid. The HRESIMS of compound **183** exhibited a signal at *m/z* 625.2539 $[M + H]^+$ (calcd. 625.2505) matching the chemical formula $C_{36}H_{36}N_2O_8$.

The ^{1}H NMR profile displayed signals for two oxygenated methyl substituents (δ_H 3.92 and 3.77) in this compound. The NMR spectra (Table 4.7, Appendix 10) displayed two batches of tyramine moieties. One of these moieties appeared at δ_H 7.00 (H-2‴/6‴), 6.70 (H-3‴/5‴), 2.72 (H-7‴) and 3.43-337 (H-8‴), while the second one resonated at δ_H 6.84 (H-2″/6″), 6.67 (H-3″/5″), 2.50 (H-7″) and 3.25 (H-8″) in the ^{1}H NMR. The ^{1}H NMR showed signals of ferulic acid (δ_H 6.90 (H-2, *s*), 6.54 (H-5, *s*), 7.22 (H-7, *s*)) derivative substituted at α–position by ethyl (δ_H 4.36 (1H, H-7′) and 3.70 (1H, H-8′), $J_{7',8'}$ = 4.0 Hz) chain. The ethyl chain cyclized to form a naphthalene derivative. This funding was confirmed through ^2J and ^3J correlations observed between the signal at δ_H 4.36 (H-7′) with carbons at δ_C 124.9 (C-1), 117.2 (C-5) and 127.6 (C-6). In addition, the ^{1}H NMR exhibited signals for an ABX coupling partner at δ_H 6.72 (H-2′), 6.66 (H-5′) and 6.43 (H-6′) corresponding for 1,3,4-trisubstituted benzene ring. This benzene ring is connected to the modified naphthalene ring through C-7′, this is evident from the HMBC correlation observed between signal at δ_H 4.36 (H-7′) with carbon at δ_C 135.9 (C-1′). The connections of the tyramine moieties with the naphthalene derivative at C-8 and C-8′ is determined as a result of ^3J correlations between H-7 (δ_H 7.22) and H-7′ (δ_H 4.36) with C-9 (δ_C 170.4) and C-9′ (δ_C 174.5), respectively. The position of the methoxy groups was established based on the long range correlations between signals at δ_H 3.92 and 3.77 with carbons at δ_C 148.2 (C-3) and 148.9 (C-3′), respectively. Therefore **183** was unambiguously identified as 7-hydroxy-1-(4-hydroxy-3-methoxyphenyl)-N_2,N_3-*bis*(4-

hydroxyphenethyl)-6-methoxy-1,2-dihydronaphthalene-2,3-dicarboxamide. This compound and its diastereomer have been previously reported from *Aptenia cordifolia* (DellaGreca *et al.*, 2006) and *Solanum nigrum* L (Li *et al.*, 2019), respectively.

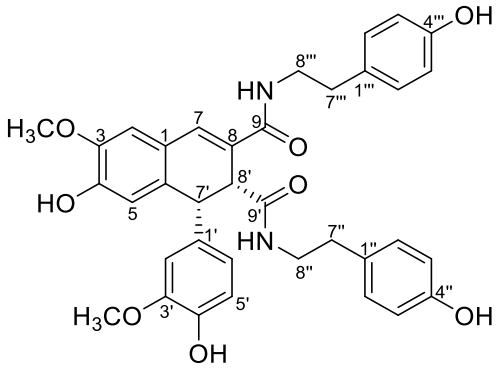

183

4.1.11: Grossamide (184)

Compound **184** was purified as a brown solid. The chemical formula of **184** was elucidated as $C_{36}H_{36}N_2O_8$ as evidence of HRESIMS (*m/z* 625.2539 $[M + H]^+$ (calcd. 625.2505)) and ^{13}C NMR spectra. This implied twenty degrees of unsaturation. The UV (λ_{max} 344, 262 and 228 nm), MS as well as the NMR (Table 4.7, Appendix 11) indicated compounds **183** and **184** are structurally closely similar isomers. Despite these similarities, the two compounds are different as evidenced by their differing retention times (t_R) of 19.3 min and 17.4 min for **184** and **183**, respectively, in their LC-MS spectra.

Just as in compound **184**, in this compound there are two sets of tyramine moieties. There are also two ferulic acid (phenylpropanoid) moieties dimerizing to give a lignan as in **183**, except that the phenylpropanoid unit are joined differently in this compound. In this compound, one of the carbons of the ethyl unit (C-7′) is joined to the other phenylpropanoid unit through oxygen. The other carbon of this unit (C-8′) is joined to the aromatic carbon of the second ferulic acid unit forming a

five membered heterocyclic ring. Basing on this and comparison of the data with literature, this compound was identified as grossamide (**184**) (Wenjie *et al.*, 2017). A compound previously isolated from *Alocasia macrorrhiza* (Wenjie *et al.*, 2017).

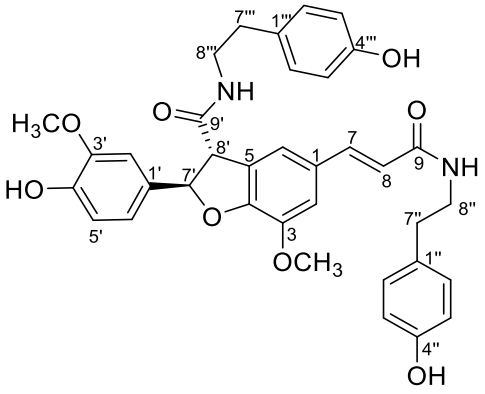

184

Table 4.7: NMR data for compounds **183** and **184** in CD_3OD

No	**183**[a]			**184**[b]		
	δ_C	δ_H (*m, Hz*)	HMBC	δ_C	δ_H (*m, Hz*)	HMBC
1	124.9	-	-	130.4	-	-
2	113.2	6.90 *s*	C- 4, 7	113.7	7.14 *d* (1.5)	C- 3, 4, 6, 7
3	148.2	-	-	146.1	-	-
4	149.6	-	-	151.2	-	-
5	117.2	6.54 *s*	C- 1, 3, 7′	129.4	-	-
6	127.6	-	-	118.1	6.77 *br s*	C- 2, 4, 7, 8′
7	134.6	7.22 *s*	C- 2, 8, 8′, 9	141.8	7.45 *d* (15.7)	C- 1, 2, 6, 8, 9
8	132.6	-	-	119.4	6.41 *d* (15.7)	C- 1, 9
9	170.4	-	-	169.0	-	-
1′	135.9	-	-	132.6	-	-
2′	112.5	6.72 *d* (2.1)	C- 3′, 4′, 6′, 7′	110.5	6.93 *d* (1.9)	C- 3′, 4′, 6′, 7′
3′	148.9	-	-	149.3	-	-
4′	146.3	-	-	148.1	-	-
5′	116.0	6.66 *d* (8.4)	C- 1′, 3′, 4′	116.3	6.82 *d* (8.2)	C- 1′, 3′
6′	121.4	6.43 *dd* (8.4, 2.1)	C- 2′, 4′, 7′	120.0	6.79 *dd* (8.2, 1.9)	C- 2′, 4′, 7′
7′	47.6	4.36 *d* (4.0)	C- 1, 1′, 2′, 5, 6, 6′, 8, 8′, 9′	90.0	5.91 *d* (8.3)	C- 1′, 2′, 6′, 8′, 9′
8′	51.0	3.70 *d* (4.0)	C- 1′, 6, 7, 7′, 8, 9, 9′	58.7	4.16 *d* (8.3)	C- 1′, 4, 5, 7′, 9′
9′	174.5	-	-	172.9	-	-
1″	131.2	-	-	131.3	-	-
2″/6″	130.7	6.84 *d* (8.4)	C- 4″, 3″/5″, 2″/6″, 7″	130.7	7.08 *d* (8.4)	C- 4″, 3″/5″, 2″/6″, 7″
3″/5″	114.6	6.67 *d* (8.4)	C- 1″, 4″, 3″/5″	116.5	6.73 *d* (8.4)	C- 1″, 4″, 3″/5″
4″	156.9	-	-	157.0	-	-
7″	35.5	2.50 *m*	C- 2″/6″, 8″	35.8	2.79 *t* (8.1)	C- 2″/6″, 8″
8″	42.4	3.25 *m*	C- 1″, 7″, 9′	42.6	3.51 *t* (8.1)	C- 1″, 7″, 9
1‴	131.4	-	-	131.1	-	-
2‴/6‴	130.8	7.00 *d* (8.5)	C- 4‴, 2‴/6‴, 7‴	130.9	7.05 *d* (8.4)	C- 4‴, 3‴/5‴, 2‴/6‴, 7‴
3‴/5‴	116.2	6.70 *d* (8.5)	C- 1‴, 4‴, 3‴/5‴	115.0	6.75 *d* (8.4)	C- 1‴, 3‴/5‴, 4‴
4‴	156.8	-	-	156.9	-	-

Table 4.7: continued

No	**183**[a]			**184**[b]		
	δ_C	δ_H (*m*, *Hz*)	HMBC	δ_C	δ_H (*m*, *Hz*)	HMBC
7‴	35.7	2.72 *t* (7.3)	C- 8‴, 2‴/6‴	35.3	2.76 *m*	C- 8‴, 2‴/6‴
8‴	42.7	3.43 *m*, 3.37 *m*	C- 1‴, 7‴, 9	42.2	3.56 *m*, 3.47 *m*	C- 1‴, 7‴, 9′
3-OCH_3	56.6	3.92 *s*	C- 3	56.8	3.92 *s*	C- 3
3′-OCH_3	56.3	3.77 *s*	C- 3′	56.4	3.84 *s*	C- 3′

[a,b] Recorded at 700 and 600 MHz, respectively

4.1.12: Methylparaben (185)

Compound **185** was purified as white solid. The chemical formula ($C_8H_8O_3$) was as results of MS (*m*/*z* 153.0544 $[M + H]^+$ (calcd. 153.0507)) and NMR evidence (Table 4.8, Appendix 12). The UV (λ_{max} 284 and 230 nm) spectrum together with the five degrees of unsaturation indicated this compound is a phenyl derivative. In agreement with this, the ^{1}H NMR exhibited signals with an AA′BB′ spin system at δ_H 7.89 (H-2/6) and 6.84 (H-3/5) for a symmetrical phenyl ring. The NMR also showed a signal ascribable to methoxy protons at δ_H 3.86 (CH_3O-) which showed HSQC connectivity with carbon at δ_C 50.8. Further, the presence of a chemical shift at δ_C 168.7 (C=O) indicated this compound is an ester. The ^3J correlation observed between signal at δ_H 7.89 (H-2/6) and δ_C 168.7 (C-7) established the connectivity of the ester carbonyl to the benzene ring. Furthermore, the position of the methoxy substituent was established with the aid of the HMBC which exhibited correlation between protons resonating at δ_H 3.86 (CH_3O-) and the ester carbonyl (δ_C 168.7). Using this and comparing the data with literature, compound **185** was identified as methylparaben (Soni *et al.*, 2002). Methylparaben (**185**) has been previously reported from *Abutilon indicum* (Kuo *et al.*, 2008).

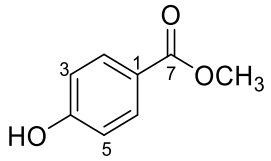

185

Table 4.8: NMR data for compound **185** in CD_3OD

No	**185**[a]		
	δ_C	δ_H (*m, Hz*)	HMBC
1	122.2	-	-
2/6	132.7	7.89 *d* (8.7)	C- 2/6, 3/5, 4, 7
3/5	116.2	6.84 *d* (8.7)	C- 1, 3/5, 4
4	163.5	-	-
7	168.7	-	-
CH_3O-	52.2	3.86 *s*	C- 7

[a] Recorded at 600 MHz

4.2: Characterization of Compounds Isolated from the Roots of *Dracaena usambarenis*

Chromatographic separation of *D. usambarenis* crude roots extract yielded seven secondary metabolites among which two were new. Their structure elucidation is discussed herein.

4.2.1: Usambarin (186)

Compound **186** was isolated as a yellow solid substance. It is an optically active compound with an optical rotation $[\alpha]_D^{25} = -10.7$ (*c* 0.01, MeOH) which had a UV absorption at λ_{max} 366, 298 and 244 nm. The signals observed in the IR spectrum at 3400 cm^{-1} indicated the existence of a free hydroxyl and while signal at 1645 cm^{-1} was ascribed to an α,β-unsaturated carbonyl group. A molecular formula of $C_{17}H_{16}O_7$ was established for this compound based on ^{13}C NMR and the HRESIMS (*m/z* 333.0970 $[M + H]^+$ (calcd. 3333.0930)).

The NMR (Table 4.9, Appendix 13) displayed the occurrence of a methoxy group (δ_H 3.92, δ_C 55.4). The ^1H NMR displayed signals at δ_H 7.11 and 6.73 (2H, J = 8.5 Hz) ascribable to the protons of a *para*-disubstituted benzene ring. In addition, the ^1H NMR in the aromatic region showed a sharp peak at δ_H 6.24 (H-8) indicating the presence of a *penta*-substituted aromatic ring. The ^1H NMR in the aliphatic region displayed signals for two mutually coupling non-equivalent protons for an oxymethylene (δ_H 4.16 and 4.01) and a methylene group (δ_H 2.96 and 2.90). The ^{13}C NMR

and HSQC spectrum indicated a total of seventeen carbons. Based on this data, compound **186** was identified as homoisoflavone (Liu *et al.*, 2009; Ning *et al.*, 2012). The aliphatic methylene protons at δ_H 4.16 and 4.01 (2H) were assigned to C-2, while the methylene protons at δ_H 2.96 and 2.90 (2H) were assigned to C-9 of the homoisoflavonoid skeleton. The corresponding carbons resonated at δ_C 73.0 and 40.6, respectively. The signal at δ_C 73.9 and 200.7 in the ^{13}C NMR were assignable to C-3 and C-4, respectively. Therefore, this compound is a 3-hydroxyhomoisoflavonoid. In the HMBC correlation (Table 4.9), a cross-peak was detected between the methoxy protons (δ_H 3.92) and an oxygenated carbon at δ_C 158.5 indicating the placement of the methoxy substituent at C-7 in ring A. This implied that there are two hydroxyls and one methoxy substituent in ring A and a hydroxyl group in ring B. This substitution pattern was supported from an MS^2 fragment ion peak observed at *m/z* 183.0287 $[M + H- C_9H_{10}O_2]^+$ (Scheme 4.1) arising from the Retro-Diels Alder (RDA) fragmentation of the pyrone ring (ring C) of the 3-hydroxyhomoisoflavone skeleton.

What is left now is to propose the absolute configuration of the compound as there are two possible stereoisomers, 3*R* or 3*S*. To resolve this, the Circular Dichroism (CD) spectrum (Figure 4.2) was generated and the results showed this compound had a negative cotton effect at 294 nm. Comparison of this data with literature indicated that the configuration of this compound is *S* at C-3 position (Dai *et al.*, 2013; El-Elimat *et al.*, 2018). Based on this, compound **186** was newly identified as usambarin.

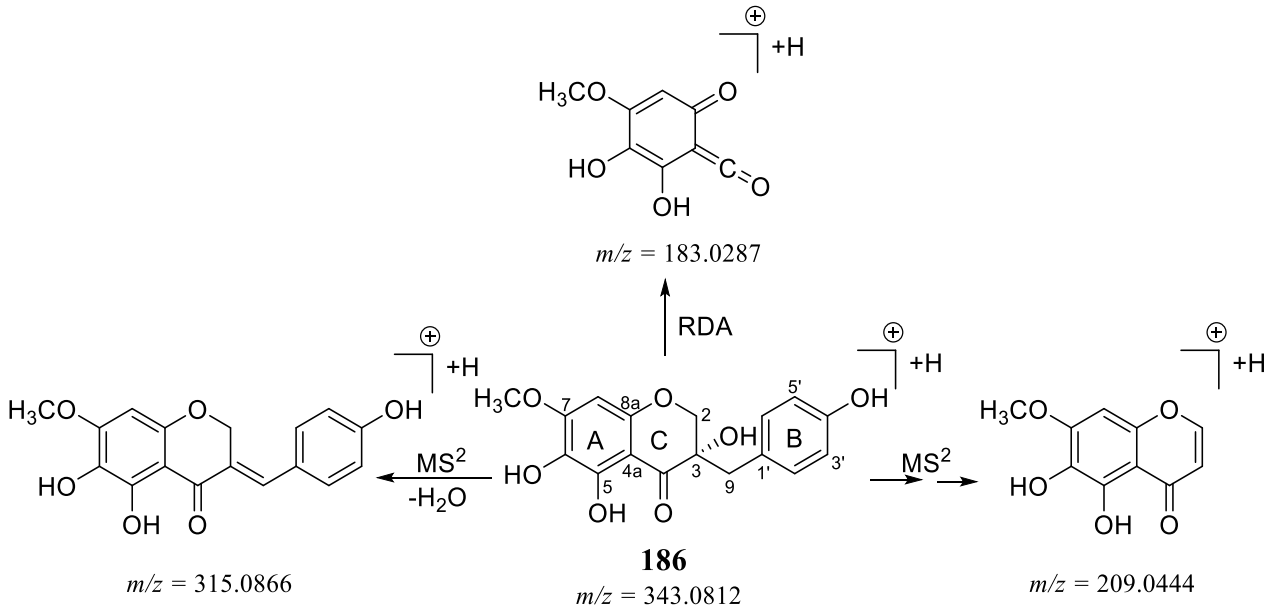

Scheme 4.1: Different fragmentation pathway of compound **186**

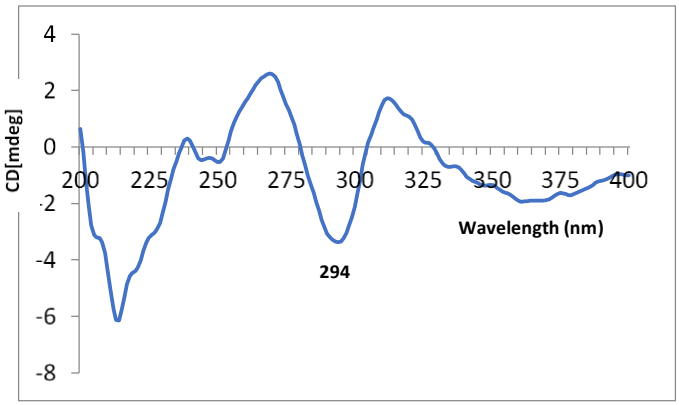

Figure 4.2: CD spectrum of compound **186**

4.2.2: (3S)-3,4',5-Trihydroxy-7-methoxyhomoisoflavanone (187)

Compound **187** was purified as a cream solid. The chemical formula $C_{17}H_{17}O_6$ was elucidated from the UV (λ_{max} 294 and 232 nm), NMR (Table 4.9, Appendix 14) and MS (*m/z* 317.1021 $[M + H]^+$ (calcd. 317.0980)) spectra. The NMR spectra showed that, this compound is 3-hydroxyhomoisoflavone derivative just as compound **186**. Comparison of the molecular weight of this compound with **186** indicated that, the molecular weight of this compound is less by 16 Dalton implying that this compound has one less hydroxy group compared to **186**.

The NMR displayed signal of a methoxy unit (δ_H 3.81, δ_C 56.0). Similarly, signals of three exchangeable protons were observed at δ_H 9.25 (HO-4′), 6.00 (HO-3) and a chelated hydroxyl at δ_H 11.93 (HO-5). The ^{1}H NMR displayed signals with an AA′BB′ spin system (δ_H 7.03 and 6.67 (2H, J = 8.5 Hz)) assignable to ring B protons. In addition to this, the ^{1}H NMR displayed an AX spin system (δ_H 6.12 and 6.11 (1H, J = 2.3 Hz)) indicating a disubstituted ring A. With this there are two possible structure for this compound depending on whether the methoxy is at C-7 or C-4′. A NOESY correlation was detected between signal at δ_H 3.81 and the *meta* coupled protons (δ_H 6.12 and 6.11 (1H, J = 2.3 Hz)) placing the methoxy at C-7. Likewise, the CD spectrum (Figure 4.3) of **187** displayed a negative absorption at 294 nm as was the case in **186**. Based on this, compound **187** was identified as (3*S*)-4′,5-dihydroxy-7-methoxyhomoisoflavanone. A compound previously isolated from *Bellevalia eigii* (Alali *et al.*, 2015).

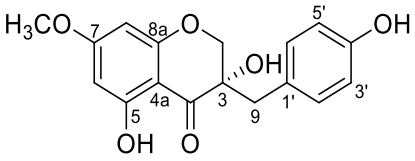

187

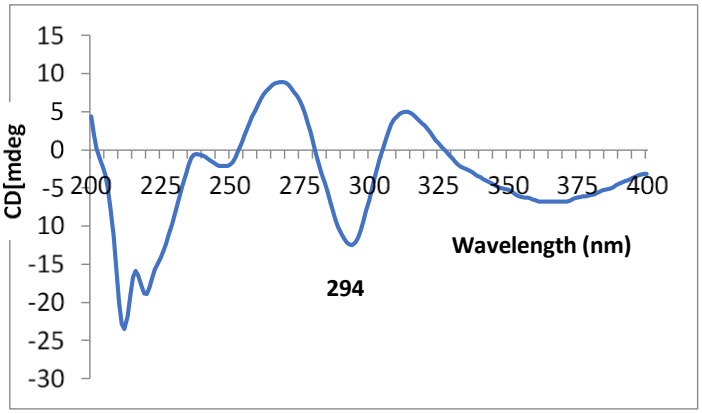

Figure 4.3: CD spectrum of compound **187**

Table 4.9: NMR data for compounds **186** and **187**

No	**186**[ab]			**187**[ac]		
	δ_C	δ_H (*m*, *Hz*)	HMBC	δ_C	δ_H (*m*, *Hz*)	HMBC
2	73.0	4.16 *d* (11.2)	C- 3, 4, 8a, 9	71.7	4.00 *d* (11.5)	C- 3, 4, 8a, 9
	-	4.01 *d* (11.2)	C- 3, 4, 8a, 9	-	3.98 *d* (11.5)	C- 3, 4, 8a, 9
3	73.9	-	-	71.6	-	-
4	200.7	-	-	198.9	-	-
4a	101.8	-	-	100.8	-	-
5	158.3	-	-	163.6	-	-
6	127.9	-	-	95.0	6.12 *d* (2.3)	C- 4a, 5, 7, 8
7	158.5	-	-	167.5	-	-
8	93.9	6.24 *s*	C- 4, 4a, 6, 7, 8a	93.7	6.11 *d* (2.3)	C- 4a, 6, 7, 8a
8a	148.8	-	-	162.4	-	-
9	40.6	2.96 *d* (14.1)	C- 1′, 3, 4, 2′/6′	38.5	2.82 *s*	C- 1′, 3, 4, 2′/6′
	-	2.90 *d* (14.1)	C- 1′, 3, 4, 2′/6′	-	-	-
1′	126.8	-	-	125.0	-	-
2′/6′	132.9	7.11 *d* (8.5)	C- 4′, 2′/6′, 3′/5′, 9	131.5	7.03 *d* (8.5)	C- 4′, 2′/6′, 3′/5′, 9
3′/5′	115.9	6.73 *d* (8.5)	C- 1′, 3′/5′, 4′	114.7	6.67 *d* (8.5)	C- 1′, 4′, 3′/5′
4′	157.5	-	-	156.1	-	-
CH_3O-7	56.8	3.92 *s*	C- 7	56.0	3.81 *s*	C- 7
HO-3	-	-	-	-	6.00 *s*	C- 1, 2, 3, 9
HO-5	-	-	-	-	11.93 *s*	C- 4a, 5, 6
HO-4′	-	-	-	-	9.25 *s*	C- 4′, 3′/5′

[a] Recorded at 600 MHz
[b] in CD_3OD, [c] in DMSO-d_6

4.2.3: Loureiriol (188)

Compound **188** was purified as a yellow solid. The NMR (Table 4.10, Appendix 15) displayed characteristic signals for a 3-hydroxyhomoisoflavone as observed in **186** and **187**. The molecular weight of **188** was less by 14 amu compared to that of **187**, implying in this compound there is a hydroxy substituent instead of a methoxy as in **187**. Based on this and comparing the data with literature, compound **188** was identified as (3*R*)-4′,5,7-trihydroxyhomoisoflavanone (Kittisak *et al*., 2002). A compound previously reported as loureiriol from the stem wood of *D. loureirin* (Kittisak *et al*., 2002).

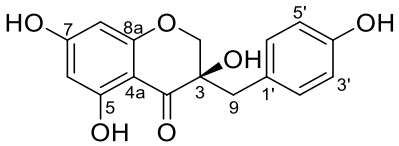

188

Table 4.10: NMR data for compound **188** in CD_3OD

No	**188**[a]		
	δ_C	δ_H (*m*, *Hz*)	HMBC
2	73.5	4.07 *d* (11.3)	C- 3, 4, 8a, 9
		3.98 *d* (11.3)	C- 3, 4, 8a, 9
3	72.8	-	-
4	199.8	-	-
4a	101.4	-	-
5	166.4	-	-
6	97.5	5.94 *d* (2.0)	C- 4a, 5, 7, 8
7	168.8	-	-
8	96.2	5.92 *d* (2.0)	C- 4a, 6, 7, 8a
8a	164.4	-	-
9	40.7	2.93 *d* (14.1)	C-1′, 3, 4, 2′/6′
		2.89 *d* (14.1)	-
1′	126.9	-	-
2′/6′	132.8	7.08 *d* (8.4)	C- 4′, 2′/6′, 3′/5′, 9
3′/5′	115.9	6.74 *d* (8.4)	C- 1′, 3′/5′, 4′
4′	157.3	-	-

[a] Recorded at 500 MHz

*4.2.4: 4′,4-Dihydroxy-2,3-dimethoxyretrodihydrochalcone (***189***)*

Compound **189** was purified as a yellow liquid. The chemical formula $C_{17}H_{18}O_5$ was established from NMR and HRESIMS (*m/z* 303.1221 $[M + H]^+$ (calcd. 303.1232)) spectra. The UV (λ_{max} 279 and 206 nm) (Qin *et al.*, 2015) and NMR ((δ_H 3.16 (H-α) and 2.89 (H-β)) and ^{13}C (δ_C 40.5 (C-α), 26.6 (C-β), 201.2 (C=O)) indicated that this compound had a retrodihydrochalcone skeleton.

The NMR (Table 4.11, Appendix 16) exhibited signals of two oxygenated methyl groups (δ_H 3.87 and 3.83; δ_C 61.1 and 60.9). The ^1H NMR displayed resonances for an AA′BB′ spin system (δ_H 7.89 (H-2′/6′) and 6.84 (H-3′/5′), 2H, *J* = 8.7 Hz) which are assigned to ring B. It also displayed signals for two *ortho*-coupled protons (δ_H 6.54 (H-5) and δ_H 6.76 (H-6), 1H, *J* = 8.4 Hz) which are assigned to ring A. Based on this, compound **189** was identified as 4′,4-dihydroxy-2,3-dimethoxyretrodihydrochalcone. Consistent with the proposed structure, the MS^2 profile displayed

fragment ions resulting from β- (**189a**) and γ- cleavages (**189b**), (Scheme 4.2), this places one of the hydroxyl substituent in ring B and the other groups in ring A. This is a new compound.

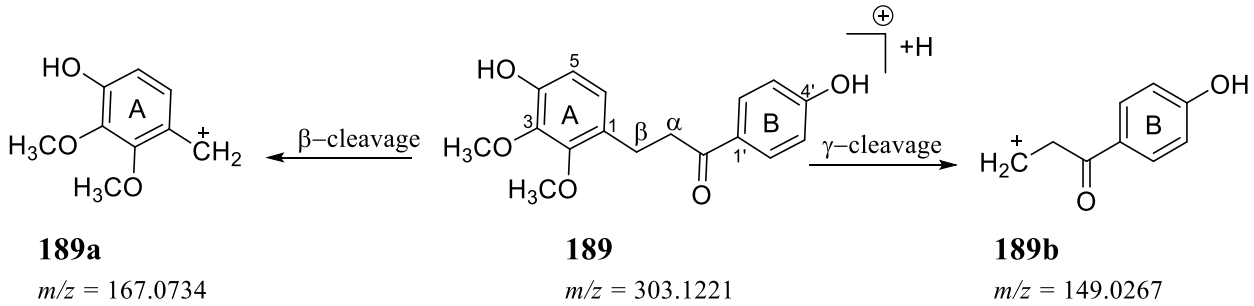

Scheme 4.2: Different fragmentation pathway of compound **189**

Table 4.11: NMR data for compound **189** in CD_3OD

No	**189**[a]		
	δ_C	δ_H (*m*, *Hz*)	HMBC
1′	130.0	-	-
2′/6′	131.9	7.89 *d* (8.7)	C- 2′/6′, 4′, 3′/5′, C=O
3′/5′	116.2	6.84 *d* (8.7)	C- 1′, 3′/5′, 4′
4′	163.7	-	-
α	40.5	3.16 *t* (6.2)	C- 1, C-β, C=O
β	26.6	2.89 *t* (6.2)	C- 1, 2, C-α, C=O
1	126.7	-	-
2	152.9	-	-
3	142.2	-	-
4	150.7	-	-
5	112.4	6.54 *d* (8.4)	C- 1, 3, 4
6	125.4	6.76 *d* (8.4)	C- 2, 4, 5, C-β
CH_3O-2	61.1	3.87 *s*	C- 2
CH_3O-3	60.9	3.83 *s*	C- 3
C=O	201.2	-	-

[a] Recorded at 500 MHz

*4.2.5: (25S)-Spirosta-1,4-dien-3-one (*190*)*

Compound **190** was identified as white needles. The mass spectrum exhibited a molecular ion at *m/z* 410.2768 $[M]^+$ (calcd. 410.2821) matching the chemical formula $C_{27}H_{38}O_3$ accounting for nine

degrees of unsaturation. Analysis of the spectroscopic data (Table 4.12, Appendix 17) suggested **190** to be a steroid type spirostanol derivative (Higano *et al.*, 2007).

The spectroscopic data of **190** was superimposable with that of dracaenogenin C (**176**) except that the oxygenated tertiary carbon at C-17 was substituted by a methine (δ_C 62.1 (C-17)) in this compound. The above findings were further supported by the cross peak detected in the HSQC between signal at δ_H 1.76 (H-17) to carbon at δ_C 62.1 (C-17). The occurrence of this methine group was further supported with correlations depicted in the HMBC between signal at δ_H 0.89 (Me-18) with carbons at δ_C 39.5 (C-12), 40.6 (C-13), 55.2 (C-14) and 62.1 (C-17) and that between the proton at δ_H 1.01 (Me-21) with carbons at δ_C 62.1 (C-17), 42.1 (C-20) and 109.5 (C-22). Based on this and by comparing the data with literature **190** was identified as (25*S*)-spirosta-1,4-dien-3-one (Huang *et al.*, 2008). This compound has been previously documented from *Asparagus officinalis* (Huang *et al.*, 2008).

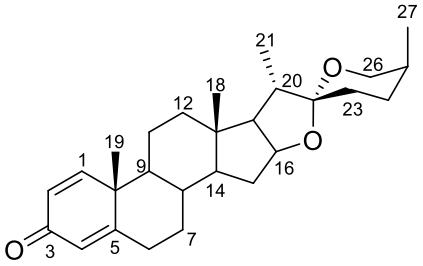

190

Table 4.12: NMR data for compound **190** in CD_2Cl_2

No	**190**[a]		
	δ_C	δ_H (*m*, *Hz*)	HMBC
1	156.1	7.11 *d* (10.2)	C- 3, 5, 6, 9, 10, 19
2	127.1	6.22 *dd* (10.2, 1.9)	C- 4, 10
3	185.9	-	-
4	123.5	6.07 *t* (1.9)	C- 2, 6, 10
5	169.6	-	-
6	32.8	2.54 *m*, 2.41 *m*	C- 4, 5, 7, 8, 10
7	33.8	2.02 *m*, 1.10 *m*	-
8	35.2	1.89 *m*	-
9	52.5	1.12 *m*	C- 15, 19
10	43.7	-	-
11	22.7	1.74 *m*	-
12	39.5	1.82 *m*, 1.21 *m*	-
13	40.6	-	-
14	55.2	1.16 *m*	-
15	31.8	2.03 *m*, 1.36 *m*	-
16	80.6	4.40 *ddd* (8.6, 7.5, 6.3)	C- 13
17	62.1	1.76 *m*	-
CH_3-18	16.2	0.89 *s*	C- 12, 13, 14, 17
CH_3-19	18.6	1.28 *s*	C- 1, 5, 9, 10
20	42.1	1.87 *m*	-
CH_3-21	14.1	1.01 *d* (7.0)	C- 17, 20, 22
22	109.5	-	-
23	25.9	1.92 *m*	-
24	25.8	2.02 *m*, 1.44 *m*	-
25	27.2	1.72 *m*	-
26	65.0	3.94 *dd* (10.9, 2.8)	C- 27
	-	3.28 *d* (10.9)	C- 22, 24
CH_3-27	15.8	1.10 *d* (7.1)	C- 25, 26

[a] Recorded at 500 MHz

4.2.6: Stigmasterol (191)

Compound **191** was purified as white solid. Its chemical formula ($C_{29}H_{48}O$) was deduced from the 1D and 2D NMR spectra (Table 4.13, Appendix 18). The ^{13}C NMR displayed twenty-nine signals among which two tertiary methyl (δ_C 11.9 (C-18), 19.4 (C-19)), four secondary methyl (δ_C 21.1 (C-21), 19.0 (C-26), 21.2 (C-27) and 12.0 (C-29)), oxymethine carbon (δ_C 71.6 (C-3)) and signals of an sp^2 carbons (δ_C 121.4 (C-6), 138.4 (C-22) and 129.3 (C-23)). These signals were

characteristic of steroid compound (Kamboj and Saluja, 2011). The ^{1}H NMR showed signals of three sets of double doublets at δ_H 5.21 (H-22), 5.07 (H-23) and 5.38 (H-6) in the olefinic region, as well as a signal of an oxymethine proton at δ_H 3.49 (H-3). All these data led to the conclusion that **191** is stigmasterol (Chaturvedula and Prakash, 2012). Stigmasterol (**191**) is ubiquitous steroid in plants.

*4.2.7: Stigmasterol 3-O-β-*D*-glucopyranoside (192)*

Compound **192** was identified as white solid. Its chemical formula was elucidated as $C_{35}H_{58}O_6$. The NMR (Table 4.13, Appendix 19) of this compound was closely related to compound **191** implying that it is a stigmasterol derivative. Comparison of ^{13}C NMR of **192** with that of **191** indicated the existence of six additional carbon signals at δ_C 78.4 - 62.6 (C-2′ - C-6′) and an anomeric carbon peak at δ_C 102.4 (C-1′) indicating the existence of sugar moiety in **192**. Based on their coupling constant $J_{1',2'}$ = 7.7 Hz and comparison with similar sugars described in the literature, the monosaccharide unit was, therefore, identified as *β*-D-glucopyranoside (Xu *et al.*, 2000). Its linkage to the aglycone was confirmed with the aid of an HMBC correlation observed between the oxymethine proton (δ_H 5.10 (H-1′)) and carbon at δ_C 78.1 (C-3). Hence, **192** was identified as a monodesmoside saponin known as stigmasterol 3-*O*-*β*-D-glucopyranoside (Debella *et al.*, 2000). This compound is very common in plant species.

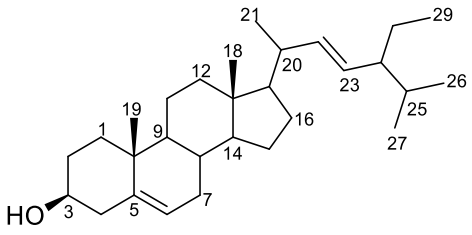

191

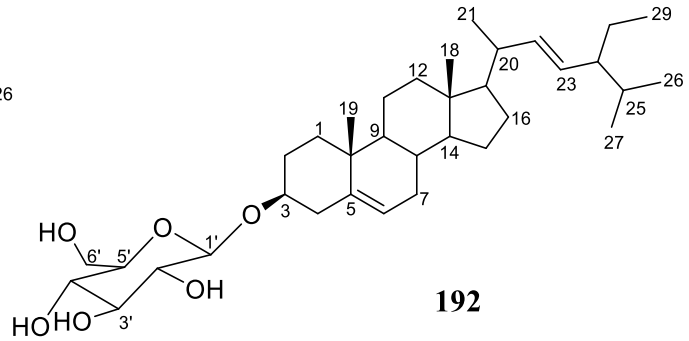

192

Table 4.13: NMR data for compounds **191** and **192** in DMSO-d_6

No	**191**[a]			**192**[a]		
	δ_C	δ_H (*m*, *Hz*)	HMBC	δ_C	δ_H (*m*, *Hz*)	HMBC
1	37.3	-	-	37.2	-	-
2	31.8	-	-	31.8	-	-
3	71.6	3.49 *m*	C- 1, 2, 5	78.1	4.02 *m*	C- 1, 2
4	41.3	-	-	42.2	-	-
5	141.0	-	-	140.7	-	-
6	121.4	5.38 *dd* (5.3, 2.6)	C- 1, 4, 8, 10	121.7	5.37 *dd* (5.1, 2.2)	C- 4, 8, 10
7	31.8	-	-	31.7	-	-
8	31.9	-	-	31.8	-	-
9	50.2	-	-	49.8	-	-
10	36.6	-	-	36.6	-	-
11	21.2	-	-	19.8	-	-
12	39.8	-	-	38.7	-	-
13	42.3	-	-	42.2	-	-
14	56.9	-	-	56.7	-	-
15	24.3	-	-	24.2	-	-
16	29.1	-	-	28.1	-	-
17	56.1	-	-	55.9	-	-
CH_3-18	11.9	-	-	11.7	-	-
CH_3-19	19.4	-	-	18.7	-	-
20	40.5	-	-	39.7	-	-
CH_3-21	21.1	-	-	20.9	-	-
22	138.4	5.21 *dd* (15.2, 8.7)	C- 17, 21 23, 24	138.6	5.24 *dd* (15.2, 8.7)	C- 17, 21 23, 24
23	129.3	5.07 *dd* (15.2, 8.7)	C- 20, 21 24	129.2	5.08 *dd* (15.2, 8.7)	C- 20, 21 24, 25
24	51.2	-	-	51.2	-	-
25	31.7	-	-	31.8	-	-
CH_3-26	19.0	-	-	19.2	-	-
CH_3-27	21.2	-	-	18.9	-	-
28	25.4	-	-	24.9	-	-
CH_3-29	12.0	-	-	12.3	-	-

Table 4.13: Continued

No	**191**[a]			**192**[a]		
	-			*β*-D-glucopyranoside		
1′	-	-	-	102.4	5.10 *d* (7.7)	C- 3, 3′, 5′
2′	-	-	-	75.1	4.61-4.11 *m*	-
3′	-	-	-	78.4	4.61-4.11 *m*	-
4′	-	-	-	71.5	4.61-4.11 *m*	-
5′	-	-	-	69.9	4.61-4.11 *m*	-
6′	-	-	-	62.6	4.61-4.11 *m*	-

[a] Recorded at 600 MHz

4.3: Characterization of Compounds Isolated from the Whole plant of *Dracaena aletriformis*

The air-dry whole plant of *D. aletriformis* was chromatographically separated to afford three previously reported phenolic amides. The structure elucidation of these compounds will be discussed.

4.3.1: 3-(4′′′-hydroxyphenyl)-N-[2′-(4′′-hydroxyphenyl)-2′-methoxyethyl]acrylamide (193)

Compound **193** was purified as a white powder. The MS profile showed a pseudo-molecular ion at *m/z* 314.1387 $[M+H]^+$ (calcd. 314.1348) equivalent to the molecular formula $C_{18}H_{19}NO_4$, accounting for ten ring double bond equivalents. Further, the signal observed at *m/z* 282.1125 $[M+H]^+$ indicated a neutral loss of one molecule of methanol suggesting the presence of a methoxy substituent in this compound. The NMR spectra (Table 4.14, Appendix 20) of this compound is closely similar to that of **170** except for the presence of an additional methoxy substituent in this compound. In agreement with this, the molecular weight of **193** was 30 amu more than that of **170** (OCH_3). The HMBC correlation between the methoxy (δ_H 3.10) protons and C-2′ (δ_C 82.0) allowed the placement of this substituent at C-2′. Hence, **193** was identified as 3-(4′′′-hydroxyphenyl)-*N*-[2′-(4′′-hydroxyphenyl)-2′-methoxyethyl]acrylamide (Sun *et al.*, 2015). This compound was also isolated from the root extract of *Dracaena usambarensis*.

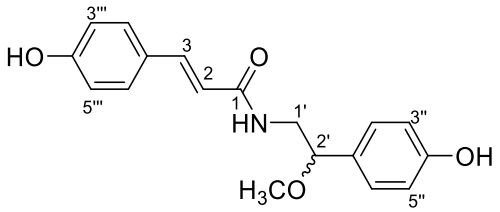

193

4.3.2: N-Trans-p-coumaroyloctopamine (194)

Compound **194** was purified as a white powder. The MS profile of this compound (**194**) exhibited a molecular ion at *m/z* 300.1231 $[M+H]^+$ (calcd. 300.1191) matching the chemical formula $C_{17}H_{17}NO_4$. The NMR data (Table 4.14, Appendix 21) of **194** were comparable to those of **193**, the notable difference being the methoxy group at C-2′ in **193** has been replaced by a hydroxyl group. The above findings were further supported with the aid of ^{13}C NMR spectrum of **194** which displayed seventeen signals *versus* eighteen in **193**. The 2D NMR data of **194** showed the same connectivity as **193**. This compound (**194**) was identified as a phenolic amide *N-trans-p-*coumaroyloctopamine. A compound previously isolated from the stems of *Solanum verbascifolium* (Zhou and Ding, 2002). This compound was also isolated from the stem of *Dracaena usambarensis.*

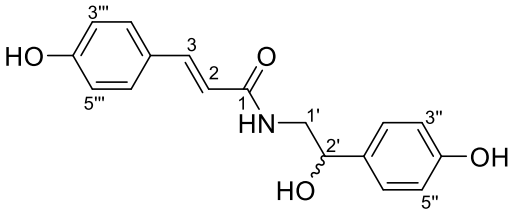

194

Table 4.14: NMR data for compounds **193** and **194**

No	**193**[ac]			**194**[bd]		
	δ_C	δ_H (*m, Hz*)	HMBC	δ_C	δ_H (*m, Hz*)	HMBC
1	165.4	-	-	169.6	-	-
2	119.2	6.49 *d* (15.7)	-	118.3	6.46 *d* (15.7)	-
3	139.2	7.31 *d* (15.7)	C- 1, 2, 2‴/6‴	141.5	7.47 *d* (15.7)	C- 1, 2, 2‴/6‴
1′	44.6	3.38 *m*	C- 1, 1″, 2′	48.3	3.55 *dd* (13.6, 4.9)	C- 1, 1″, 2′
		3.27 *ddd* (13.5, 8.2, 5.1)	C- 1, 1″, 2′,		3.45 *dd* (13.6, 8.0)	C- 1, 1″, 2′,
2′	82.0	4.16 *dd* (8.2, 5.1)	C- 1′, 1″, 2″/6″	73.5	4.74 *dd* (8.0, 4.9)	C- 1′, 1″, 2″/6″
1″	130.3	-	-	134.8	-	-
2″/6″	128.4	7.11 *d* (8.5)	C- 2′, 2″/6″, 4″, 3″/5″	128.5	7.24 *d* (8.6)	C- 2′, 2″/6″, 4″, 3″/5″
3″/5″	115.6	6.76f *d* (8.5)	C- 1″, 4″, 3″/5″	116.1	6.80 *d* (8.6)	C- 1″, 4″, 3″/5″
4″	157.5	-	-	158.1	-	-
1‴	126.4	-	-	127.2	-	-
2‴/6‴	129.7	7.38 *d* (8.6)	C- 3, 4‴, 3‴/5‴, 2‴/6‴	130.6	7.42 *d* (8.6)	C- 3, 4‴, 3‴/5‴, 2‴/6‴
3‴/5‴	116.2	6.79 *d* (8.6)	C- 1‴, 4‴, 3‴/5‴	116.8	6.81 *d* (8.6)	C- 1‴, 4‴, 3‴/5‴
4‴	159.3	-	-	160.7	-	-
CH_3O-2′	56.2	3.10 *s*	C- 2′	-	-	-
HO-4″	-	9.40 *s*	C- 3″/5″, 4″		-	-
HO-4‴	-	9.83 *s*	C- 3‴/5‴		-	-
NH	-	8.05 *t* (1.3)	C- 1, 2, 2′		-	-

[a,b] Recorded at 600 and 500 MHz, respectively
[c] in DMSO-d_6, [d] in CD_3OD

4.3.3: N-Trans-feruloylphenethylamine (195)

Compound **195** (UV λ_{max} 319 and 228 nm) was purified as a white powder. This compound was deduced as $C_{18}H_{19}NO_3$ as evidence of MS (*m/z* 298.1437 $[M+H]^+$ (calcd. 298.1398)) spectrum. The NMR (Table 4.15, Appendix 22) of **195** and **171** are closely related. Just as in **171**, in this compound there is a ferulic moiety. However, instead of tyramine moiety as in **171** this compound has a phenethylamine moiety (δ_H 7.26 (H-2″/6″), 7.31 (H-3″/5″) and 7.21 (H-4″)). Using this and comparing the data with literature, **195** was identified as *N-trans*-feruloyl phenethylamine (Siyu *et al.*, 2017). A compound previously reported from *Lycium barbarum* (Siyu *et al.*, 2017).

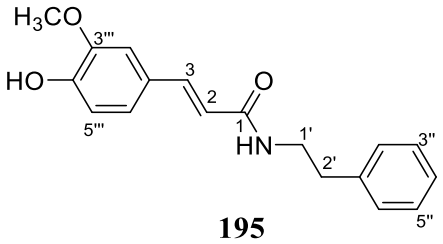

195

Table 4.15: NMR data for compound **195** in CD_3OD

No	**195**[a]		
	δ_C	δ_H (*m*, *Hz*)	HMBC
1	169.2	-	-
2	118.7	6.42 *d* (15.7)	C- 1, 1‴
3	142.1	7.46 *d* (15.7)	C- 1, 2, 2‴, 6‴
1′	42.2	3.54 *t* (7.4)	C- 1, 1″
2′	36.7	2.88 *t* (7.4)	C- 1″, 2″/6″
1″	140.6	-	-
2″/6″	129.8	7.26 *m*	C- 2′, 4″, 2″/6″
3″/5″	129.5	7.31 *m*	C- 1″, 3″/5″
4″	127.4	7.21 *m*	-
1‴	128.3	-	-
2‴	111.5	7.14 *d* (2.0)	C- 3, 4‴, 6‴
3‴	149.3	-	-
4‴	149.9	-	-
5‴	116.5	6.82 *d* (8.2)	C- 1‴, 4‴
6‴	123.2	7.04 *dd* (8.2, 2.0)	C- 2‴, 3, 4‴
CH_3O-3‴	56.4	3.91 *s*	C- 3‴

[a] Recorded at 700 MHz

4.4: Characterization of Compounds Isolated from the Seeds of *Dracaena steudneri*

Repeated column chromatography in silica gel and further purification through semi-preparative HPLC of the seeds of *D. steudneri* yielded seven previously reported secondary metabolites. The structure elucidation of these compounds is discussed herein.

4.4.1: Isorhamnetin 3-O-rungioside (196)

Compound **196** was purified as a yellow solid. The MS profile exhibited a protonated molecular ion at *m*/*z* 625.1760 $[M + H]^+$ (calcd. 625.1724) which was consistent with the molecular formula $C_{28}H_{32}O_{16}$ indicating thirteen rings double bond equivalents. The UV (λ_{max} 356 and 254 nm) and ^{13}C NMR (δ_C 157.9 (C-2), 134.2 (C-3) and 179.1 (C-4)) spectra indicated that compound **196** is a flavonol derivative (Awouafack *et al.*, 2013; Gao *et al.*, 2010; Yang *et al.*, 2015).

The NMR (Table 4.16, Appendix 23) showed signals of a oxygenated methyl substituent (δ_H 3.99, δ_C 56.9). In addition, the NMR displayed signals for a disaccharide with their two anomeric protons resonating at δ_H 5.90 (H-1″, J = 7.6 Hz) and 5.20 (H-1‴, J = 1.6 Hz) in the ^1H NMR and the corresponding carbons showing at δ_C 100.2 and 102.8, respectively. Based on their coupling constants and comparison of ^{13}C NMR data of carbon of the sugars with literature, the two monosaccharide units were identified as *β*-D-glucopyranose (Xu *et al.*, 2000) and *α*-L-rhmanopyranose (Fouedjou *et al.*, 2014). The monosaccharide sequence and their linkage site to the aglycone moiety were established using HMBC and tandem mass spectra. The ^3J correlation identified in the HMBC flanked by the signal at δ_H 5.20 (α-rhm) with carbon at δ_C 80.3 (C-3″) indicating the inter-glycosidic linkage of the two monosaccharides as (1‴ → 3″). Further, the signal at *m*/*z* 479.1180 $[(M + H) - Rhm]^+$ was consistent with a rhamnose as the terminal sugar.

The aglycone part displayed signals for three mutually coupling aromatic protons with an ABX spin system (δ_H 7.99 (J = 2.0 Hz), 6.93 (J = 8.4 Hz) and 7.56 (J = 8.4, 2.0 Hz)) and two *meta*-coupled protons with an AX spin system (δ_H 6.17 and 6.35 (J = 2.0 Hz)). Two of the protons of the ABX spin system (δ_H 7.99 and 7.56) showed HMBC correlations with C-2 (δ_C 157.9) allowing the placement of this system in ring B and therefore, the AX protons at H-6 and H-8 in ring A.

The *meta* proton (7.56 (J = 8.4, 2.0 Hz)) of the ABX system showed HMBC correlation with an oxygenated carbon (δ_C 148.4) which in turn showed HMBC correlation with signal at δ_H 3.99 (CH_3O-) placed the methoxy group (CH_3O-) at C-3′ (δ_C 148.4). A NOESY correlation between H-2′ with the methoxy substituent confirming the placement of the methoxy at C-3′. An HMBC correlation between the anomeric proton of the β-glycoside (δ_H 5.90) with C-3 (δ_C 134.2) fixed the disaccharide unit at C-3. Based on the foregoing, **196** was identified as isorhamnetin 3-*O*-rungioside, a compound reported from *Alhagi maurorum* (Ahmad *et al.*, 2010).

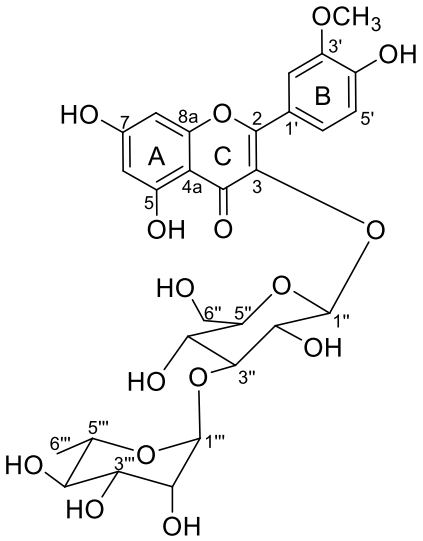

196

4.4.2: Kaempferol 3-O-rungioside (197)

Compound **197** was purified as a yellow solid. The chemical formula $C_{27}H_{30}O_{15}$ was deduced from the MS (*m*/*z* 595.1655 $[M + H]^+$ (calcd. 595.1618)) and NMR spectrums. This compound was consistent with thirteen degrees of unsaturation. Just like the previous compound, this compound (**197**) displayed UV (λ_{max} 350, 266 and 232 nm) and ^{13}C NMR (δ_C 158.3 (C-2), 134.3 (C-3) and 179.3 (C-4)) (Table 4.16, Appendix 24) spectra characteristic of flavonol derivative (Awouafack *et al.*, 2013; Gao *et al.*, 2010; Yang *et al.*, 2015). As in **197**, there is a disaccharide (Glu-rham) (δ_H 5.76 (H-1″, *J* = 7.6 Hz), δ_C 100.2 and δ_H 5.25 (H-1‴, *J* = 1.6 Hz), δ_C 100.6) unit at C-3 position. This was further reinforced from the MS profile which displayed fragments ions at *m*/*z* 449.1078 $[(M + H) - Rhm]^+$ and 287.0551 $[(M + H) – (Glu+Rhm)]^+$ consistent with the loss of a rhamnose and a disaccharide (Glu+Rhm) units, respectively. The ^1H NMR displayed signals for an AA′BB′ spin system (δ_H 8.06 (H-2′/6′) and 6.91 (H-3′/5′), *J* = 8.8 Hz) assigned to ring B and an AX spin system (δ_H 6.18 and 6.36 (*J* = 2.0 Hz)) representing ring A protons. Therefore, **197** was identified as kaempferol 3-*O*-rungioside. This compound has been previously reported from the flowers of *Rungia repens* (Seshadri and Vydeeswaran, 1972).

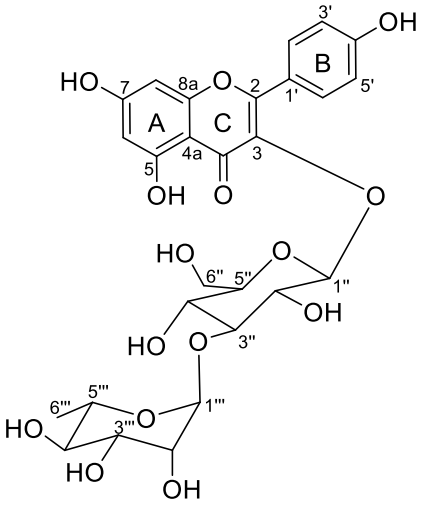

197

Table 4.16: NMR data for compounds **196** and **197** in CD_3OD

No	**196**[a]			**197**[a]		
	δ_C	δ_H (*m*, *Hz*)	HMBC	δ_C	δ_H (*m*, *Hz*)	HMBC
2	157.9	-	-	158.3	-	-
3	134.2	-	-	134.3	-	-
4	179.1	-	-	179.3	-	-
4a	105.4	-	-	105.5	-	-
5	163.1	-	-	163.1	-	-
6	100.4	6.17 *d* (2.1)	C- 4a, 5, 7, 8	100.3	6.18 *d* (2.0)	C- 4a, 5, 8
7	165.6	-	-	165.7	-	-
8	95.0	6.35 *d* (2.1)	C- 4a, 6, 7, 8a	94.9	6.36 *d* (2.0)	C- 4a, 6, 8a
8a	158.6	-	-	158.5	-	-
1′	122.0	-	-	123.2	-	-
2′	114.5	7.99 *d* (2.0)	C- 2, 3′, 4′, 6′	132.1	8.06 *d* (8.8)	C- 2, 4′, 6′
3′	148.4	-	-	116.1	6.91 *d* (8.8)	C- 1′, 4′, 5′
4′	150.6	-	-	161.3	-	-
5′	116.0	6.93 *d* (8.4)	C- 3′, 4′, 6′	116.1	6.91 *d* (8.8)	C- 1′, 3′, 4′
6′	123.4	7.56 *dd* (8.4, 2.0)	C- 2, 2′, 4′	132.1	8.06 *d* (8.8)	C- 2, 2′, 4′
CH_3O-3′	56.9	3.99 *s*	C- 3′	-	-	-
	β-D-Glucopyranose			*β*-D-Glucopyranose		
1″	100.2	5.90 *d* (7.6)	C- 3	100.2	5.76 *d* (7.6)	C- 3
2″	71.8	4.01-3.76 *m*	-	71.8	4.01-3.30 *m*	-
3″	80.3	3.65 *m*	-	80.1	3.62 *m*	-
4″	78.9	3.59 *m*	-	79.0	3.57 *m*	-
5″	78.4	3.27 *m*	-	78.4	3.23 *m*	-
6″	62.4	3.78-3.57 *m*	-	62.6	3.75-3.52 *m*	-

Table 4.16: Continued

No	**196**[a]			**197**[a]		
	α-L-Rhamnopyranose			*α*-L-Rhamnopyranose		
1‴	102.8	5.20 *d* (1.6)	C- 3″, 3‴, 5‴	102.6	5.25 *d* (1.6)	C- 3″, 3‴, 5‴
2‴	72.4	4.01-3.76 *m*	-	72.4	4.01-3.30 *m*	-
3‴	72.3	4.01-3.76 *m*	-	72.3	4.01-3.30 *m*	-
4‴	74.0	3.31 *m*	-	74.0	3.34 *m*	-
5‴	69.9	4.01-3.76 *m*	-	69.9	4.01-3.30 *m*	-
6‴	17.4	0.90 *d* (6.2)	C- 4‴, 5‴	17.5	0.98 *d* (6.1)	C- 4‴, 5‴

[a] Recorded at 600 MHz

4.4.3: Hirsutrin (198)

Compound **198** was isolated as a yellow solid. This compound (**198**) had a molecular formula $C_{21}H_{20}O_{12}$ based on NMR and MS observed at *m*/*z* 465.1023 $[M + H]^+$ (calcd. 465.0988). This compound was isolated as a flavonol derivative similar to **196** and **197** based on signal observed in the UV (λ_{max} 354 and 260 nm) and the ^{13}C NMR spectra (Awouafack *et al.*, 2013; Gao *et al.*, 2010; Yang *et al.*, 2015).

The NMR (Table 4.17, Appendix 25) displayed signals for a sugar moiety (δ_H 5.26, δ_C 104.3). Comparing the NMR (**Table 4.17)** data of the sugar unit with literature, the monosaccharide was identified as glucose (Lanzotti *et al.*, 2012). The ^1H NMR displayed signals of five aromatic protons ascribable to ring B (δ_H 7.73 (H-2′), 6.89 (H-5′) and 7.61 (H-6′)) and ring A (δ_H 6.22 (H-6) and 6.40 (H-8)). An HMBC between δ_H 5.26 (H-1″)) and C-3 (δ_C 135.6) placed the *β*-D-glucopyranoside ($J_{1'',2''}$ = 7.7 Hz) unit at C-3. Hence, **198** was proposed as quercetin-3-*O*-*β*-D-glucoside (hirsutrin). Hirsutrin (**198**) was reported from *Acer barbinerve* (Kwon and Bae, 2011).

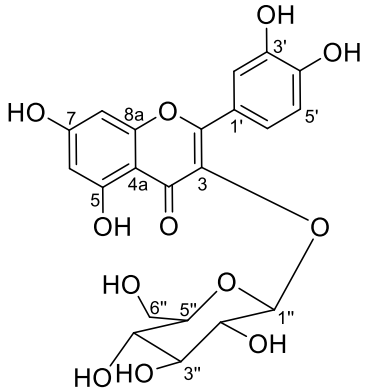

198

4.4.4: Isorhamnetin 3-O-β-D-glucopyranoside (199)

Compound **199** was purified as a yellow solid. The MS (*m*/*z* 479.1179 $[M + H]^+$ (calcd. 479.1145)) profile was consistent the chemical formula $C_{22}H_{22}O_{12}$ indicating twelve sites of unsaturation. Its UV (λ_{max} 356 and 264 nm) and NMR data (Table 4.17, Appendix 26) are characteristics of a flavonol scaffold (Awouafack *et al.*, 2013; Gao *et al.*, 2010; Yang *et al.*, 2015). The spectroscopic data (Table 4.17) of **199** was superimposable to **196** except that instead of a disaccharide unit as in **196**, this compound has a monosaccharide (*β*-D-glucopyranoside) substituent at position C-3. Based on these data, **199** was elucidated as isorhamnetin 3-*O*-*β*-D-glucopyranoside (Touil *et al.*, 2006).

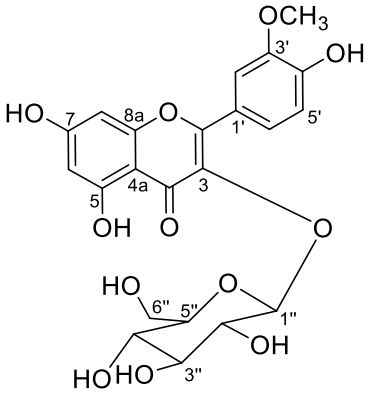

199

Table 4.17: NMR data for compounds **198** and **199** in CD_3OD

No	**198**[a]			**199**[a]		
	δ_C	δ_H (*m*, *Hz*)	HMBC	δ_C	δ_H (*m*, *Hz*)	HMBC
2	158.9	-	-	158.5	-	-
3	135.6	-	-	135.3	-	-
4	179.4	-	-	179.5	-	-
4a	105.5	-	-	105.8	-	-
5	163.0	-	-	163.1	-	-
6	100.1	6.22 *d* (2.0)	C- 4a, 5, 7, 8	99.9	6.23 *d* (2.1)	C- 4a, 5, 7, 8
7	166.7	-	-	166.0	-	-
8	94.8	6.40 *d* (2.0)	C- 4a, 6, 7, 8a	94.7	6.43 *d* (2.1)	C- 4a, 6, 7, 8a
8a	158.5	-	-	158.7	-	-
1′	123.1	-	-	123.1	-	-
2′	117.5	7.73 *d* (2.2)	C- 1′, 2, 3′, 4′	113.0	7.95 *d* (2.0)	C- 1′, 2, 3′, 4′
3′	145.9	-	-	148.4	-	-
4′	149.9	-	-	150.8	-	-
5′	116.0	6.89 *d* (8.5)	C- 1′, 3′, 4′	116.0	6.93 *d* (8.5)	C- 1′, 3′, 4′
6′	123.2	7.61 *dd* (8.5, 2.2)	C- 2, 2′, 4′	123.8	7.61 *dd* (8.5, 2.2)	C- 2, 2′, 4′
CH_3O-3′	-	-	-	56.8	3.97 *s*	C- 3′
	β-D-Glucopyranose			*β*-D-Glucopyranose		
1″	104.3	5.26 *d* (7.7)	C- 3	103.6	5.44 *d* (7.1)	C- 3
2″	75.7	3.50 *dd* (9.0, 7.7)	C- 1″, 3″	75.9	3.47 *m*	-
3″	78.1	3.44 *t* (9.0)	C- 2″, 4″	78.0	3.45	-
4″	71.2	3.37 *t* (9.0)	C- 3″, 5″, 6″,	70.1	3.37	-
5″	78.4	3.24 *ddd* (9.0, 5.4, 2.3)	-	78.6	3.26 *ddd* (9.8, 5.5, 2.3)	-
6″	62.5	3.73 *dd* (11.9, 2.3)	C- 4″, 5″	62.5	3.75 *dd* (11.9, 2.3)	-
		3.59 *dd* (11.9, 5.4)	C- 4″, 5″		3.58 *dd* (11.9, 5.5)	-

[a] Recorded at 600 MHz

*4.4.5: 3,3′-Di-O-methylquercetin 4′-O-β-*D*-glucoside (200)*

Compound **200** (UV (λ_{max} 350 and 268 nm)) was purified as a yellow solid. The HRESIMS of this compound (**200**) exhibited a protonated molecular ion at *m/z* 493.1333 $[M + H]^+$ (calcd. 493.1301) corresponding to $C_{23}H_{24}O_{12}$. Its UV and NMR data are characteristics of a flavonol (Awouafack *et al.*, 2013; Gao *et al.*, 2010; Yang *et al.*, 2015).

The NMR (Table 4.18, Appendix 27) data indicated the occurrence of two oxygenated methyl (δ_H/δ_C 3.71/60.7; δ_H/δ_C 3.85/56.9) and β-D-glucopyranoside (δ_H 4.96, δ_C 102.1) substituents. Collision induced dissociation MS^2 of the parent ion gave a fragment *m/z* 331.0816 $[(M + H) - Glu]^+$ confirming the presence of the *β*-D-glucopyranoside substituent. The ^1H NMR displayed signals for five aromatic protons ascribable to ring B (δ_H 7.65 (H-2′), 7.21 (H-5′) and 7.61 (H-6′)) and ring A (δ_H 6.10 (H-6) and 6.31 (H-8)). One of the methoxy substituents (δ_H/δ_C 3.71/60.7) displayed an HMBC correlation with C-3 (δ_C 140.1) and thus placed at C-3. While the second methoxy group at δ_H/δ_C 3.85/56.9 was located at δ_C 150.6 (C-3′). Similarly, the doublet observed at δ_H 4.96 (H-1″) displayed a cross-peak in the HMBC spectrum with carbon at δ_C 150.4 establishing the location of the sugar unit at C-4′ position. The location of the sugar unit was further confirmed with NOESY spectrum between H-1″ and H-5′. Therefore, **200** was unambiguously proposed as 3,3′-*di-O*-methylquercetin 4′-*O-β*-D-glucoside (Woo *et al.*, 1983). This compound (**200**) was previously obtained from *Typha latifolia* (Woo *et al.*, 1983).

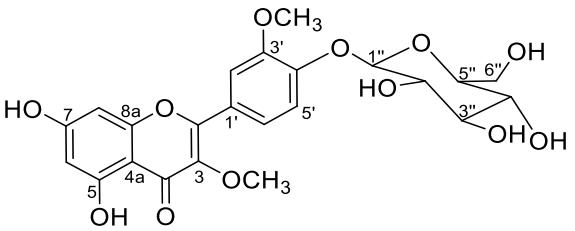

200

4.4.6: Quercetin (201)

Compound **201** was elucidated as $C_{15}H_{10}O_7$, as evidence of NMR and HRESIMS (*m*/*z* 303.0501 $[M + H]^+$ (calcd, 303.0460)) data. Compound **201** (UV λ_{max} 372 and 256 nm) was purified as yellow solid. This UV and the NMR (Table 4.18, Appendix 28) data were typical of a flavonol core (Awouafack *et al.*, 2013; Gao *et al.*, 2010; Yang *et al.*, 2015).

The ^{1}H NMR (Table 4.18) displayed signals for three mutually coupling siganls type ABX and AX spin system. The HMBC correlations observed between C-2 (δ_C 146.2) and signals at δ_H 7.76 and 7.66 allowed the assignment of the ABX system to ring B and thus the AX protons are assigned to ring A (H-6 and H-8).

The total assignment of the protons and carbons of this compound was achieved using COSY, HSQC and HMBC correlations. Using this and comparing the data with literature, **201** was elucidated as 3,3′,4′,5,7-pentahydroxyflavone (**201**), quercetin. Quercetin has been reported in many plants (Teponno *et al.*, 2006).

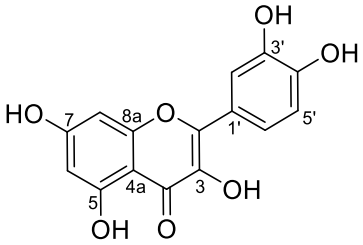

201

Table 4.18: NMR data for compounds **200** and **201** in CD_3OD

No	**200**[a]			**201**[a]		
	δ_C	δ_H (*m*, *Hz*)	HMBC	δ_C	δ_H (*m*, *Hz*)	HMBC
2	157.0	-	-	146.2	-	-
3	140.1	-	-	137.2	-	-
4	179.9	-	-	177.3	-	-
4a	105.7	-	-	104.5	-	-
5	163.1	-	-	162.5	-	-
6	100.2	6.10 *d* (2.1)	C- 4a, 5, 7, 8	99.3	6.20 *d* (2.1)	C- 4a, 5, 7, 8
7	167.1	-	-	165.7	-	-
8	95.1	6.31 *d* (2.1)	C- 4a, 6, 7, 8a	94.4	6.41 *d* (2.1)	C- 4a, 6, 7, 8a
8a	158.6	-	-	158.2	-	-
1′	125.9	-	-	124.1	-	-
2′	113.5	7.65 *d* (2.1)	C- 1′, 2, 3′, 6′	116.2	7.76 *d* (2.2)	C- 1′, 2, 3′, 6′
3′	150.6	-	-	148.0	-	-
4′	150.4	-	-	148.8	-	-
5′	117.0	7.21 *d* (8.6)	C- 1′, 2, 3′	116.0	6.91 *d* (8.5)	C- 1′, 2, 3′
6′	123.3	7.61 *dd* (8.6, 2.1)	C- 2, 2′, 4′	121.7	7.66 *dd* (8.5, 2.2)	C- 2, 2′, 4′
CH_3O-3	60.7	3.71 *s*	C- 3	-	-	-
CH_3O-3′	56.9	3.85 *s*	C- 3′	-	-	-
	β-D-Glucopyranose			-	-	-
1″	102.1	4.96 *d* (7.6)	C- 4′	-	-	-
2″	74.8	3.50 *dd* (9.2, 7.6)	-	-	-	-
3″	77.9	3.39 *m*	-	-	-	-
4″	71.3	3.32 *m*	-	-	-	-
5″	78.4	3.39 *m*	-	-	-	-
6″	62.5	3.81 *dd* (12.1, 2.2)	-	-	-	-
		3.61 *dd* (12.1, 5.7)	-	-	-	-

[a] Recorded at 600 MHz

4.4.7: 4-(2′-Formyl-1′-pyrrolyl)butanoic acid (202)

Compound **202** was purified as yellow solid. The chemical formula $C_9H_{11}NO_3$ was interpreted from the HRESIMS (*m*/*z* 182.0811 $[M + H]^+$ (calcd, 182.0772)) and NMR spectra. The NMR data (Table 4.19, Appendix.29) displayed signals for an aldehyde (δ_H 9.48, δ_C 180.9) and a carboxyl (δ_C 179.4) substituents. The NMR also displayed signals for a disubstituted pyrrole moiety (δ_H 7.04 (H-3′), 6.26 (H-4′) and 7.20 (H-5′); δ_C 126.5 (C-3′), 110.8 (C-4′) and 133.8 (C-5′)).

An HMBC correlation between the aldehyde (δ_H 9.48) and one of the carbons of the pyrrole resonating at δ_C 132.6 (C-2′) allowed the placement of this group at C-2′. The NMR further displayed signals for three mutually coupling (*J* = 7.4 Hz) methylene protons resonating at δ_H 2.19 (*t*), 2.03 (*p*) and 4.38 (*t*). The methylene protons at δ_H 4.38 are most deshielded among the methylenes due their attachment to the nitrogen. The 2D NMR correlations analysis revealed, these methylenes are attached to the carboxyl. Thus, based on this and comparison of the data with literature, **202** was identified as 4-(2′-formyl-l′-pyrrolyl)butanoic acid (Tressl *et al.*, 1993).

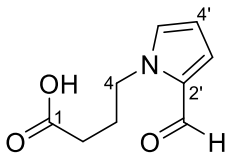

202

Table 4.19: NMR data for compound **202** in CD_3OD

No	**202**[a]		
	δ_C	δ_H (*m*, *Hz*)	HMBC
1	179.4	-	-
2	33.9	2.19 *t* (7.4)	C- 1, 3, 4
3	28.7	2.03 *p* (7.4)	C- 1, 2, 4
4	48.7	4.38 *t* (7.4)	C- 2, 3, 5′
2′	132.6	-	-
3′	126.5	7.04 *dd* (4.1, 1.7)	C- 5′
4′	110.8	6.26 *dd* (4.1, 2.5)	C- 5′
5′	133.8	7.20 *dd* (4.1, 1.7)	C- 2′, 3′, 4′
CHO-2′	180.8	9.48 *s*	C- 2′

[a] Recorded at 600 MHz

4.5: Characterization of the Compounds Isolated from the Leaves of *Dracaena steudneri*

The air-dried leaves of *D. steudneri* were extracted with methanol/dichloromethane (1:1) and chromatographically separated to yield twenty-one secondary metabolites. Six of them were novel. Their structure elucidation is discussed herein.

4.5.1: 3,5,7-Trihydroxy-6-methyl-3',4'-methylenedioxyflavone (203)

Compound **203** (λ_{max} 368 and 260 nm) was purified as a yellow solid. The chemical formula was elucidated as $C_{17}H_{12}O_7$ on the basis of IR (3345, 2987, 1610, 1481, 1250, 1066 and 669 cm^{-1}), NMR and MS (*m/z* 329.0659 $[M+H]^+$ (calcd, 329.0617)) spectra. The UV and ^{13}C NMR (δ_C 146.6 (C-2), 137.6 (C-3) 177.3 (C-4)) spectra were characteristic of a flavonol framework (Awouafack *et al.*, 2013; Gao *et al.*, 2010; Yang *et al.*, 2015).

The NMR (Table 4.20, Appendix 30) displayed signals for a methyl (δ_H 2.09, δ_C 7.4) and a methylenedioxy (δ_H 6.06, δ_C 103.0) substituents. In addition to this, signals for an ABX spin system (δ_H 7.73, 6.99 and 7.81) together with a sharp singlet (δ_H 6.45) were observed. An HMBC connectivity observed between the protons at δ_H 7.73 (J = 1.7 Hz) and 7.81 (J = 1.7, 8.4 Hz) of the ABX system with a carbon at δ_C 146.6 (C-2) allowed the assignment of the ABX system to ring

B. This also allowed the assignment of the aromatic protons at δ_H 7.73 and 7.81 to H-2′ and H-6′, respectively. Thus, the singlet aromatic proton was assigned to ring A. HMBC correlation was observed between H-2′ and H-5′ with the oxygenated carbons at δ_C 150.3 and 149.3 which also had HMBC correlations with the methylenedioxy protons (δ_H 6.06) placed the methylenedioxy substituents at C-3′/C-4′. The aromatic singlet proton in ring A displayed HMBC correlations with δ_C 104.1 (C-4a), 108.3 (C-6), 156.1 (C-8a), and 164.5 (C-7) indicating that the proton can be either at C-6 or C-8 position. Therefore, the substitution pattern in ring A could be 5,7-dihydroxy-8-methyl or 5,7-dihydroxy-6-methyl. The latter possibility (5,7-dihydroxy-6-methyl) was taken because the NMR data of ring A of this compound were superimposable with those of 6-methylquercetin 3-*O*-α-L-rhamnopyranoside (Quang *et al.*, 2008). Collisionally activated dissociation (CAD) displayed a predominant ion peak at *m/z* 299.0551 $[M + H\text{-}CH_2O]^+$ which underwent further division to give a signal at *m/z* 271.0603 $[M + H\text{-}CO]^+$ and *m/z* 243.0653 $[M + H\text{-}CO]^+$(Scheme 4.3) confirming the proposed structure. Thus, **203** was characterized as 3,5,7-trihydroxy-6-methyl-3′,4′-methylenedioxyflavone, which is a new compound.

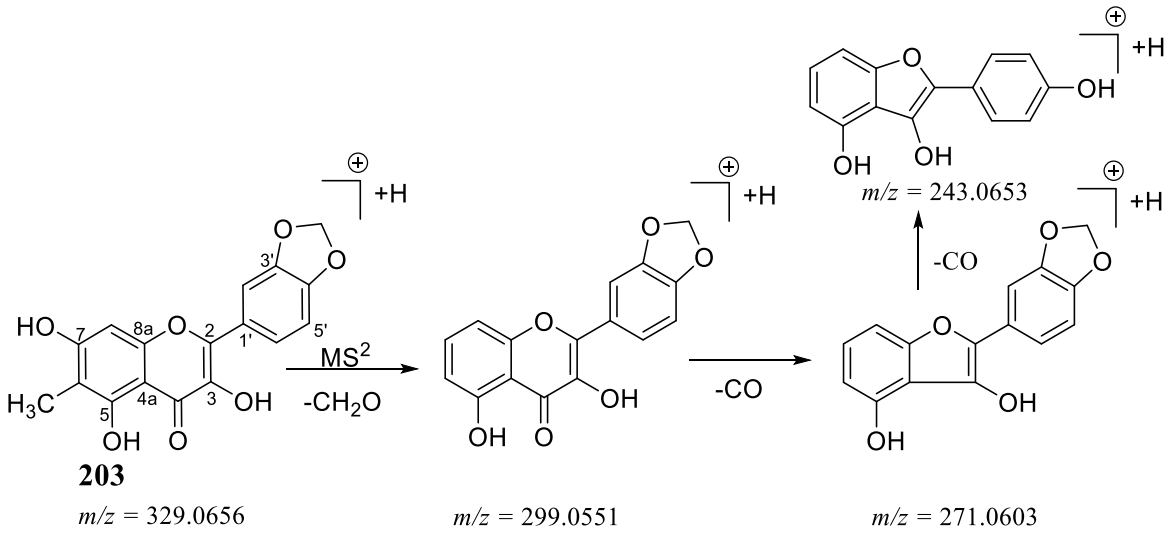

Scheme 4.3: Different fragmentation pathway of compound **203**

4.5.2: 5,7-Dihydroxy-3-methoxy-6-methyl-3',4'-methylenedioxyflavone (204)

Compound **204** (UV λ_{max} 351 and 269 nm) was isolated as a off-white solid. It exhibited a pseudo molecular ion at *m/z* 343.0812 $[M + H]^+$ (calcd. 343.0773) which corroborated the chemical formula $C_{18}H_{14}O_7$. Collision induced fragmentation (MS^2) of the parent ion produced signal at *m/z* 328.0579 $[M + H]^+$ (for a loss of CH_3), indicating the presence of a methyl substituents in this compound. The IR (3345, 2987, 1610, 1481, 1250, 1066 and 669 cm^{-1}), UV and NMR (δ_H 12.85 (HO-5), δ_C 155.3 (C-2), 138.5 (C-3) 176.3 (C-4)) data indicated that **204** is a 5-hydroxyflavonol derivative (Awouafack *et al.*, 2013; Gao *et al.*, 2010; Yang *et al.*, 2015).

The NMR (Table 4.20, Appendix 31) exhibited signal of a methyl (δ_H 2.00, δ_C 7.8) and a methylenedioxy (δ_H 6.16, δ_C 102.3) substituents as in compound **203** in addition to a methoxy (δ_H 3.79, δ_C 60.3) substituent. The NMR data of **204** mirrors that of **203** except for the additional methoxy substituents in this compound. The methoxy substituents was located at C-3 (δ_C 138.5) due to the HMBC correlation of this protons with C-3. Therefore, **204** was unambiguously characterized as 5,7-dihydroxy-3-methoxy-6-methyl-3′,4′-methylenedioxyflavone, which is a new compound.

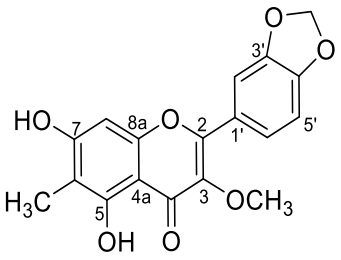

204

Table 4.20: NMR data for compounds **203** and **204**

No	**203**[ac]			**204**[bd]		
	δ_C	δ_H (*m*, *Hz*)	HMBC	δ_C	δ_H (*m*, *Hz*)	HMBC
2	146.6	-	-	155.3	-	-
3	137.6	-	-	138.5	-	-
4	177.3	-	-	176.3	-	-
4a	104.1	-	-	104.0	-	-
5	159.2	-	-	158.6	-	-
6	108.3	-	-	107.2	-	-
7	164.5	-	-	163.5	-	-
8	93.6	6.45 *s*	C- 4a, 6, 8a, 7	93.4	6.53 *s*	C- 4a, 6, 8a
8a	156.1	-	-	154.5	-	-
1′	126.7	-	-	124.2	-	-
2′	108.7	7.73 *d* (1.7)	C- 2, 4′, 6′	108.5	7.56 *d* (1.8)	C- 4′, 6′
3′	149.3	-	-	148.1	-	-
4′	150.3	-	-	149.9	-	-
5′	109.2	6.99 *d* (8.4)	C- 1′, 3′	109.1	7.13 *d* (8.4)	C- 1′, 3′
6′	123.7	7.81 *dd* (8.4, 1.7)	C- 2, 2′, 4′,	123.9	7.63 *dd* (8.4, 1.8)	C- 2, 2′, 4′
$-OCH_2O-$	103.0	6.06 *s*	C- 3′, 4′	102.3	6.16 *s*	C- 3′, 4′
CH_3-6	7.4	2.09 *s*	C- 5, 6, 7	7.8	2.00 *s*	C- 5, 6, 7
CH_3O-3	-	-	-	60.3	3.79 *s*	C- 3
HO-5	-	-	-	-	12.85 *s*	-

[a,b] Recorded at 600 and 700 MHz, respectively
[c] in CD_3OD, [d] in DMSO-d_6

4.5.3: 3,5,7-Trihydroxy-6-methoxy-3',4'-methylenedioxyflavone (205)

Compound **205** was purified as a yellow solid. The chemical formula $C_{17}H_{12}O_8$ was elucidated from its NMR and MS (*m/z* 345.0605 $[M + H]^+$ (calcd. 345.0566)) spectra. The UV (λ_{max} 368 and 258 nm) and NMR data (Table 4.21, Appendix 32) indicated **205** to be a flavonol derivative (Awouafack *et al.*, 2013; Gao *et al.*, 2010; Yang *et al.*, 2015). The NMR of **205** were similar as those observed in **203**. The only difference emanated from the fact that, the methyl group at C-6 in **203** was exchanged by a oxygenated methyl group (δ_H 3.77, δ_C 60.9) in **205**. Hence **205** was characterized as 3,5,7-trihydroxy-6-methoxy-3′,4′-methylenedioxyflavone, which is a new compound.

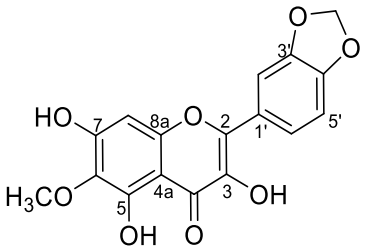

205

4.5.4: (2S,3S)-3,7-Dihydroxy-6-methoxy-3',4'-methylenedioxyflavanone (206)

Compound **206** (λ_{max} 341, 282 and 238 nm) was isolated as a off-white solid. It is an optically active compound with an optical rotation $[\alpha]_D^{21}$ = + 6.2 (*c* 0.010, MeOH). The MS profile exhibited signal of a molecular ion at *m/z* 331.0813 (calcd. 331.0773) matching the molecular formula $C_{17}H_{14}O_7$. Signals observed in the UV, ^{1}H NMR (δ_H 5.01 and 4.50, *J* = 12.0 Hz) and ^{13}C NMR (δ_C 85.9 (C-2), 74.7 (C-3) and 194.2 (C-4)) were characteristic of a flavanonol backbone (Wu *et al.*, 2003). Collision induced dissociation (CID) of **206** yielded daughter ion at *m/z* 313.0709 $[M+H-H_2O]^+$ and 285.0760 $[M+H-CH_2O_2]^+$. Furthermore, signal at *m/z* 167.0337 $[M+H-C_9H_8O_3]^+$ arising from a RDA fragmentation of ring C was also observed (Scheme 4.4). The NMR (Table

4.21, Appendix 33) showed signals for a methoxy (δ_H 3.88, δ_C 56.6) and methylenedioxy (δ_H 6.00, δ_C 102.6) substituents. Further inspection of the NMR spectrum showed the occurence of two singlets (δ_H 7.29 and 6.41) and ABX spin system (δ_H 7.08 (J = 1.7 Hz), 6.87 (J = 7.9 Hz) and 7.03 (J = 1.7, 7.9 Hz)).

An HMBC connectivity observed between the protons at δ_H 7.08 (J = 1.7 Hz) and 7.03 (J = 1.7, 7.9 Hz) of the ABX system with a carbon at δ_C 85.9 (C-2) allowed the assignment of the ABX system to ring B. This also allowed the assignment of the aromatic signals at δ_H 7.29 and 6.41 to ring A. The deshieled proton at δ_H 7.29 was ascribe to H-5 due to the *peri* effect of the carbonyl.

The $ESIMS^2$ profile showed a fragment ion peak at *m/z* 209.0445 $[(M+H) – ring B]^+$ indicated the existence of a hydroxy and methoxy substituents in ring A, thus, placing the methylenedioxy substituent in ring B (Scheme 4.4). The HMBC correlation that was observed between H-2′ and H-5′ with the oxygenated carbons at δ_C 149.2 and 149.5 which also had HMBC correlations with the methylenedioxy protons (δ_H 6.00) placed the methylenedioxy substituents at C-3′/C-4′. NOESY correlation between signals at δ_H 7.29 (H-5) and 3.88 (OCH_3) showing the proximity of these protons in space allowed the placement of the methoxy substituent at C-6.

What is remaining to be determined now is the absolute configuration around the stereogenic center as there are four possible stereoisomers; (2*R*,3*S*), (2*S*,3*R*), (2*R*,3*R*) and (2*S*,3*S*). These set was reduced to a pair of *cis* or *trans* enantiomers using the coupling constant of the two vicinal oxymethine protons. The coupling constant observed between these protons in this compound is large (J = 12.0 Hz) indicating their *trans* axial relationship ((2*R*,3*R*) and (2*S*,3*S*)) (Yin *et al.*, 2010). To resolve this, the CD spectrum (Figure 4.4) of this compound was generated and the results showed **206** exhibited a negative cotton effect at 312 nm suggesting 2*S*,3*S* arrangement (Slade *et*

al., 2005). Therefore **206** was characterized as (2*S*,3*S*)-3,7-dihydroxy-6-methoxy-3′,4′-methylenedioxyflavanone, which is a new compound.

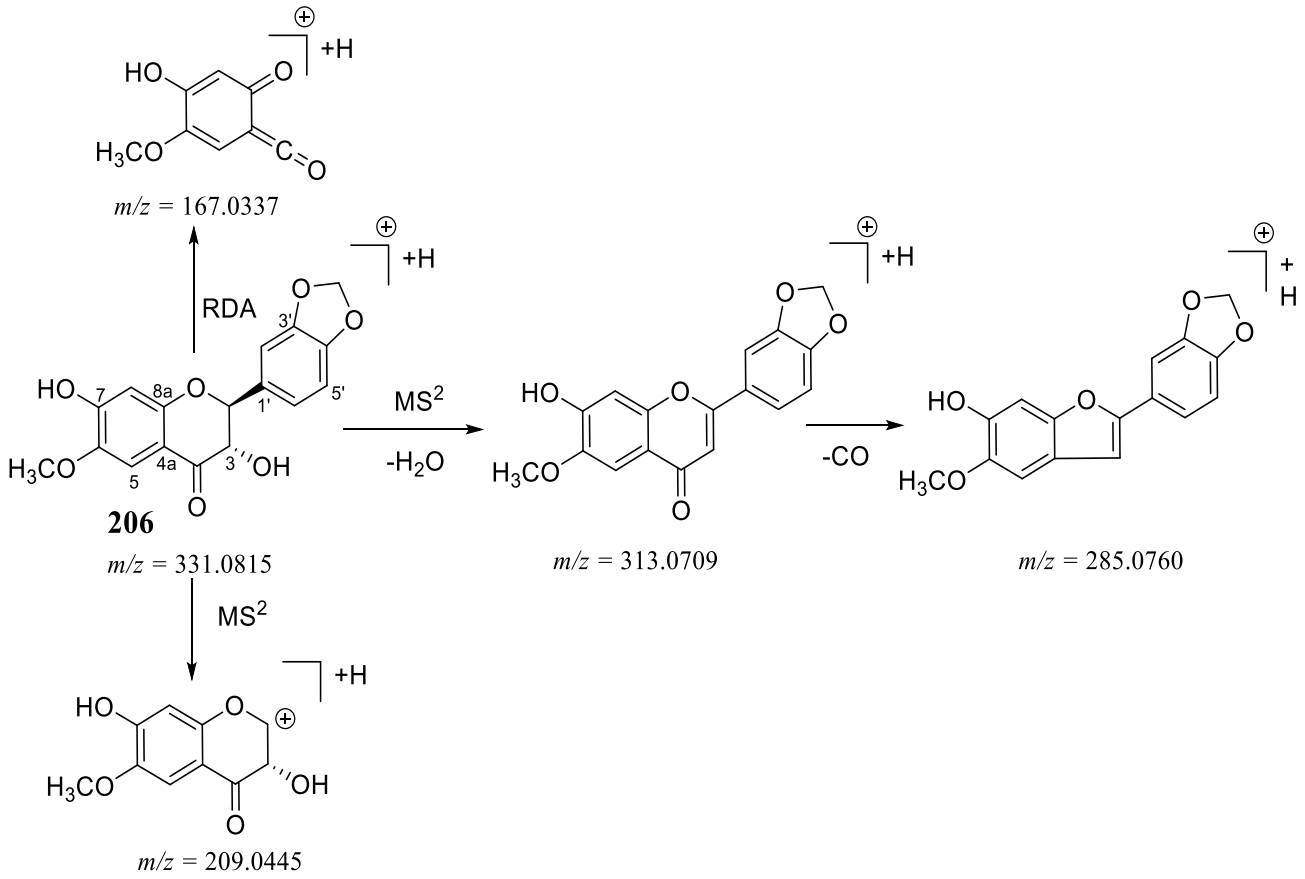

Scheme 4.4: Different fragmentation pathway of compound **206**

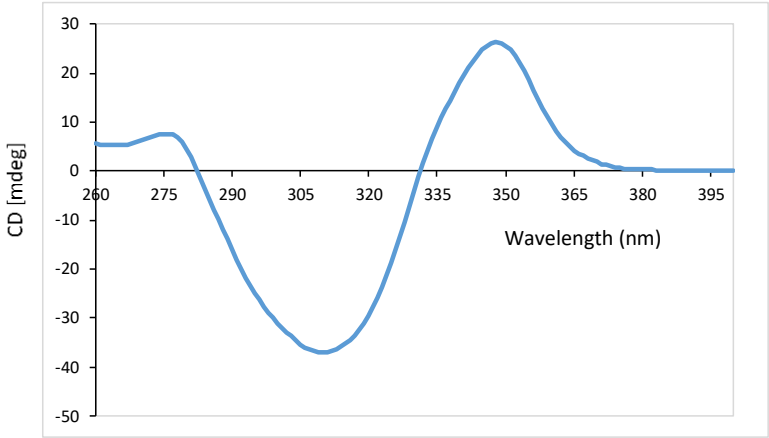

Figure 4.4: CD spectrum of compound **206**

Table 4.21: NMR data for compounds **205** and **206** in CD_3OD

No	**205**[a]			**206**[a]		
	δ_C	δ_H (*m*, *Hz*)	HMBC	δ_C	δ_H (*m*, *Hz*)	HMBC
2	146.8	-	-	85.9	5.01 *d* (12.0)	C- 1′, 2′, 3, 4, 6′
3	137.3	-	-	74.7	4.50 *d* (12.0)	C- 1′, 2, 4
4	177.5	-	-	194.2	-	-
4a	104.3	-	-	111.9	-	-
5	152.9	-	-	108.1	7.29 *s*	C- 4, 4a, 6, 7, 8a
6	132.9	-	-	145.8	-	-
7	159.6	-	-	159.8	-	-
8	95.3	6.36 *s*	C- 4, 4a, 6, 8a	104.6	6.41 *s*	C- 4a, 6, 7, 8a
8a	153.9	-	-	157.5	-	-
1′	126.6	-	-	132.7	-	-
2′	108.8	7.62 *d* (1.7)	C- 2, 4′, 6′	108.9	7.08 *d* (1.7)	C- 2, 4′, 6′
3′	149.3	-	-	149.2	-	-
4′	150.4	-	-	149.5	-	-
5′	109.2	6.87 *d* (8.4)	C- 1′, 3′	108.9	6.87 *d* (7.9)	C- 1′, 3′
6′	123.8	7.70 *dd* (8.4, 1.7)	C- 2, 2′, 4′,	123.1	7.03 *dd* (7.9, 1.7)	C- 2, 4′, 5′
$-OCH_2O-$	103.0	5.95 *s*	C- 3′, 4′	102.6	6.00 *s*	C- 3′, 4′
CH_3O-6	60.9	3.77 *s*	C- 6	56.6	3.88 *s*	C- 6

[a]Recorded at 600 MHz

4.5.5: 4′,5,7-Trihydroxy-3,3′,8-trimethoxy-6-methylflavone (207)

Compound was obtained as a yellow solid. The presence of flavonol backbone in this compound (**207)** was established based on IR (λ_{max} 341, 282 and 238 nm), UV (352 and 274 nm) and NMR spectra (Awouafack *et al.*, 2013; Gao *et al.*, 2010; Yang *et al.*, 2015). The chemical formula of $C_{19}H_{18}O_8$ was inferred from its HRESIMS (*m/z* 375.1073 (calcd. 375.1035)) indicating twelve unsaturation sites. The HRESIMS^2 profile, displayed signal at *m/z* 360.0840 $[(M+H) - CH_3]^+$, showing the occurrence of a methyl substituent.

The ^{1}H NMR data (Table 4.22, Appendix 34) of **207** revealed signals of one methyl (δ_H 2.21) and three methoxy (δ_H 3.72, 3.80 and 3.85) substituents alongside signals of an ABX spin system. An HMBC correlation observed between two of the ABX protons at δ_H 7.68 (*J* = 2.1 Hz) and 7.61 (*J* = 2.1, 8.4 Hz) with C-2 (δ_C 157.6) resulted in the assignment of this spin system to ring B. As a consequence, the ABX protons resonating at δ_H 7.68 (*J* = 2.1 Hz), 6.87 (*J* = 8.4 Hz) and 7.61 (*J* = 2.1, 8.4 Hz) were assigned to H-2′, H-5′ and H-6′, respectively. Since there are no other aromatic protons ring A is fully substituted.

One of the methoxy substituents (δ_H 3.72) was fixed at C-3 due to its ^3J correlation with C-3 (δ_C 139.2). The NOESY experiment displayed a relationship between a signals at δ_H 7.68 (H-2′) and 3.85 (3′-OCH_3) placing the second methoxy substituent at C-3′. Thus, the other two substituents, a methyl and the third methoxy, are placed in ring A. The methyl and the third methoxy substituents were placed at C-6 and C-8, respectively, by comparing their NMR data with a compound with similar substitution pattern for ring A. This compound was, therefore, characterized as 4′,5,7-trihydroxy-3,3′,8-trimethoxy-6-methylflavone which is a new compound.

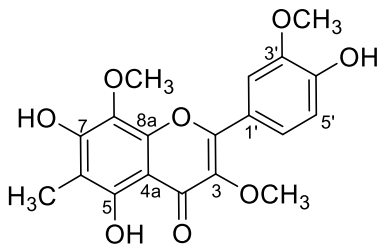

207

4.5.6: (2R) 7-Hydroxy- 2',8-dimethoxyflavanone (208)

Compound **208** (UV λ_{max} 306 and 240 nm) was isolated as a yellow solid. It is an optically active compound with an optical rotation of $[\alpha]_D^{21}$ = −14.4 (*c* 0.010, MeOH). The HRESIMS (*m/z* 301.1071 (calcd. 301.1031)) consistent with a molecular formula of $C_{17}H_{16}O_5$ accounting for ten rings double bond equivalents. The IR (3385, 2987, 2901, 1650, 1066 and 669 cm^{-1}), UV and NMR (δ_H 5.58 (H-2), 3.15 (H-3ax) and 3.30 (H-3eq)); δ_C 66.9 (C-2), 47.6 (C-3), and 204.9 (C-4)) data indicated that **208** is a flavanone (Cui *et al.*, 2008). The NMR data (Table 4.22, Appendix 35) displayed signals for two methoxy substituents (δ_H 3.86 and 3.85; δ_C 60.8 and 55.7). In addition to these, the ^{1}H NMR displayed resonances for two sets of mutually coupling protons with AB spin system (δ_H 7.58 and 6.44, *J* = 8.9 Hz) and four protons (δ_H 6.95 (*J* = 7.6 Hz), 7.26 (*J* = 1.8, 7.6 Hz), 6.99 (*J* = 1.8, 7.6 Hz) and 7.52 (*J* = 1.8, 7.6 Hz)). The deshielded proton (δ_H 7.58) of the AB spin system was assigned to H-5 due to the *peri* effect of the carbonyl as well as its HMBC correlation with C-4. This, therefore, led to the placement of the four aromatic protons to ring B. Correlation observed in the HMBC between H-2 (δ_H 5.58) and δ_C 157.2 which in turn correlated with the methoxy protons at δ_H 3.85 (δ_C 55.7) placed this methoxy substituent at C-2′. The ^{13}C NMR resonance for the other methoxy substituent, δ_C 60.8, implied that this group is di *ortho*-substituted, this is consistent with placing it at C-3. This is further confirmed from the MS^2 (Scheme 4.5) of the parent ion produced at *m/z* 167.0337 (**208a**) and 193.0495 (**208b**).

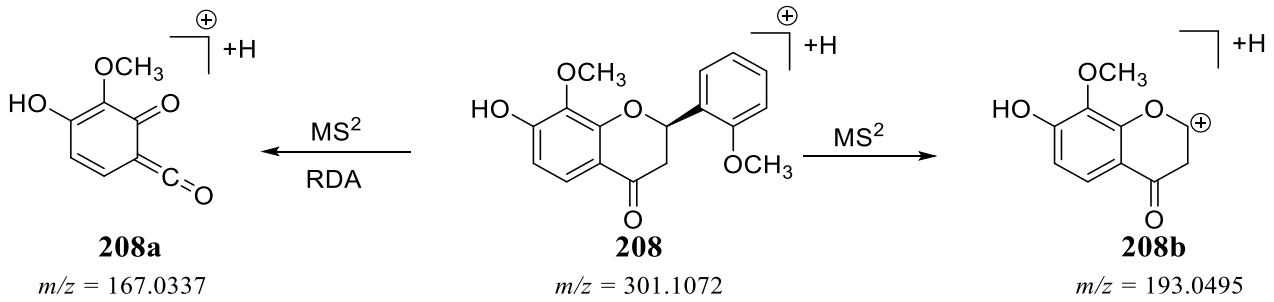

Scheme 4.5: Different fragmentation pathway of compound **208**

The CD spectrum (Figure 4.5) of **208** displayed a positive and negative cotton effect at 288 (π→π∗) and 324 nm (n→π∗), respectively, indicating an *R* configuration at C-2 (Slade *et al.*, 2005). Thus, **208** was elucidated as (2*R*) 7-hydroxy-2′,8-dimethoxyflavanone which is a new compound.

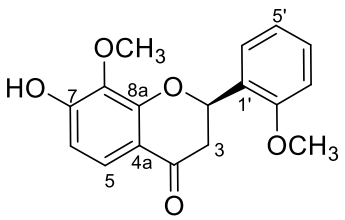

208

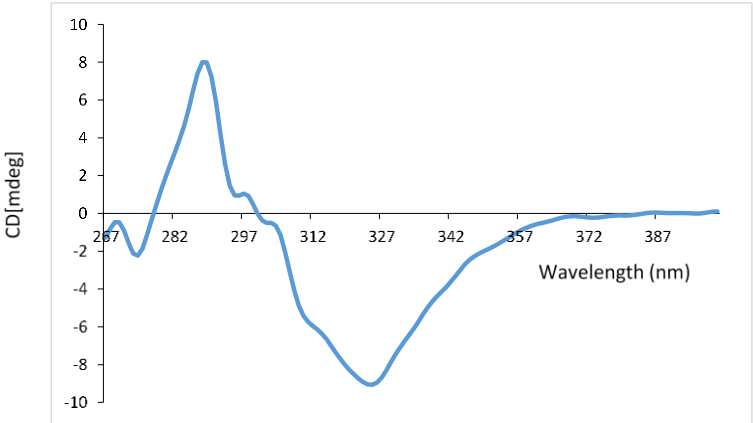

Figure 4.5: CD spectrum of compound **208**

Table 4.22: NMR data for compounds **207** and **208** in CD_3OD

No	**207**[a]			**208**[a]		
	δ_C	δ_H (*m*, *Hz*)	HMBC	δ_C	δ_H (*m*, *Hz*)	HMBC
2	157.6	-	-	66.9	5.58 *dd* (9.0, 3.7)	C- 1′, 2′, 3, 4, 6′
3	139.2	-	-	47.6	3.30 *dd* (14.9, 3.7)	C- 1′, 2, 4
	-	-	-		3.15 *dd* (14.9, 9.0)	C- 1′, 2, 4
4	180.6	-	-	204.9	-	-
4a	105.9	-	-	115.2	-	-
5	151.5	-	-	128.5	7.58 *d* (8.9)	C- 4, 4a, 7
6	103.7	-	-	108.8	6.44 *d* (8.9)	C- 4a, 8, 8a
7	156.7	-	-	158.8	-	-
8	132.3	-	-	136.0	-	-
8a	151.0	-	-	158.4	-	-
1′	123.3	-	-	133.5	-	-
2′	112.7	7.68 *d* (2.1)	C- 2, 4′, 6′	157.2	-	-
3′	149.0	-	-	111.3	6.95 *d* (7.6)	C- 1′, 2′, 5′
4′	151.1	-	-	129.4	7.26 *td* (7.6, 1.8)	C- 2′, 3′, 6′
5′	116.6	6.87 *d* (8.4)	C- 1′, 3′, 4′	121.7	6.99 *td* (7.6, 1.8)	C- 1′, 3′
6′	123.6	7.61 *dd* (8.4, 2.1)	C- 2, 2′, 4′	127.0	7.52 *dd* (7.6, 1.8)	C- 2, 2′, 4′
CH_3O-3	60.6	3.72 *s*	C- 3	-	-	-
CH_3O-8	61.0	3.80 *s*	C- 8	60.8	3.86 *s*	C- 8
CH_3O-2′	-	-	-	55.7	3.85 *s*	C- 2′
CH_3O-3′	56.5	3.85 *s*	C- 3′	-	-	-
CH_3-6	8.0	2.21 *s*	C- 6, 5, 7	-	-	-

[a] Recorded at 700 MHz

4.5.7: Dihydrooroxylin A (209)

Compound **209** was purified as yellow solid. The HRESIMS of this compound (**209**, *m/z* 287.0914 (calcd. 287.0875)) indicated that this molecule had a chemical formula of $C_{16}H_{14}O_5$. The UV (λ_{max} 300 and 236 nm) and NMR data (Table 4.23, Appendix 36) are consistent with a flavanone skeleton (Cui *et al.*, 2008).

The NMR displayed a signal for one di *ortho*-substituted methoxy group (δ_H 3.80; δ_C 60.9). The ^{1}H NMR displayed signals for five mutually coupling aromatic protons (δ_H 7.51, 7.43 and 7.38) which were allocated to an unsubstituted ring B and a singlet proton (δ_H 5.98) assigned to ring A. The methoxy substituent was assigned to C-6 by comparing the NMR data with flavonoids having similar substitution pattern for ring A (Tran *et al.*, 2012). Based on this data, this compound was named as dihydrooroxylin A. Dihydrooroxylin A has been isolated from *Sunipia scariosa* (Jiazhu *et al.*, 2014).

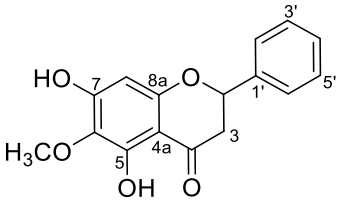

209

4.5.8: 7-Hydroxy-6-methoxyflavanone (210)

Compound **210** was purified as a yellow solid. Its MS (*m/z* 271.0965 $[M + H]^+$ (calcd. 271.0926)) profile was consistent with the chemical formula of $C_{16}H_{14}O_4$, ten unsaturation sites. The UV (λ_{max} 280 and 240 nm) and NMR data (Table 4.23, Appendix 37) are consistent with a flavanone framework (Cui *et al.*, 2008).

The substitution pattern of ring B of **210** and **209** were the same (**Table 4.23**). In ring A, this molecule has two singlet aromatic protons resonating at δ_H 7.27 and 6.40. These aromatic protons were assigned to H-5 and H-8, respectively. This compound just as in **209** has a methoxy group (δ_H 3.86; δ_C 56.5). A NOESY correlation between the methoxy protons and H-5 allowed the placement of the methoxy substituent at C-6. This was further confirmed from the HMBC correlation observed between H-5 and C-6. Hence, based on this data and comparison with literature, **210** was identified as 7-hydroxy-6-methoxyflavanone (Yoon *et al.*, 2004). 7-Hydroxy-6-methoxyflavanone (**210**) is known compound reported from *Spatholobus suberectus* (Yoon *et al.*, 2004).

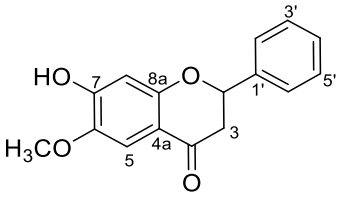

210

Table 4.23: NMR data for compounds **209** and **210** in CD_3OD

No	**209**[a]			**210**[a]		
	δ_C	δ_H (*m*, *Hz*)	HMBC	δ_C	δ_H (*m*, *Hz*)	HMBC
2	80.5	5.45 *dd* (12.8, 3.3)	C- 1′, 4, 2′/6′	81.1	5.47 *dd* (13.1, 3.1)	C- 1′, 3, 2′/6′, 4
3	44.2	3.09 *dd* (17.1, 12.8)	C- 1′, 2, 4	45.0	3.01 *dd* (16.9, 13.1)	C- 1′, 2, 4
		2.78 *dd* (17.1, 3.3)	C- 4, 4a		2.76 *dd* (16.9, 3.1)	-
4	197.4	-	-	192.7	-	-
4a	102.8	-	-	112.5	-	-
5	156.5	-	-	107.6	7.27 *s*	C- 4, 4a, 6, 8a
6	131.0	-	-	146.2	-	-
7	163.4	-	-	161.9	-	-
8	97.0	5.98 *s*	C- 4(W), 4a, 6, 7, 8a	104.8	6.40 *s*	C- 4a, 6, 8a,
8a	160.1	-	-	160.7	-	-
1′	140.6	-	-	140.9	-	-
2′/6′	127.3	7.51 *m*	C- 2, 2′/6′, 3′/5′	127.3	7.52 *m*	C- 2, 2′/6′, 3′/5′
3′/5′	129.7	7.43 *m*	C- 1′, 3′/5′	129.6	7.43 *m*	C- 1′, 3′/5′
4′	129.6	7.38 *m*	C- 2′/6′	129.4	7.38 *m*	C- 2′/6′
CH_3O-6	60.9	3.80 *s*	C- 6	56.5	3.86 *s*	C- 6

[a] Recorded at 600 MHz

4.5.9: 4',5,7-Trihydroxy-6-methylflavanone (211)

Compound **211** (UV λ_{max} 298 and 238 nm) was purified as a yellow solid. The MS profile (**211**, *m*/*z* 287.0914 $[M + H]^+$ (calcd. 287.0875)) corroborated the chemical formula of $C_{16}H_{14}O_5$. The UV and NMR data (Table 4.24, Appendix 38) indicated a flavanone scaffold (Cui *et al.*, 2008).

The NMR experiment displayed signals for a methyl substituent (δ_H 1.97; δ_C 7.0). In addition, the ^{1}H NMR displayed signals of an AA′BB′ spin system (δ_H 7.33 and 6.83 (2H, *J* = 8.6 Hz) assigned to a *para*-hydroxy substituted ring B and an aromatic singlet (δ_H 5.95) assigned to a trisubstituted ring A. The methyl substituent was placed to C-6 by comparing the NMR data with similar compound having similar substitution pattern for ring A (Jin-hai *et al.*, 2002). Using this data and comparison with literature, **211** was identified as 4′,5,7-trihydroxy-6-methylflavanone (Nobakht *et al.*, 2014). A compound isolated from *Corymbia torelliana* (Nobakht *et al.*, 2014).

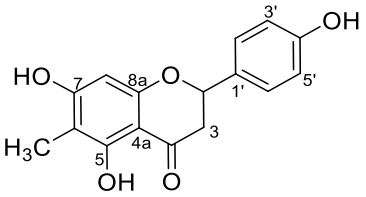

211

4.5.10: Quercetin-4'-methyl ether (212)

Compound **212** was purified as a yellow solid. The MS ($[M + H]^+$ at *m*/*z* 317.0657 (calcd. 317.0617)) profile was in agreement with the chemical formula $C_{16}H_{12}O_7$, implying eleven ring double bonds equivalents. The UV (absorption bands at λ_{max} 368 (cinnamoyl system) and 256 (benzoyl system) nm) and NMR (δ_H 12.45 (HO-5), δ_C 148.8 (C-2), 135.8 (C-3) and 175.7 (C-4)) data are characteristic of a 5-hydroxyflavonol skeleton (Awouafack *et al.*, 2013; Gao *et al.*, 2010; Yang *et al.*, 2015).

The NMR (Table 4.24, Appendix 39) exhibited signals for a methoxy group (δ_H 3.84; δ_C 55.8). In addition, the ^{1}H NMR exhibited signals of an ABX spin system (δ_H 7.76 (J = 2.1 Hz), 6.94 (J = 8.2 Hz) and 7.68 (J = 2.1, 8.2 Hz)) ascribed to a *di*- substituted ring B and a AX spin system (δ_H 6.17 and 6.44, J = 2.1 Hz) assigned to ring A. The assignment of the ABX system to ring B was further confirmed using the HMBC correlation that was observed between the ABX protons at δ_H 7.76 (J = 2.1 Hz) and 7.68 (J = 2.1, 8.5 Hz) with a carbon at δ_C 148.8 (C-2). This allowed the assignment of the ABX at δ_H 7.76, 6.94 and 7.68 to H-2′, H-5′ and H-6′, respectively.

The location of the methoxy substituent at C-4′ was established with the aid of NOESY correlation observed between the oxygenated methyl signal (δ_H 3.84) with H-5′ (δ_H 6.94). Based on these evidence and by comparison with literature (Ezenyi *et al.*, 2014), **212** was identified as quercetin-4′-methyl ether, a compound reported from *Chromolaena odorata* (Ezenyi *et al.*, 2014).

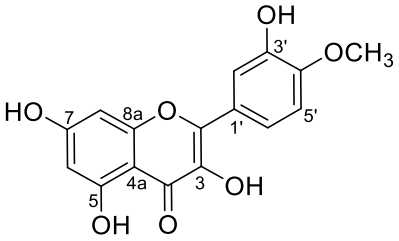

212

Table 4.24: NMR data for compounds **211** and **212**

No	**211**[ac]			**212**[bd]		
	δ_C	δ_H (*m*, *Hz*)	HMBC	δ_C	δ_H (*m*, *Hz*)	HMBC
2	80.4	5.33 *dd* (12.9, 3.0)	-	148.8	-	-
3	44.2	3.11 *dd* (17.1, 12.9)	C- 1′, 2, 4	135.8	-	-
		2.71 *dd* (17.1, 3.0)	C- 4			-
4	197.7	-	-	175.7	-	-
4a	103.0	-	-	102.7	-	-
5	162.6	-	-	160.6	-	-
6	105.4	-	-	98.4	6.17 *d* (2.1)	C- 4a, 5, 7, 8
7	166.7	-	-	164.9	-	-
8	95.4	5.95 *s*	C- 4a, 7, 6, 8a	93.7	6.44 *d* (2.1)	C- 4a, 6, 7, 8a
8a	162.4	-	-	156.2	-	-
1′	131.3	-	-	122.0	-	-
2′	129.0	7.33 *d* (8.6)	C- 2, 4′, 6′	111.7	7.76 *d* (2.1)	C- 2, 3′, 6′
3′	116.3	6.83 *d* (8.6)	C- 1′, 5′	146.4	-	-
4′	159.0	-	-	147.4	-	-
5′	116.3	6.83 *d* (8.6)	C- 1′, 3′	115.5	6.94 *d* (8.5)	C- 1′, 2(W), 4′
6′	129.0	7.33 *d* (8.6)	C- 2, 4′, 2′	121.6	7.68 *dd* (8.5, 2.1)	C- 2′, 2
CH_3-6	7.0	1.97 *s*	C- 5, 6, 7	-	-	-
CH_3O-4′	-	-	-	55.8	3.84 *s*	C- 4′
HO-5	-	-	-	-	12.45 *s*	-

[a,b] Recorded at 700 and 600 MHz, respectively
[c] in CD_3OD, [d] in DMSO-d_6

4.5.11: 3,3′-Di-O-methyl quercetin (213)

Compound **213** was purified as a yellow solid. Analysis of its HRESIMS exhibited a pseudo molecular ion peak at *m/z* 331.0812 $[M + H]^+$ (calcd. 331.0773) consistent with $C_{17}H_{14}O_7$. The UV (357 and 255 nm) and NMR (Table 4.25, Appendix 40) data indicated a flavonol skeleton (Awouafack *et al.*, 2013; Gao *et al.*, 2010; Yang *et al.*, 2015).

The NMR displayed the existence of two methoxy groups (δ_H/δ_C 3.82/60.9; 3.96/56.5) alongside signals for an ABX and AX spin systems (Table 4.25). The ABX system was assigned to ring B based on the HMBC correlations of the ABX protons at δ_H 7.74 (*J* = 2.1 Hz) and 7.66 (*J* = 2.1, 8.5 Hz) with C-2 (δ_C 157.8). As a result, the AX protons, δ_H 6.23 and 6.44 (*J* = 2.1 Hz, were assigned H-6 and H-8, respectively, to ring A.

An HMBC correlation observed between one of the methoxy substituents resonating at δ_H 3.82 with C-3 (δ_C 139.6) which allowed the placement of this substituent at C-3. A NOESY correlation observed between H-2′ (δ_H 7.74, (*J* = 2.1 Hz)) and the second methoxy substituent (δ_H 3.96) placed this group at C-3′. Hence, compound **213** was elucidated as 3,3′-di-*O*-methyl quercetin, previously isolated from *Anaxagorea luzonensis* (Pabuprapap *et al.*, 2019).

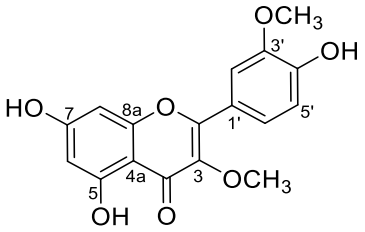

213

4.5.12: Kaempferol 3-methyl ether (214)

Compound **214** was purified as a yellow solid. The HRESIMS of compound **214** exhibited a molecular ion peak at *m/z* 301.0706 $[M + H]^+$ (calcd. 301.0667) consistent with $C_{16}H_{12}O_6$. The UV (λ_{max} 351 and 266 nm) and NMR data indicated a flavonol core (Awouafack *et al.*, 2013; Gao *et al.*, 2010; Yang *et al.*, 2015).

The NMR (Table 4.25, Appendix 41) showed signals for a methoxy group (δ_H 3.80; δ_C 60.6). Further, signals for an AA′BB′ spin system (8.01 (H-2′/6′) and 6.95 (H-3′/5′, J = 8.8 Hz)) and an AX spin system (6.23 (H-6) and 6.43 (H-8, J = 2.1 Hz)) which were assigned to ring B and A, respectively were observed. The methoxy unit (δ_H 3.80) was assigned at C-3 based on its HMBC correlation with C-3 (δ_C 139.5). Comparison of these data with similar compound reported indicated that, **214** was a kaempferol 3-methyl ether, a compound reported from the rhizome of *Acorus gramineus* (Park *et al.*, 2011).

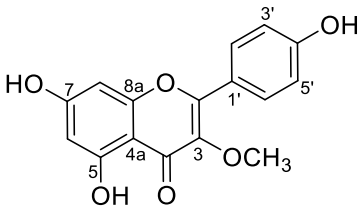

214

Table 4.25: NMR data for compounds **213** and **214** in CD_3OD

No	**213**[a]			**214**[b]		
	δ_C	δ_H (*m*, *Hz*)	HMBC	δ_C	δ_H (*m*, *Hz*)	HMBC
2	157.8	-	-	158.1	-	-
3	139.6	-	-	139.5	-	-
4	180.0	-	-	180.0	-	-
4a	105.8	-	-	105.9	-	-
5	163.1	-	-	163.1	-	-
6	99.5	6.23 *d* (2.1)	C- 4a, 5, 7, 8	99.8	6.23 *d* (2.1)	C- 4a, 8
7	166.3	-	-	166.1	-	
8	94.9	6.44 *d* (2.1)	C- 4a, 6, 7, 8a	94.8	6.43 *d* (2.1)	C- 4a, 6, 7, 8a
8a	158.5	-	-	158.5	-	-
1′	122.9	-	-	122.6	-	-
2′	112.8	7.74 *d* (2.1)	C- 2, 3′, 4′, 6′	131.4	8.01 *d* (8.8)	C- 2, 4′, 6′
3′	149.0	-	-	116.6	6.95 *d* (8.8)	C- 1′, 4′, 5′
4′	151.1	-	-	161.7	-	-
5′	116.5	6.97 *d* (8.5)	C- 1′, 3′, 4′	116.6	6.95 *d* (8.8)	C- 1′, 4′, 3′
6′	123.7	7.66 *dd* (8.5, 2.1)	C- 2, 2′, 4′	131.4	8.01 *d* (8.8)	C- 2, 4′, 2′
CH_3O-3	60.9	3.82 *s*	C- 3	60.6	3.80 *s*	-
CH_3O-3′	56.5	3.96 *s*	C- 3′	-	-	-

[a,b] Recorded at 500 and 700 MHz, respectively

4.5.13: Jaceidin (215)

Compound **215** was purified as a yellow solid. The presence of flavonol scaffold in compound **215** was evident from the UV (λ_{max} 353 and 256 nm) and NMR data (Awouafack *et al.*, 2013; Gao *et al.*, 2010; Yang *et al.*, 2015). The HRESIMS (*m/z* 361.0920 $[M + H]^+$ (calcd. 361.0879)) was consistent with a chemical formula $C_{19}H_{18}O_8$.

The NMR (Table 4.26, Appendix 42) data of **215** showed signals for three methoxy (δ_H/δ_C 3.82/60.6; 3.90/61.0 and 3.96/56.6) substituents. Further, it exhibited signals for an ABX spin system (δ_H 7.74 (*J* = 2.1 Hz), 6.96 (*J* = 8.5 Hz) and 7.66 (*J* = 2.1, 8.5 Hz)) and a sharp singlet (δ_H 6.56). An HMBC connectivity observed between the signals at δ_H 7.74 (*J* = 2.1 Hz) and 7.66 (*J* = 1.7, 8.4 Hz) of the ABX system with C-2 (δ_C 158.0) allowed the assignment of the ABX system to ring B. This also allowed the assignment of the singlet aromatic proton (δ_H 6.56) to ring A. The ABX protons at δ_H 7.74 (*J* = 2.1 Hz), 6.96 (*J* = 8.5 Hz) and 7.66 (*J* = 2.1, 8.5 Hz) were assignable to H-2′, H-5′ and H-6′, respectively.

The methoxy resonating at δ_H 3.82 (δ_C 60.6) was placed at C-3 (δ_C 139.3) due to its HMBC correlation with this carbon. A NOESY correlation observed between H-2′ (δ_H 7.68) with the methoxy substituent at δ_H 3.85 placed this group at C-3′. The third methoxy substituent was placed at C-6 by comparing the NMR data with similar compound having similar substitution pattern for ring A (Huo *et al.*, 2013; Long *et al.*, 2003). Hence, based on all these data and by comparison with literature **215** was named as jaceidin (Huo *et al.*, 2013). Jaceidin (**215**) has been isolated from *Achillea millefolium* (Huo *et al.*, 2013).

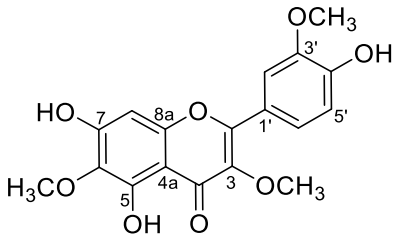

215

4.5.14: 7-Hydroxy-6-methoxyflavone (216)

Compound **216** was isolated as a yellow solid. This compound (**216)** was identified as $C_{16}H_{12}O_4$ based on HRESIMS (*m*/*z* 269.0809 (calcd. 269.0769)) and NMR spectra. The UV (λ_{max} 312 and 264 nm) and NMR (δ_H 6.85 (H-3); δ_C 165.1 (C-2), 106.8 (C-3) and 180.0 (C-4)) data led to the conclusion that this compound is a flavone (Jin *et al.*, 2007; Sathiamoorthy *et al.*, 2007).

The NMR (Table 4.26, Appendix 43) of this compound displayed signals of one methoxy (δ_H 4.00; δ_C 56.7) group. In addition, the ^{1}H NMR displayed signals for an unsubstituted aromatic ring (δ_H 8.03 and 7.58) and two singlets (δ_H 6.85 and 7.54) aromatic protons. The singlet aromatic protons, δ_H 6.85 and 7.54, were assignable to H-8 and H-5, respectively. The methoxy substituent was placed at C-6 due to its NOESY correlation with H-5. Thus, **216** was herein identified as 7-hydroxy-6-methoxyflavone, a compound which has been reported from *Dalbergia cochinchinensis* (Pathak *et al.*, 1997).

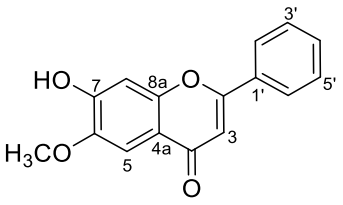

216

Table 4.26: NMR data for compounds **215** and **216** in CD_3OD

No	**215**[a]			**216**[b]		
	δ_C	δ_H (*m*, *Hz*)	HMBC	δ_C	δ_H (*m*, *Hz*)	HMBC
2	158.0	-	-	165.1	-	-
3	139.3	-	-	106.8	6.85 *s*	C- 1′, 2, 4, 4a
4	180.3	-	-	180.0	-	-
4a	106.4	-	-	118.9	-	-
5	153.7	-	-	105.0	7.54 *s*	C- 4, 6, 7
6	132.6	-	-	148.7	-	-
7	158.8	-	-	155.3	-	-
8	95.1	6.56 *s*	C- 4(w), 4a, 6, 7, 8a	104.3	7.11 *s*	C- 4a, 6, 7
8a	153.8	-	-	165.0	-	-
1′	122.9	-	-	132.8	-	-
2′	112.9	7.74 *d* (2.1)	C- 2, 4′, 6′	127.3	8.03 *m*	C- 1′, 2
3′	149.0	-	-	130.2	7.58 *m*	-
4′	151.2	-	-	130.2	7.58 *m*	-
5′	116.5	6.96 *d* (8.5)	C- 1′, 3′, 4′	130.2	7.58 *m*	-
6′	123.7	7.66 *dd* (8.5, 2.1)	C- 2, 2′, 4′	127.3	8.03 *m*	C- 1′, 2
CH_3O-3	60.6	3.82 *s*	C- 3	-	-	-
CH_3O-6	61.0	3.90 *s*	C- 6	56.7	4.00 *s*	C- 6
CH_3O-3′	56.6	3.96 *s*	C- 3′	-	-	-

[a,b] Recorded at 700 and 600 MHz, respectively

4.5.15: 6,8-Dimethylchrysin (217)

Compound **217** was purified as a yellow solid. The MS profile of this compound (**217)** showed a quasi-molecular ion peak at *m/z* 283.0965 $[M + H]^+$ (calcd. 283.0926) matching with $C_{17}H_{14}O_4$, eleven unsaturation sites. The flavone backbone was evident in this compound from its UV (λ_{max} 321 and 278 nm) and NMR data (Jin *et al.*, 2007; Sathiamoorthy *et al.*, 2007).

The NMR (Table 4.27, Appendix 44) of this compound exhibited signals of two methyl substituents (δ_H 2.15 and 2.38; δ_C 7.9 and 8.3). The ^{1}H NMR showed signals for an unsubstituted aromatic ring (δ_H 7.53, 7.60 and 8.04) which were assigned to ring B. In the absence of any other aromatic protons, ring A is fully substituted. The two methyl substituents were placed at C-6 and C-8 by comparing the NMR data with similar compound having similar substitution pattern for ring A (Nobakht *et al.*, 2014). With this and comparison of the data with literature, **217** was identified as 6,8-dimethylchrysin, a compound reported from *Matteuccia orientalis* (Basnet *et al.*, 1995).

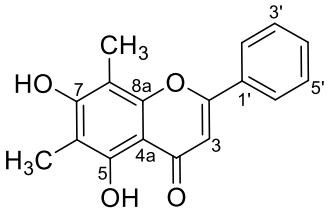

217

4.5.16: Strobochrysin (218)

Compound **218** was purified as a yellow solid. The chemical formula was elucidated as $C_{16}H_{12}O_4$ from HRESMS (*m/z* 269.0810 $[M + H]^+$ (calcd. 269.0769)) and NMR spectra. The UV (λ_{max} 320 and 272 nm) and NMR (δ_H 13.05 (HO-5) and 6.91 (H-3); δ_C 162.4 (C-2), 105.0 (C-3) and 181.3

(C-4)) data indicated a 5-hydroxyflavone core for this compound (Jin *et al.*, 2007; Sathiamoorthy *et al.*, 2007).

In the NMR (Table 4.27, Appendix 45) spectra signal of one methyl substituent (δ_H 1.97, δ_C 7.5) was observed. In addition to this, the ^{1}H NMR exhibited signals for an unsubstituted aromatic ring (δ_H 7.58, 7.59 and 8.05) and a singlet (δ_H 6.54). Correlation observed between the methyl protons (δ_H 1.97) and C-5 (δ_C 158.3) placed this substituent at C-6. Thus, all these data were superimposable with 5,7-dihydroxy-6-methylflavone**,** strobochrysin (Fang *et al.*, 1987). Strobochrysin (**218**) was reported from *Pinus morrisonicola* (Fang *et al.*, 1987).

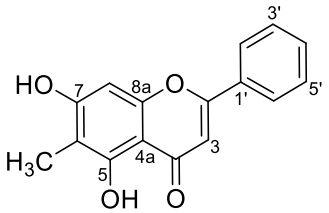

218

Table 4.27: NMR data for compounds **217** and **218**

No	**217**[ac]			**218**[bd]		
	δ_C	δ_H (*m*, *Hz*)	HMBC	δ_C	δ_H (*m*, *Hz*)	HMBC
2	165.3	-	-	162.4	-	-
3	105.6	6.78 *s*	C- 1′, 2, 4a, 4	105.0	6.91 *s*	C- 1′, 2, 4, 4a
4	184.4	-	-	181.3	-	-
4a	105.6	-	-	102.9	-	-
5	157.8	-	-	158.3	-	-
6	108.9	-	-	107.3	-	-
7	162.2	-	-	165.0	-	-
8	103.5	-	-	93.4	6.54 *s*	C- 4a, 6, 8a
8a	154.7	-	-	155.3	-	-
1′	133.0	-	-	131.0	-	-
2′/6′	130.3	7.60 *m*	C- 3′/5′	126.3	8.05 *m*	C- 2, 4′, 2′/6′
3′/5′	127.4	8.04 *m*	C- 1′	129.1	7.58 *m*	C- 1′, 3′/5′
4′	129.5	7.53 *m*	-	131.8	7.59 *m*	C- 2′/6′
CH_3-6	7.9	2.15 *s*	C- 5, 6, 7	7.5	1.97 *s*	C- 5, 6, 7
CH_3-8	8.3	2.38 *s*	C- 7, 8, 8a	-	-	-
HO-5	-	-	-	-	13.05 *s*	-

[a,b] Recorded at 700 and 600 MHz, respectively
[c] in CD_3OD, [d] in DMSO-d_6

4.5.17: 3,5,7-Trihydroxy-6-methylflavanone (219)

Compound **219** was purified as a off-white solid. The HRESIMS spectrum showed molecular ion peak at *m/z* 287.0915 $[M + H]^+$ (calcd. 287.0875) consistent with $C_{16}H_{14}O_5$. Signals observed in the ^1H (δ_H 5.06 and 4.55, J = 11.5 Hz), ^{13}C (δ_C 85.1 (C-2), 73.8 (C-3) and 198.0 (C-4)) NMR as well as the UV (λ_{max} 280 and 236 nm) were characteristic of a flavanonol backbone (Wu *et al.*, 2003).

Signals of a methyl (δ_H 1.99; δ_C 7.0) substituent was observed in the NMR (Table 4.28, Appendix 46). In addition to this, the ^1H NMR exhibited signals for an unsubstituted aromatic ring B (δ_H 7.42, 7.43 and 7.55) and a singlet (δ_H 5.96) assigned to ring A. An HMBC correlation between the methyl protons (δ_H 1.99) and C-5 (δ_C 162.4) placed this substituent at C-6. The magnitude of the coupling constant ($^3J_{2,3}$ = 11.5 Hz) between H-2 and H-3 indicated their *trans*-axial relationship with a dihedral angle of 180 degrees. Based on all data, compound **219** was named as 3,5,7-trihydroxy-6-methylflavanone, a compound isolated from *Pinus morrisonicola* (Fang *et al.*, 1987).

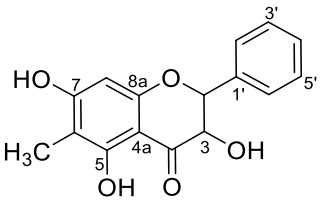

219

4.5.18: 3,5,7-Trihydroxy-6-methoxyflavanone (220)

Compound **220** was ipurified as a off-white solid. The MS profile showed a quasi-molecular ion peak at *m/z* 303.0864 $[M + H]^+$, consistent with $C_{16}H_{14}O_6$, ten degrees of unsaturation. A flavanonol core in this compound was evident based on its ^1H NMR (δ_H 4.94 (H-2) and 4.43 (H-

3, J = 11.5 Hz)), ^{13}C NMR (δ_C 85.2 (C-2), 73.8 (C-3) and 198.1 (C-4)) and UV (λ_{max} 296 and 236 nm) spectra (Wu *et al.*, 2003).

The NMR (Table 4.28, Appendix 47) exhibited signals of an oxygenated methyl (δ_H 3.69; δ_C 60.9) substituent. Further, signals for an unsubstituted aromatic ring B (δ_H 7.29, 7.32 and 7.43) and a sharp singlet (δ_H 5.83) assignable to ring A were observed. The singlet aromatic proton at δ_H 5.83 was placed at C-8 position by comparison with spectroscopic data of similar ring A compound reported in the literature (Muhammad *et al.*, 2012). The large coupling constant ($^3J_{2,3}$ = 11.5 Hz) between H-2 and H-3 indicated these two protons were *trans* oriented. Hence **220** was unambiguously identified as 3,5,7-trihydroxy-6-methoxyflavanone (Asakawa, 1971).

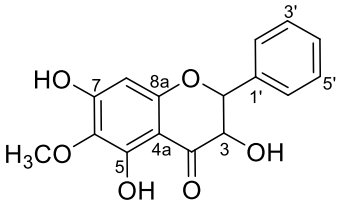

220

Table 4.28: NMR data for compounds **219** and **220** in CD_3OD

No	**219**[a]			**220**[b]		
	δ_C	δ_H (*m*, *Hz*)	HMBC	δ_C	δ_H (*m*, *Hz*)	HMBC
2	85.1	5.06 *d* (11.5)	C- 1′, 3, 2′/6′, 4	85.2	4.94 *d* (11.5)	C- 1′, 3, 2′/6′, 4
3	73.8	4.55 *d* (11.5)	C- 1′, 2, 4	73.8	4.43 *d* (11.5)	C- 1′, 2, 4
4	198.0	-	-	198.1	-	-
4a	101.4	-	-	101.3	-	-
5	162.4	-	-	156.3	-	-
6	105.9	-	-	131.4	-	-
7	167.4	-	-	163.6	-	-
8	95.6	5.96 *s*	C- 4, 4a, 6, 7, 8a	97.2	5.83 *s*	C- 4, 4a, 6, 7, 8a
8a	161.9	-	-	159.9	-	-
1′	138.7	-	-	138.7	-	-
2′/6′	128.9	7.55 *m*	C- 2, 3′/5′	128.9	7.43 *m*	C- 2, 3′/5′
3′/5′	129.4	7.43 *m*	C- 1′, 3′/5′	129.4	7.32 *m*	C- 1′, 3′/5′
4′	129.8	7.42 *m*	C- 2′/6′	129.8	7.29 *m*	C- 2′/6′
CH_3-6	7.0	1.99 *s*	C- 5, 6, 7	-	-	-
CH_3O-6	-	-	-	60.9	3.69 *s*	C- 6

[a,b] Recorded at 600 and 700 MHz, respectively

4.5.19: 3,7-Dihydroxy-6-methoxyflavanone (221)

Compound **221** was purified as a off-white solid. Its chemical formula was elucidated as $C_{16}H_{14}O_5$ as evidence from NMR and HRESIMS (*m*/*z* 287.0915 $[M + H]^+$ (calcd. 287.0875)). The compound showed signals in ^1H (δ_H 5.14 (H-2) and 4.58 (H-3, J = 12.0 Hz); ^{13}C (δ_C 85.5 (C-2), 74.4 (C-3) and 193.2 (C-4)) NMR and UV (λ_{max} 298 and 232 nm) characteristic of a flavanonol scaffold (Wu *et al.*, 2003).

In the NMR (Table 4.29, Appendix 48) spectra signals of a methoxy (δ_H 3.91; δ_C 56.9) substituent was observed. Further inspection of the mass spectrum profile indicated the occurrence of daughter ion peaks at *m*/*z* 241.0859 $[M +H- CH_2O]^+$ indicated the existence of a methoxy group in this compound. An unsubstituted aromatic ring B (δ_H 7.43, 7.46 and 7.63) and two singlets (δ_H 7.29 and 6.50) assigned to ring A were depicted in the NMR. The downfield shifted singlet (δ_H 7.29) was placed at C-5 due to the *peri* effect of the carbonyl group.

An NOESY correlation depicted between the methoxy substituent (δ_H 3.91) with the aromatic singlet (δ_H 7.29) allowed the placement of the methoxy group at C-6. Signal at *m*/*z* 167.0340 $[M +H- C_8H_8O]^+$arising from RDA fragmentation of ring C were observed which further confirmed the placement of the methoxy in ring A. Likewise, a large coupling constant ($^3J_{2,3}$ = 12.0 Hz) indicated that the arrangement of H-2 and H-3 is *trans*. Thus, compound **221** was identified as 3,7-dihydroxy-6-methoxyflavanone, a compound previously reported from *Brazilian* red propolis (Li *et al.*, 2008).

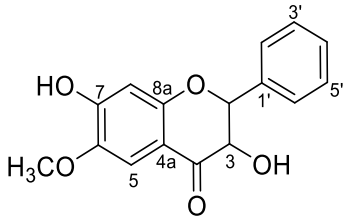

221

Table 4.29: NMR data for compound **221** in $(CD_3)_2CO$

No	**221**[a]		
	δ_C	δ_H (*m*, *Hz*)	HMBC
2	85.5	5.14 *d* (12.0)	C- 2, 4′, 2′/6′
3	74.4	4.58 *d* (12.0)	C- 2, 4′, 2′/6′
4	193.2	-	-
4a	112.0	-	-
5	108.3	7.29 *s*	C- 4, 4a, 6, 7, 8a
6	145.0	-	-
7	159.3	-	-
8	104.6	6.50 *s*	C- 4(w), 4a, 6, 7, 8a
8a	156.1	-	-
1′	138.9	-	-
2′/6′	129.3	7.46 *m*	C- 1′, 3′/5′
3′/5′	129.1	7.63 *m*	C- 2, 2′/6′
4′	129.7	7.43 *m*	C- 3′/5′
CH_3O-6	56.9	3.91 *s*	C- 6

[a] Recorded at 700 MHz

4.5.20: Para-hydroxybenzoic acid (222)

Compound **222** (UV λ_{max} 264) was purified as a white solid. The HRESIMS showed a molecular ion peak at *m*/*z* 139.0387 (calcd. 139.0350), representing $C_7H_7O_3$, five degree of unsaturation.

The ^{13}C NMR showed a signal for a carboxyl (δ_C 168.0) group. The ^{1}H NMR data (Table 4.30, Appendix 49) displayed two aromatic signals of a *para*-disubstituted benzene with resonance at δ_H 7.73 (H-2/6) and 6.75 (H-3/56, 2H, J = 8.6 Hz). Using these data and comparison with literature enabled the identification of **222** as *para*-hydroxybenzoic acid, a compound reported from *Celosia argentea* (Perveen *et al.*, 2014).

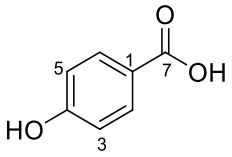

222

Table 4.30: NMR data for compound **222** in DMSO-d_6

No	**222**[a]		
	δ_C	δ_H (*m*, *Hz*)	HMBC
1	124.7	-	-
2/6	131.1	7.73 *d* (8.6)	C- 2/6, 3/5, 4, 7
3/5	114.6	6.75 *d* (8.6)	C- 1, 3/5, 4, 7(W)
4	160.0	-	-
7	168.0	-	-

[a] Recorded at 700 MHz

4.5.21: Indole-3-carboxaldehyde (223)

Compound **223** (Table 4.31, Appendix 50) was purified as a white solid. The MS (*m*/*z* 146.0602 $[M + H]^+$ (calcd. 146.0561)) was consistent the chemical formula C_9H_7ON, seven unsaturation sites. The ^{1}H NMR data displayed a signal of an aldehyde group at δ_H 9.93 with its ^{13}C NMR signal at δ_C 185.5 based on HSQC spectrum.

The ^{1}H NMR displayed resonances for four mutually coupling aromatic protons (Table 4.31) assigned to a 1,2-disubstituted benzene ring. In addition to this, the ^{1}H NMR indicated the existence of a singlet aromatic proton (δ_H 8.28). This deshielded aromatic proton was assigned to a proton attached to a nitrogen as in pyrrole. The foregoing, is consistent with an indole skeleton for this compound, where a benzene and a pyrrole had fused. This will therefore, place the aldehyde substituent in the pyrrole ring at C-3. The placement of this group at C-3 was confirmed using HMBC correlations of the aldehydic proton with C-3 which in turn correlated with H-2.

Based on this and comparison of the data with literature, **223** was identified as indole-3-carboxaldehyde (El-Sawy *et al.*, 2018). Indole-3-carboxaldehyde (**223**) is uncommon compound found in plant kingdom which is synthesized by microorganism (*Lactobacillus genus*) (Zhang and Davies, 2016).

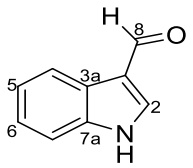

223

Table 4.31: NMR data for compound **223** in DMSO-d_6

No	**223**[a]		
	δ_C	δ_H (*m*, *Hz*)	HMBC
2	139.0	8.28 *s*	C- 3, 3a, 7a, 8
3	118.6	-	-
3a	124.6	-	-
4	121.3	8.09 *d* (7.7)	C- 6, 7a
5	122.6	7.21 *dd* (7.7, 7.4)	C- 3a, 7
6	123.9	7.25 *dd* (7.7, 7.4)	C- 4, 7a
7	112.9	7.51 *d* (7.4)	C- 3a, 5
7a	137.5	-	-
8	185.4	9.93 *s*	C- 3

[a] Recorded at 600 MHz

4.6: Anti-inflammatory Assay

4.6.1: Anti-inflammatory Activity of Compounds from the Stems of Dracaena usambarensis

At the end of phytochemical study, the isolated compounds as well as the standard drug were tested for their potential to decrease four different inflammatory mediators (IL-1β, IL-2, GM-CSF and TNF-α) in the supernatant media of human peripheral blood mononuclear cells (PBMCs) stimulated by lipopolysaccharide (LPS). As shown in Figure 4.6 (Table S1 see Appendix), LPS led to the improved production of all the inflammatory mediators except for IL-2 in comparison to the untreated cells. In the presence of the standard anti-inflammatory drug (ibuprofen), the release

of three biomarkers (IL-1β, GM-CSF and TNF-α) was reduced in comparison to the LPS control except for IL-2 whose production was not affected.

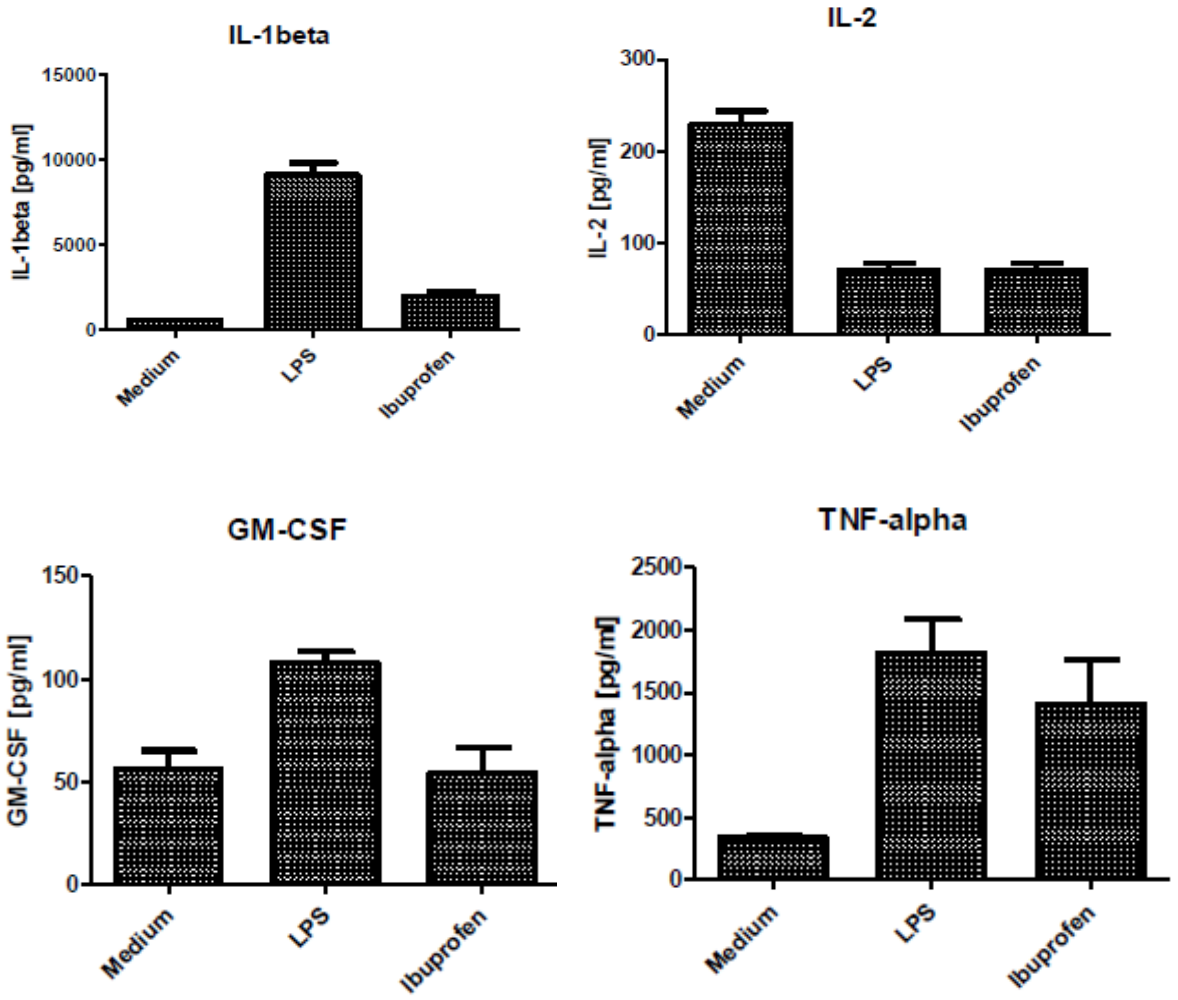

Figure 4.6: Concentration of different mediators after incubation of PBMCs with lipopolysaccharide (LPS, 10 µg/mL) and co-incubation with LPS (10 µg/mL) and ibuprofen (100 µM), respectively, compared to the medium (mean ± SD, n = 3)

Among the tested compounds (Figure 4.7 and Table S2 see Appendix) strong activities were observed for compounds **180, 182** and **184** at 100 µM. These test substances inhibited the production of all pro-inflammatory cytokines between 0.06 – 58.04% compared to the positive

control used as inflammation (LPS control). These three compounds (**180**, **182** and **184**) inhibited the release of all inflammatory cytokines compared to the standard drug, ibuprofen (21.97 – 100.00% of LPS control).

Compounds **170**, **171**, **177**, **179**, **180**, **182** – **184**, **190** and **194** showed a decrease of IL-1β compared to the LPS control (2.14 – 68.84% of LPS control). While the release of IL-1β was not affected in presence of **176**, **178** and **181** (Table 4.32). However, the release of IL-2 in presence of compounds **170**, **171**, **176**, **177**, **180 – 184**, **190** and **194** was reduced in comparison to positive control used for inflammation (LPS control) (11.6 – 94.03% of LPS control). Compounds **171**, **176**, **177**, **180** – **184** and **194** decreased the production of GM-CSF release from the PBMCs (1.61 – 78.31% of LPS control) with the strongest inhibition occurring in the presence of **180** and **184** (1.61% of LPS control). Compound **181** equally showed strongest inhibition against production of GM-CSF just as compounds **180** and **184** in comparison to the other compounds as evidenced in Figure 4.7. Compounds **180**, **181** and **184** were able to decrease GM-CSF with inhibition of 98.39, 93.86 and 98.39%, respectively as compared to the standard antibiotic 49.79 %. While compounds **170**, **178**, **179** and **190** had virtually no effect in comparison to the LPS control. Interestingly, the release of TNF-*α* was clearly affected in presence of all isolated compounds by comparison of the LPS control (0.06 – 72.50% of LPS control). Compounds **177**, **180**, **183** and **184** showed a clear reduction of TNF-α release of 14.72, 1.79, 11.32 and 0.06%, respectively. Compounds **180** and **184** showing best results against reduction of TNF-α release as evidenced in Figure 4.7. It was not obvious to established a clear structure-activity relationship (SAR) among related isoforms.

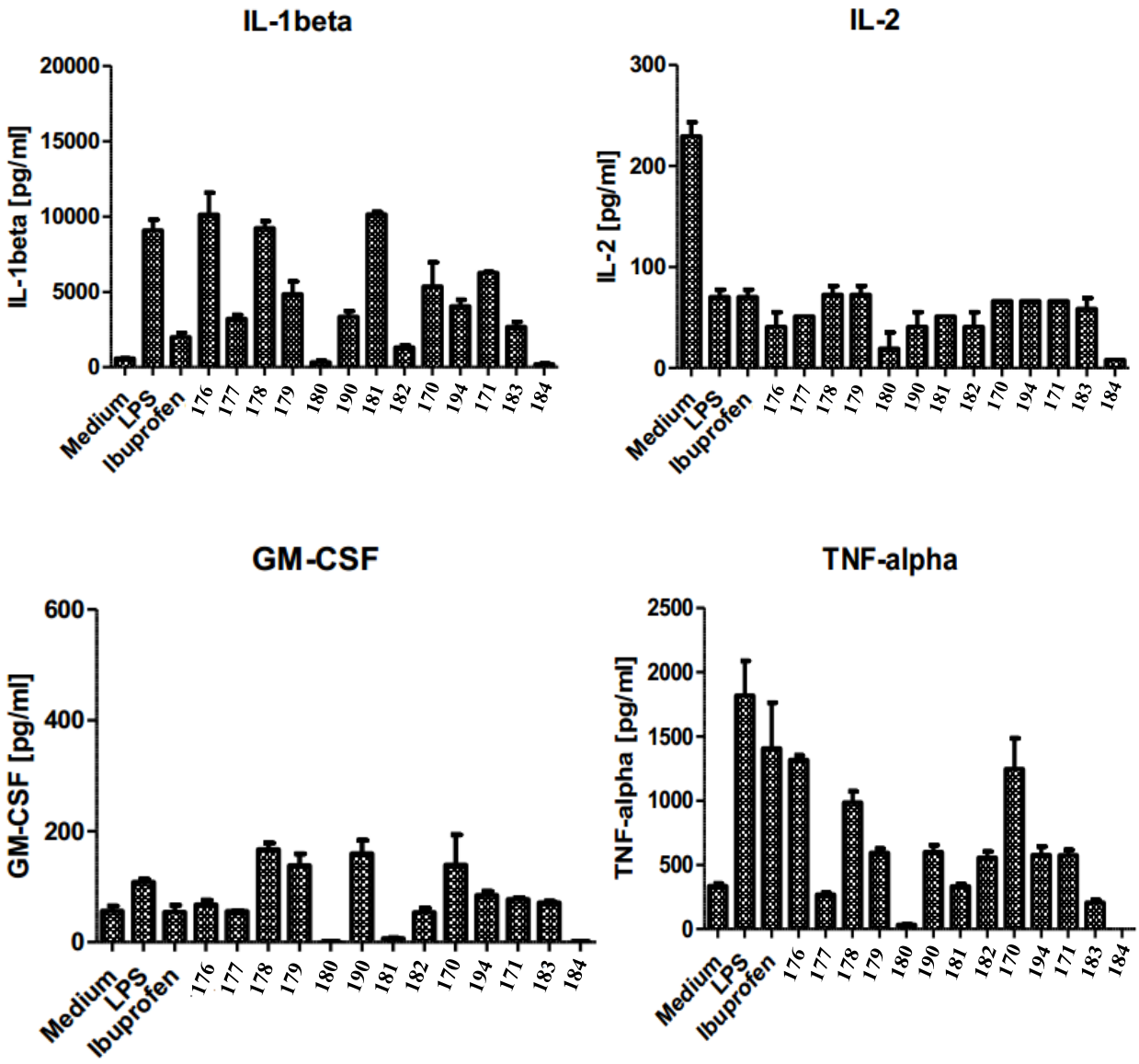

Figure 4.7: Concentration of different mediators after co-incubation of PBMCs with lipopolysaccharide (LPS, 10 µg/mL) and the test compounds or ibuprofen (100 µM), respectively, compared to the medium and to the medium incubated with LPS (10 µg/mL) only (mean ± SD, n = 2)

Table 4.32: Effects of isolated compounds and ibuprofen (100 µM) on LPS-induced release of biomarkers

	Inflammatory mediators [% of LPS control]			
Compounds	IL-1β	IL-2	GM-CSF	TNF-α
170	59.05	94.03	128.77	68.58
171	68.84	94.03	71.48	31.67
176	111.43	58.04	62.86	72.50
177	35.24	72.61	51.74	14.72
178	101.53	102.98	154.81	54.23
179	53.28	102.98	128.09	32.69
180	3.51	27.53	1.61	1.79
181	111.65	72.61	6.11	18.35
182	14.48	58.04	49.76	30.64
183	29.54	83.32	66.09	11.32
184	2.14	11.61	1.61	0.06
190	36.87	58.04	147.88	32.97
194	44.60	94.03	78.31	31.76
Ibuprofen	21.97	100.00	50.21	77.40

4.6.2: Anti-Inflammatory Activity of Compounds from the Leaves of Dracaena steudneri

The anti-inflammatory activities of the compounds (Figure 4.8 and Table S3 see Appendix) isolated from the leaves of *D. steudneri* were tested at 100 µM against the four inflammation modulators under study. The results showed compounds **207** – **211**, **214** – **216**, **219** and **220** (Figure 4.8 and Table 4.33), decreased the release of IL-1β in the range of 0.35 – 87.96%, compared to the LPS control with compounds **207** and **216** causing significant inhibition (12.25 and 0.35%, respectively). The results obtained for **216** are consistent with previous investigations (Li *et al.*, 2014). In contrast, **206**, **212**, **217**, **218** and **221** showed very minimal inhibition effect (93.54 – 98.60% of LPS control). Ibuprofen, the standard anti-inflammatory drug, decreased production of the four inflammation modulators with the exception of IL-2.

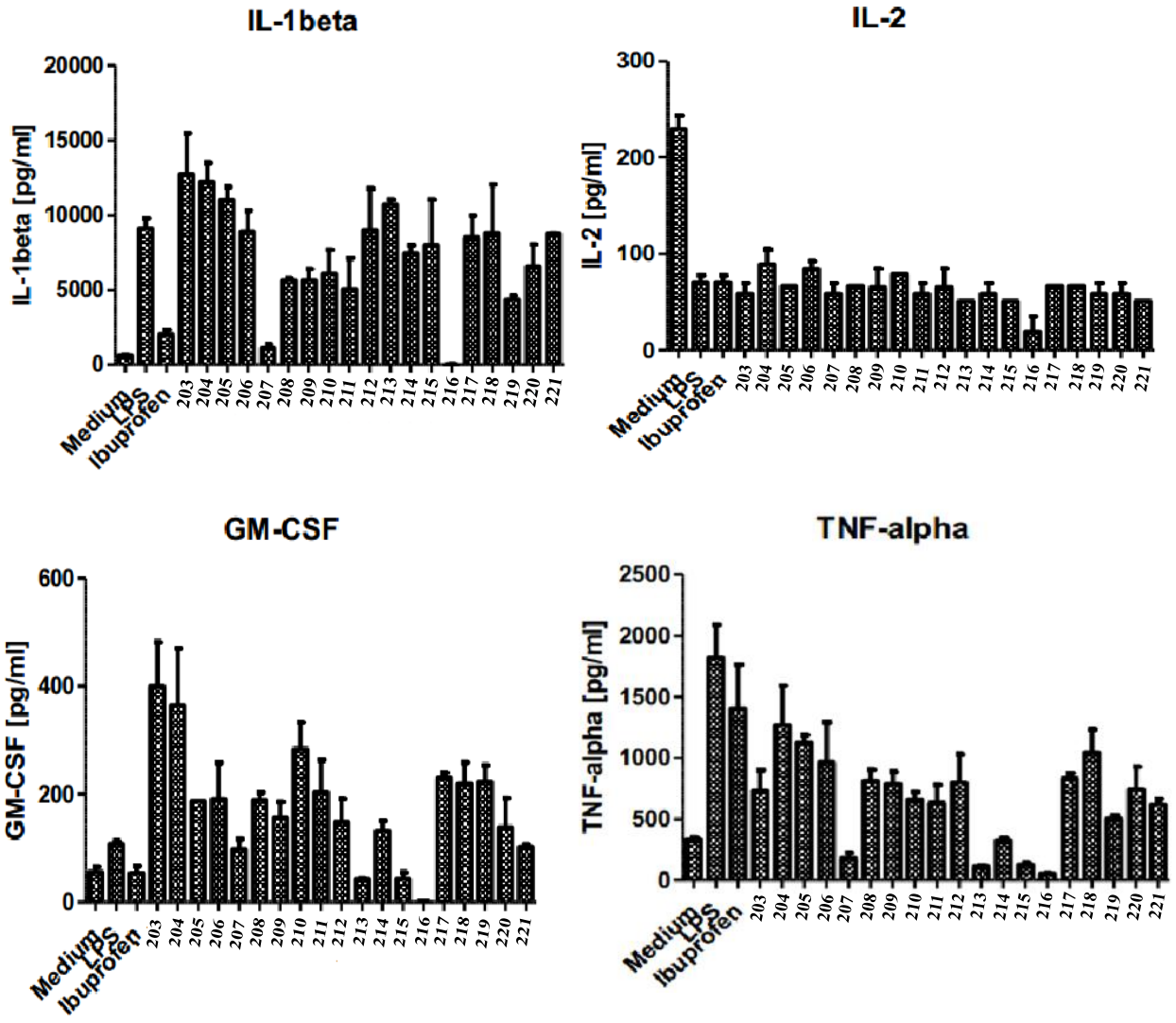

Figure 4.8: Concentration of different mediators after co-incubation of PBMCs with lipopolysaccharide (LPS, 10 µg/mL) and the test compounds or ibuprofen (100 µM), respectively, compared to the medium and to the medium incubated with LPS (10 µg/mL) only (mean ± SD, n = 2)

Table 4.33: Effects of isolated compounds and ibuprofen (100 µM) on LPS-induced release of biomarkers

	Inflammatory mediators [% of LPS control]			
Compounds	IL-1β	IL-2	GM-CSF	TNF-α
203	140.20	83.32	369.34	40.42
204	134.22	126.97	338.04	69.87
205	121.20	94.03	173.28	62.08
206	97.61	119.83	176.82	53.04
207	12.25	83.32	90.59	9.89
208	61.84	94.03	175.18	44.83
209	61.80	92.28	145.17	43.37
210	66.85	111.94	262.69	36.22
211	55.75	83.32	187.96	34.89
212	98.60	92.28	136.57	44.05
213	117.77	72.61	39.35	6.18
214	81.72	83.32	122.60	17.86
215	87.96	72.61	39.82	6.80
216	0.35	27.53	1.61	2.70
217	93.54	94.03	212.47	45.93
218	96.47	94.03	203.71	57.33
219	47.82	83.32	206.83	27.73
220	72.44	83.32	128.54	41.05
221	96.04	72.61	94.76	34.18
Ibuprofen	21.97	100.00	50.21	77.40

The results were analyzed to see if there is any SAR. Among the flavanones tested (**203** – **221**), the basic substitution pattern required for moderate IL-1β cytokine inhibition activity seemed to be the presence of 7-OH and C-6 OMe moieties in ring A as elaborated in compound **210** (66.85% of LPS control). The effect of additional oxygenation on inhibitory effect against IL-1β cytokine was dependent on the location of this substituent in rings A-C in the flavanone skeleton.

It was observed that additional oxygenation of **210**, in either ring A resulting to **209** (61.80% of LPS control) or ring B to **208** (61.84% of LPS control) led to minimal improvement in IL-1β cytokine release inhibition. These three flavanones, **208** – **210** showed inhibitory activity of similar magnitude. Additional oxygenation of **210** in ring C resulted in a significant reduction in inhibition

activity as exhibited in **221** with inhibition of 96.04% of LPS control. However, further oxygenation of **209** (61.80% of LPS control) at C-3 in ring C led to a decrease in inhibition activity as observed in **220** (72.44% of LPS control). Replacement of the C-6 methoxy group of **220** with a methyl group increased the lipophilicity of the molecule leading to a substantial improvement of inhibitory activity as elaborated in **219** with inhibition activity of 47.82% of LPS control versus **220** with much lower activity of 72.44% of LPS control. The placement of a hydroxyl substituent at C-4′ as compared to C-3 position in the flavanone skeleton led to a minimal decrease in inhibition activity as elaborated in **219** (47.82% of LPS control) and **211** (55.75% of LPS control). The activity profiles for flavones varied depending mainly on the substitution patterns. From these results, the presence of methylenedioxy substituent in ring B as in **203** – **205** led to substantial increase in production of IL-1β cytokine as compared to LPS control (121.20 – 140.20% of LPS control). Several previous studies have revealed the potency of quercetin and kaempferol and their derivatives in decreasing the expression of interleukines (IL-6 and IL-1β) and cyclooxygenase (COX-2) amongst others (Lesjak *et al.*, 2018; Spagnuolo *et al.*, 2018). In the current study, it was not obvious to determine the structural features that were responsible for IL-1β cytokine inhibitory activity of the isolated quercetin and kaempferol derivatives except for **213** and **215**. These two compounds displayed a similar substitution pattern except for an additional C-6 methoxy group in **215**. However, it was obvious that an additional methoxy group in ring A at C-6 position was pivotal to a substantial improvement of inhibitory activity against IL-1β as demonstrated by the two closely related derivatives of quercetin, **213** (117.77% of LPS control) and **215** (87.96% of LPS control).

Compounds **207**, **213** and **215** were all quercetin derivatives with similar substitution patterns in both rings B and C. The difference emanated from the substitution pattern of ring A, with **207**

exhibiting a substantially higher inhibitory activity against IL-1β cytokine attributable to additional C-6 Me and C-8 OMe groups. It is not clear whether the strong inhibitory activity was linked to the complete substitution in ring A as shown in **207** or the presence of these particular groups in the respective positions. The strong inhibitory activity of **207** as compared to **213** and **215** could be due to the equilibrium between the lipophilicity and hydrophilicity requirements the C-6 Me and C-8 OMe groups imparts on the molecule when in the respective positions.

The results showed that compared to flavanones, some of the flavones with similar substitution patterns showed relatively higher inhibitory activity against IL-1β cytokine as elaborated in **210** (66.85% of LPS control) and **216** (0.35% of LPS control), the most active compounds. The current study corroborates with earlier findings that highlighted the importance of the olefinic group at C-2/C-3 positions in ring C for strong activity (Middleton *et al.*, 2000). For the rest of the flavonoids, the inhibitory effect was found to be independent of the occurrence of the double bond as flavonoids from the two subclasses effected similar inhibitory activities against IL-1β cytokine. There seems to be other factors other than the substitution patterns on the flavonoid moiety together with the positioning of specific substituents in rings A-C that contributes to inhibitory potency of flavones against this specific cytokine. The hydrophilicity or lipophilicity imparted onto the flavonoid subclasses elaborates different substituent in different positions in the skeleton seems to also contribute to inhibitory activity against IL-1β cytokine production.

All the isolated compounds except **204** – **206**, **208** – **210**, **212**, **217** and **218** exhibited a reduction of IL-2 release compared to the LPS control. However, the most active compounds included the flavones, 7-hydroxy-6-methoxyflavone (**216**) (27.53% of LPS control) and quercetin and kaempferol derivatives, **207**, **213** – **215** (72.61 – 83.32% of LPS control) together with the

flavanones **211** (83.32% of LPS control) and **221** (72.61% of LPS control). It was not possible to determine an elaborate structure-activity relationship towards inhibition of IL-2 cytokine as was the case for IL-1β cytokine as compounds from the two flavonoid subclasses, flavones and flavanones exhibited similar potency profiles.

Compounds **207**, **213**, **215** and **216** were sensitive to GM-CSF release from the PBMCs (1.61 – 90.59% of LPS control). In comparison, the presence of ibuprofen reduced the cytokine release by 50.21% of LPS control. The inhibitory activity pattern against GM-CSF was similar to that against IL-1β for compounds **203** – **206**, all with methylenedioxy substituent in ring B, leading to increased production of cytokine GM-CSF (173.28 – 369.34% of LPS control). All the derivatives of quercetin including **207**, **213** and **215** except **212** showed promising inhibitory activities (39.35 – 90.59% of LPS control) as was the case against IL-1β and IL-2.

The results for these compounds against these cytokines are in agreement with previous related studies which demonstrated that flavonoids with guaiacol-like B ring displayed good anti-inflammatory activity (Pelzer *et al.*, 1998). For quercetin derivatives the major structural feature necessary for inhibitory activity against GM-CSF was established to be the presence of a free C-4′ hydroxyl group. This was clearly elaborated by **207**, **213** and **215** all with C-4′ OH displaying interesting inhibitory activity (39.35 – 90.59% of LPS control) contrary to **212** with a C-4′ OMe group showing increased production of GM-CSF (136.57% of LPS control).

All isolates, **203** – **221**, decreased the production of TNF-α (2.70 – 69.87% of LPS control). The decrease was in the similar range with the standard drug, ibuprofen (77.40% of LPS control). In addition to the flavone **216**, marked inhibitory activity against TNF-α was observed for quercetin

derivatives **207**, **213** and **215** exhibiting a hydroxyl group at C-4′ position and kaempferol derivative, compound (**214**) (17.86% of LPS control).

In conclusion, the current study is in agreement with previous work that demonstrated that not all flavonoids possess the ability to inhibit the release of inflammatory mediators (Hougee *et al.*, 2005). Overall, the sensitivity of the four pro-inflammatory cytokines to the isolated flavonoids (**203** – **221**) varied based on the types of substituents (-OH, -OMe, Me-, -OCH_2O-), the substitution pattern and levels of oxygenation on the flavonoid skeletal.

For quercetin derivatives isolated from *D. steudneri*, the presence of hydroxyl groups at C-5, C-7, C-4′ and methoxy groups at C-3 and C-3′ seemed to be important features for the anti-inflammatory activity. Hence, compounds **207**, **213** and **215** having these characteristics inhibited the production of the three among the four pro-inflammatory cytokines. Compound **207** bearing additional substituents at C-6 (Me) and C-8 (OMe) was the most active quercetin derivative against IL-1β. However, **213** and **215** that were not fully substituted in ring A showed the strongest anti-inflammatory activity against the other three inflammatory mediators, IL-2, GM-CSF and TNF-α. It is worth nothing that flavones (double bond between C-2/C-3) have better anti-inflammatory activity than flavanones (lacking double bond between C-2/C-3). For example, compounds **210** and **216** have identical substitutions pattern. The only difference between the two compounds is the fact that **210** is a flavanone while **216** is a flavone. Despite their close structure similarity, **216** is more active than **210**. For flavones the presence of a methylenedioxy group at C-3′/4′ led to substantial increase in the production of the pro-inflammatory cytokines relative to LPS control in two out of four cytokines.

4.7: Anticancer Assay

4.7.1: Anticancer Activity of Crude extract and Compounds from the Roots of Dracaena usambarensis

In this study, the root extract of *D. usambarensis* (50% MeOH in CH_2Cl_2) and isolates purified from this plant were screened for their potencies against two leukemia cell lines (CCRF-CEM and CEM/ADR5000). Doxorubicin was used as reference drug (Table 4.34).

The crude extract (10 µg/mL) had inhibited cancer cell growth by 13.04 – 22.43%, while the isolated compounds (10 µM) inhibited the growth of cancer cells by 6.45 – 55.11%. Among the compounds tested, **186** and **192** exhibited the highest activities against both drug-sensitive and multidrug-resistant leukemia cell lines in the preliminary screening, Table 4.34. The cell inhibitions were: 55.11% and 46.03% for **186** while for **192**, 53.72% and 42.58% against CCRF-CEM and CEM/ADR5000 leukemia cells, respectively. Following this preliminary screening, the IC_{50} and the anticancer activity against other cancer cell lines (CEM/ADR5000, MDA-MB-231-pcDNA3, MDA-MB-231-*BCRP* clone 23, U87.MG, U87.MGΔ*EGFR*, HepG2 and the normal AML12 cells) of the most active compound, **186**, was determined. The results showed that this compound had an IC_{50} value of 40.43 ± 10.26 µM against CCRF-CEM cells, but was inactive against the other tested cell lines, IC_{50} >100 µM (Nyaboke *et al*., 2018). The results of the present studies for **186** are in agreement with previous ones for a related homoisoflavone, which showed 50% cancer growth inhibition (GI_{50} value) at 7 µg /mL against MCF7 breast cancer cells (Lin *et al*., 2014).

Preliminary cytotoxicity results of the structurally related homoisoflavonoids, **186** – **188**, enabled structure-activity relationship studies. In support of investigations by Dai et al (2013), the importance of oxygenation of homoisoflavonoids at C-6 for good activity with these skeletal

structures was further established. This is elaborated for compounds **186** – **188**. It is clear that compounds **187** and **188** lacking oxygenation at C-6 exhibited substantially lower potencies than **186** bearing a hydroxyl group at the same position. It seems that additional oxygenation of **187** at C-6 resulted in a substantial improvement of cytotoxicity as evidenced in **186** with cell inhibition of 55.11% and 46.03% *vs.* 48.60% and 33.83% against CCRF-CEM and CEM/ADR5000, respectively.

This study further concurs with previous research findings by Alali et al (2015) and Dai et al (2013), which showed that a reduction in hydrophilicity mainly through methylation led to increased cytotoxicity. This is elaborated for compounds **187** and **188**, which have a similar substitution or oxygenation pattern except that **187** is methylated at C-7 probably resulting in increased cytotoxicity. The cell inhibition of **187** is 48.60% and 33.83% *vs.* 15.27% and 25.09% for **188** against CCRF-CEM and CEM/ADR5000 cell lines, respectively. This could be due to increased lipophilicity required for the interaction with cell membranes.

Table 4.34: Cell inhibition of test compounds against CCRF-CEM, CEM/ADR5000

Compounds	Cell inhibition (%)	
	CCRF-CEM	CEM/ADR5000
186	55.11 ± 2.31	46.03 ± 0.70
187	48.60 ± 4.08	33.83 ± 4.79
188	15.27 ± 10.36	25.09 ± 1.46
189	8.12 ± 4.27	20.26 ± 1.77
190	20.20 ± 1.30	46.33 ± 0.84
191	18.89 ± 2.31	6.45 ± 2.51
192	53.72 ± 0.84	42.58 ± 2.68
193	49.45 ± 2.46	35.71 ± 2.40
Crude extract	13.04 ± 4.86	22.43 ± 2.84
Doxorubicin	97.36 ± 0.86	21.03 ± 2.89

4.7.2: Anticancer Activity of Crude extracts and Compounds from Dracaena Species

The crude extracts (*D. usambarensis* (stems), *D. aletriformis* (whole plant) and *D. steudneri* (leaves and seeds)) as well as compounds obtained from these extracts were preliminarily screened for their cytotoxicity potencies against the drug sensitive leukemia (CCRF-CEM) cell line (Table 4.35). The crude extracts and compounds with ≤ 30 % cell viability were selected and further serially diluted (10, 3, 1, 0.3, 0.1, 0.03, 0.01 and 0.003 µM) and their IC_{50} values were determined. As shown in Table 4.35, all the compounds except **200** and **213** displayed cell viability of more than 30% against CCRF-CEM cell line. It is only compounds **200** and **213** that displayed cells inhibition of more than 70% and were selected and tested against the multi-drug resistant (CEM/ADR5000) leukemia cell lines and their IC_{50} were calculated (Table 4.36). Compound **200** displayed strong cytotoxic activity against both leukemia cell lines with IC_{50} values 7.88 ± 0.74 µM and 5.28 ± 0.85 µM against CCRF-CEM and CEM/ADR5000, respectively. Compound **213** showed equally strong inhibition with IC_{50} values 8.80 ± 0.74 µM, 3.31 ± 0.36 µM against CCRF-CEM and CEM/ADR5000, respectively. These compounds (**200** and **213**) are quercetin derivative bearing a methoxy substituent at C-3. Their activities are consistent with other such compounds described in the literature (Beutler *et al.*, 1998; Díaz *et al.*, 2003). Compounds **196**, **199** and **200** shared the same substitution pattern in rings A and B with the only difference being in ring C. It is clear that the existence of the sugar unit at C-3 position in **199** had virtually no effect since the cell inhibition was less than 10% living 90% of cell alive. The same trend can be applied to **196** (101.75% cell viability against CCRF-CEM). On the basis of results obtained in this study, the basic requirement for a flavonol hydroxylated at C-5 and C-7 position in ring A for cytotoxic activity seems to be methylation at C-3, whereas in ring B, the requirement for activity is 3′-methoxy-4′-hydroxy substitution which facilitated cellular uptake (Beutler *et al.*, 1998; Díaz *et al.*,

2003). Compound **201** lacking these features exhibited substantially no cytotoxicity effect compared to **213** (IC_{50} < 10 µM).

Table 4.35: Cell viability of test compounds against CCRF-CEM cell line

Compounds	Cell Viability (%)	Compounds	Cell Viability (%)
170	86.89 ± 4.38	**200**	17.54 ± 4.44
171	100.22 ± 4.54	**201**	86.88 ± 13.49
176	57.28 ± 12.74	**202**	91.26 ± 15.48
180	102.40 ± 1.63	**208**	103.92 ± 4.56
181	89.90 ± 3.86	**213**	23.02 ± 7.35
183	98.81 ± 4.98	**220**	96.67 ± 2.16
185	105.97 ± 1.65	**221**	94.52 ± 8.97
195	99.63 ± 2.44	**DUS***	87.02 ± 1.68
196	101.75 ± 14.50	**DAW***	97.88 ± 11.09
197	100.55 ± 18.95	**DSS***	98.82 ± 2.33
198	93.71 ± 15.05	**DSL***	100.39 ± 2.33
199	92.00 ± 15.26		

***Crude extract, DUS: *Dracaena usambarensis* stems; DAW: *Dracaena aletriformis* whole plant; DSS: *Dracaena steudneri* seeds; DSL: *Dracaena steudneri* leaves

Table 4.36: Cytotoxicity of compounds **200** and **213** against CCRF-CEM, CEM/ADR5000 as determined by resazurin assay

Compounds	CCRF-CEM	CEM/ADR5000	[a]Degree of resistance (D.R)
	IC_{50} in µM	IC_{50} in µM	
200	7.88 ± 0.74	5.28 ± 0.85	0.67
213	8.80 ± 0.74	3.31 ± 0.36	0.37
Doxorubicin	0.01 ± 0.14	26.78 ± 3.30	2.67

[a]D.R= IC_{50} CEM/ADR5000/ IC_{50} CCRF-CEM

CHAPTER 5: CONCLUSIONS AND RECOMMENDATIONS

5.1: Conclusions

In this study three *Dracaena* species (*Dracaena usambarensis*, *Dracaena aletriformis*, and *Dracaena steudneri*) were investigated phytochemically and the crude extract as well as the isolates were screened for their potential anti-inflammatory and anticancer properties. The conclusion drawn from the study are summarized herein.

i. The three *Dracaena* species afforded fifty (50) compounds of which nineteen (19) were characterized from *D. usambarensis*, three (3) from *D. aletriformis* and twenty eight (28) from *D. steudneri*. Among these, thirteen (13) were novel compounds (**176** – **179, 180**, **186**, **189, 203, 204, 205, 206, 207** and **208**)

ii. In the anti-inflammatory assay, compounds **180**, **182**, **184** and **216** decreased the level of all mediators (IL-1β, IL-2, GM-CSF and TNF-α) from as low as 0.06 to 90.59% compared to the LPS control.

iii. In the resazurin reduction assay, compounds **200** and **213** exhibited the strongest cytotoxic activity against both leukemia cell lines with an $IC_{50} < 10$ µM. Compound **186** displayed moderate activity towards CCRF-CEM leukemia cancer cell line with IC_{50} value of 40.43 ± 10.26 µM.

5.2: Recommendations

On the basis of the results obtained in this study, the study recommends that:

i. The phytochemicals from the other Kenyan *Dracaena* species be determined.

ii. Structure analogues of the most active compounds should be synthesized and assayed for their anti-inflammatory and anticancer potential to determine Structure-Activity Relationship (SAR).

iii. The synergistic effect of the isolated compounds should be explored.

iv. The cytotoxicity of the most active compounds should be performed against a panel of drug-sensitive and multi-drug resistant cancer cell lines in parallel with normal cells.

REFERENCES

Abegaz, B. M., Mutanyatta-Comar, J. and Nindi, M. (2007). Naturally occurring homoisoflavonoids: Phytochemistry, biological activities and synthesis. *Natural product communications* **2**: 475-498.

Adinolfi, M., Lanzetta, R., Laonigro, G., Parrilli, M. and Breitmaier, E. (1986). 1H and 13C chemical shift assignments of homoisoflavanones. *Magnetic resonance in chemistry* **24**: 663-666.

Aggarwal, B. B., Vijayalekshmi, R. and Sung, B. (2009). Targeting inflammatory pathways for prevention and therapy of cancer: short-term friend, long-term foe. *Clinical Cancer Research* **15**: 425-430.

Ahmad, S., Riaz, N., Saleem, M., Jabbar, A., Nisar-Ur-Rehman and Ashraf, M. (2010). Antioxidant flavonoids from Alhagi maurorum. *Journal of Asian natural products research* **12**: 138-143.

Alali, F., El-Elimat, T., Albataineh, H., Al-Balas, Q., Al-Gharaibeh, M., Falkinham III, J. O., Chen, W.-L., Swanson, S. M. and Oberlies, N. H. (2015). Cytotoxic homoisoflavones from the bulbs of Bellevalia eigii. *Journal of Natural Products* **78**: 1708-1715.

Antonelli, M. and Kushner, I. (2017). It's time to redefine inflammation. *The FASEB Journal* **31**: 1787-1791.

APG. (2016). An update of the Angiosperm Phylogeny Group classification for the orders and families of flowering plants: APG IV. *Botanical Journal of the Linnean Society* **181**: 1-20.

Arif, T., Bhosale, J., Kumar, N., Mandal, T., Bendre, R., Lavekar, G. and Dabur, R. (2009). Natural products–antifungal agents derived from plants. *Journal of Asian natural products research* **11**: 621-638.

Armstrong, H., Bording-Jorgensen, M., Dijk, S. and Wine, E. (2018). The complex interplay between chronic inflammation, the microbiome, and cancer: understanding disease progression and what we can do to prevent it. *Cancers* **10**: 83.

Asakawa, Y. (1971). Chemical constituents of Alnus sieboldiana (Betulaceae) II. The isolation and structure of flavonoids and stilbenes. *Bulletin of the Chemical Society of Japan* **44**: 2761-2766.

Awouafack, M. D., Tane, P. and Eloff, J. N. (2013). Two new antioxidant flavones from the twigs of Eriosema robustum (Fabaceae). *Phytochemistry Letters* **6**: 62-66.

Basnet, P., Kadota, S., Hase, K. and Namba, T. (1995). Five new C-methyl flavonoids, the potent aldose reductase inhibitors from Matteuccia orientalis TREV. *Chemical and Pharmaceutical Bulletin* **43**: 1558-1564.

Beard, E. L., Jr. (2001). The American Society of Health System Pharmacists. *JONA's Healthcare Law, Ethics and Regulation* **3**: 78-79.

Bedane, K. G., Zühlke, S. and Spiteller, M. (2020). Bioactive constituents of Lobostemon fruticosus: Anti-inflammatory properties and quantitative analysis of samples from different places in South Africa. *South African Journal of Botany* **131**: 174-180.

Beentje, H. (1994). Kenya trees, shrubs, and lianas. National Museums of Kenya, P.O.Box 40658, Nairobi, Kenya.

Bektas, S. and Iscimen, S. (2005). Antibiotic Resistance of Aeromonas hydrophila Strains Isolated from Karasu Stream (Sinop/Turkey). *environment* **1**: 10-21.

Beutler, J. A., Hamel, E., Vlietinck, A. J., Haemers, A., Rajan, P., Roitman, J. N., Cardellina, J. H. and Boyd, M. R. (1998). Structure− activity requirements for flavone cytotoxicity and binding to tubulin. *Journal of medicinal chemistry* **41**: 2333-2338.

Bray, F., Ferlay, J., Soerjomataram, I., Siegel, R. L., Torre, L. A. and Jemal, A. (2018). Global cancer statistics 2018: GLOBOCAN estimates of incidence and mortality worldwide for 36 cancers in 185 countries. *CA: a cancer journal for clinicians* **68**: 394-424.

Bu, H., He, X., Zhang, Z., Yin, Q., Yu, H. and Li, Y. (2014). A TPGS-incorporating nanoemulsion of paclitaxel circumvents drug resistance in breast cancer. *International journal of pharmaceutics* **471**: 206-213.

Butler, M. S., Robertson, A. A. and Cooper, M. A. (2014). Natural product and natural product derived drugs in clinical trials. *Natural Product Reports* **31**: 1612-1661.

Chase, M. W., Reveal, J. L. and Fay, M. F. (2009). A subfamilial classification for the expanded asparagalean families Amaryllidaceae, Asparagaceae and Xanthorrhoeaceae. *Botanical Journal of the Linnean Society* **161**: 132-136.

Chaturvedula, V. S. P. and Prakash, I. (2012). Isolation of Stigmasterol and?-Sitosterol from the dichloromethane extract of Rubus suavissimus. *International Current Pharmaceutical Journal* **1**: 239-242.

Chau, V. M., Dat, N. T., Dang, N. H., Nam, N. H., Ban, N. K., Van Tuyen, N., Huong, L. M., Huong, T. T. and Van Kiem, P. (2009). Unusual 22S-spirostane steroids from Dracaena cambodiana. *Natural product communications* **4**: 1197-1200.

Chen, H.-Q., Zuo, W.-J., Wang, H., Shen, H.-Y., Luo, Y., Dai, H.-F. and Mei, W.-L. (2012). Two new antimicrobial flavanes from dragon's blood of Dracaena cambodiana. *Journal of Asian natural products research* **14**: 436-440.

Chen, J.-J., Chung, C.-Y., Hwang, T.-L. and Chen, J.-F. (2009). Amides and benzenoids from Zanthoxylum ailanthoides with inhibitory activity on superoxide generation and elastase release by neutrophils. *Journal of Natural Products* **72**: 107-111.

Chilakamarthi, U. and Giribabu, L. (2017). Photodynamic therapy: past, present and future. *The Chemical Record* **17**: 775-802.

Christenhusz, M. J. and Byng, J. W. (2016). The number of known plants species in the world and its annual increase. *Phytotaxa* **261**: 201-217.

Cipollone, F., Cicolini, G. and Bucci, M. (2008). Cyclooxygenase and prostaglandin synthases in atherosclerosis: recent insights and future perspectives. *Pharmacology & Therapeutics* **118**: 161-180.

Coussens, L. M. and Werb, Z. (2002). Inflammation and cancer. *Nature* **420**: 860-867.

Croteau, R., Kutchan, T. M. and Lewis, N. G. (2000). Natural products (secondary metabolites). *Biochemistry and molecular biology of plants* **24**: 1250-1319.

Cui, L., Thuong, P. T., Lee, H. S., Ndinteh, D. T., Mbafor, J. T., Fomum, Z. T. and Oh, W. K. (2008). Flavanones from the stem bark of Erythrina abyssinica. *Bioorganic & Medicinal Chemistry* **16**: 10356-10362.

Dai, H.-f., Wang, H., Liu, J., Wu, J. and Mei, W.-l. (2012). Two new biflavonoids from the stem of Dracaena cambodiana. *Chemistry of natural compounds* **48**: 376-378.

Dai, Y., Harinantenaina, L., Brodie, P. J., Goetz, M., Shen, Y., TenDyke, K. and Kingston, D. G. (2013). Antiproliferative homoisoflavonoids and bufatrienolides from Urginea depressa. *Journal of Natural Products* **76**: 865-872.

Damen, T. H., Van der Burg, W., Wiland-Szymańska, J. and Sosef, M. (2018). Taxonomic novelties in African Dracaena (Dracaenaceae). *Blumea-Biodiversity, Evolution and Biogeography of Plants* **63**: 31-53.

Dat, N. T., Binh, P. T. X., Van Minh, C., Huong, H. T. and Lee, J. J. (2010). Cytotoxic prenylated flavonoids from Morus alba. *Fitoterapia* **81**: 1224-1227.

Debella, A., Haslinger, E., Schmid, M. G., Bucar, F., Michl, G., Abebe, D. and Kunert, O. (2000). Triterpenoid saponins and sapogenin lactones from Albizia gummifera. *Phytochemistry* **53**: 885-892.

DellaGreca, M., Previtera, L., Purcaro, R. and Zarrelli, A. (2006). Cinnamic acid amides and lignanamides from Aptenia cordifolia. *Tetrahedron* **62**: 2877-2882.

Dias, D. A., Urban, S. and Roessner, U. (2012). A historical overview of natural products in drug discovery. *Metabolites* **2**: 303-336.

Díaz, F., Chávez, D., Lee, D., Mi, Q., Chai, H.-B., Tan, G. T., Kardono, L. B., Riswan, S., Fairchild, C. R. and Wild, R. (2003). Cytotoxic flavone analogues of vitexicarpin, a constituent of the leaves of Vitex negundo. *Journal of Natural Products* **66**: 865-867.

Doyle, L. A., Yang, W., Abruzzo, L. V., Krogmann, T., Gao, Y., Rishi, A. K. and Ross, D. D. (1998). A multidrug resistance transporter from human MCF-7 breast cancer cells. *Proceedings of the National Academy of Sciences* **95**: 15665-15670.

Durmowicz, A. G. and Stenmark, K. R. (1999). Mechanisms of structural remodeling in chronic pulmonary hypertension. *Pediatr Rev* **20**: e91-e102.

Edward, H. G., de Oliveira, L. F. C. and Quye, A. (2001). Raman spectroscopy of coloured resins used in antiquity: dragon's blood and related substances. *Spectrochimica Acta Part A: Molecular and Biomolecular Spectroscopy* **57**: 2831-2842.

Efferth, T., Sauerbrey, A., Olbrich, A., Gebhart, E., Rauch, P., Weber, H. O., Hengstler, J. G., Halatsch, M.-E., Volm, M. and Tew, K. D. (2003). Molecular modes of action of artesunate in tumor cell lines. *Molecular pharmacology* **64**: 382-394.

El-Elimat, T., Rivera-Chávez, J., Burdette, J. E., Czarnecki, A., Alhawarri, M. B., Al-Gharaibeh, M., Alali, F. and Oberlies, N. H. (2018). Cytotoxic homoisoflavonoids from the bulbs of Bellevalia flexuosa. *Fitoterapia* **127**: 201-206.

El-Sawy, E. R., Abdelwahab, A. B. and Kirsch, G. (2018). Utilization of 1H-Indole-3-carboxaldehyde as a Precursor for the Synthesis of Bioactive Indole Alkaloids. *Synthesis* **50**: 4525-4538.

Ezenyi, I., Salawu, O., Kulkarni, R. and Emeje, M. (2014). Antiplasmodial activity-aided isolation and identification of quercetin-4'-methyl ether in Chromolaena odorata leaf fraction with high activity against chloroquine-resistant Plasmodium falciparum. *Parasitology research* **113**: 4415-4422.

Fang, J.-M., Chang, C.-F. and Cheng, Y.-S. (1987). Flavonoids from Pinus morrisonicola. *Phytochemistry* **26**: 2559-2561.

Ferrero-Miliani, L., Nielsen, O., Andersen, P. and Girardin, S. (2007). Chronic inflammation: importance of NOD2 and NALP3 in interleukin-1β generation. *Clinical & Experimental Immunology* **147**: 227-235.

Fitzmaurice, C., Allen, C., Barber, R. M., Barregard, L., Bhutta, Z. A., Brenner, H., Dicker, D. J., Chimed-Orchir, O., Dandona, R. and Dandona, L. (2017). Global, regional, and national cancer incidence, mortality, years of life lost, years lived with disability, and disability-adjusted life-years for 32 cancer groups, 1990 to 2015: a systematic analysis for the global burden of disease study. *JAMA oncology* **3**: 524-548.

Fouedjou, R. T., Teponno, R. B., Quassinti, L., Bramucci, M., Petrelli, D., Vitali, L. A., Fiorini, D., Tapondjou, L. A. and Barboni, L. (2014). Steroidal saponins from the leaves of Cordyline fruticosa (L.) A. Chev. and their cytotoxic and antimicrobial activity. *Phytochemistry Letters* **7**: 62-68.

Fürst, R. and Zündorf, I. (2014). Plant-derived anti-inflammatory compounds: hopes and disappointments regarding the translation of preclinical knowledge into clinical progress. *Mediators of inflammation* **2014**: 146832.

Gao, Y., Su, Y., Yan, S., Wu, Z., Zhang, X., Wang, T. and Gao, X. (2010). Hexaoxygenated flavonoids from Pteroxygonum giraldii. *Natural product communications* **5**: 223-226.

Ghaly, N. S., Nabil, M., Miyase, T. and Melek, F. R. (2014). Steroidal saponins from the roots of Dracaena marginata tam. *Der Pharmacia Lettre* **6**: 132-141.

Gidey, M., Beyene, T., Signorini, M. A., Bruschi, P. and Yirga, G. (2015). Traditional medicinal plants used by Kunama ethnic group in Northern Ethiopia. *Journal of Medicinal Plants Research* **9**: 494-509.

González, A. G., Hernández, J. C., León, F., Padrón, J. I., Estévez, F., Quintana, J. and Bermejo, J. (2003). Steroidal Saponins from the Bark of Dracaena d raco and Their Cytotoxic Activities. *Journal of Natural Products* **66**: 793-798.

González, A. G., León, F., Sánchez-Pinto, L., Padrón, J. I. and Bermejo, J. (2000). Phenolic Compounds of Dragon's Blood from Dracaena d raco. *Journal of Natural Products* **63**: 1297-1299.

Gori, A., Cesari, F., Marcucci, R., Giusti, B., Paniccia, R., Antonucci, E., Gensini, G. and Abbate, R. (2009). The balance between pro-and anti-inflammatory cytokines is associated with platelet aggregability in acute coronary syndrome patients. *Atherosclerosis* **202**: 255-262.

Gottesman, M. M. (2002). Mechanisms of Cancer Drug Resistance. *Annual Review of Medicine* **53**: 615-627.

Grivennikov, S. I., Greten, F. R. and Karin, M. (2010). Immunity, inflammation, and cancer. *Cell* **140**: 883-899.

Grotewold, E. (2006). The science of flavonoids. *New York, Springer* **239-267**.

Gupta, D., Bleakley, B. and Gupta, R. K. (2008). Dragon's blood: botany, chemistry and therapeutic uses. *Journal of Ethnopharmacology* **115**: 361-380.

Gupta, D., Verma, N., Das, H. R. and Gupta, R. K. (2014). Evaluation of anti-inflammatory activity of Dracaena cinnabari Balf. f. resin. *Indian Journal of Natural Products and Resources* **5**: 218-222.

Handral, H. K., Pandith, A. and Shruthi, S. (2012). A review on Murraya koenigii: multipotential medicinal plant. *Asian Journal of pharmaceutical and clinical research* **5**: 5-14.

Hao, Q., Saito, Y., Matsuo, Y., Li, H.-Z. and Tanaka, T. (2015). Chalcane–stilbene conjugates and oligomeric flavonoids from Chinese Dragon’s Blood produced from Dracaena cochinchinensis. *Phytochemistry* **119**: 76-82.

Harris, R. E., Beebe-Donk, J., Doss, H. and Doss, D. B. (2005). Aspirin, ibuprofen, and other non-steroidal anti-inflammatory drugs in cancer prevention: a critical review of non-selective COX-2 blockade. *Oncology reports* **13**: 559-583.

Harris, R. E., Chlebowski, R. T., Jackson, R. D., Frid, D. J., Ascenseo, J. L., Anderson, G., Loar, A., Rodabough, R. J., White, E. and McTiernan, A. (2003). Breast cancer and nonsteroidal anti-inflammatory drugs: prospective results from the Women’s Health Initiative. *Cancer research* **63**: 6096-6101.

Havsteen, B. H. (2002). The biochemistry and medical significance of the flavonoids. *Pharmacology & Therapeutics* **96**: 67-202.

Hernández, J. C., León, F., Estévez, F., Quintana, J. and Bermejo, J. (2006). A Homo-Isoflavonoid and a Cytotoxic Saponin from Dracaena draco. *Chemistry & biodiversity* **3**: 62-68.

Hernandez, J. C., León, F., Quintana, J., Estevez, F. and Bermejo, J. (2004). Icogenin, a new cytotoxic steroidal saponin isolated from Dracaena draco. *Bioorganic & Medicinal Chemistry* **12**: 4423-4429.

Higano, T., Kuroda, M., Sakagami, H. and Mimaki, Y. (2007). Convallasaponin A, a new 5β-spirostanol triglycoside from the rhizomes of Convallaria majalis. *Chemical and Pharmaceutical Bulletin* **55**: 337-339.

Hostettmann, K., Potterat, O. and Wolfender, J.-L. (1998). The potential of higher plants as a source of new drugs. *Chimia International Journal for Chemistry* **52**: 10-17.

Hougee, S., Sanders, A., Faber, J., Graus, Y. M., van den Berg, W. B., Garssen, J., Smit, H. F. and Hoijer, M. A. (2005). Decreased pro-inflammatory cytokine production by LPS-stimulated PBMC upon in vitro incubation with the flavonoids apigenin, luteolin or chrysin, due to selective elimination of monocytes/macrophages. *Biochemical Pharmacology* **69**: 241-248.

Hu, L., Wang, F.-F., Wang, X.-H., Yang, Q.-S., Xiong, Y. and Liu, W.-X. (2015). Phytoconstituents from the leaves of Dracaena cochinchinensis (Lour.) S. C. Chen. *Biochemical systematics and ecology* **63**: 1-5.

Huang, H.-C., Lin, M.-K., Hwang, S.-Y., Hwang, T.-L., Kuo, Y.-H., Chang, C.-I., Ou, C.-Y. and Kuo, Y.-H. (2013). Two Anti-inflammatory Steroidal Saponins from Dracaena angustifolia Roxb. *Molecules* **18**: 8752-8763.

Huang, X. F., Lin, Y. Y. and Kong, L. Y. (2008). Steroids from the roots of Asparagus officinalis and their cytotoxic activity. *Journal of integrative plant biology* **50**: 717-722.

Huo, C.-H., Li, Y., Zhang, M.-L., Wang, Y.-F., Zhang, Q., Qin, F., Shi, Q.-W. and Kiyota, H. (2013). Cytotoxic flavonoids from the flowers of Achillea millefolium. *Chemistry of natural compounds* **48**: 958-962.

Ichikawa, K., Kitaoka, M., Taki, M., Takaishi, S., Boriboon, M. and Akiyama, T. (1997). Retrodihydrochalcones and homoisoflavones isolated from Thai medicinal plant Dracaena loureiri and their estrogen agonist activity. *Planta medica* **63**: 540-543.

Jemal, A., Bray, F., Forman, D., O'Brien, M., Ferlay, J., Center, M. and Parkin, D. M. (2012). Cancer burden in Africa and opportunities for prevention. *Cancer* **118**: 4372-4384.

Jeong, R.-H., Wu, Q., Cho, J.-G., Lee, D.-Y., Shrestha, S., Lee, M.-H., Lee, K.-T., Choi, M.-S., Jeong, T.-S. and Ahn, E.-M. (2013). Isolation and Identification of Flavonoids from the Roots of Brassica rapa ssp. *Journal of Applied Biological Chemistry* **56**: 23-27.

Jiazhu, Y., Jiang, J., Huang, G., Liu, B., Liu, Y., Zhan, R. and Chen, Y. (2014). Two new flavanone glycosides from Sunipia scariosa. *Biochemical systematics and ecology* **100**: 317-321.

Jin-hai, Y., Zhang, G.-l. and LI, B.-g. (2002). Studies on the chemical constituents of Pseudotsuga sinensis. *Acta Pharmaceutica Sinica* **37**: 352-354.

Jin, J.-M., Zhang, Y.-J. and Yang, C.-R. (2004). Four new steroid constituents from the waste residue of fibre separation from Agave americana leaves. *Chemical and Pharmaceutical Bulletin* **52**: 654-658.

Jin, L., Chen, H. S., Xiang, Z. B., Liang, S., Jin, Y. S. and Liu, J. G. (2007). New flavone and isoflavone glycoside from Belamcanda chinensis. *Chinese Chemical Letters* **18**: 158-160.

Jung, S., Lee, M.-S., Choi, A.-J., Kim, C.-T. and Kim, Y. (2019). Anti-Inflammatory effects of high hydrostatic pressure extract of mulberry (Morus alba) fruit on LPS-stimulated RAW264. 7 cells. *Molecules* **24**: 1425.

Kaileh, M., Berghe, W. V., Boone, E., Essawi, T. and Haegeman, G. (2007). Screening of indigenous Palestinian medicinal plants for potential anti-inflammatory and cytotoxic activity. *Journal of Ethnopharmacology* **113**: 510-516.

Kale, R. D., Taye, M. and Chaudhary, B. (2019). Extraction and characterization of cellulose single fiber from native Ethiopian Serte (Dracaena steudneri Egler) plant leaf. *Journal of Macromolecular Science, Part A* **56**: 837-844.

Kamboj, A. and Saluja, A. K. (2011). Isolation of stigmasterol and β-sitosterol from petroleum ether extract of aerial parts of Ageratum conyzoides (Asteraceae). *International Journal of Pharmacy and Pharmaceutical Sciences* **3**: 94-96.

Kamtcha, D.W., Tene, M., Bedane, K.G., Knauer, L., Strohmann, C., Tane, P., Kusari, S., Spiteller, M. (2018). Cardenolides from the stem bark of Salacia staudtiana, *Fitoterapia*. **127**: 402–409.

Karin, M. (2006). Nuclear factor-κB in cancer development and progression. *Nature* **441**: 431-436.

Karin, M. (2009). NF-κB as a critical link between inflammation and cancer. *Cold Spring Harbor perspectives in biology* **1**: 1-41.

Kawai, T. and Akira, S. (2011). Toll-like receptors and their crosstalk with other innate receptors in infection and immunity. *Immunity* **34**: 637-650.

Keglevich, P., Hazai, L., Kalaus, G. and Szántay, C. (2012). Modifications on the basic skeletons of vinblastine and vincristine. *Molecules* **17**: 5893-5914.

Kimmig, A., Gekeler, V., Neumann, M., Frese, G., Handgretinger, R., Kardos, G., Diddens, H. and Niethammer, D. (1990). Susceptibility of multidrug-resistant human leukemia cell lines to human interleukin 2-activated killer cells. *Cancer research* **50**: 6793-6799.

Kittisak, L., Sawasdee, K. and Kirtikara, K. (2002). Flavonoids and stilbenoids with COX-1 and COX-2 inhibitory activity from Dracaena loureiri. *Planta medica* **68**: 841-843.

Kokwaro, J. O. (2009). *Medicinal plants of east Africa,Third Edition*: University of Nairobi press.

Kosala, K., Widodo, M. A., Santoso, S. and Karyono, S. (2018). In vitro and In vivo Anti-inflammatory Activities of Coptosapelta flavescens Korth Root's Methanol Extract. *Journal of Applied Pharmaceutical Science* **8**: 42-48.

Kougan, G. B., Miyamoto, T., Tanaka, C., Paululat, T., Mirjolet, J.-F., Duchamp, O., Sondengam, B. L. and Lacaille-Dubois, M.-A. (2010). Steroidal saponins from two species of Dracaena. *Journal of Natural Products* **73**: 1266-1270.

Kuete, V., Mbaveng, A. T., Sandjo, L. P., Zeino, M. and Efferth, T. (2017). Cytotoxicity and mode of action of a naturally occurring naphthoquinone, 2-acetyl-7-methoxynaphtho [2, 3-b] furan-4, 9-quinone towards multi-factorial drug-resistant cancer cells. *Phytomedicine* **33**: 62-68.

Kuete, V., Sandjo, L. P., Wiench, B. and Efferth, T. (2013a). Cytotoxicity and modes of action of four Cameroonian dietary spices ethno-medically used to treat cancers: Echinops giganteus, Xylopia aethiopica, Imperata cylindrica and Piper capense. *Journal of Ethnopharmacology* **149**: 245-253.

Kuete, V., Tchakam, P. D., Wiench, B., Ngameni, B., Wabo, H. K., Tala, M. F., Moungang, M. L., Ngadjui, B. T., Murayama, T. and Efferth, T. (2013b). Cytotoxicity and modes of action

of four naturally occuring benzophenones: 2, 2′, 5, 6′-tetrahydroxybenzophenone, guttiferone E, isogarcinol and isoxanthochymol. *Phytomedicine* **20**: 528-536.

Kuo, P.-C., Yang, M.-L., Wu, P.-L., Shih, H.-N., Thang, T. D., Dung, N. X. and Wu, T.-S. (2008). Chemical constituents from Abutilon indicum. *Journal of Asian natural products research* **10**: 689-693.

Kwon, D.-J. and Bae, Y.-S. (2011). Chemical constituents from the stem bark of Acer barbinerve. *Chemistry of natural compounds* **47**: 636-638.

Lacroix, D., Prado, S., Kamoga, D., Kasenene, J., Namukobe, J., Krief, S., Dumontet, V., Mouray, E., Bodo, B. and Brunois, F. (2011). Antiplasmodial and cytotoxic activities of medicinal plants traditionally used in the village of Kiohima, Uganda. *Journal of Ethnopharmacology* **133**: 850-855.

Lang, G.-Z., Li, C.-J., Gaohu, T.-Y., Li, C., Ma, J., Yang, J.-Z., Zhou, T.-T., Yuan, Y.-H., Ye, F. and Wei, J.-H. (2020). Bioactive flavonoid dimers from Chinese dragon's blood, the red resin of Dracaena cochinchinensis. *Bioorganic Chemistry* **97**: 103659.

Lanzotti, V., Barile, E., Antignani, V., Bonanomi, G. and Scala, F. (2012). Antifungal saponins from bulbs of garlic, Allium sativum L. var. Voghiera. *Phytochemistry* **78**: 126-134.

Lawrence, T. and Gilroy, D. W. (2007). Chronic inflammation: a failure of resolution? *International journal of experimental pathology* **88**: 85-94.

Lee, Y.-Y., Kwon, S.-H., Kim, H.-J., Park, H.-J., Yang, E.-J., Kim, S.-K., Yoon, Y.-H., Kim, C.-G., Park, J.-W. and Song, K.-S. (2009). Isolation of oleanane triterpenes and trans-resveratrol from the root of peanut (Arachis hypogaea). *Journal of the Korean Society For Applied Biological Chemistry* **52**: 40-44.

Lesjak, M., Beara, I., Simin, N., Pintać, D., Majkić, T., Bekvalac, K., Orčić, D. and Mimica-Dukić, N. (2018). Antioxidant and anti-inflammatory activities of quercetin and its derivatives. *Journal of Functional Foods* **40**: 68-75.

Li, C.-X., Song, X.-Y., Zhao, W.-Y., Yao, G.-D., Lin, B., Huang, X.-X., Li, L.-Z. and Song, S.-J. (2019). Characterization of enantiomeric lignanamides from Solanum nigrum L. and their neuroprotective effects against MPP+-induced SH-SY5Y cells injury. *Phytochemistry* **161**: 163-171.

Li, F., Awale, S., Tezuka, Y. and Kadota, S. (2008). Cytotoxic constituents from Brazilian red propolis and their structure–activity relationship. *Bioorganic & Medicinal Chemistry* **16**: 5434-5440.

Li, F., Wang, Y., Parkin, K. L., Nitteranon, V., Liang, J., Yang, W., Li, Y., Zhang, G. and Hu, Q. (2011). Isolation of quinone reductase (QR) inducing agents from ginger rhizome and their in vitro anti-inflammatory activity. *Food research international* **44**: 1597-1603.

Li, N., Ma, Z., Li, M., Xing, Y. and Hou, Y. (2014). Natural potential therapeutic agents of neurodegenerative diseases from the traditional herbal medicine Chinese Dragon′ s Blood. *Journal of Ethnopharmacology* **152**: 508-521.

Li, Y.-S., Wang, J.-X., Jia, M.-M., Liu, M., Li, X.-J. and Tang, H.-B. (2012). Dragon’s blood inhibits chronic inflammatory and neuropathic pain responses by blocking the synthesis and release of substance P in rats. *Journal of Pharmacological Sciences* **118**: 43-54.

Liang, S., Shen, Y.-H., Feng, Y., Tian, J.-M., Liu, X.-H., Xiong, Z. and Zhang, W.-D. (2010). Terpenoids from Daphne aurantiaca and their potential anti-inflammatory activity. *Journal of Natural Products* **73**: 532-535.

Lin, L.-G., Liu, Q.-Y. and Ye, Y. (2014). Naturally occurring homoisoflavonoids and their pharmacological activities. *Planta medica* **80**: 1053-1066.

Liu, H., Lv, L. and Yang, K. (2015). Chemotherapy targeting cancer stem cells. *American journal of cancer research* **5**: 880–893.

Liu, J., Dai, H.-F., Wu, J., Zeng, Y.-B. and Mei, W.-L. (2008). Flavanes from Dracaena cambodiana. *Zeitschrift für Naturforschung B* **63**: 1407-1410.

Liu, J., Mei, W.-L., Wu, J., Zhao, Y.-X., Peng, M. and Dai, H.-F. (2009). A new cytotoxic homoisoflavonoid from Dracaena cambodiana. *Journal of Asian natural products research* **11**: 192-195.

Liu, Q.-L., Chen, A.-H., Tang, J.-Y., Ma, Y.-L., Jiang, Z.-H., Liu, Y.-P., Chen, G.-Y., Fu, Y.-H. and Xu, W. (2017). A new indole alkaloid with anti-inflammatory activity from Nauclea officinalis. *Natural product research* **31**: 2107-2112.

Liu, X., Zhang, H., Niu, X.-F., Xin, W. and Qi, L. (2012). Steroidal saponins from Smilacina japonica. *Fitoterapia* **83**: 812-816.

Long, C., Sauleau, P., David, B., Lavaud, C., Cassabois, V., Ausseil, F. and Massiot, G. (2003). Bioactive flavonoids of Tanacetum parthenium revisited. *Phytochemistry* **64**: 567-569.

Lu, P.-L. and Morden, C. (2010). Phylogenetics of the plant genera Dracaena and Pleomele (Asparagaceae). *Botanica Orientalis: Journal of Plant Science* **7**: 64-72.

Lu, P.-L. and Morden, C. W. (2014). Phylogenetic relationships among Dracaenoid genera (Asparagaceae: Nolinoideae) inferred from chloroplast DNA loci. *Systematic Botany* **39**: 90-104.

Luo, Y., Dai, H.-F., Wang, H. and Mei, W.-L. (2011b). Chemical Constituents from Dragon's Blood of Dracaena cambodiana. *Chinese Journal of Natural Medicines* **9**: 112-114.

Luo, Y., Shen, H.-Y., Zuo, W.-J., Wang, H., Mei, W.-L. and Dai, H.-F. (2015). A new steroidal saponin from dragon's blood of Dracaena cambodiana. *Journal of Asian natural products research* **17**: 409-414.

Luo, Y., Wang, H., Zhao, Y.-X., Zeng, Y.-B., Shen, H.-Y., Dai, H.-F. and Mei, W.-L. (2011a). Cytotoxic and antibacterial flavonoids from dragon's blood of Dracaena cambodiana. *Planta medica* **77**: 2053-2056.

Manthey, J. A., Guthrie, N. and Grohmann, K. (2001). Biological properties of citrus flavonoids pertaining to cancer and inflammation. *Current medicinal chemistry* **8**: 135-153.

Masaoud, M., Himmelreich, U., Ripperger, H. and Adam, G. (1995b). New biflavonoids from dragon's blood of Dracaena cinnabari. *Planta medica* **61**: 341-344.

Masaoud, M., Ripperger, H., Porzel, A. and Adam, G. (1995a). Flavonoids of dragon's blood from Dracaena cinnabari. *Phytochemistry* **38**: 745-749.

Medić-Šarić, M., Jasprica, I., Smolčić-Bubalo, A. and Mornar, A. (2004). Optimization of chromatographic conditions in thin layer chromatography of flavonoids and phenolic acids. *Croatica Chemica Acta* **77**: 361-366.

Meng, C.-W., Peng, C., Zhou, Q.-m., Yang, H., Guo, L. and Xiong, L. (2015). Spirostanols from the roots and rhizomes of Trillium tschonoskii. *Phytochemistry Letters* **14**: 134-137.

Middleton, E., Kandaswami, C. and Theoharides, T. C. (2000). The effects of plant flavonoids on mammalian cells: implications for inflammation, heart disease, and cancer. *Pharmacological reviews* **52**: 673-751.

Mimaki, Y., Kuroda, M., Takaashi, Y. and Sashida, Y. (1997). Concinnasteoside A, a New Bisdesmosidic Cholestane Glycoside from the Stems of Dracaena concinna. *Journal of Natural Products* **60**: 1203-1206.

Min, X., Yang, C. R. and Zhang, Y. J. (2010). New C27 steroidal bisdesmosides from the fresh stems of Dracaena cambodiana. *Helvetica Chimica Acta* **93**: 302-308.

Mirossay, L., Varinská, L. and Mojžiš, J. (2018). Antiangiogenic effect of flavonoids and chalcones: An update. *International Journal of Molecular Sciences* **19**: 27.

Mishra, B. B. and Tiwari, V. K. (2011). Natural products: an evolving role in future drug discovery. *European Journal of Medicinal Chemistry* **46**: 4769-4807.

Modi, C., Mody, S., Patel, H., Dudhatra, G., Kumar, A. and Avale, M. (2012). Toxicopathological overview of analgesic and anti-inflammatory drugs in animals. *Journal of Applied Pharmaceutical Science* **2**: 149-157.

Mortensen, M. E., Cecalupo, A. J., Lo, W. D., Egorin, M. J. and Batley, R. (1992). Inadvertent intrathecal injection of daunorubicin with fatal outcome. *Pediatric Blood & Cancer* **20**: 249-253.

Moshi, M. J., Otieno, D. F. and Weisheit, A. (2012). Ethnomedicine of the Kagera Region, north western Tanzania. Part 3: plants used in traditional medicine in Kikuku village, Muleba District. *Journal of Ethnobiology and Ethnomedicine* **8**: 1-11.

Muhammad, A., Anis, I., Khan, A., Marasini, B. P., Choudhary, M. I. and Shah, M. R. (2012). Biologically active C-alkylated flavonoids from Dodonaea viscosa. *Archives of pharmacal research* **35**: 431-436.

Mukavi, J., Omosa, L. K., Nchiozem-Ngnitedem, V.-A., Nyaga, J., Omole, R., Bitchagno, G. T. M. and Spiteller, M. (2020). Anti-inflammatory norhopanes from the root bark of Fagaropsis angolensis (Engl.) HM Gardner. *Fitoterapia*: 104690.

Mukazayire, M.-J., Minani, V., Ruffo, C. K., Bizuru, E., Stévigny, C. and Duez, P. (2011). Traditional phytotherapy remedies used in Southern Rwanda for the treatment of liver diseases. *Journal of Ethnopharmacology* **138**: 415-431.

Mulholland, D. A., Schwikkard, S. L. and Crouch, N. R. (2013). The chemistry and biological activity of the Hyacinthaceae. *Natural Product Reports* **30**: 1165-1210.

Nayak, A. K., Mallick, S. and Babu, B. K. (2019). First report of Aspergillus terreus causing sunken leaf spot on Dracaena aletriformis in India. *Australasian Plant Pathology*: 1-3.

Newman, D. J. and Cragg, G. M. (2007). Natural products as sources of new drugs over the last 25 years. *Journal of Natural Products* **70**: 461-477.

Ning, L., Zhang, J.-Y., Zeng, K.-W., Zhang, L., Che, Y.-Y. and Tu, P.-F. (2012). Anti-inflammatory homoisoflavonoids from the tuberous roots of Ophiopogon japonicus. *Fitoterapia* **83**: 1042-1045.

Nobakht, M., Grkovic, T., Trueman, S. J., Wallace, H. M., Katouli, M., Quinn, R. J. and Brooks, P. R. (2014). Chemical constituents of kino extract from Corymbia torelliana. *Molecules* **19**: 17862-17871.

Noumi, E., Zollo, A. and Lontsi, D. (1998). Aphrodisiac plants used in Cameroon. *Fitoterapia (Milano)* **69**: 125-134.

Nyaboke, H. O., Moraa, M., Omosa, L. K., Mbaveng, A. T., Vaderament-Alexe, N.-N., Masila, V., Okemwa, E., Heydenreich, M., Efferth, T. and Kuete, V. (2018). Cytotoxicity of lupeol from the stem bark of Zanthoxylum gilletii against multi-factorial drug resistant cancer cell lines. *Invest Med Chem Pharmacol* **1**: 10.

O'brien, J., Wilson, I., Orton, T. and Pognan, F. (2000). Investigation of the Alamar Blue (resazurin) fluorescent dye for the assessment of mammalian cell cytotoxicity. *European Journal of Biochemistry* **267**: 5421-5426.

Oleszek, W., Sitek, M., Stochmal, A., Piacente, S., Pizza, C. and Cheeke, P. (2001). Resveratrol and other phenolics from the bark of Yucca schidigera roezl. *Journal of Agricultural and Food Chemistry* **49**: 747-752.

Omosa, L. K., Midiwo, J. O., Masila, V. M., Gisacho, B. M., Munayi, R., Chemutai, K. P., Elhaboob, G., Saeed, M. E., Hamdoun, S. and Kuete, V. (2016). Cytotoxicity of 91 Kenyan indigenous medicinal plants towards human CCRF-CEM leukemia cells. *Journal of Ethnopharmacology* **179**: 177-196.

Owor, R. O., Bedane, K. G., Zühlke, S., Derese, S., Ong'amo, G. O., Ndakala, A. and Spiteller, M. (2020). Anti-inflammatory Flavanones and Flavones from Tephrosia linearis. *Journal of Natural Products* **83**: 996-1004.

Oyekachukwu, A., Elijah, J., Eshu, O. and Nwodo, O. (2017). Anti-inflammatory effects of the chloroform extract of Annona muricata leaves on phospholipase A2 and prostaglandin synthase activities. *Translational Biomedicine* **8**: 137.

Pabuprapap, W., Wassanatip, Y., Khetkam, P., Chaichompoo, W., Kunkaewom, S., Senabud, P., Hata, J., Chokchaisiri, R., Svasti, S. and Suksamrarn, A. (2019). Quercetin analogs with high fetal hemoglobin-inducing activity. *Medicinal Chemistry Research* **28**: 1755-1765.

Panche, A., Diwan, A. and Chandra, S. (2016). Flavonoids: an overview. *Journal of nutritional science* **5**: 1-15.

Pandey, G. and Madhuri, S. (2009). Some medicinal plants as natural anticancer agents. *Pharmacognosy Reviews* **3**: 259-266.

Pang, D.-R., Pan, B., Sun, J., Sun, H., Yao, H.-N., Song, Y.-L., Zhao, Y.-F., Tu, P.-F., Huang, W.-Z. and Zheng, J. (2018). Homoisoflavonoid derivatives from the red resin of Dracaena cochinchinensis. *Fitoterapia* **131**: 105-111.

Pang, D.-R., Su, X.-Q., Zhu, Z.-X., Sun, J., Li, Y.-T., Song, Y.-L., Zhao, Y.-F., Tu, P.-F., Zheng, J. and Li, J. (2016). Flavonoid dimers from the total phenolic extract of Chinese dragon's blood, the red resin of Dracaena cochinchinensis. *Fitoterapia* **115**: 135-141.

Paramita, S. and Kosala, K. (2017). Anti-inflammatory activities of ethno medicinal plants from Dayak Abai in North Kalimantan, Indonesia. *Indonesia. Biodiversitas* **18**: 1556-1561.

Park, C. H., Kim, K. H., Lee, I. K., Lee, S. Y., Choi, S. U., Lee, J. H. and Lee, K. R. (2011). Phenolic constituents of Acorus gramineus. *Archives of pharmacal research* **34**: 1289-1296.

Parkin, D. M., Hämmerl, L., Ferlay, J. and Kantelhardt, E. J. (2020). Cancer in Africa 2018: the role of infections. *International journal of cancer* **146**: 2089-2103.

Pathak, V., Shirota, O., Sekita, S., Hirayama, Y., Hakamata, Y., Hayashi, T., Yanagawa, T. and Satake, M. (1997). Antiandrogenic phenolic constituents from Dalbergia cochinchinensis. *Phytochemistry* **46**: 1219-1223.

Pelzer, L. E., Guardia, T., Juarez, A. O. and Guerreiro, E. (1998). Acute and chronic antiinflammatory effects of plant flavonoids. *Il Farmaco* **53**: 421-424.

Perveen, S., Yousaf, M., Zahoor, A. F., Rasool, N. and Jabber, A. (2014). Extraction, isolation, and identification of various environment friendly components from cock's comb (Celosia argentea) leaves for allelopathic potential. *Toxicological & Environmental Chemistry* **96**: 1523-1534.

Qin, X., Xing, Y. F., Zhou, Z. and Yao, Y. (2015). Dihydrochalcone compounds isolated from crabapple leaves showed anticancer effects on human cancer cell lines. *Molecules* **20**: 21193-21203.

Quang, T. H., Cuong, N. X., Van Minh, C. and Van Kiem, P. (2008). New flavonoids from Baeckea frutescens and their antioxidant activity. *Natural product communications* **3**: 755-758.

Ragasa, C. Y., De Luna, R. D. and Hofilena, J. G. (2005). Antimicrobial terpenoids from Pterocarpus indicus. *Natural product research* **19**: 305-309.

Raguz, S. and Yagüe, E. (2008). Resistance to chemotherapy: new treatments and novel insights into an old problem. *British journal of cancer* **99**: 387-391.

Rayburn, E. R., Ezell, S. J. and Zhang, R. (2009). Anti-inflammatory agents for cancer therapy. *Molecular and cellular pharmacology* **1**: 29-43.

Rey-Ladino, J., Ross, A. G., Cripps, A. W., McManus, D. P. and Quinn, R. (2011). Natural products and the search for novel vaccine adjuvants. *Vaccine* **29**: 6464-6471.

Rocca, G., Chiarandini, P. and Pietropaoli, P. (2005). Analgesia in PACU: nonsteroidal anti-inflammatory drugs. *Current drug targets* **6**: 781-787.

Roy, A. and Bharadvaja, N. (2017). Medicinal Plants in the Management of Cancer: A Review. *International Journal of Complementary & Alternative Medicine* **9**: 1-6.

Sando, Z., Fouelifack, Y. F., Fouogue, T. J., Fouedjio, J. H. and Essame-Oyono, J. L. (2015). Trends in breast and cervical cancer incidence in Cameroon (Central Africa) from 2004 to 2011Incidences des cancers du sein et du col de l'utérus au Cameroun: évolution sur 8 ans (2004–2011). *Journal Africain du Cancer/African Journal of Cancer* **7**: 118-121.

Sathiamoorthy, B., Gupta, P., Kumar, M., Chaturvedi, A. K., Shukla, P. and Maurya, R. (2007). New antifungal flavonoid glycoside from Vitex negundo. *Bioorganic & medicinal chemistry letters* **17**: 239-242.

Schäfer, H. and Wink, M. (2009). Medicinally important secondary metabolites in recombinant microorganisms or plants: progress in alkaloid biosynthesis. *Biotechnology Journal: Healthcare Nutrition Technology* **4**: 1684-1703.

Seshadri, T. and Vydeeswaran, S. (1972). Chrysoeriol glycosides and other flavonoids of Rungia repens flowers. *Phytochemistry* **11**: 803-806.

Shaikh, R., Pund, M., Dawane, A. and Iliyas, S. (2014). Evaluation of anticancer, antioxidant, and possible anti-inflammatory properties of selected medicinal plants used in Indian traditional medication. *Journal of traditional and complementary medicine* **4**: 253-257.

Shaikh, R. U., Pund, M. M. and Gacche, R. N. (2016). Evaluation of anti-inflammatory activity of selected medicinal plants used in Indian traditional medication system in vitro as well as in vivo. *Journal of traditional and complementary medicine* **6**: 355-361.

Shen, C.-C., Tsai, S.-Y., Wei, S.-L., Wang, S.-T., Shieh, B.-J. and Chen, C.-C. (2007). Flavonoids isolated from draconis resina. *Natural product research* **21**: 377-380.

Shen, H.-Y., Zuo, W.-J., Wang, H., Zhao, Y.-X., Guo, Z.-K., Luo, Y., Li, X.-N., Dai, H.-F. and Mei, W.-L. (2014). Steroidal saponins from dragon's blood of Dracaena cambodiana. *Fitoterapia* **94**: 94-101.

Singh, S., Pandey, M., Singh, A., Singh, U. and Pandey, V. (2008). A new chalcone glycoside from Rhamnus nipalensis. *Natural product research* **22**: 1657-1659.

Siyu, W., Suh, J. H., Zheng, X., Wang, Y. and Ho, C.-T. (2017). Identification and quantification of potential anti-inflammatory hydroxycinnamic acid amides from wolfberry. *Journal of Agricultural and Food Chemistry* **65**: 364-372.

Slade, D., Ferreira, D. and Marais, J. P. (2005). Circular dichroism, a powerful tool for the assessment of absolute configuration of flavonoids. *Phytochemistry* **66**: 2177-2215.

Song, Y. H., Kim, D. W., Curtis-Long, M. J., Park, C., Son, M., Kim, J. Y., Yuk, H. J., Lee, K. W. and Park, K. H. (2016). Cinnamic acid amides from Tribulus terrestris displaying uncompetitive α-glucosidase inhibition. *European Journal of Medicinal Chemistry* **114**: 201-208.

Soni, M., Taylor, S., Greenberg, N. and Burdock, G. (2002). Evaluation of the health aspects of methyl paraben: a review of the published literature. *Food and Chemical Toxicology* **40**: 1335-1373.

Souto, A. L., Tavares, J. F., Da Silva, M. S., Diniz, M. d. F. F. M., Athayde-Filho, D., Filgueiras, P. and Barbosa Filho, J. M. (2011). Anti-inflammatory activity of alkaloids: an update from 2000 to 2010. *Molecules* **16**: 8515-8534.

Spagnuolo, C., Moccia, S. and Russo, G. L. (2018). Anti-inflammatory effects of flavonoids in neurodegenerative disorders. *European Journal of Medicinal Chemistry* **153**: 105-115.

Stevigny, C., Bailly, C. and Quetin-Leclercq, J. (2005). Cytotoxic and antitumor potentialities of aporphinoid alkaloids. *Current Medicinal Chemistry-Anti-Cancer Agents* **5**: 173-182.

Su, X.-Q., Song, Y.-L., Zhang, J., Huo, H.-X., Huang, Z., Zheng, J., Zhang, Q., Zhao, Y.-F., Xiao, W. and Li, J. (2014). Dihydrochalcones and homoisoflavanes from the red resin of Dracaena cochinchinensis (Chinese dragon's blood). *Fitoterapia* **99**: 64-71.

Sun, J., Huo, H.-X., Zhang, J., Huang, Z., Zheng, J., Zhang, Q., Zhao, Y.-F., Li, J. and Tu, P.-F. (2015). Phenylpropanoid amides from the roots of Solanum melongena L.(Solanaceae). *Biochemical systematics and ecology* **58**: 265-269.

Sun, J., Liu, J.-N., Fan, B., Chen, X.-N., Pang, D.-R., Zheng, J., Zhang, Q., Zhao, Y.-F., Xiao, W. and Tu, P.-F. (2019). Phenolic constituents, pharmacological activities, quality control, and metabolism of Dracaena species: A review. *Journal of Ethnopharmacology* **244**: 112138.

Tang, Y., Su, G., Li, N., Li, W., Chen, G., Chen, R., Zhou, D. and Hou, Y. (2019). Preventive agents for neurodegenerative diseases from resin of Dracaena cochinchinensis attenuate LPS-induced microglia over-activation. *Journal of natural medicines* **73**: 318-330.

Taniguchi, K. and Karin, M. (2014). IL-6 and related cytokines as the critical lynchpins between inflammation and cancer. *Seminars in Immunology* **26**: 54-74. .

Tapondjou, L. A., Ponou, K. B., Teponno, R. B., Mbiantcha, M., Djoukeng, J. D., Nguelefack, T. B., Watcho, P., Cadenas, A. G. and Park, H.-J. (2008). In vivo anti-inflammatory effect of a new steroidal saponin, mannioside A, and its derivatives isolated from Dracaena mannii. *Archives of pharmacal research* **31**: 653-658.

Teponno, R. B., Dzoyem, J. P., Nono, R. N., Kauhl, U., Sandjo, L. P., Tapondjou, L. A., Bakowsky, U. and Opatz, T. (2017). Cytotoxicity of Secondary Metabolites from Dracaena viridiflora Engl & Krause and their Semisynthetic Analogues. *Records of Natural Products* **11**: 421-430.

Teponno, R. B., Tapondjou, A. L., Djoukeng, J. D., Abou-Mansour, E., Tabacci, R., Tane, P., Lontsi, D. and Park, H.-J. (2006). Isolation and NMR assignment of a pennogenin glycoside from Dioscorea bulbifera L. var sativa. *Natural Product Sciences* **12**: 62-66.

Thiengsusuk, A., Chaijaroenkul, W. and Na-Bangchang, K. (2013). Antimalarial activities of medicinal plants and herbal formulations used in Thai traditional medicine. *Parasitology research* **112**: 1475-1481.

Thu, Z. M., Myo, K. K., Aung, H. T., Armijos, C. and Vidari, G. (2020). Flavonoids and Stilbenoids of the Genera Dracaena and Sansevieria: Structures and Bioactivities. *Molecules* **25**: 1-26.

Thun, M. J., DeLancey, J. O., Center, M. M., Jemal, A. and Ward, E. M. (2010). The global burden of cancer: priorities for prevention. *Carcinogenesis* **31**: 100-110.

Thun, M. J., Henley, S. J. and Patrono, C. (2002). Nonsteroidal anti-inflammatory drugs as anticancer agents: mechanistic, pharmacologic, and clinical issues. *Journal of the National Cancer Institute* **94**: 252-266.

Topazian, H., Cira, M., Dawsey, S. M., Kibachio, J., Kocholla, L., Wangai, M., Welch, J., Williams, M. J., Duncan, K. and Galassi, A. (2016). Joining forces to overcome cancer: the Kenya cancer research and control stakeholder program. *Journal of cancer policy* **7**: 36-41.

Touil, A., Rhouati, S. and Creche, J. (2006). Flavonoid glycosides from Pituranthos chloranthus. *Chemistry of natural compounds* **42**: 104-105.

Tran, Q. L., Tezuka, Y., Banskota, A. H., Tran, Q. K., Saiki, I. and Kadota, S. (2001). New Spirostanol Steroids and Steroidal Saponins from Roots and Rhizomes of Dracaena a ngustifolia and Their Antiproliferative Activity. *Journal of Natural Products* **64**: 1127-1132.

Tran, V. H., Duke, R. K., Abu-Mellal, A. and Duke, C. C. (2012). Propolis with high flavonoid content collected by honey bees from Acacia paradoxa. *Phytochemistry* **81**: 126-132.

Tressl, R., Kersten, E. and Rewicki, D. (1993). Formation of pyrroles, 2-pyrrolidones, and pyridones by heating of 4-aminobutyric acid and reducing sugars. *Journal of Agricultural and Food Chemistry* **41**: 2125-2130.

Vane, J. R., Mitchell, J. A., Appleton, I., Tomlinson, A., Bishop-Bailey, D., Croxtall, J. and Willoughby, D. A. (1994). Inducible isoforms of cyclooxygenase and nitric-oxide synthase in inflammation. *Proceedings of the National Academy of Sciences* **91**: 2046-2050.

Vazquez-Tello, A., Halwani, R., Hamid, Q. and Al-Muhsen, S. (2013). Glucocorticoid receptor-beta up-regulation and steroid resistance induction by IL-17 and IL-23 cytokine stimulation in peripheral mononuclear cells. *Journal of clinical immunology* **33**: 466-478.

Vikrant, A. and Arya, M. (2011). A review on anti-inflammatory plant barks. *International Journal of PharmTech Research* **3**: 899-908.

Vincken, J.-P., Heng, L., de Groot, A. and Gruppen, H. (2007). Saponins, classification and occurrence in the plant kingdom. *Phytochemistry* **68**: 275-297.

Volk-Draper, L., Hall, K., Griggs, C., Rajput, S., Kohio, P., DeNardo, D. and Ran, S. (2014). Paclitaxel therapy promotes breast cancer metastasis in a TLR4-dependent manner. *Cancer research* **74**: 5421-5434.

Vorobiof, D. A. and Abratt, R. (2007). The cancer burden in Africa. *South African Medical Journal* **97**: 937-939.

Waller, C. P., Thumser, A. E., Langat, M. K., Crouch, N. R. and Mulholland, D. A. (2013). COX-2 inhibitory activity of homoisoflavanones and xanthones from the bulbs of the Southern African Ledebouria socialis and Ledebouria ovatifolia (Hyacinthaceae: Hyacinthoideae). *Phytochemistry* **95**: 284-290.

Wang, Q., Li, Z., Yang, Z., Fang, Y., Ouyang, H., Liao, H., Feng, Y. and Yang, S. (2016a). New alkaloids with anti-inflammatory activities from Corydalis decumbens. *Phytochemistry Letters* **18**: 83-86.

Wang, Y., Li, C., Xiang, L., Huang, W. and He, X. (2016b). Spirostanol saponins from Chinese onion (Allium chinense) exert pronounced anti-inflammatory and anti-proliferative activities. *Journal of Functional Foods* **25**: 208-219.

Wenjie, H., Li, C., Wang, Y., Yi, X. and He, X. (2017). Anti-inflammatory lignanamides and monoindoles from Alocasia macrorrhiza. *Fitoterapia* **117**: 126-132.

WHO. (2020). WHO report on cancer: setting priorities, investing wisely and providing care for all. 13.

Witschi, H., Espiritu, I., Ly, M. and Uyeminami, D. (2005). The chemopreventive effects of orally administered dexamethasone in Strain A/J mice following cessation of smoke exposure. *Inhalation toxicology* **17**: 119-122.

Woo, W. S., Choi, J. S. and Kang, S. S. (1983). A flavonol glucoside from Typha latifolia. *Phytochemistry* **22**: 2881-2882.

Wu, T.-S., Hsu, M.-Y., Kuo, P.-C., Sreenivasulu, B., Damu, A. G., Su, C.-R., Li, C.-Y. and Chang, H.-C. (2003). Constituents from the Leaves of Phellodendron a murense var. w ilsonii and Their Bioactivity. *Journal of Natural Products* **66**: 1207-1211.

Xu, M., Zhang, Y.-J., Li, X.-C., Jacob, M. R. and Yang, C.-R. (2010). Steroidal saponins from fresh stems of Dracaena angustifolia. *Journal of Natural Products* **73**: 1524-1528.

Xu, X., Cheng, K., Cheng, W., Zhou, T., Jiang, M. and Xu, J. (2016). Isolation and chatacterization of homoisoflavonoids from Dracaena cochinchinensis and their osteogenic activities in mouse mesenchymal stem cells. *Journal of pharmaceutical and biomedical analysis* **129**: 466-472.

Xu, Y.-X., Chen, H.-S., Liang, H.-Q., Gu, Z.-B., Liu, W.-Y., Leung, W.-N. and Li, T.-J. (2000). Three new saponins from Tribulus terrestris. *Planta medica* **66**: 545-550.

Yang, D.-S., Peng, W.-B., Yang, Y.-P., Liu, K.-C., Li, X.-L. and Xiao, W.-L. (2015). Cytotoxic prenylated flavonoids from Macaranga indica. *Fitoterapia* **103**: 187-191.

Yin, S., Sykes, M. L., Davis, R. A., Shelper, T., Avery, V. M., Camp, D. and Quinn, R. J. (2010). New galloylated flavanonols from the Australian plant Glochidion sumatranum. *Planta medica* **76**: 1877-1881.

Yokosuka, A., Mimaki, Y. and Sashida, Y. (2000). Steroidal Saponins from Dracaena surculosa. *Journal of Natural Products* **63**: 1239-1243.

Yoon, J. S., Sung, S. H., Park, J. H. and Kim, Y. C. (2004). Flavonoids fromSpatholobus suberectus. *Archives of pharmacal research* **27**: 589-592.

Zaki, A. A., Ali, Z., Wang, Y.-H., El-Amier, Y. A., Khan, S. I. and Khan, I. A. (2017). Cytotoxic steroidal saponins from Panicum turgidum Forssk. *Steroids* **125**: 14-19.

Zaynab, M., Fatima, M., Abbas, S., Sharif, Y., Umair, M., Zafar, M. H. and Bahadar, K. (2018). Role of secondary metabolites in plant defense against pathogens. *Microbial pathogenesis* **124**: 198-202.

Zhang, J., Liao, X.-J., Wang, K.-L., Deng, Z. and Xu, S.-H. (2013). Cytotoxic cholesta-1, 4-dien-3-one derivatives from soft coral Nephthea sp. *Steroids* **78**: 396-400.

Zhang, L. S. and Davies, S. S. (2016). Microbial metabolism of dietary components to bioactive metabolites: opportunities for new therapeutic interventions. *Genome medicine* **8**: 1-18.

Zhang, X. (2004). Traditional medicine: its importance and protection. *Protecting and promoting traditional knowledge: systems, national experiences and international dimensions.* **1**: 3-6.

Zhao, D., Islam, M. N., Ahn, B. R., Jung, H. A., Kim, B.-W. and Choi, J. S. (2012). In vitro antioxidant and anti-inflammatory activities of Angelica decursiva. *Archives of pharmacal research* **35**: 179-192.

Zhao, T., Nong, X.-H., Zhang, B., Tang, M.-M., Huang, D.-Y., Wang, J.-L., Xiao, J.-L. and Chen, G.-Y. (2020). New flavones from the stems of Dracaena angustifolia. *Phytochemistry Letters* **36**: 115-119.

Zheng, Q.-A., Li, H.-Z., Zhang, Y.-J. and Yang, C.-R. (2006a). Dracaenogenins A and B, new spirostanols from the red resin of Dracaena cochinchinensis. *Steroids* **71**: 160-164.

Zheng, Q.-A., Zhang, Y.-J. and Yang, C.-R. (2006b). A new meta-homoisoflavane from the fresh stems of dracaena cochinchinensis: Note. *Journal of Asian natural products research* **8**: 571-577.

Zhou, L.-X. and Ding, Y. (2002). A cinnamide derivative from solanum verbascifolium L. *Journal of Asian natural products research* **4**: 185-187.

Zhu, Y., Zhang, P., Yu, H., Li, J., Wang, M.-W. and Zhao, W. (2007). Anti-Helicobacter pylori and Thrombin Inhibitory Components from Chinese Dragon's Blood, Dracaena cochinchinensis. *Journal of Natural Products* **70**: 1570-1577.

APPENDICES

Appendix 1: NMR spectra for dracaenogenin C (**176**)

Appendix 1A: HRESIMS of compound **176**

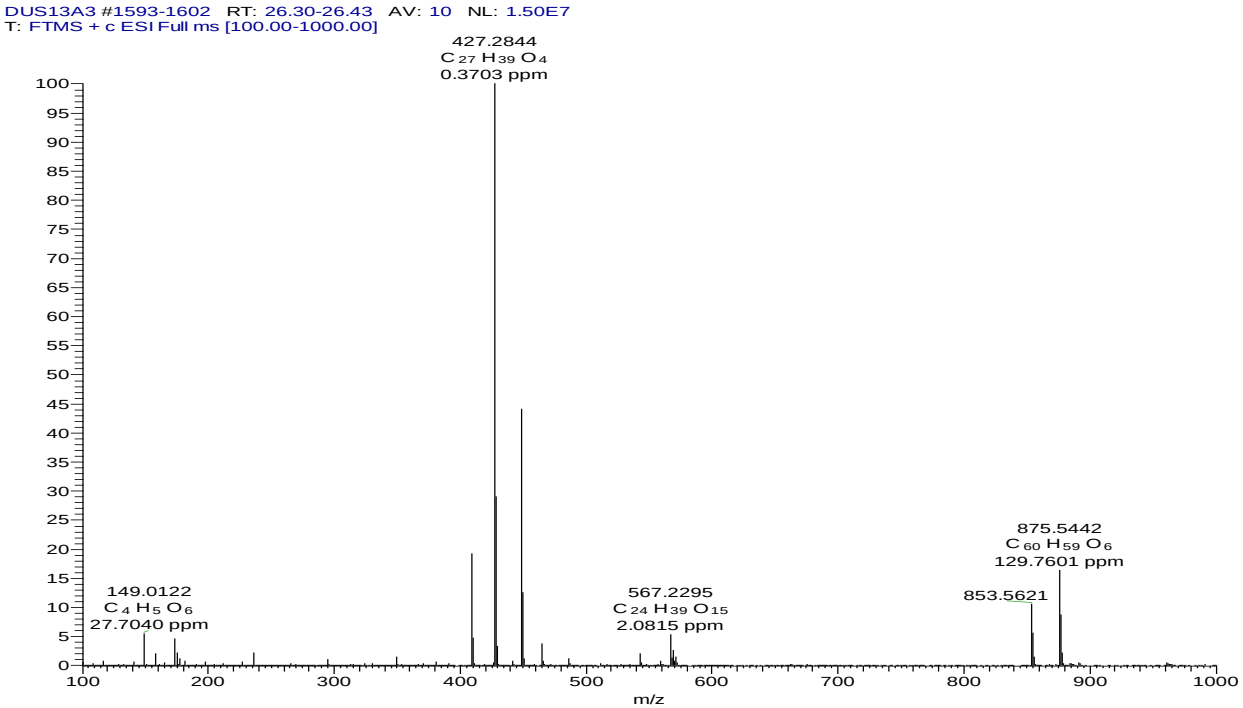

Appendix 1B: LC-UV spectrum of compound **176**

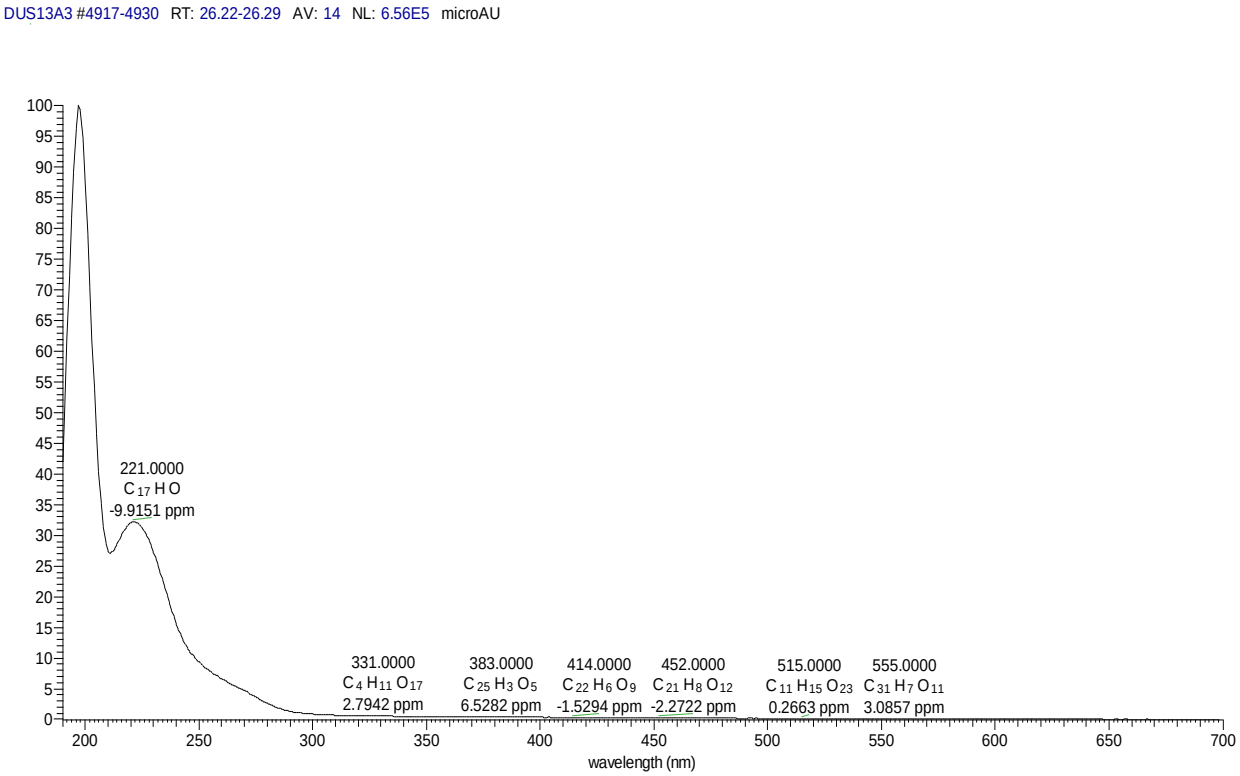

Appendix 1C: FT-IR spectrum of compound **176**

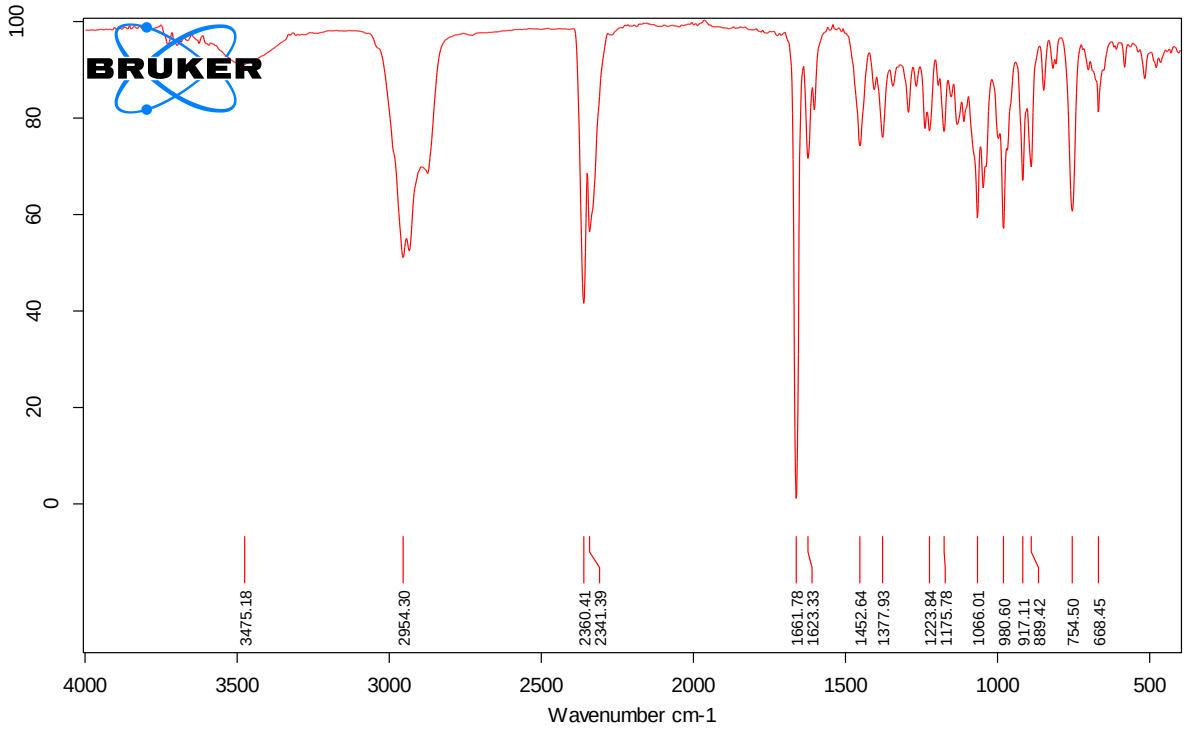

Appendix 1D: ^{1}H NMR spectrum (600 MHz, $CDCl_3$) of compound **176**

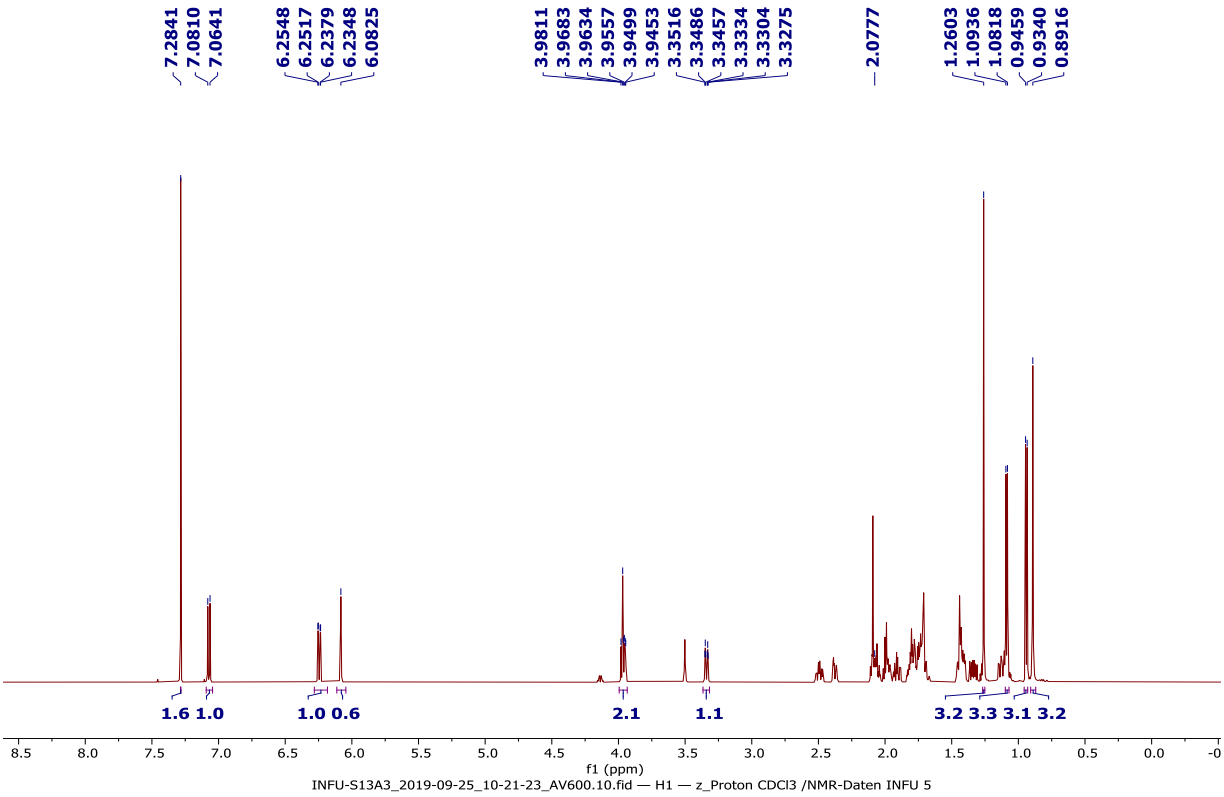

Appendix 1E: ^{13}C NMR spectrum (150 MHz, $CDCl_3$) of compound **176**

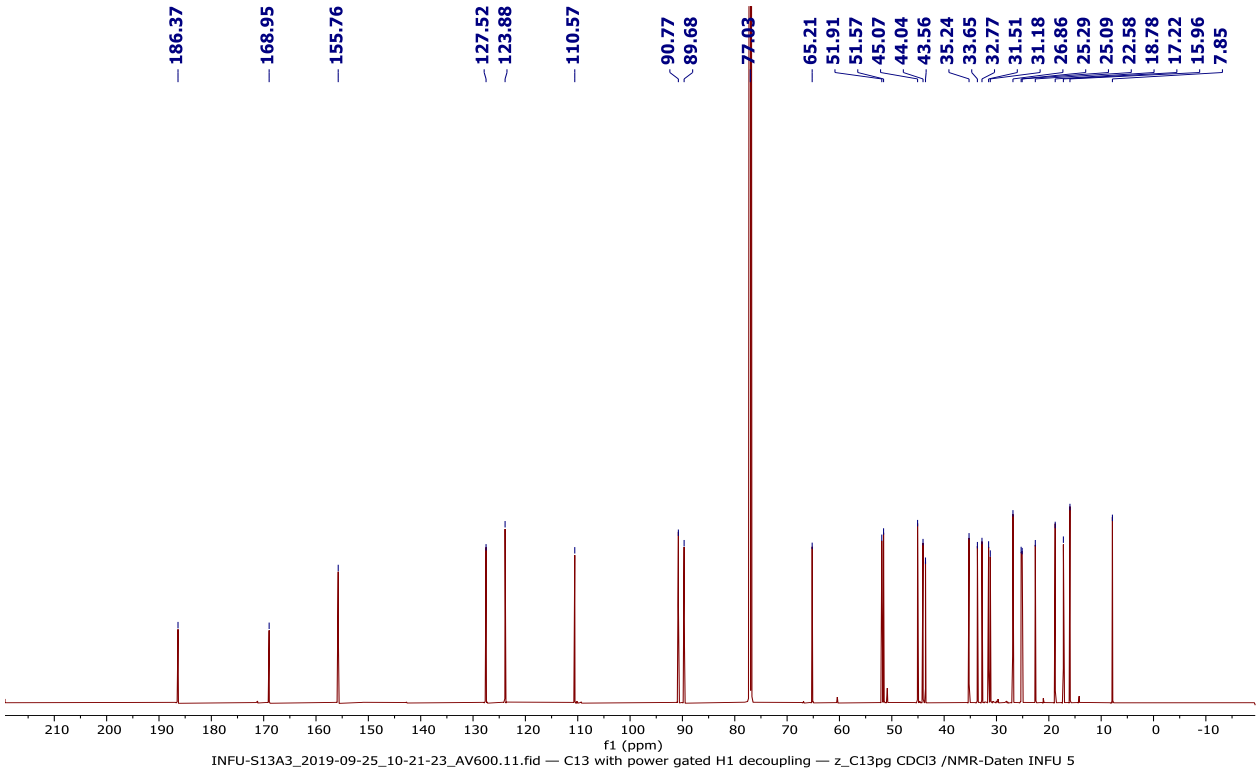

Appendix 1F: DEPT-135 spectrum (150 MHz, $CDCl_3$) of compound **176**

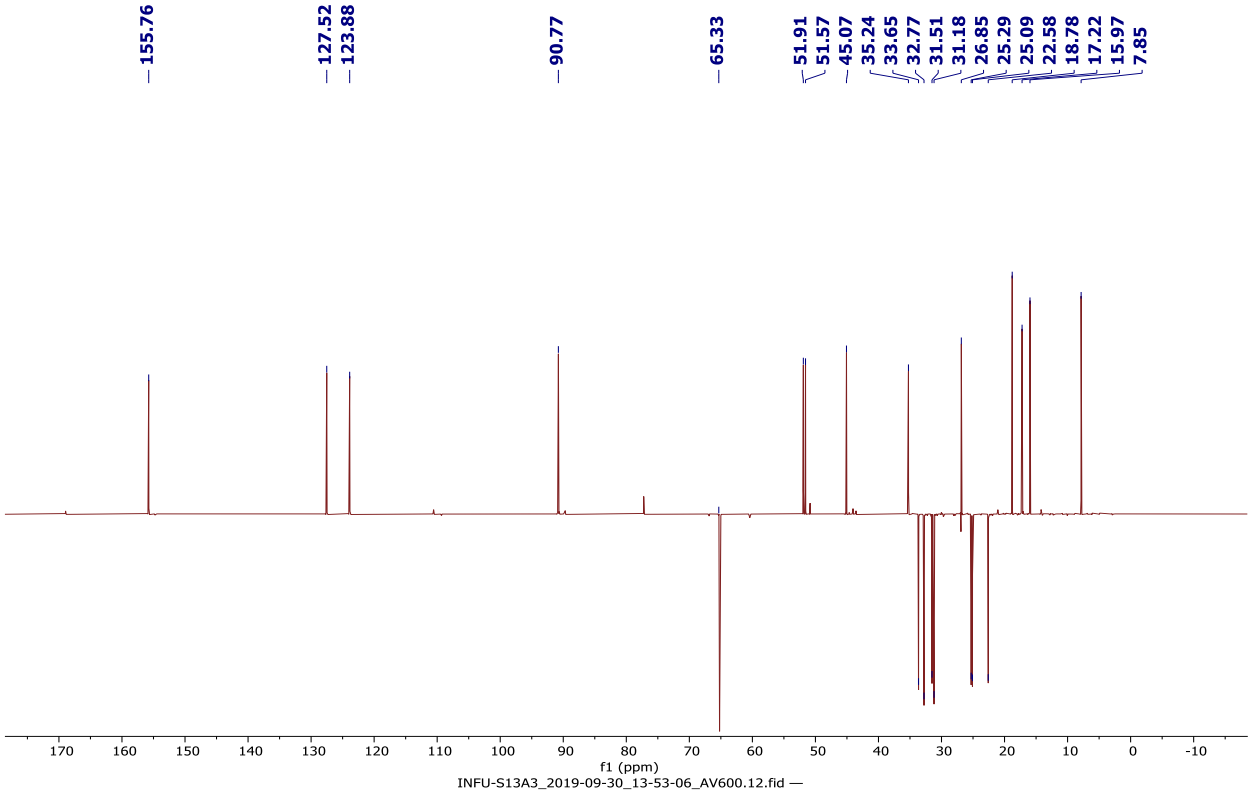

Appendix 1G: ^{1}H-^{1}H COSY spectrum ($CDCl_3$) of compound **176**

Appendix 1H: NOESY spectrum ($CDCl_3$) of compound **176**

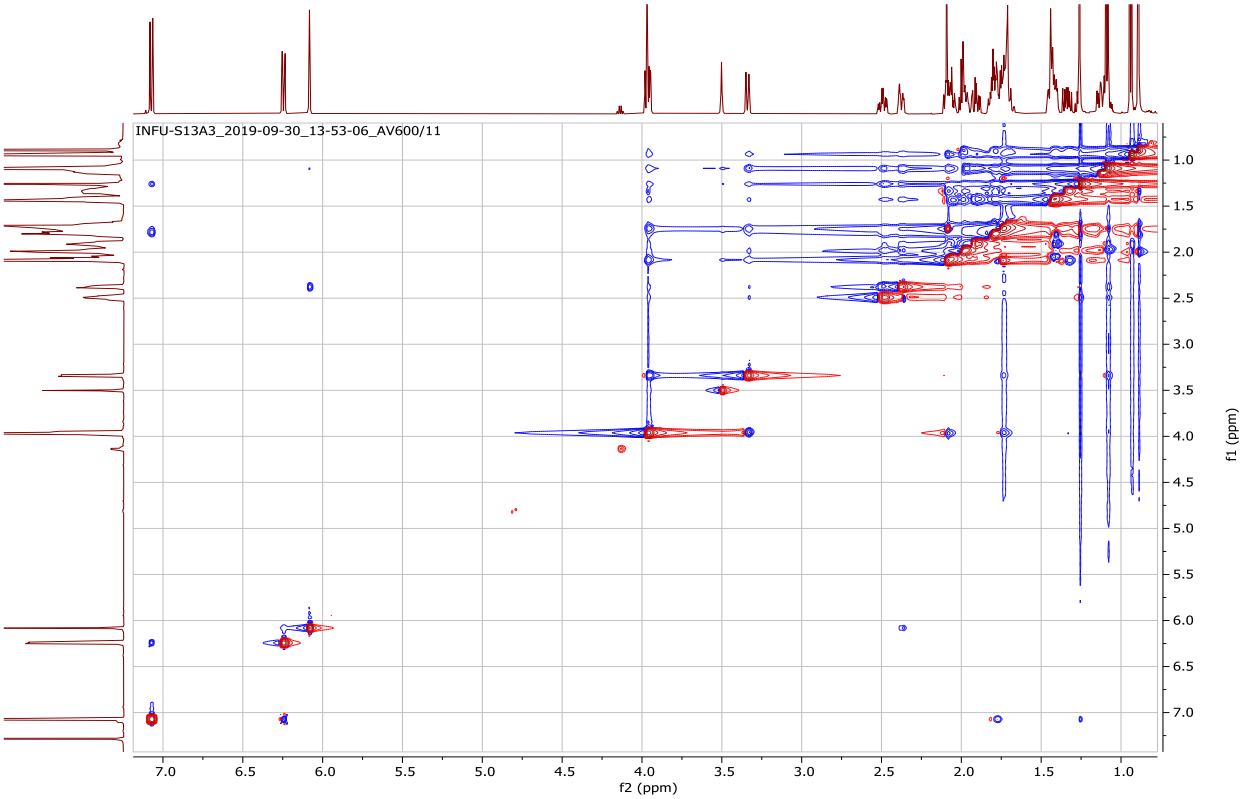

Appendix 1I: HSQC spectrum ($CDCl_3$) of compound **176**

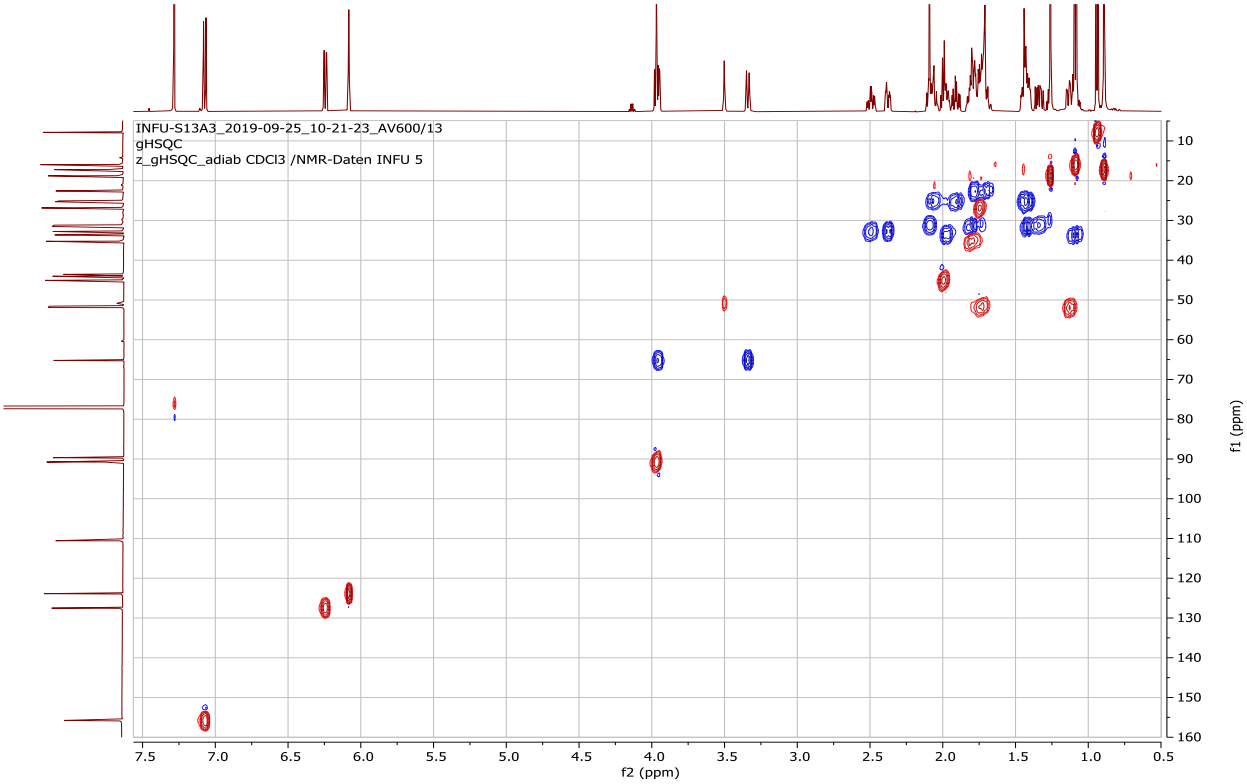

Appendix 1J: HMBC spectrum ($CDCl_3$) of compound **176**

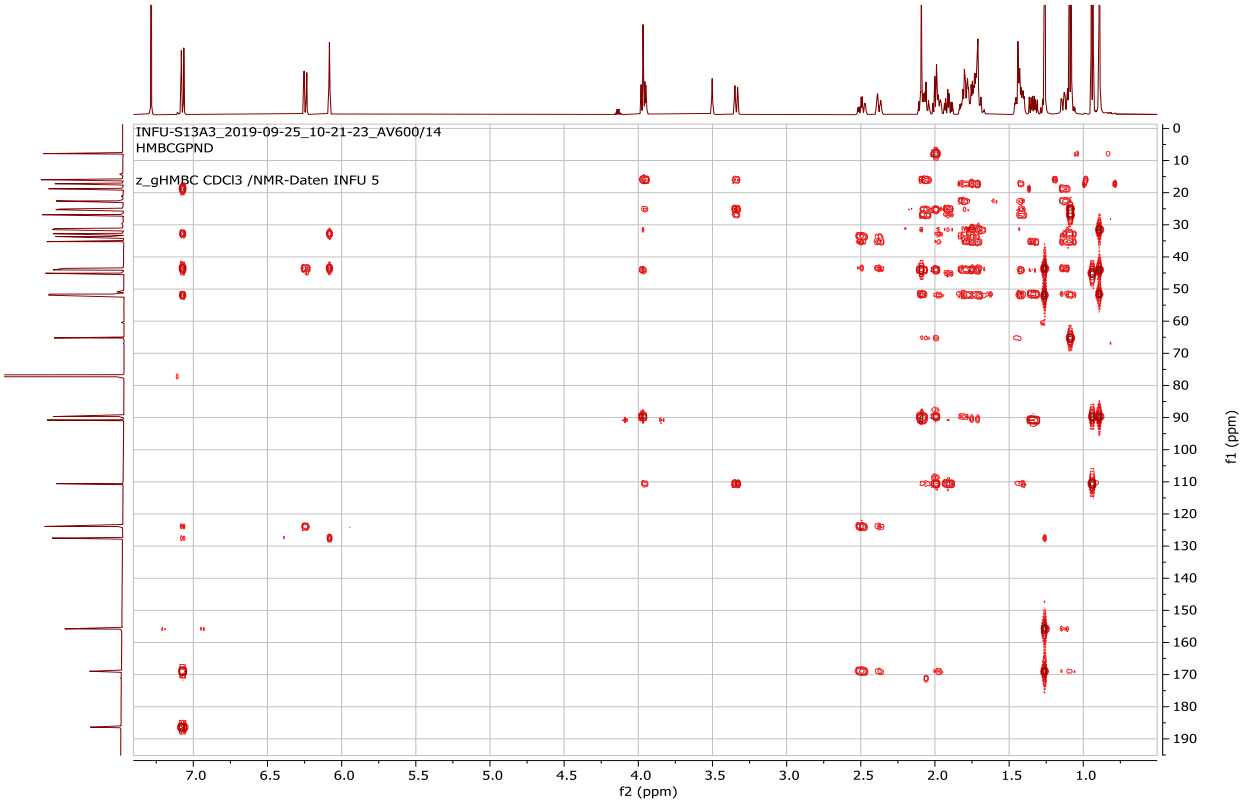

Appendix 2: NMR spectra for dracaenogenin D (**177**)

Appendix 2A: HRESIMS of compound **177**

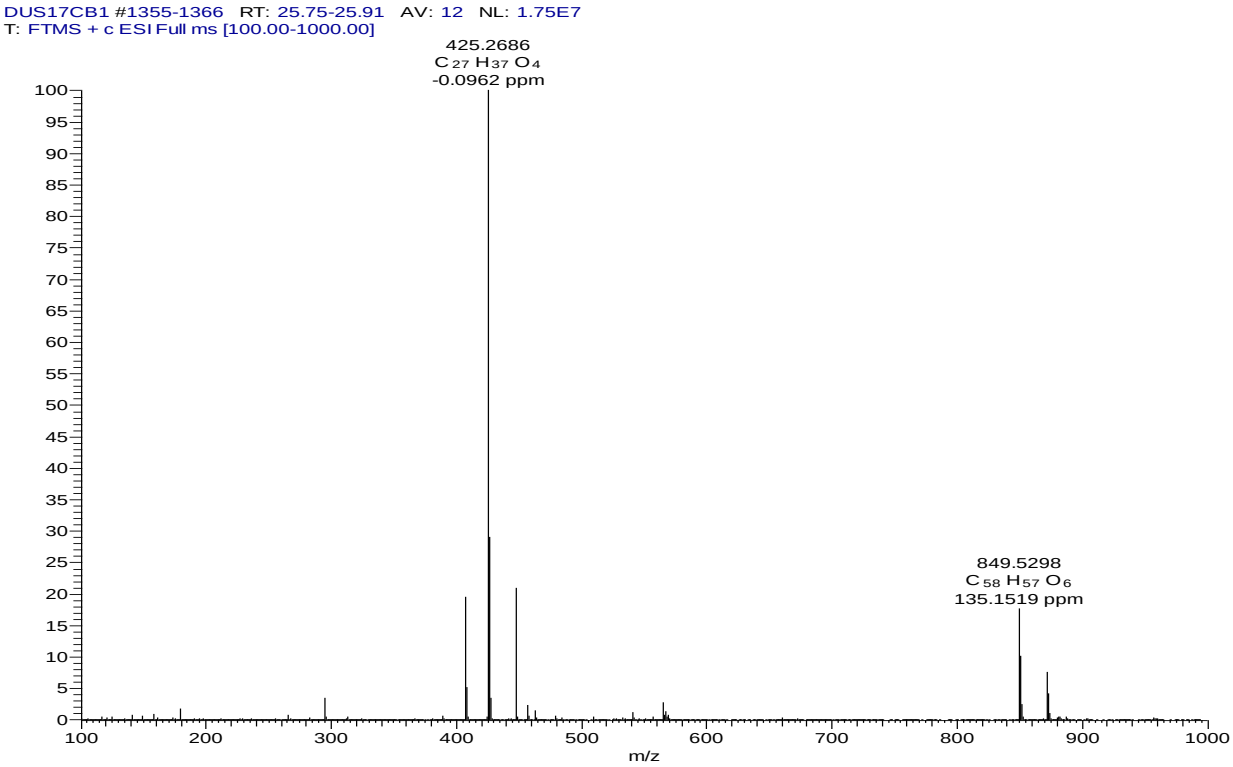

Appendix 2B: LC-UV spectrum of compound **177**

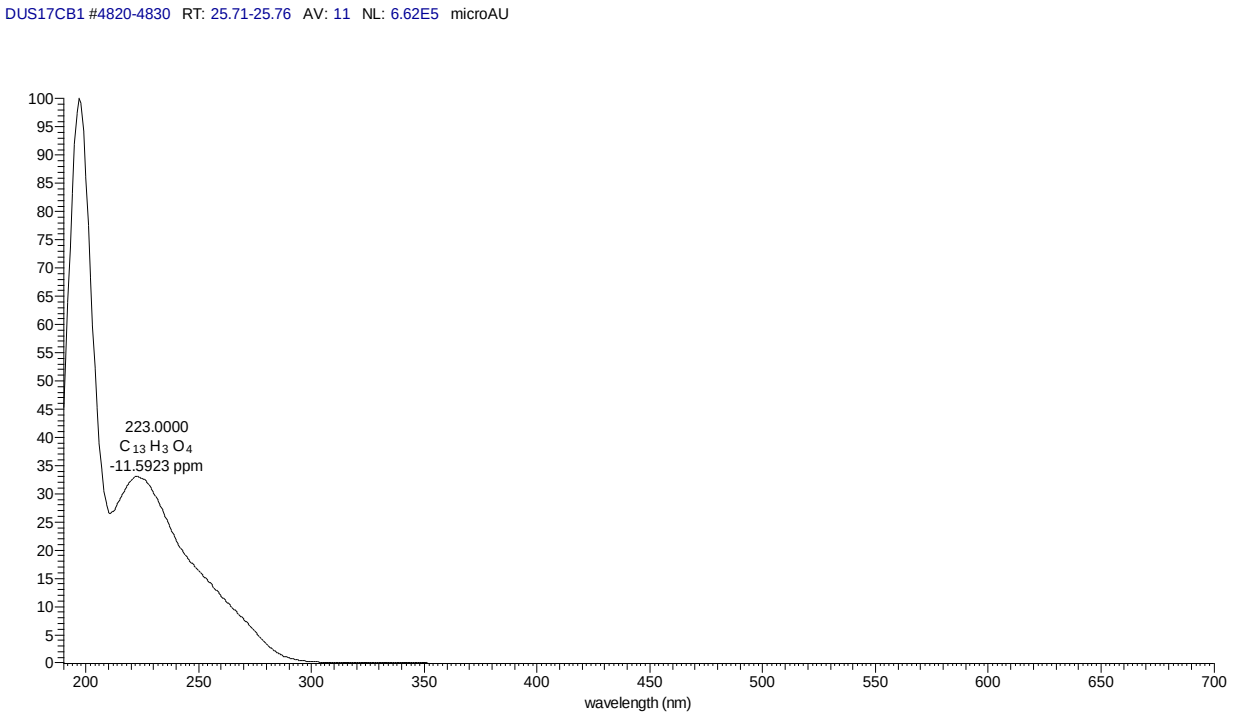

Appendix 2C: FT-IR spectrum of compound **177**

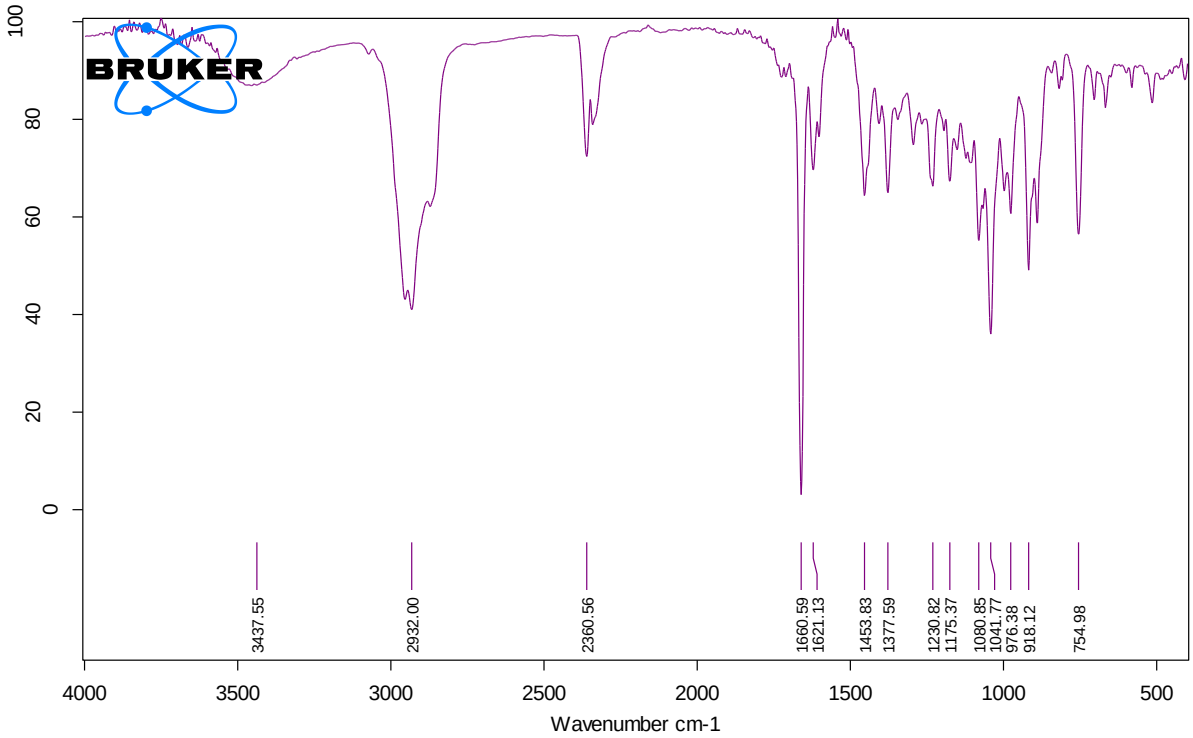

Appendix 2D: ^{1}H NMR spectrum (600 MHz, $CDCl_3$) of compound **177**

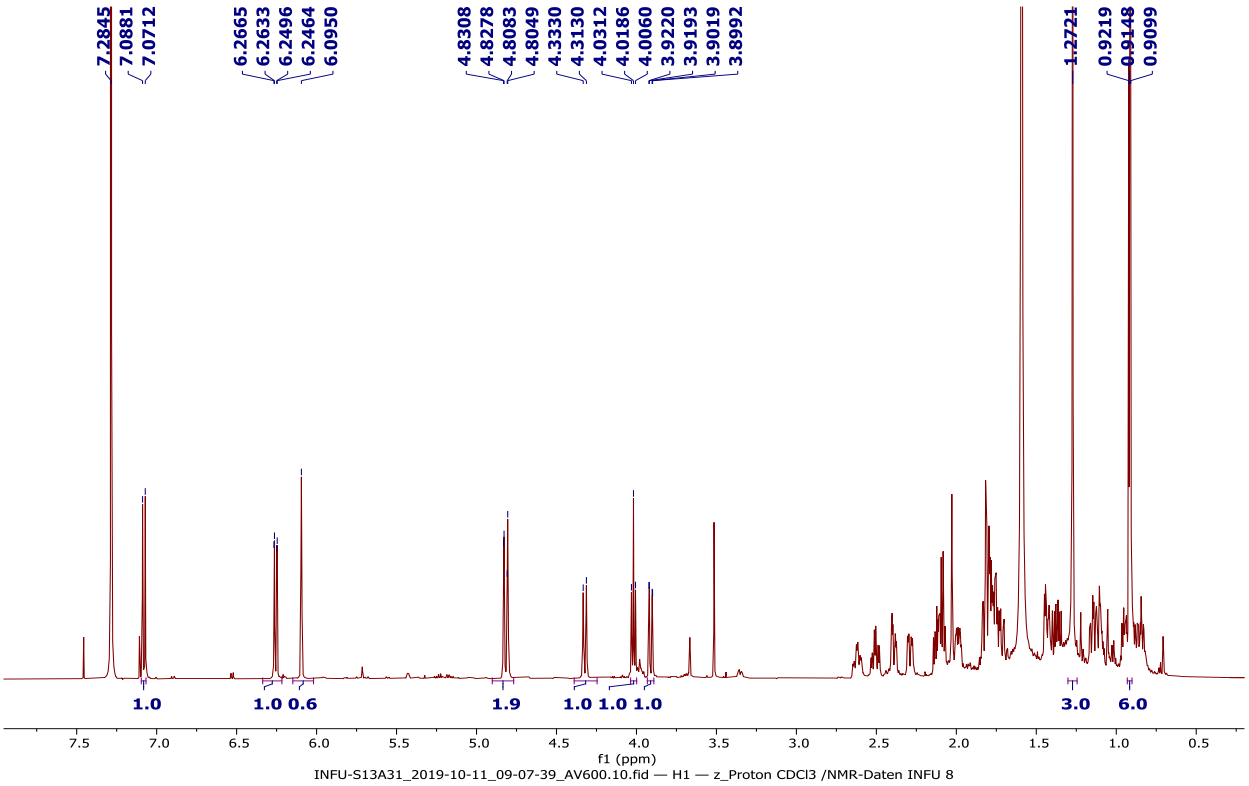

Appendix 2E: ^{13}C NMR spectrum (150 MHz, $CDCl_3$) of compound **177**

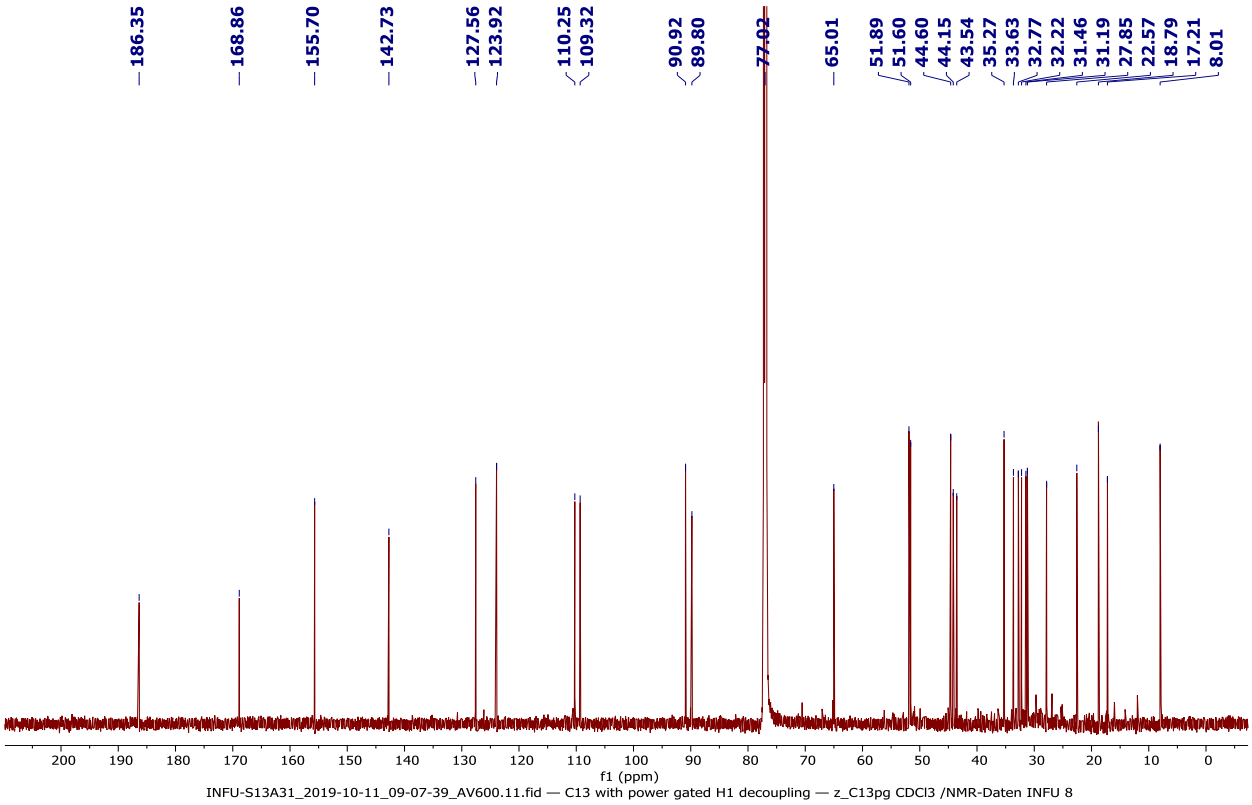

Appendix 2F: DEPT-135 spectrum (150 MHz, $CDCl_3$) of compound **177**

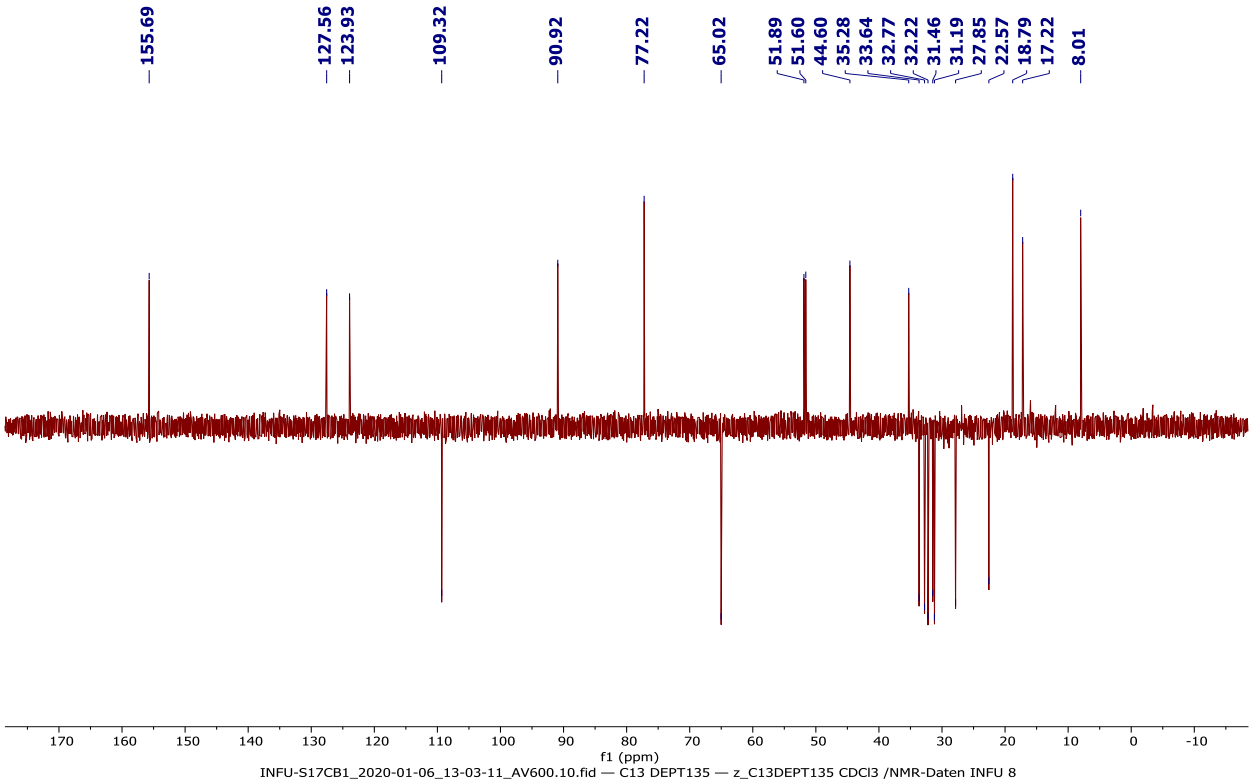

Appendix 2G: ^{1}H-^{1}H COSY spectrum ($CDCl_3$) of compound **177**

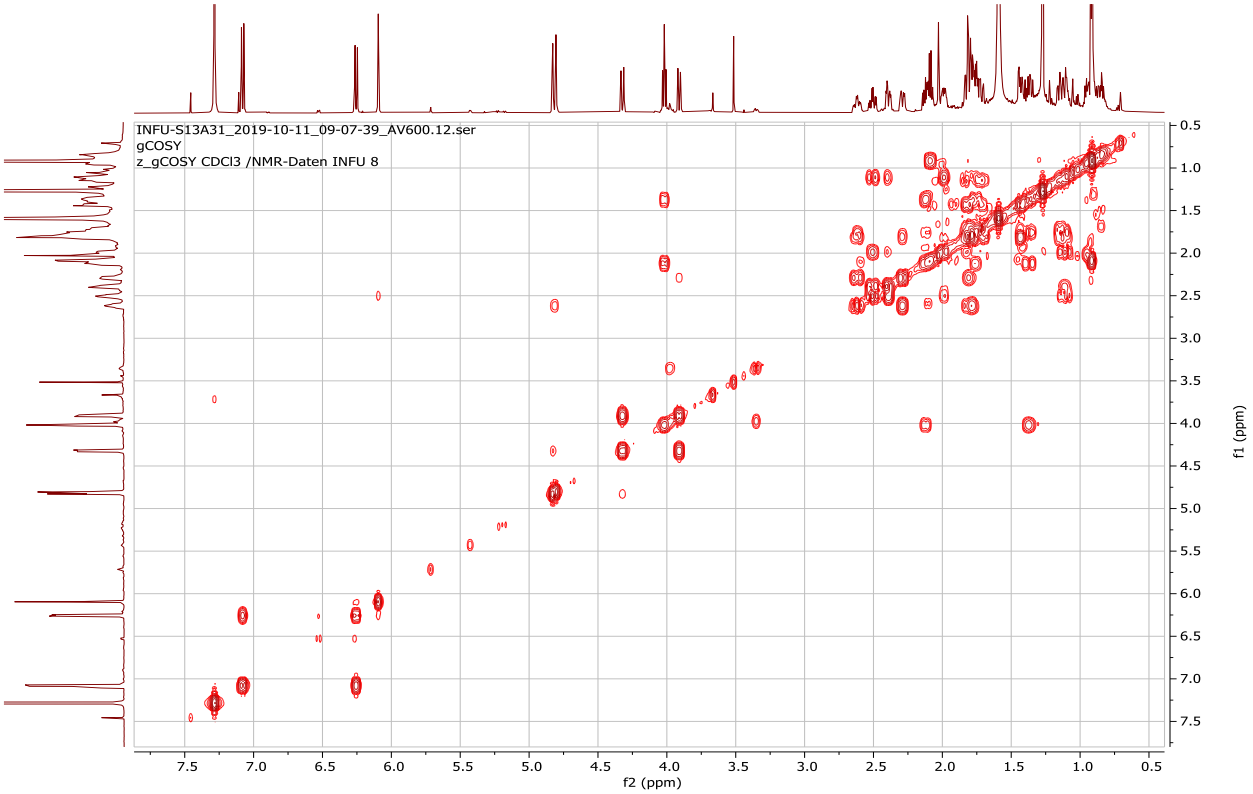

Appendix 2H: NOESY spectrum ($CDCl_3$) of compound **177**

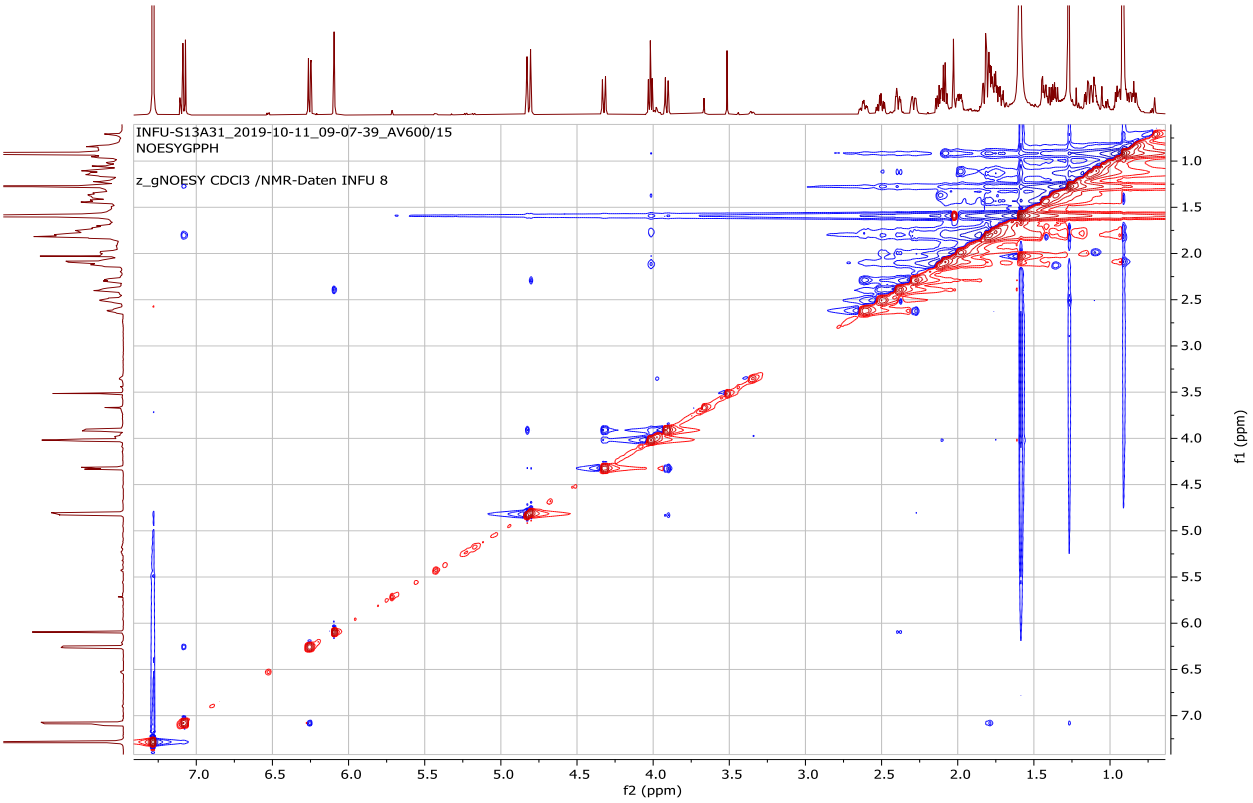

Appendix 2I: HSQC spectrum ($CDCl_3$) of compound **177**

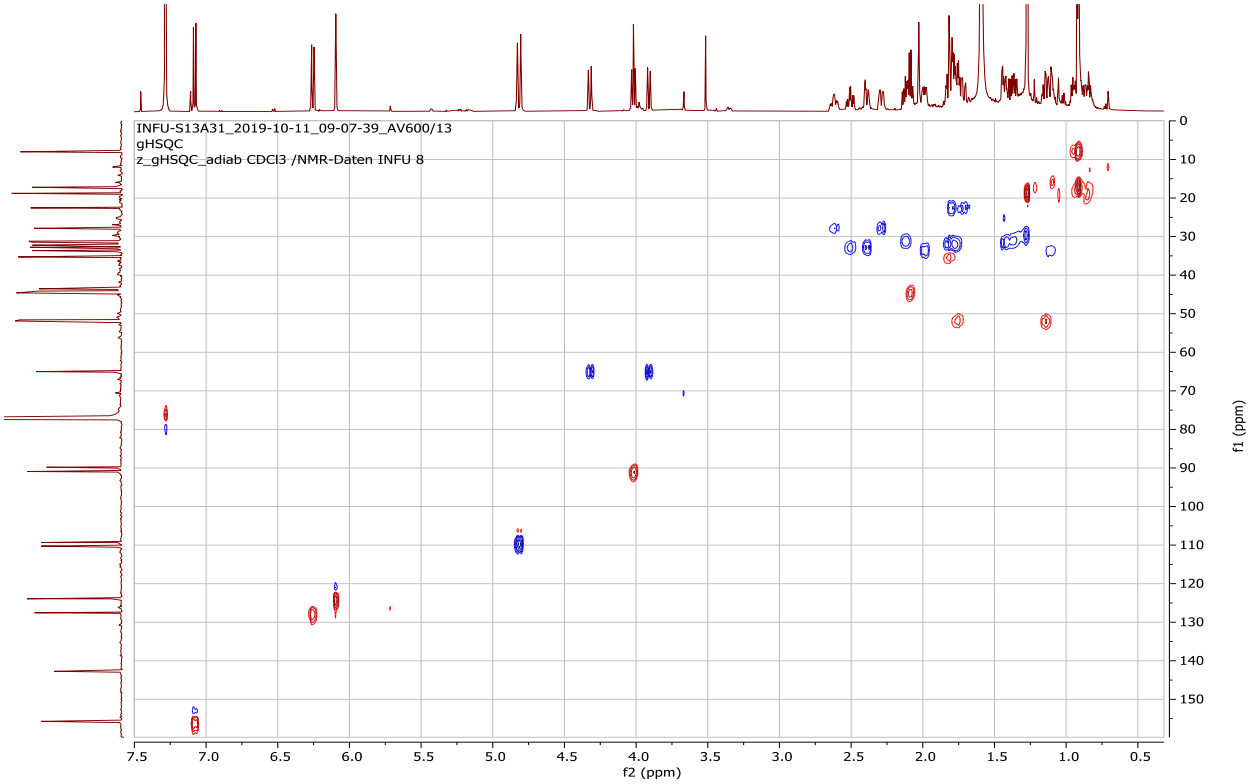

Appendix 2J: HMBC spectrum ($CDCl_3$) of compound **177**

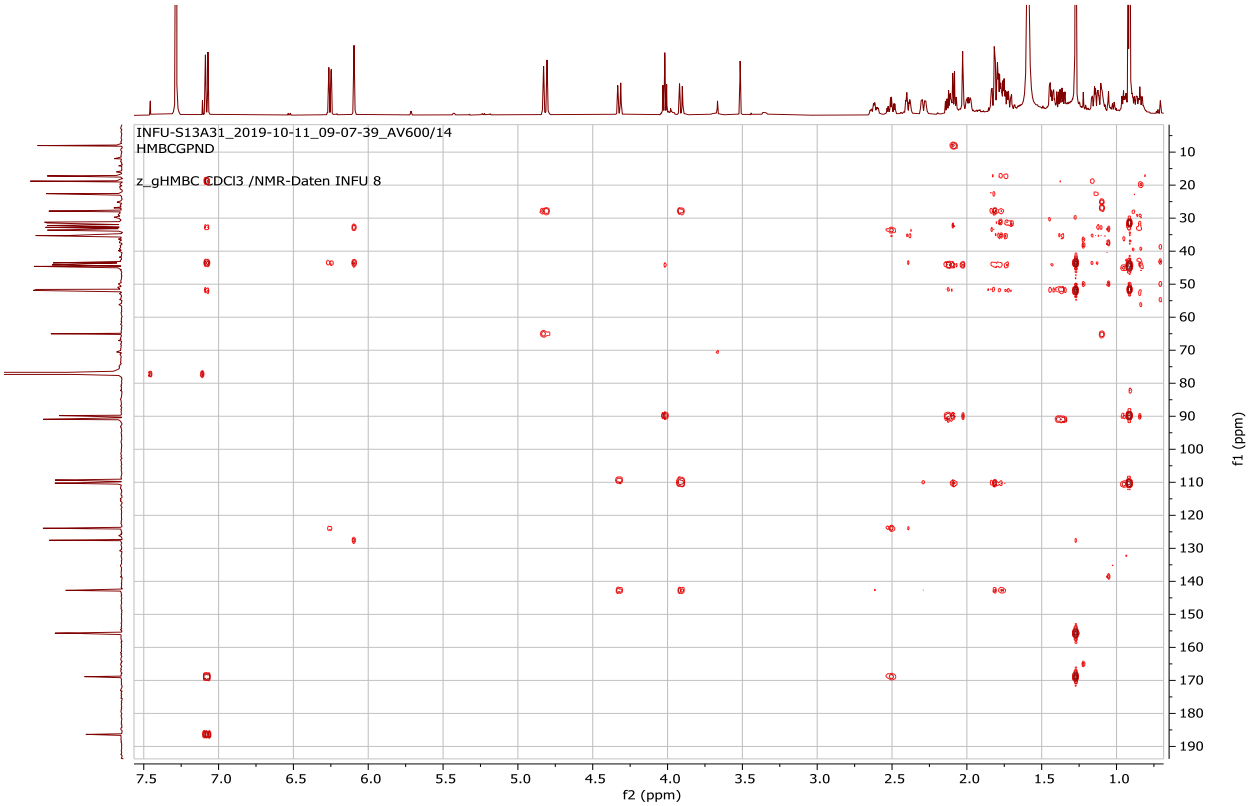

Appendix 3: NMR spectra for dracaenogenin E (**178**)

Appendix 3A: HRESIMS of compound **178**

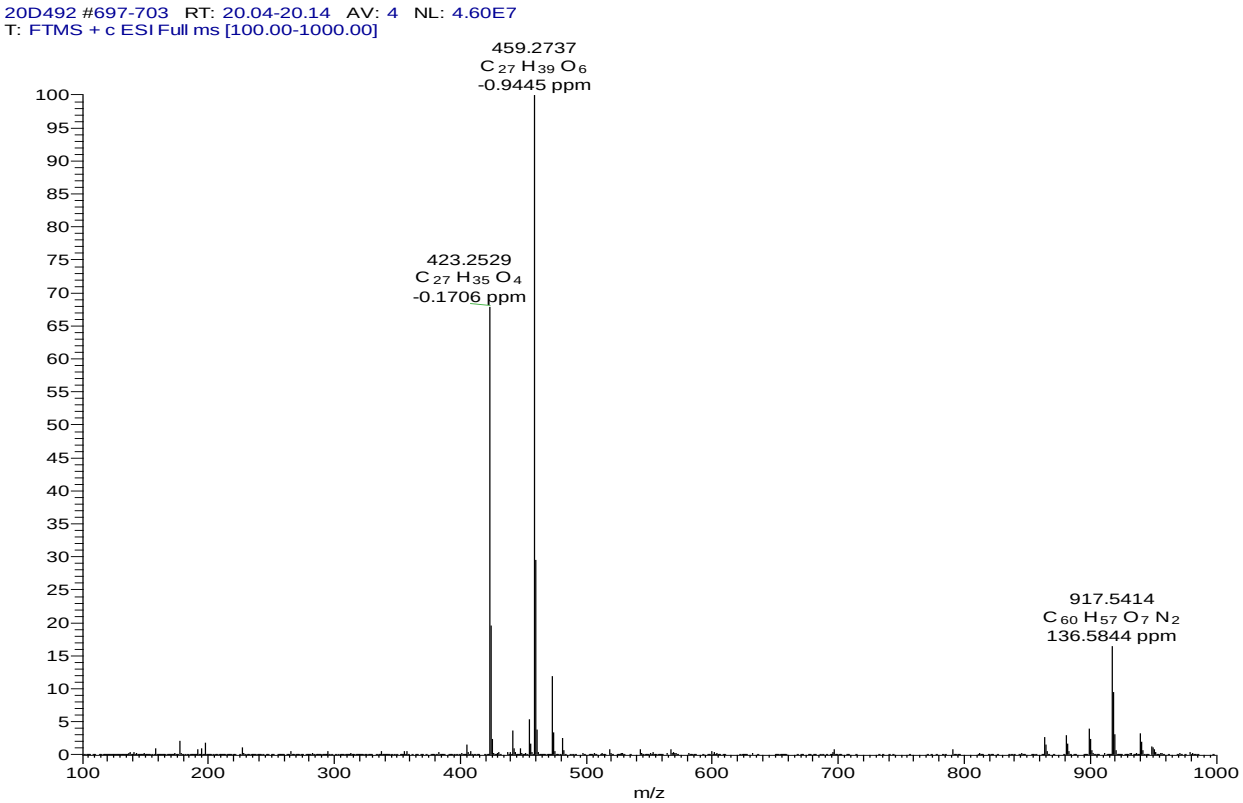

Appendix 3B: LC-UV spectrum of compound **178**

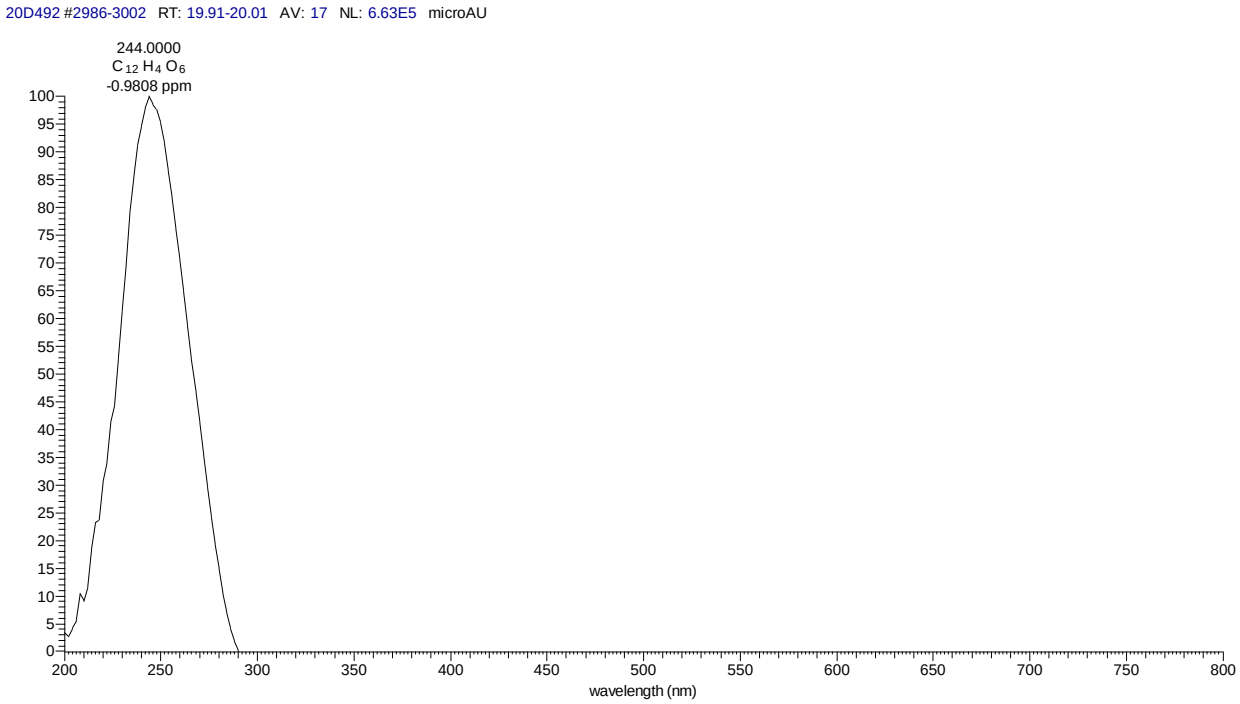

Appendix 3C: FT-IR spectrum of compound **178**

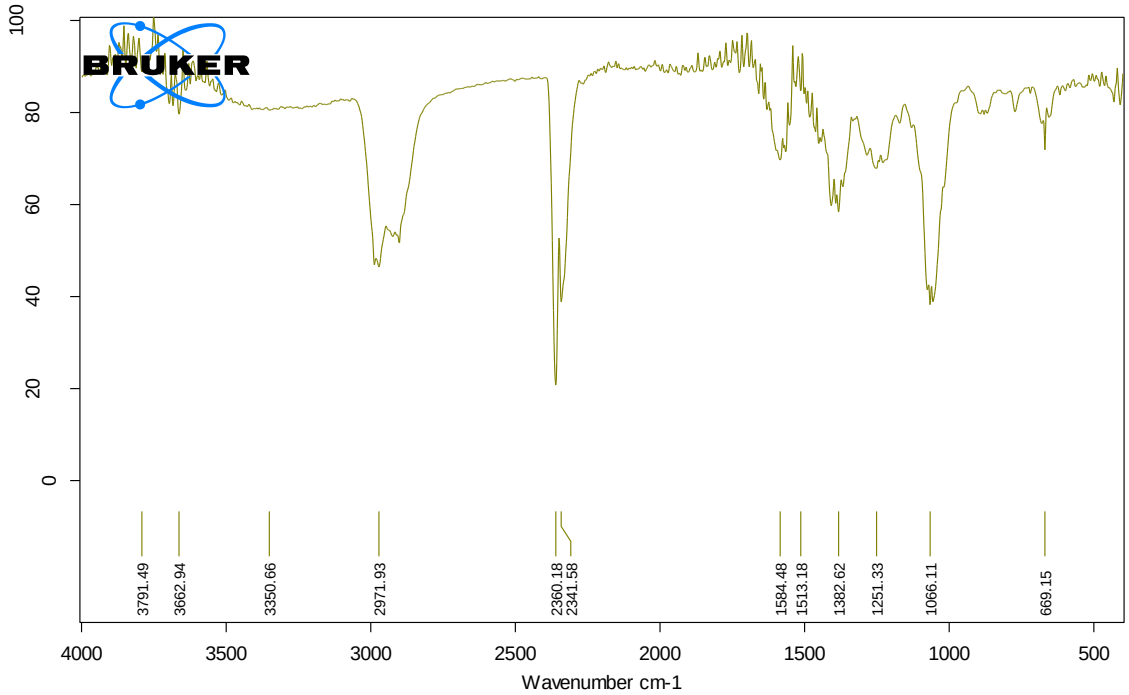

Appendix 3D: ^{1}H NMR spectrum (600 MHz, CD_3OD) of compound **178**

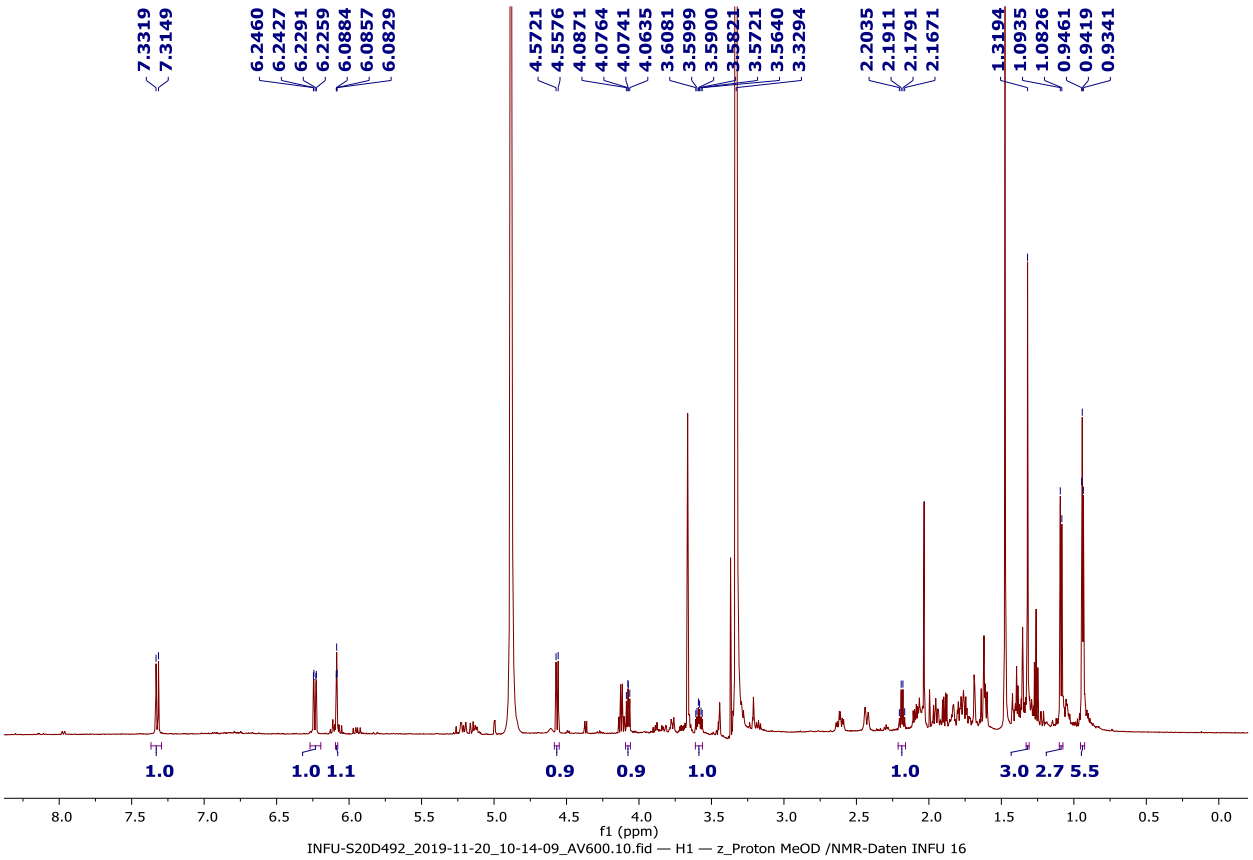

Appendix 3E: ^{13}C NMR spectrum (150 MHz, CD_3OD) of compound **178**

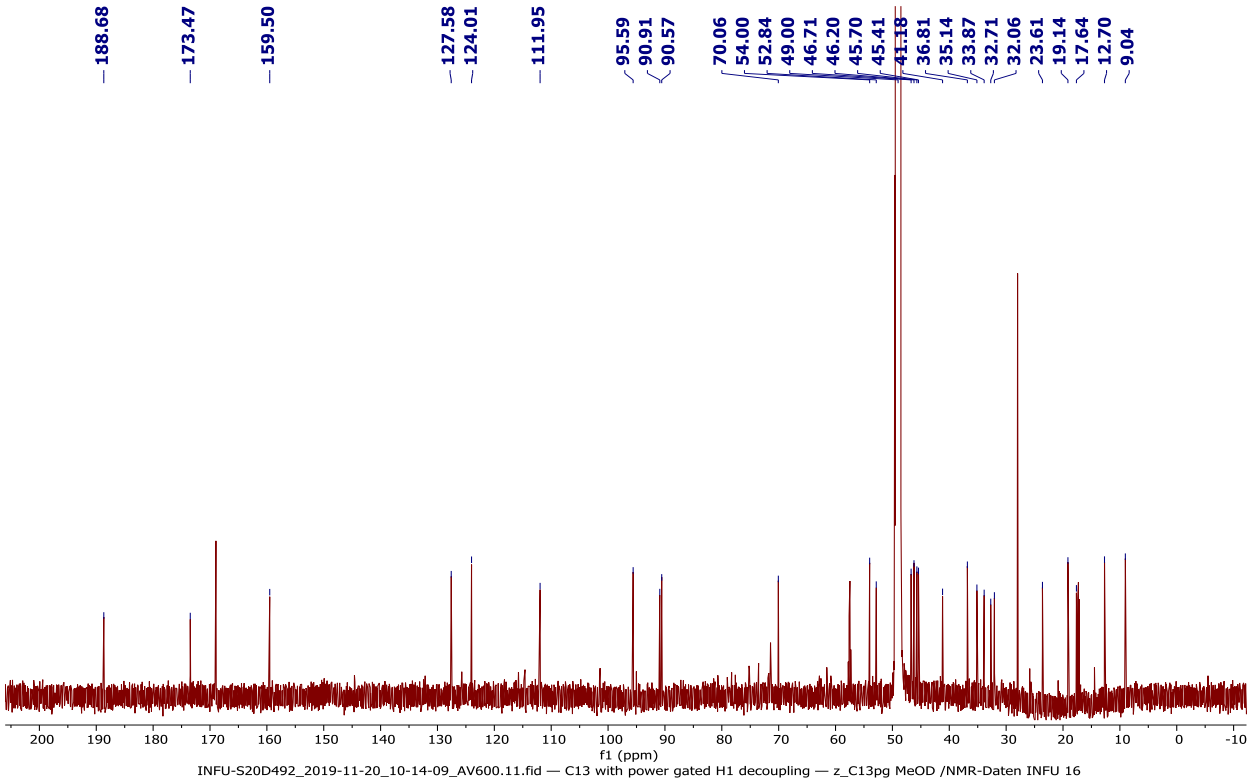

Appendix 3F: DEPT-135 spectrum (150 MHz, CD_3OD) of compound **178**

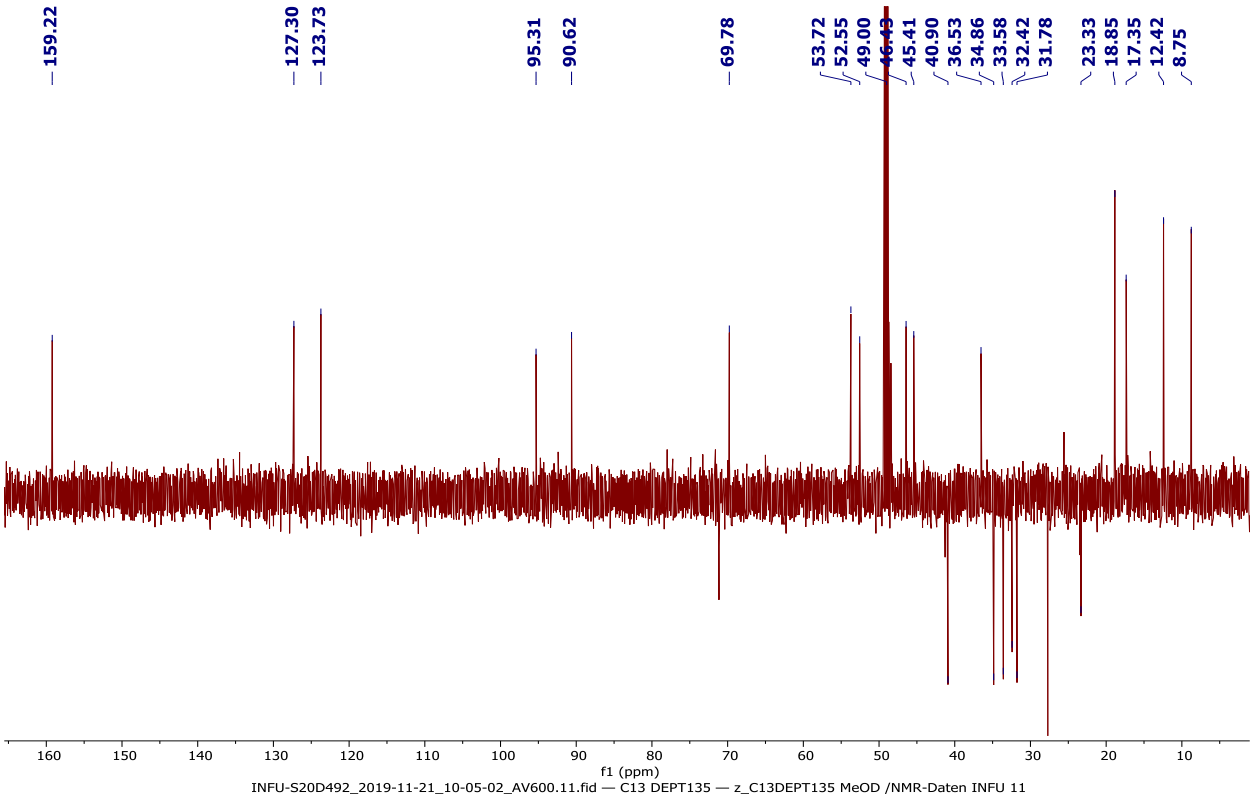

Appendix 3G: ^{1}H-^{1}H COSY spectrum (CD_3OD) of compound **178**

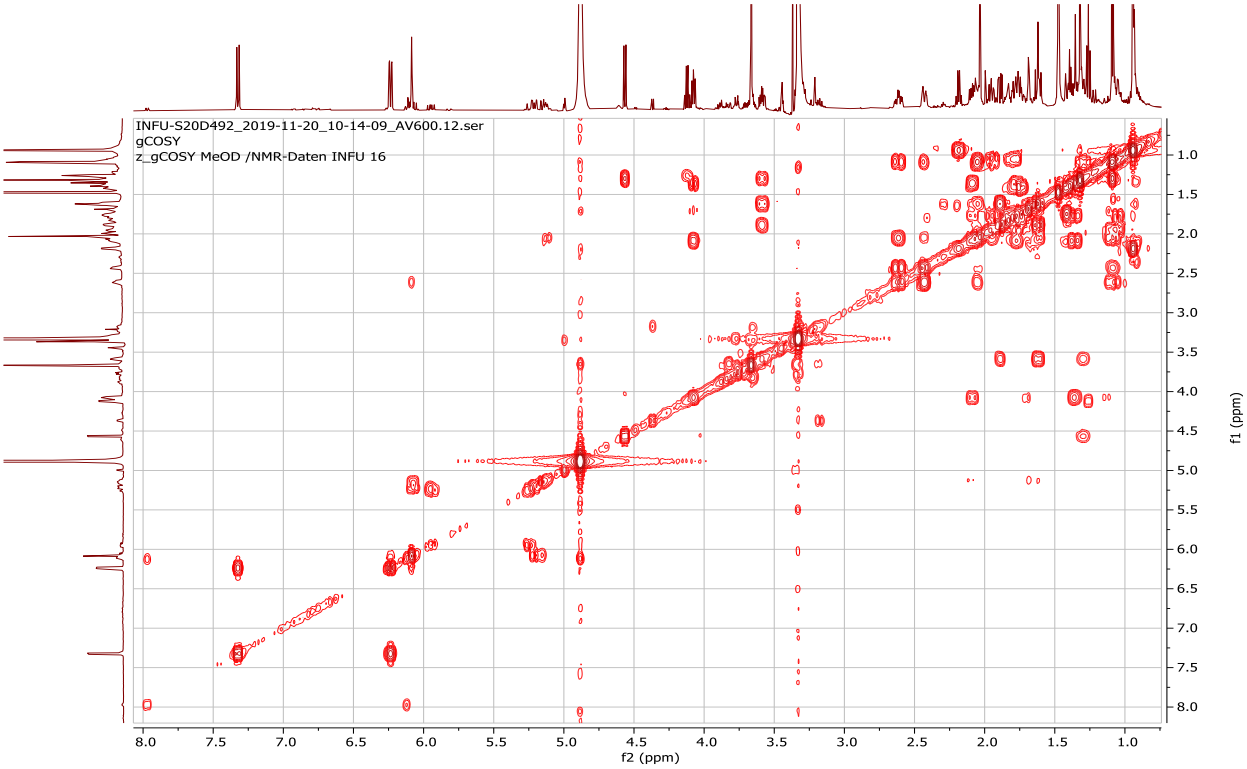

Appendix 3H: NOESY spectrum (CD_3OD) of compound **178**

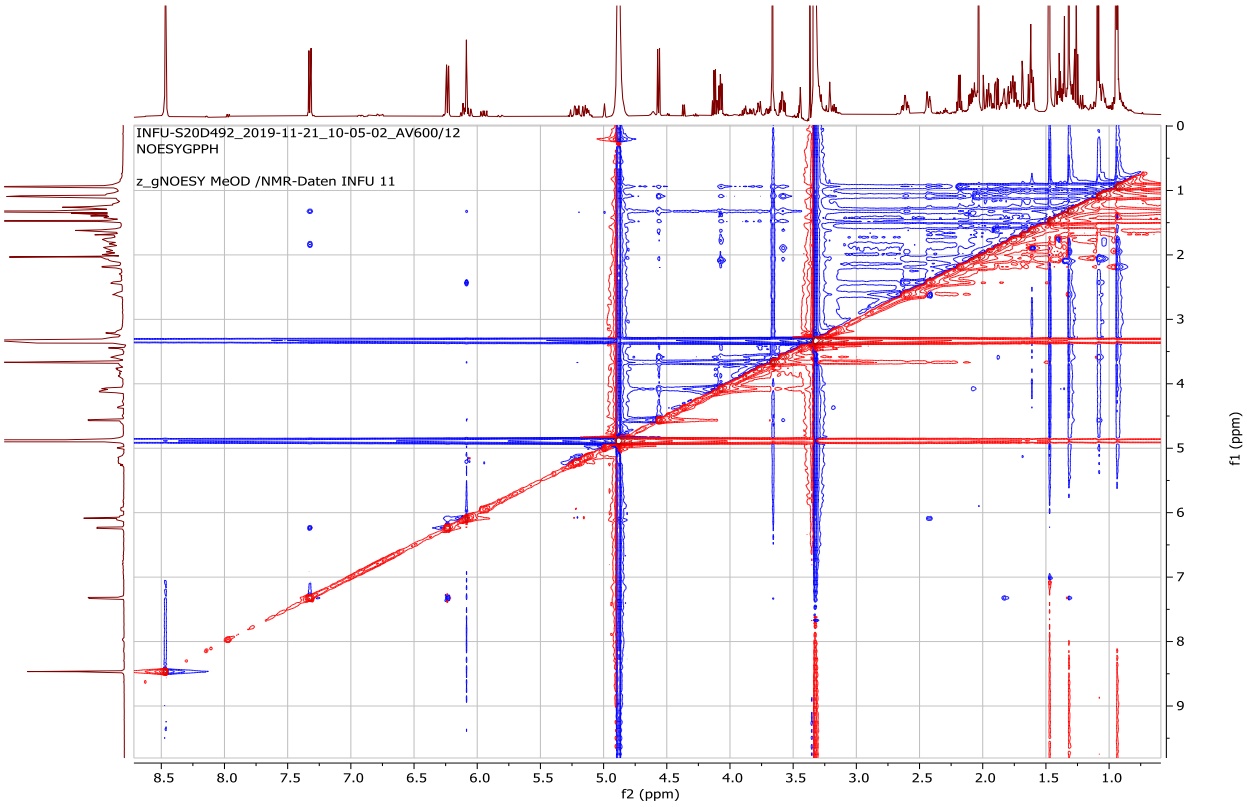

Appendix 3I: HSQC spectrum (CD_3OD) of compound **178**

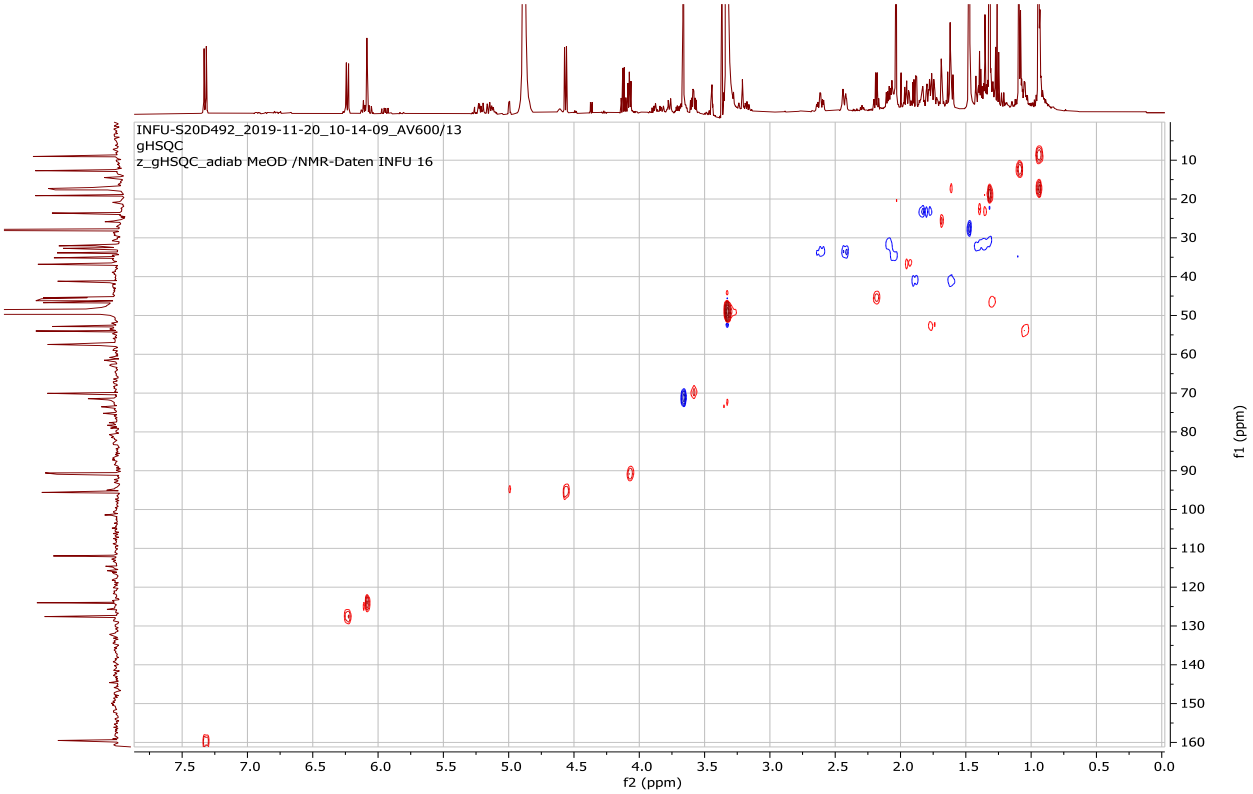

Appendix 3J: HMBC spectrum (CD_3OD) of compound **178**

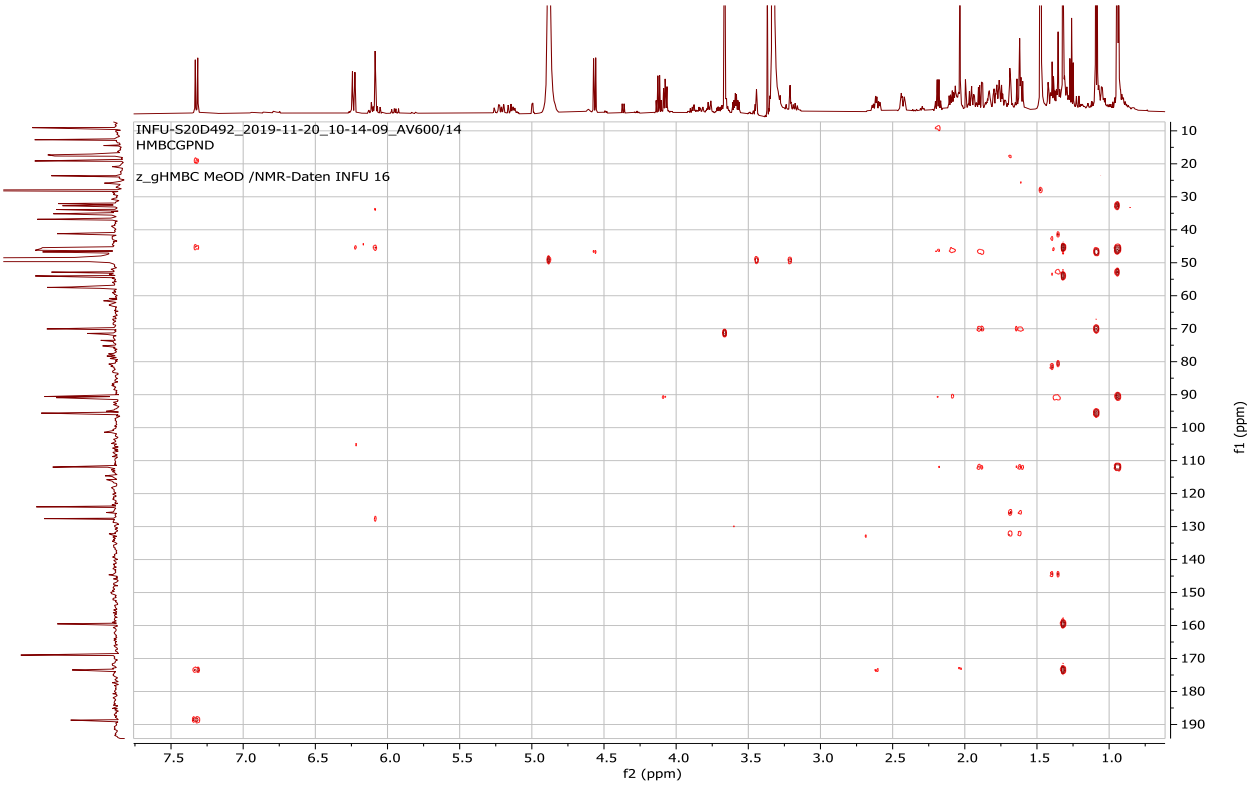

Appendix 4: NMR spectra for dracaenogenin F (**179**)

Appendix 4A: HRESIMS of compound **179**

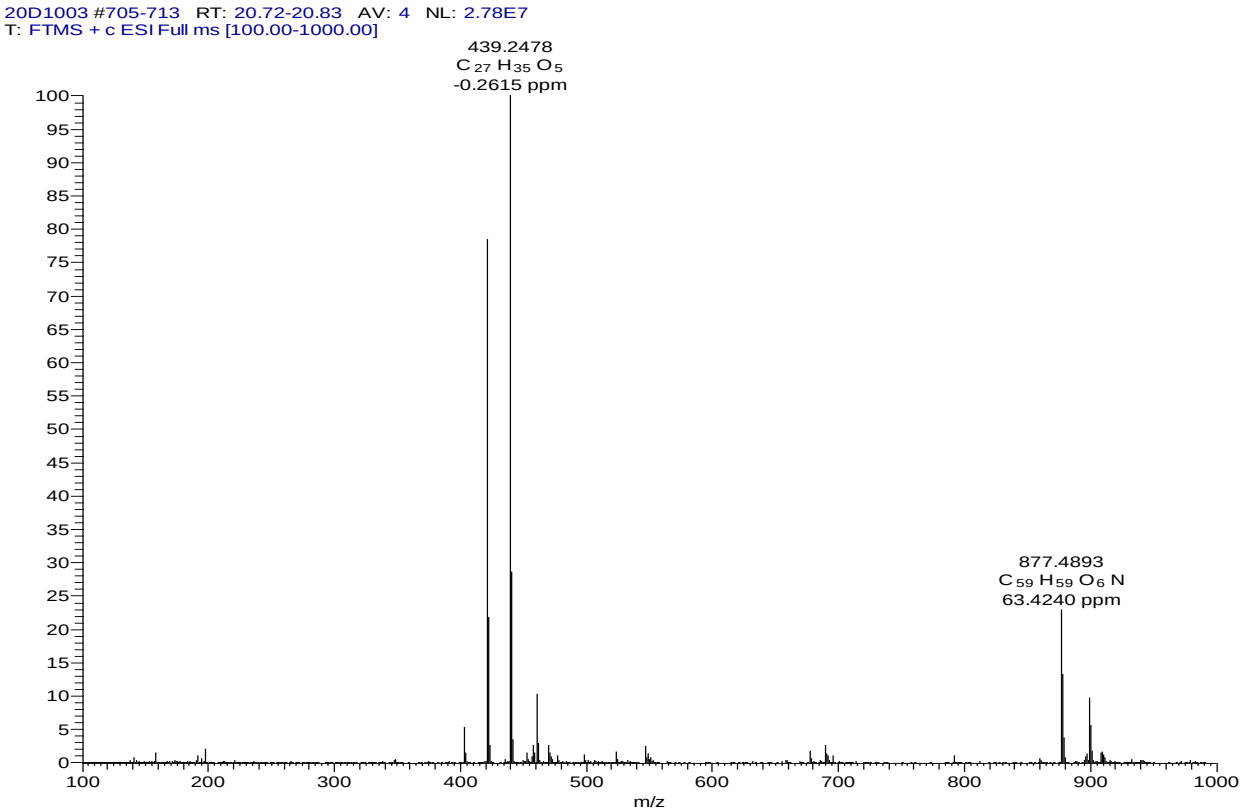

Appendix 4B: LC-UV spectrum of compound **179**

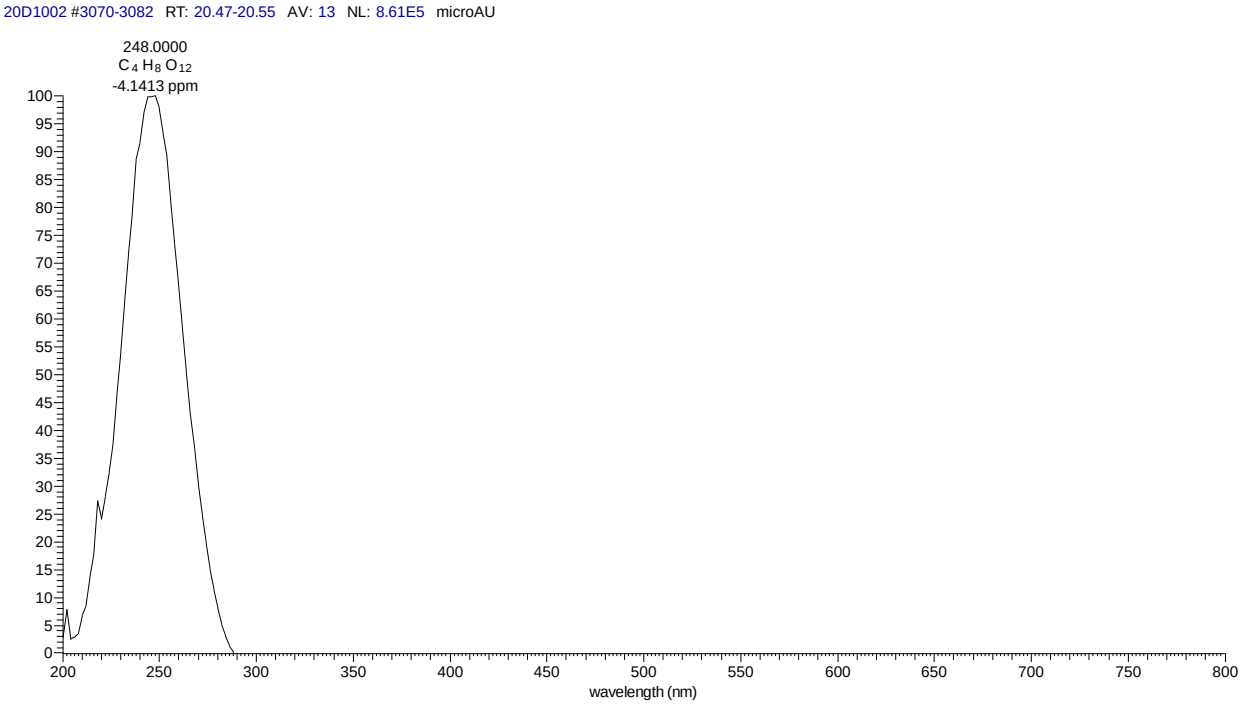

Appendix 4C: FT-IR spectrum of compound **179**

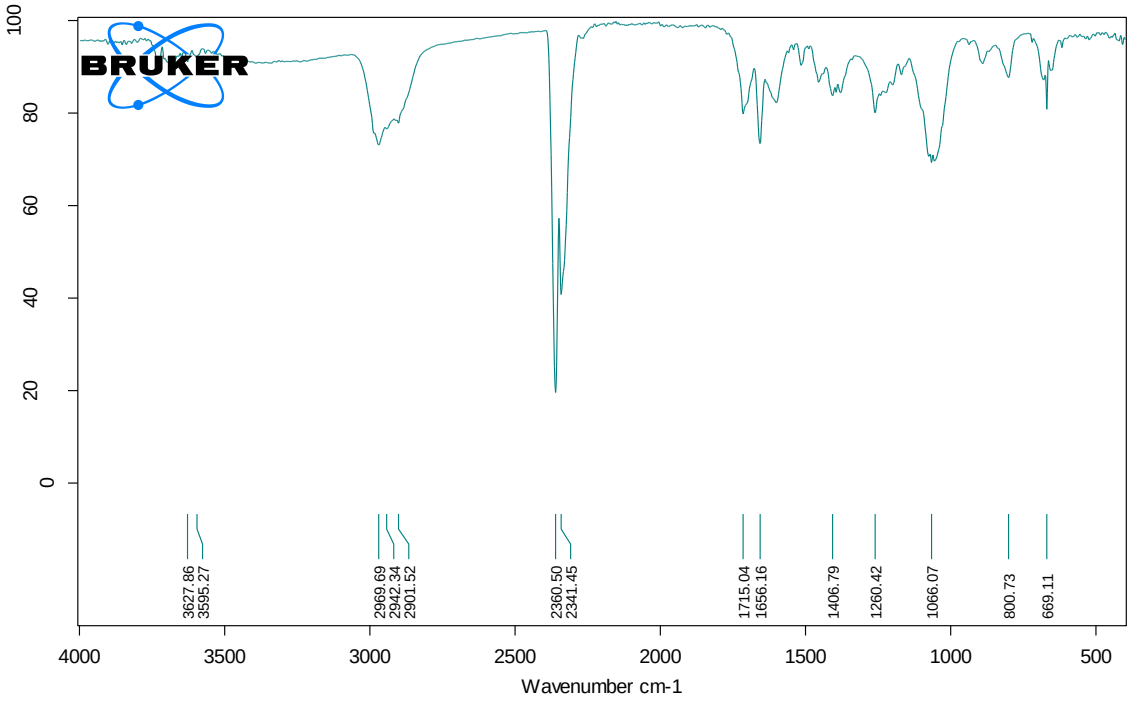

Appendix 4D: ^{1}H NMR spectrum (600 MHz, CD_3OD) of compound **179**

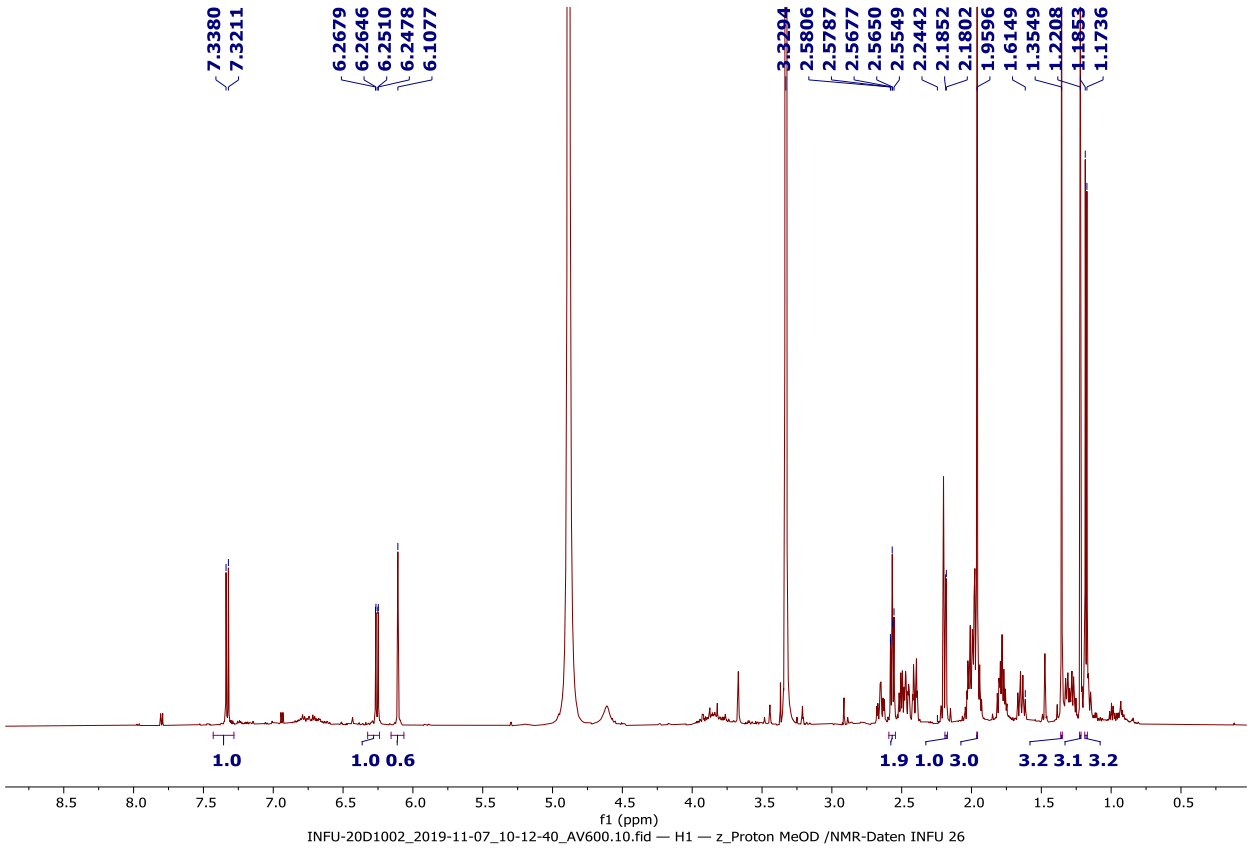

Appendix 4E: ^{13}C NMR spectrum (150 MHz, CD_3OD) of compound **179**

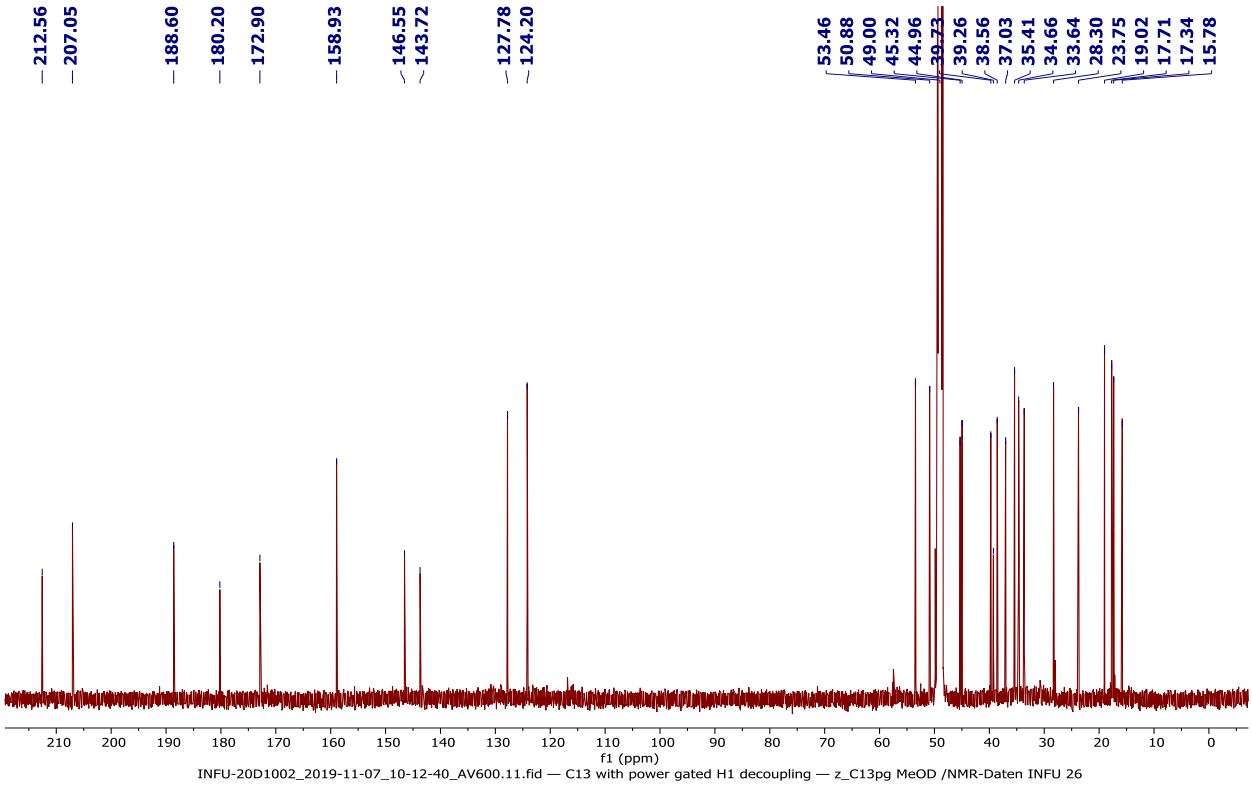

Appendix 4F: DEPT-135 spectrum (150 MHz, CD_3OD) of compound **179**

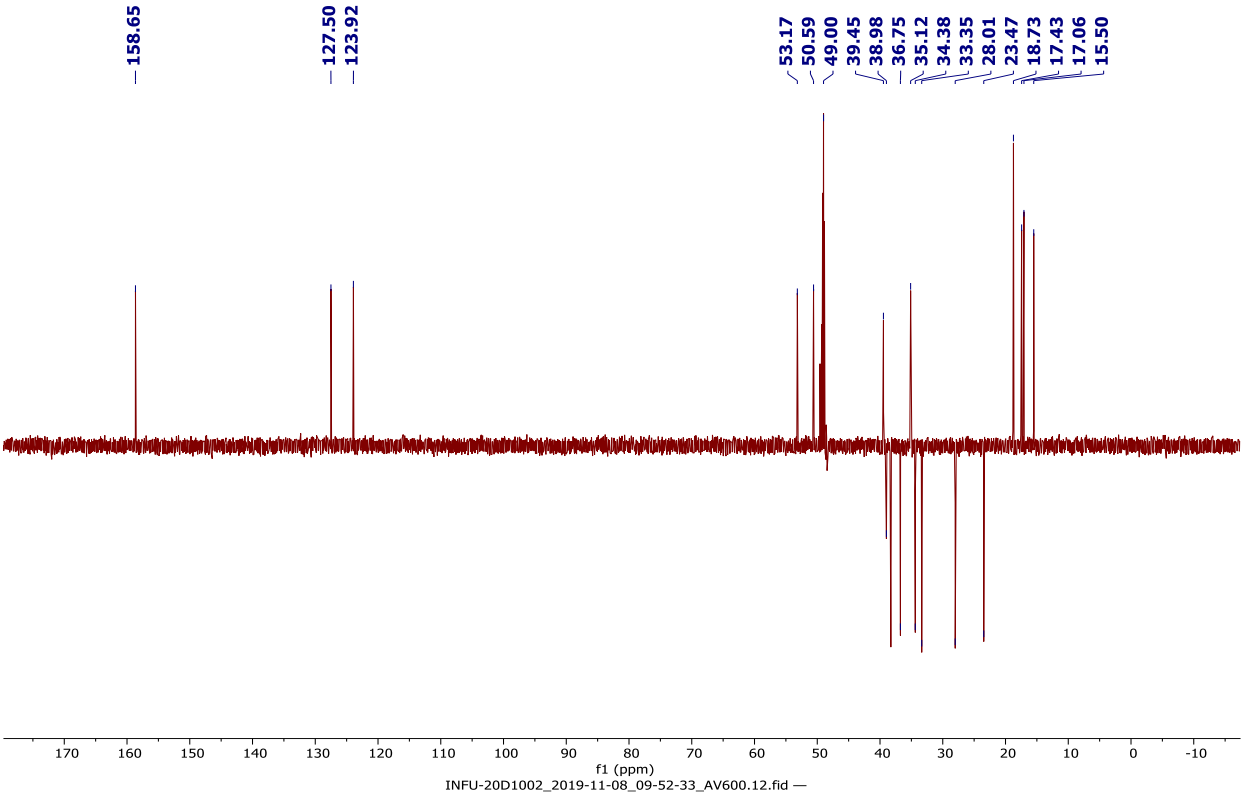

Appendix 4G: ^{1}H-^{1}H COSY spectrum (CD_3OD) of compound **179**

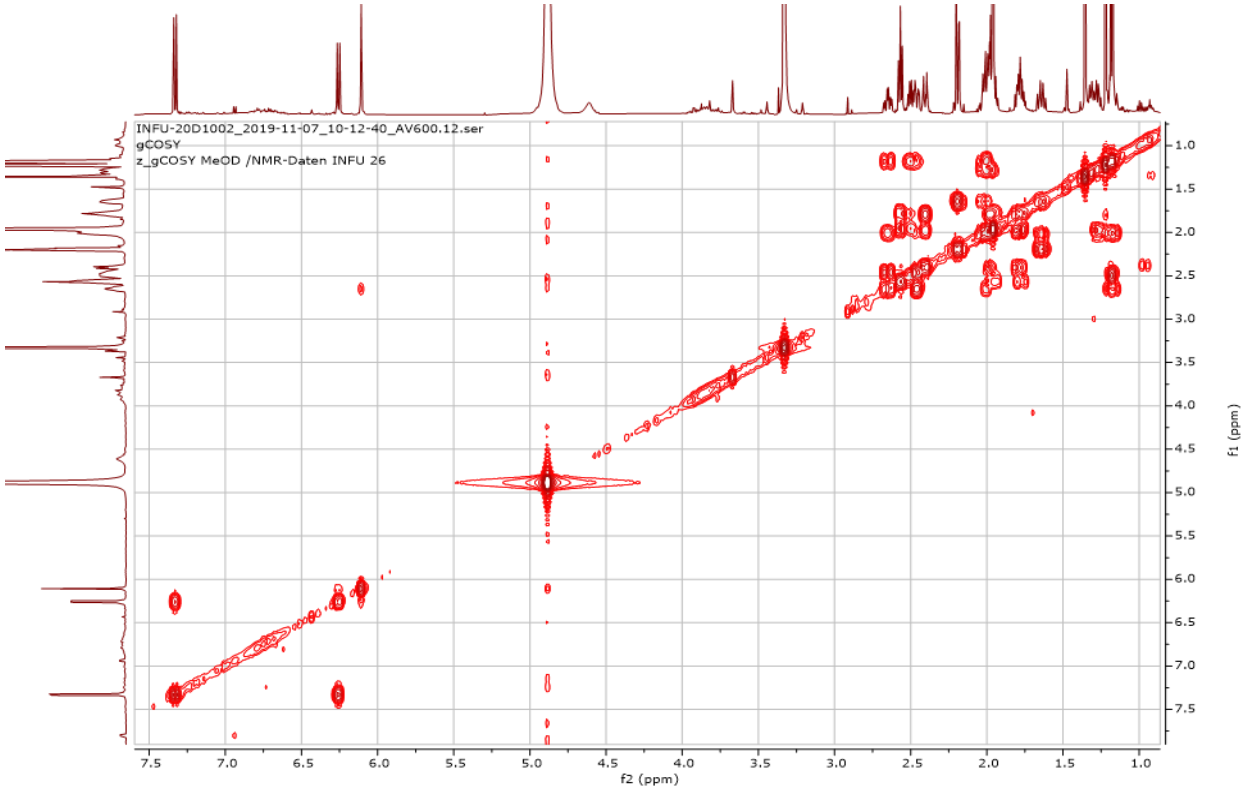

Appendix 4H: NOESY spectrum (CD_3OD) of compound **179**

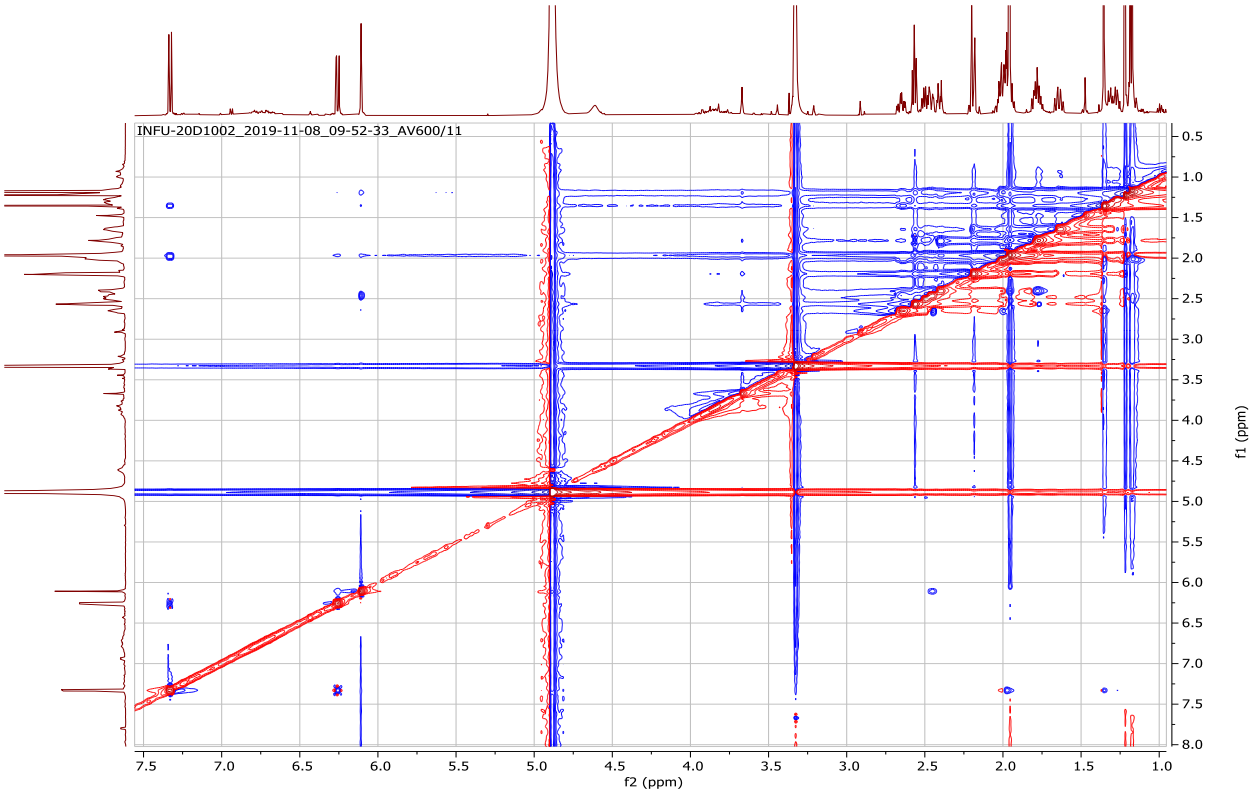

Appendix 4I: HSQC spectrum (CD_3OD) of compound **179**

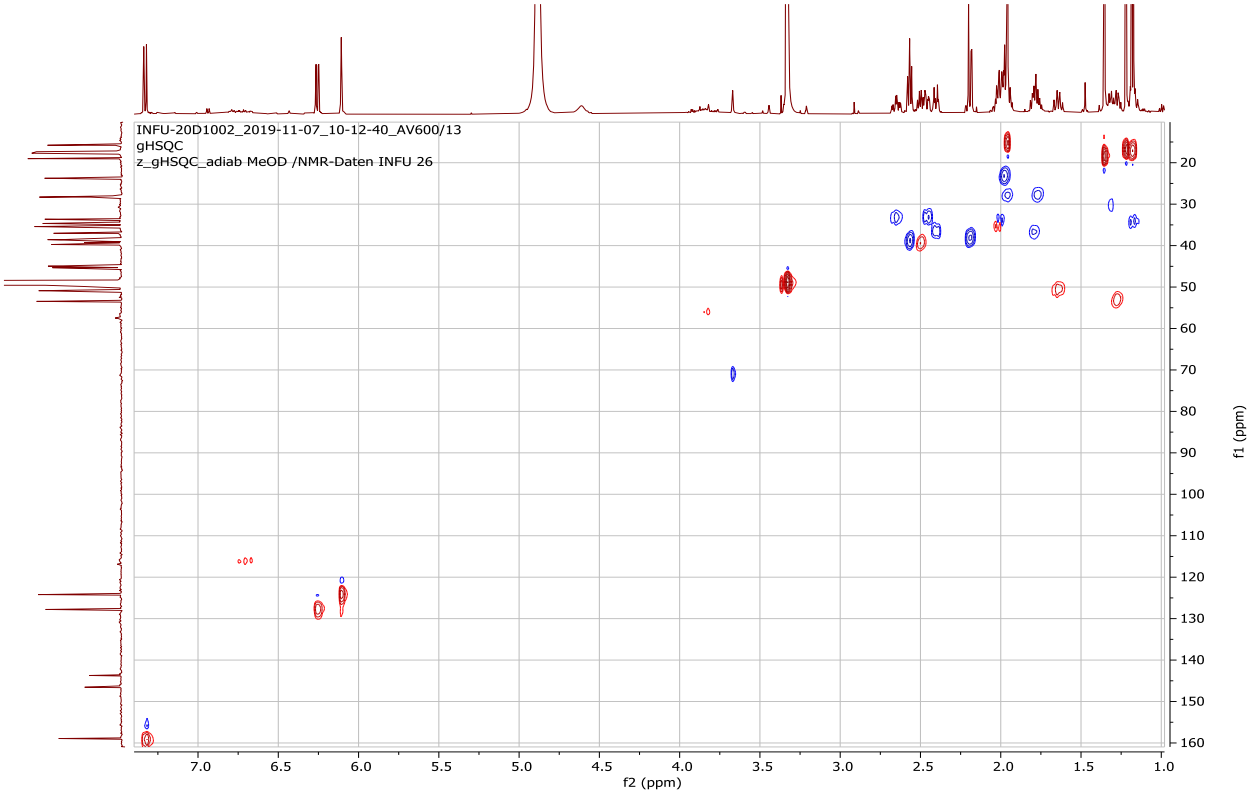

Appendix 4J: HMBC spectrum (CD_3OD) of compound **179**

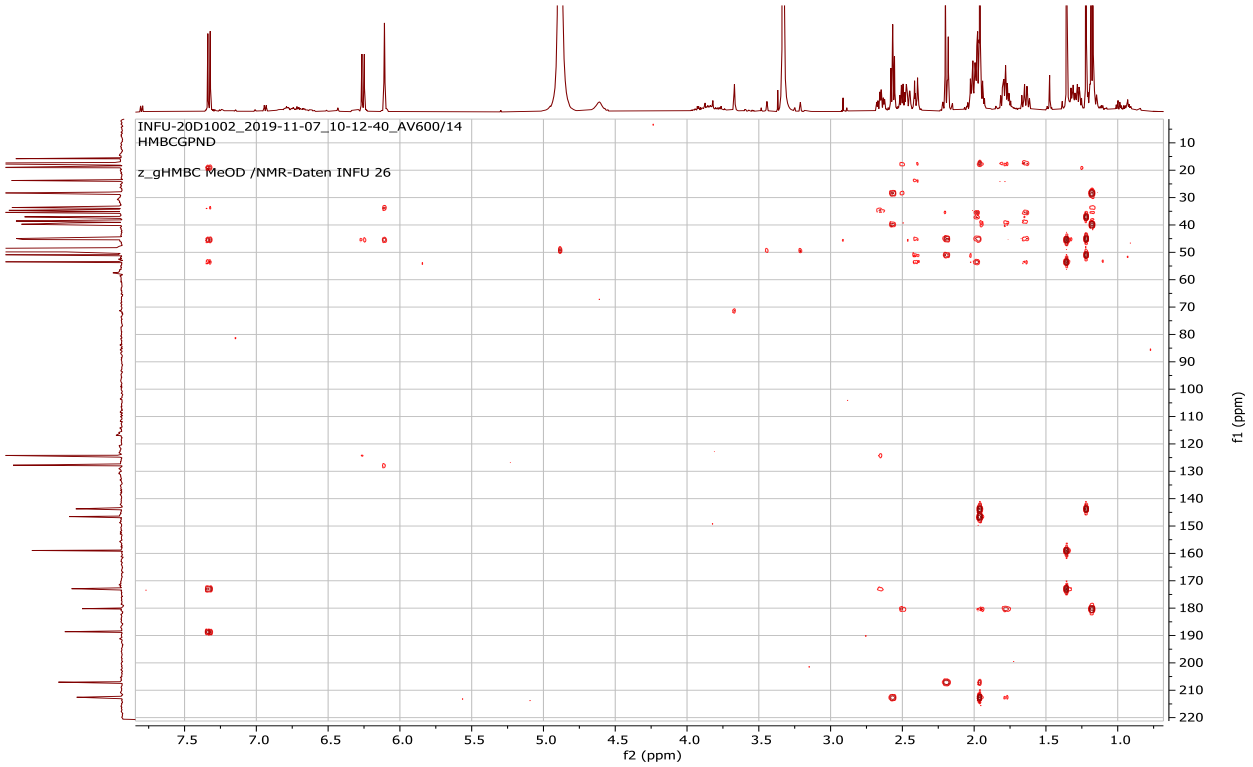

Appendix 5: NMR spectra for 3″-methoxycochinchinenene H (**180**)

Appendix 5A: HRESIMS of compound **180**

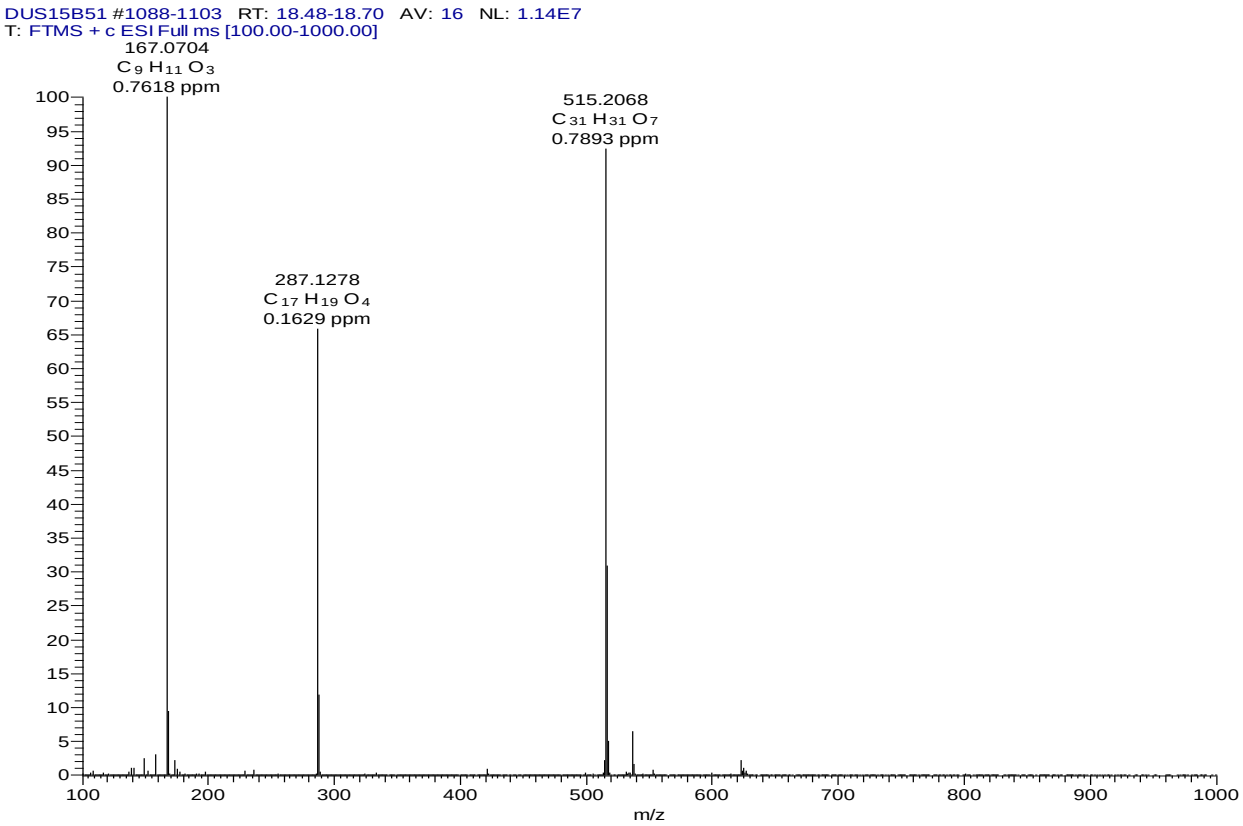

Appendix 5B: LC-UV spectrum of compound **180**

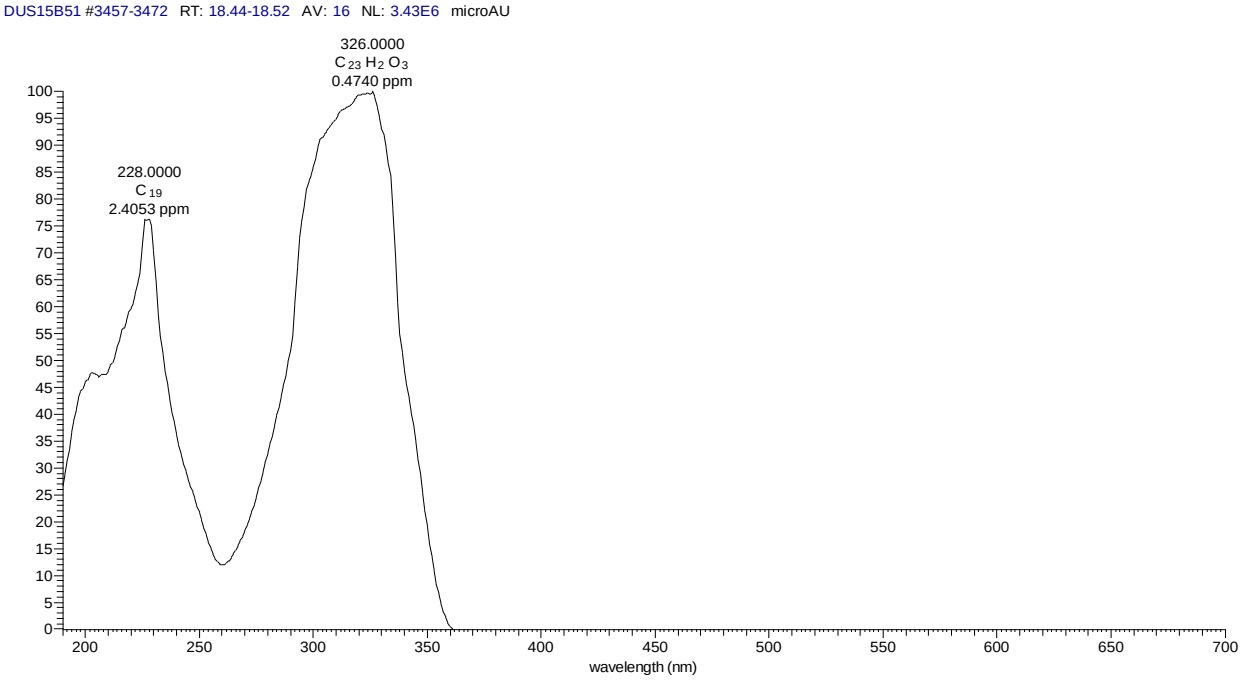

Appendix 5C: FT-IR spectrum of compound **180**

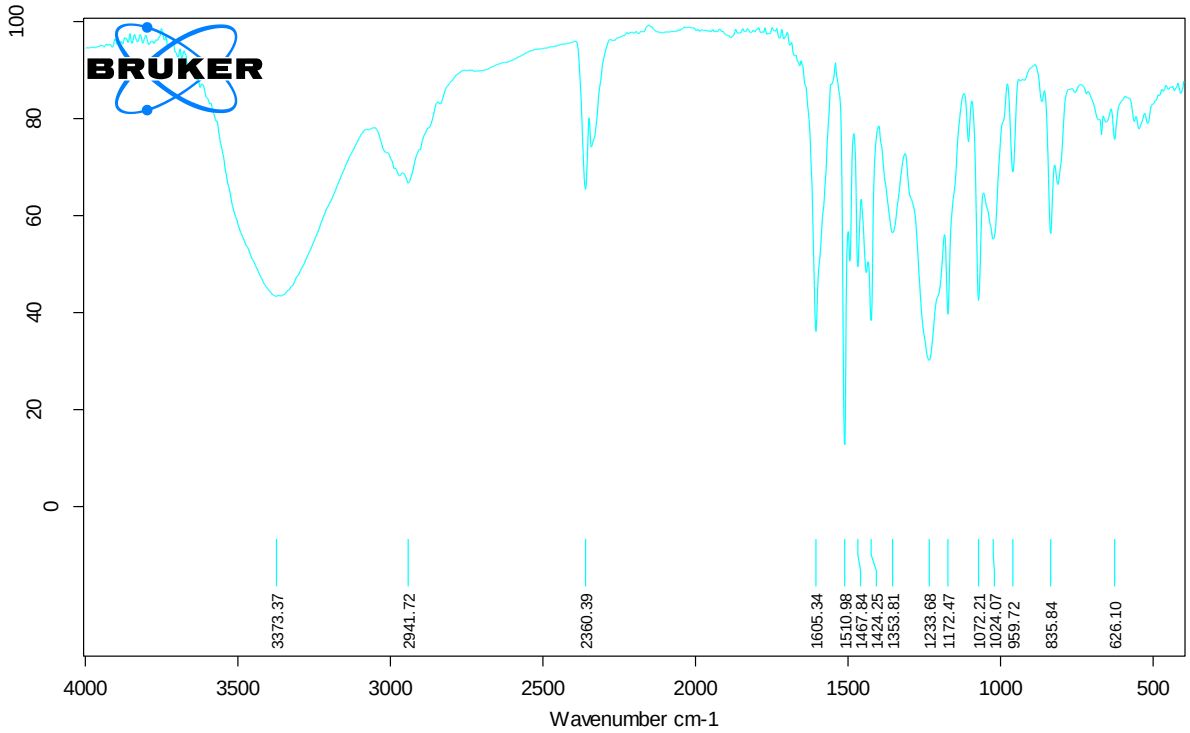

Appendix 5D: ^{1}H NMR spectrum (600 MHz, CD_3OD) of compound **180**

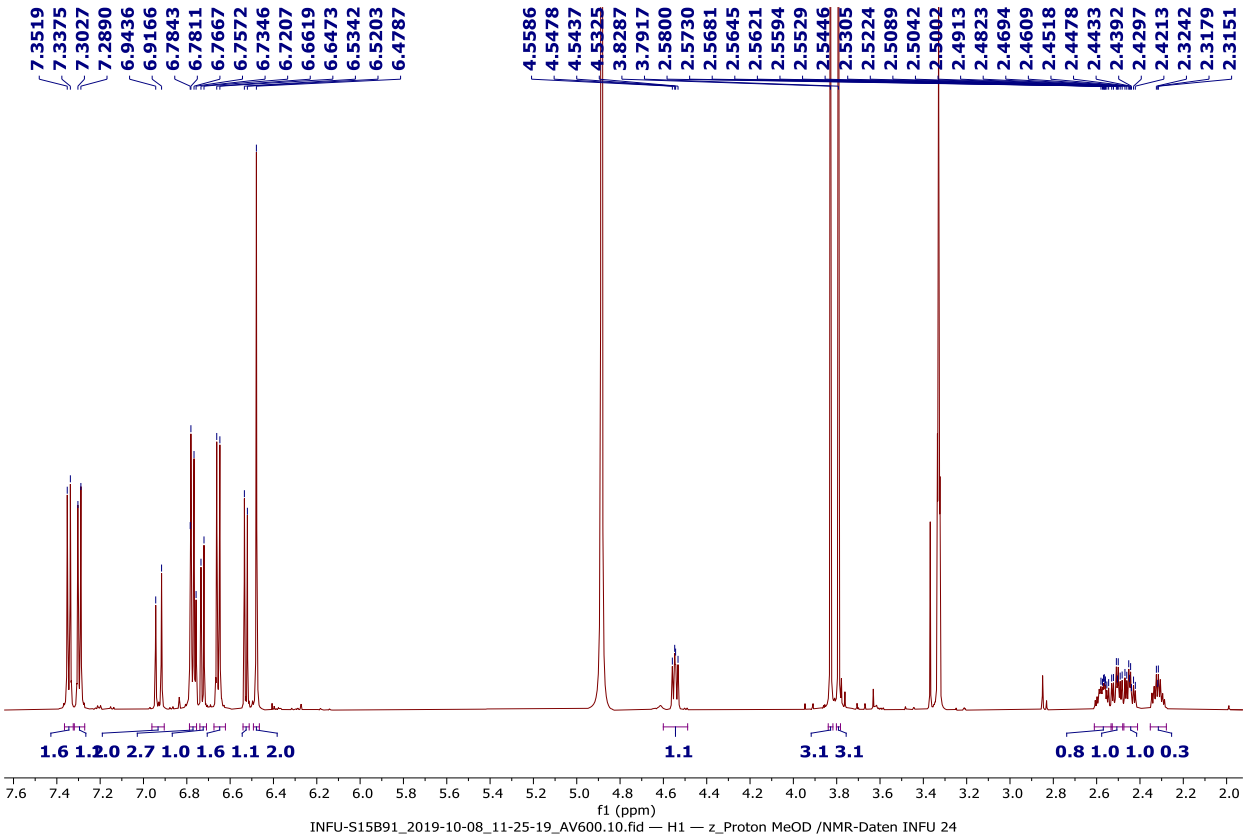

Appendix 5E: ^{13}C NMR spectrum (150 MHz, CD_3OD) of compound **180**

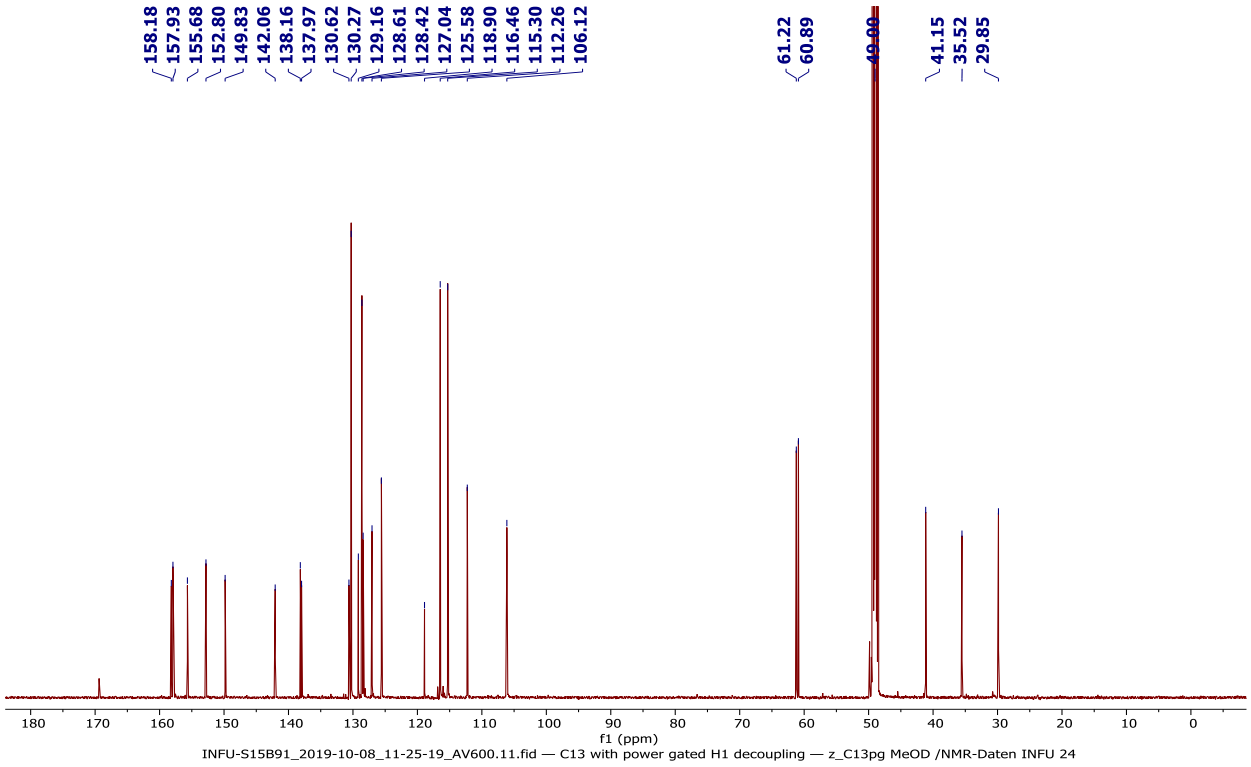

Appendix 5F: DEPT-135 spectrum (150 MHz, CD_3OD) of compound **180**

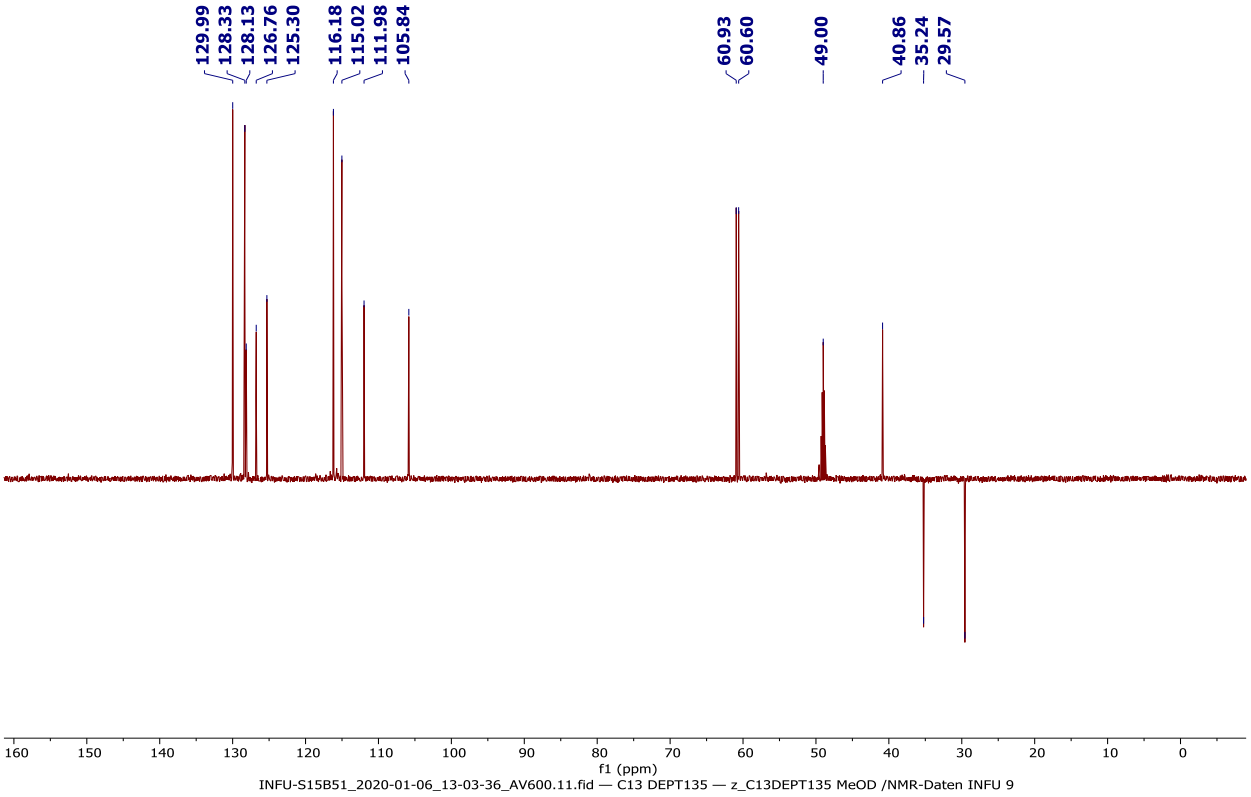

Appendix 5G: ^{1}H-^{1}H COSY spectrum (CD_3OD) of 3 compound **180**

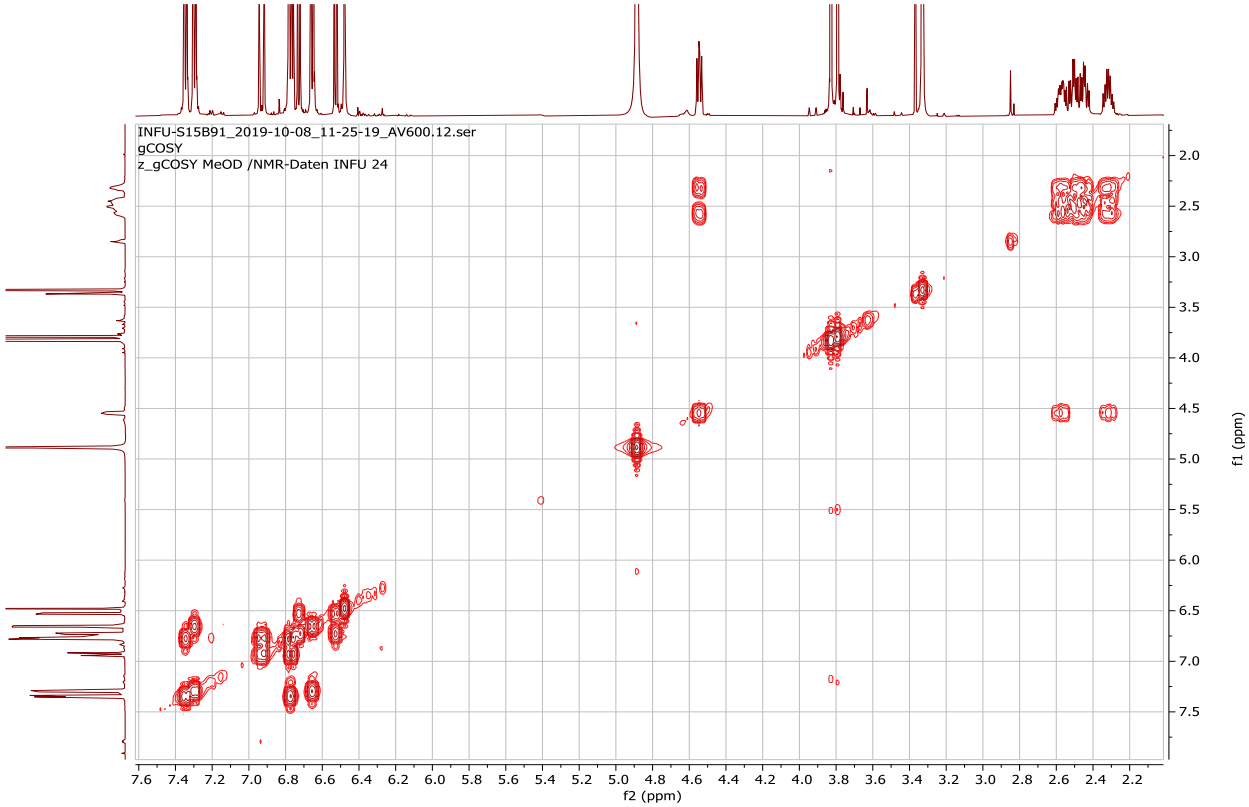

Appendix 5H: NOESY spectrum (CD_3OD) of compound **180**

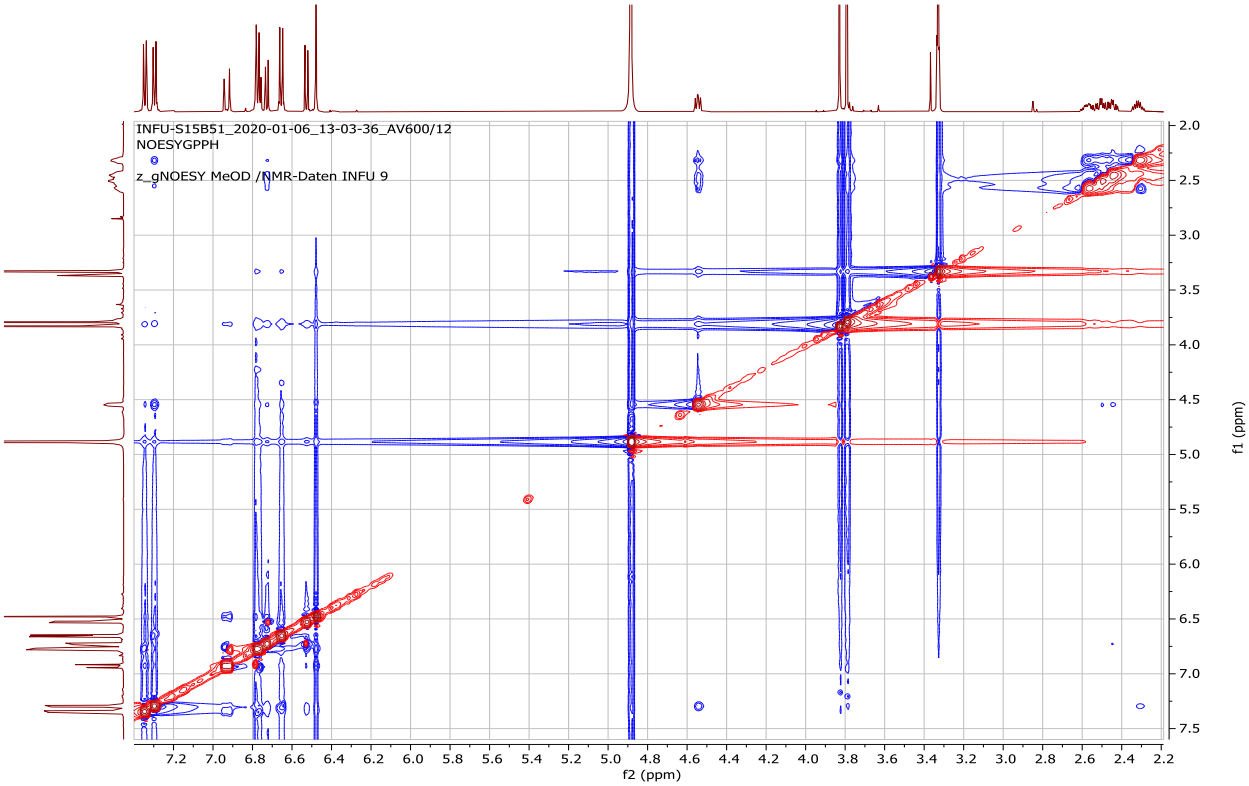

Appendix 5I: HSQC spectrum (CD_3OD) of compound **180**

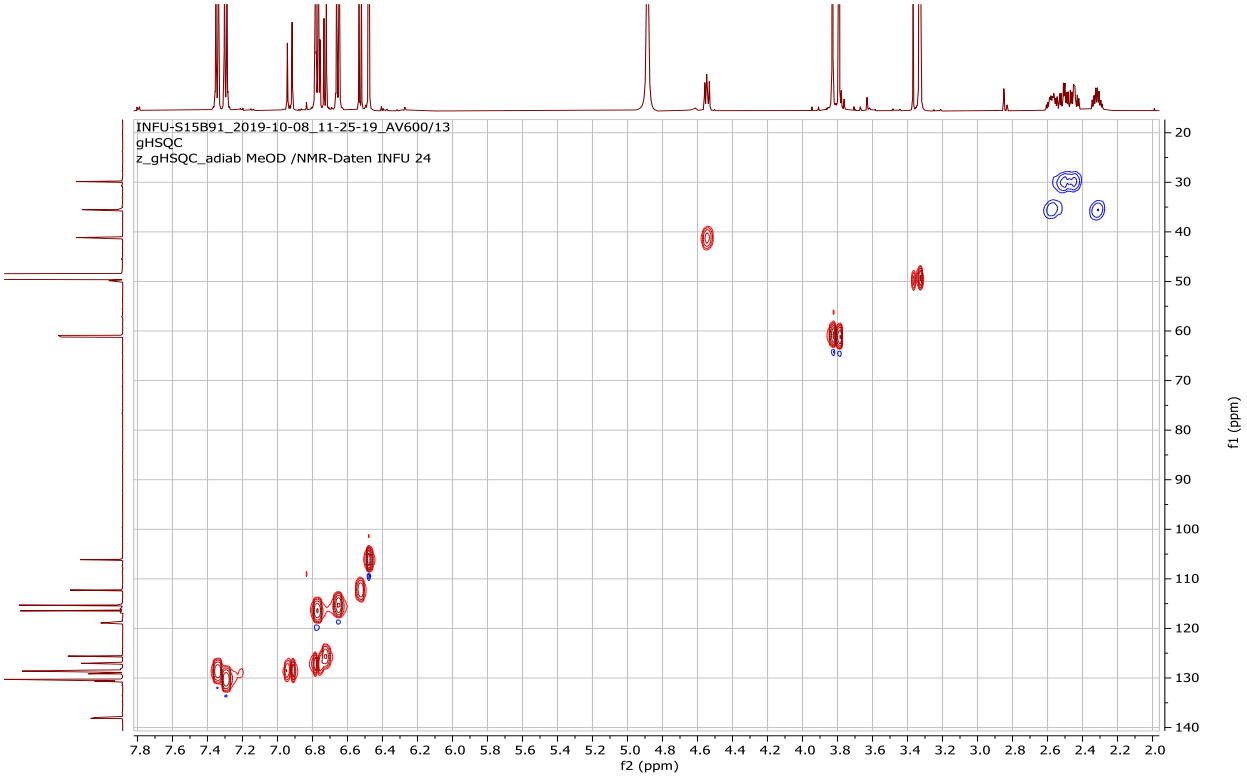

Appendix 5J: HMBC spectrum (CD_3OD) of compound **180**

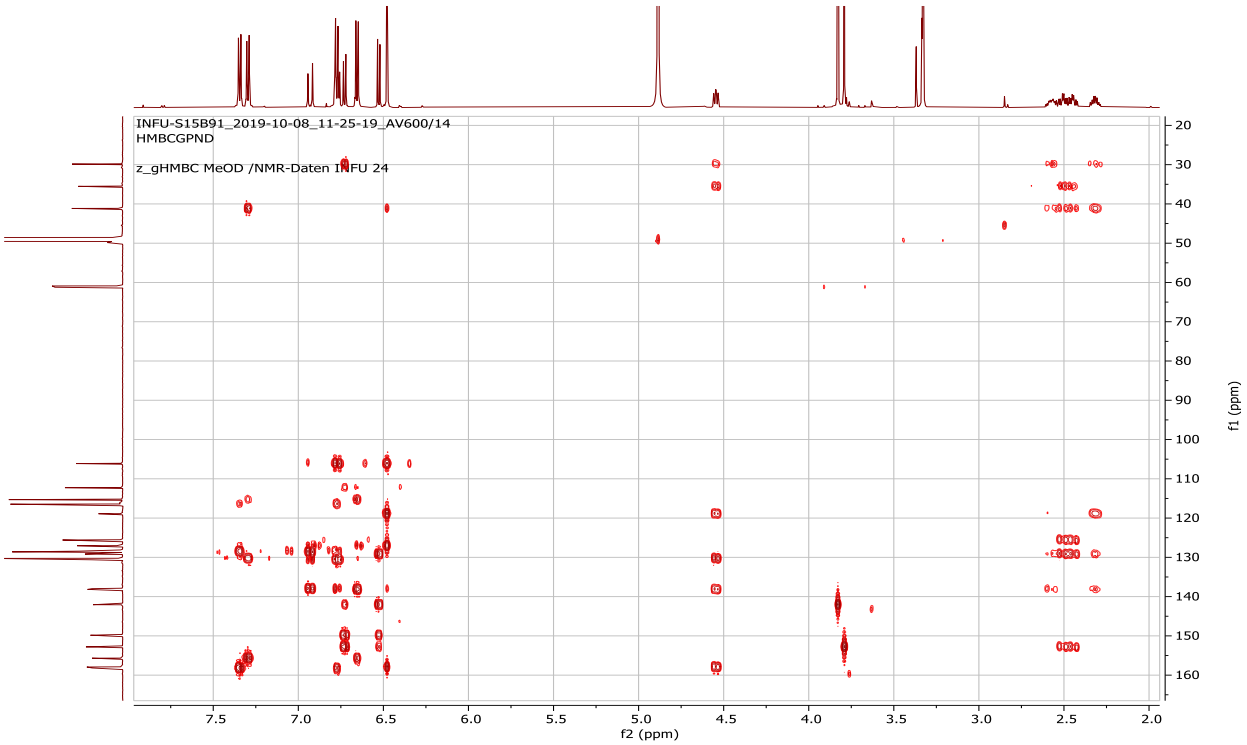

Appendix 6: NMR spectra for *trans*-resveratrol (**181**)

Appendix 6A: HRESIMS of compound **181**

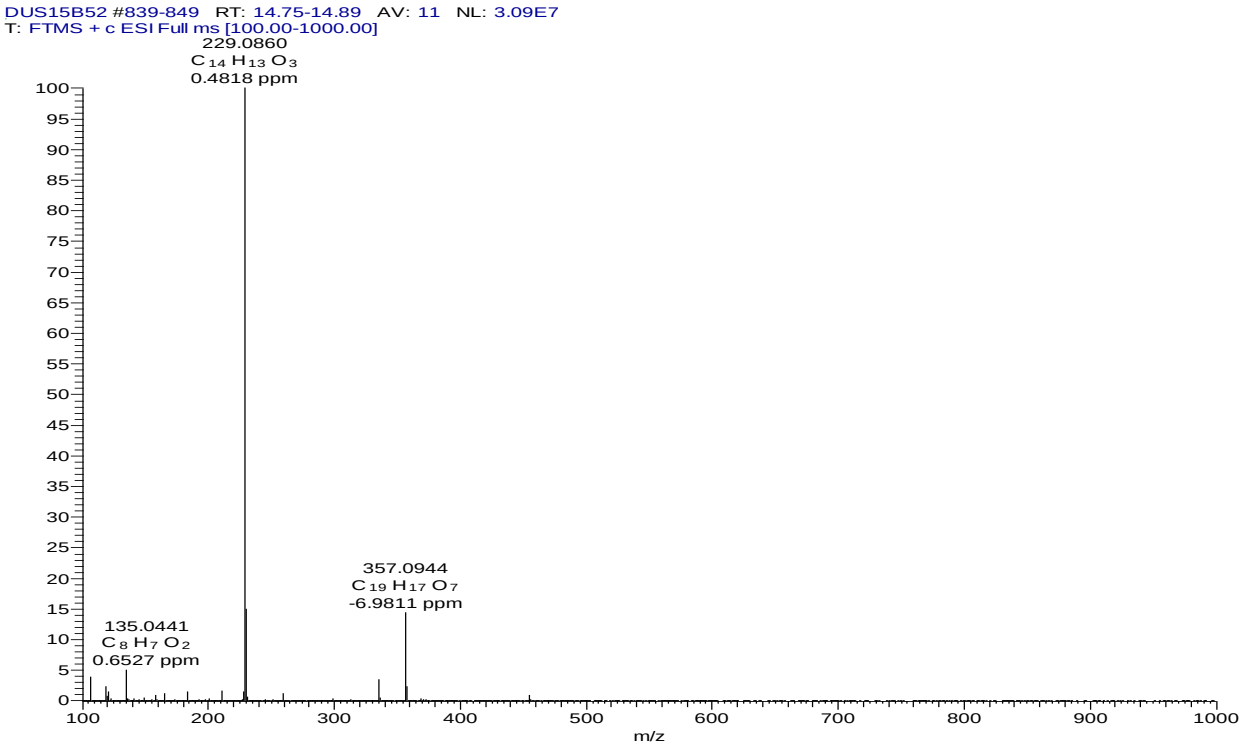

Appendix 6B: LC-UV spectrum of compound **181**

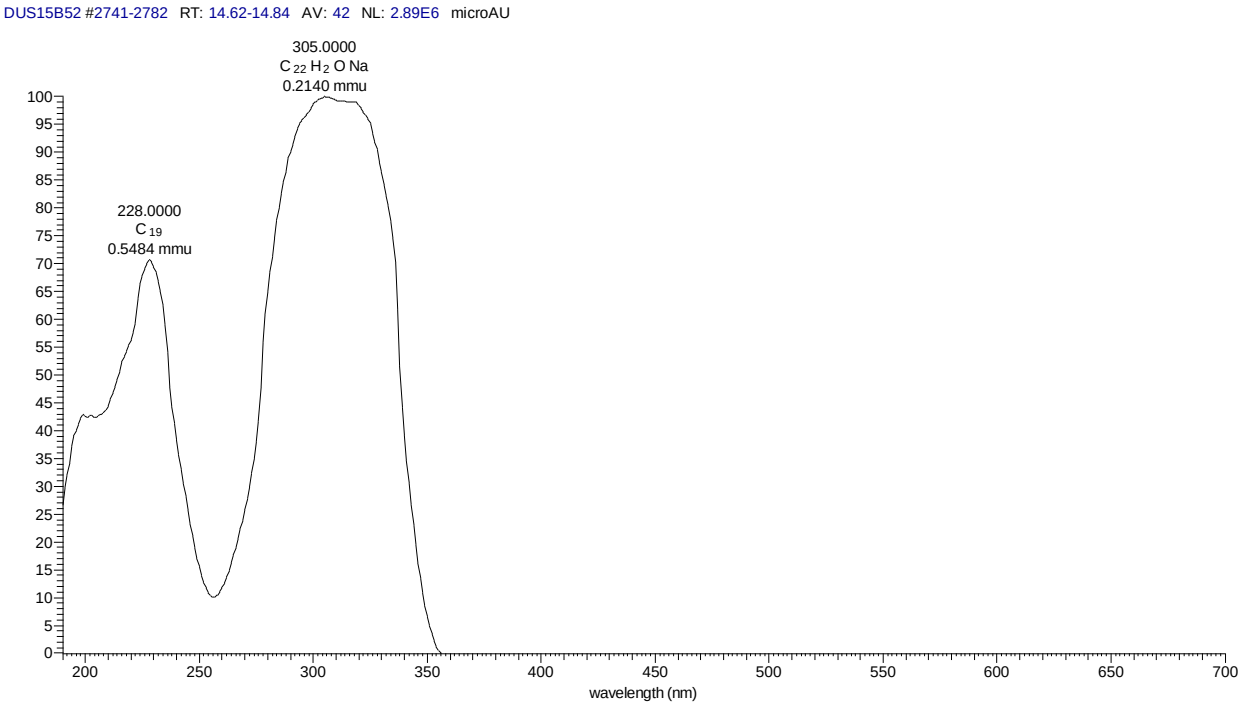

Appendix 6C: ^{1}H NMR spectrum (600 MHz, CD_3OD) of compound **181**

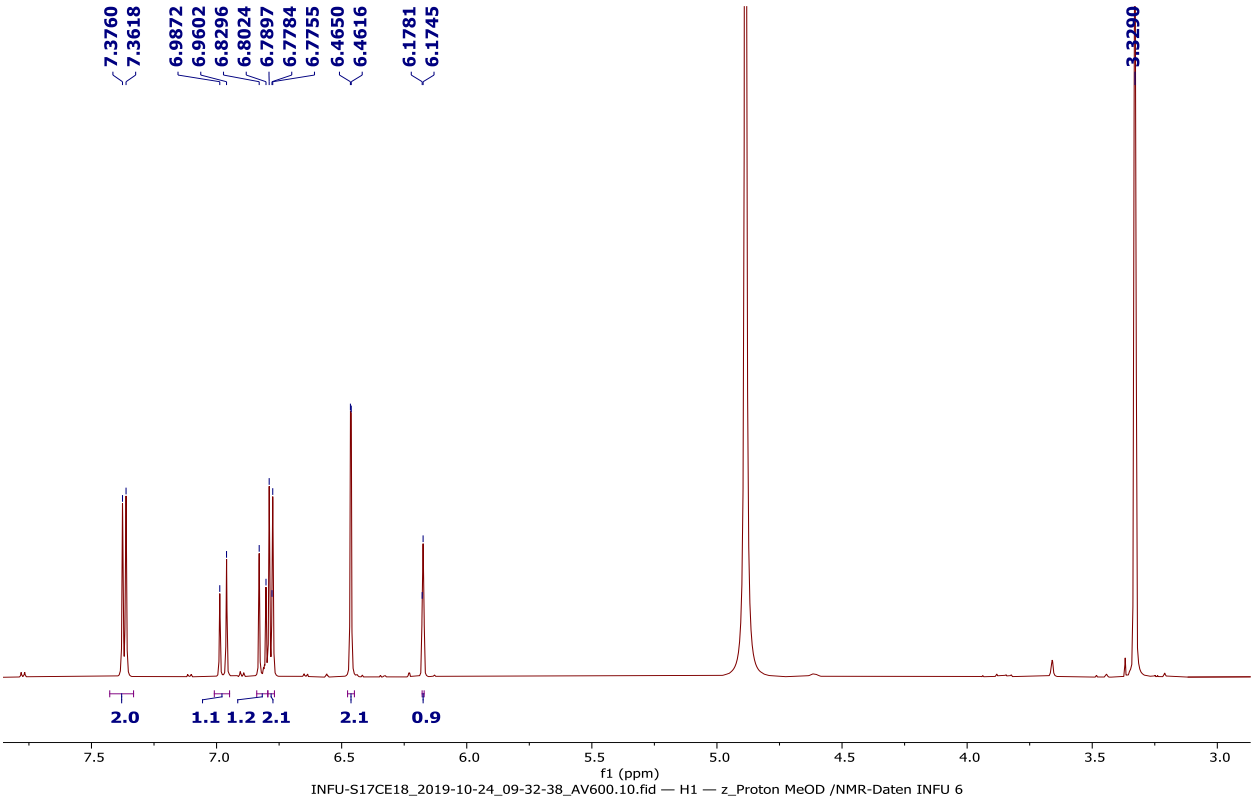

Appendix 6D: ^{13}C NMR spectrum (150 MHz, CD_3OD) of compound **181**

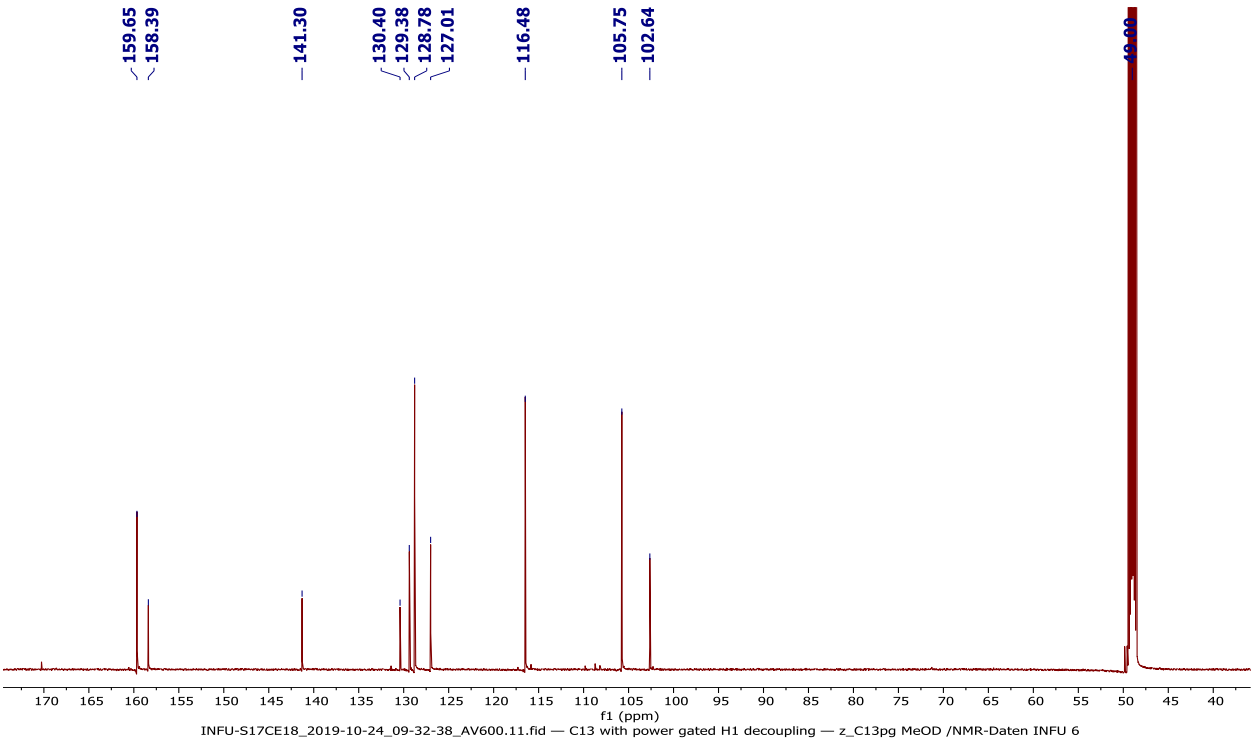

Appendix 6E: ^{1}H-^{1}H COSY spectrum (CD_3OD) of compound **181**

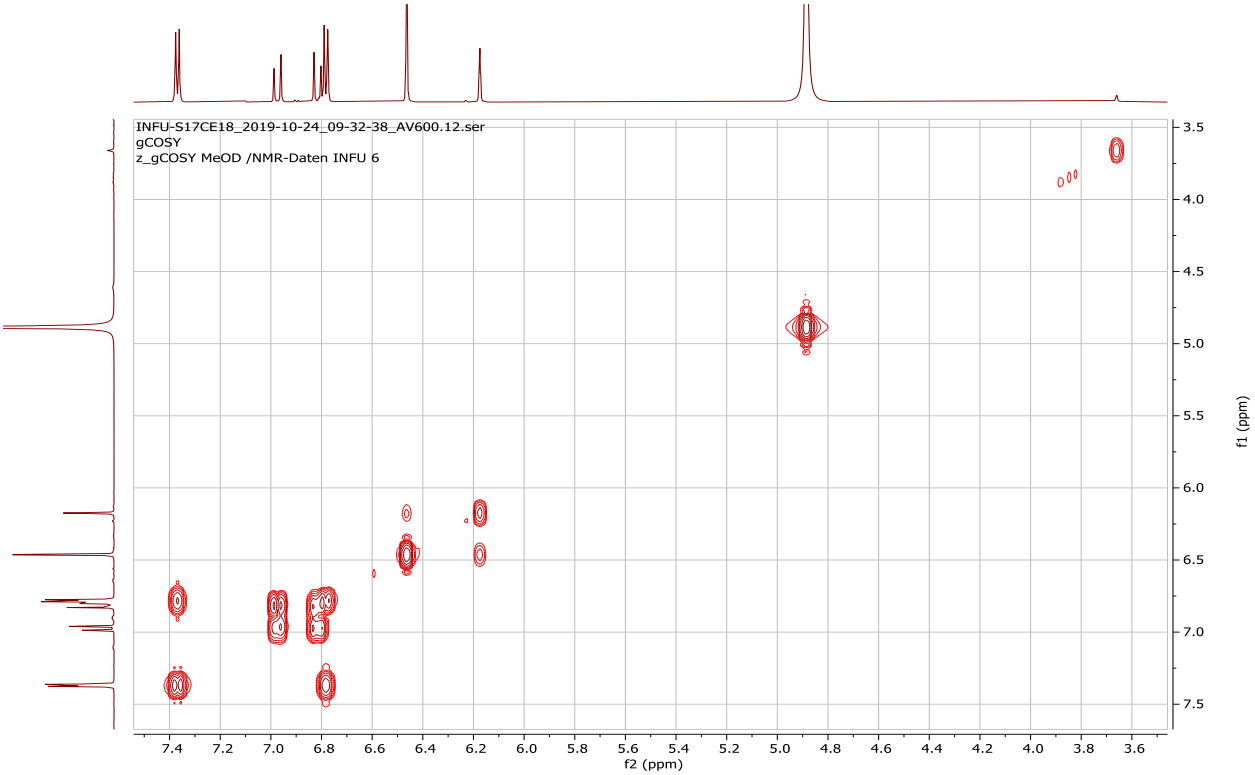

Appendix 6F: HSQC spectrum (CD_3OD) of compound **181**

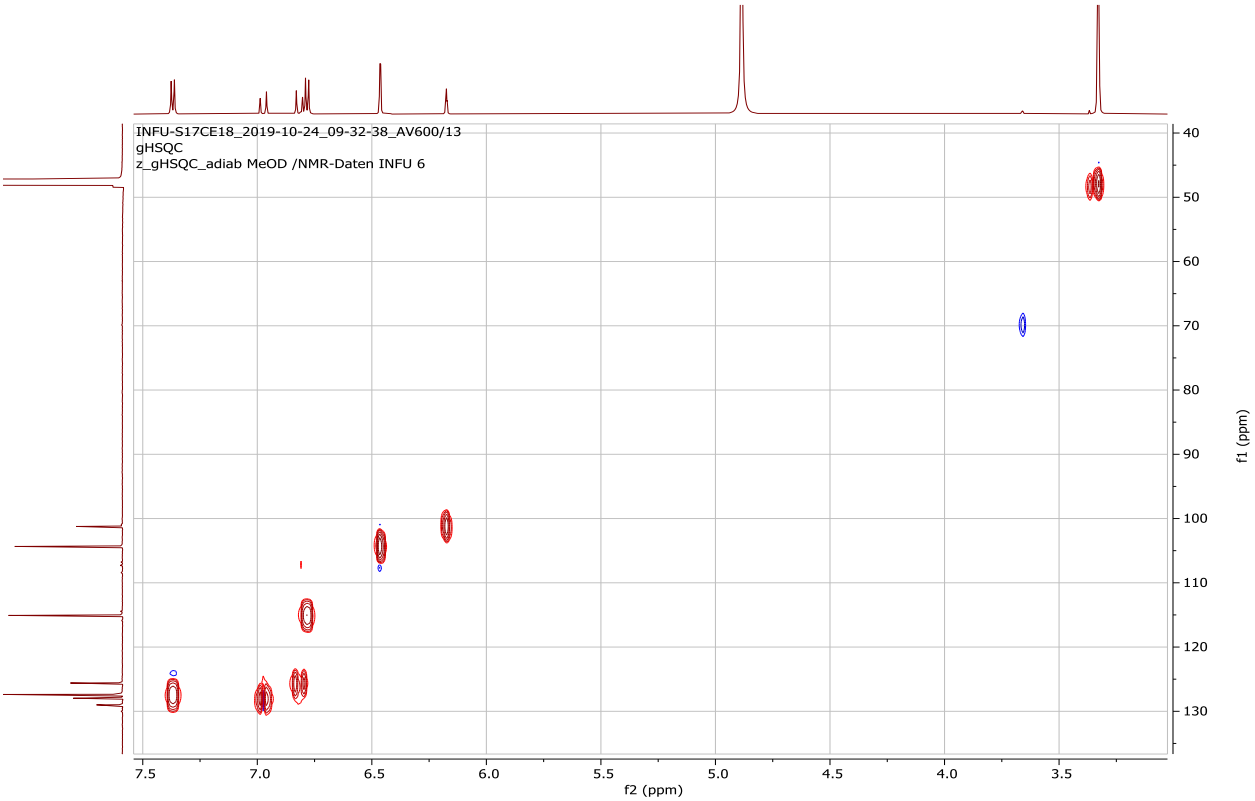

Appendix 6G: HMBC spectrum (CD_3OD) of compound **181**

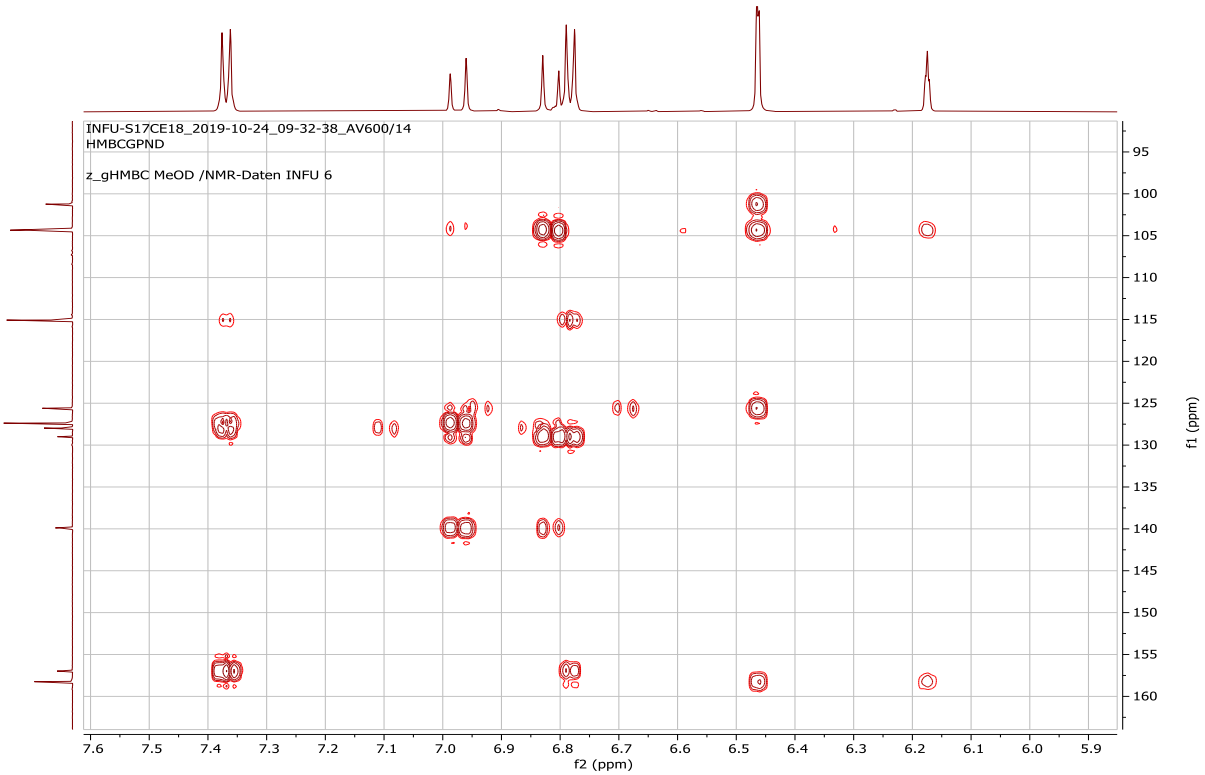

Appendix 7: NMR spectra for 4,4′-dihydroxy-3′-methoxychalcone (**182**)

Appendix 7A: HRESIMS of compound **182**

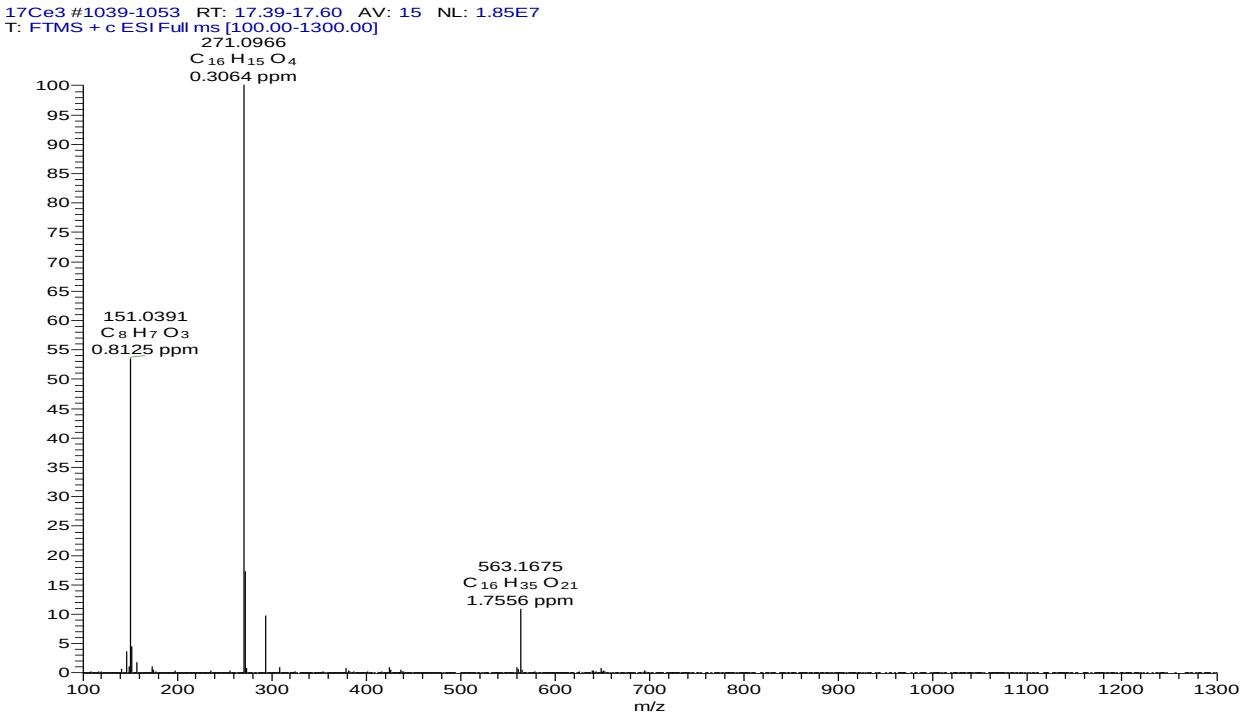

Appendix 7B: LC-UV spectrum of compound **182**

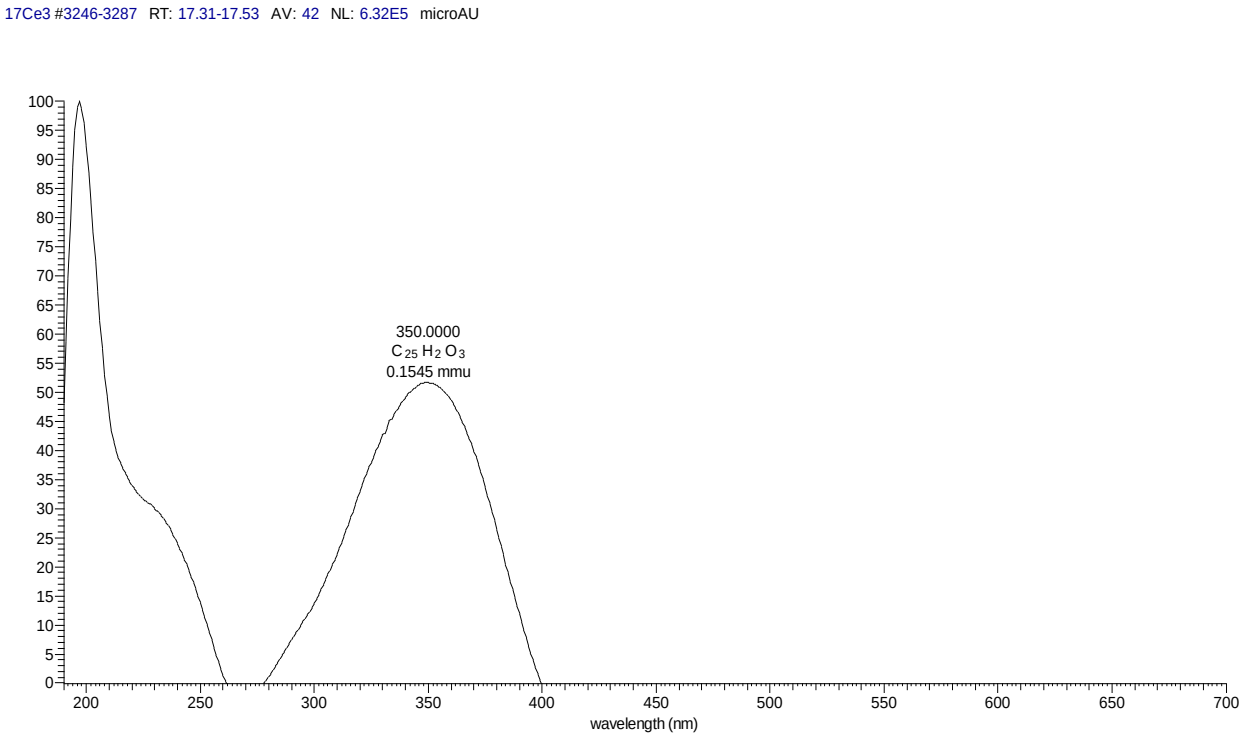

Appendix 7C: ^{1}H NMR spectrum (600 MHz, DMSO-d_6) of compound **182**

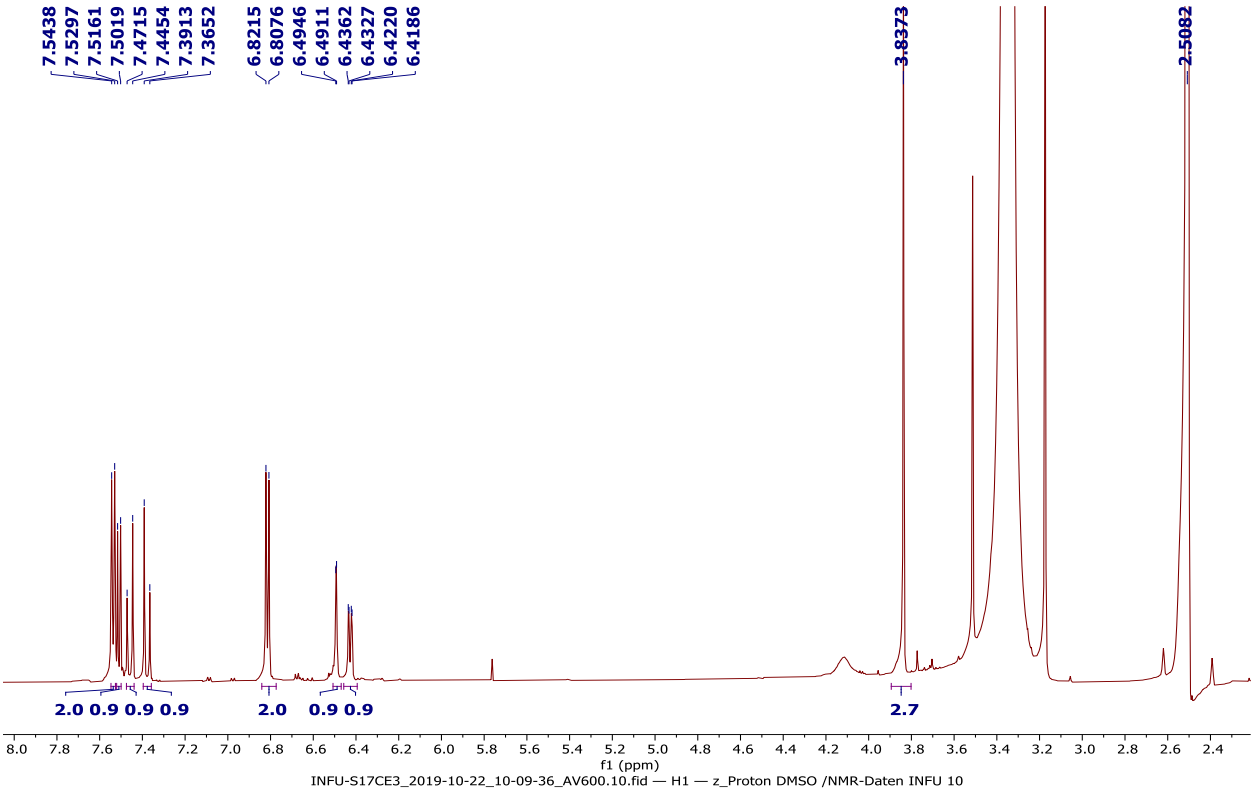

Appendix 7D: ^{13}C NMR spectrum (150 MHz, DMSO-d_6) of compound **182**

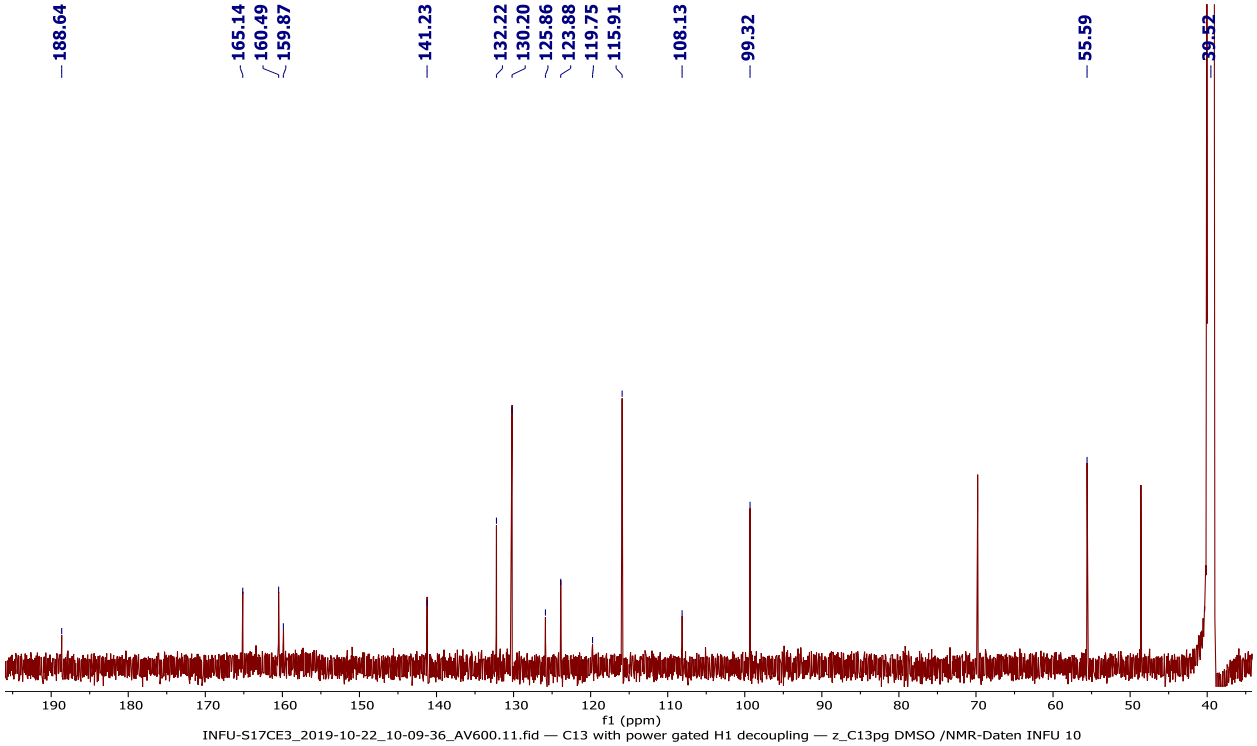

Appendix 7E: ^{1}H-^{1}H COSY spectrum (DMSO-d_6) of compound **182**

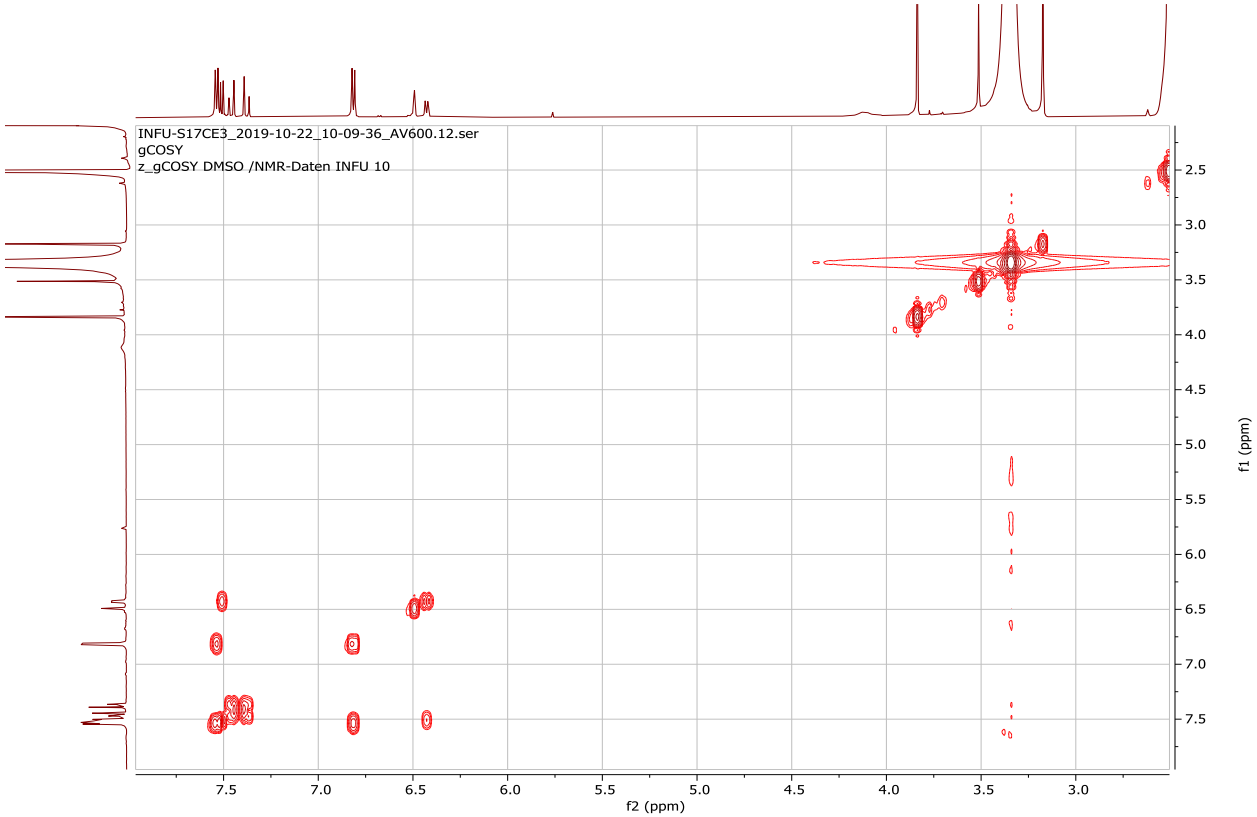

Appendix 7F: HSQC spectrum (DMSO-d_6) of compound **182**

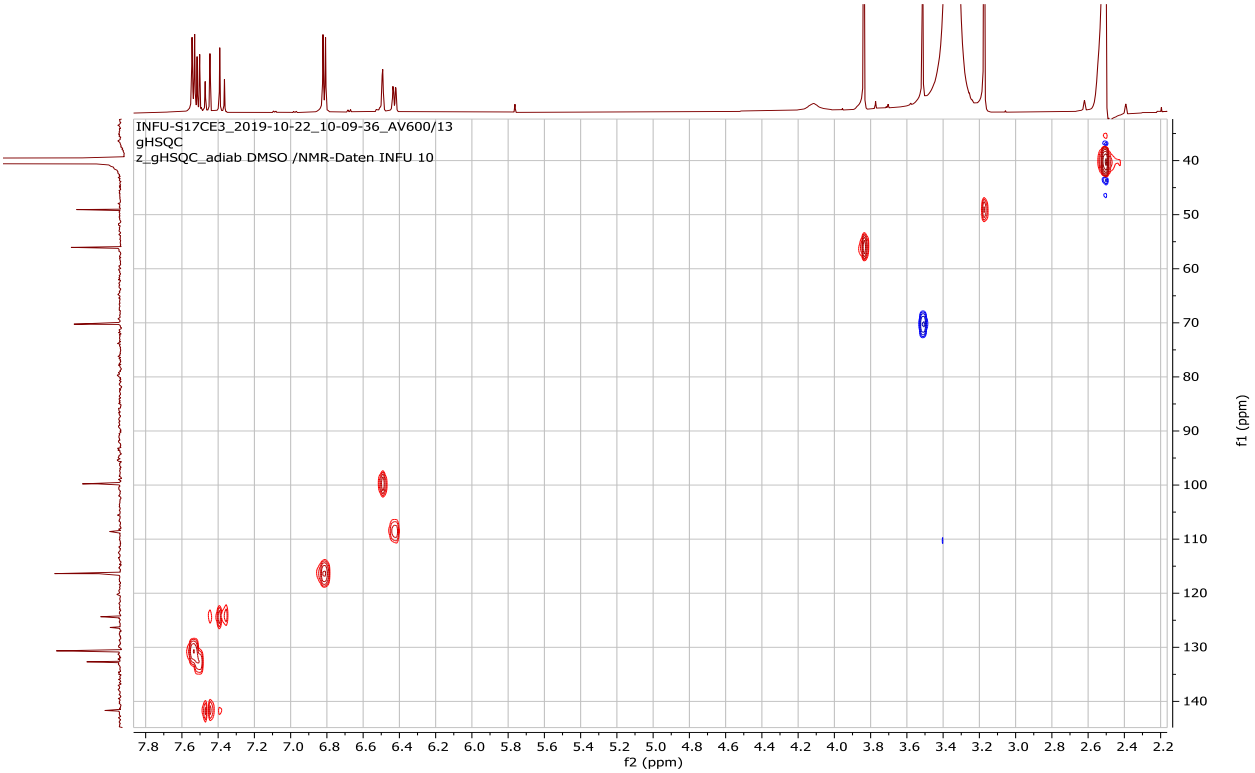

Appendix 7G: HMBC spectrum (DMSO-d_6) of compound **182**

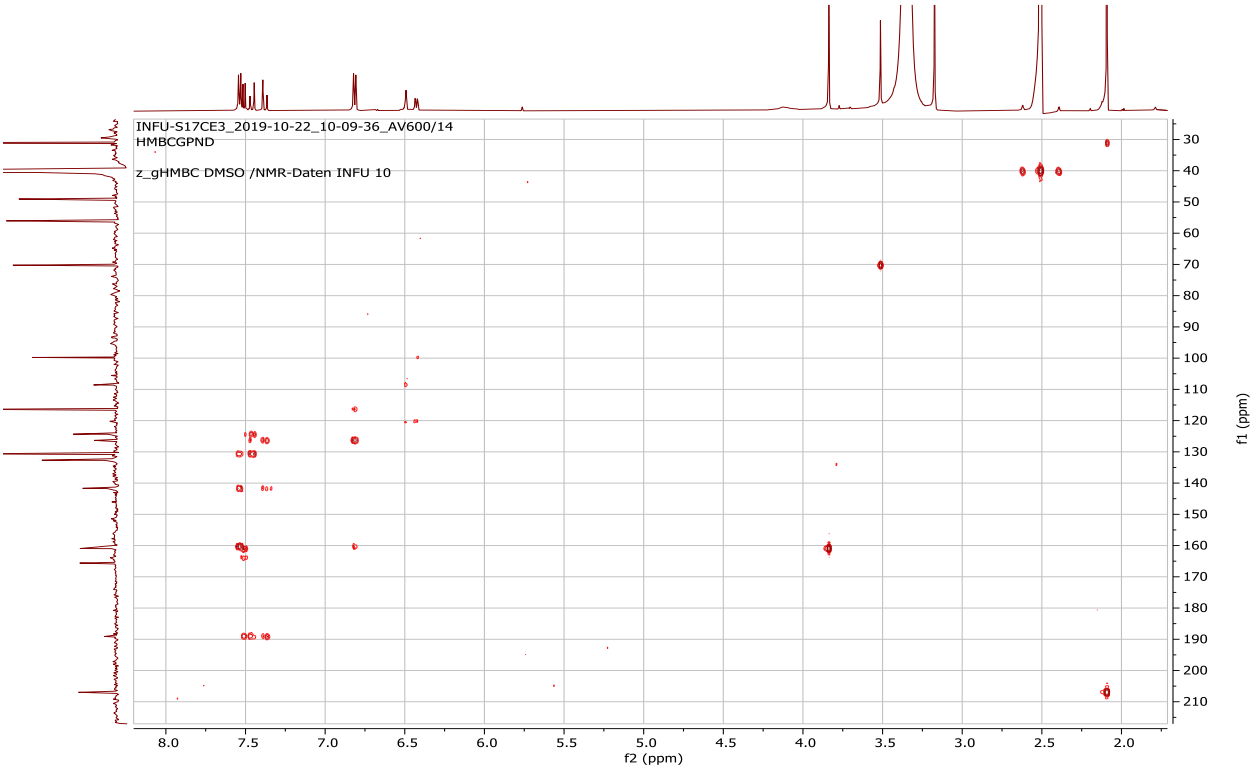

Appendix 8: NMR spectra for *N-trans*-coumaroyltyramine (**170**)

Appendix 8A: HRESIMS of compound **170**

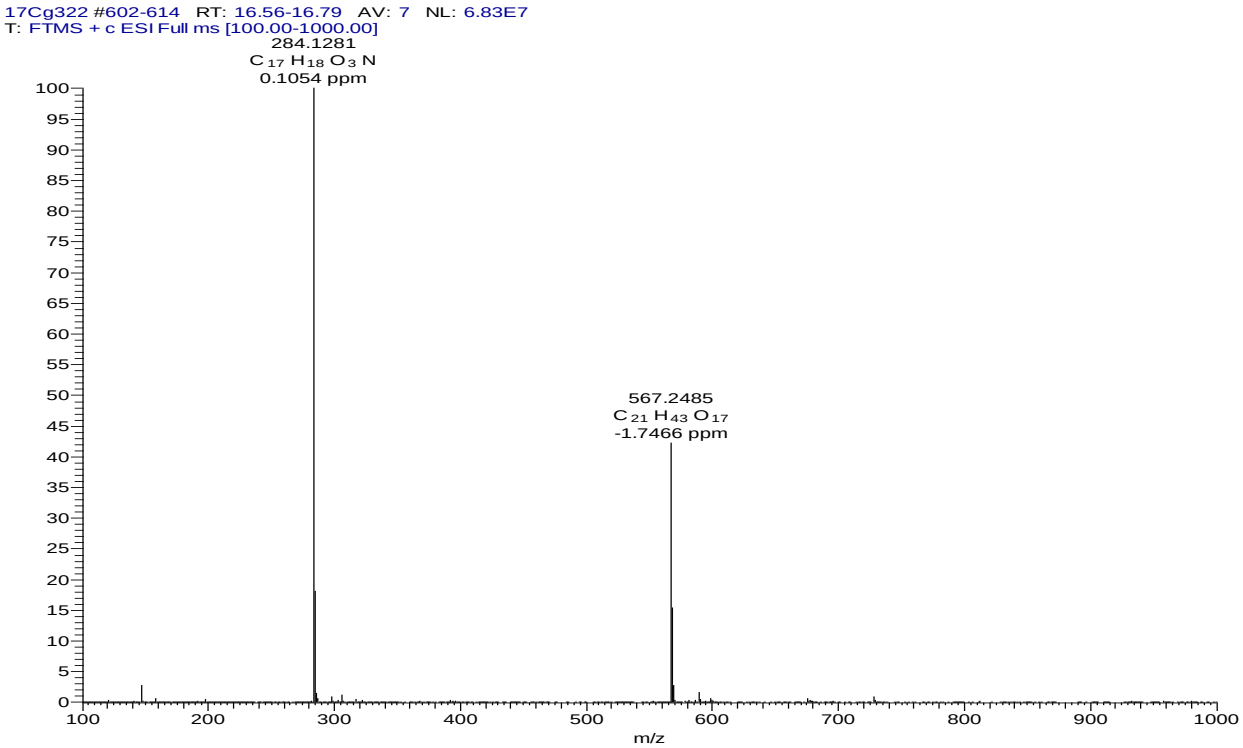

Appendix 8B: LC-UV spectrum of compound **170**

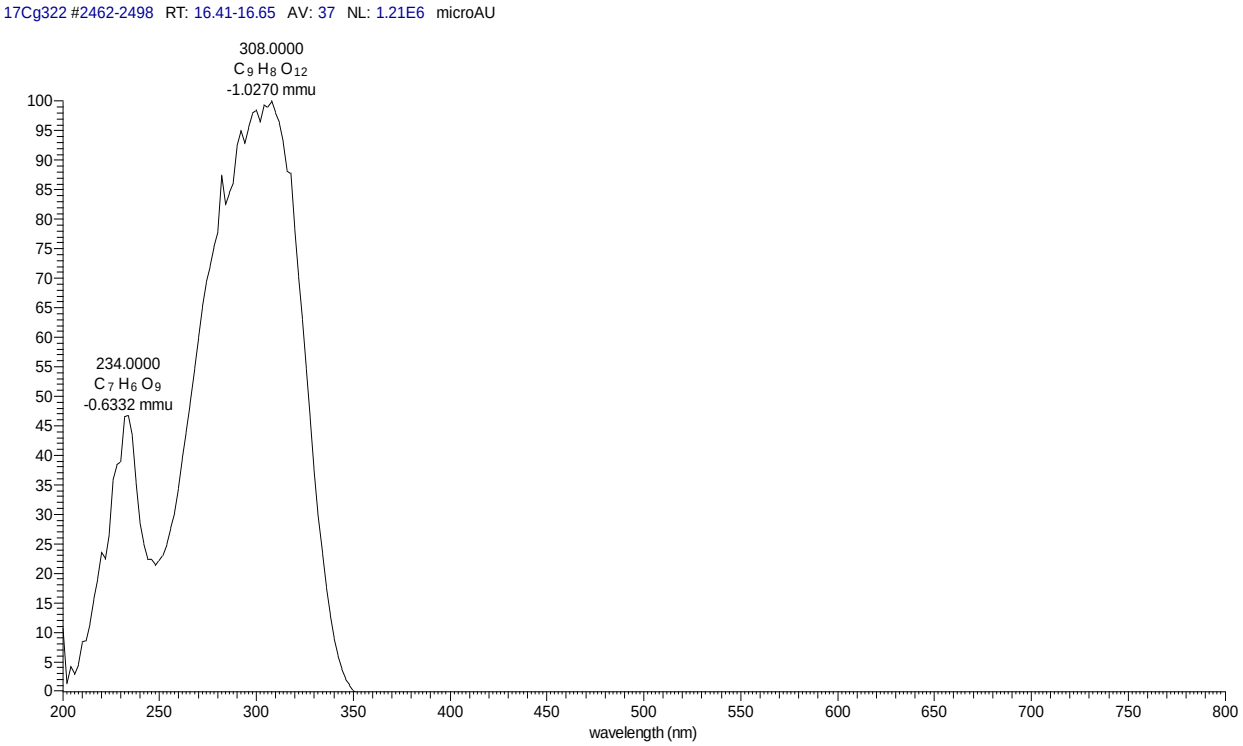

Appendix 8C: ^{1}H NMR spectrum (600 MHz, CD_3OD) of compound **170**

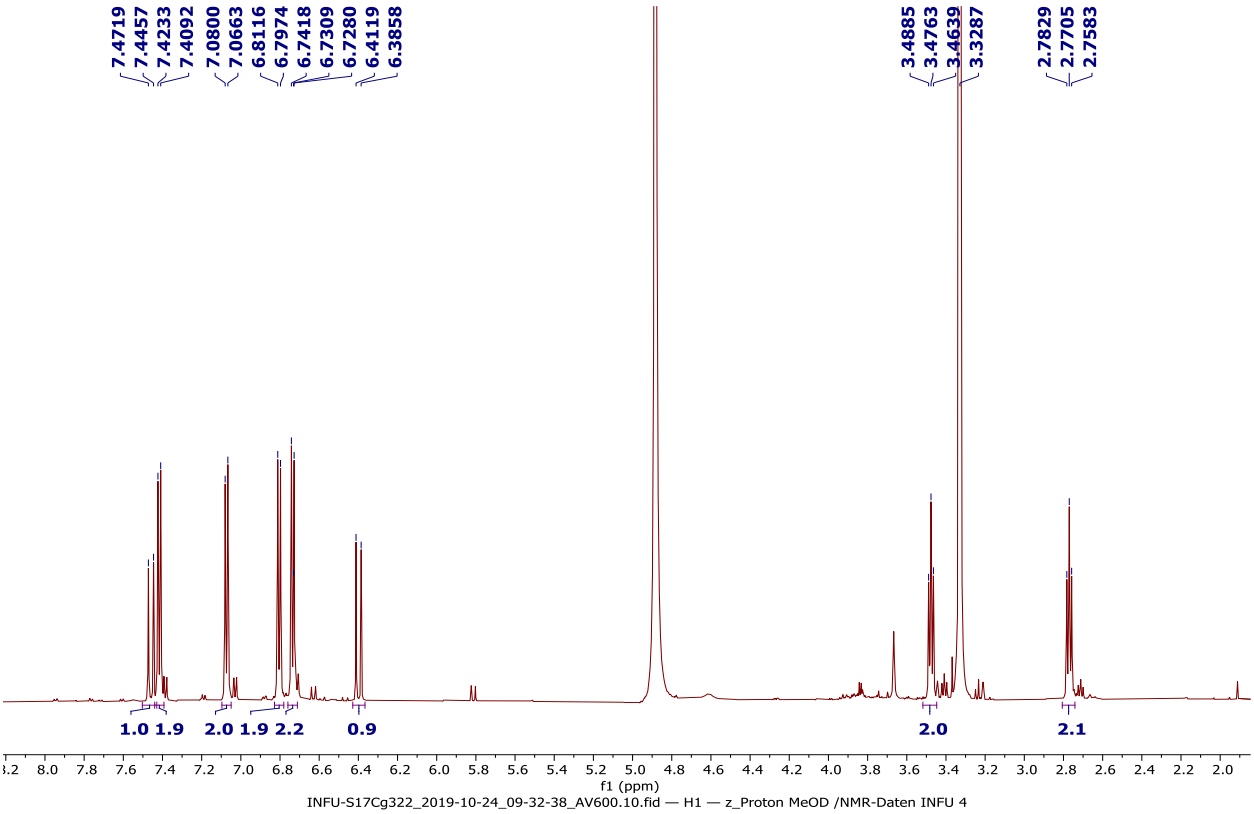

Appendix 8D: ^{13}C NMR spectrum (150 MHz, CD_3OD) of compound **170**

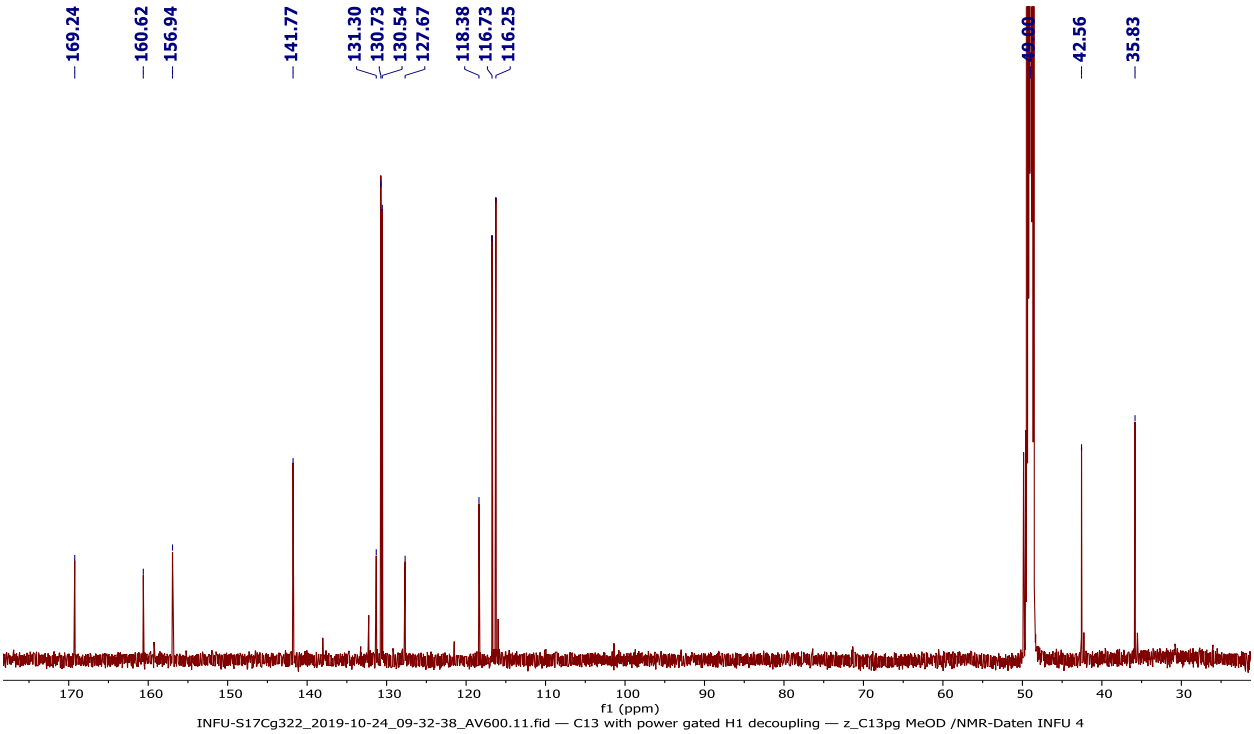

Appendix 8E: ^{1}H-^{1}H COSY spectrum (CD_3OD) of compound **170**

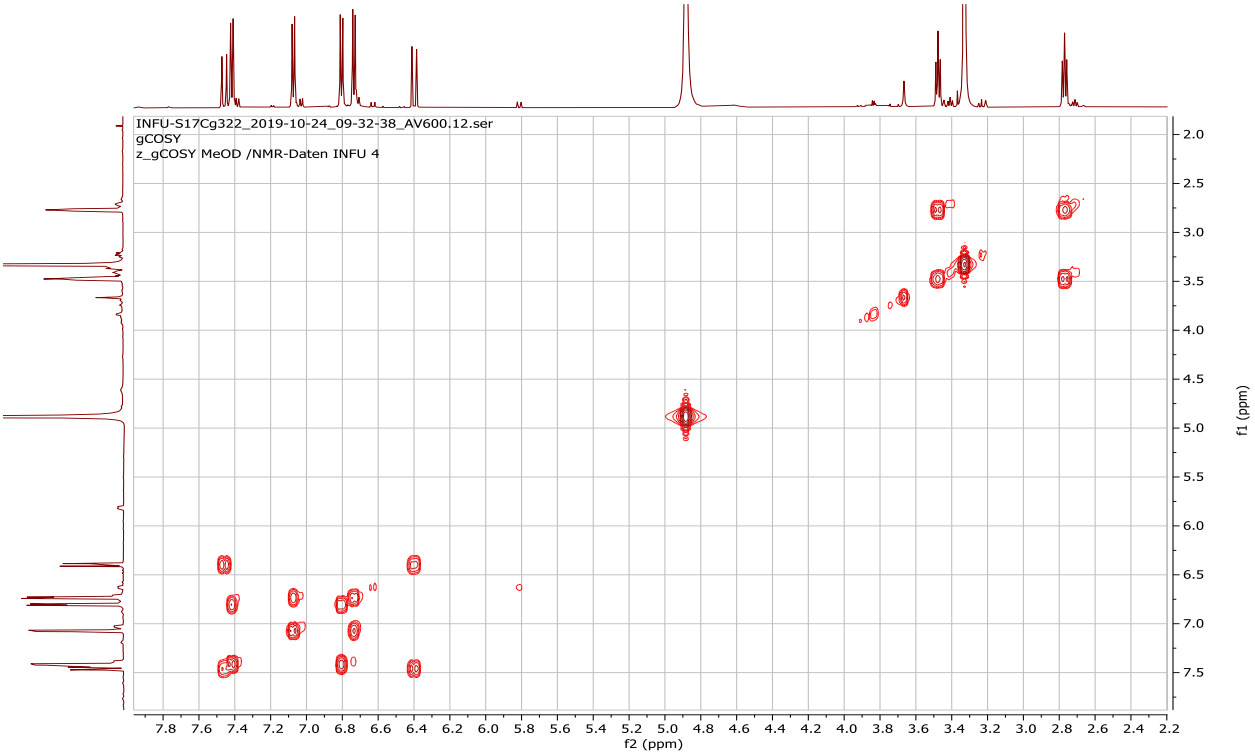

Appendix 8F: HSQC spectrum (CD_3OD) of compound **170**

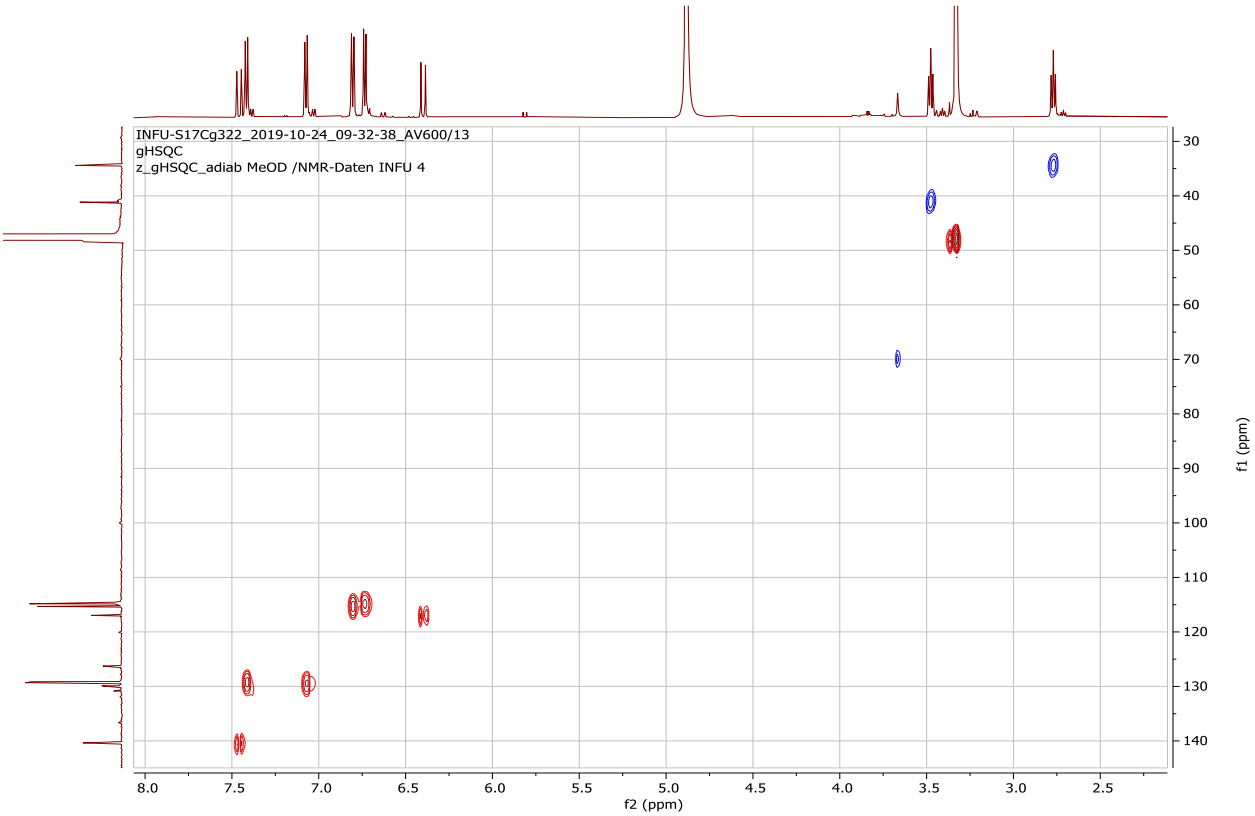

Appendix 8G: HMBC spectrum (CD_3OD) of compound **170**

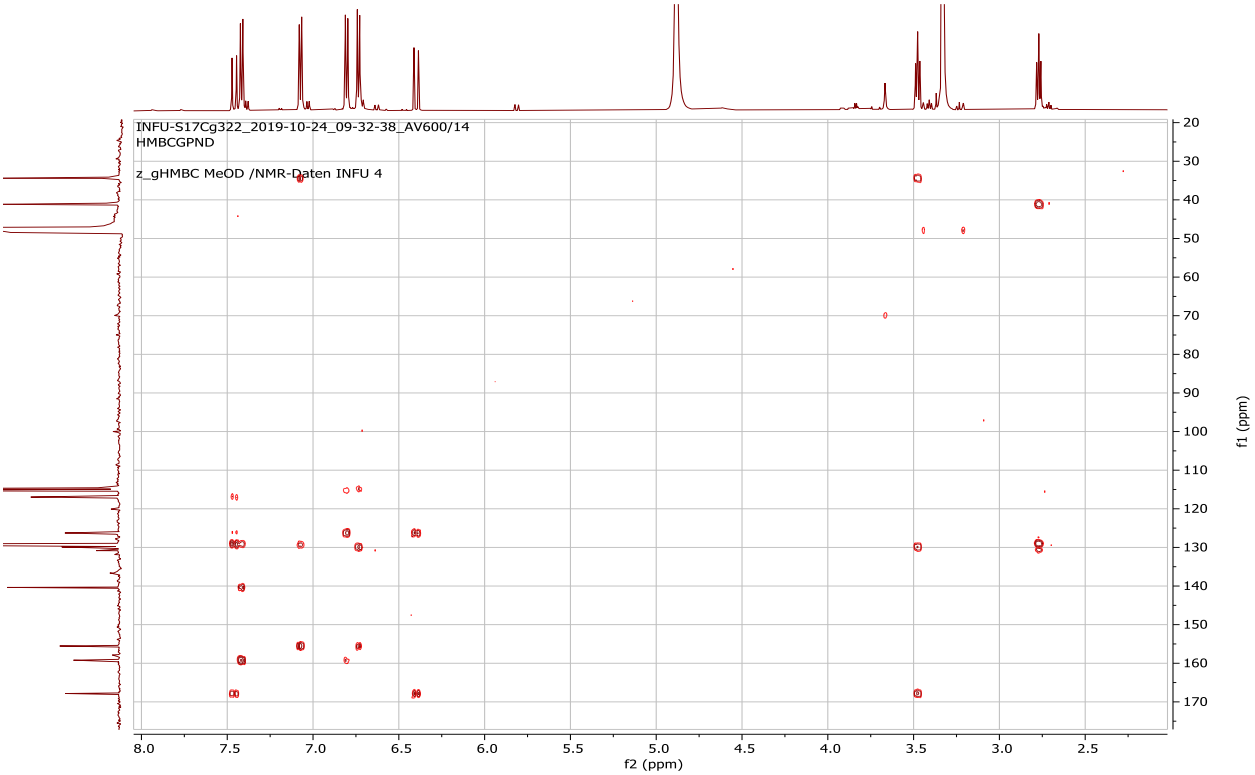

Appendix 9: NMR spectra for *N-trans*-feruloyl octopamine (**171**)

Appendix 9A: HRESIMS of compound **171**

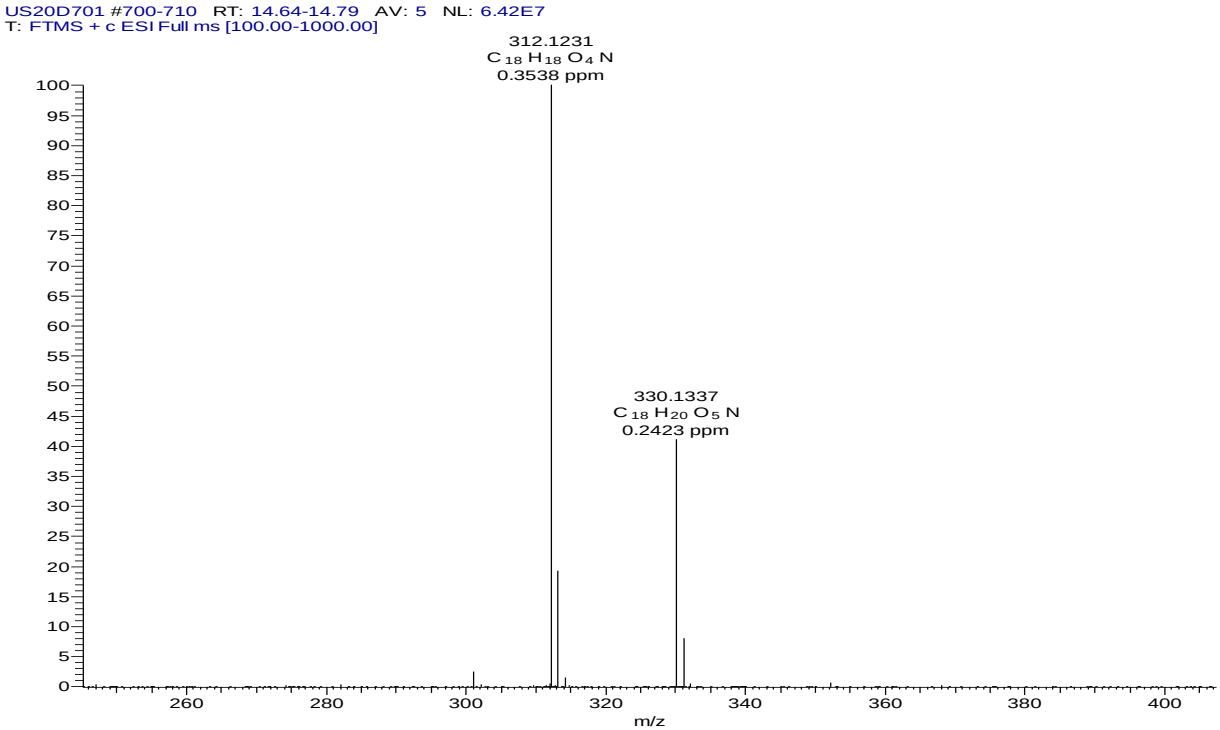

Appendix 9B: LC-UV spectrum of compound **171**

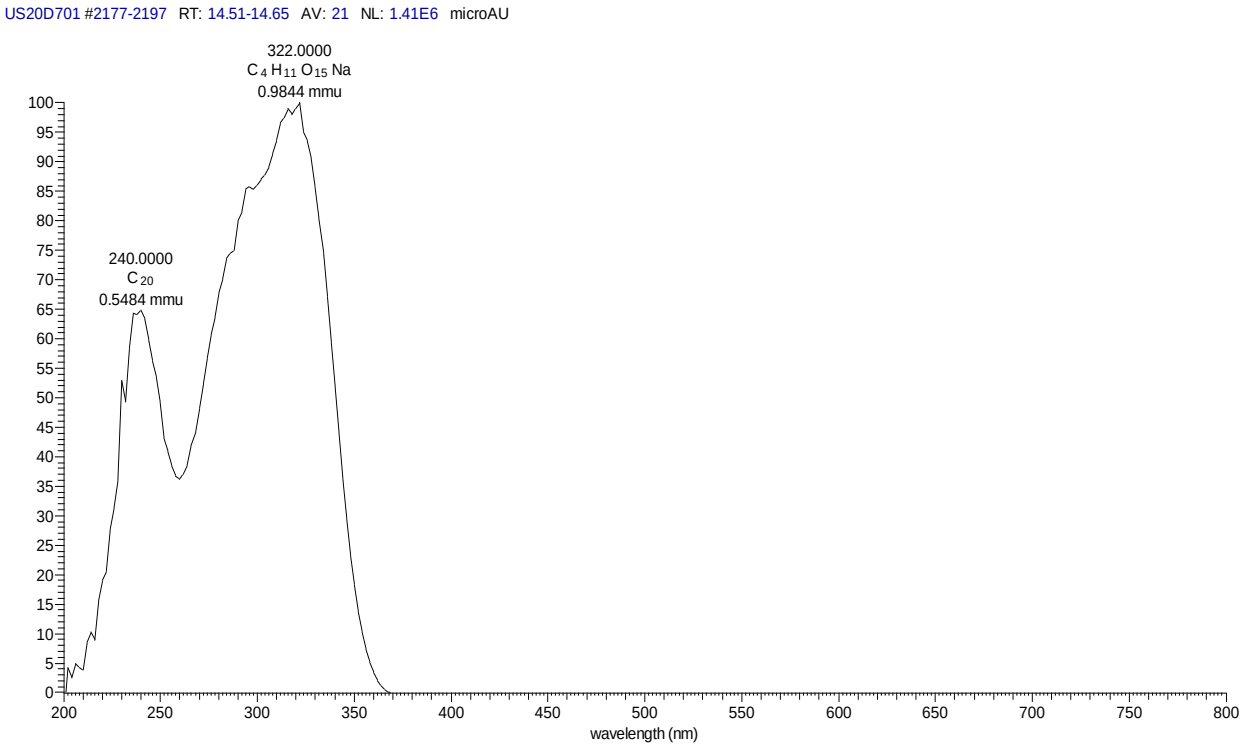

Appendix 9C: ^{1}H NMR spectrum (600 MHz, CD_3OD) of compound **171**

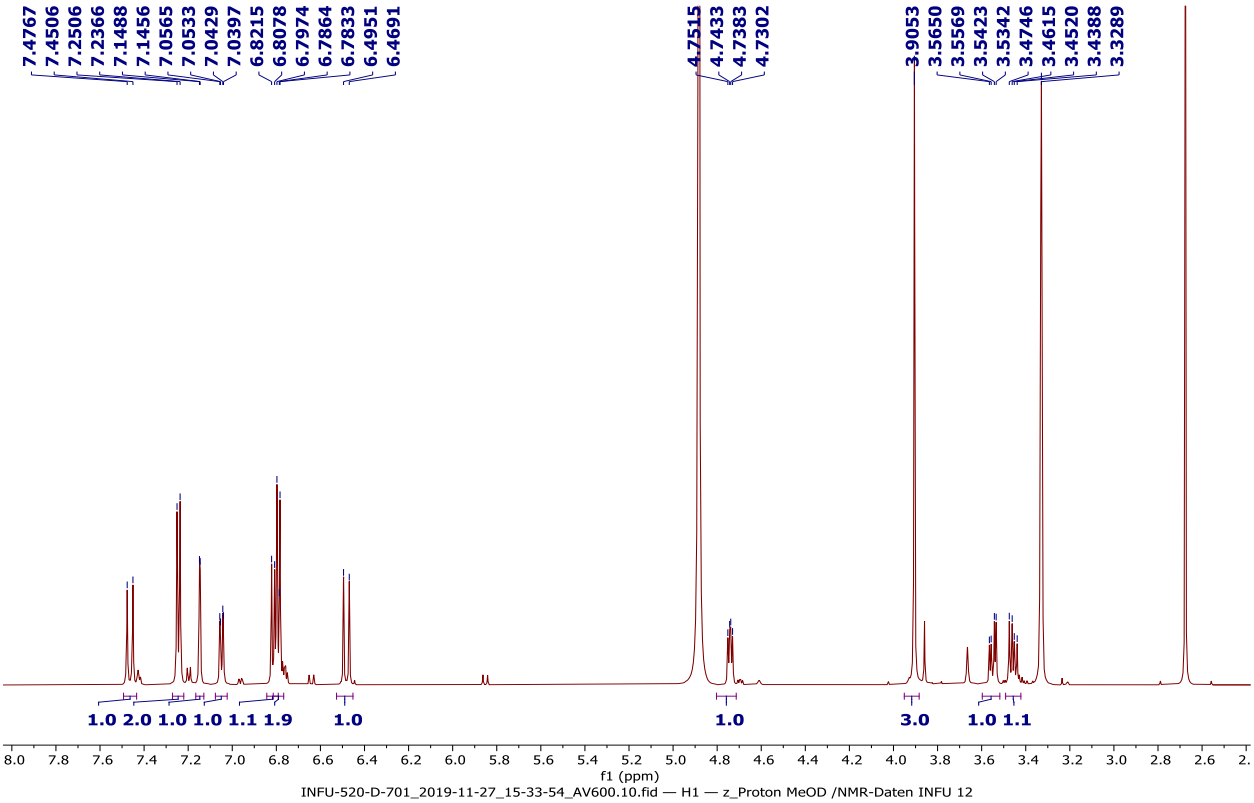

Appendix 9D: ^{13}C NMR spectrum (150 MHz, CD_3OD) of compound **171**

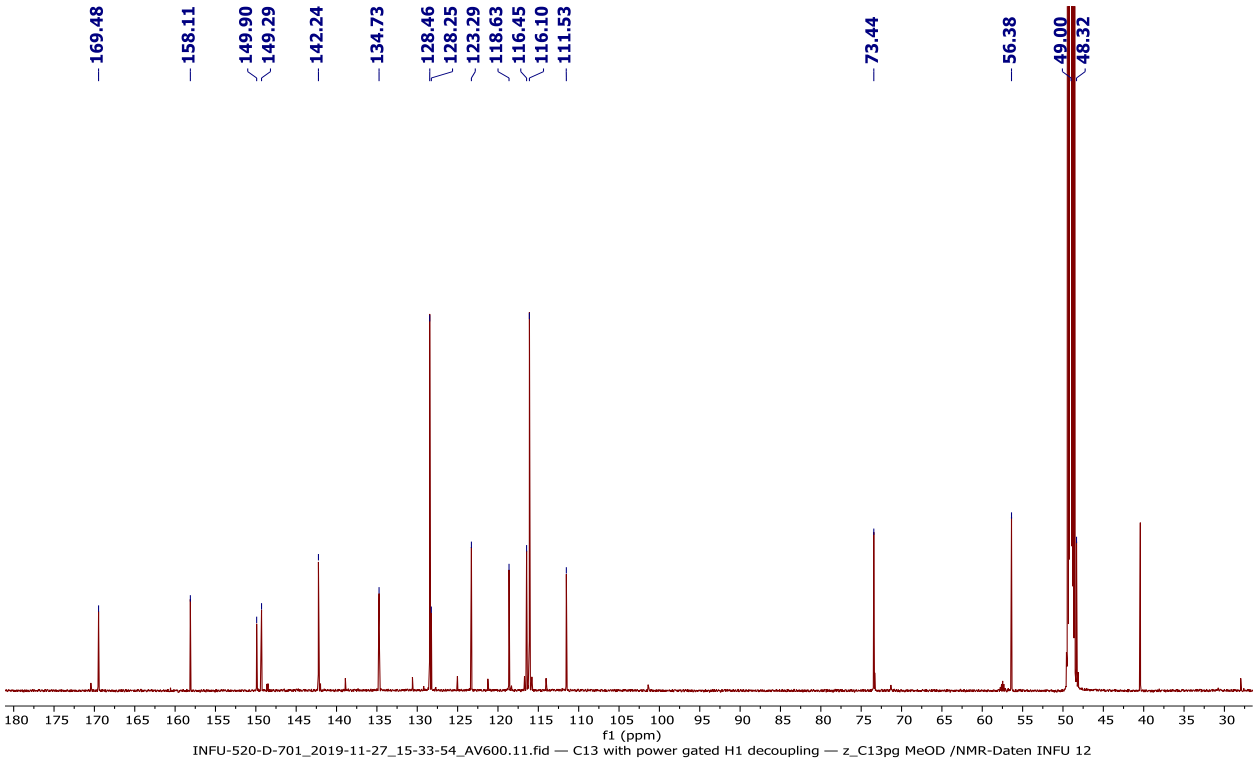

Appendix 9E: ^{1}H-^{1}H COSY spectrum (CD_3OD) of compound **171**

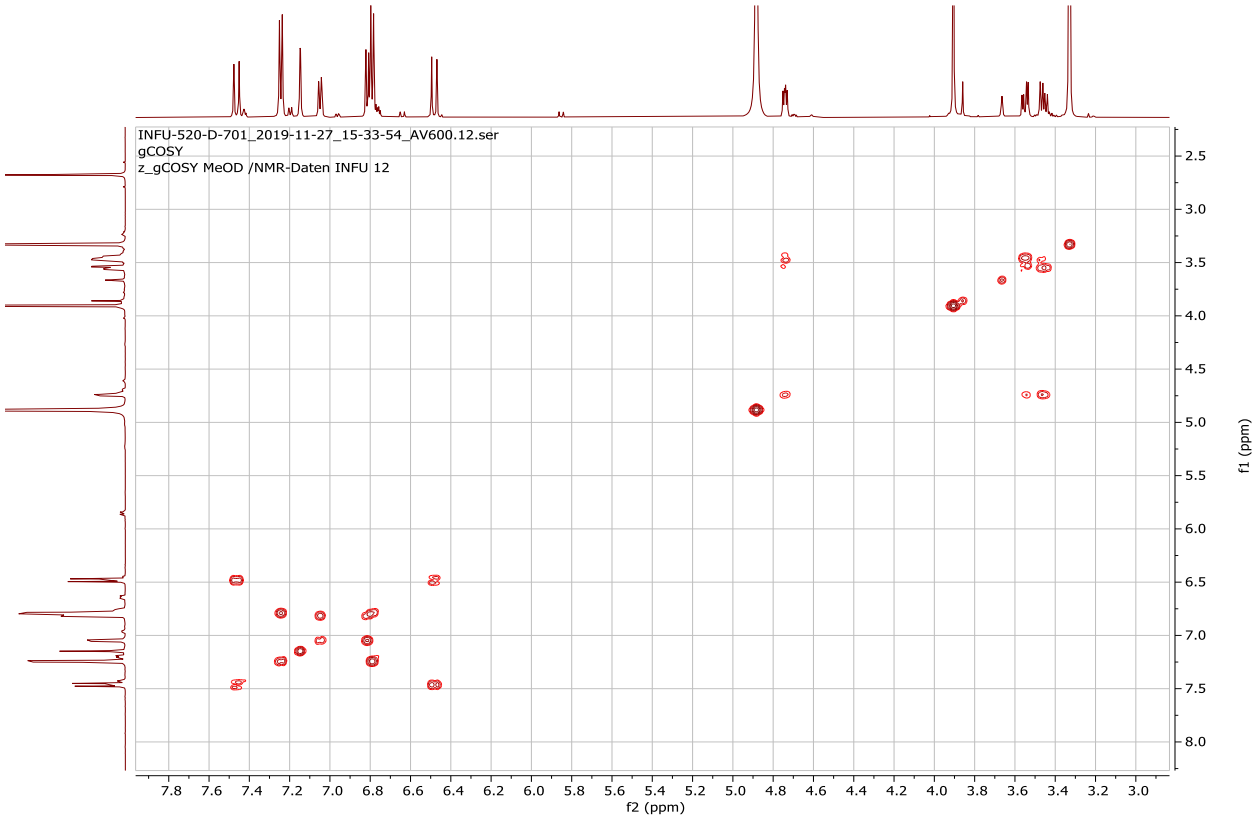

Appendix 9F: HSQC spectrum (CD_3OD) of compound **171**

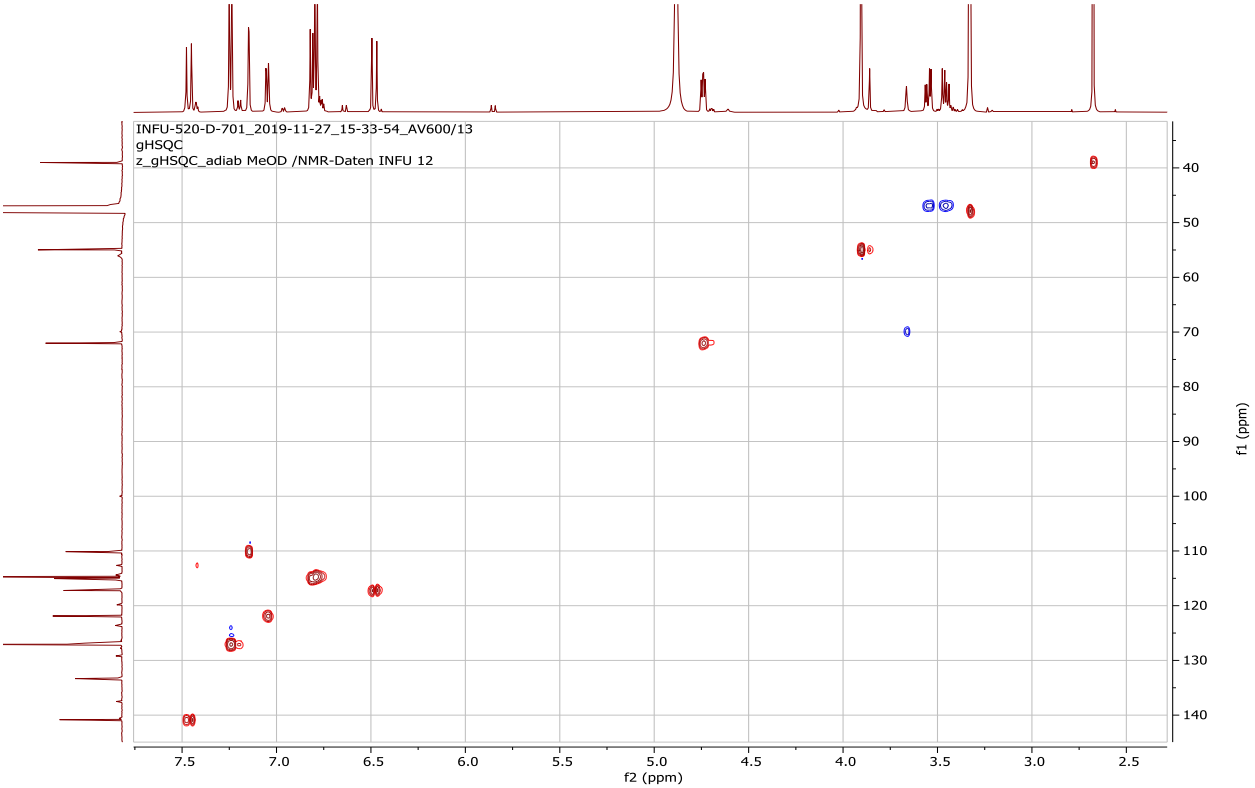

Appendix 9G: HMBC spectrum (CD_3OD) of compound **171**

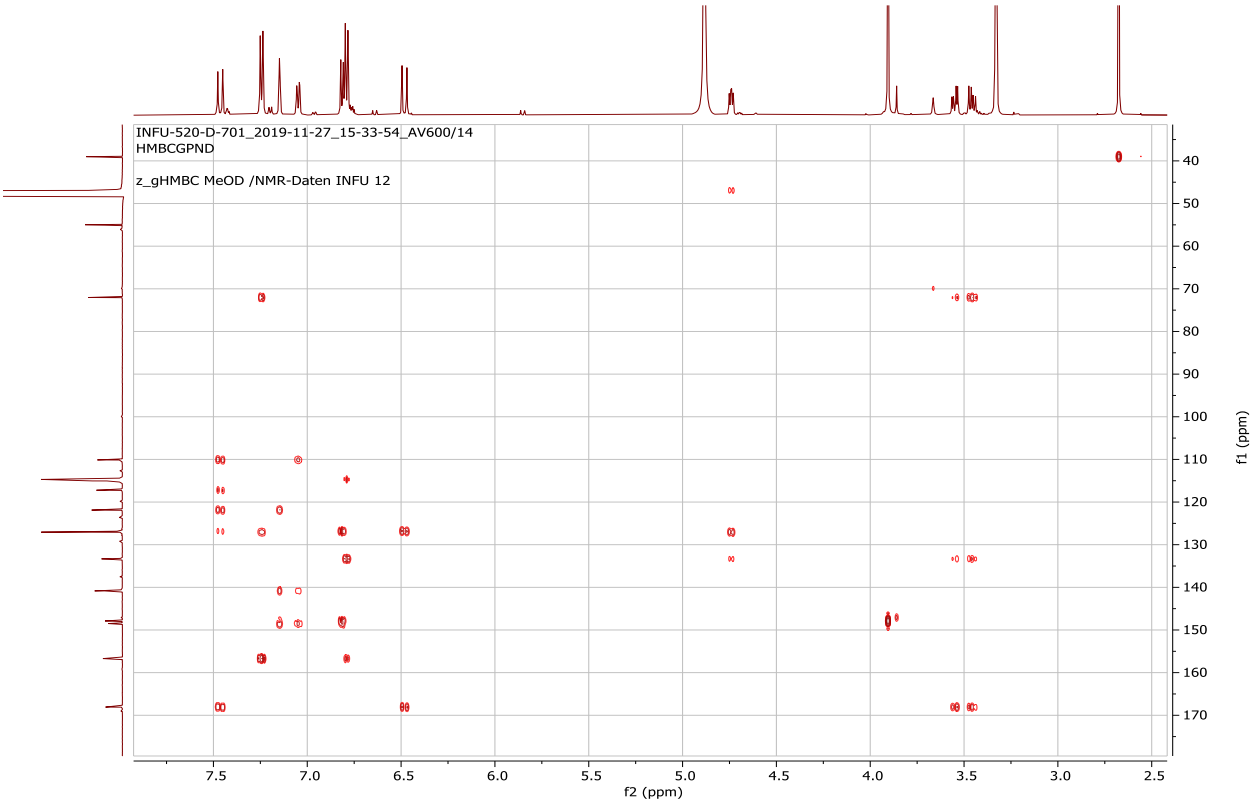

Appendix 10: NMR spectra for 7-hydroxy-1-(4-hydroxy-3-methoxyphenyl)-N_2, N_3-bis(4-hydroxyphenethyl)-6-methoxy-1,2-dihydronaphthalene-2,3-dicarboxamide (**183**)

Appendix 10A: HRESIMS of compound **183**

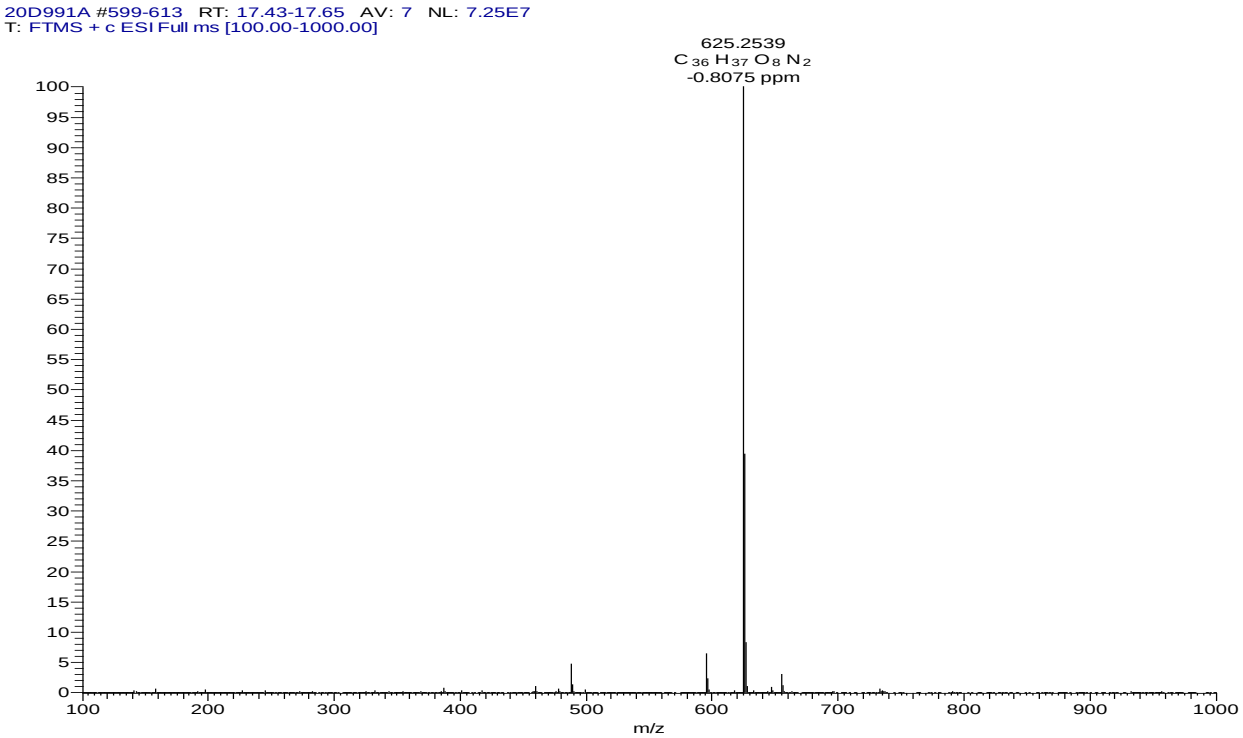

Appendix 10B: LC-UV spectrum of compound **183**

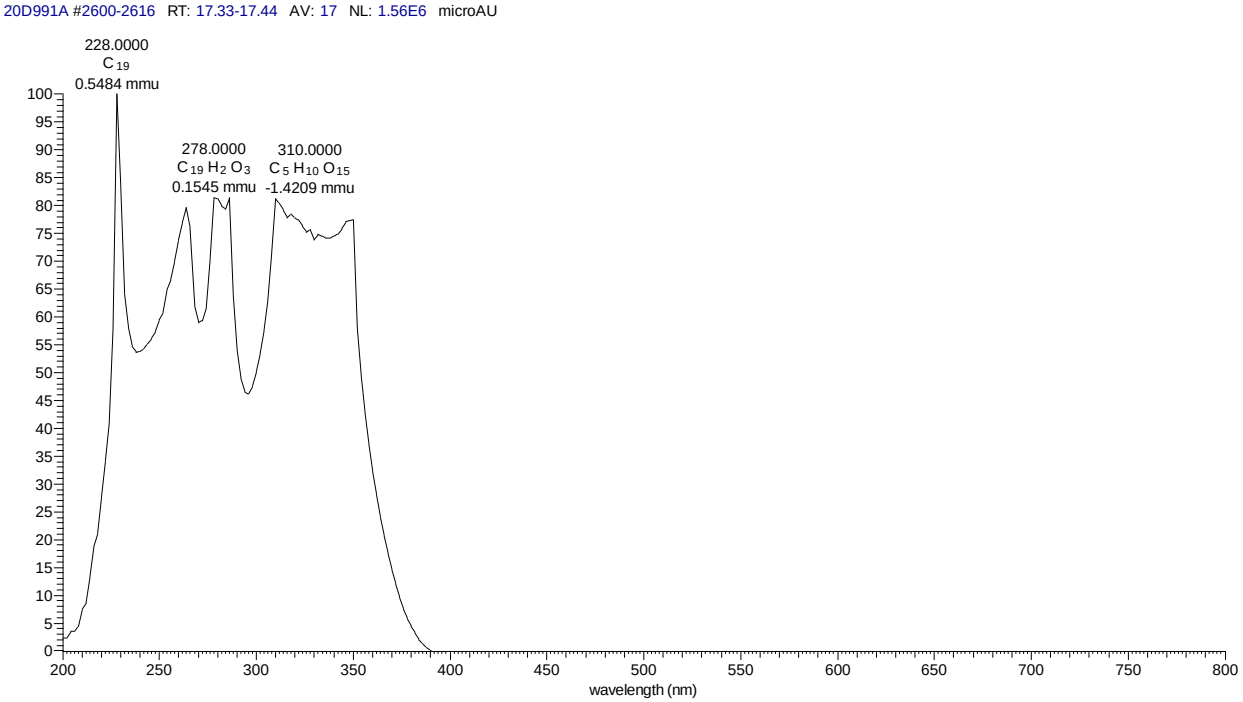

Appendix 10C: ^{1}H NMR spectrum (700 MHz, CD_3OD) of compound **183**

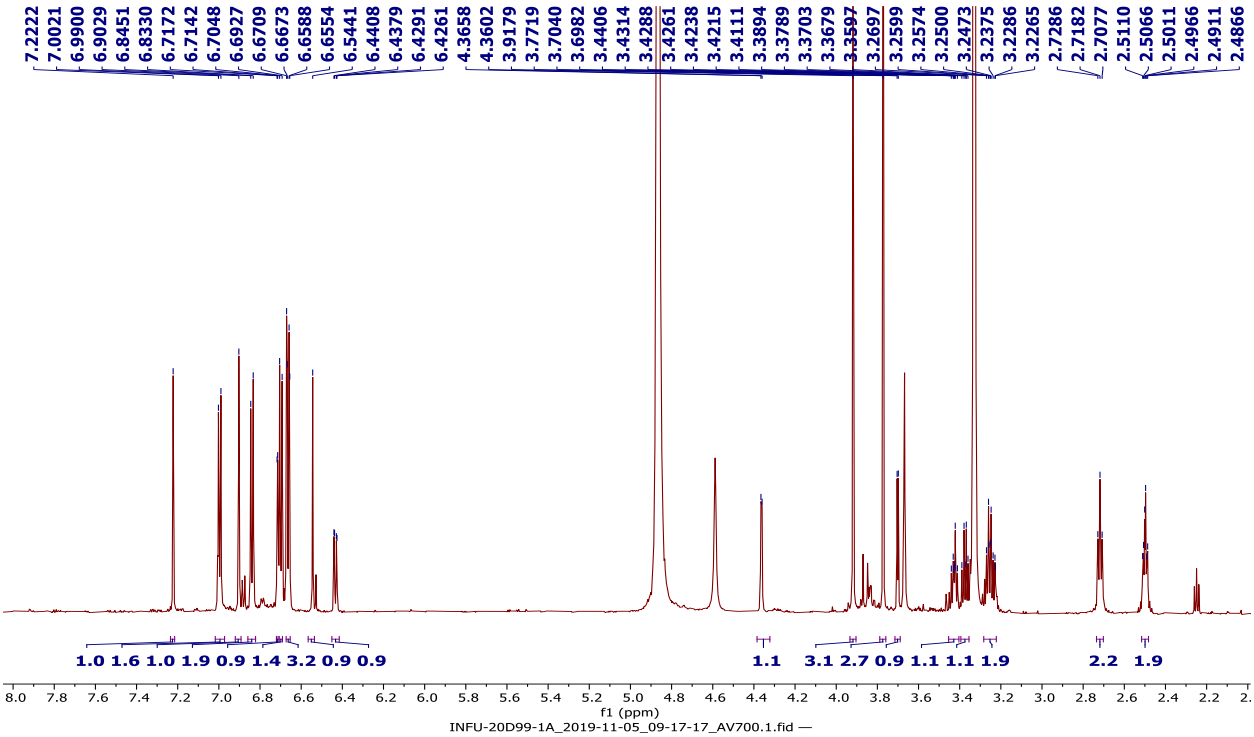

Appendix 10D: ^{13}C NMR spectrum (175 MHz, CD_3OD) of compound **183**

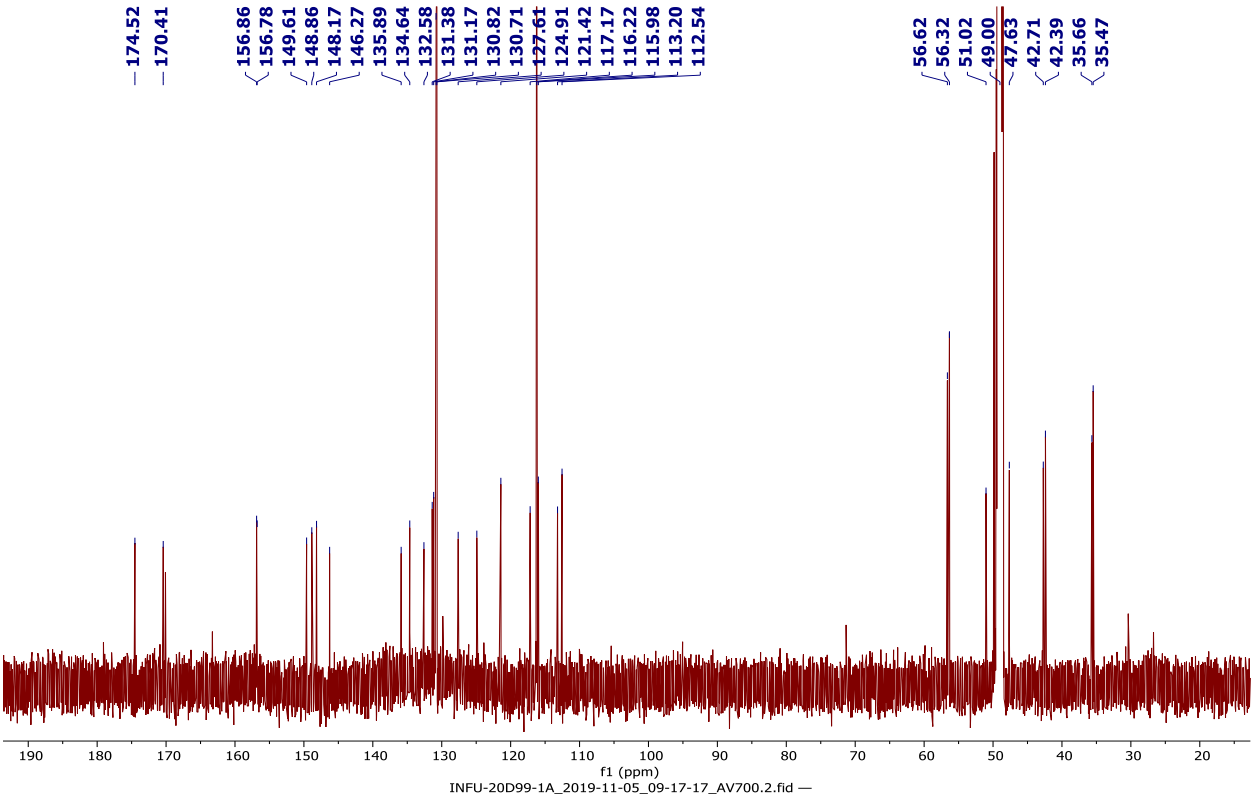

Appendix 10E: DEPT-135 spectrum (175 MHz, CD_3OD) of compound **183**

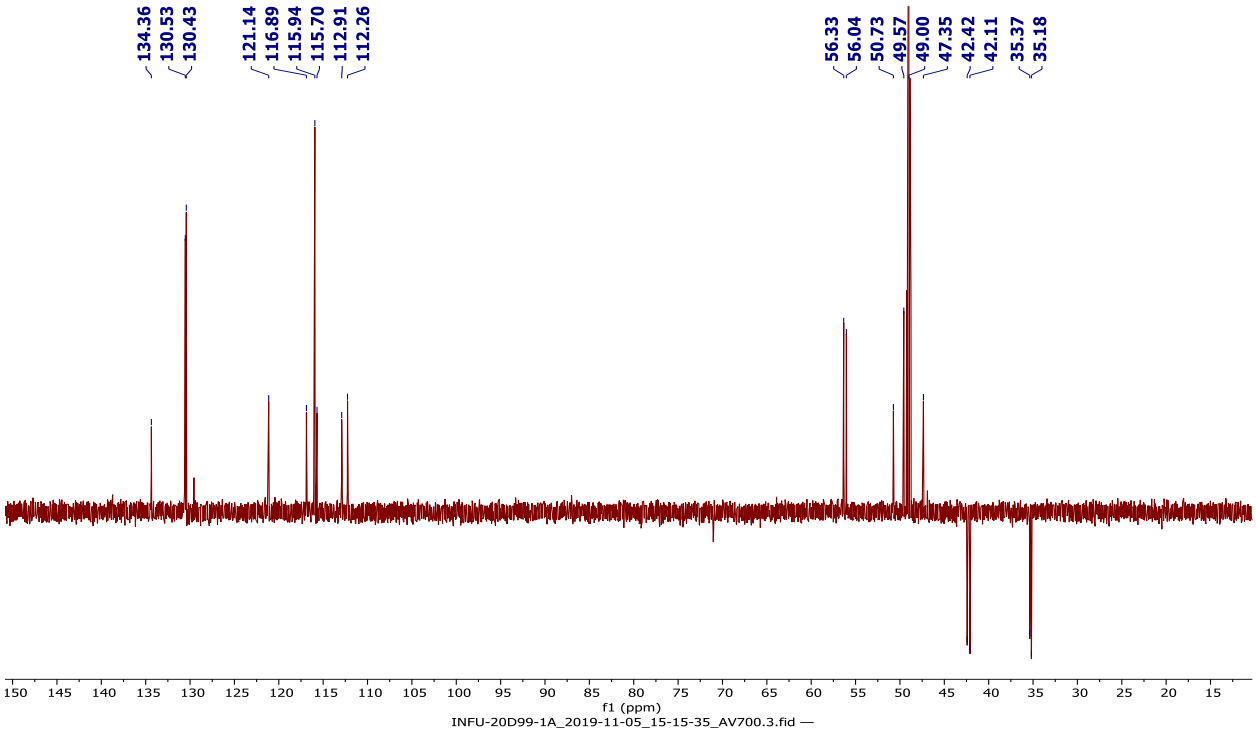

Appendix 10F: ^1H-^1H COSY spectrum (CD_3OD) of compound **183**

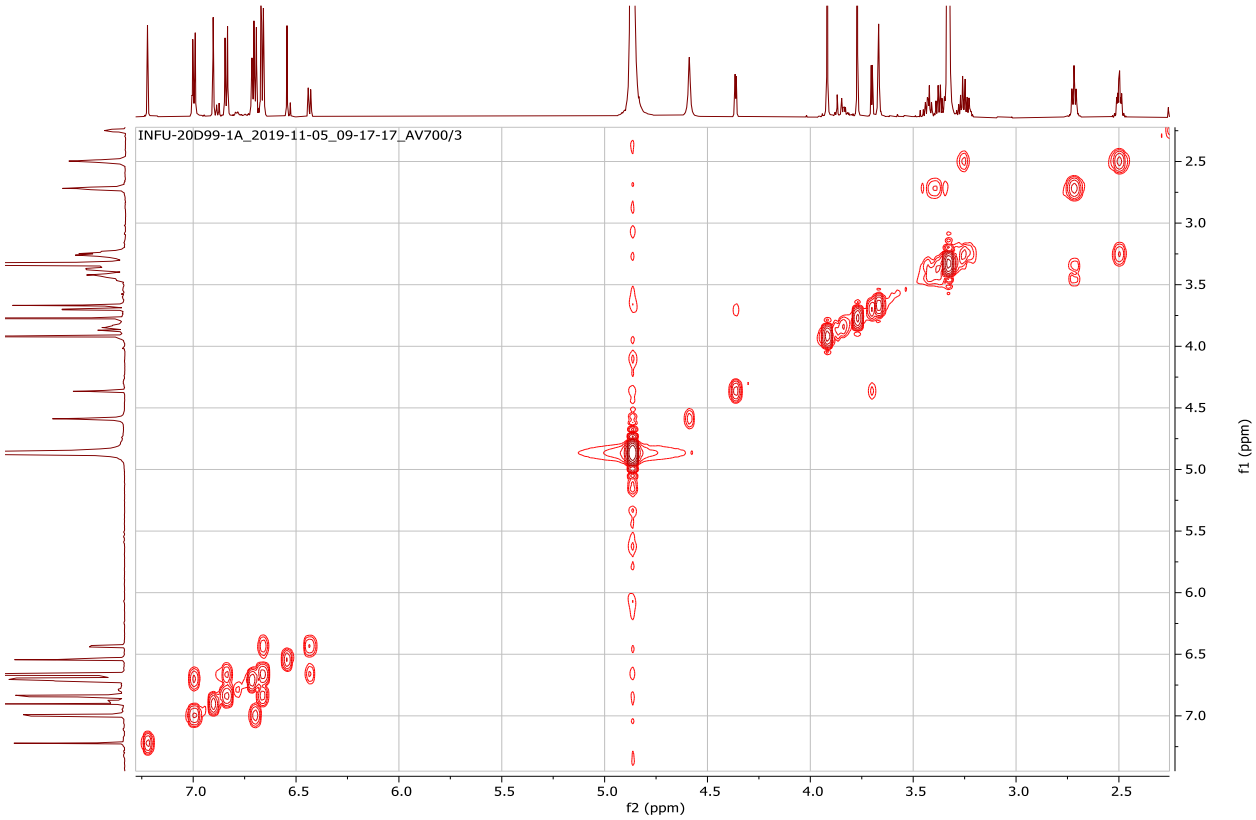

Appendix 10G: HSQC spectrum (CD_3OD) of compound **183**

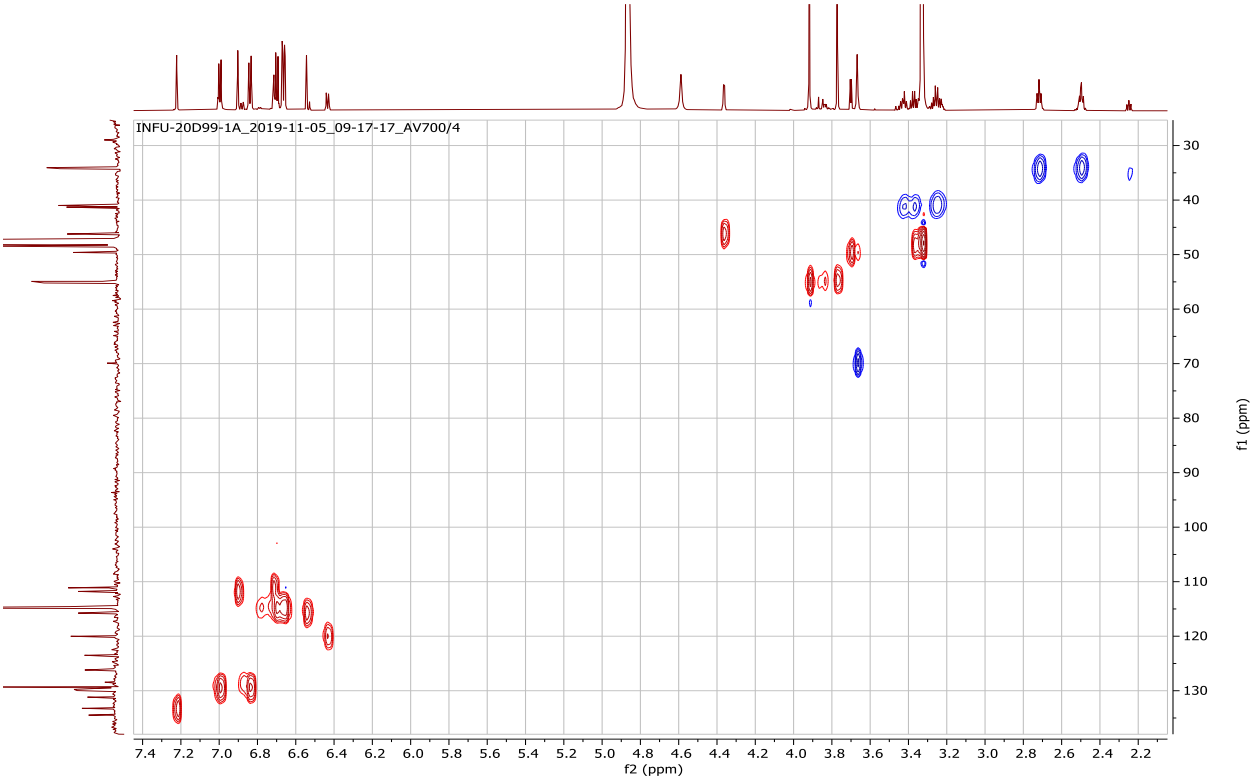

Appendix 10H: HMBC spectrum (CD_3OD) of compound **183**

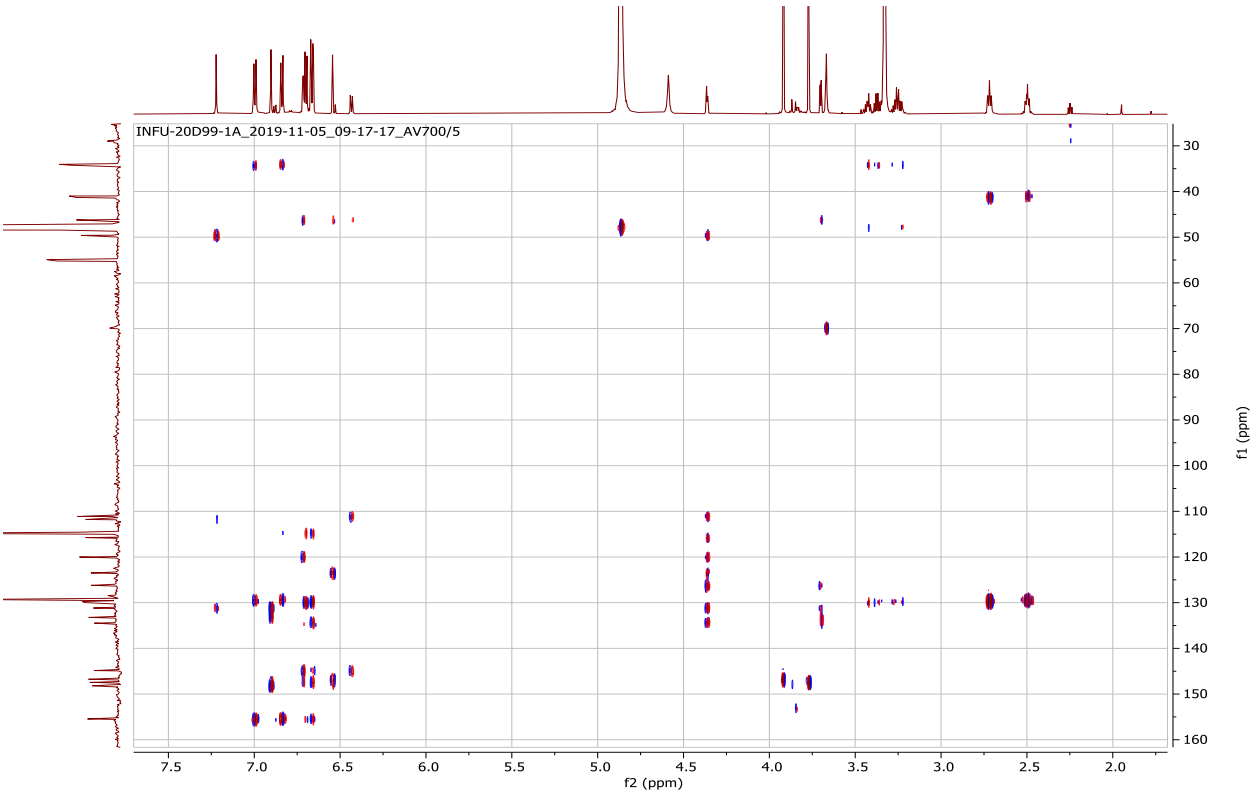

Appendix 11: NMR spectra for grossamide (**184**)

Appendix 11A: HRESIMS of compound **184**

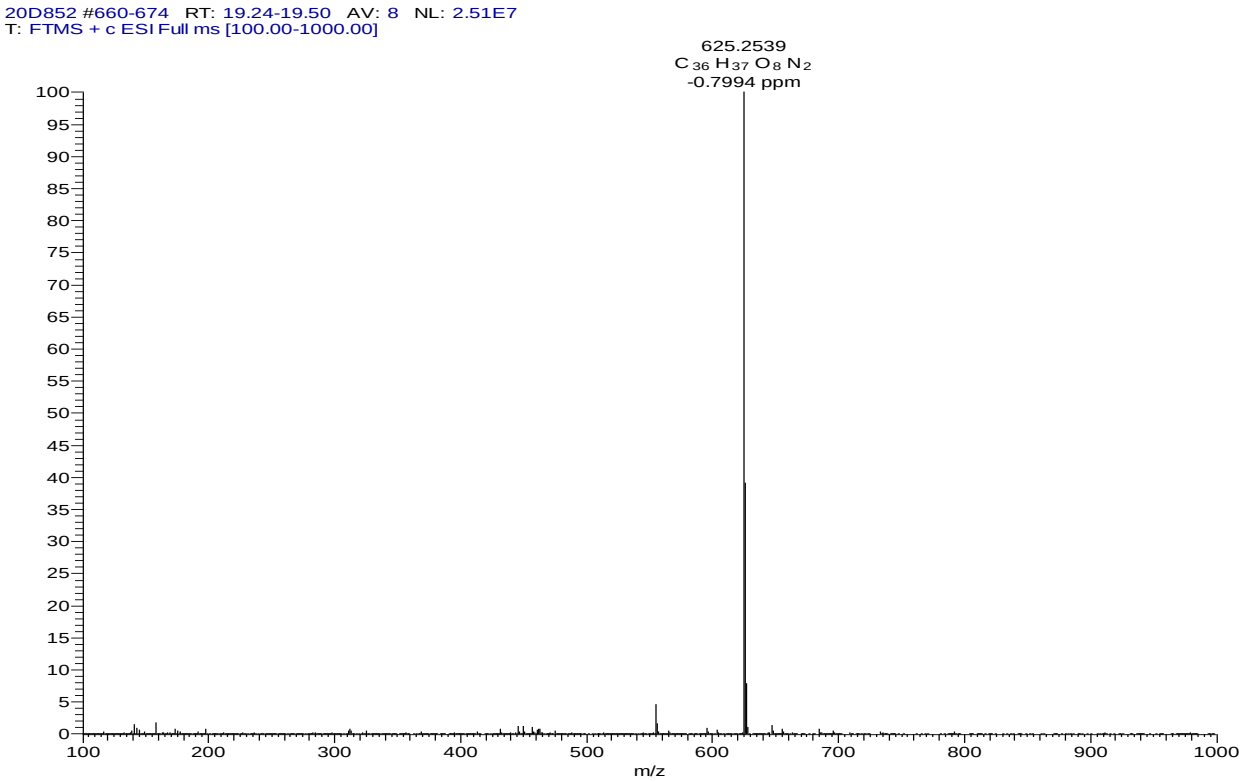

Appendix 11B: LC-UV spectrum of compound **184**

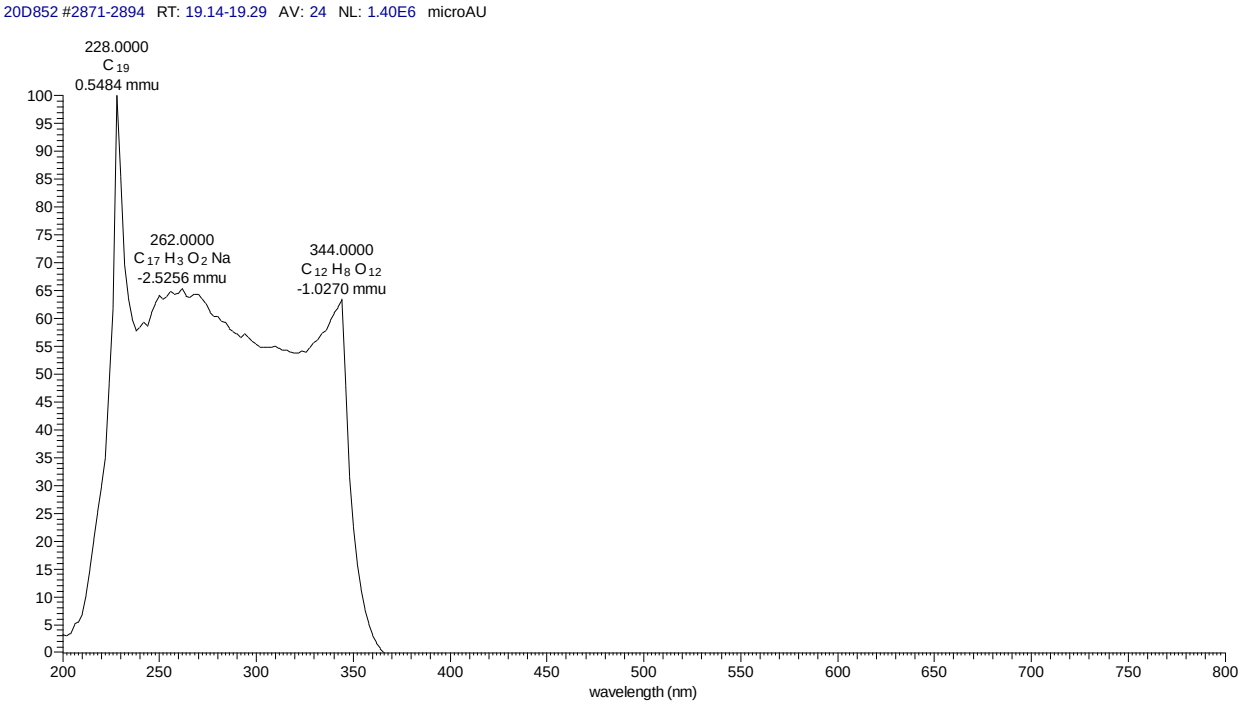

Appendix 11C: Retention time (t_R) spectrum of compounds **183** and **184**

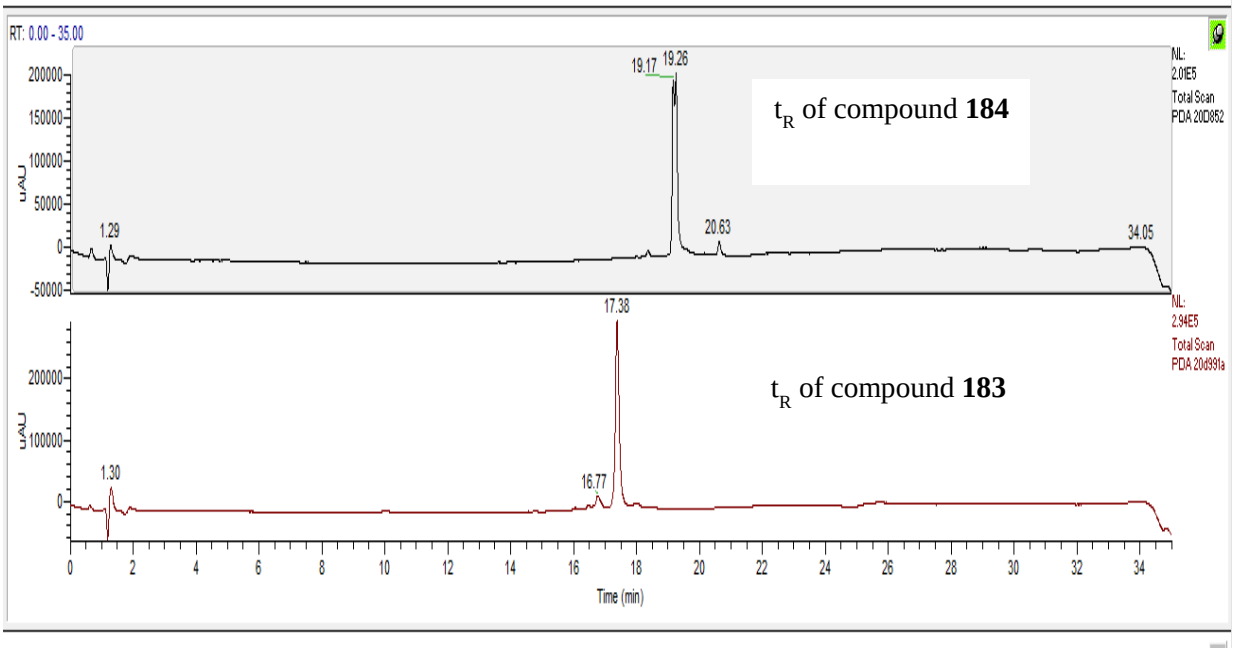

Appendix 11D: ^{1}H NMR spectrum (600 MHz, CD_3OD) of compound **184**

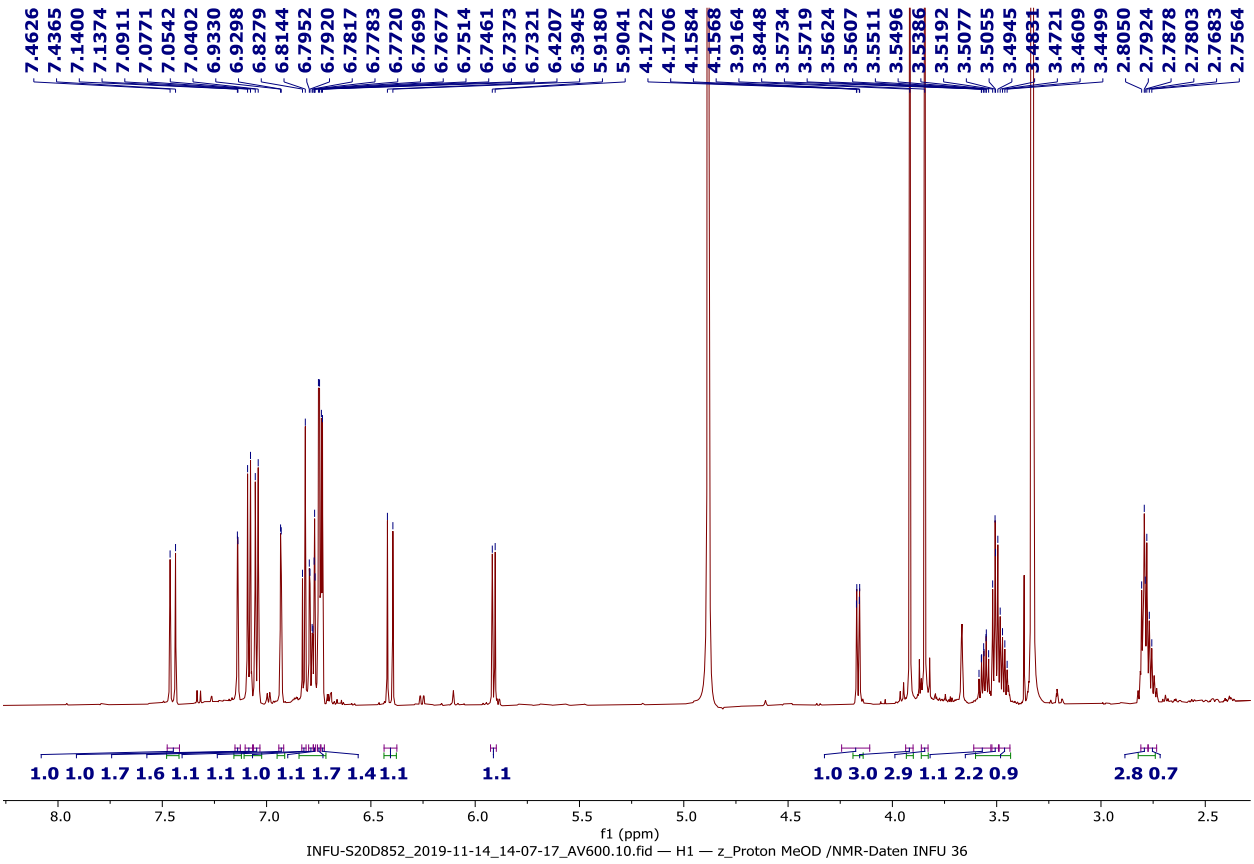

Appendix 11E: ^{13}C NMR spectrum (150 MHz, CD_3OD) of compound **184**

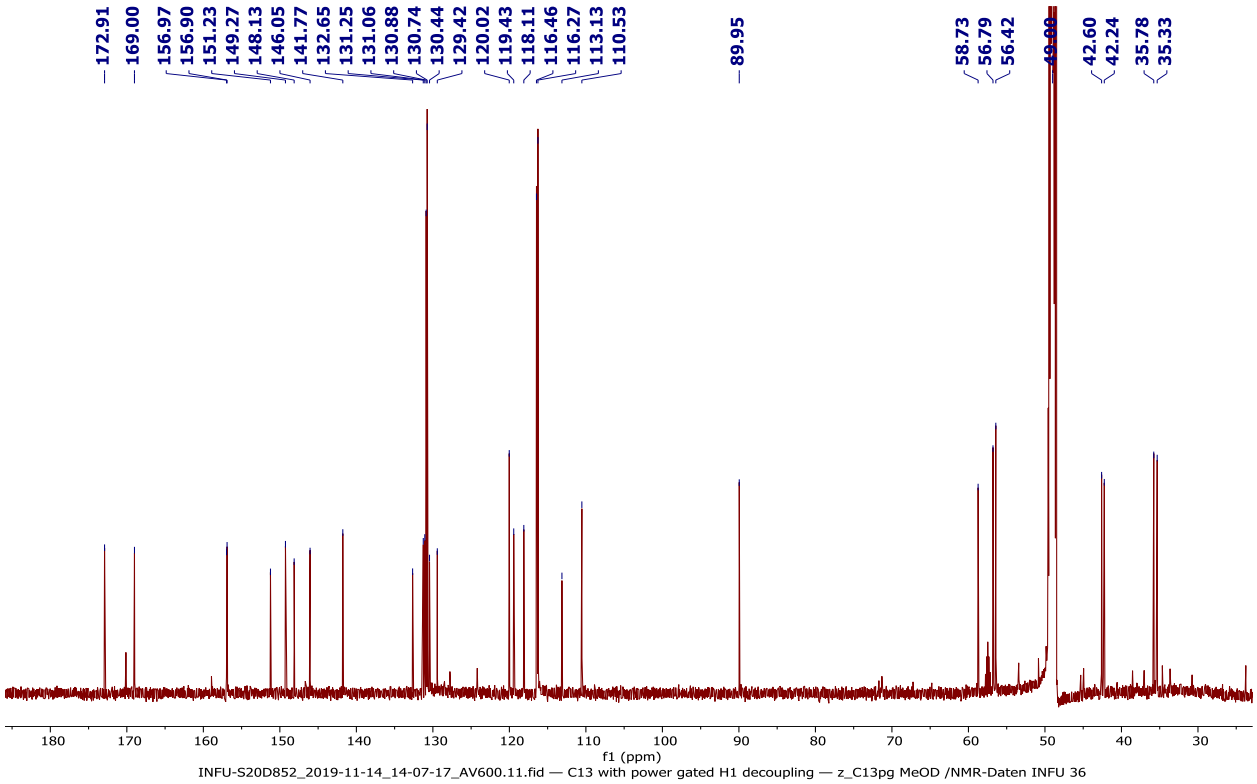

Appendix 11F: ^{1}H-^{1}H COSY spectrum (CD_3OD) of compound **184**

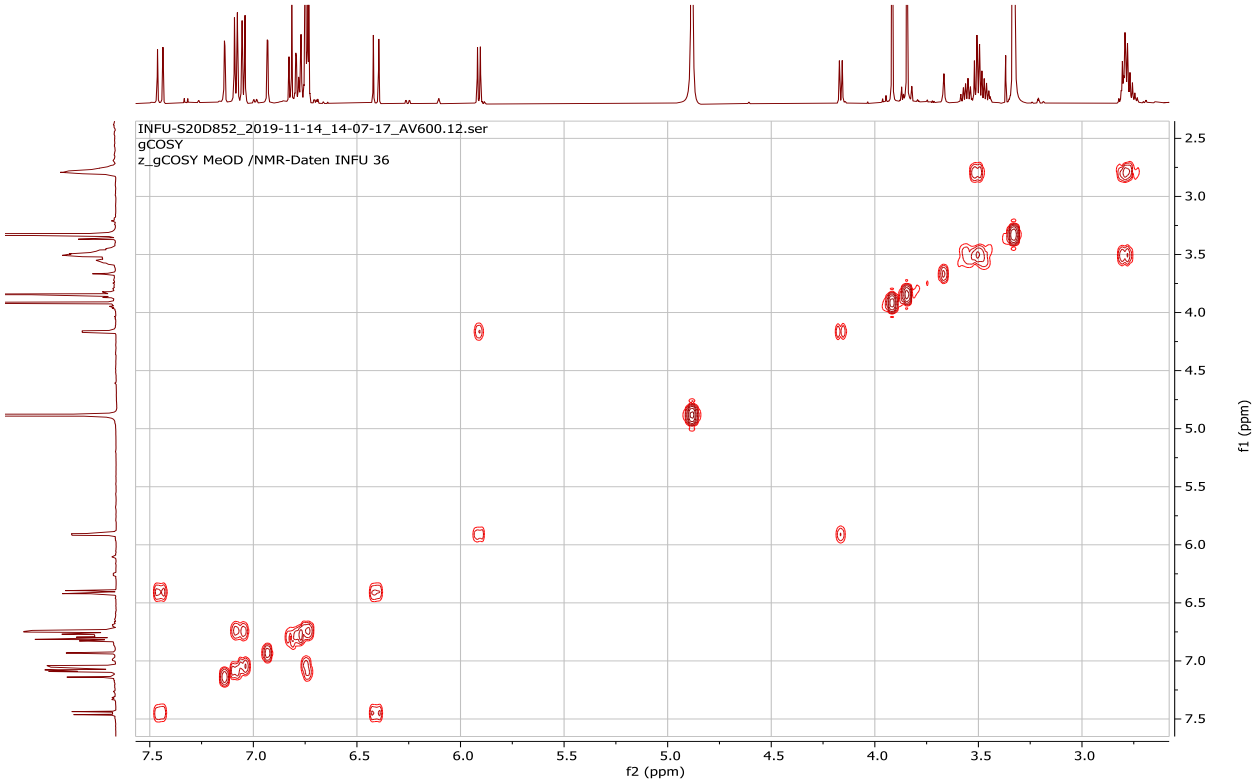

Appendix 11G: HSQC spectrum (CD_3OD) of compound **184**

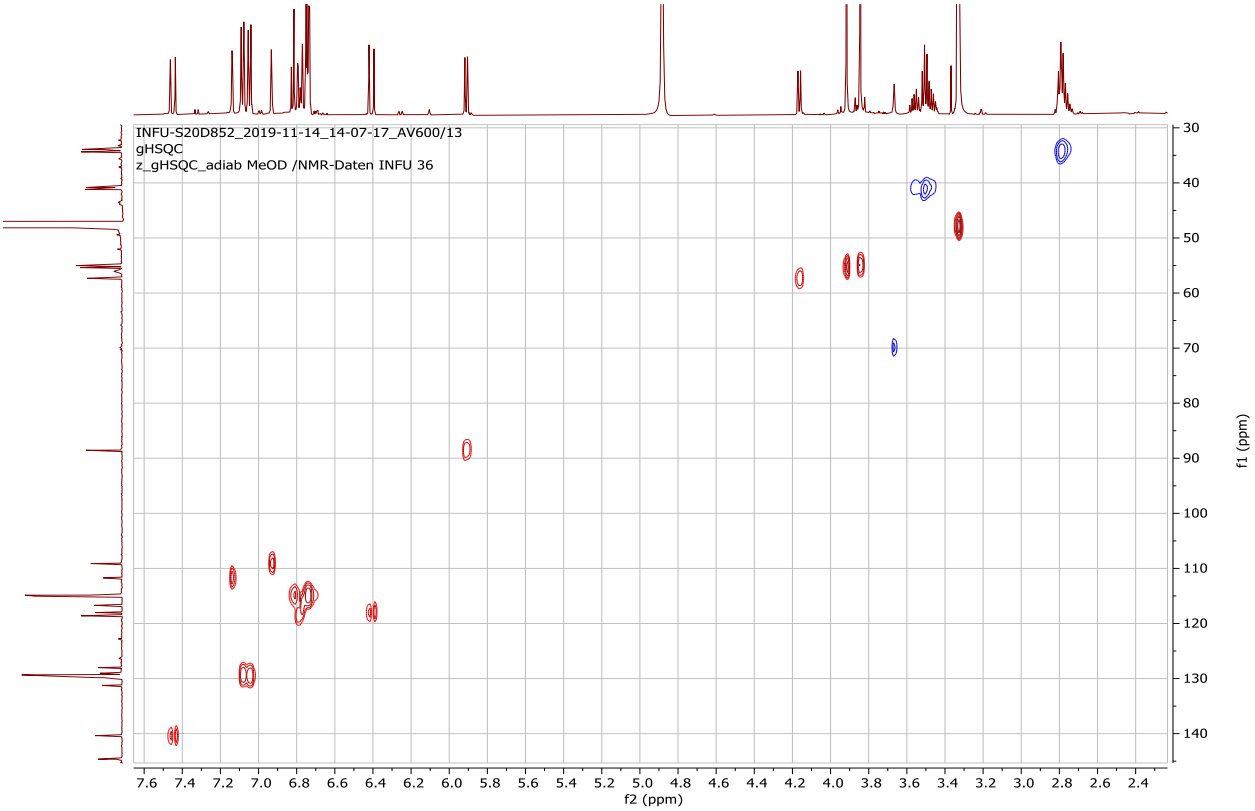

Appendix 11H: HMBC spectrum (CD_3OD) of compound **184**

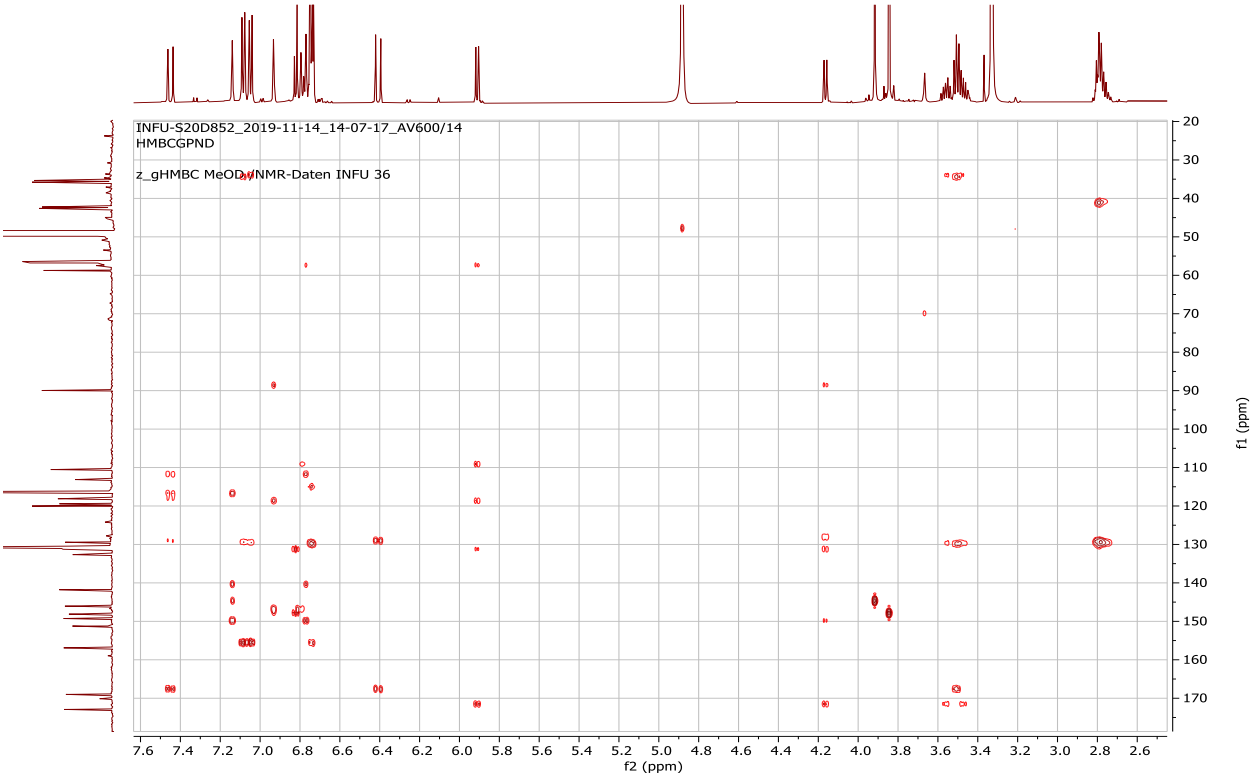

Appendix 12: NMR spectra for methylparaben (**185**)

Appendix 12A: HRESIMS of compound **185**

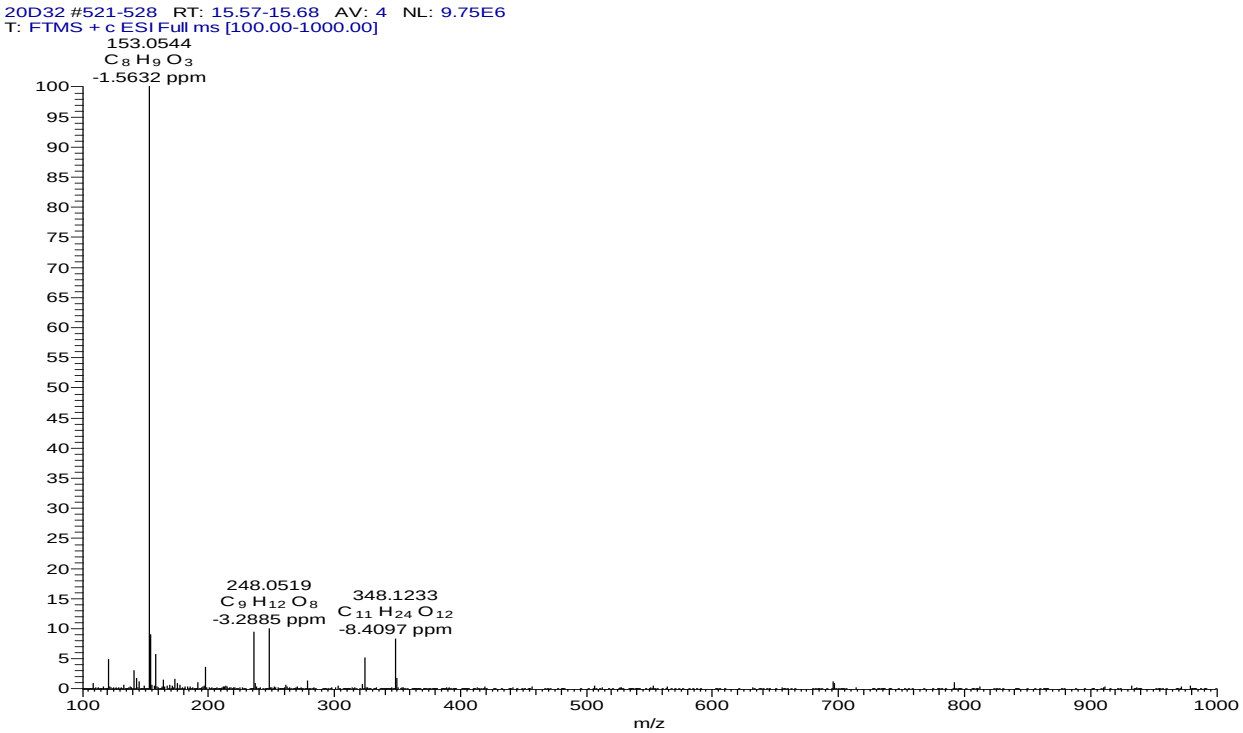

Appendix 12B: LC-UV spectrum of compound **185**

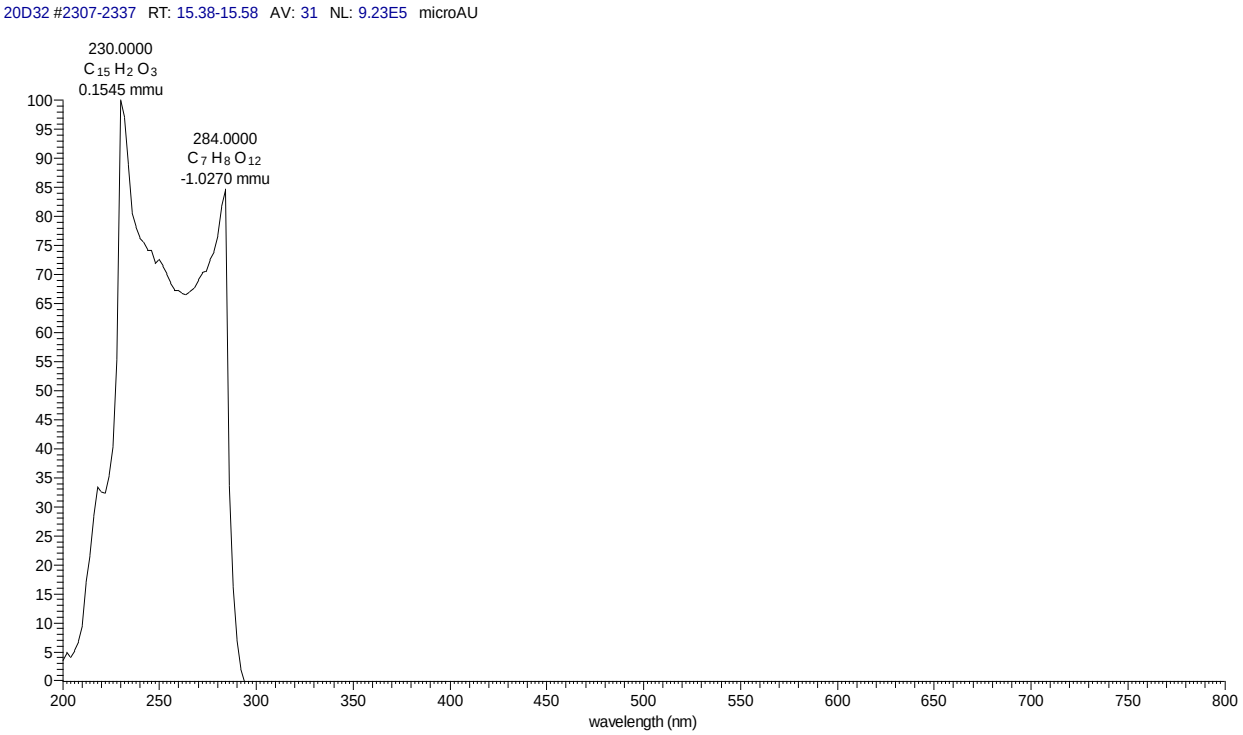

Appendix 12C: ^{1}H NMR spectrum (600 MHz, CD_3OD) of compound **185**

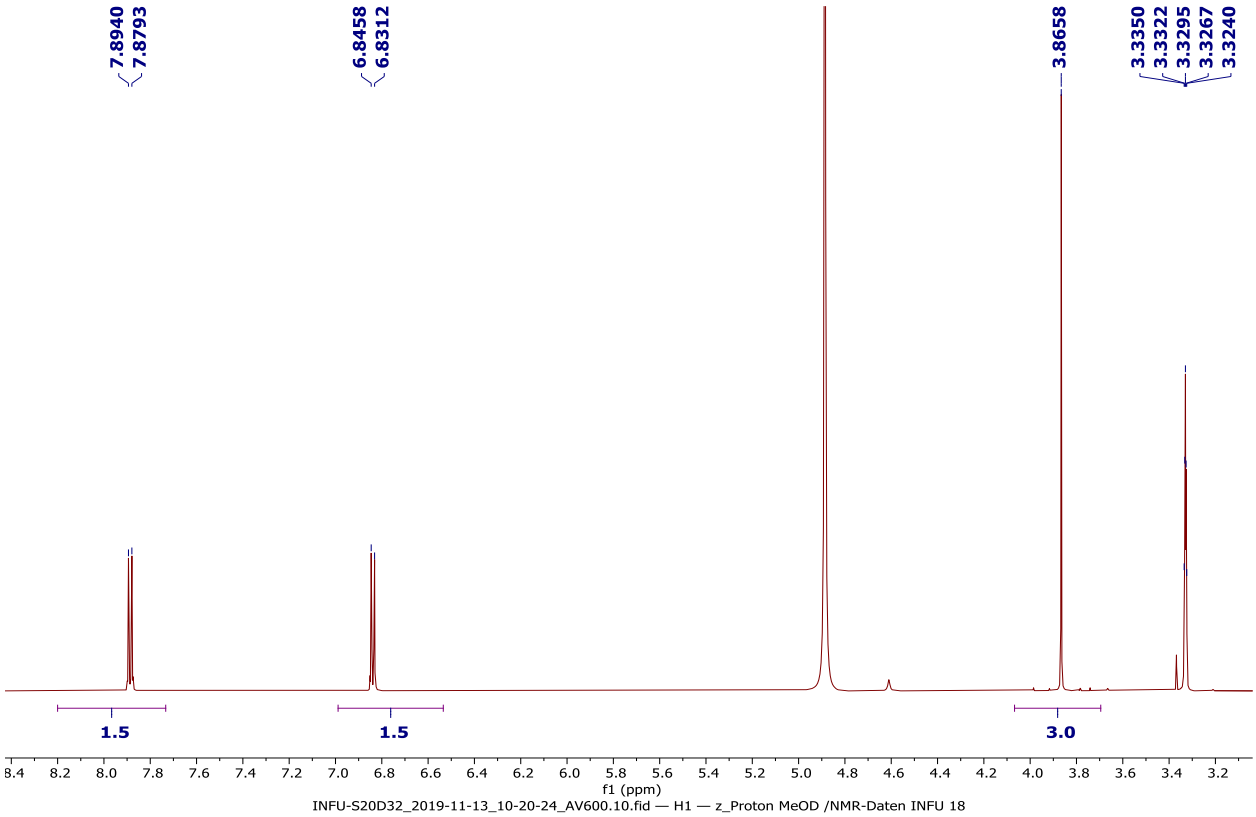

Appendix 12D: ^{13}C NMR spectrum (150 MHz, CD_3OD) of compound **185**

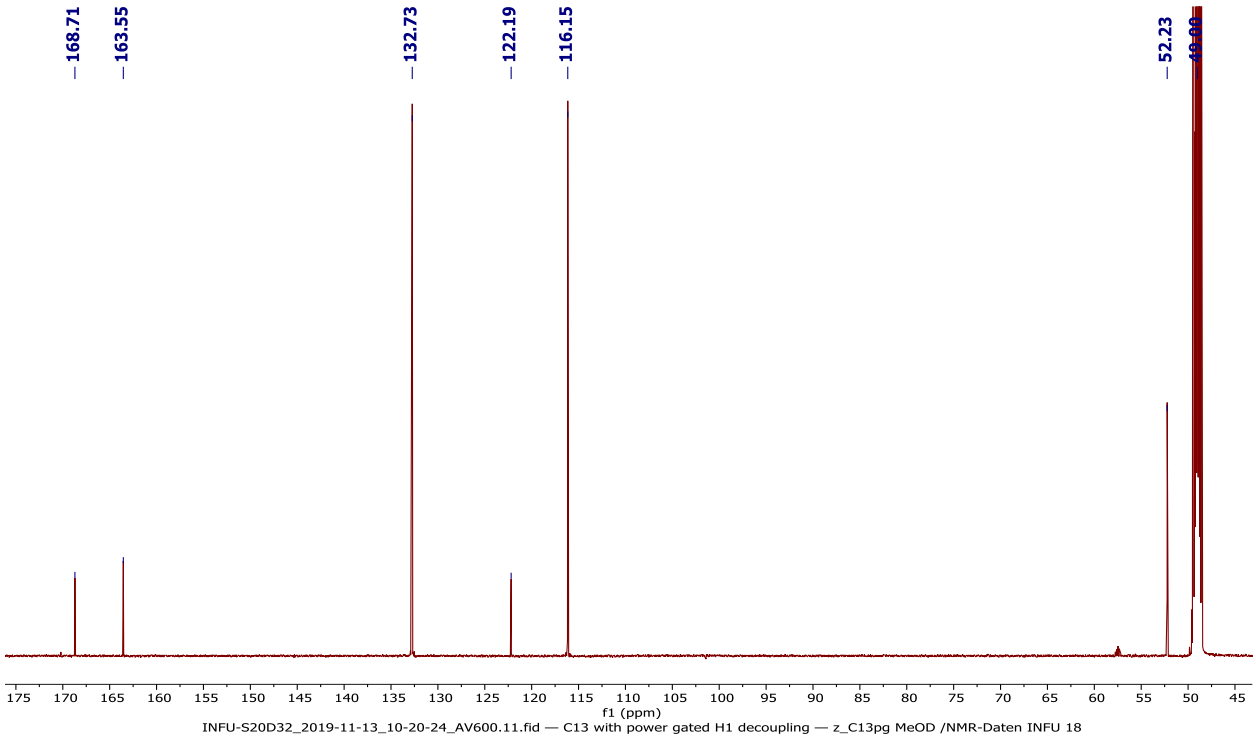

Appendix 12E: ^{1}H-^{1}H COSY spectrum (CD_3OD) of compound **185**

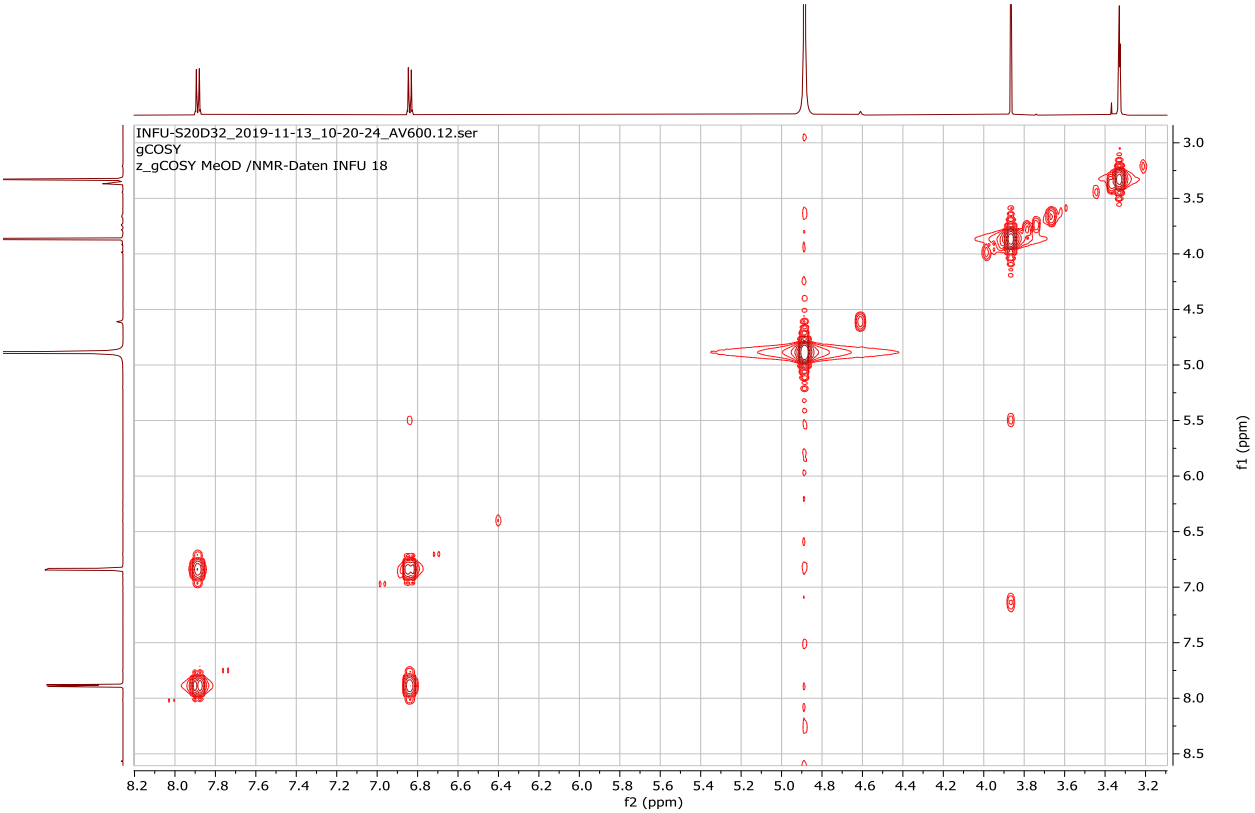

Appendix 12F: HSQC spectrum (CD_3OD) of compound **185**

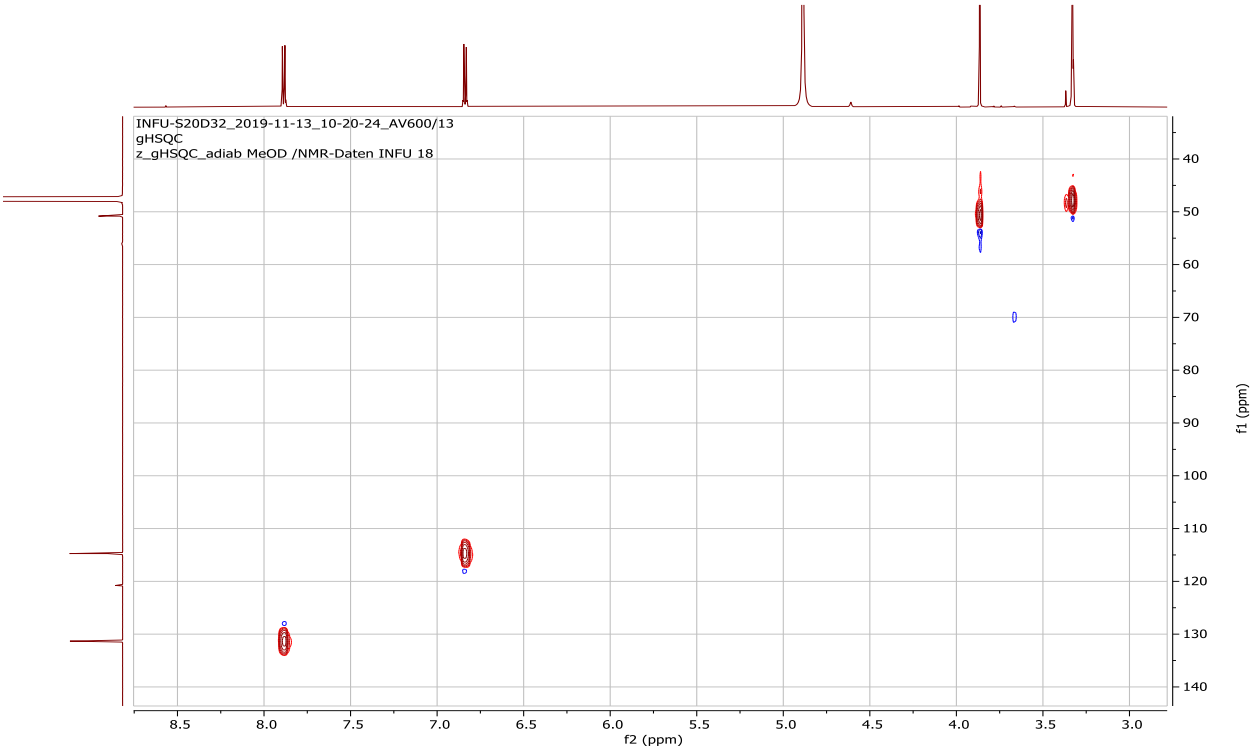

Appendix 12G: HMBC spectrum (CD_3OD) of compound **185**

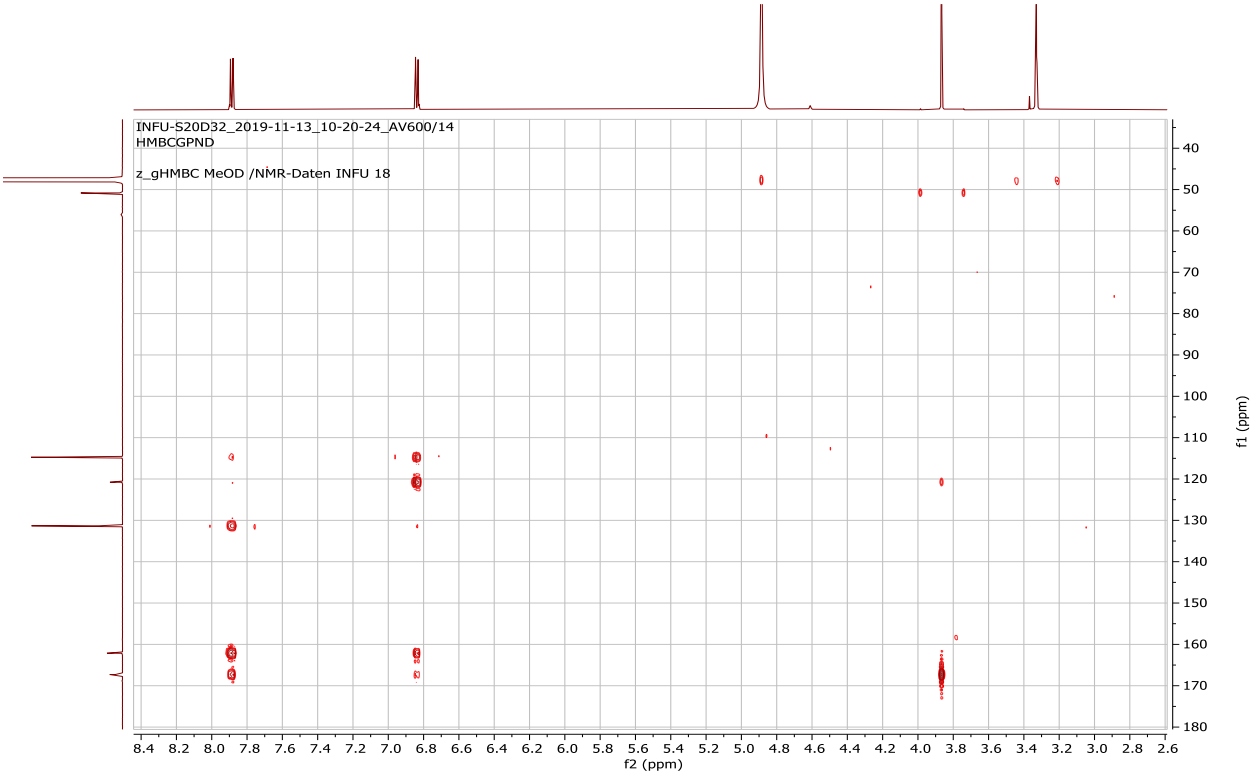

Appendix 13: NMR spectra for usambarin (**186**)

Appendix 13A: HRESIMS of compound **186**

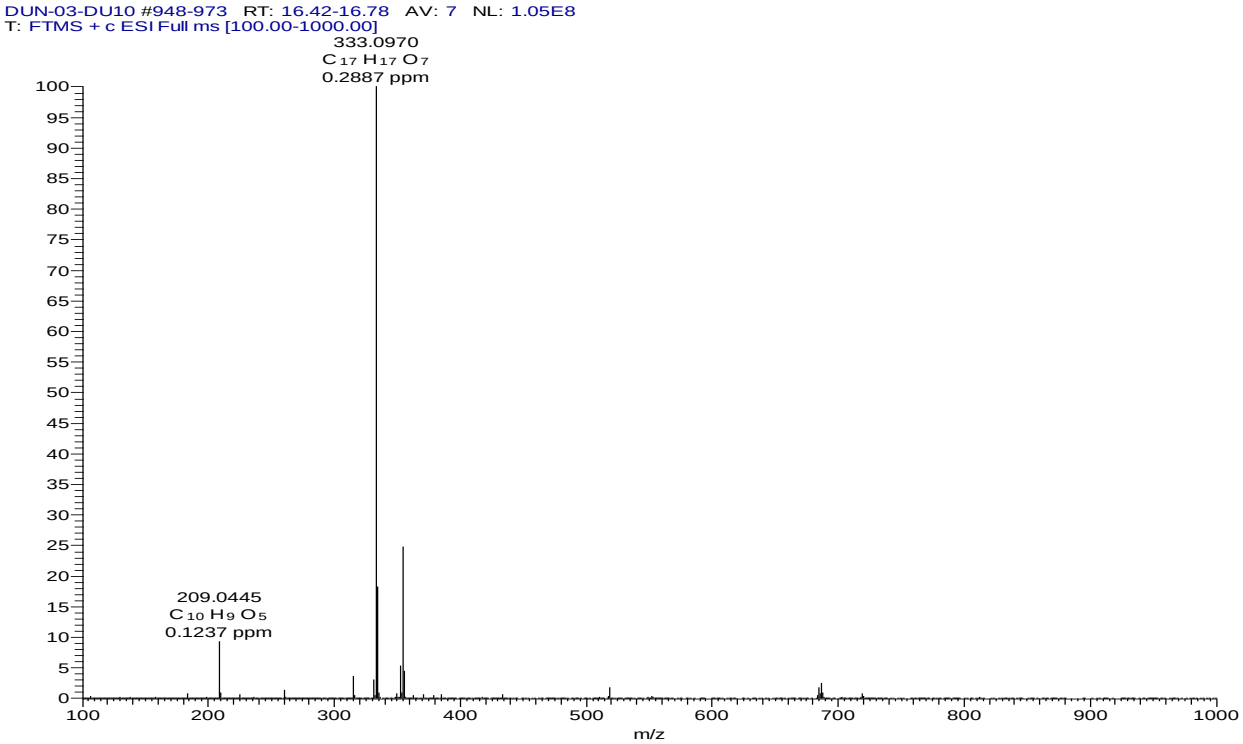

Appendix 13B: HRESIMS/MS of compound **186**

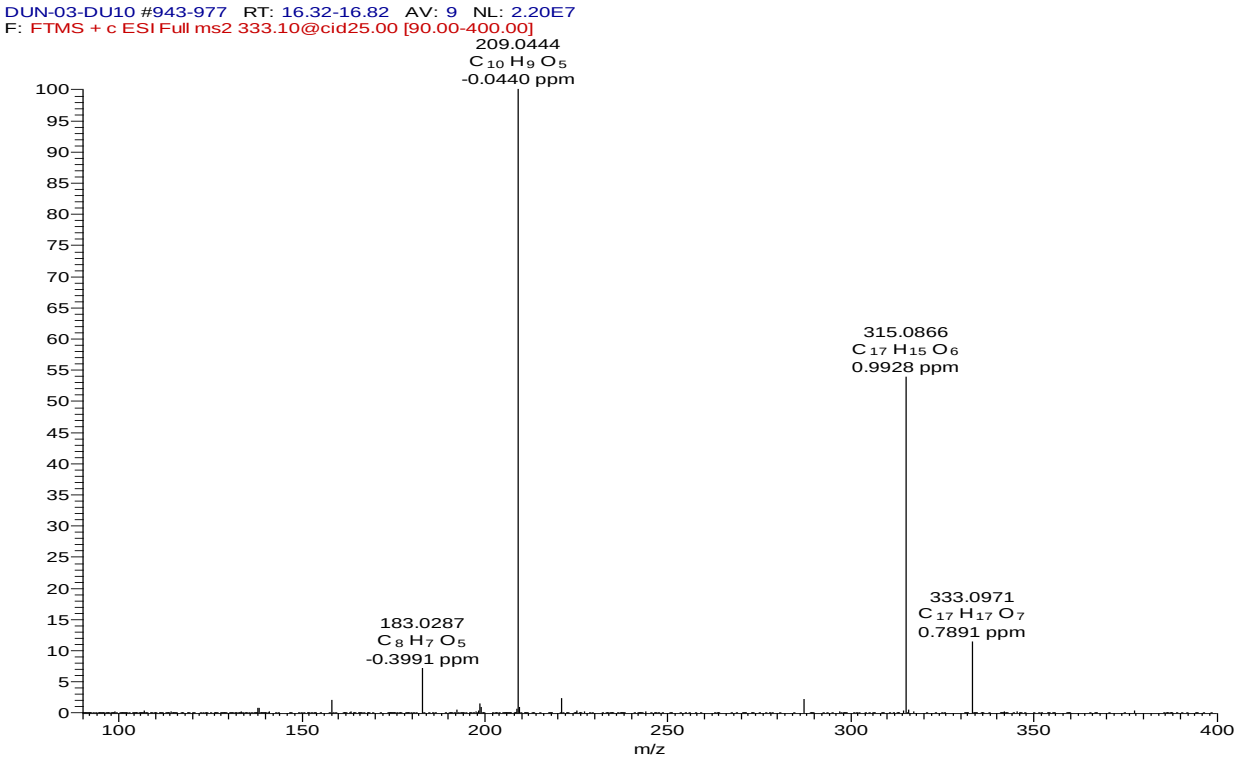

Appendix 13C: ^{1}H NMR spectrum (600 MHz, CD_3OD) of compound **186**

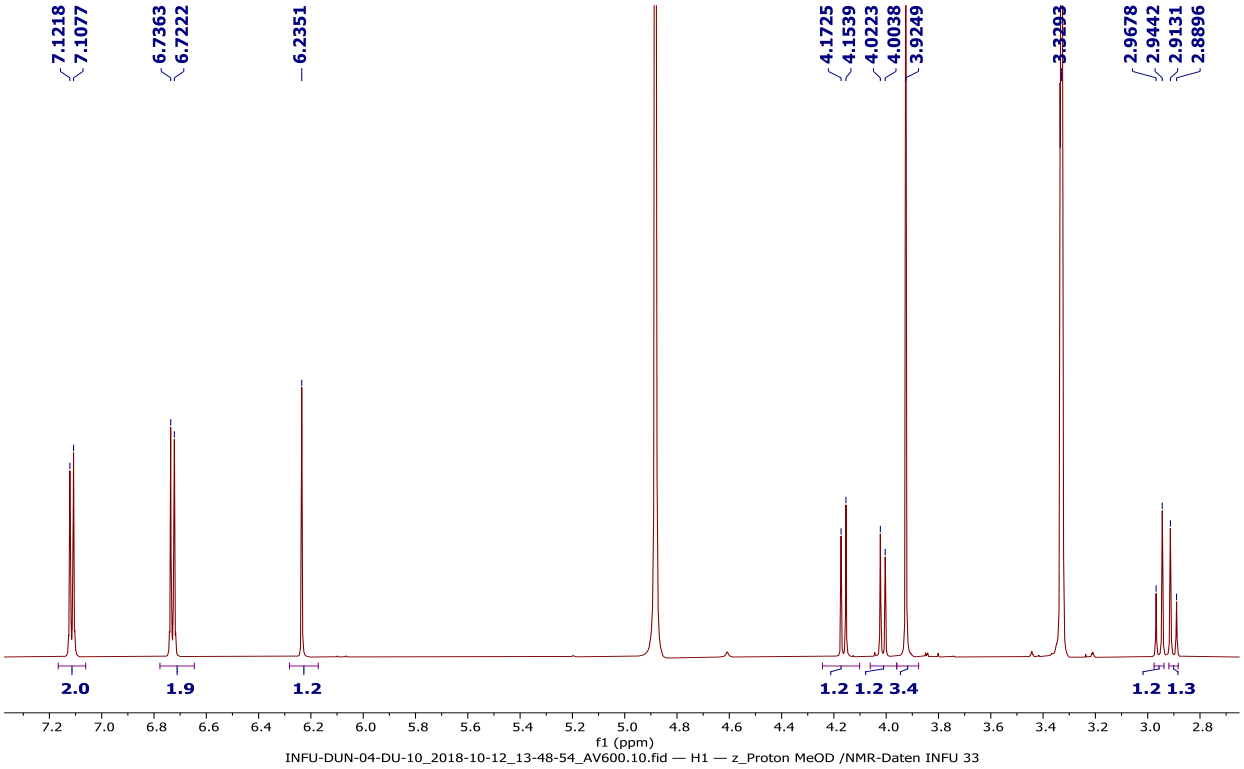

Appendix 13D: ^{13}C NMR spectrum (150 MHz, CD_3OD) of compound **186**

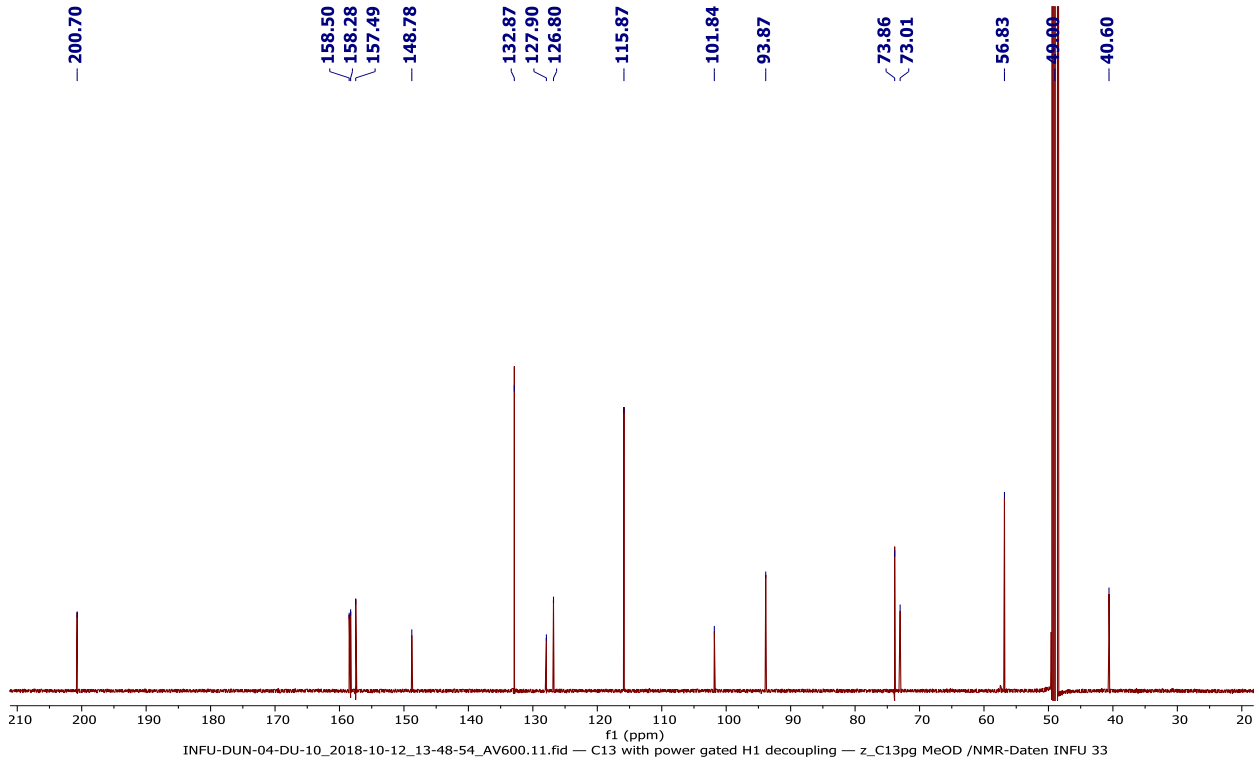

Appendix 13E: ^{1}H-^{1}H COSY spectrum (CD_3OD) of compound **186**

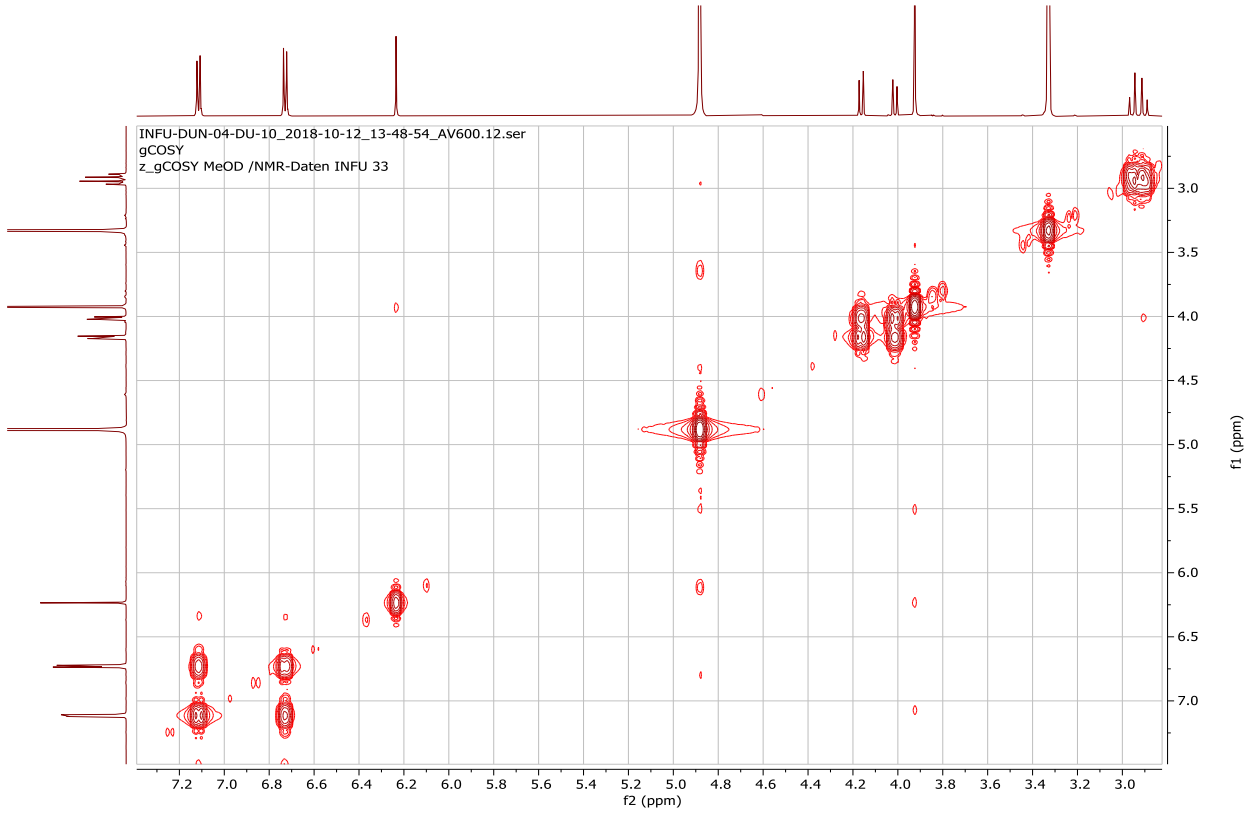

Appendix 13F: HSQC spectrum (CD_3OD) of compound **186**

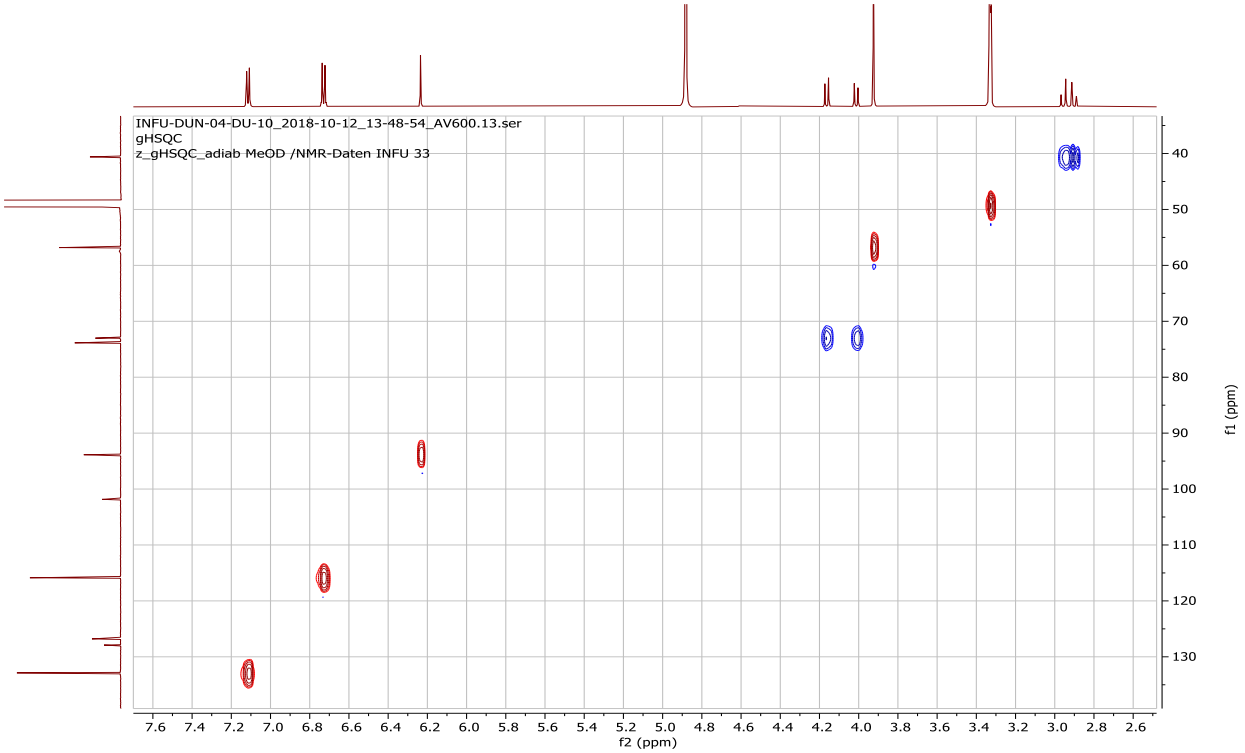

Appendix 13G: HMBC spectrum (CD_3OD) of compound **186**

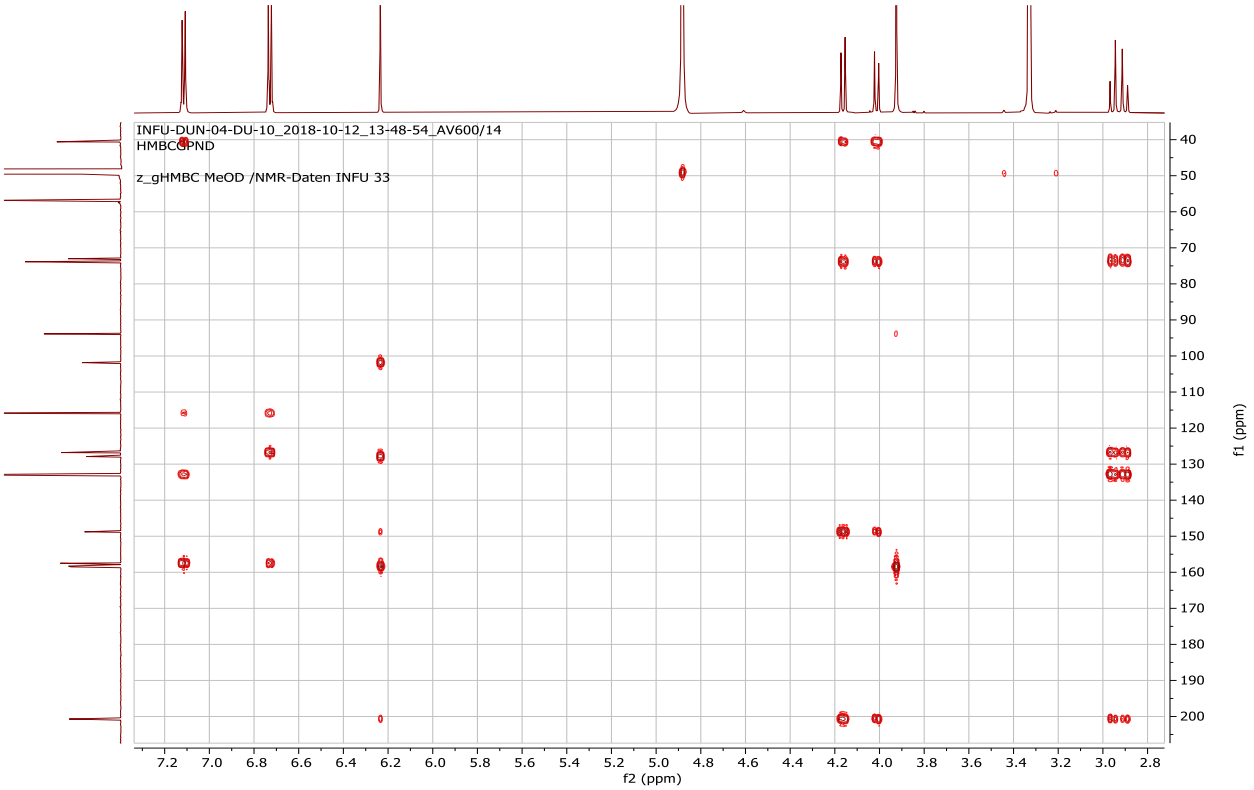

Appendix 14: NMR spectra for (3*S*)-3,4′,5-trihydroxy-7-methoxyhomoisoflavanone (**187**)

Appendix 14A: HRESIMS of compound **187**

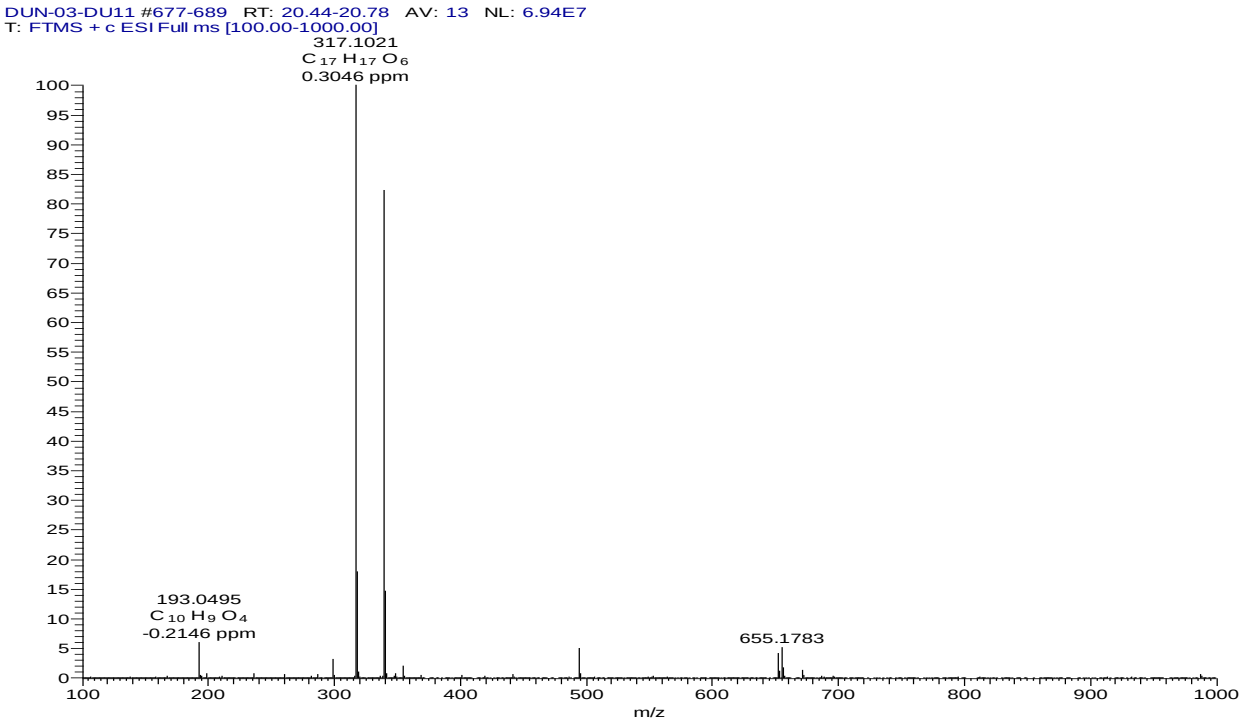

Appendix 14B: ^{1}H NMR spectrum (600 MHz, DMSO-d_6) of compound **187**

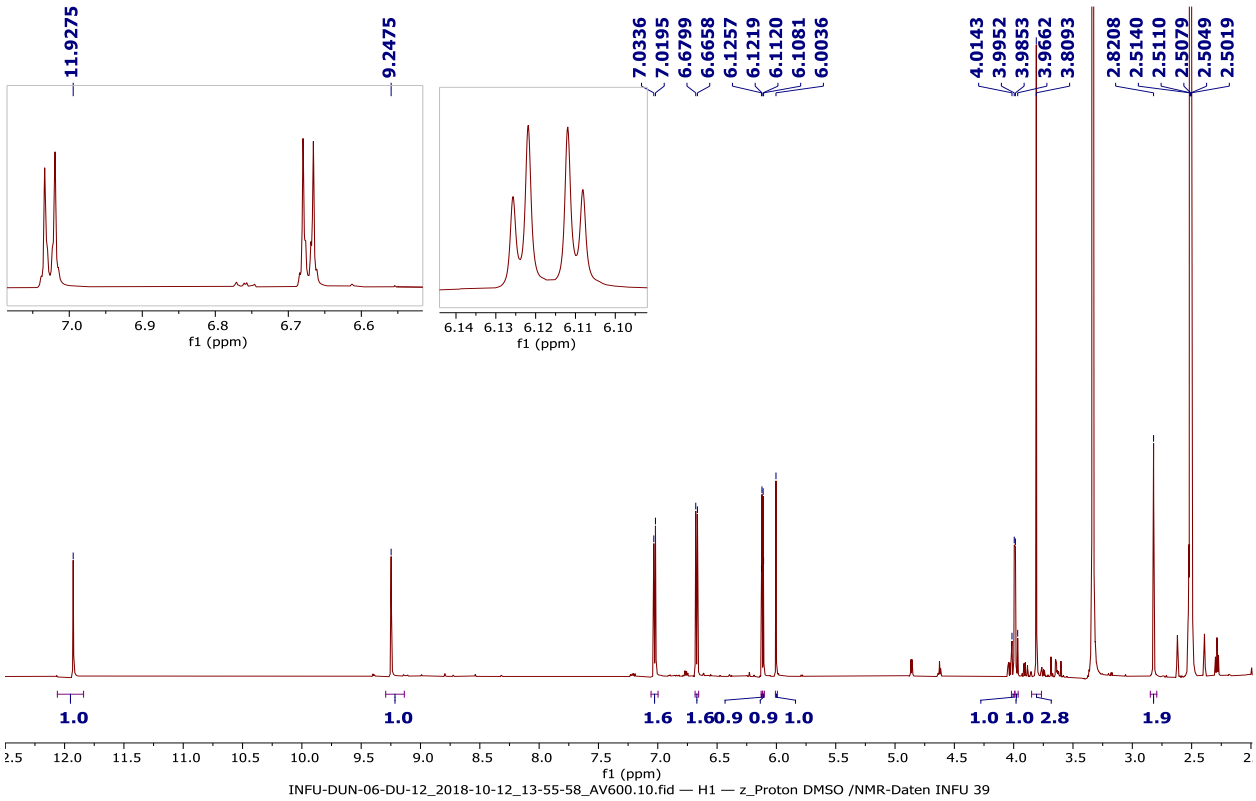

Appendix 14C: ^{13}C NMR spectrum (150 MHz, DMSO-d_6) of compound **187**

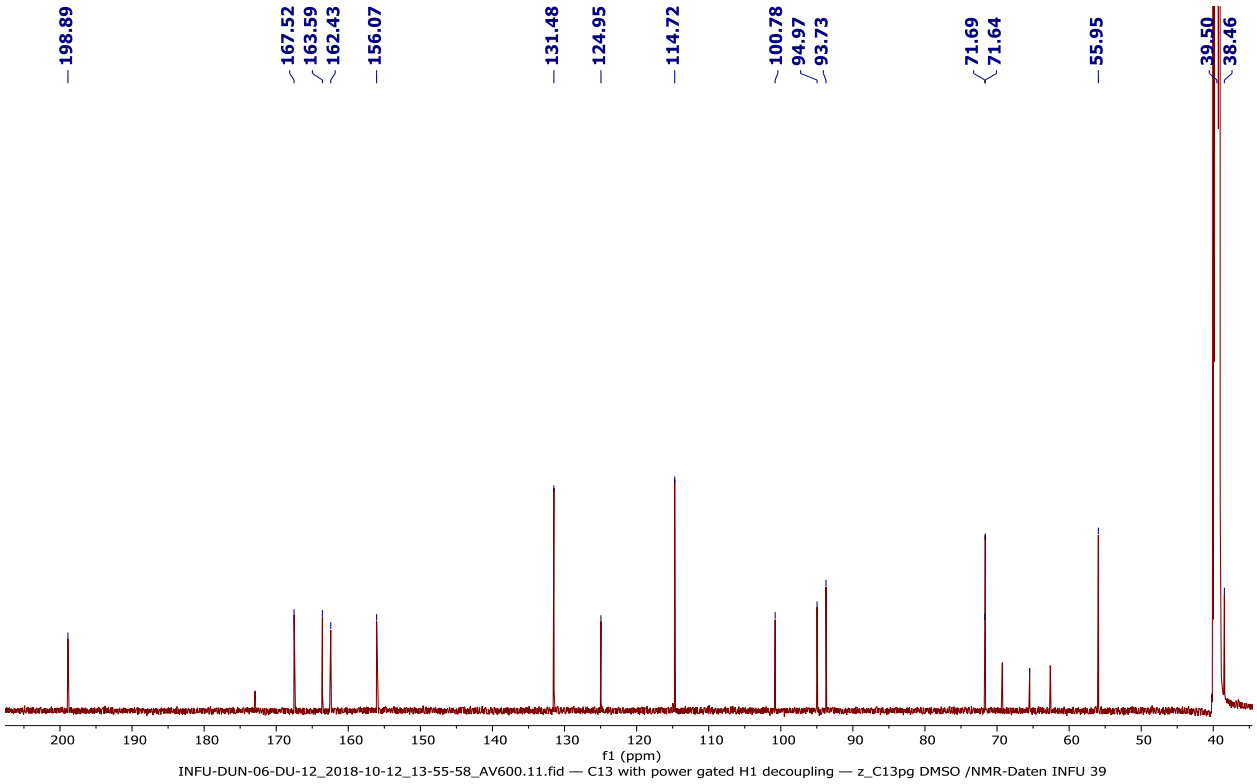

Appendix 14D: ^{1}H-^{1}H COSY spectrum (DMSO-d_6) of compound **187**

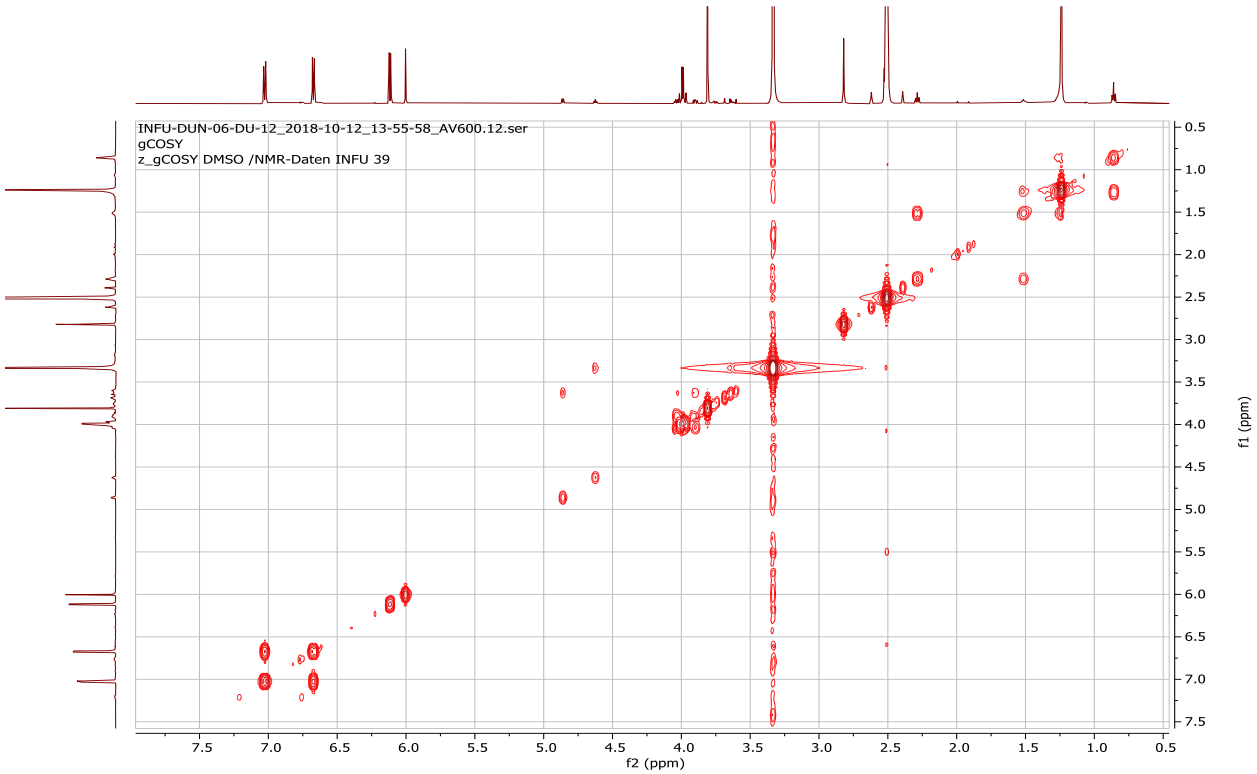

Appendix 14E: HSQC spectrum (DMSO-d_6) of compound **187**

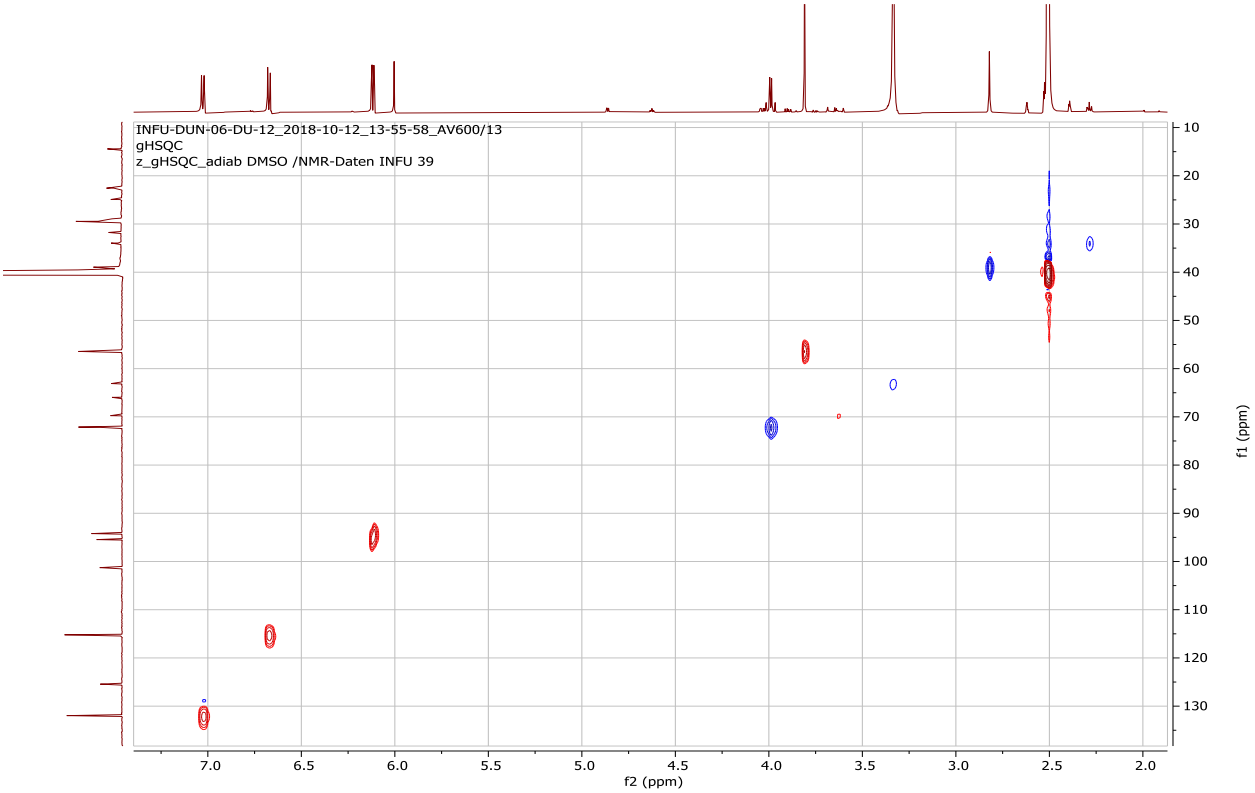

Appendix 14F: HMBC spectrum (DMSO-d_6) of compound **187**

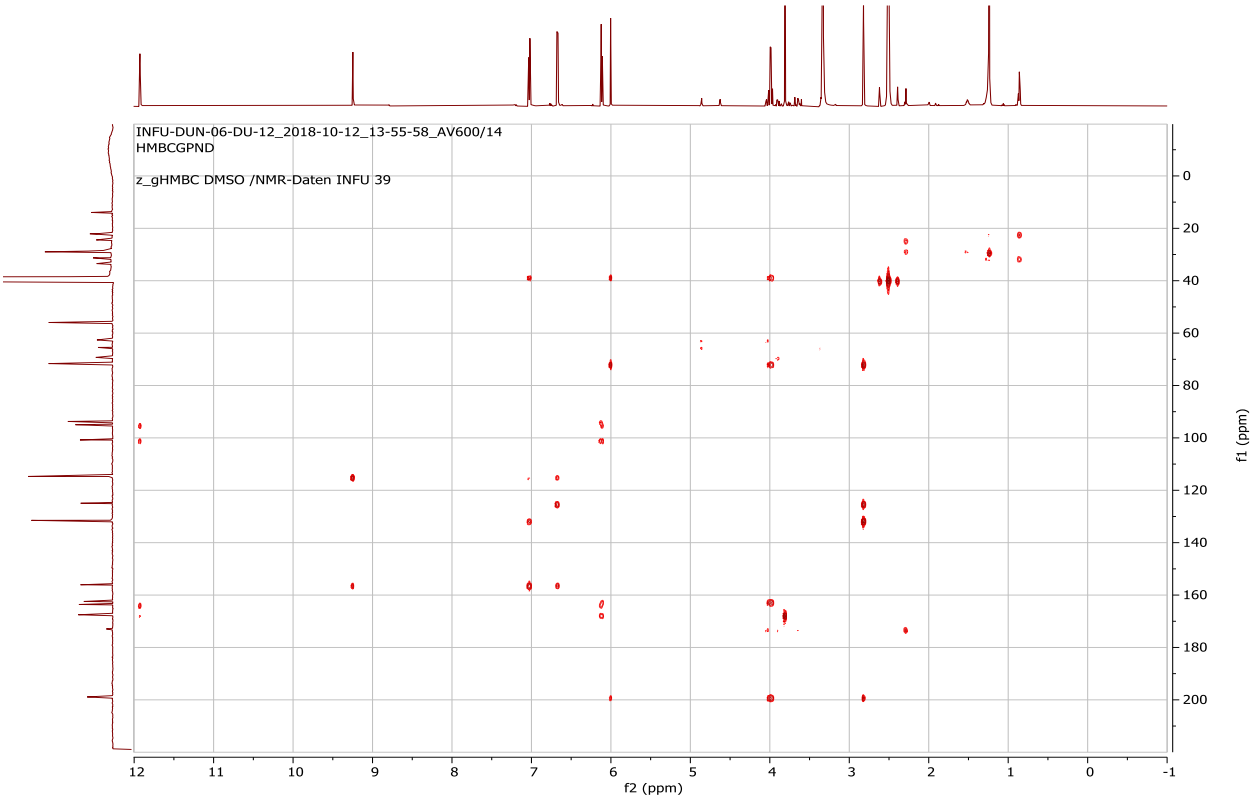

Appendix 15: NMR spectra for loureiriol (**188**)

Appendix 15A: ^{1}H NMR spectrum (500 MHz, CD_3OD) of compound **188**

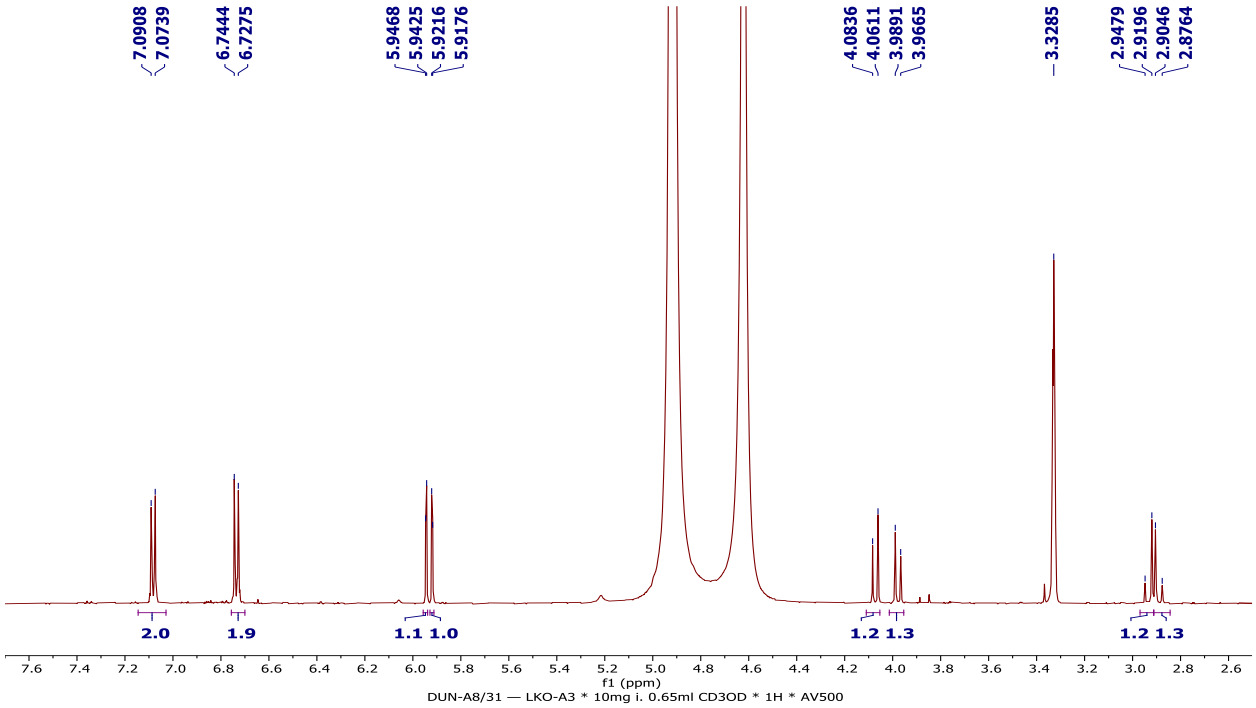

Appendix 15B: ^{13}C NMR spectrum (125 MHz, CD_3OD) of compound **188**

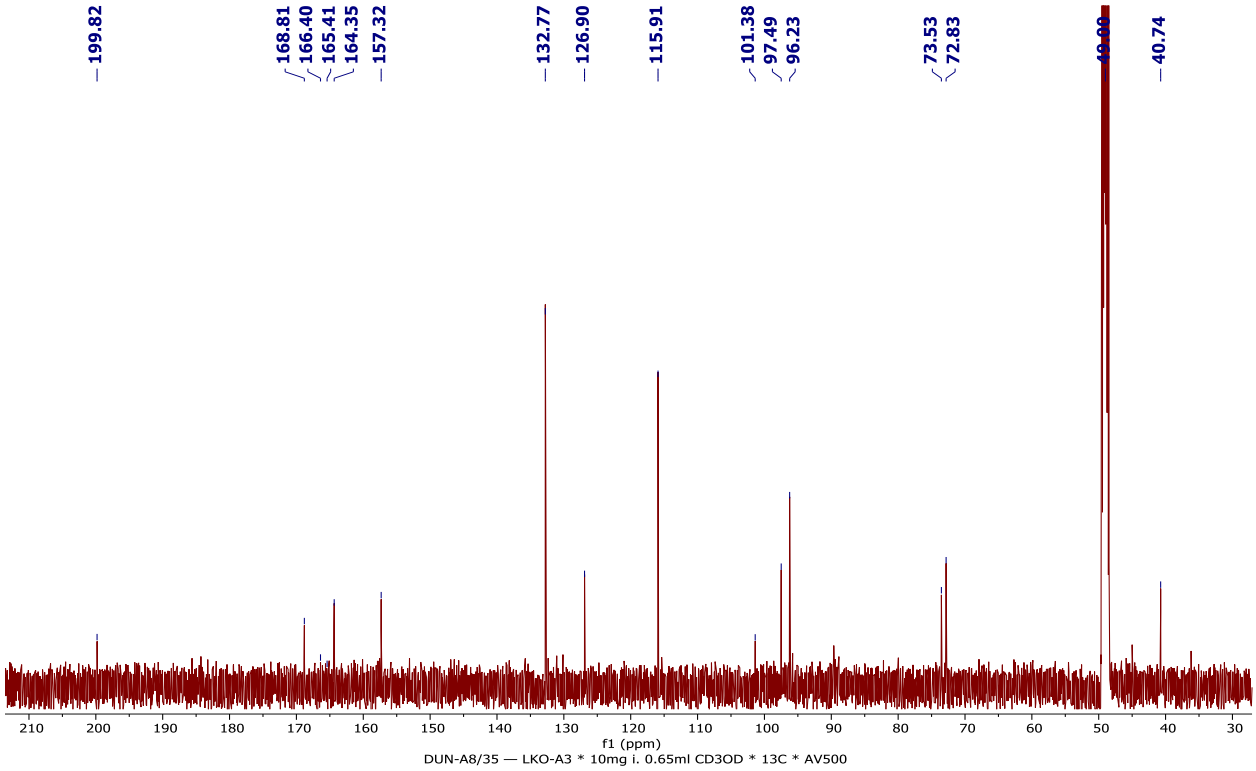

Appendix 15C: ^{1}H-^{1}H COSY spectrum (CD_3OD) of compound **188**

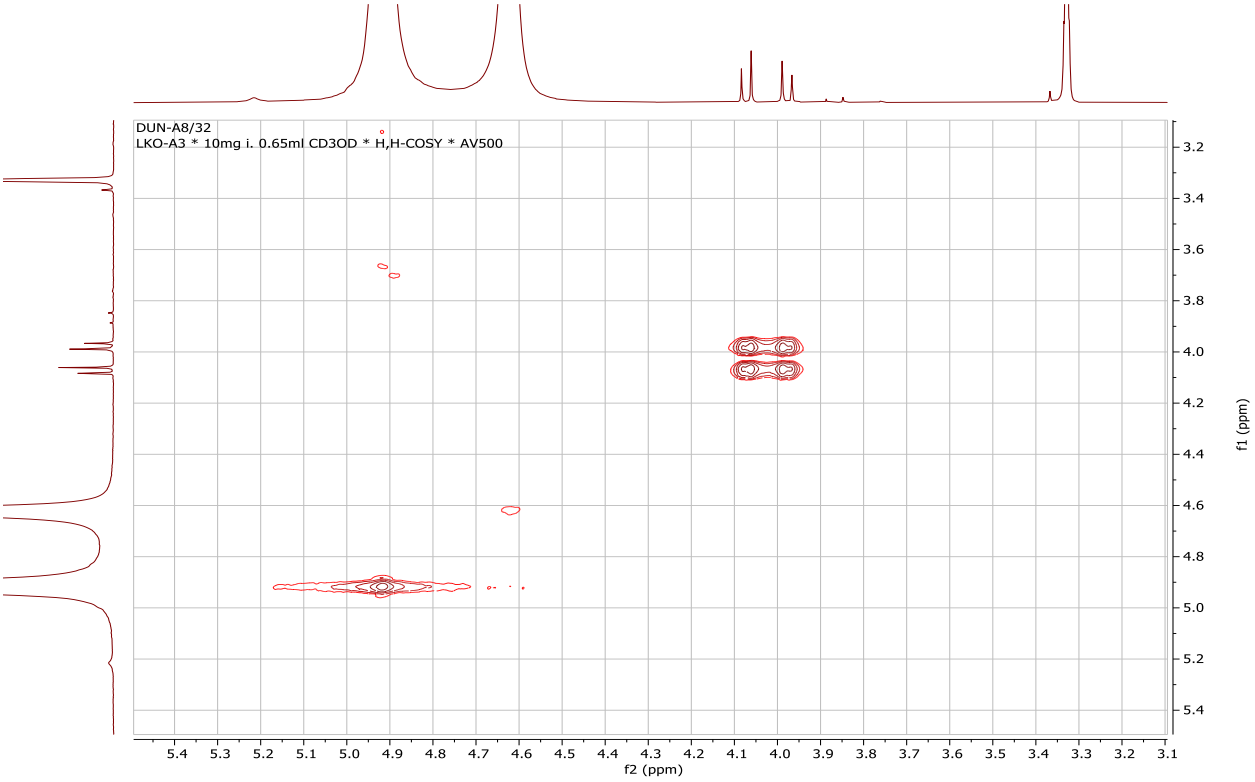

Appendix 15D: HSQC spectrum (CD_3OD) of compound **188**

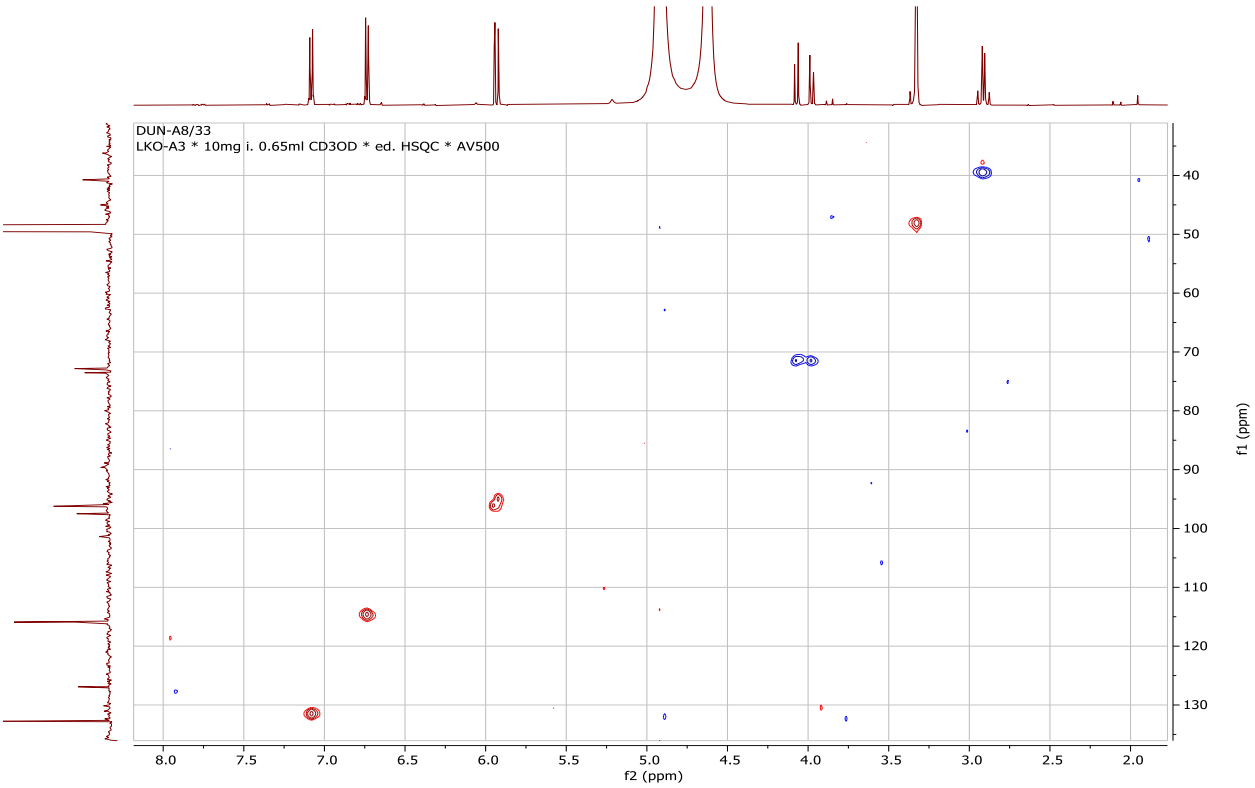

Appendix 16: NMR spectra for 4′,4-dihydroxy-2,3-dimethoxydihydrochalcone (**189**)

Appendix 16A: HRESIMS of compound **189**

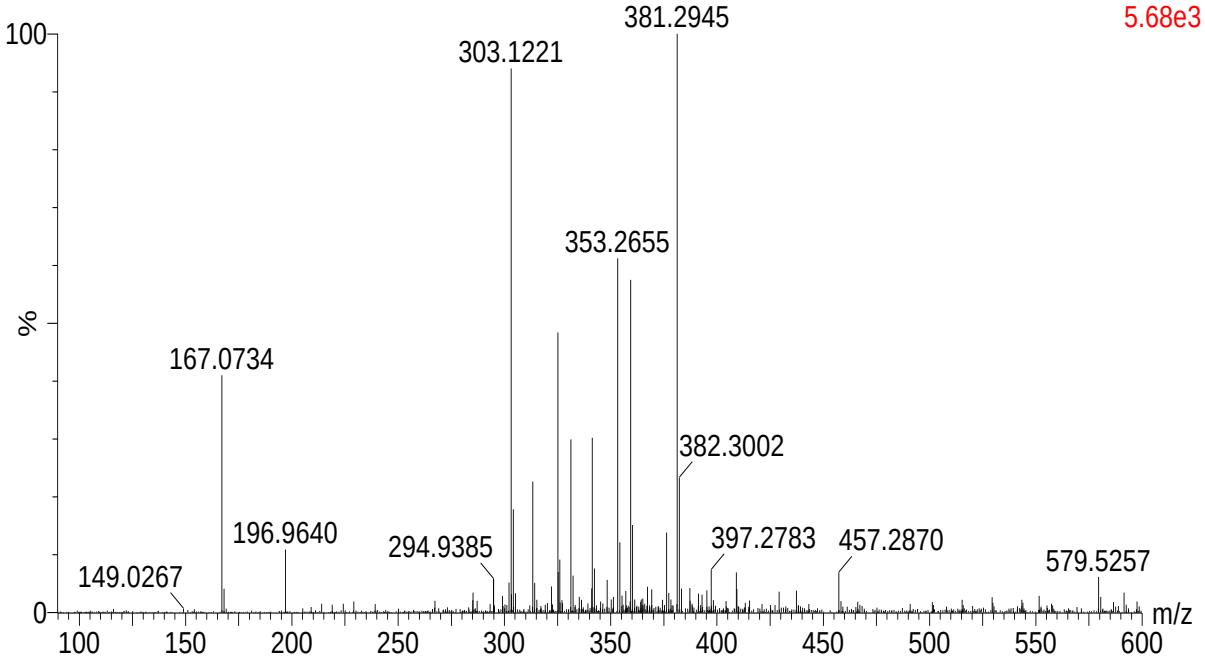

Appendix 16B: ^{1}H NMR spectrum (500 MHz, CD_3OD) of compound **189**

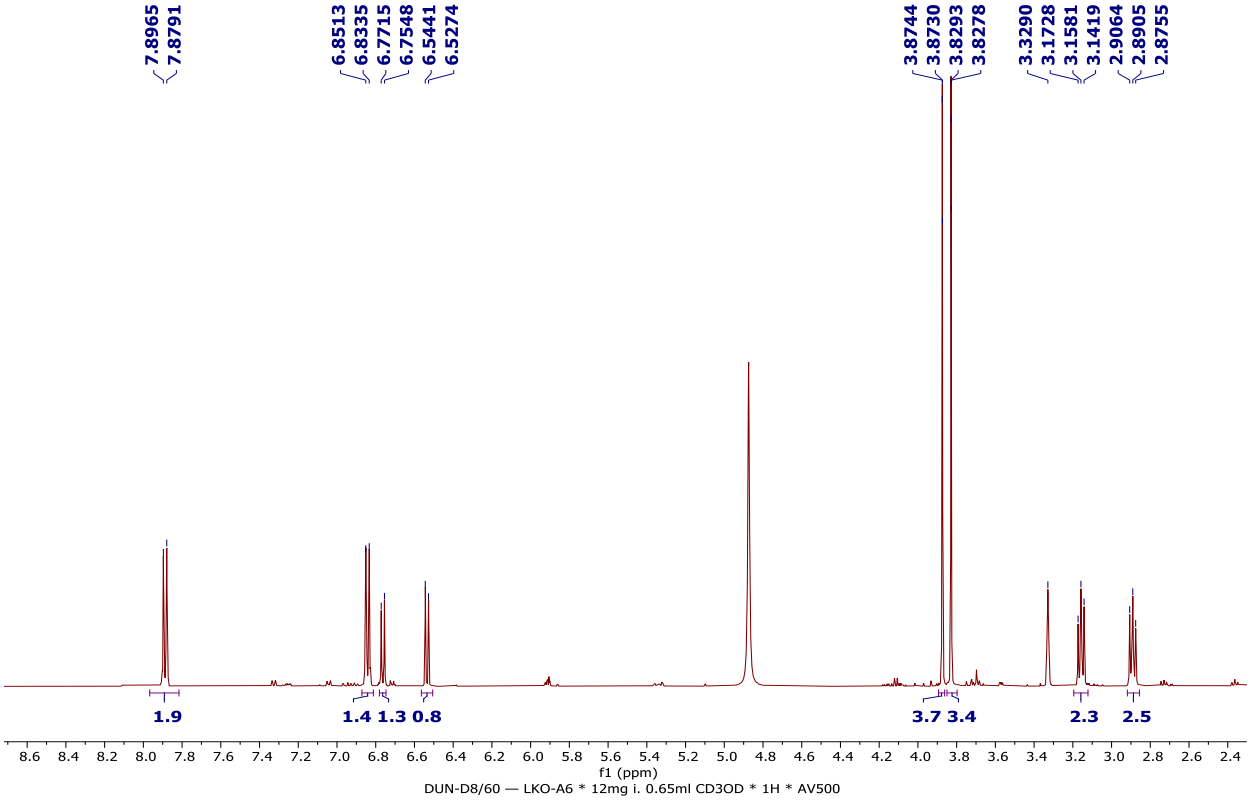

Appendix 16C: ^{13}C NMR spectrum (125 MHz, CD_3OD) of compound **189**

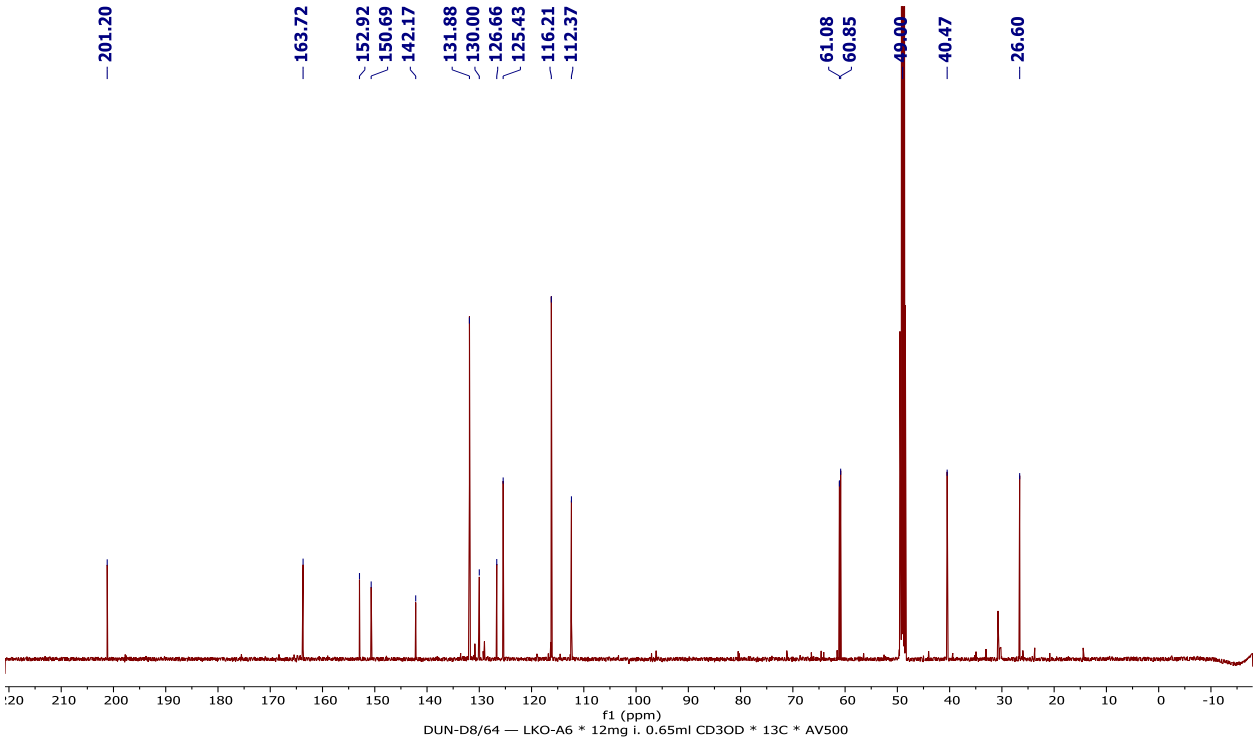

Appendix 16D: ^{1}H-^{1}H COSY spectrum (CD_3OD) of compound **189**

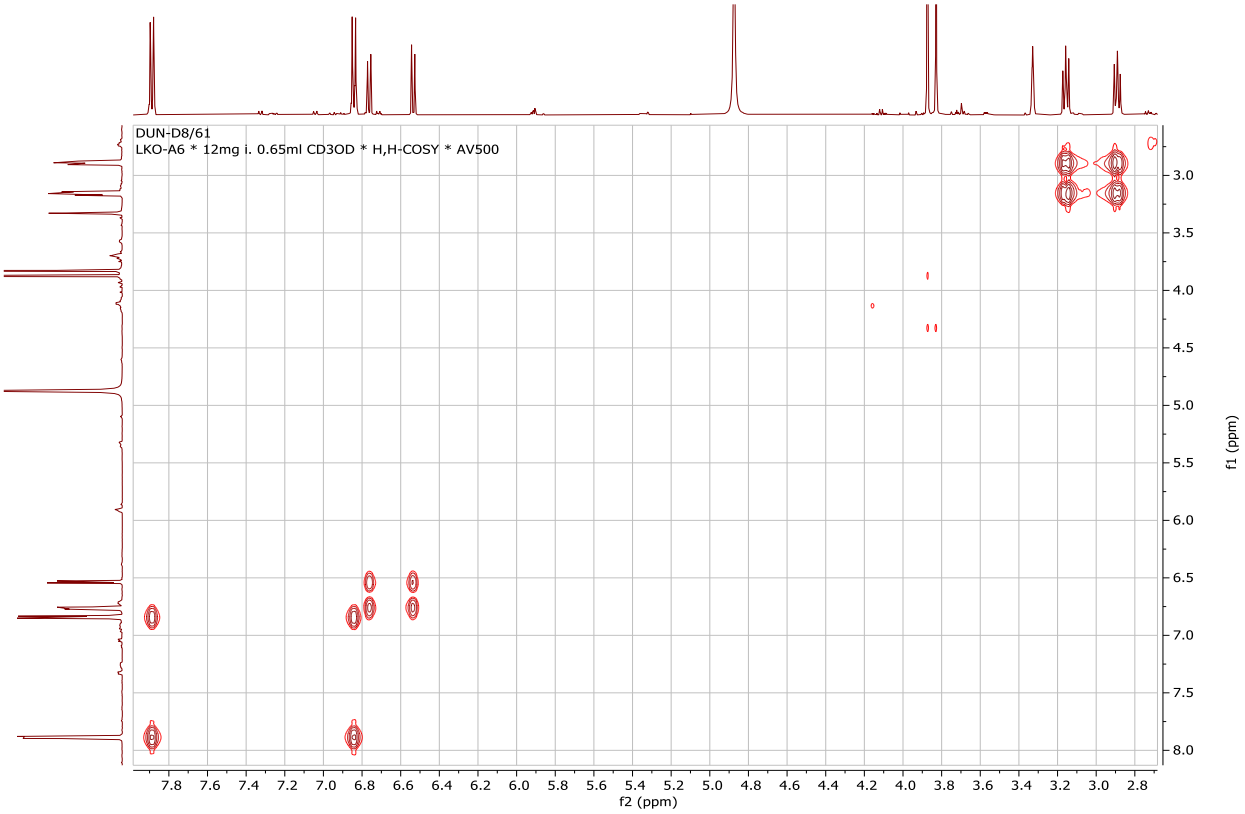

Appendix 16E: NOESY spectrum (CD_3OD) of compound **189**

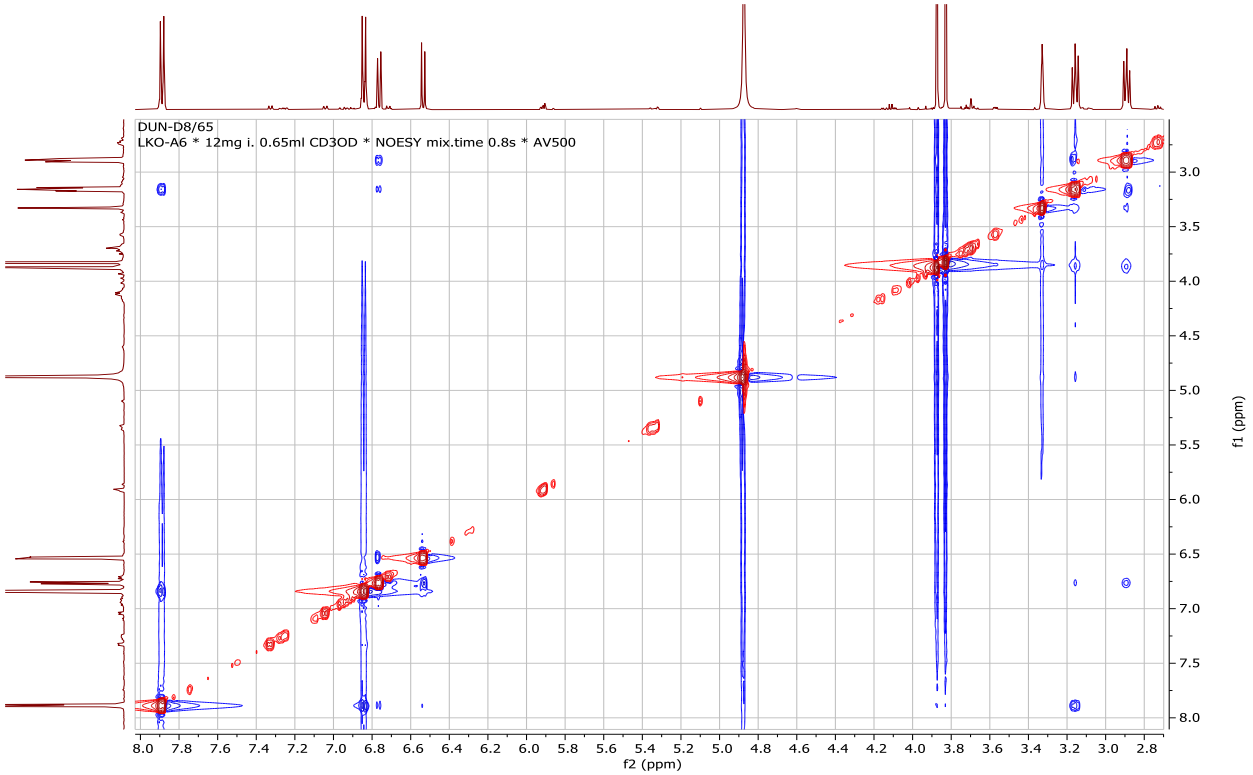

Appendix 16F: HSQC spectrum (CD_3OD) of compound **189**

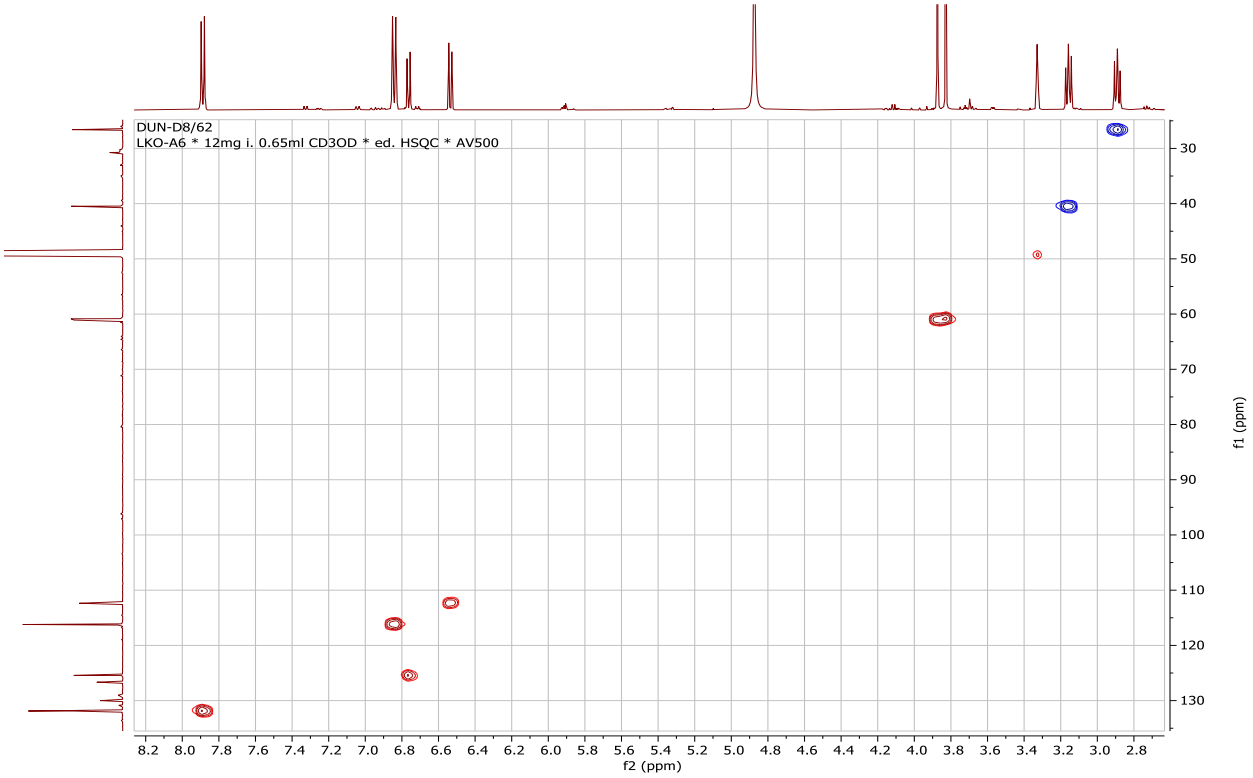

Appendix 16G: HMBC spectrum (CD_3OD) of compound **189**

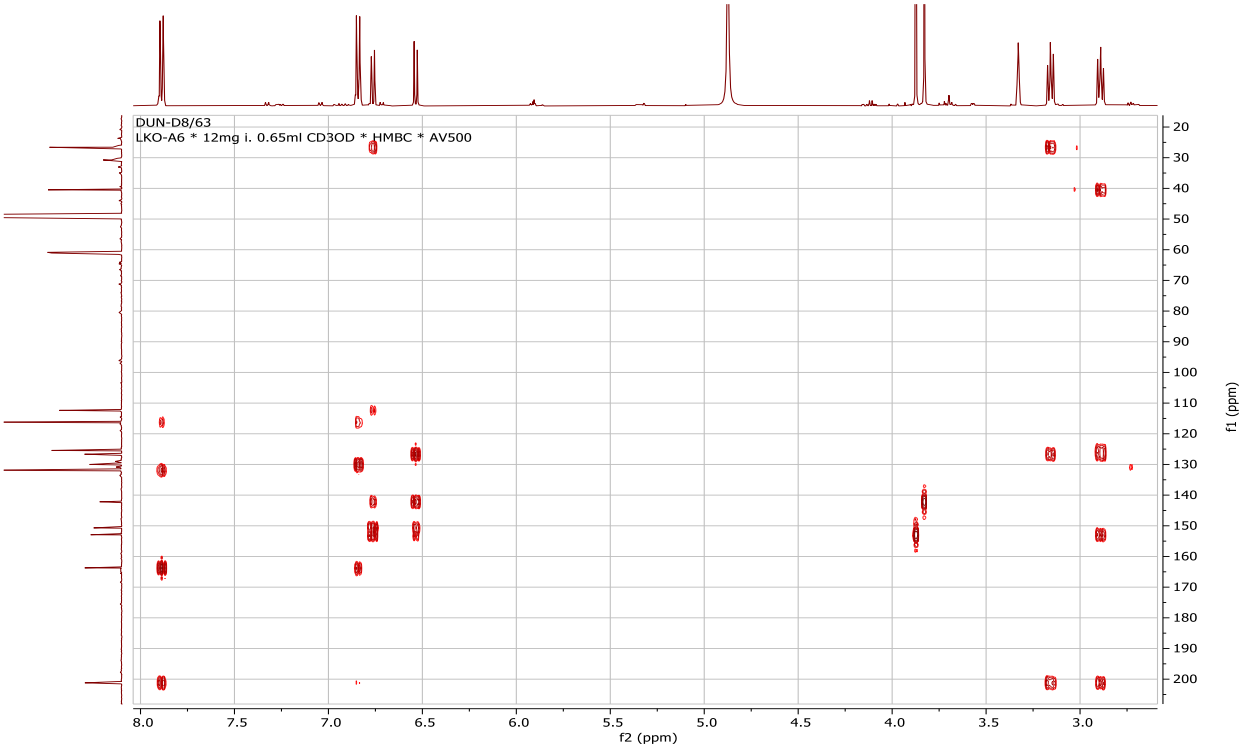

Appendix 17: NMR spectra for (25*S*)-spirosta-1,4-dien-3-one (**190**)

Appendix 17A: HRESIMS of compound **190**

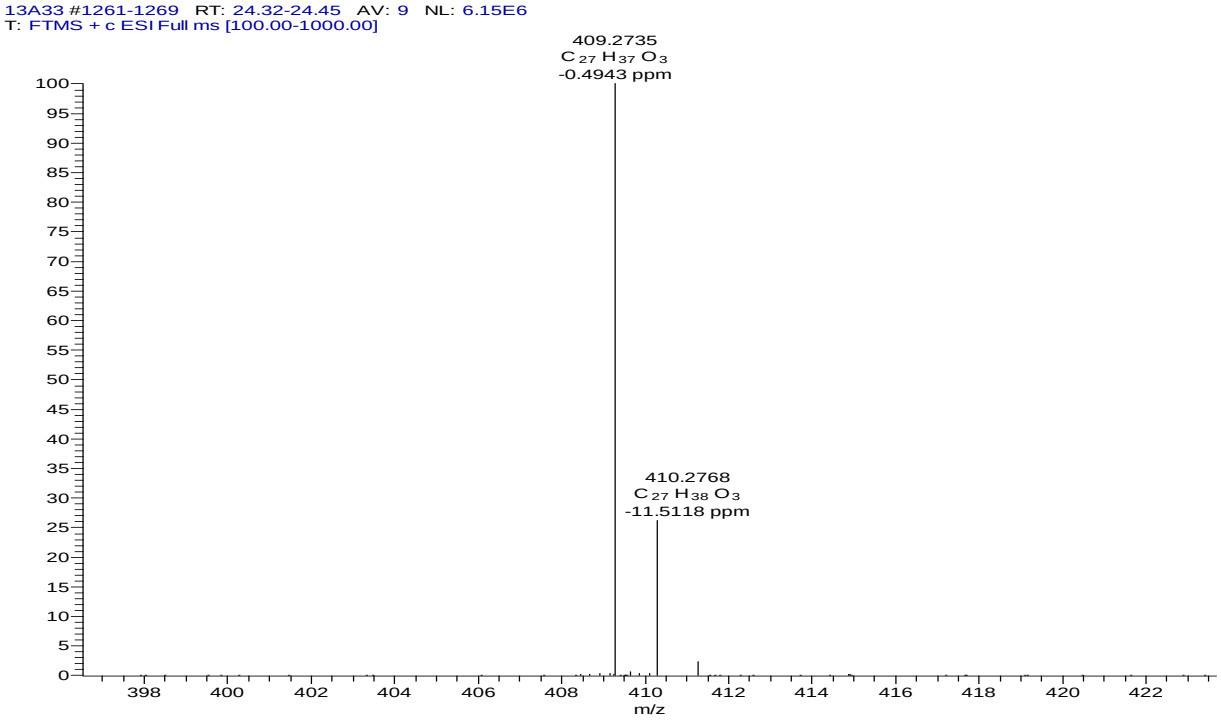

Appendix 17B: ^{1}H NMR spectrum (500 MHz, CD_2Cl_2) of compound **190**

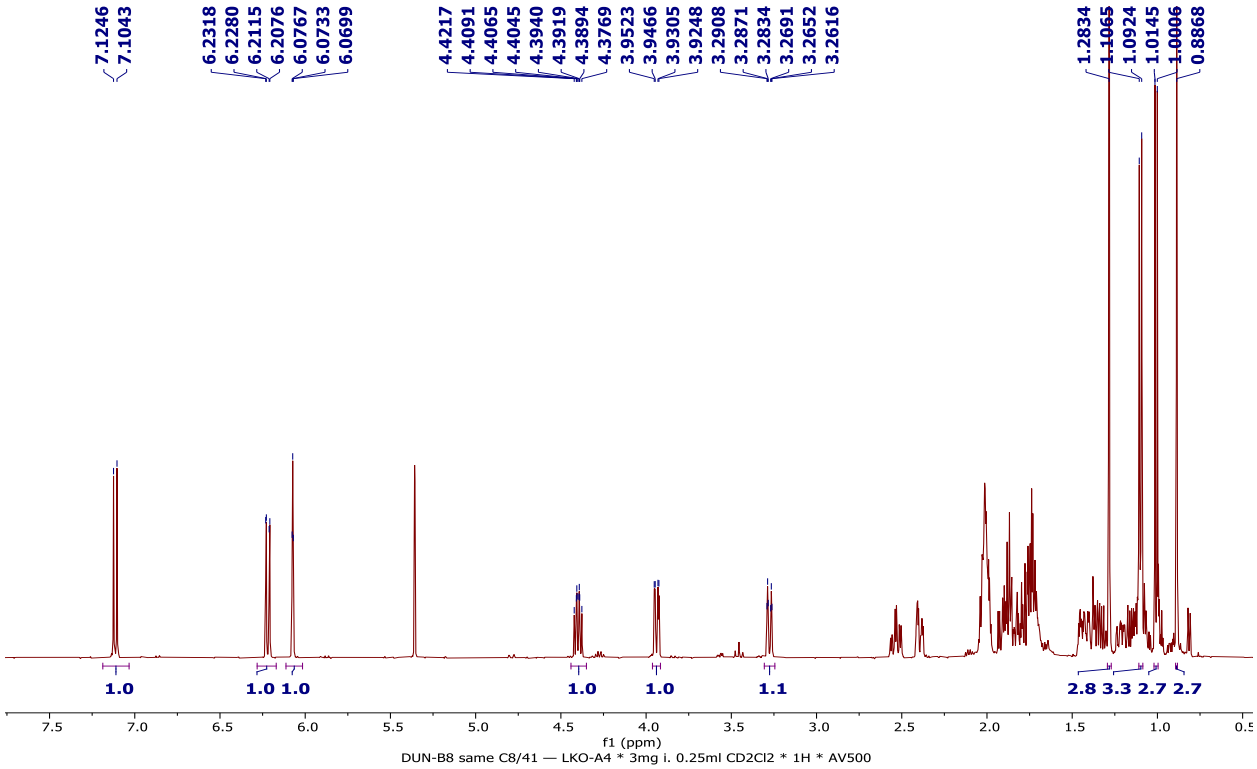

Appendix 17C: ^{13}C NMR spectrum (125 MHz, CD_2Cl_2) of compound **190**

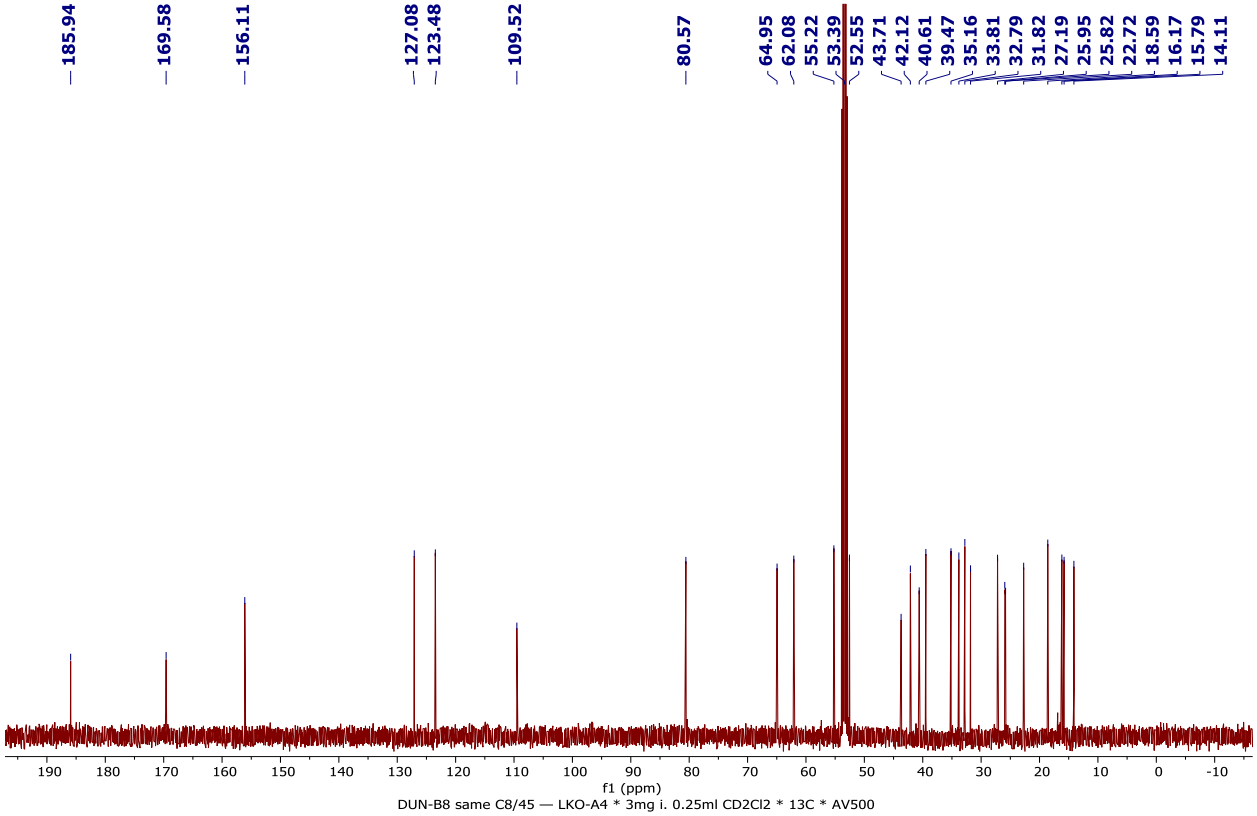

Appendix 17D: ^{1}H-^{1}H COSY spectrum (CD_2Cl_2) of compound **190**

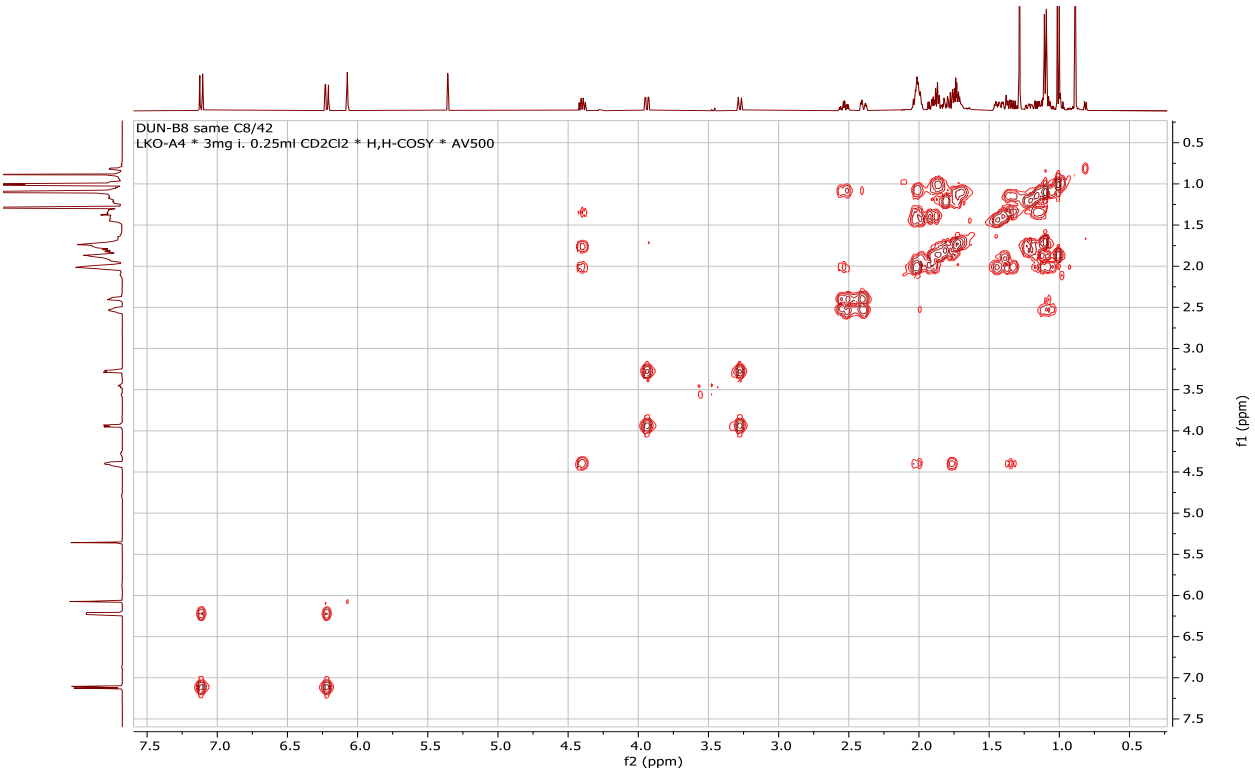

Appendix 17E: HSQC spectrum (CD_2Cl_2) of compound **190**

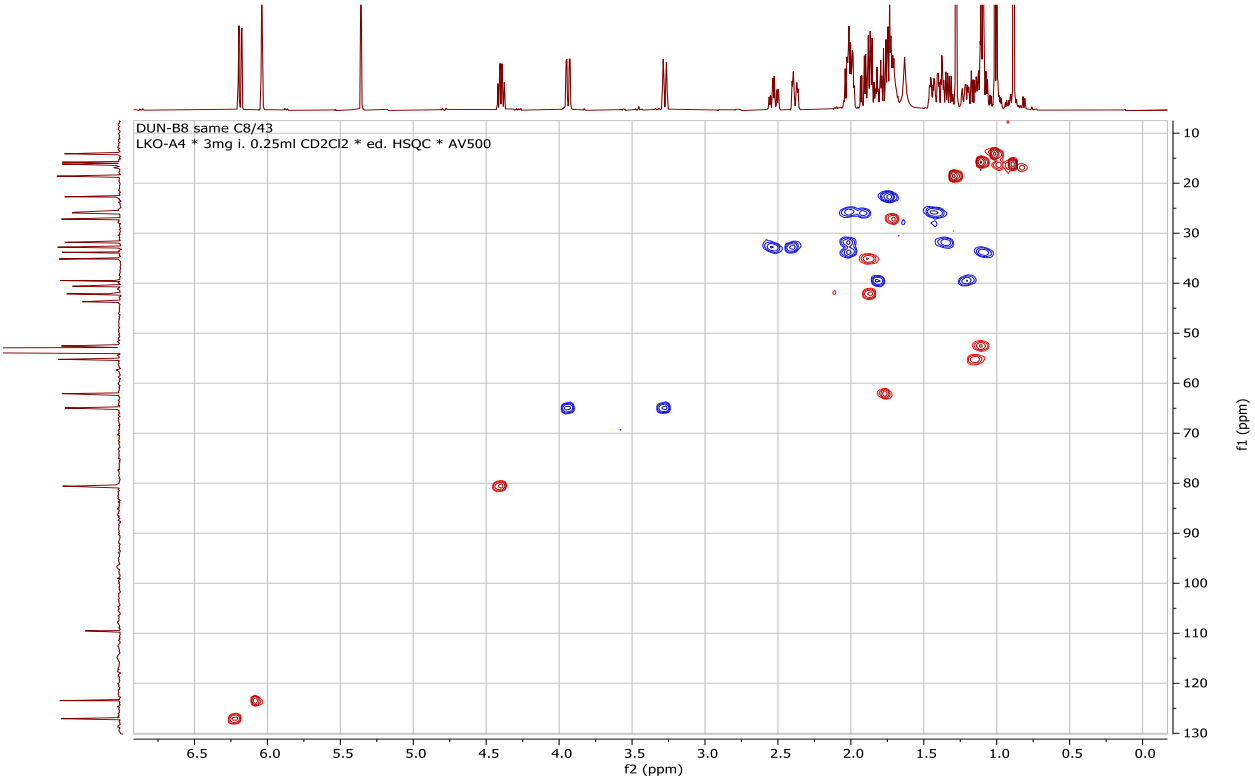

Appendix 17F: HMBC spectrum (CD_2Cl_2) of compound **190**

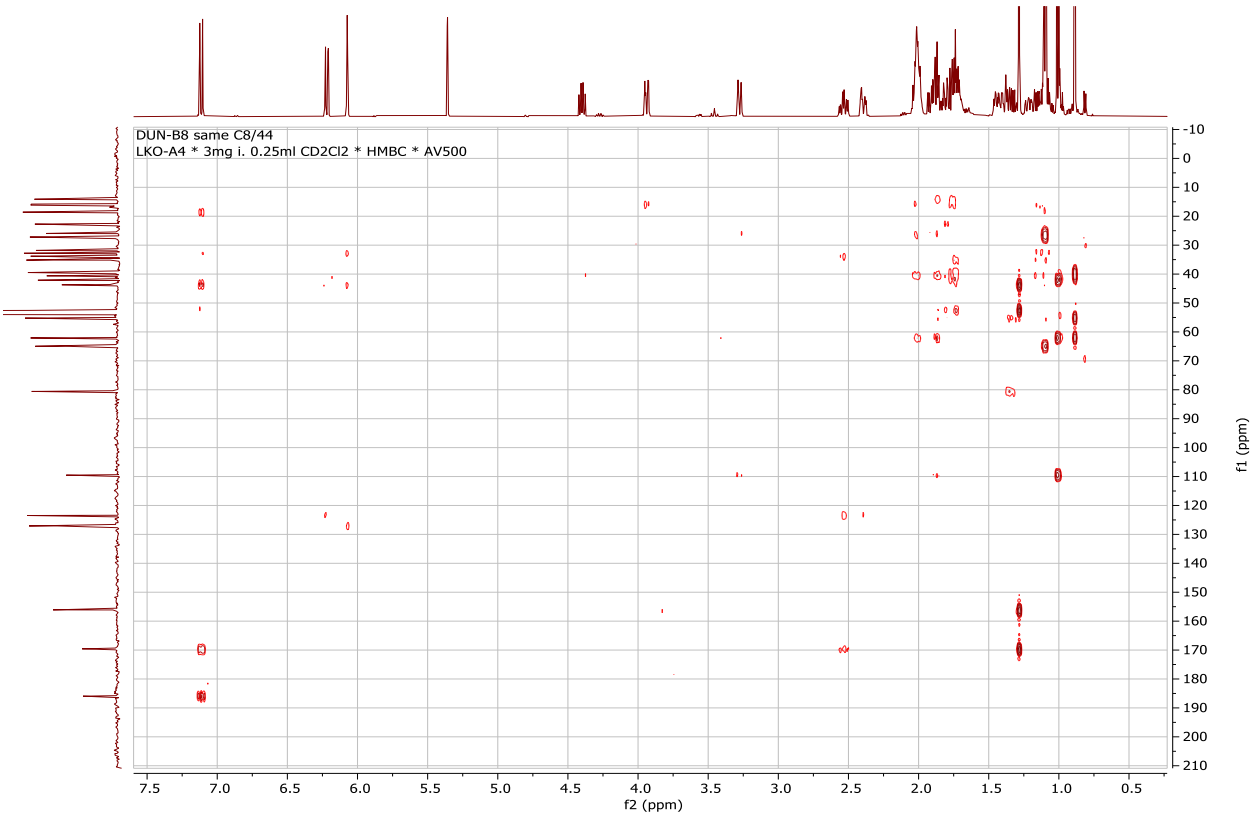

Appendix 18: NMR spectra for stigmasterol (**191**)

Appendix 18A: ^{1}H NMR spectrum (500 MHz, CD_2Cl_2) of compound **191**

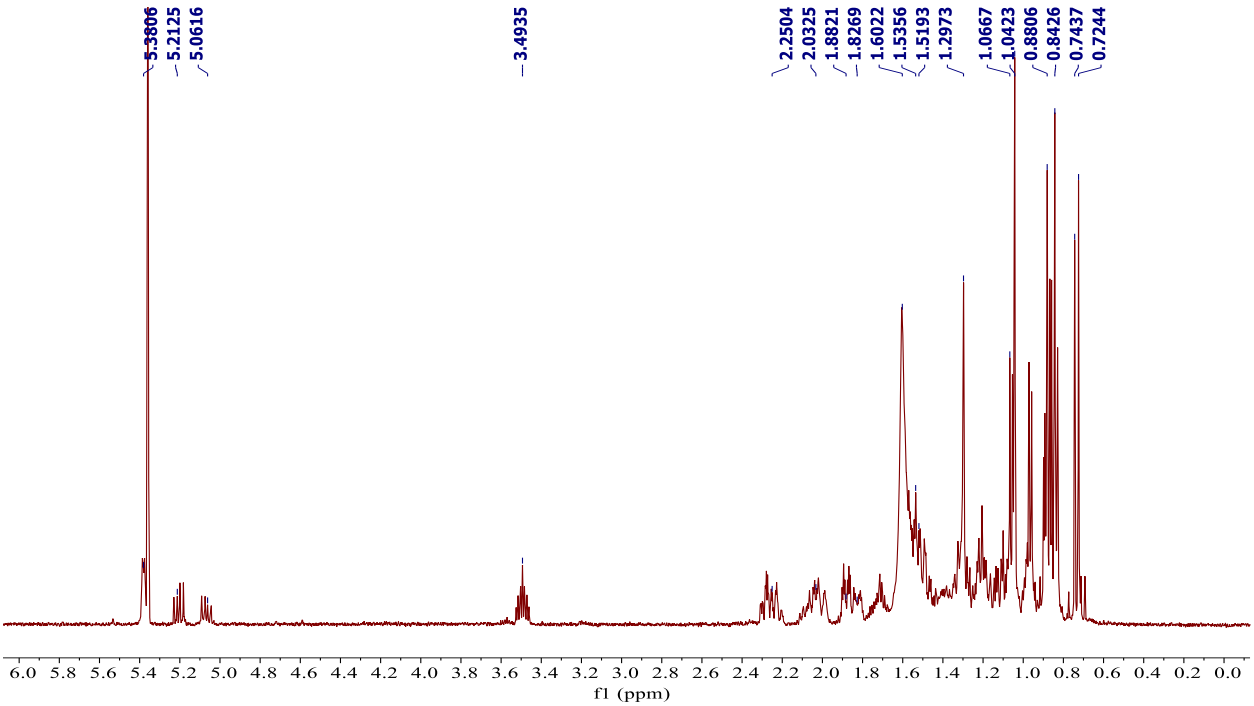

Appendix 18B: ^{13}C NMR spectrum (125 MHz, CD_2Cl_2) of compound **191**

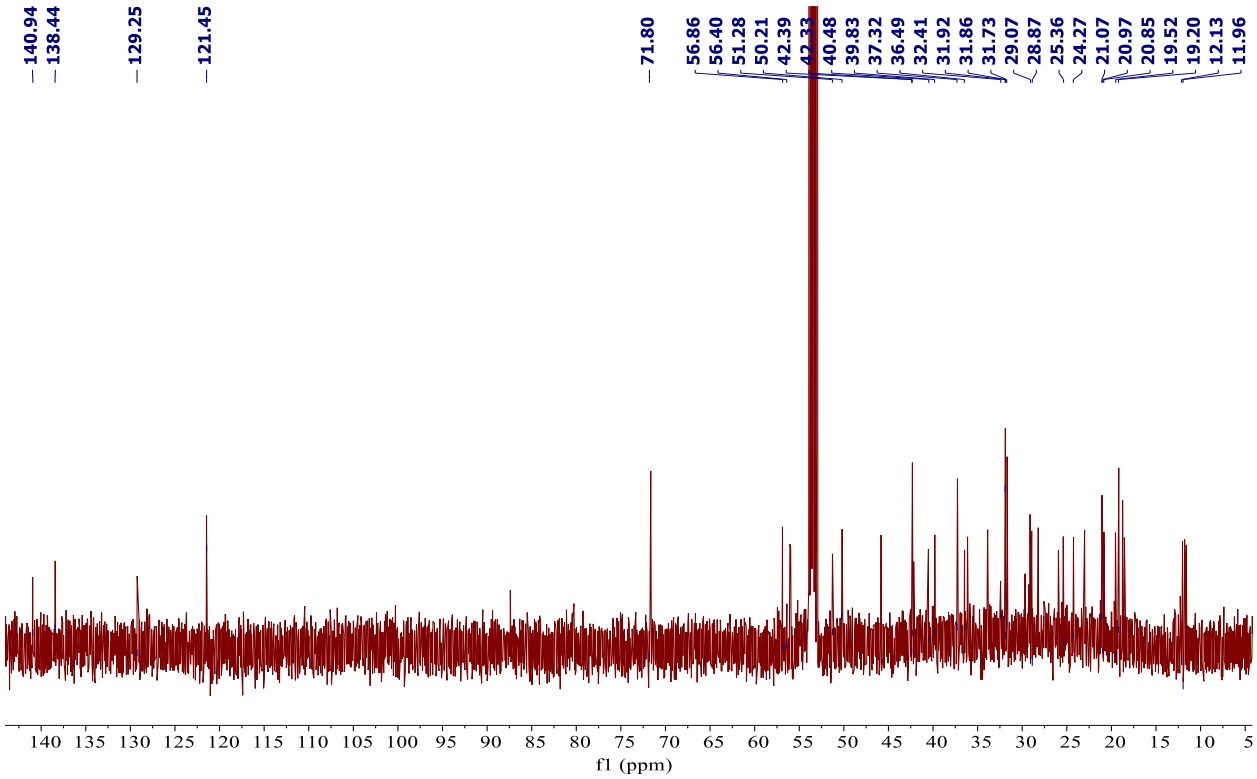

Appendix 18C: ^{1}H-^{1}H COSY spectrum (CD_2Cl_2) of compound **191**

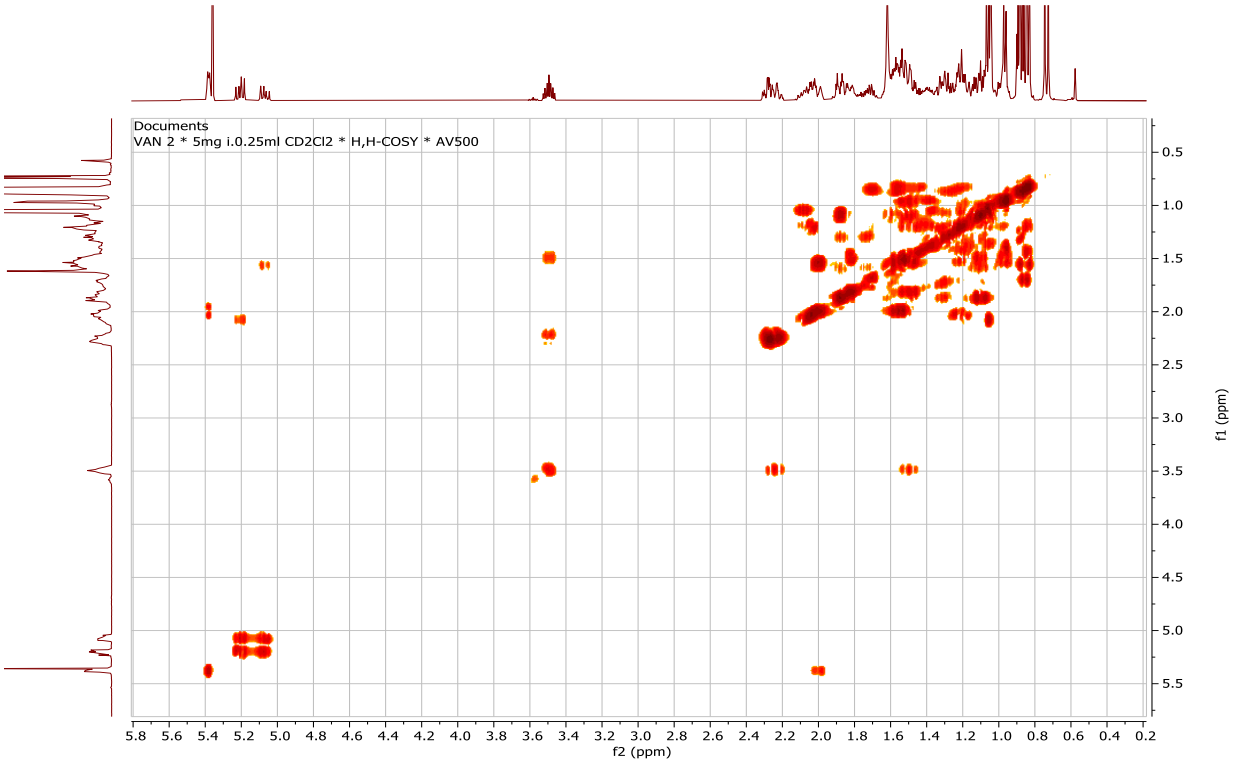

Appendix 18D: HSQC spectrum (CD_2Cl_2) of compound **191**

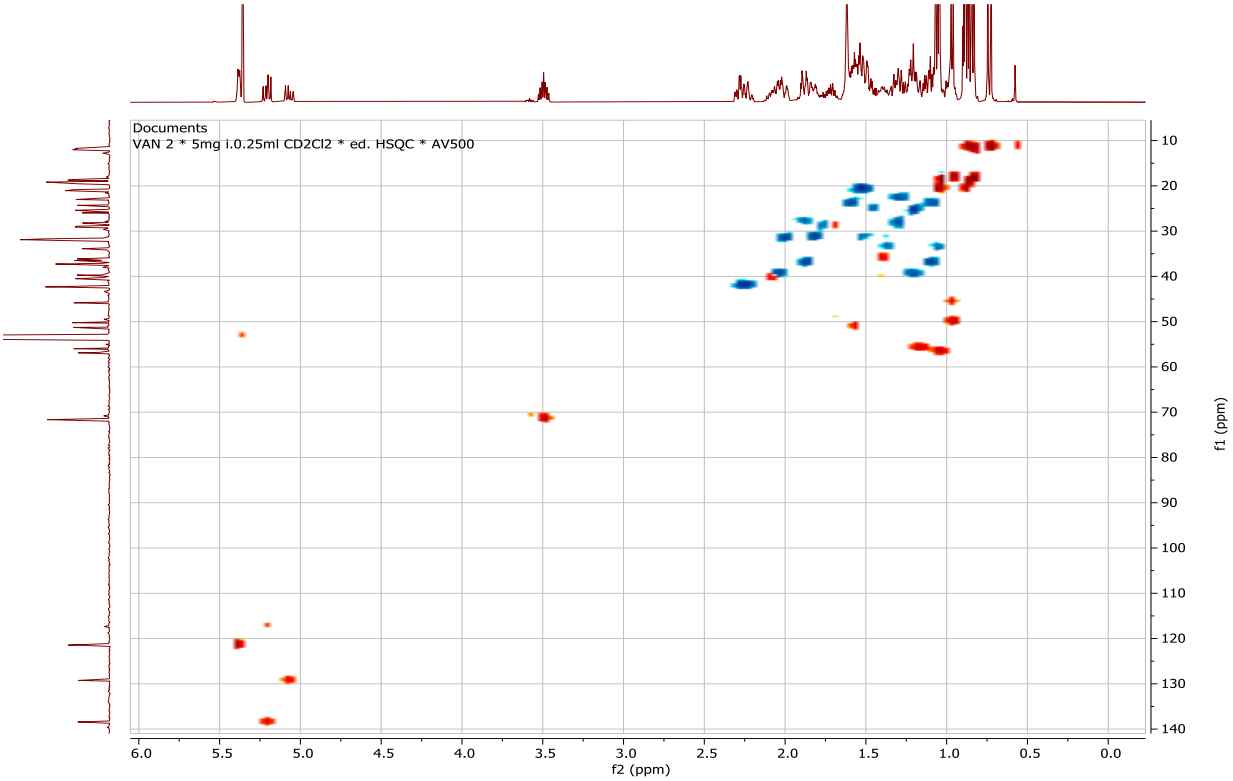

Appendix 18E: HMBC spectrum (CD_2Cl_2) of compound **191**

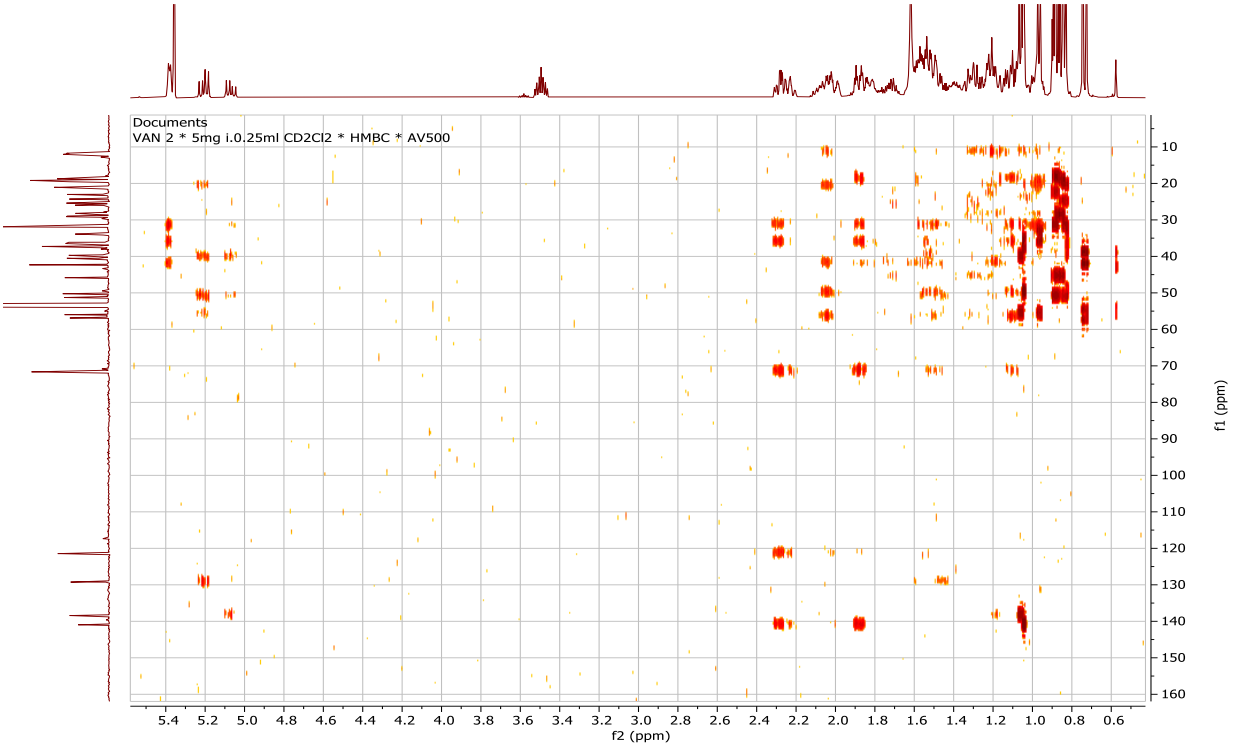

Appendix 19: NMR spectra for stigmasterol 3-*O*-*β*-D-glucopyranoside (**192**)

Appendix 19A: ^{1}H NMR spectrum (600 MHz, DMSO-d_6) of compound **192**

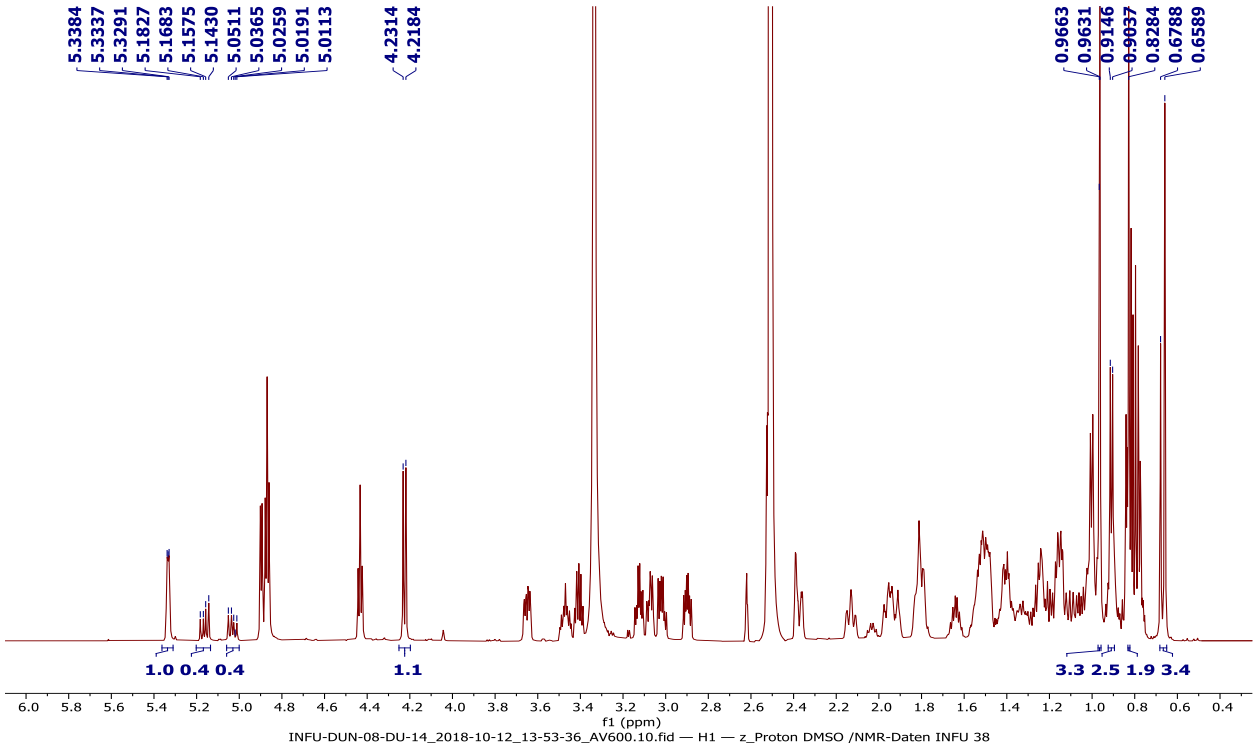

Appendix 19B: ^{13}C NMR spectrum (150 MHz, DMSO-d_6) of compound **192**

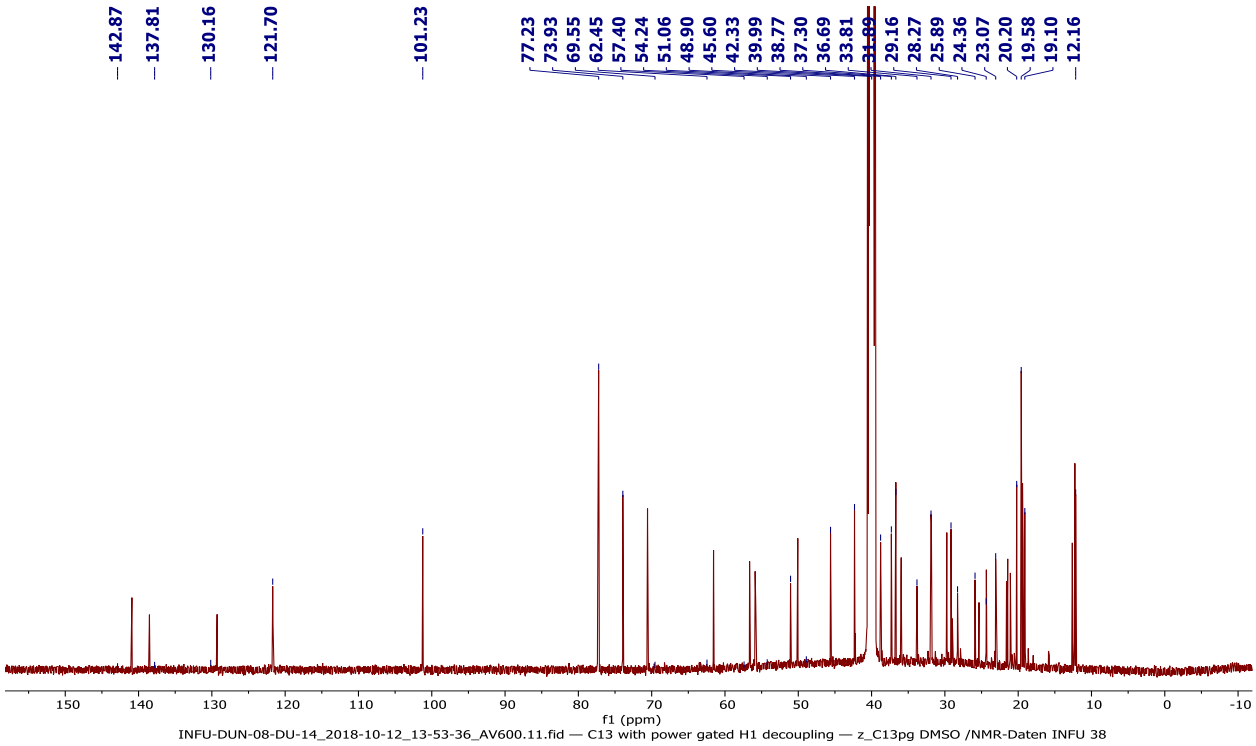

Appendix 19C: ^{1}H-^{1}H COSY spectrum (DMSO-d_6) of compound **192**

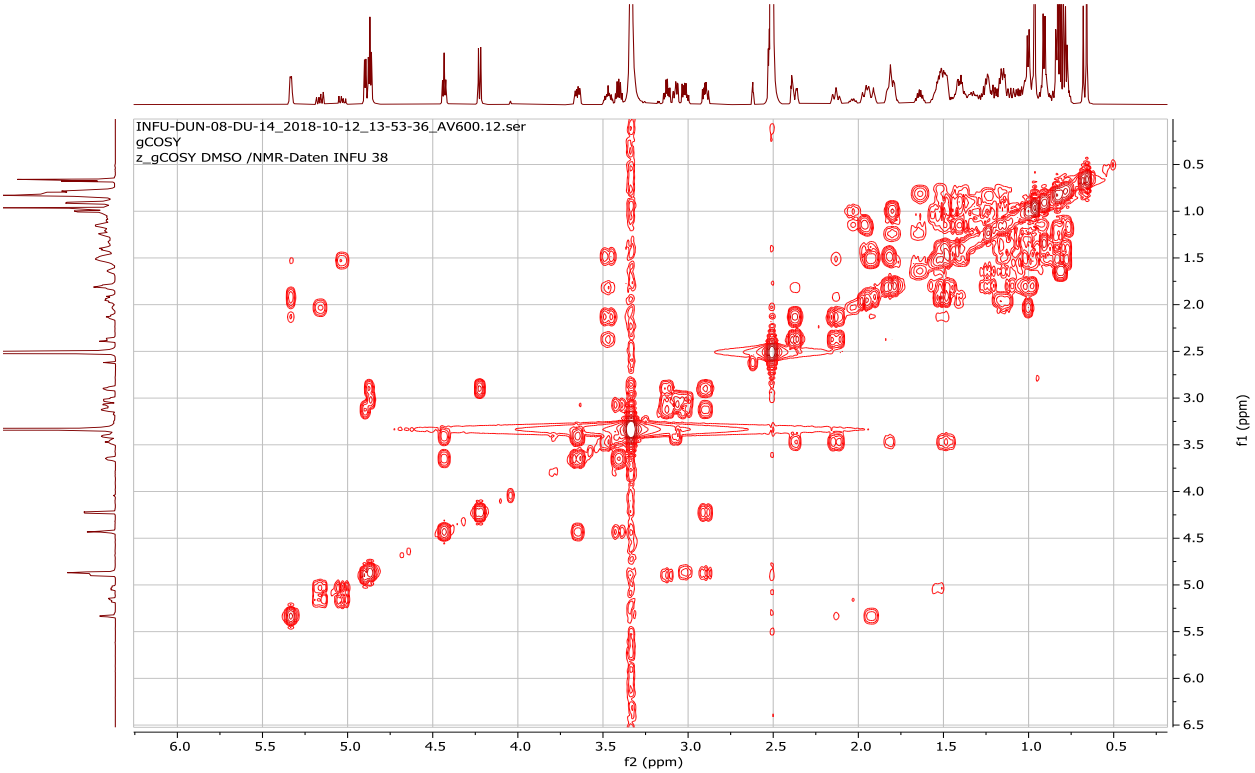

Appendix 19D: HSQC spectrum (DMSO-d_6) of compound **192**

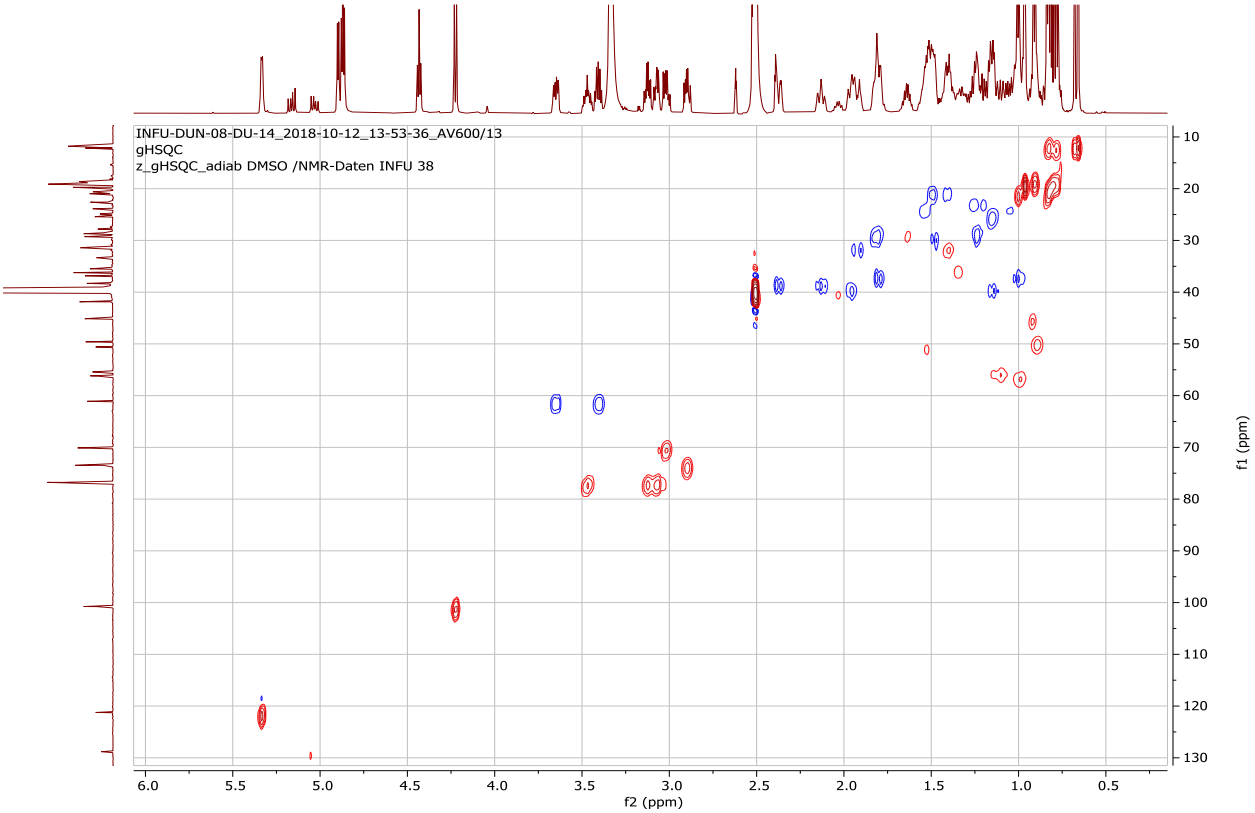

Appendix 19E: HMBC spectrum (DMSO-d_6) of compound **192**

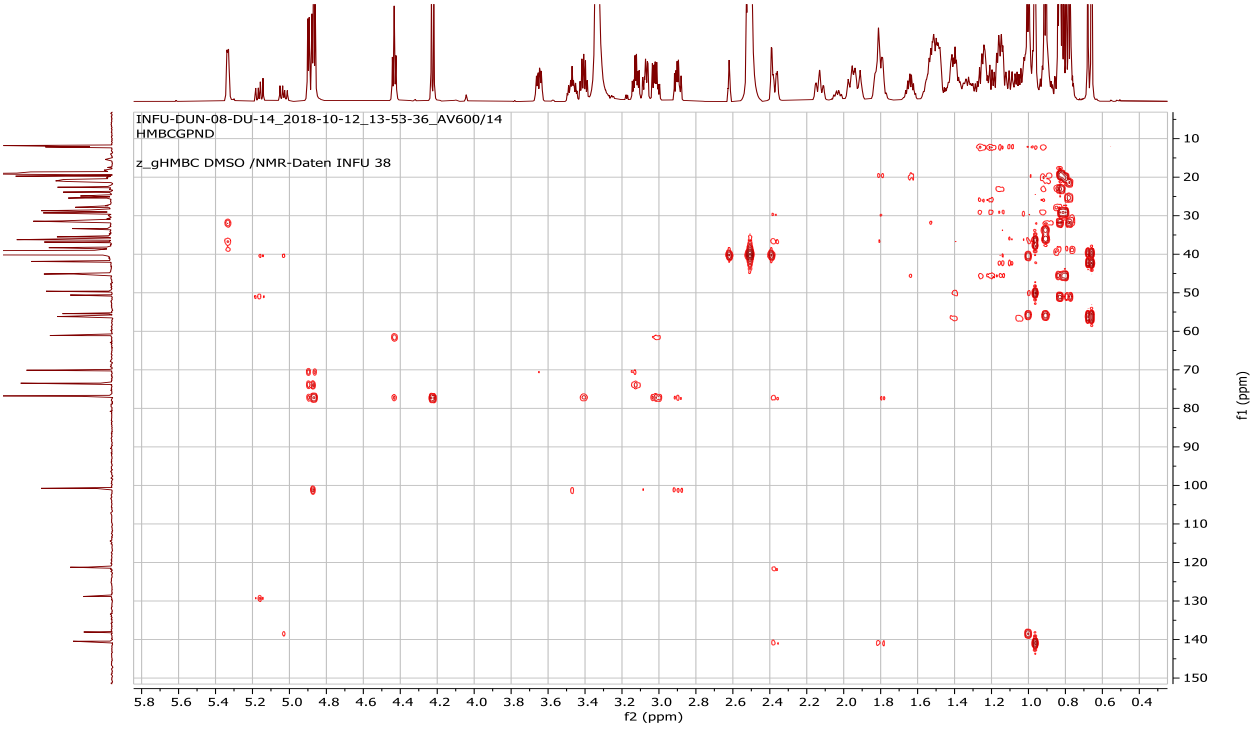

Appendix 20: NMR spectra for 3-(4‴-hydroxyphenyl)-*N*-[2′-(4″-hydroxyphenyl)-2′-methoxyethyl]acrylamide (**193**)

Appendix 20A: HRESIMS of compound **193**

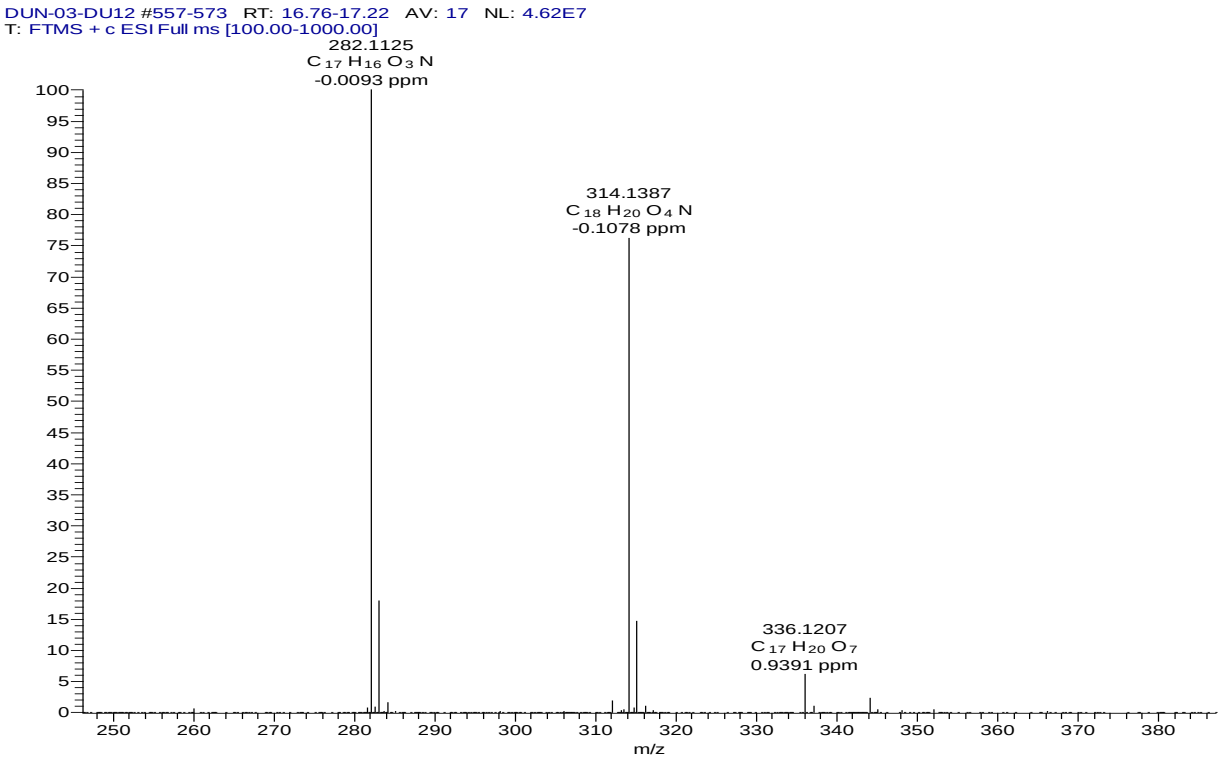

Appendix 20B: LC-UV spectrum of compound **193**

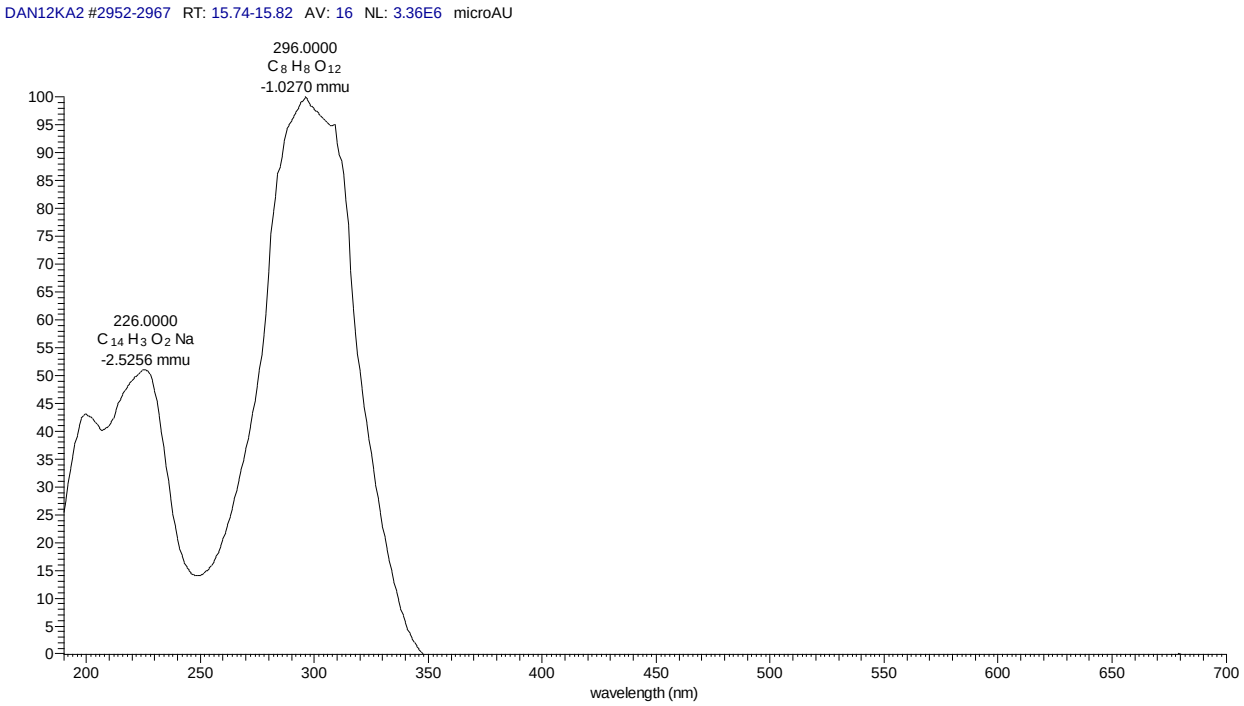

Appendix 20C: ^{1}H NMR spectrum (600 MHz, DMSO-d_6) of compound **193**

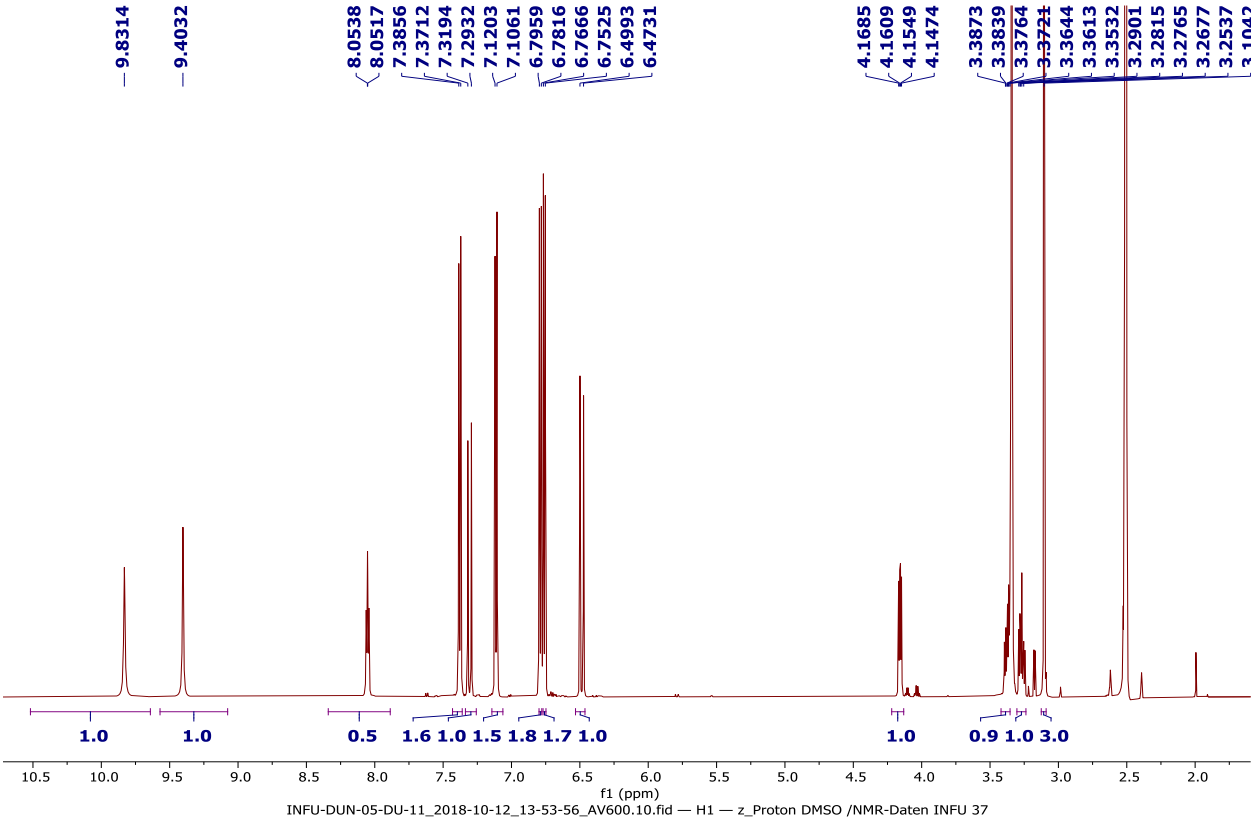

Appendix 20D: ^{13}C NMR spectrum (150 MHz, DMSO-d_6) of compound **193**

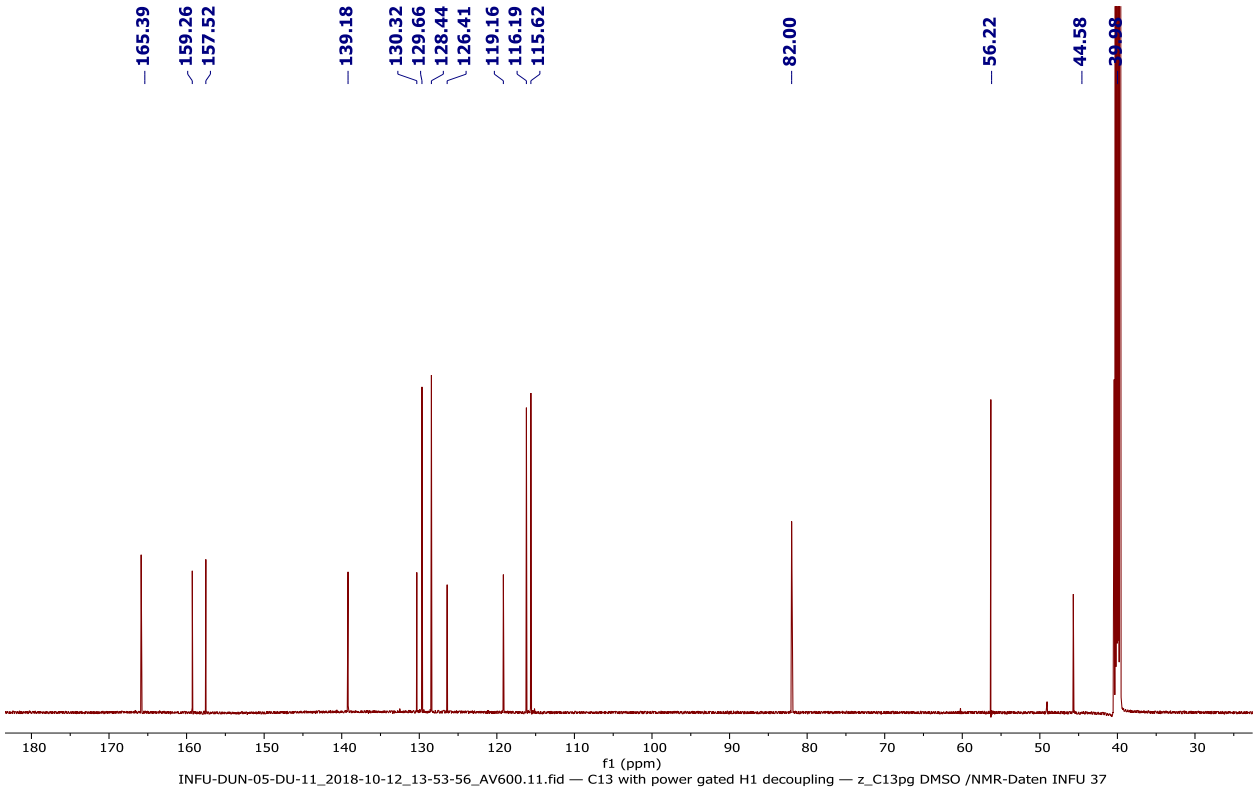

Appendix 20E: ^{1}H-^{1}H COSY spectrum (DMSO-d_6) of compound **193**

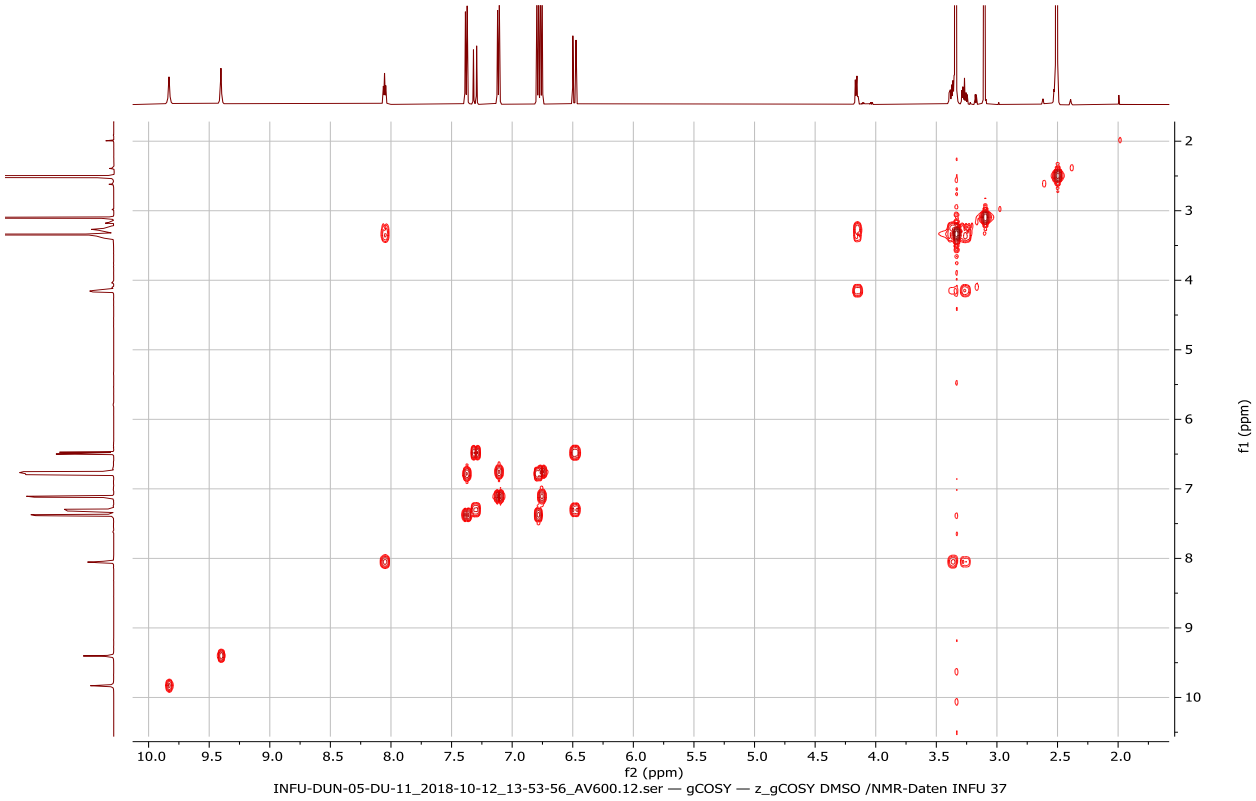

Appendix 20F: HSQC spectrum (DMSO-d_6) of compound **193**

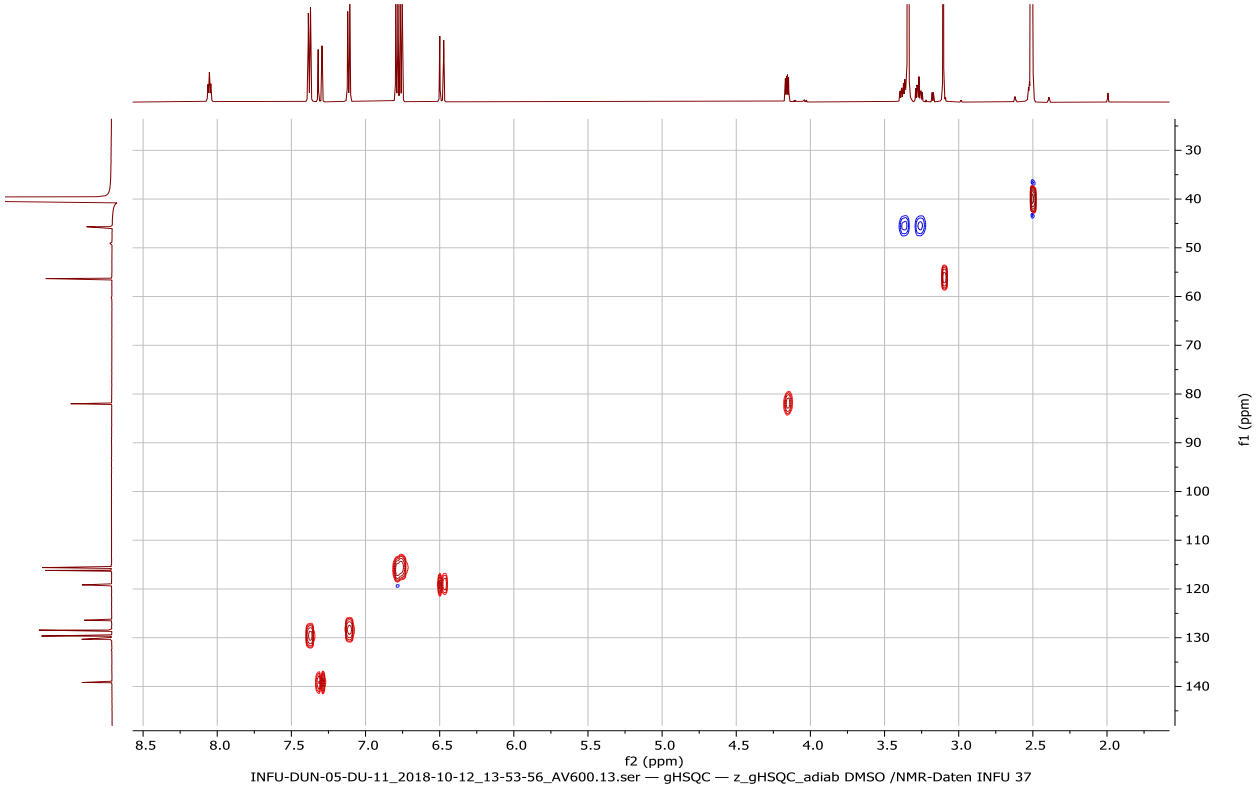

Appendix 20G: HMBC spectrum (DMSO-d_6) of compound **193**

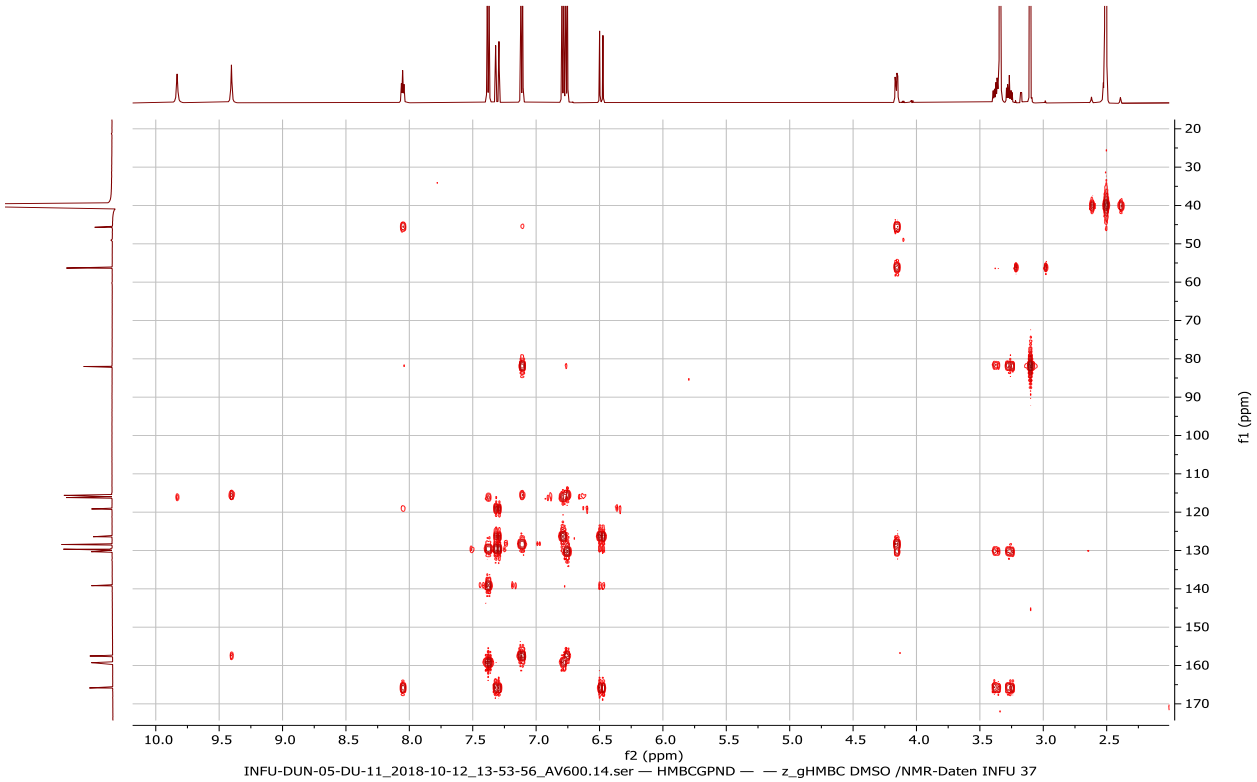

Appendix 21: NMR spectra for *N-Trans-p*-coumaroyloctopamine (**194**)

Appendix 21A: HRESIMS of compound **194**

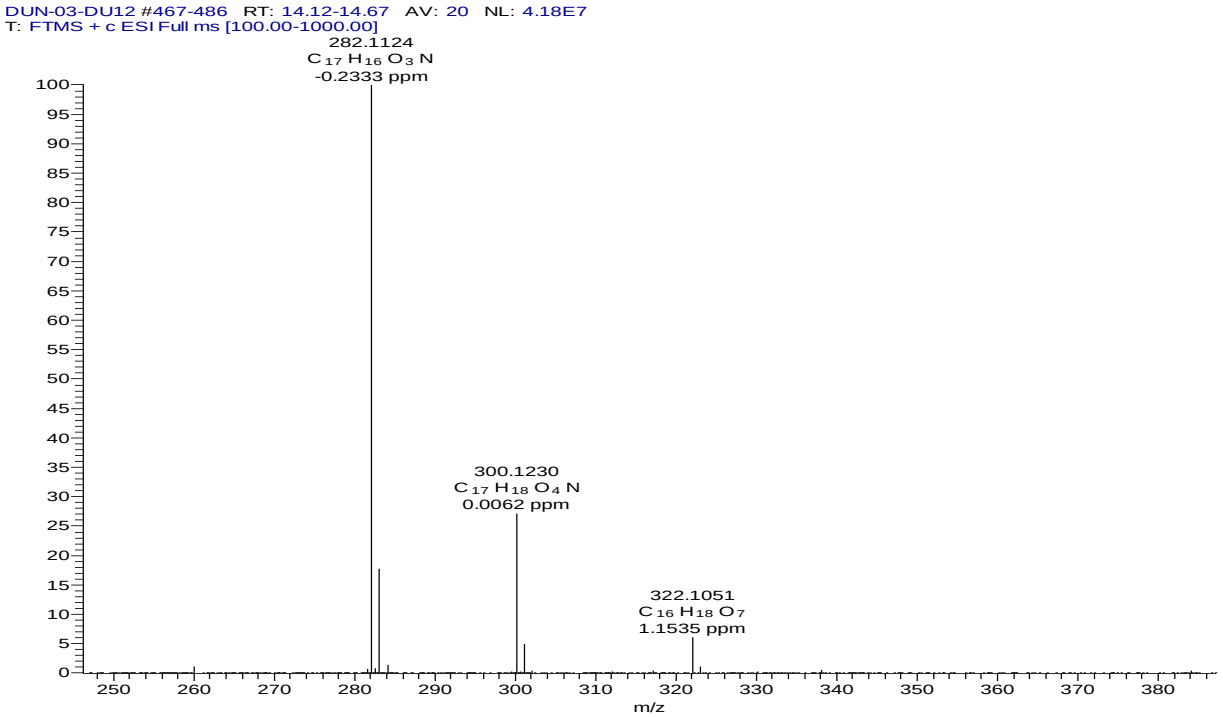

Appendix 21B: ^{1}H NMR spectrum (500 MHz, CD_3OD) of compound **194**

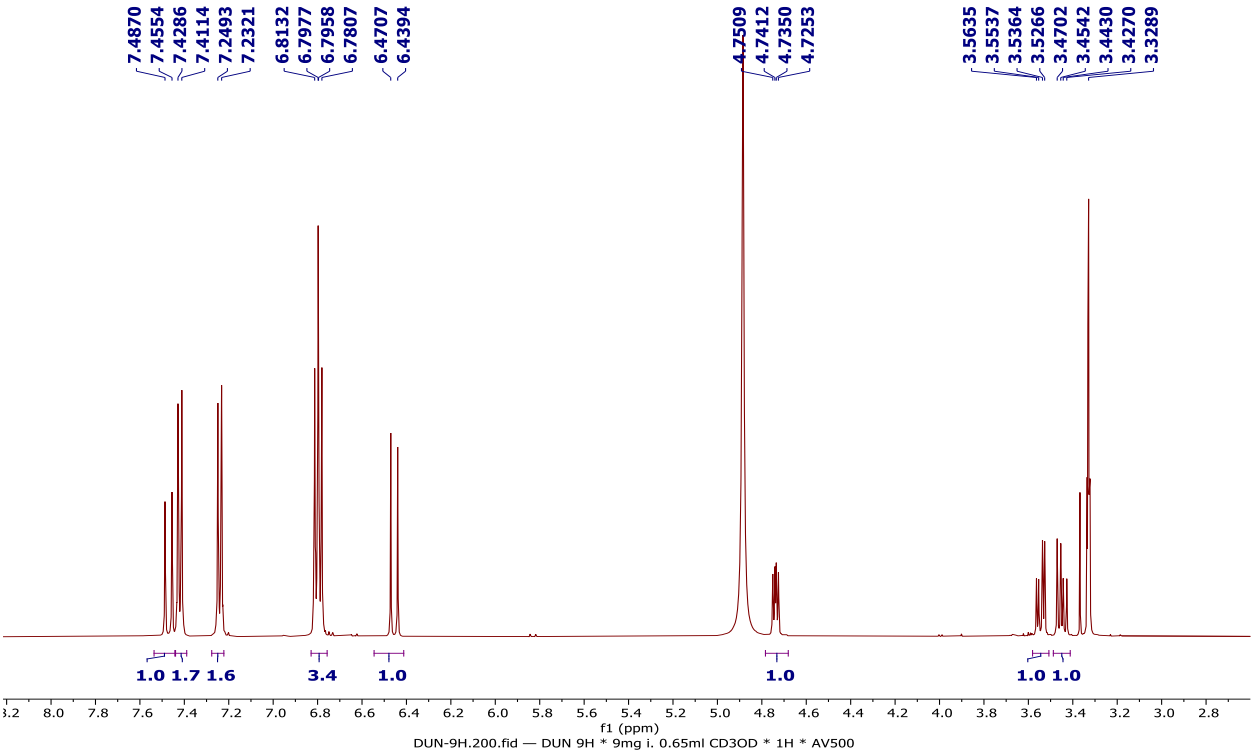

Appendix 21C: ^{13}C NMR spectrum (125 MHz, CD_3OD) of compound **194**

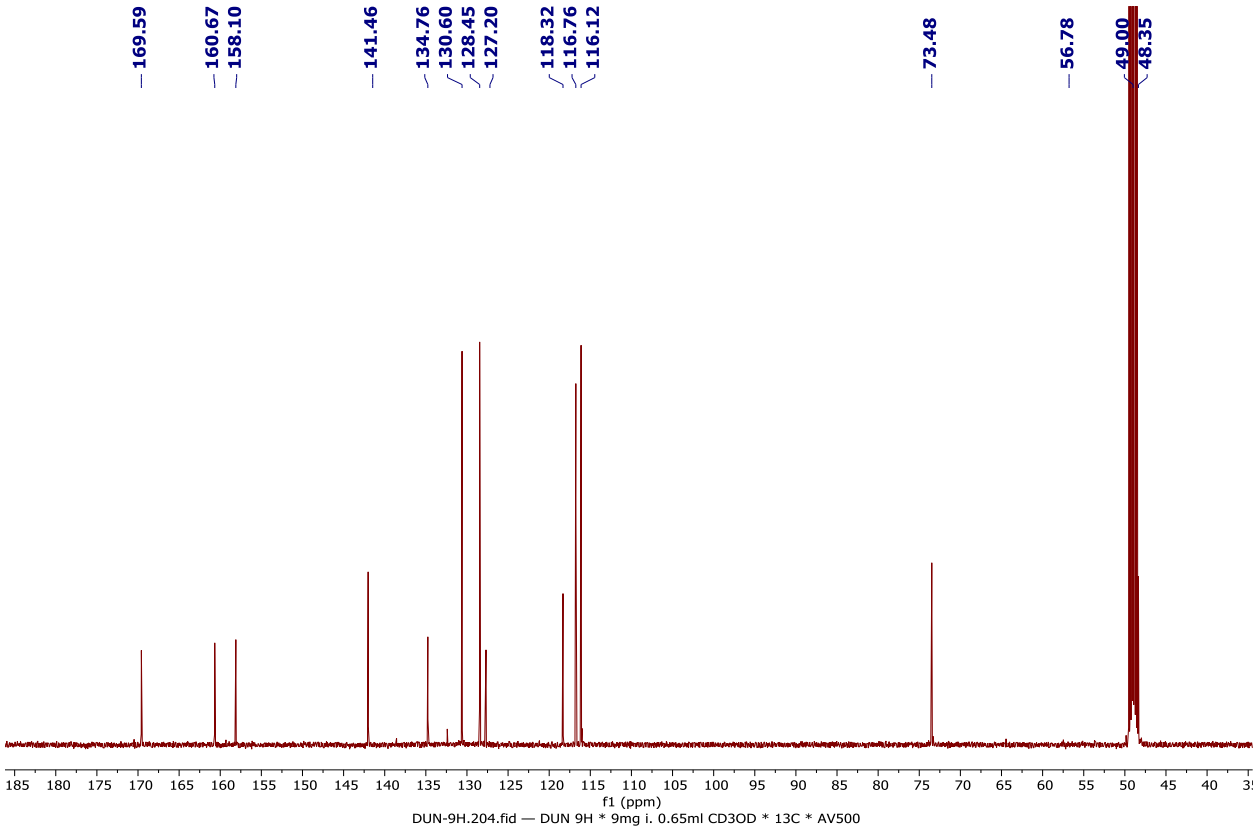

Appendix 21D: ^{1}H-^{1}H COSY spectrum (CD_3OD) of compound **194**

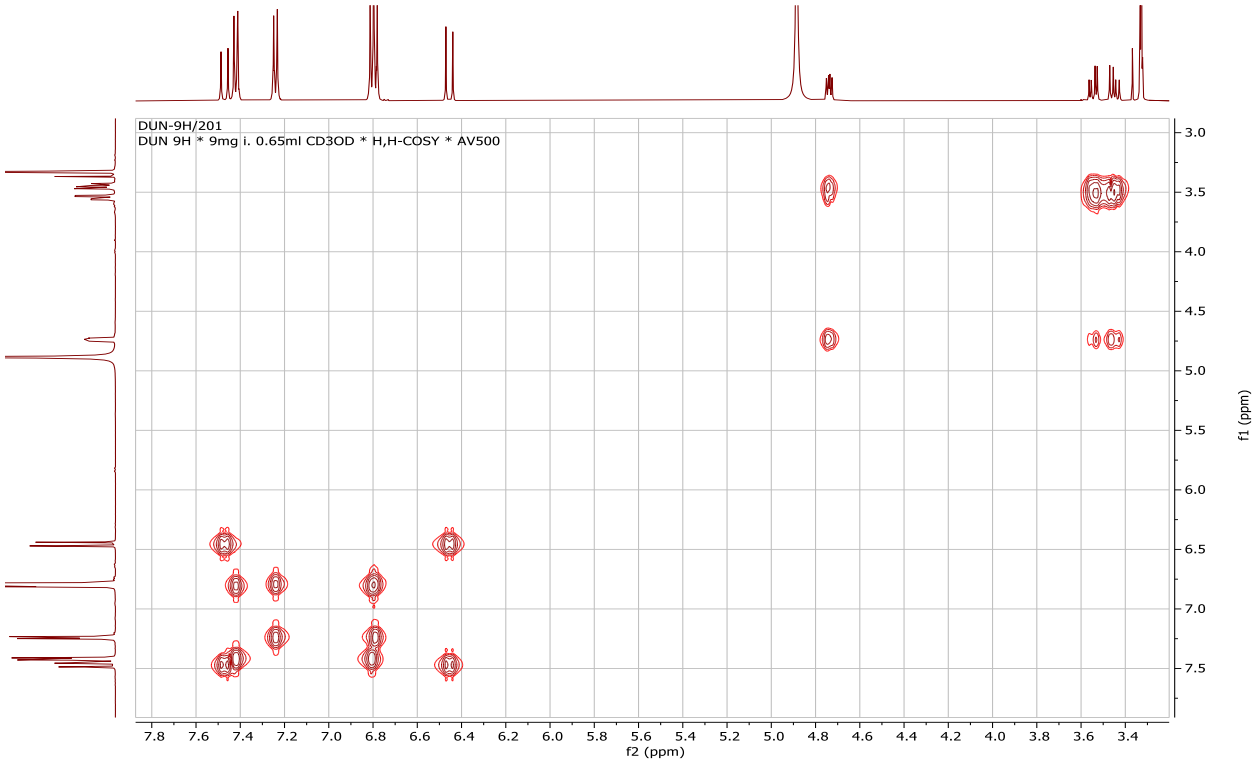

Appendix 21E: HSQC spectrum (CD_3OD) of compound **194**

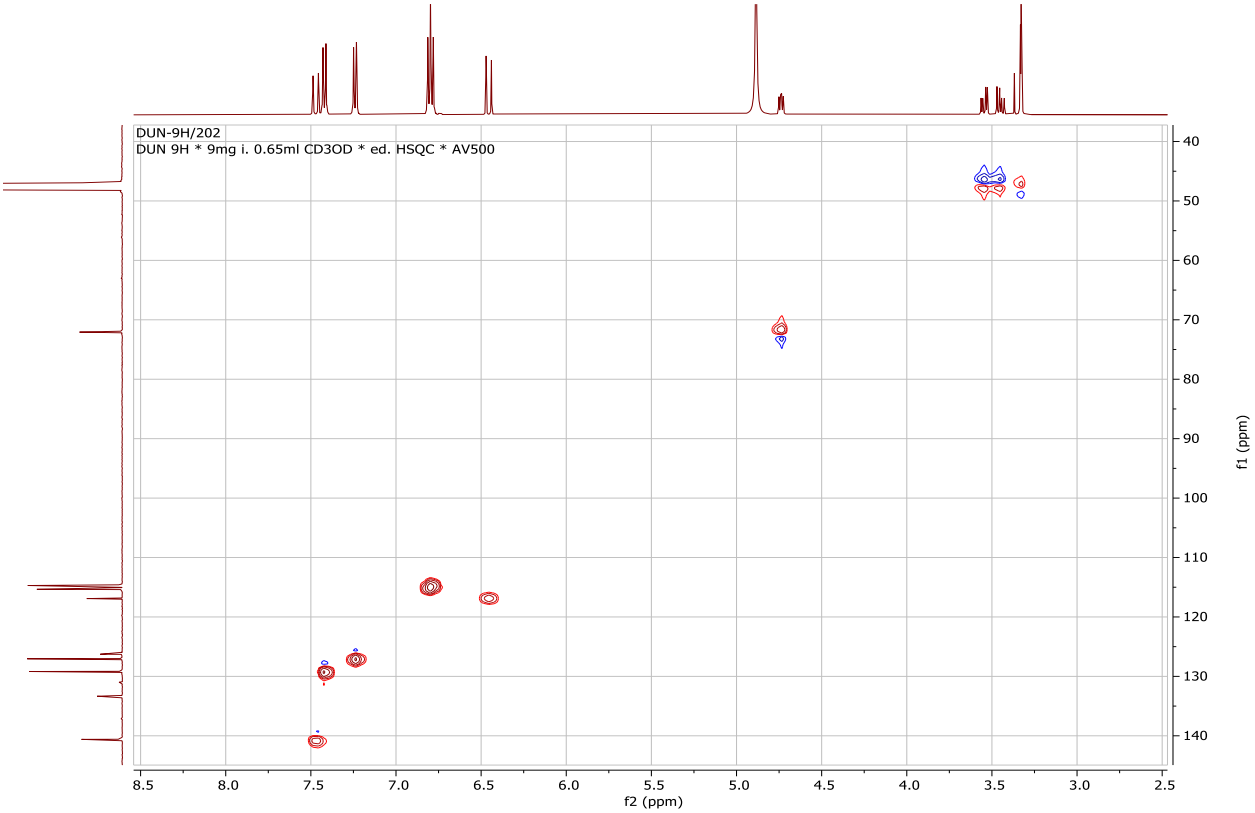

Appendix 21F: HMBC spectrum (CD_3OD) of compound **194**

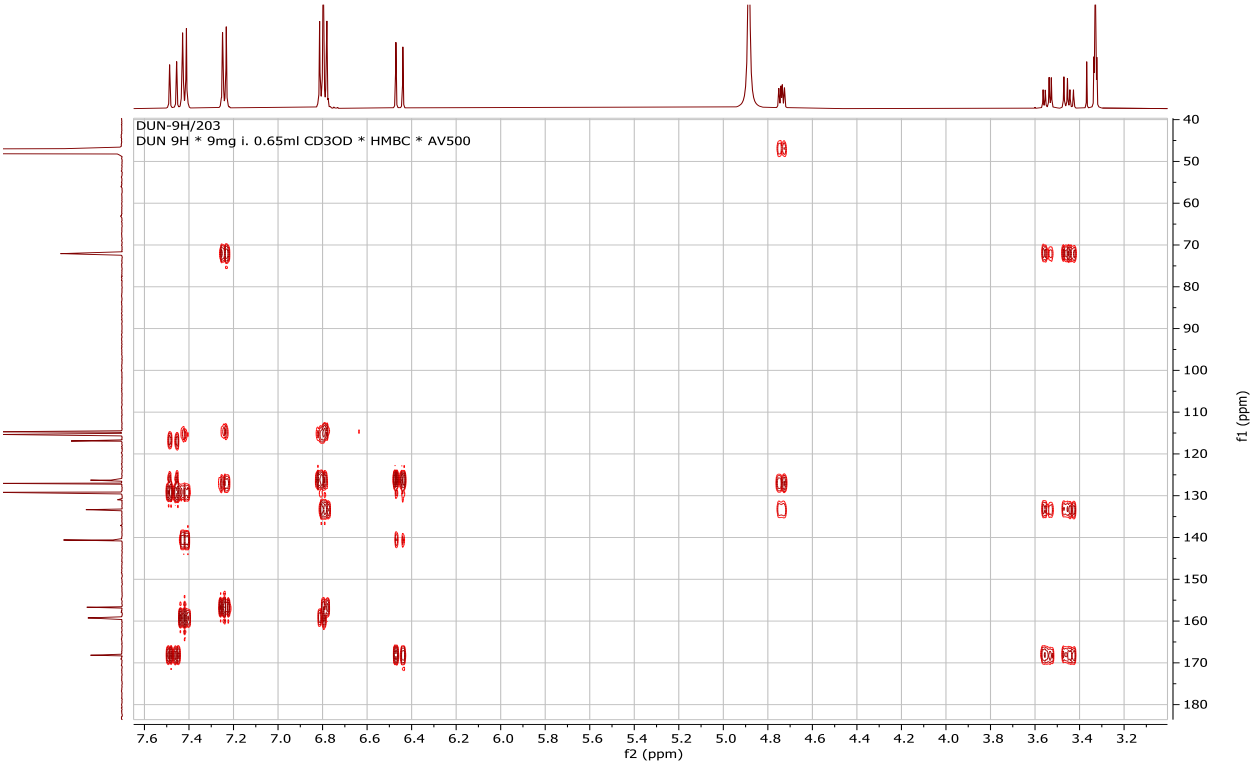

Appendix 22: NMR spectra for *N-Trans*-feruloyl phenethylamine (**195**)

Appendix 22A: HRESIMS of compound **195**

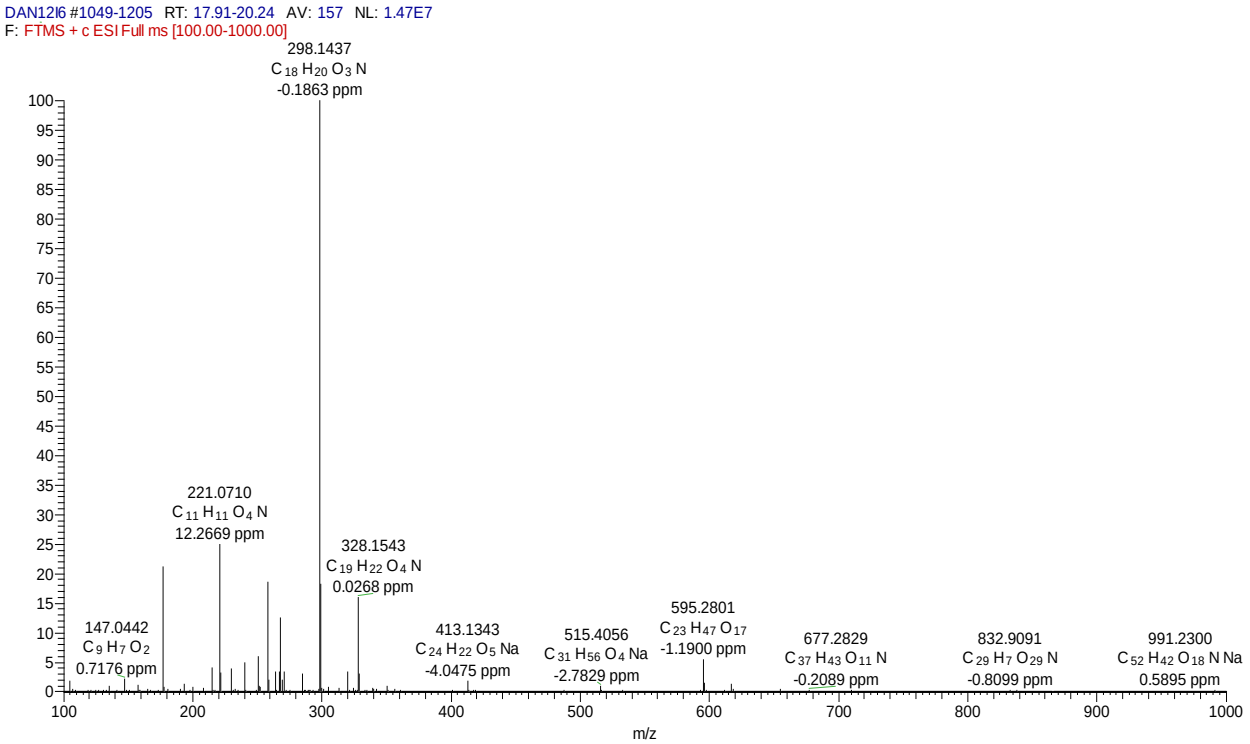

Appendix 22B: LC-UV spectrum of compound **195**

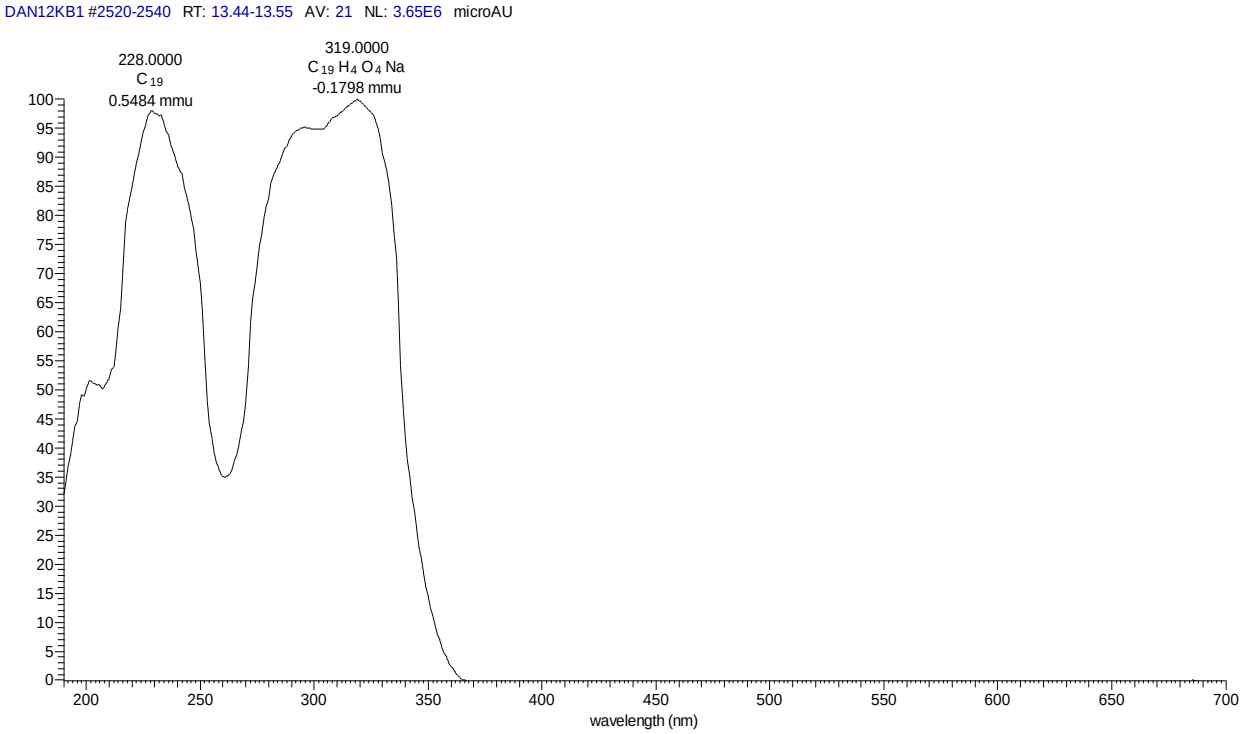

Appendix 22C: ^{1}H NMR spectrum (700 MHz, CD_3OD) of compound **195**

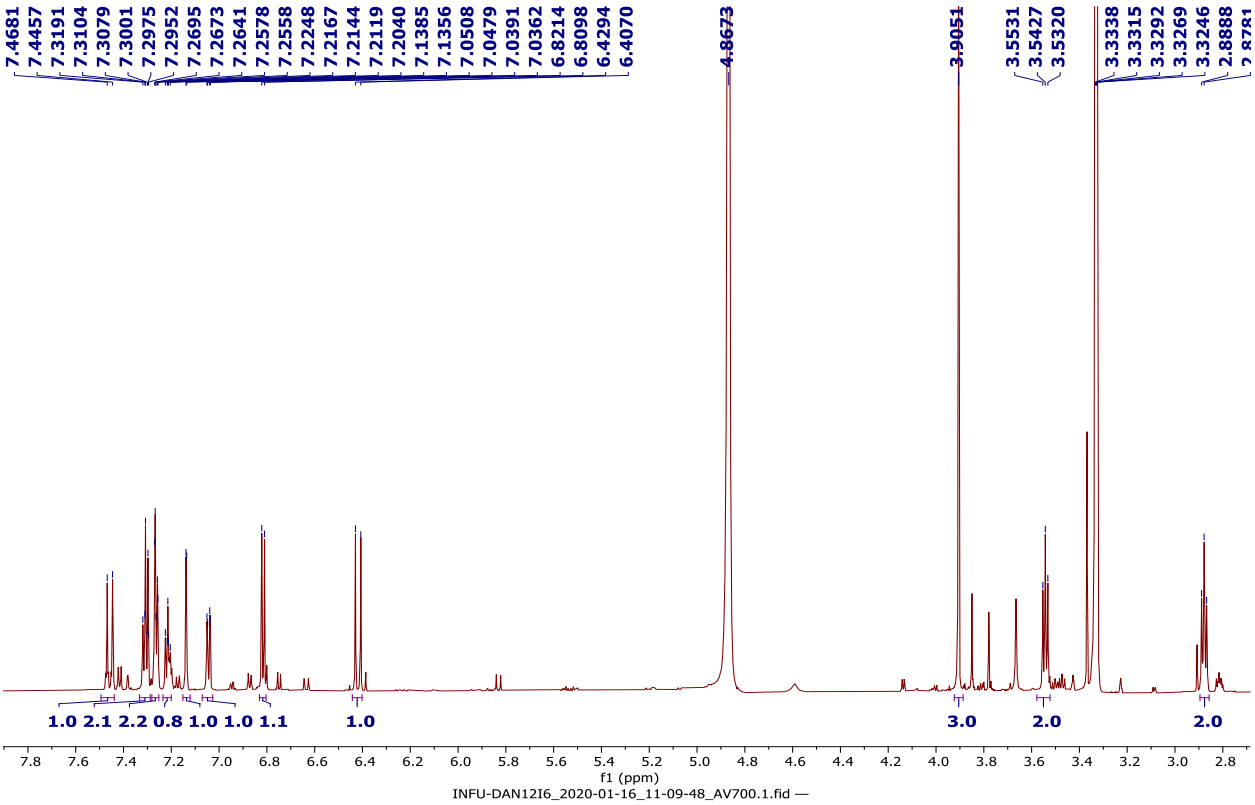

Appendix 22D: ^{13}C NMR spectrum (175 MHz, CD_3OD) of compound **195**

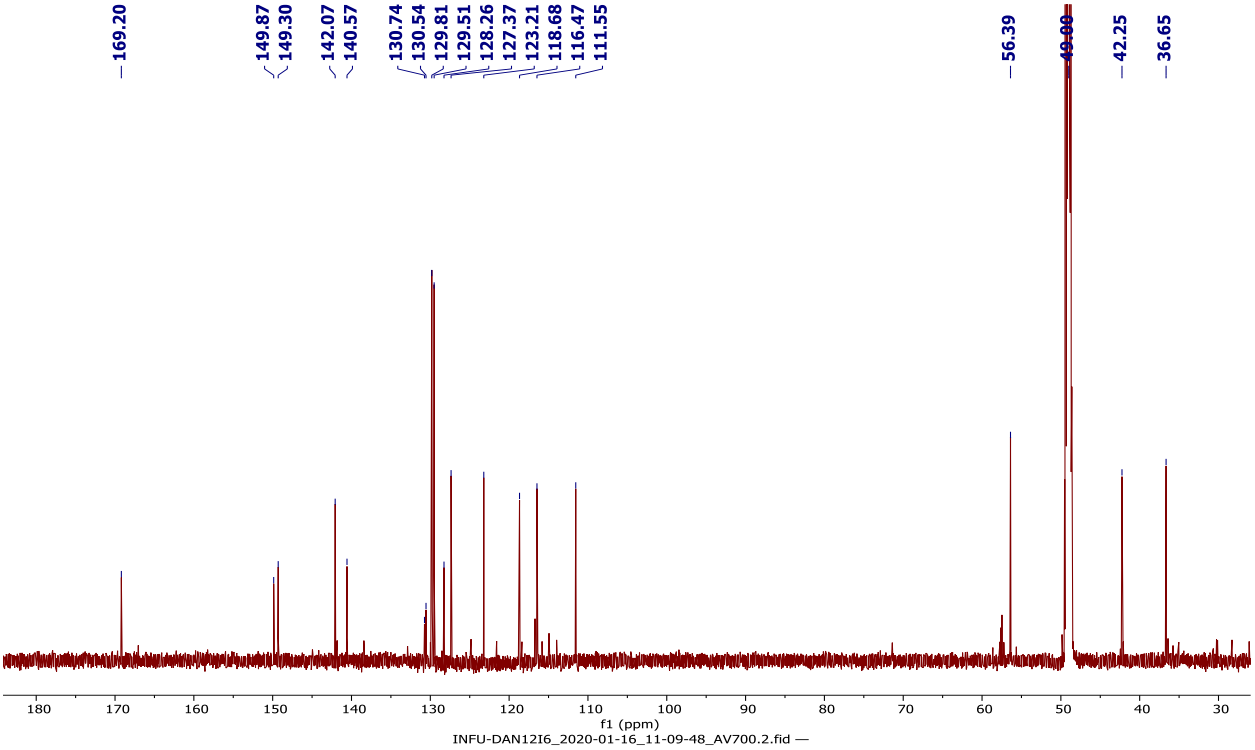

Appendix 22E: ^{1}H-^{1}H COSY spectrum (CD_3OD) of compound **195**

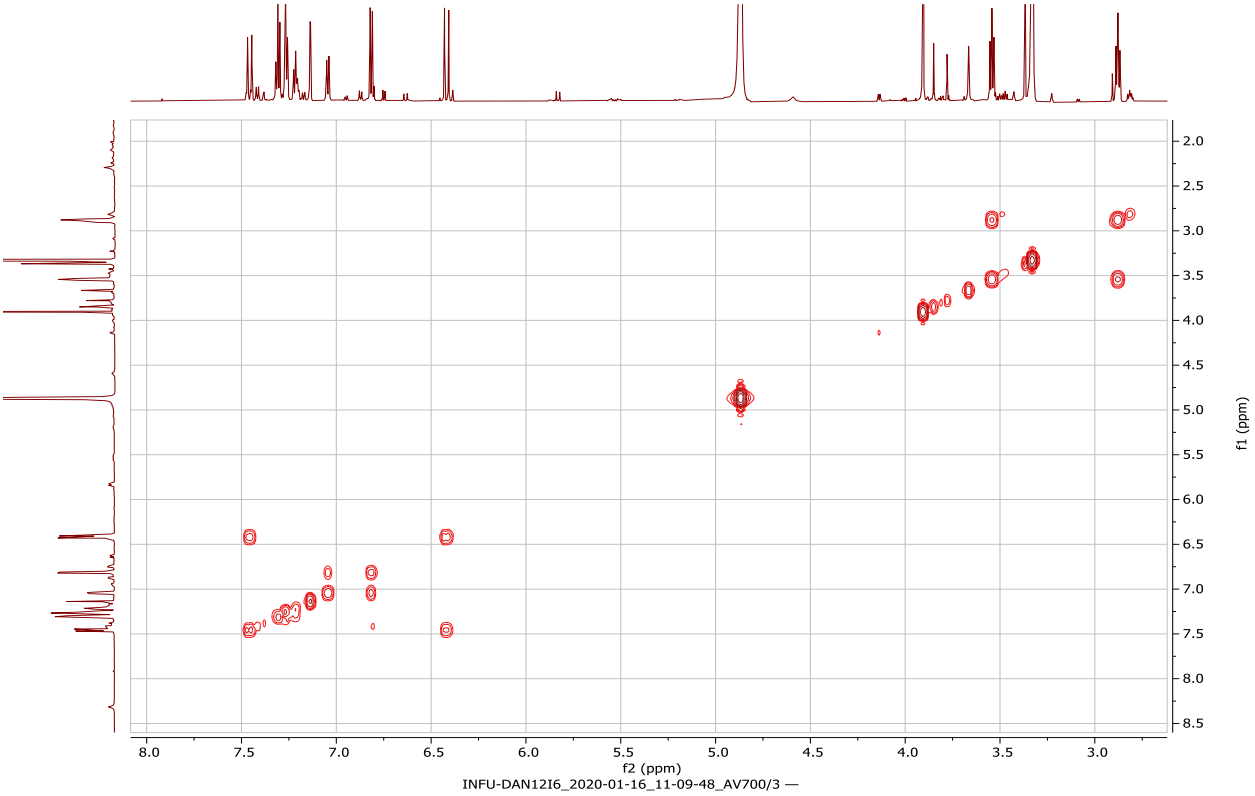

Appendix 22F: HSQC spectrum (CD_3OD) of compound **195**

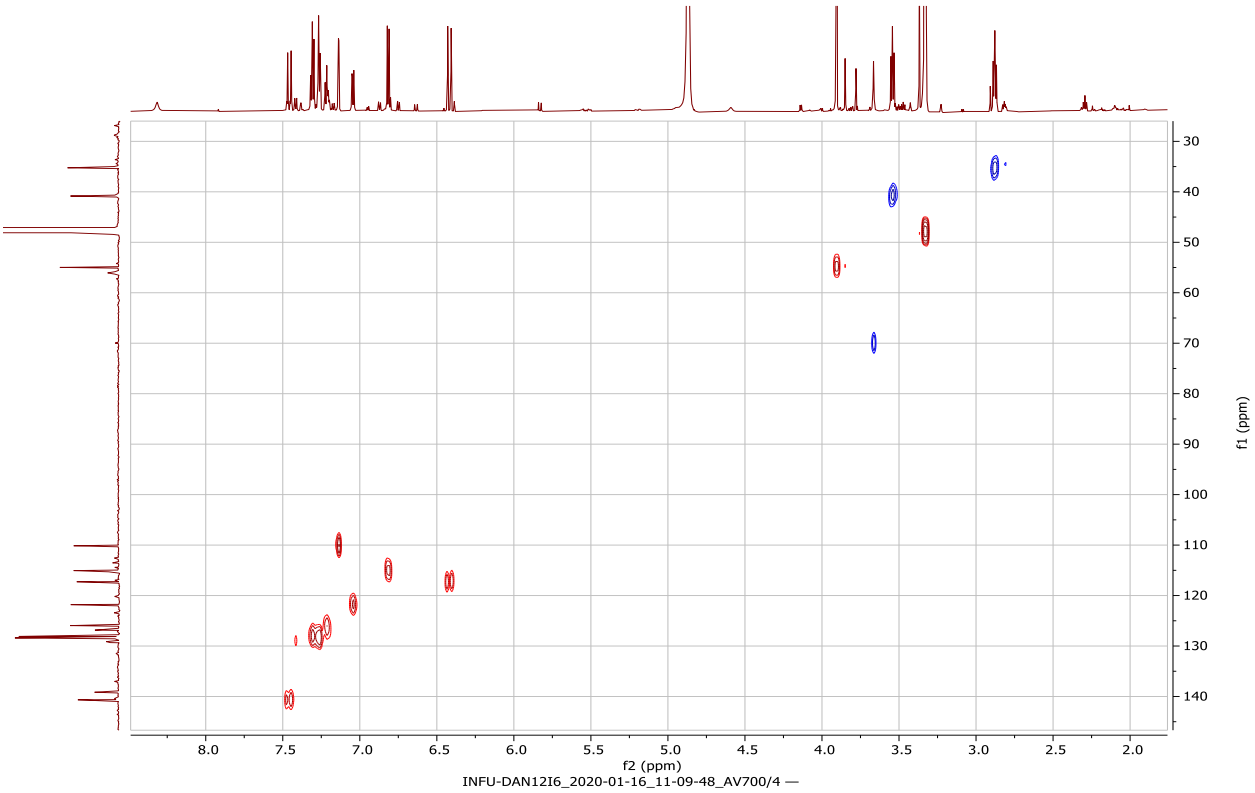

Appendix 22G: HMBC spectrum (CD_3OD) of compound **195**

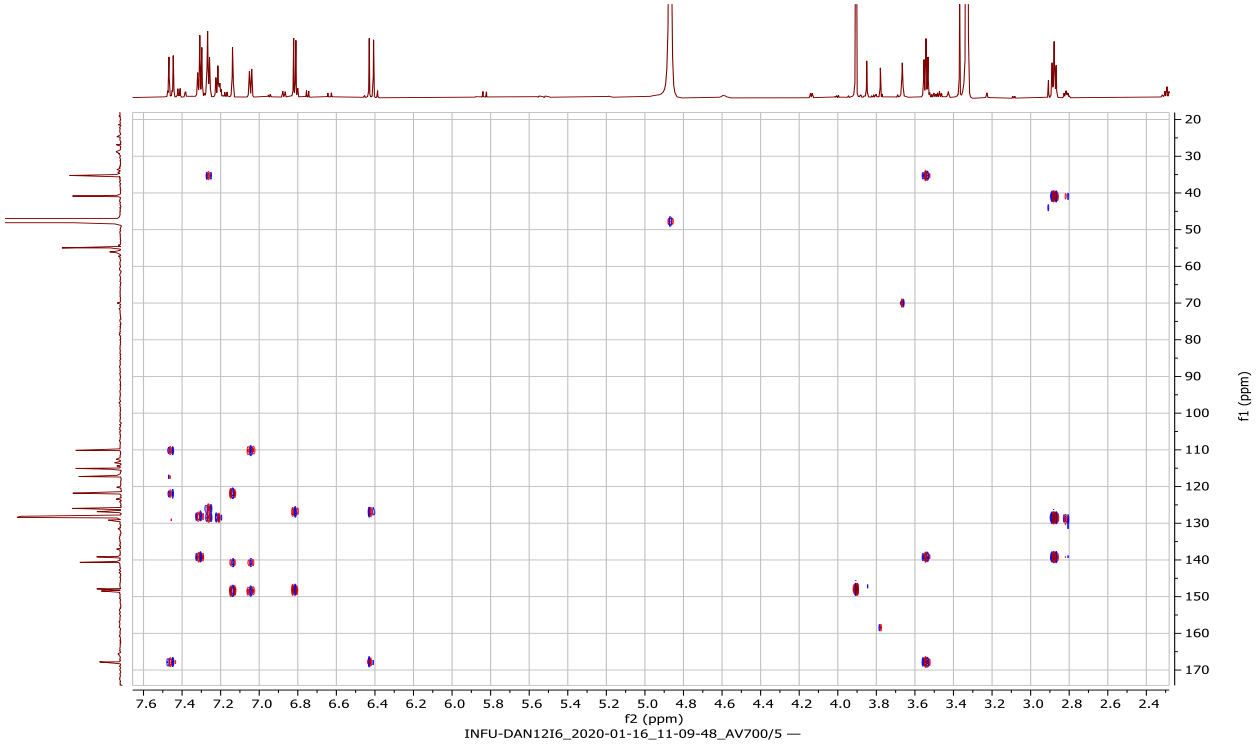

Appendix 23: NMR spectra for isorhamnetin 3-*O*-rungioside (**196**)

Appendix 23A: HRESIMS of compound **196**

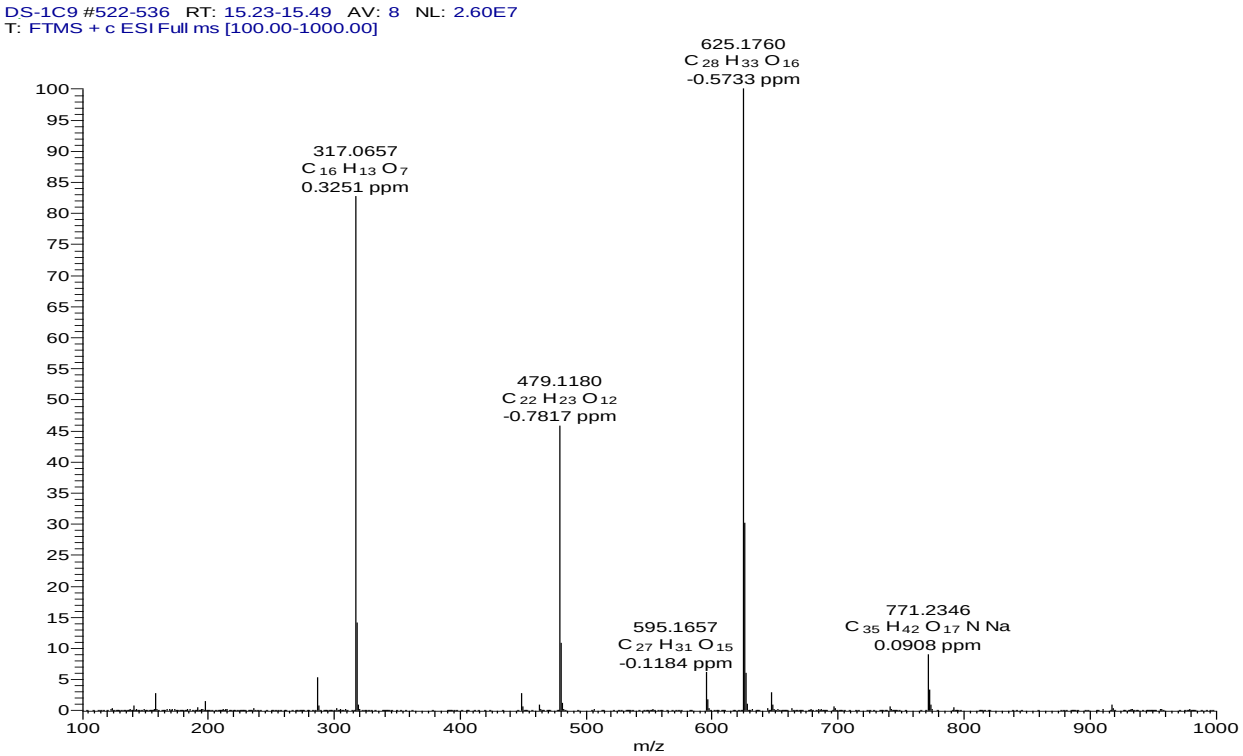

Appendix 23B: LC-UV spectrum of compound **196**

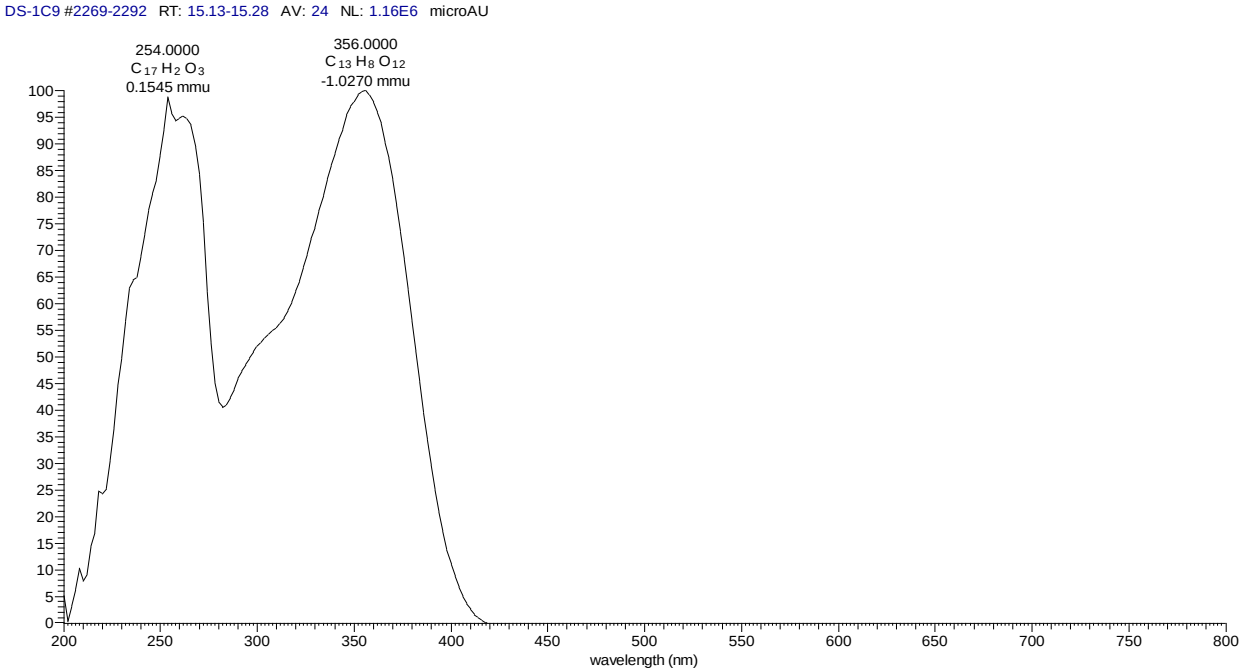

Appendix 23C: ^{1}H NMR spectrum (600 MHz, CD_3OD) of compound **196**

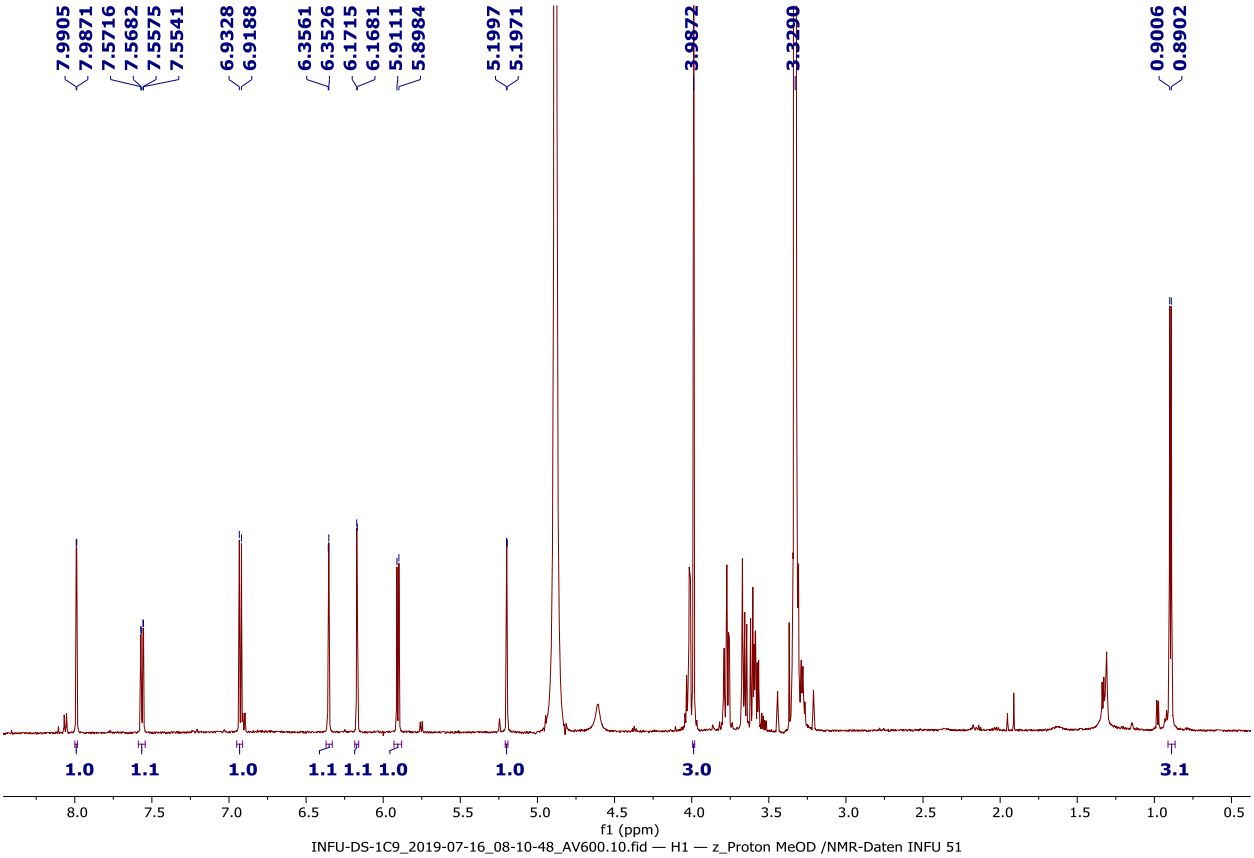

Appendix 23D: ^{13}C NMR spectrum (150 MHz, CD_3OD) of compound **196**

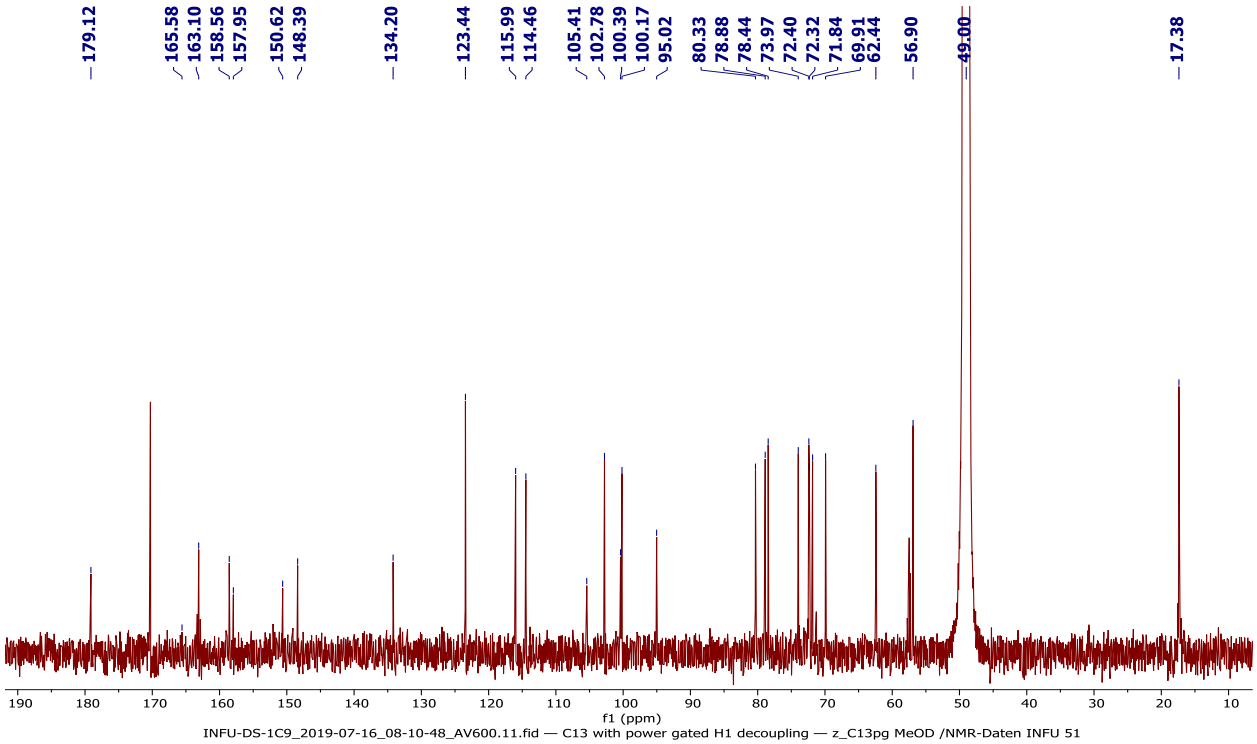

Appendix 23E: ^{1}H-^{1}H COSY spectrum (CD_3OD) of compound **196**

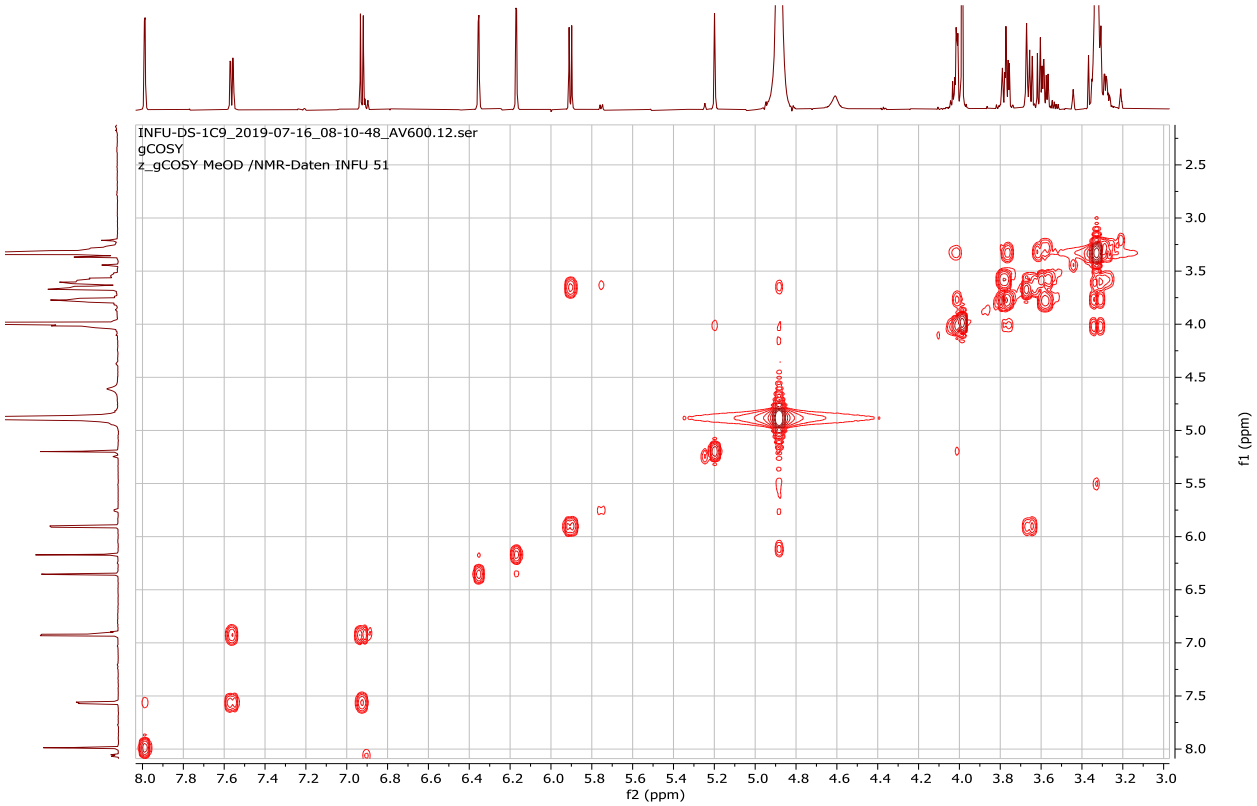

Appendix 23F: HSQC spectrum (CD_3OD) of compound **196**

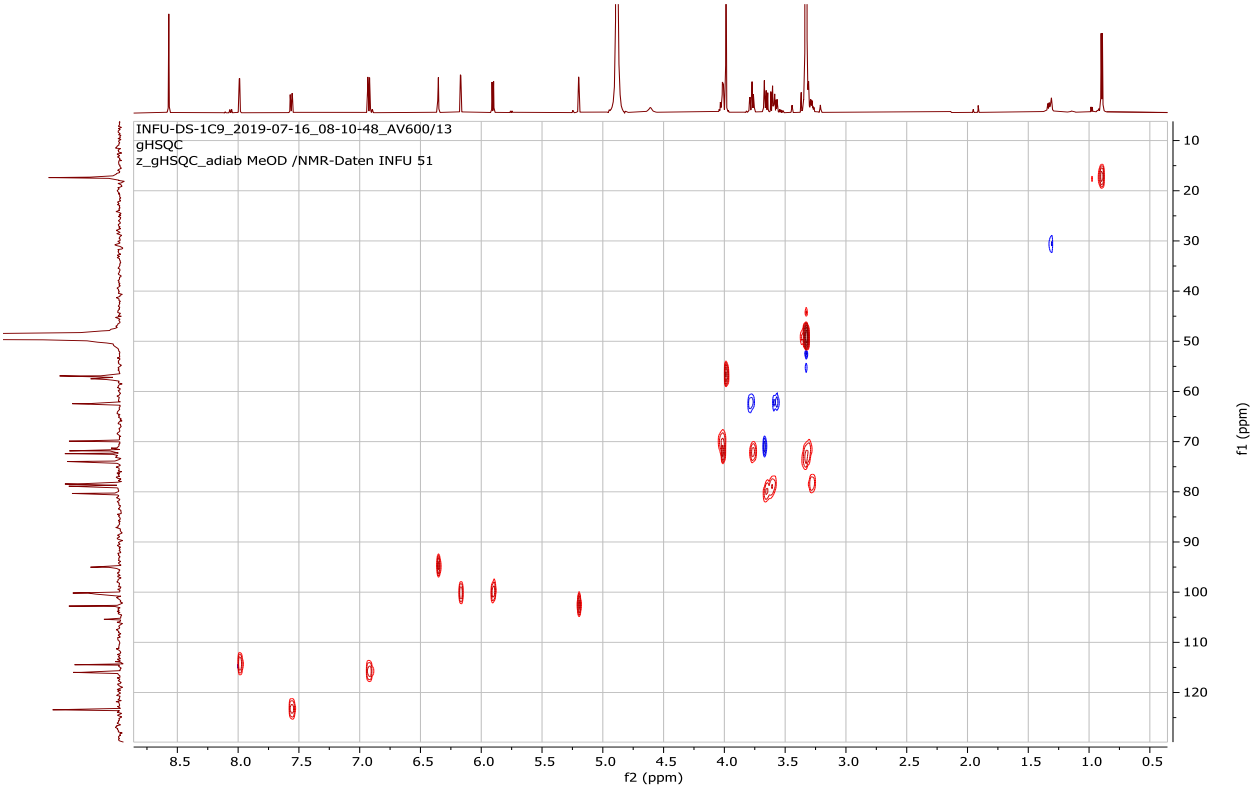

Appendix 23G: HMBC spectrum (CD_3OD) of compound **196**

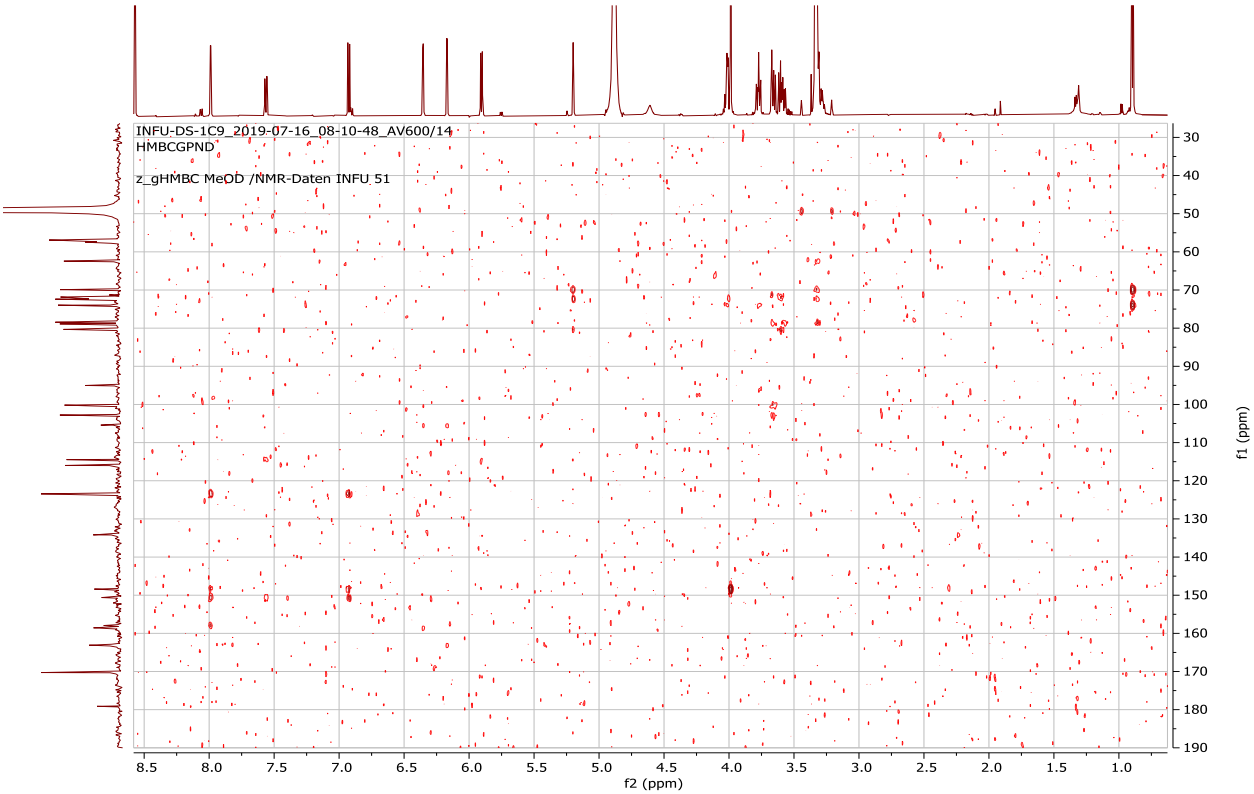

Appendix 24: NMR spectra for kaempferol 3-*O*-rungioside (**197**)

Appendix 24A: HRESIMS of compound **197**

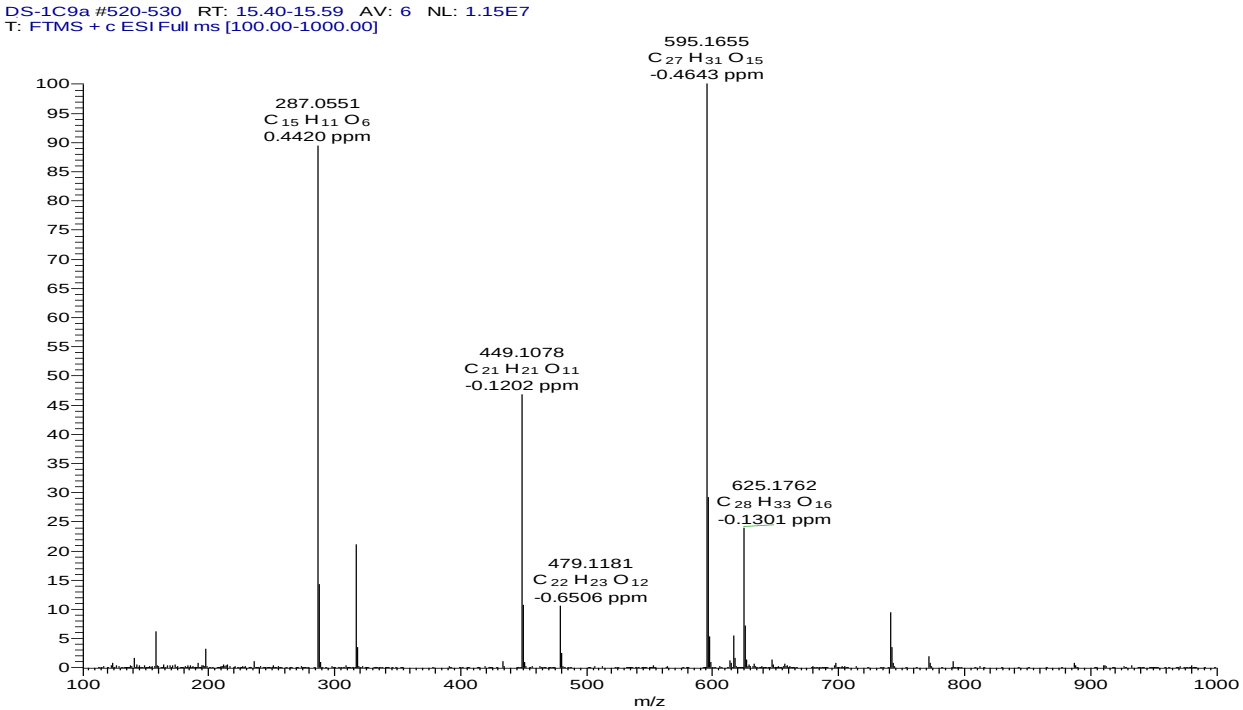

Appendix 24B: LC-UV spectrum of compound **197**

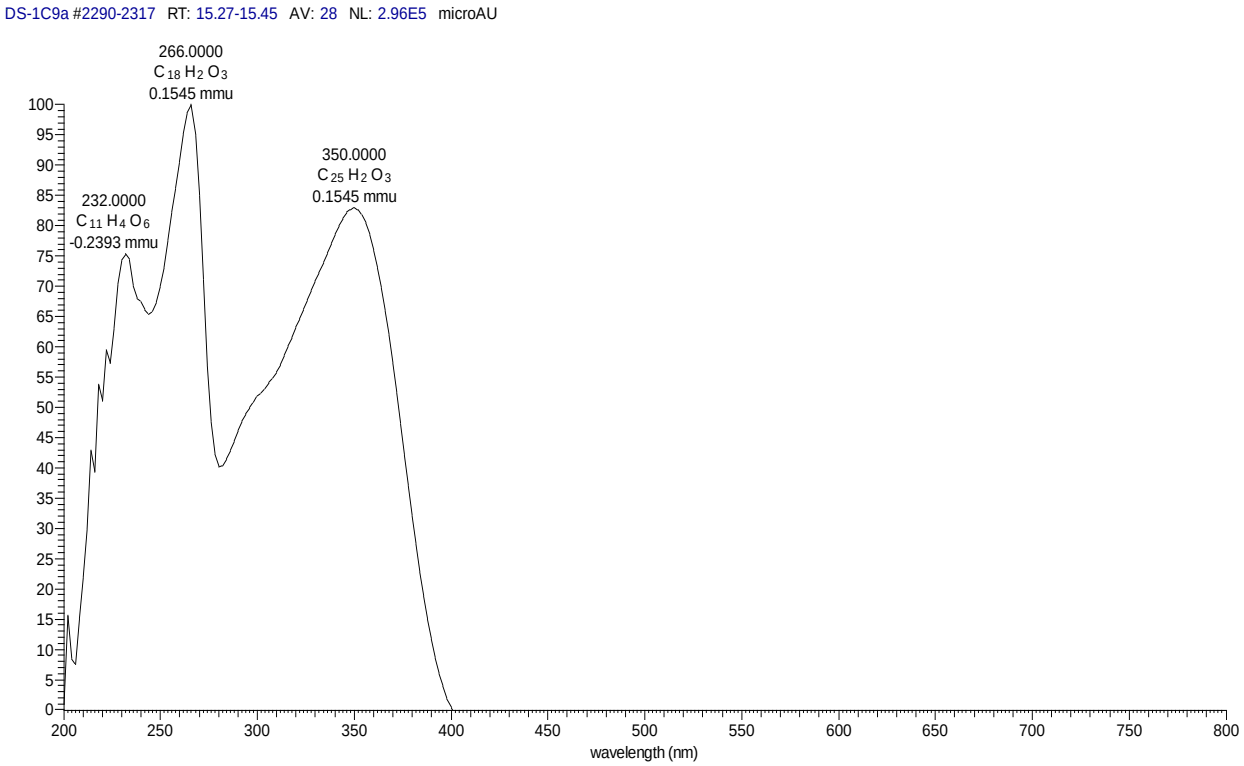

Appendix 24C: ^{1}H NMR spectrum (600 MHz, CD_3OD) of compound **197**

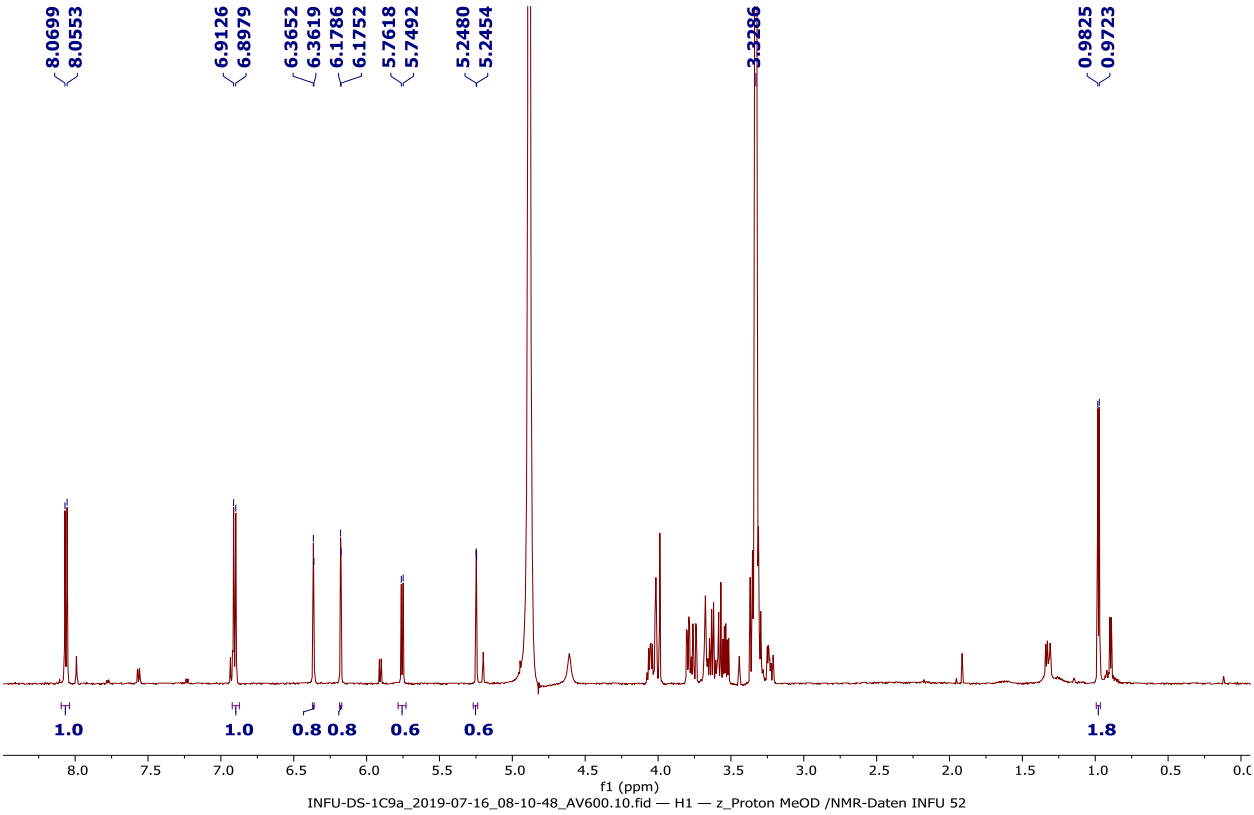

Appendix 24D: ^{13}C NMR spectrum (150 MHz, CD_3OD) of compound **197**

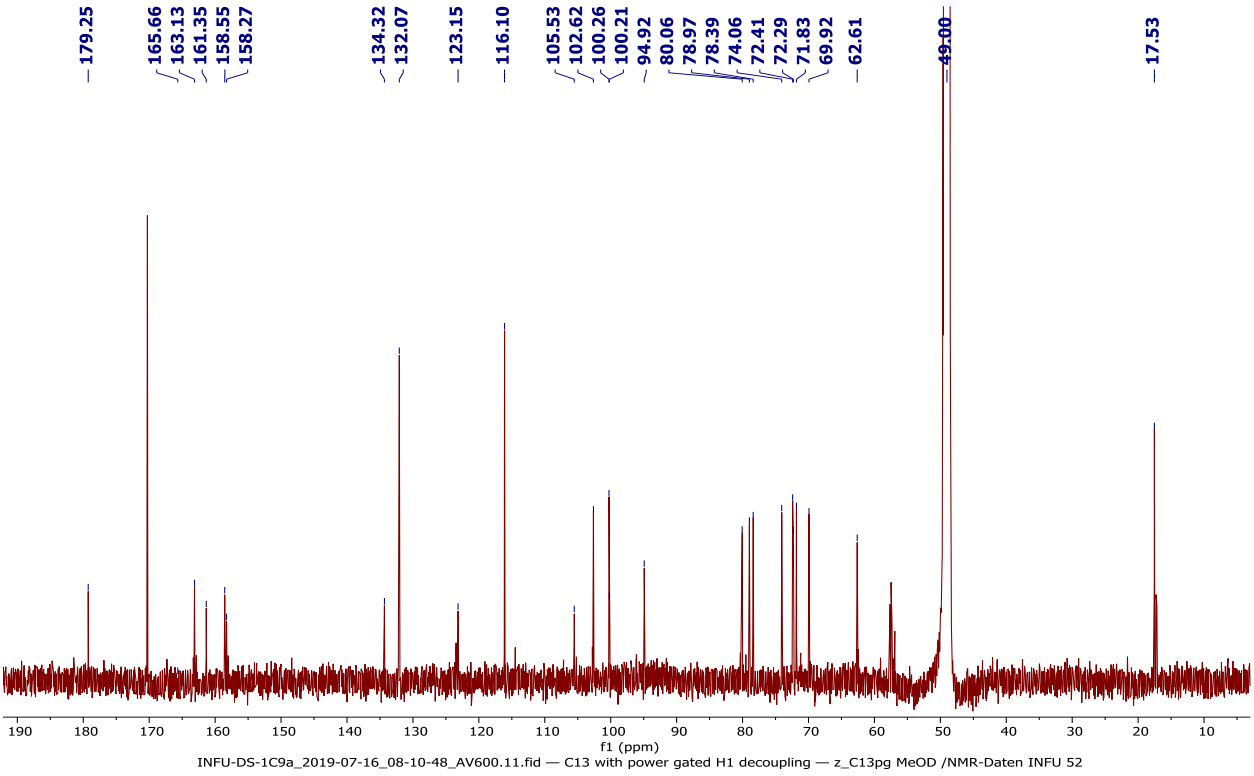

Appendix 24E: ^{1}H-^{1}H COSY spectrum (CD_3OD) of compound **197**

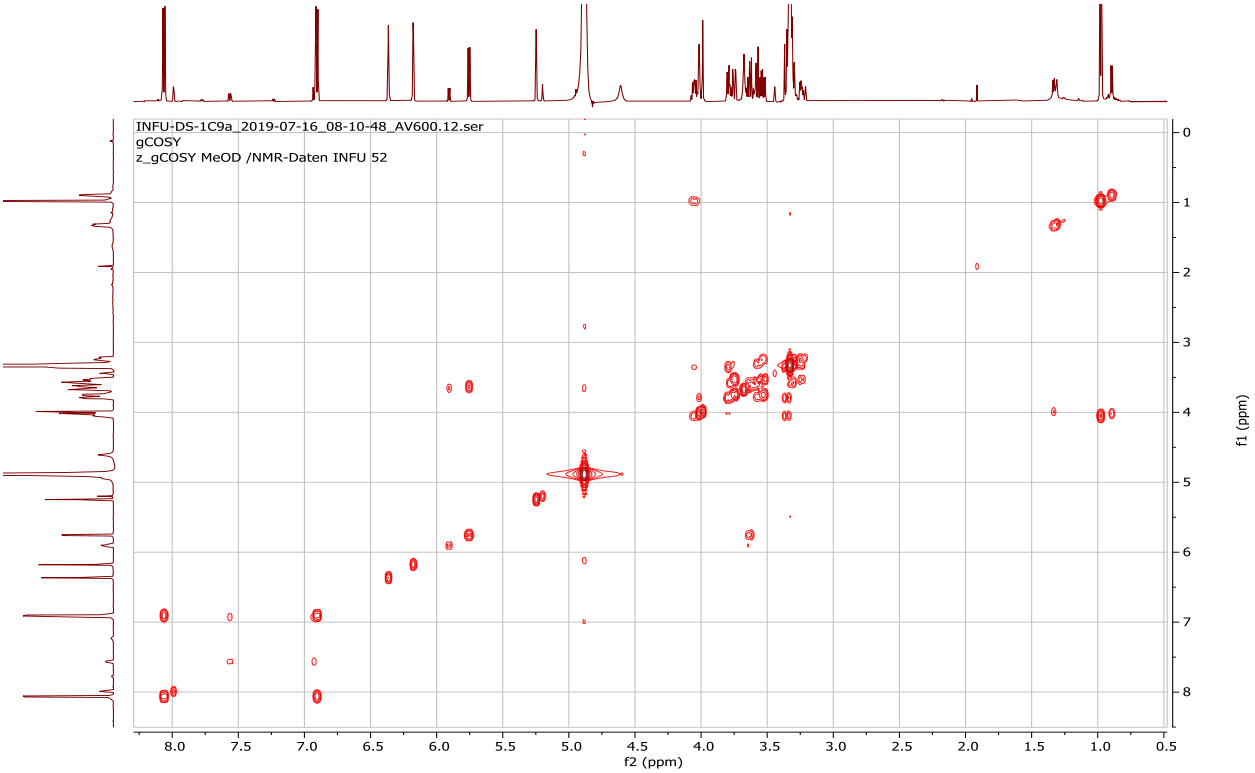

Appendix 24F: HSQC spectrum (CD_3OD) of compound **197**

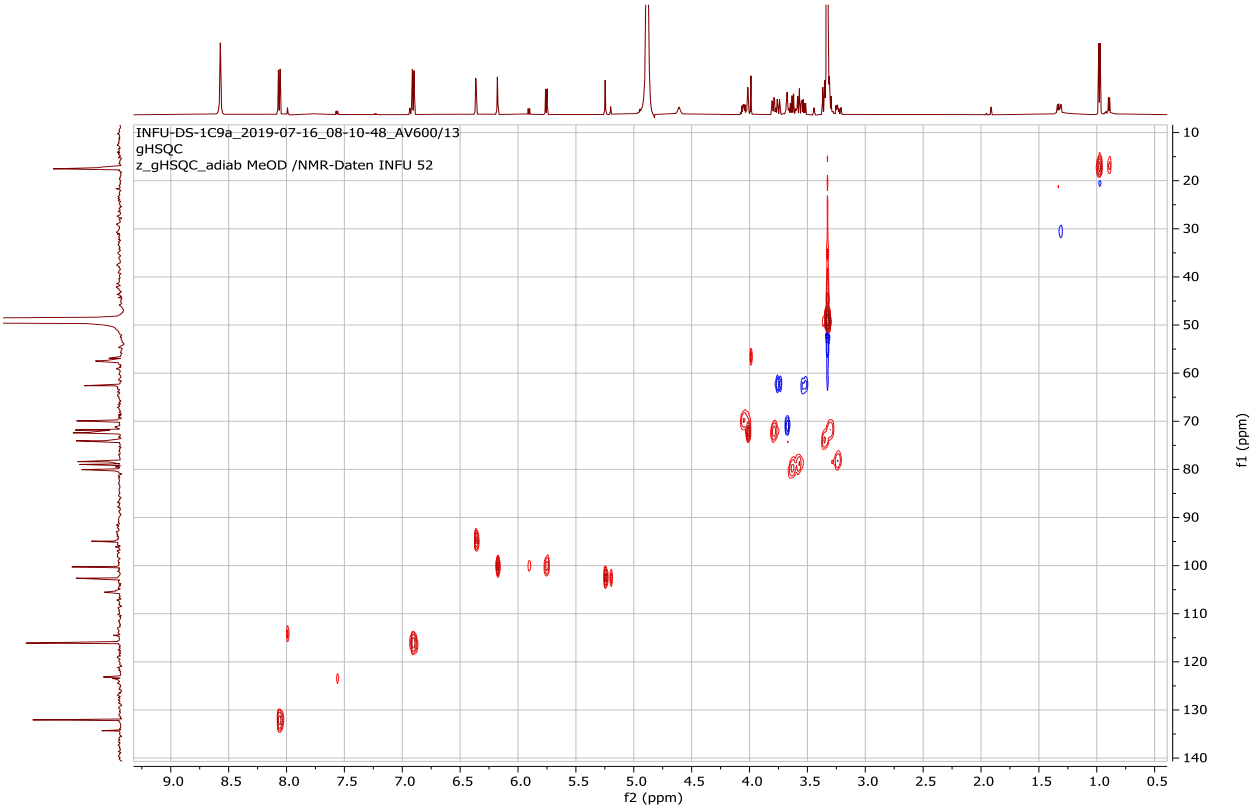

Appendix 24G: HMBC spectrum (CD_3OD) of compound **197**

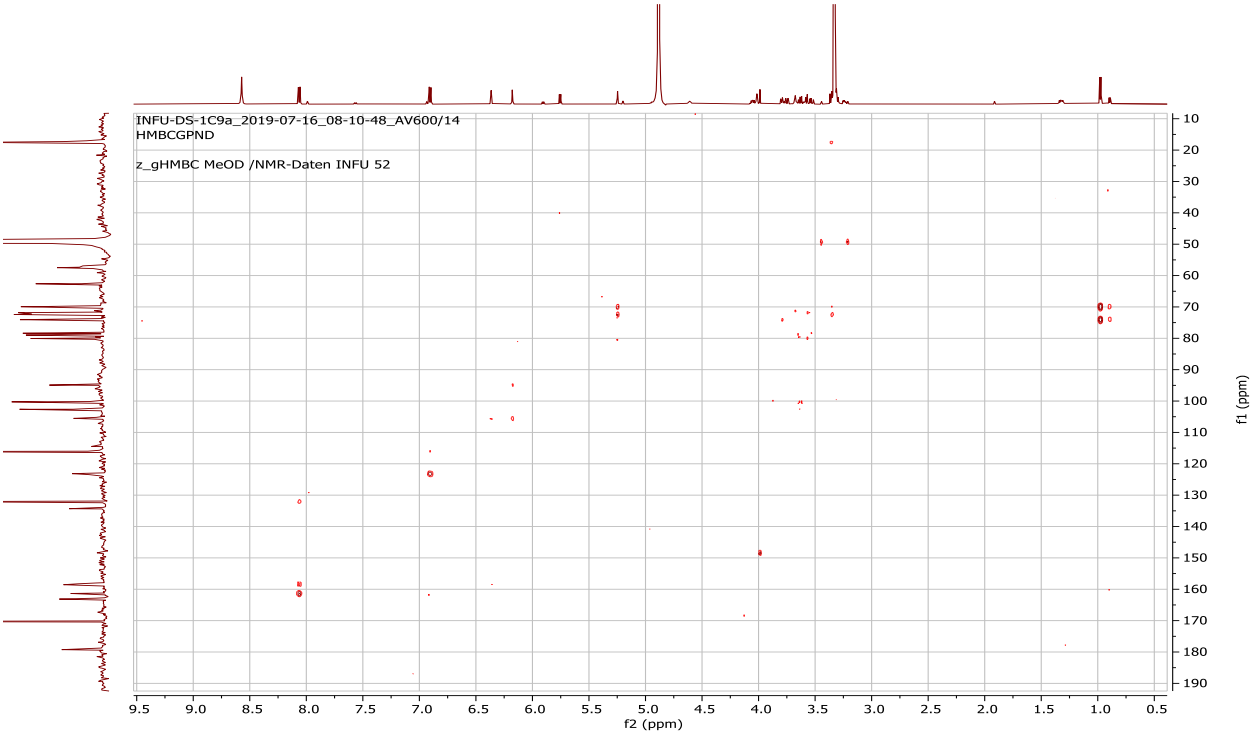

Appendix 25: NMR spectra for quercetin-3-*O*-*β*-D-glucoside (**198**)

Appendix 25A: HRESIMS of compound **198**

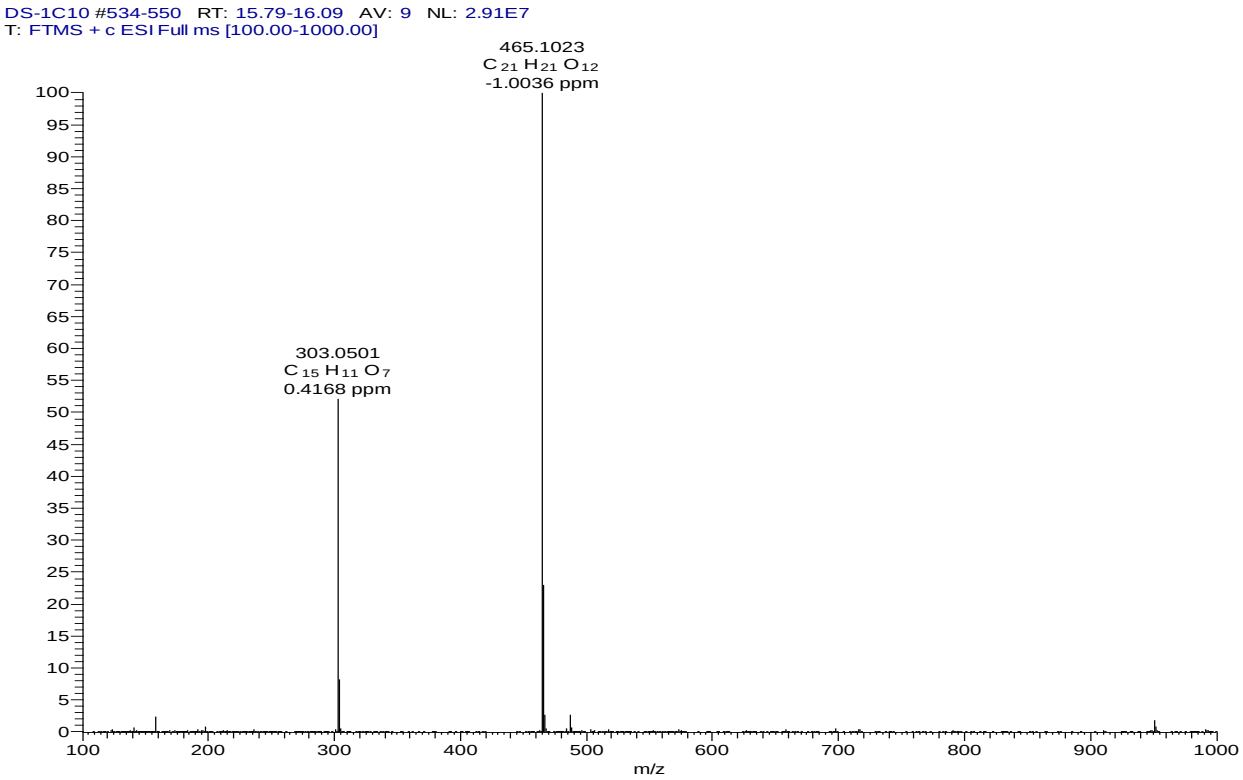

Appendix 25B: LC-UV spectrum of compound **198**

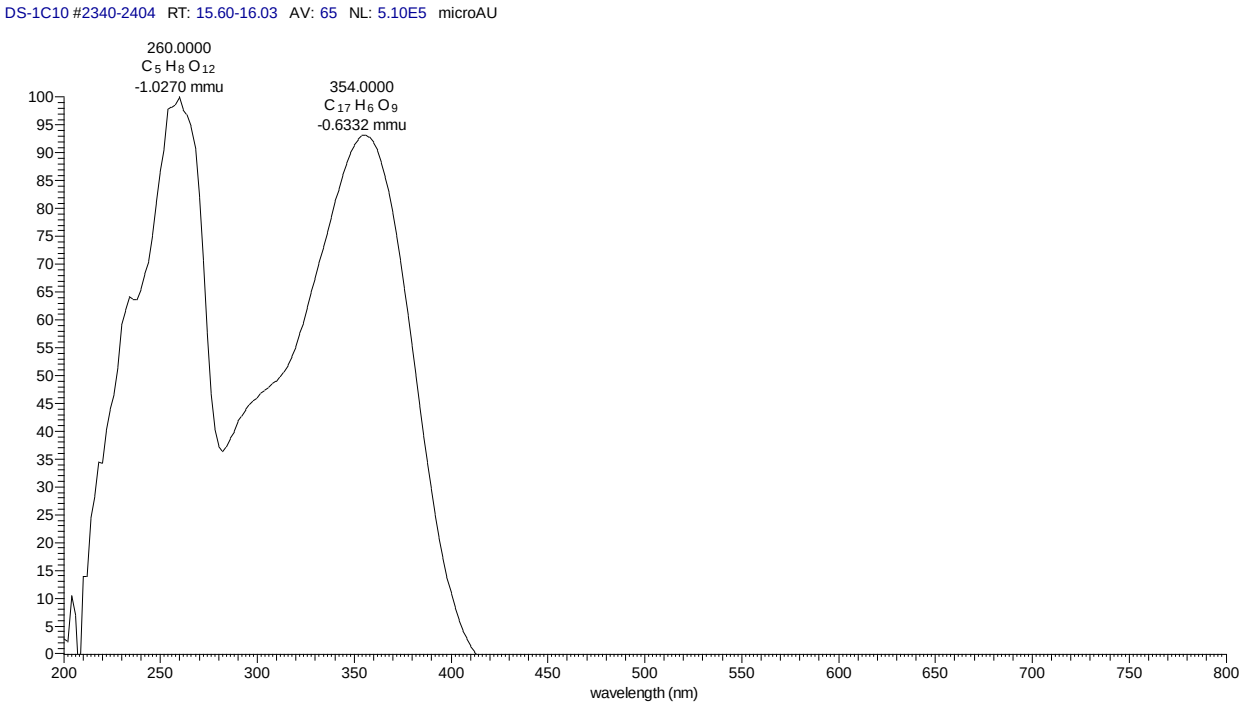

Appendix 25C: ^{1}H NMR spectrum (600 MHz, CD_3OD) of compound **198**

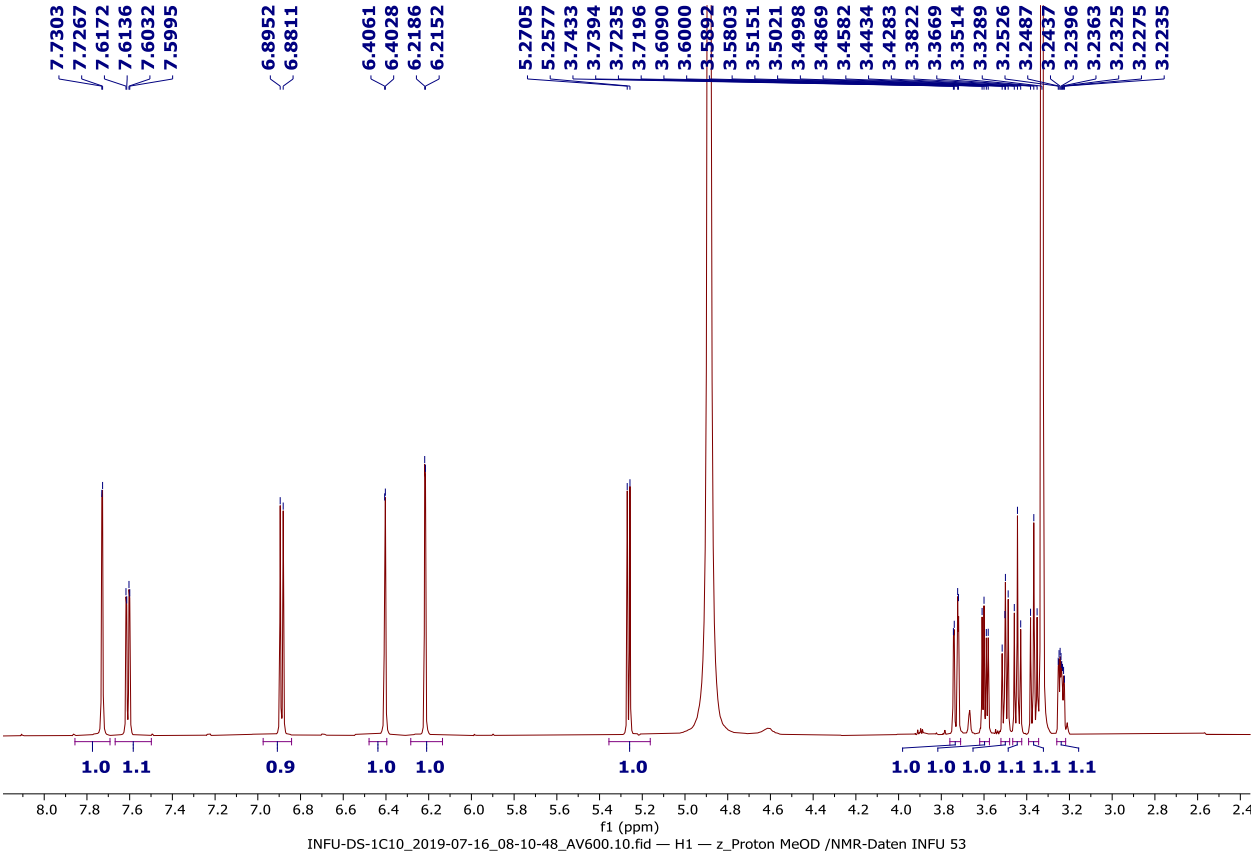

Appendix 25D: ^{13}C NMR spectrum (150 MHz, CD_3OD) of compound **198**

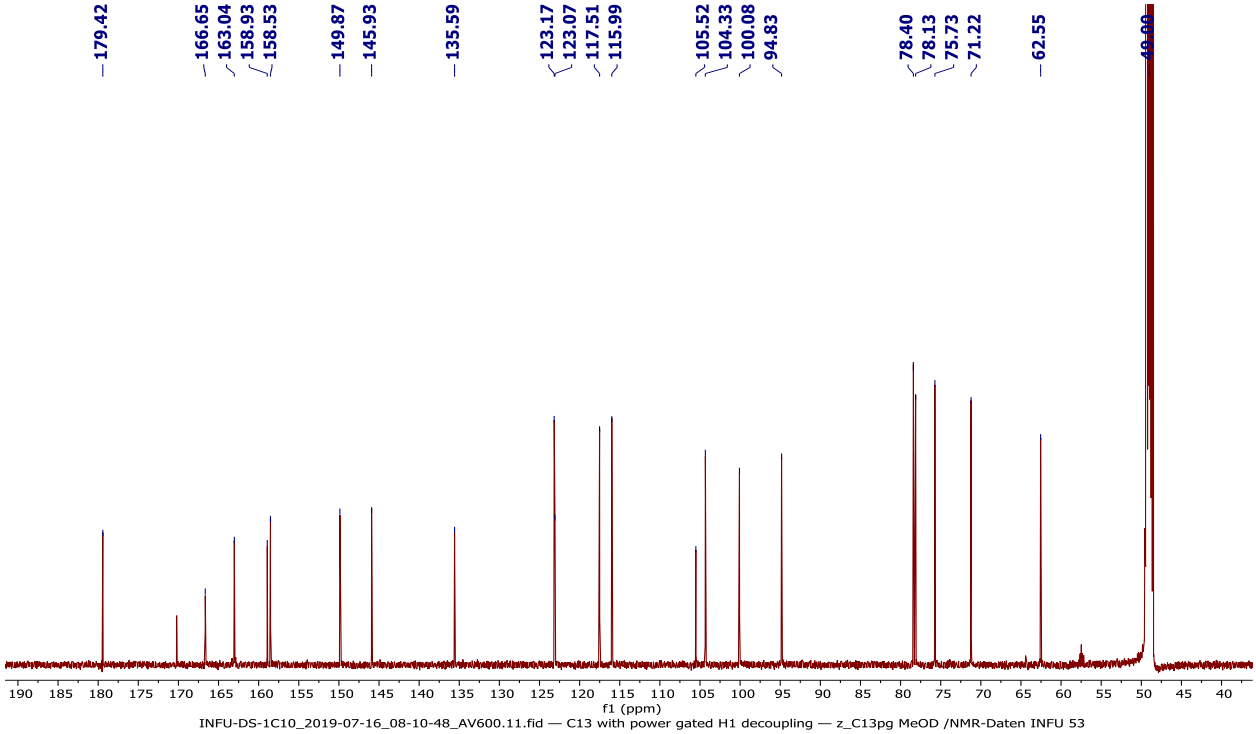

Appendix 25E: ^{1}H-^{1}H COSY spectrum (CD_3OD) of compound **198**

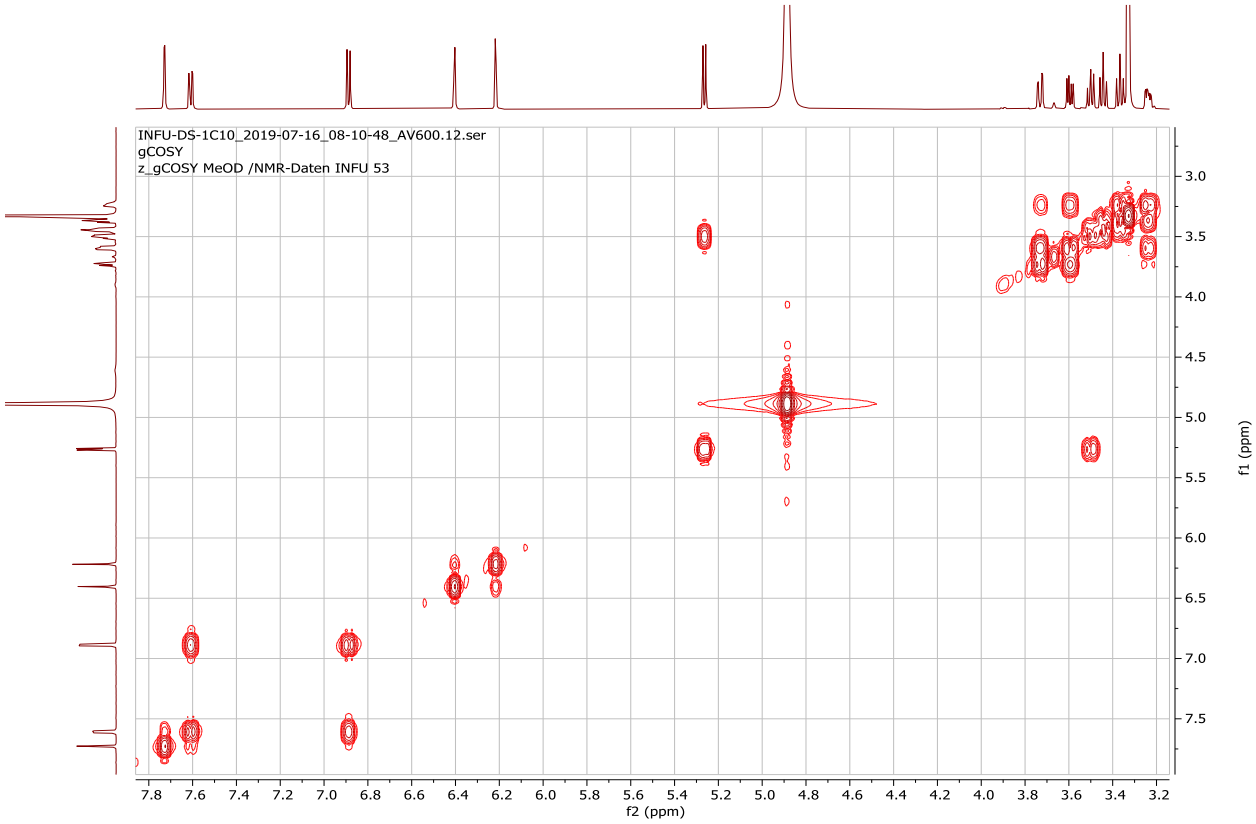

Appendix 25F: HSQC spectrum (CD_3OD) of compound **198**

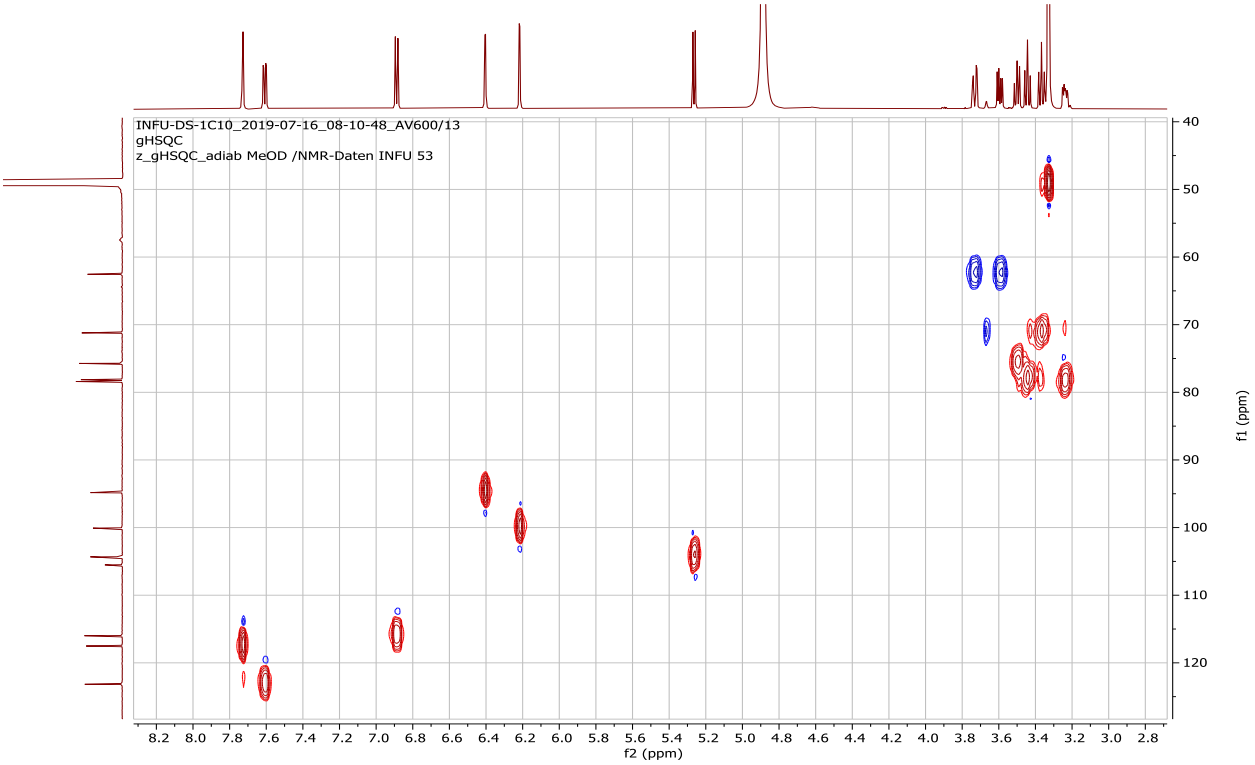

Appendix 25G: HMBC spectrum (CD_3OD) of compound **198**

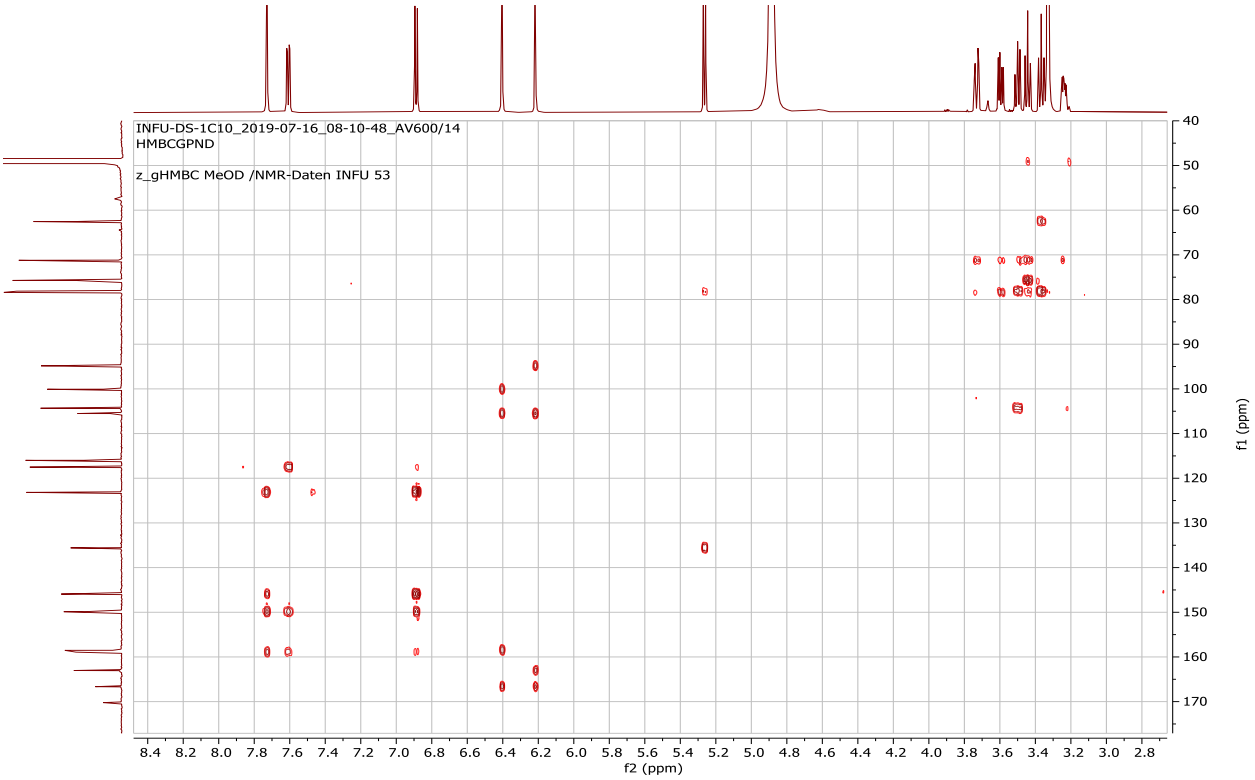

Appendix 26: NMR spectra for isorhamnetin 3-*O*-*β*-D-glucopyranoside (**199**)

Appendix 26A: HRESIMS of compound **199**

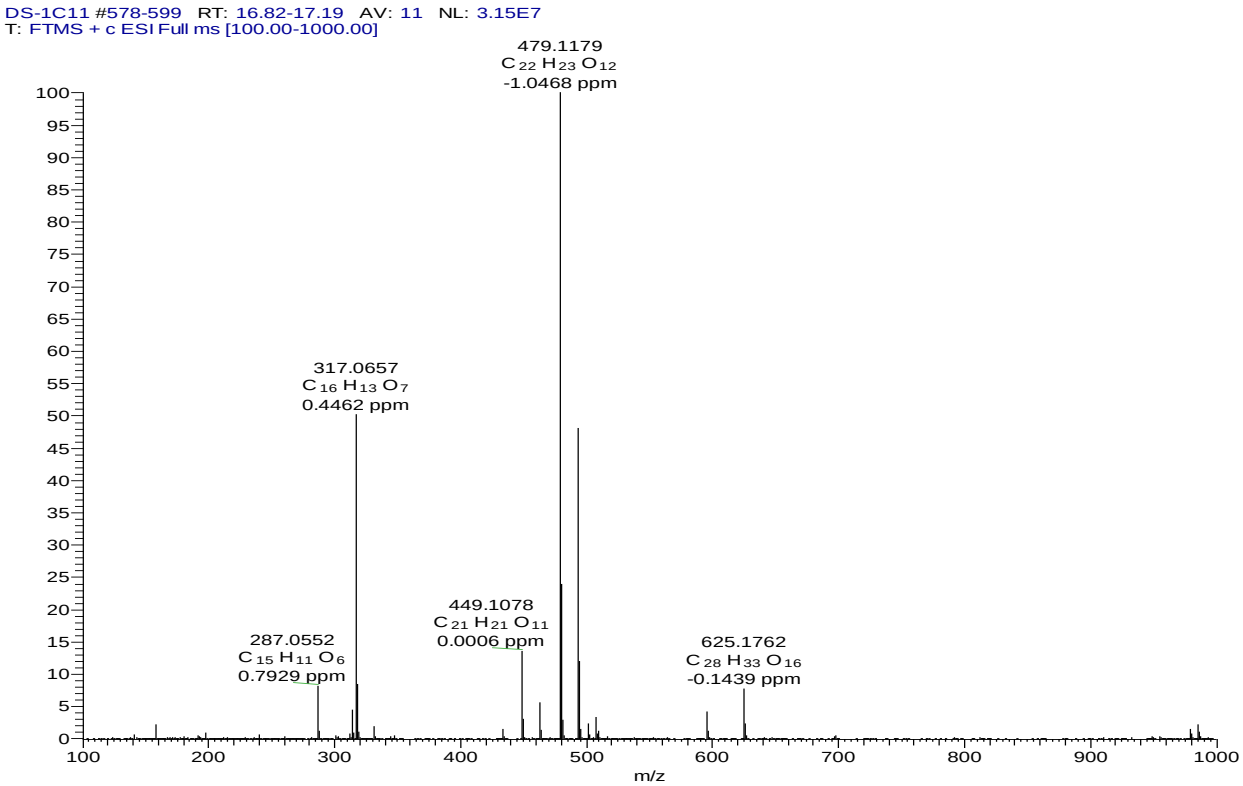

Appendix 26B: LC-UV spectrum of compound **199**

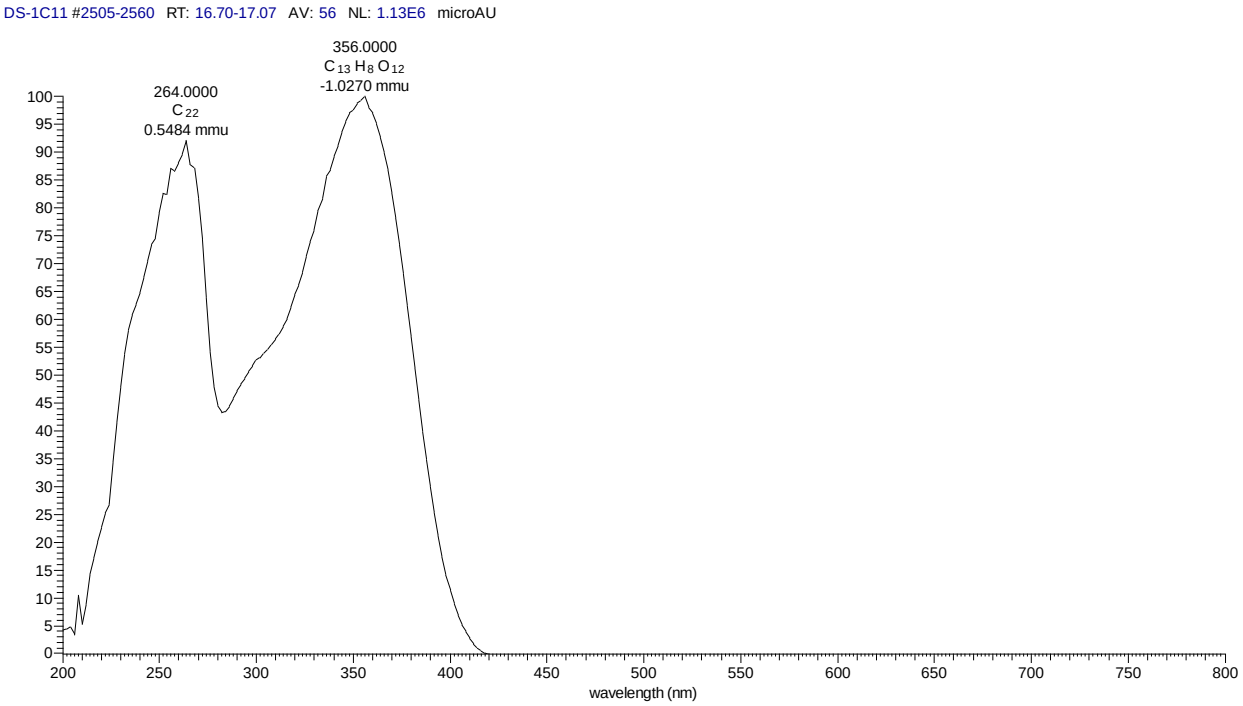

Appendix 26C: ^{1}H NMR spectrum (600 MHz, CD_3OD) of compound **199**

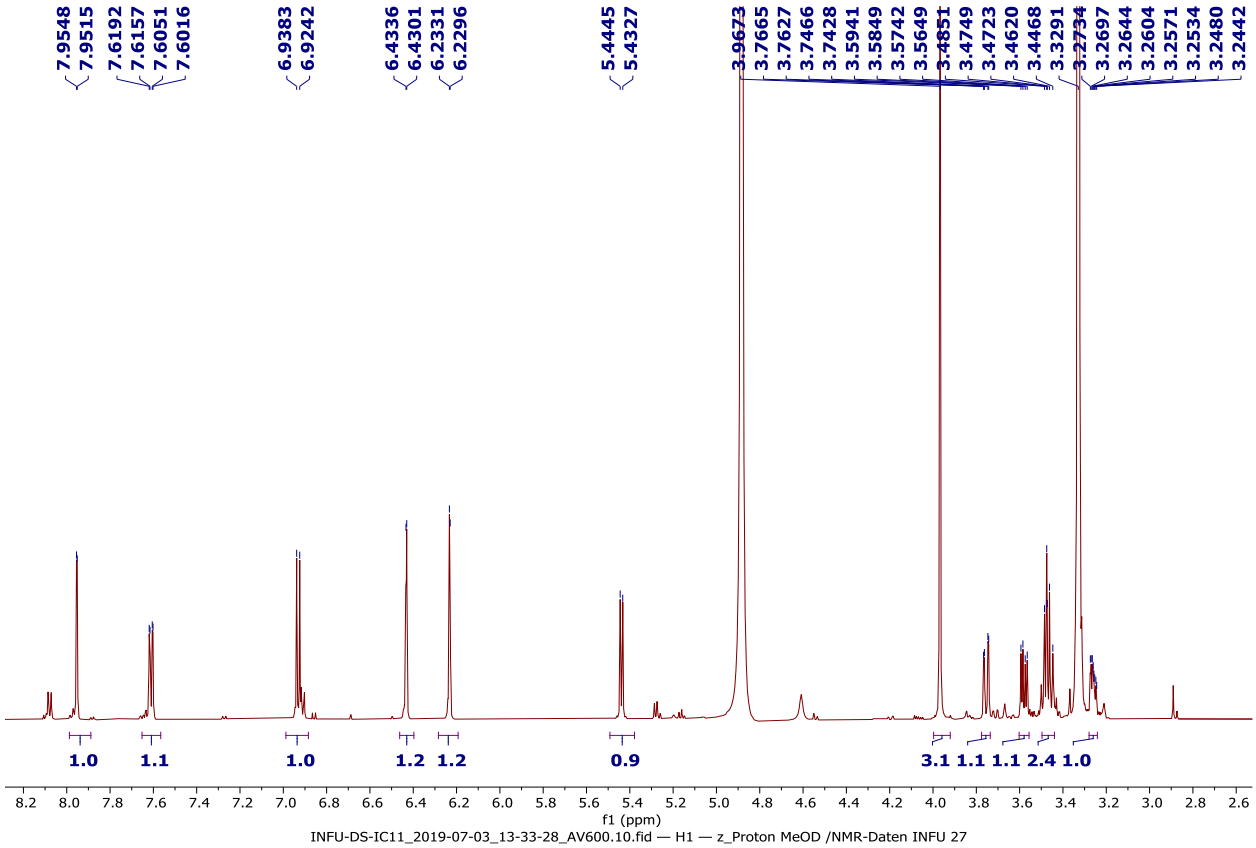

Appendix 26D: ^{13}C NMR spectrum (150 MHz, CD_3OD) of compound **199**

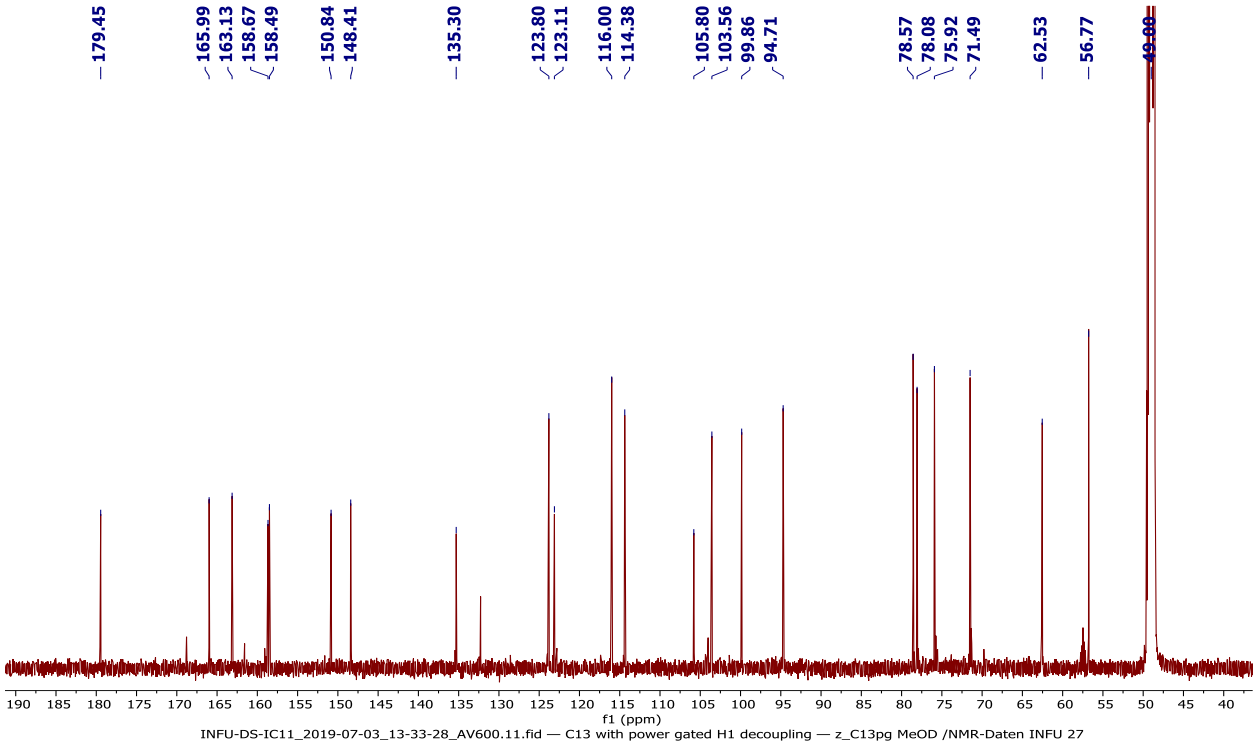

Appendix 26E: ^{1}H-^{1}H COSY spectrum (CD_3OD) of compound **199**

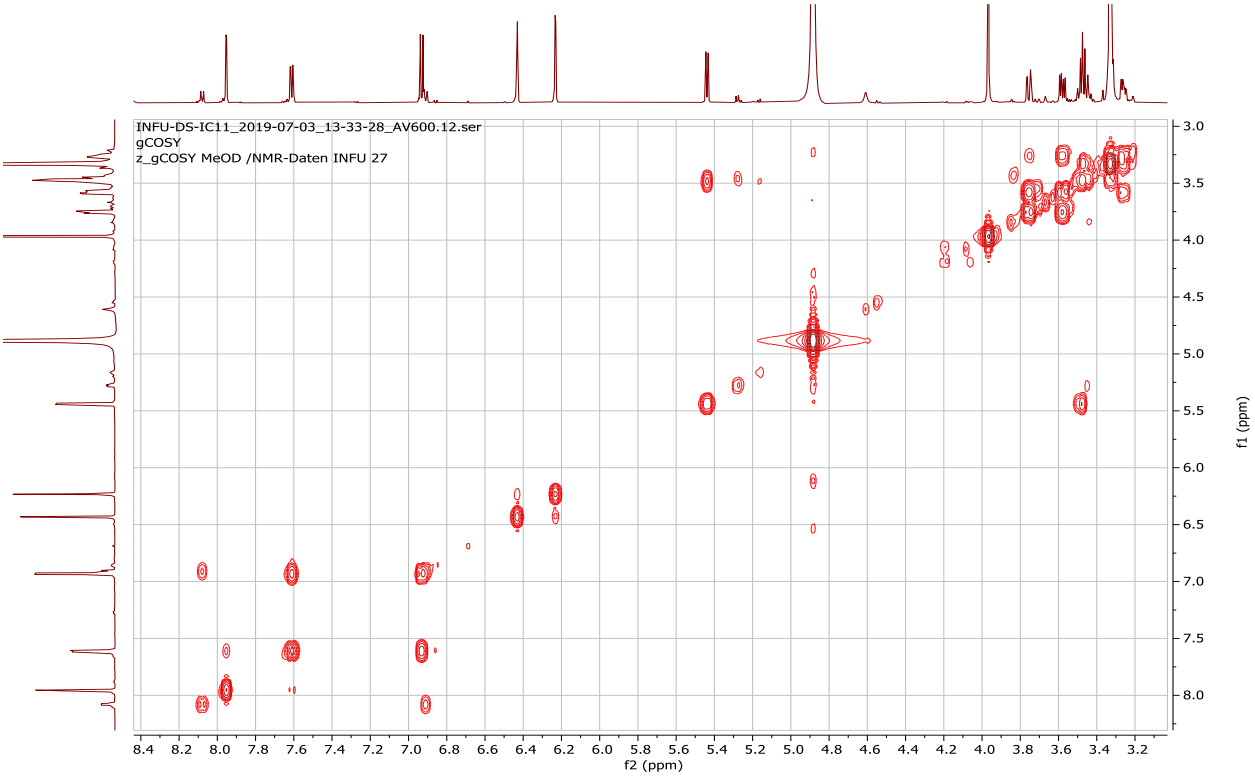

Appendix 26F: HSQC spectrum (CD_3OD) of compound **199**

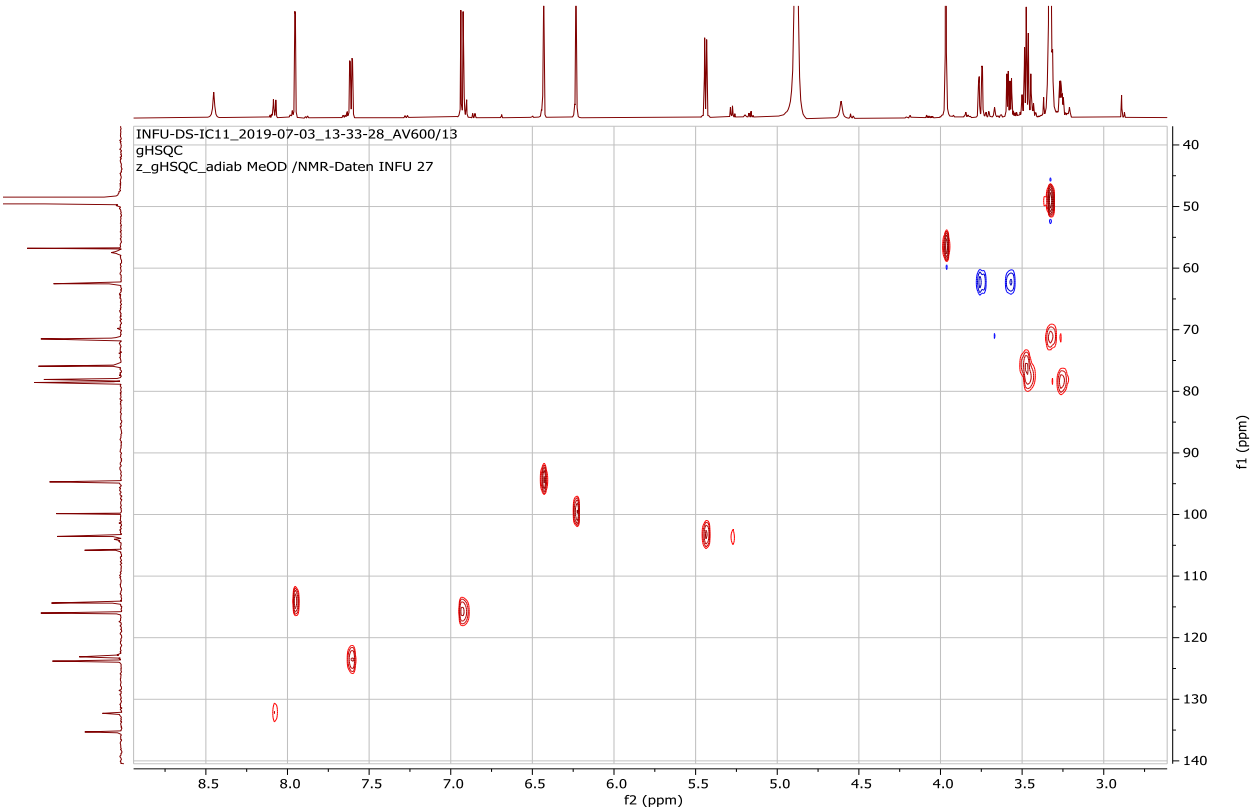

Appendix 26G: HMBC spectrum (CD_3OD) of compound **199**

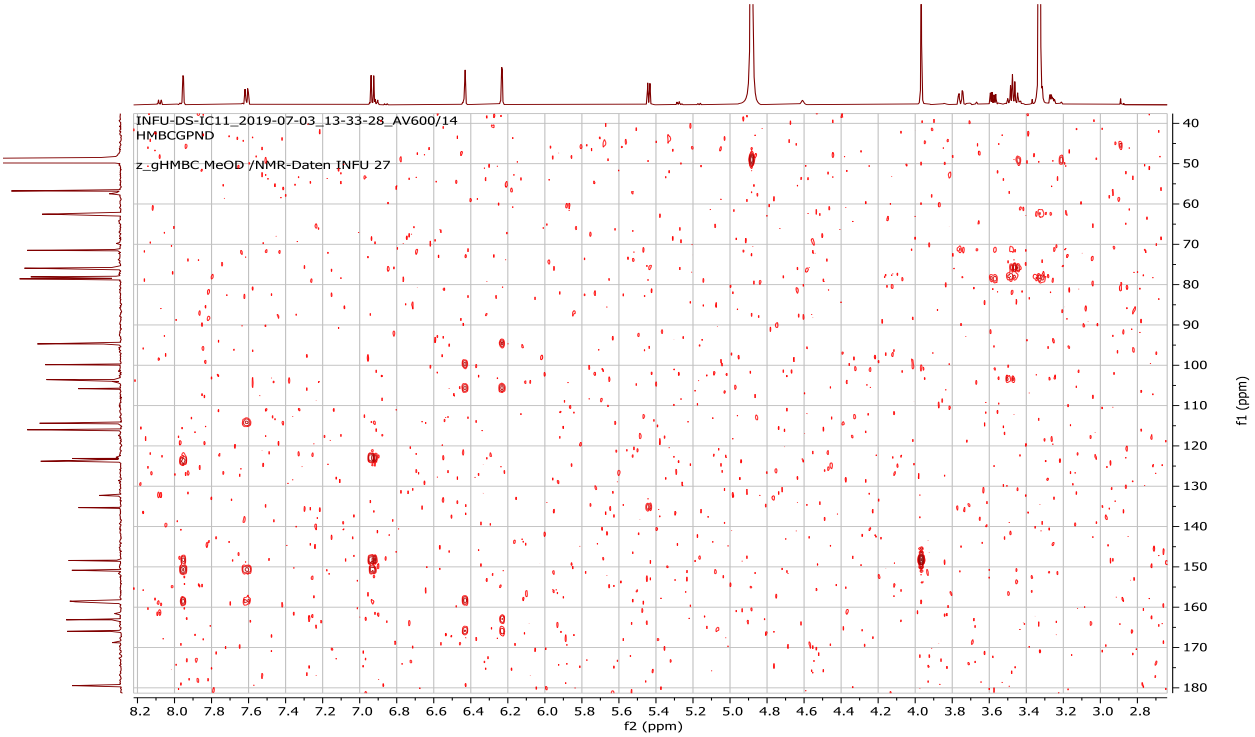

Appendix 27: NMR spectra for 3,3′-di-*O*-methylquercetin 4′-*O*-*β*-D-glucoside (**200**)

Appendix 27A: HRESIMS of compound **200**

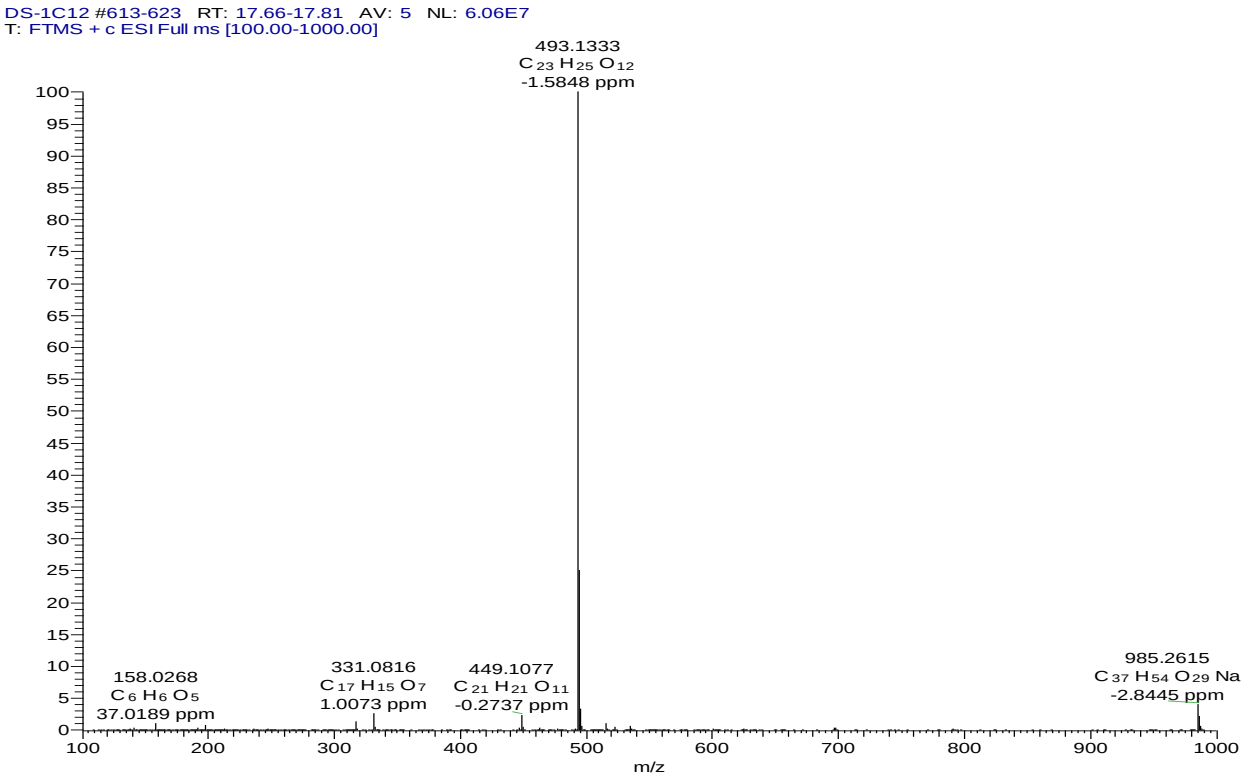

Appendix 27B: LC-UV spectrum of compound **200**

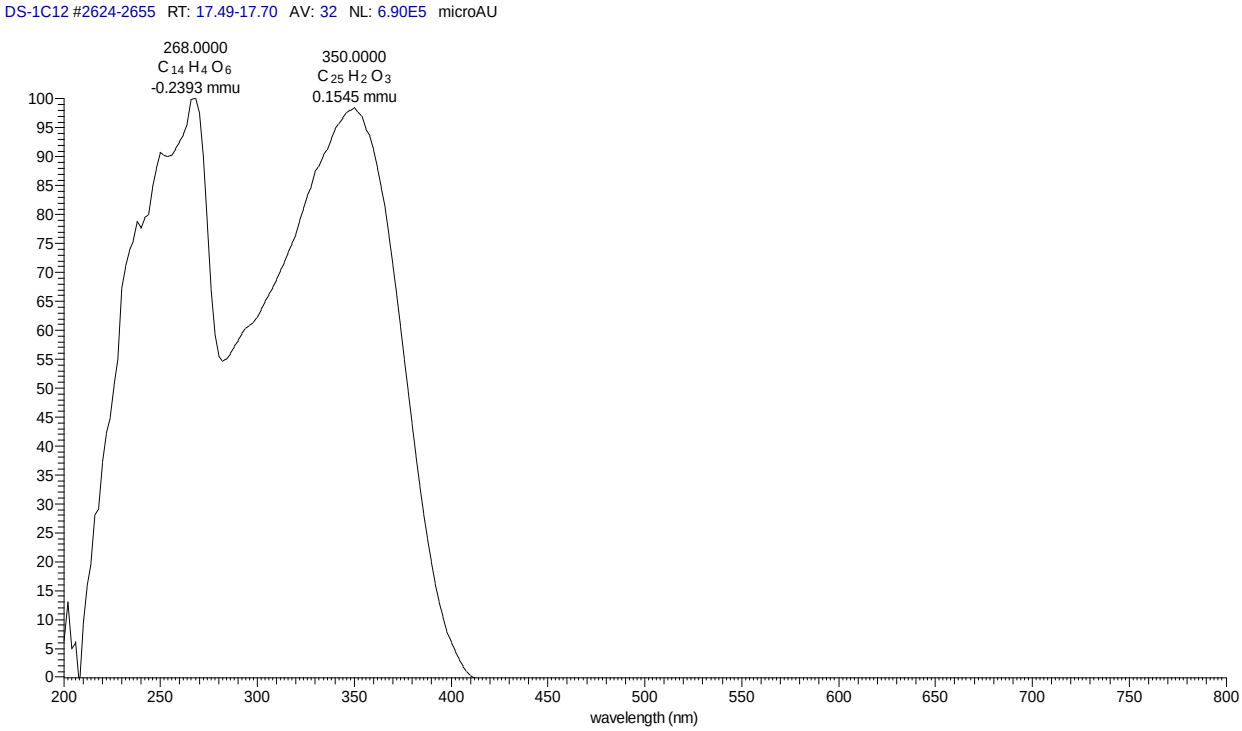

Appendix 27C: ^{1}H NMR spectrum (600 MHz, CD_3OD) of compound **200**

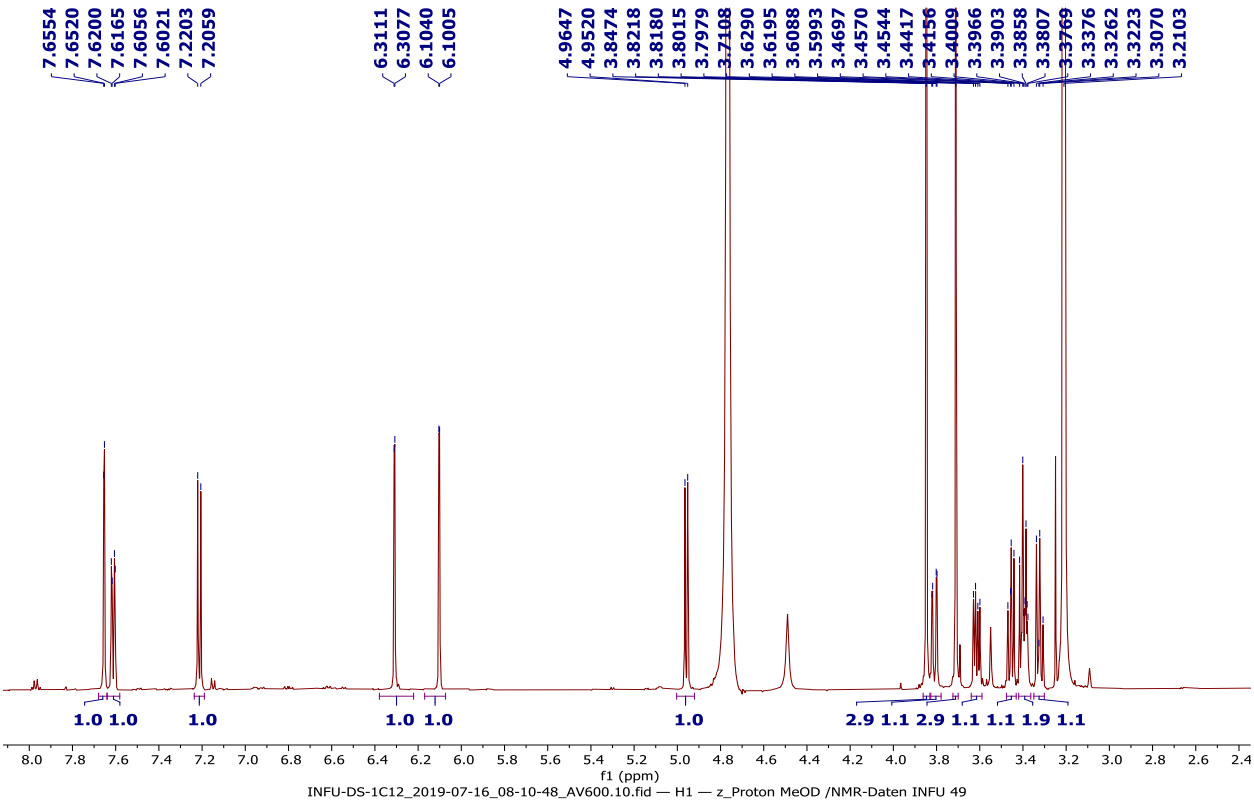

Appendix 27D: ^{13}C NMR spectrum (150 MHz, CD_3OD) of compound **200**

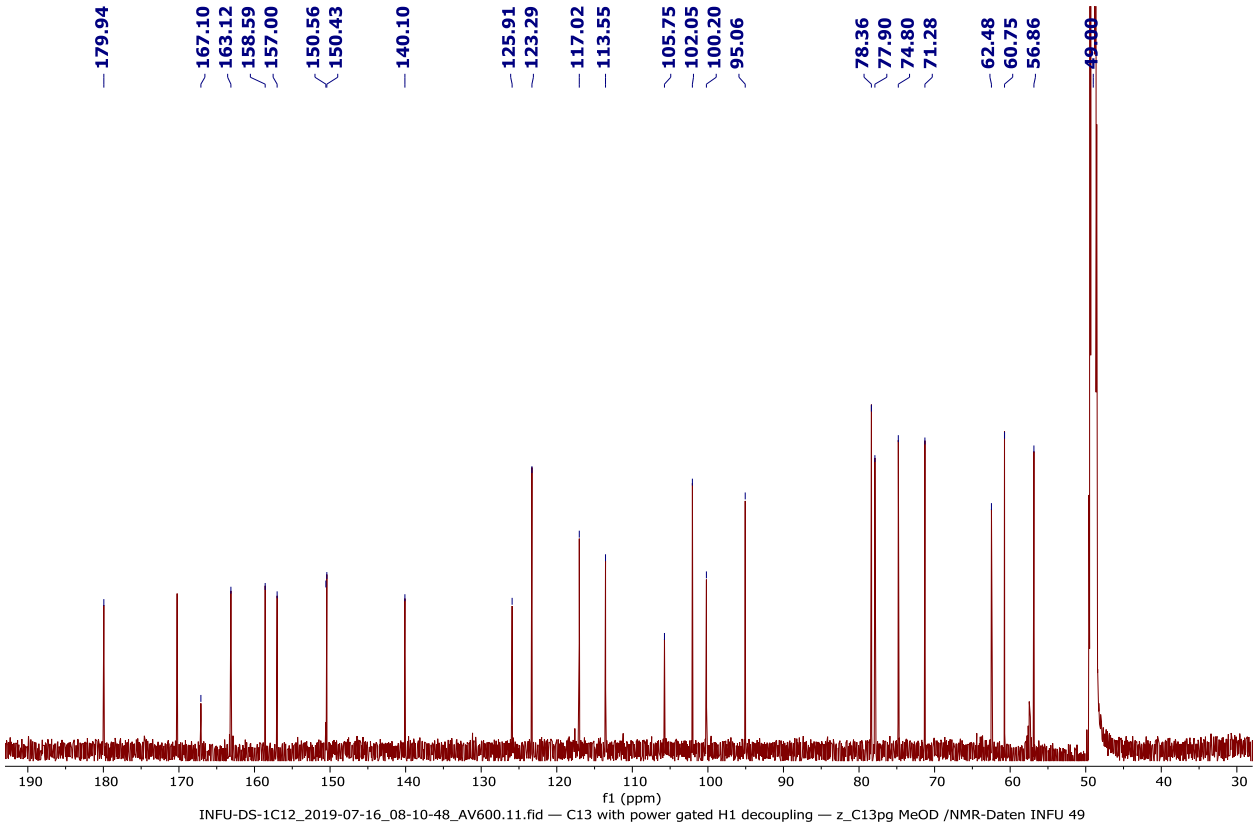

Appendix 27E: ^{1}H-^{1}H COSY spectrum (CD_3OD) of compound **200**

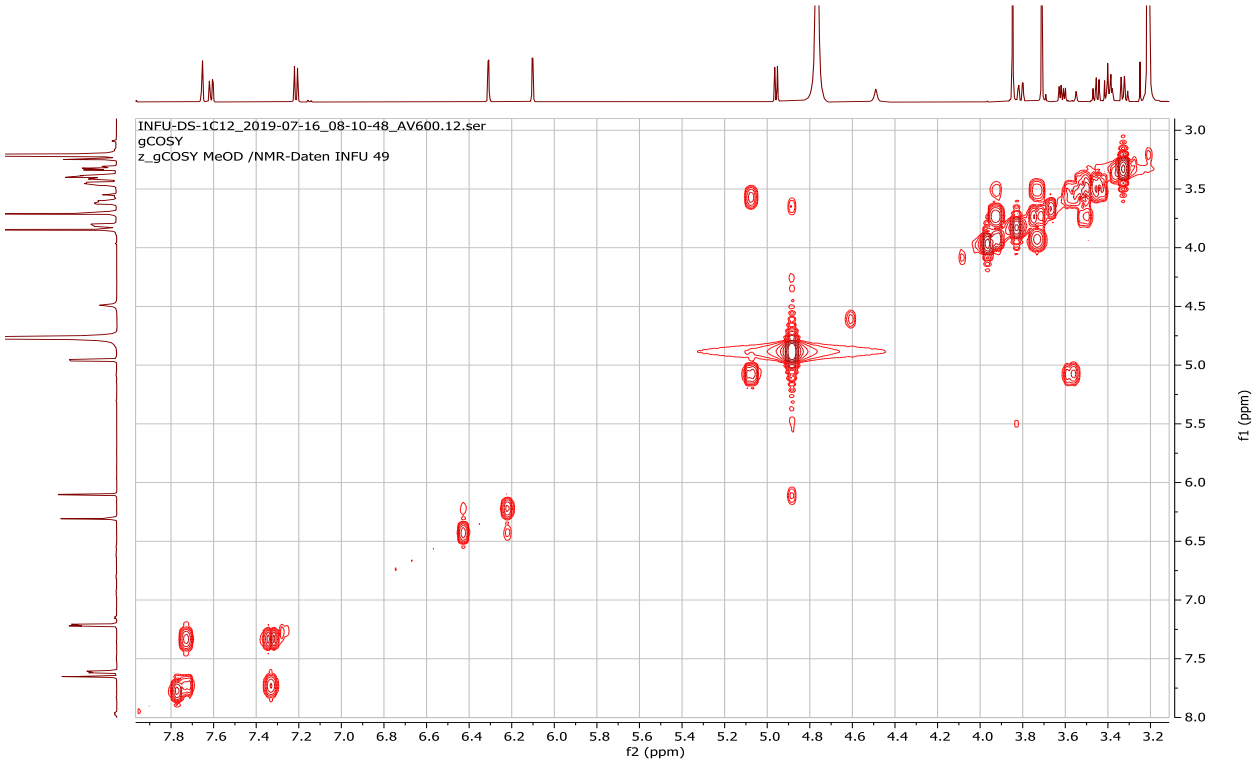

Appendix 27F: NOESY spectrum (CD_3OD) of compound **200**

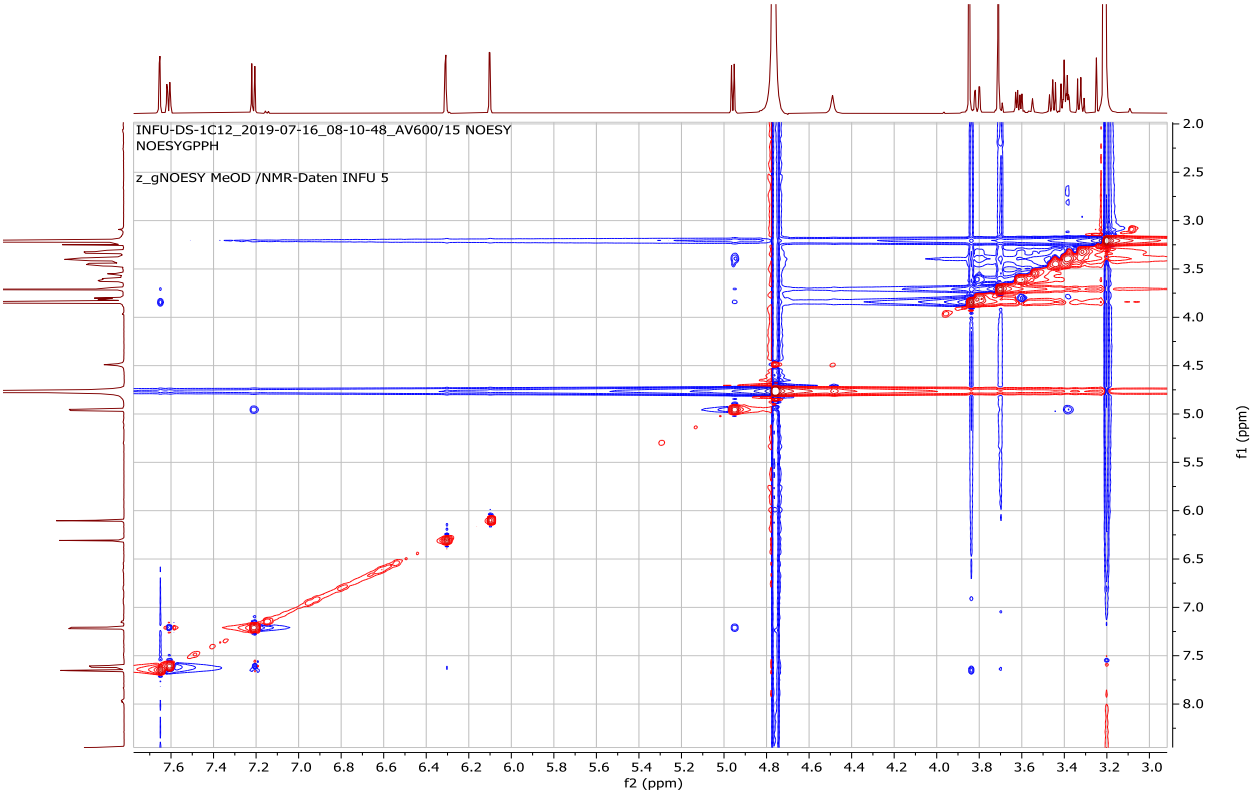

Appendix 27G: HSQC spectrum (CD_3OD) of compound **200**

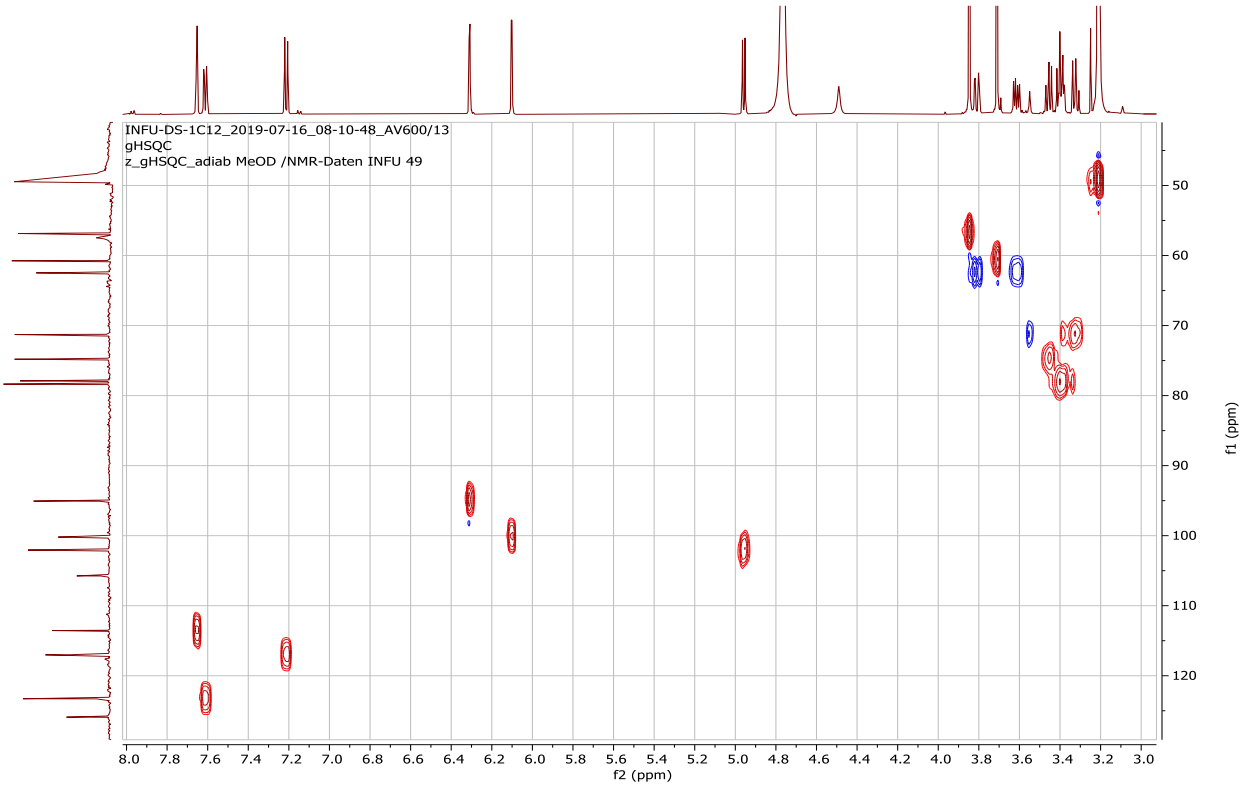

Appendix 27H: HMBC spectrum (CD_3OD) of compound **200**

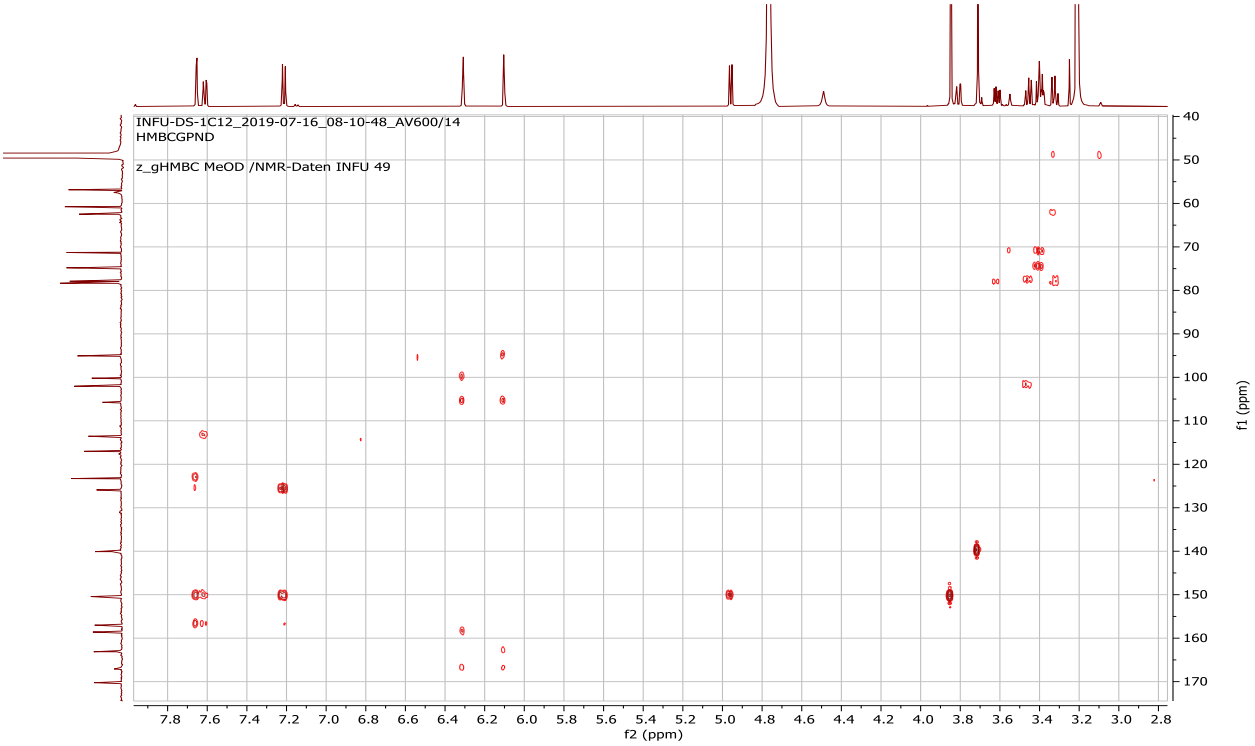

Appendix 28: NMR spectra for quercetin (**201**)

Appendix 28A: HRESIMS of compound **201**

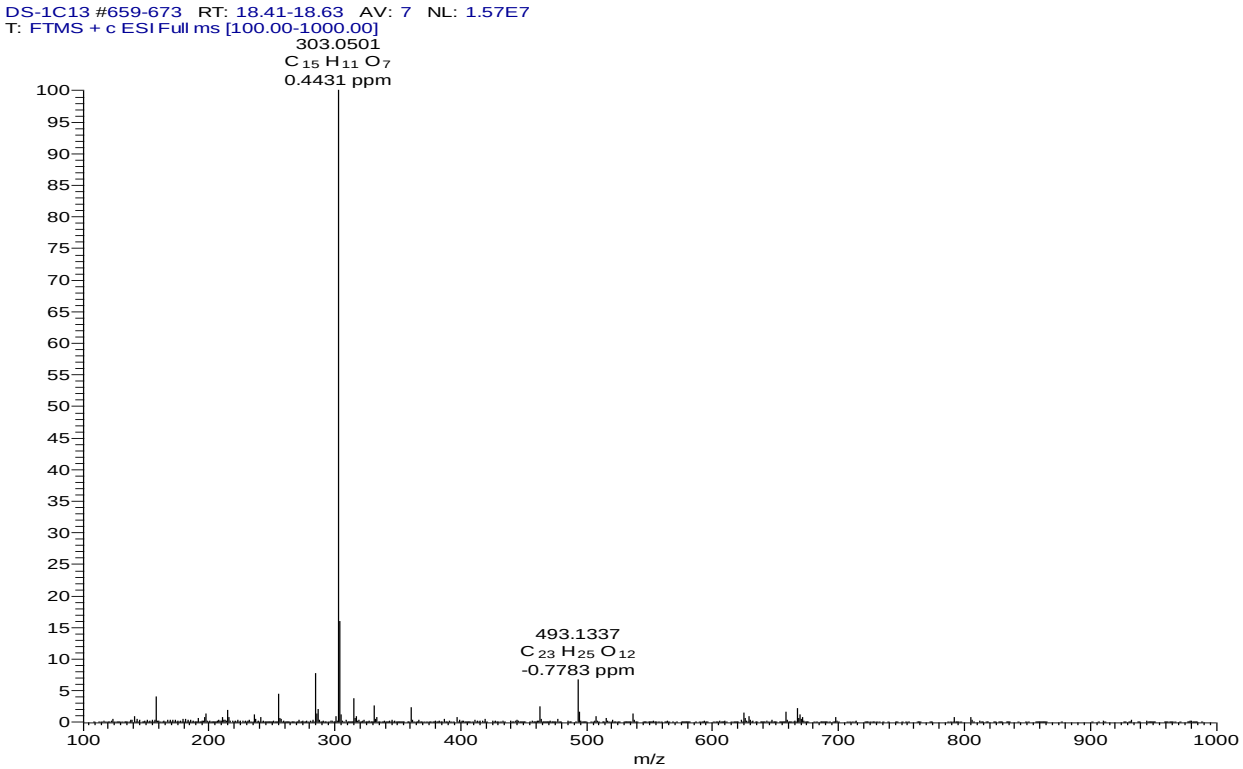

Appendix 28B: LC-UV spectrum of compound **201**

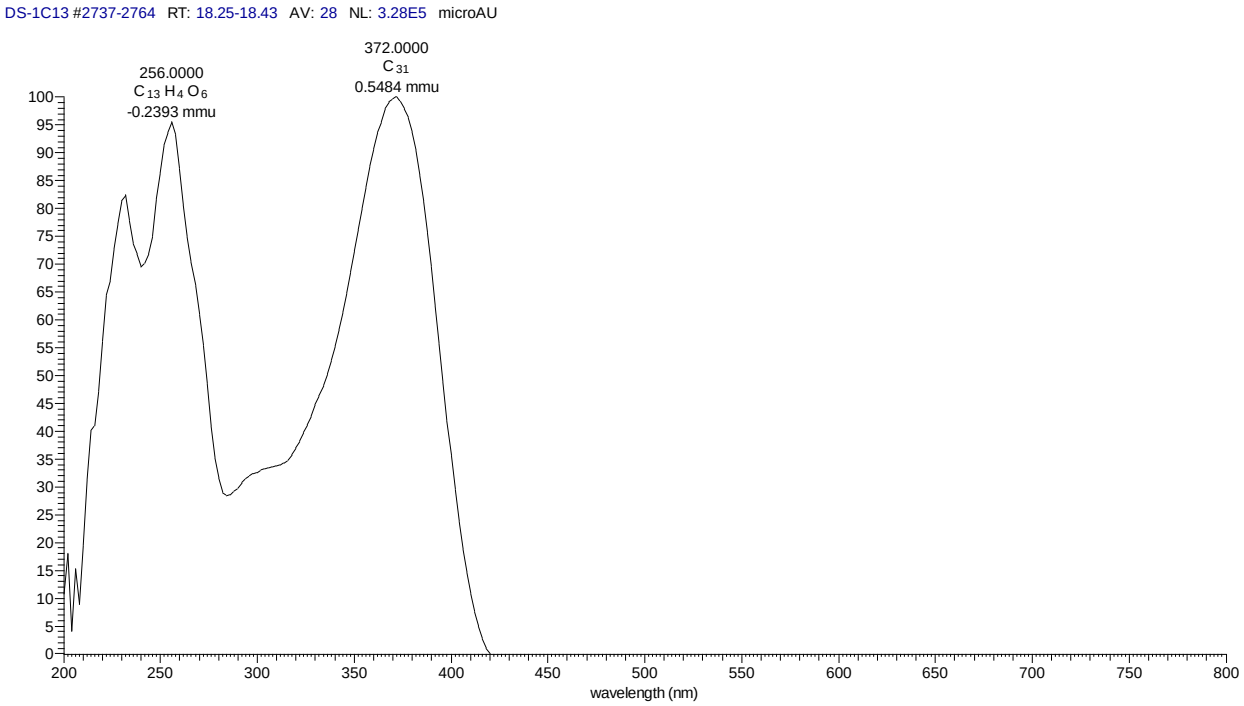

Appendix 28C: ^{1}H NMR spectrum (600 MHz, CD_3OD) of compound **201**

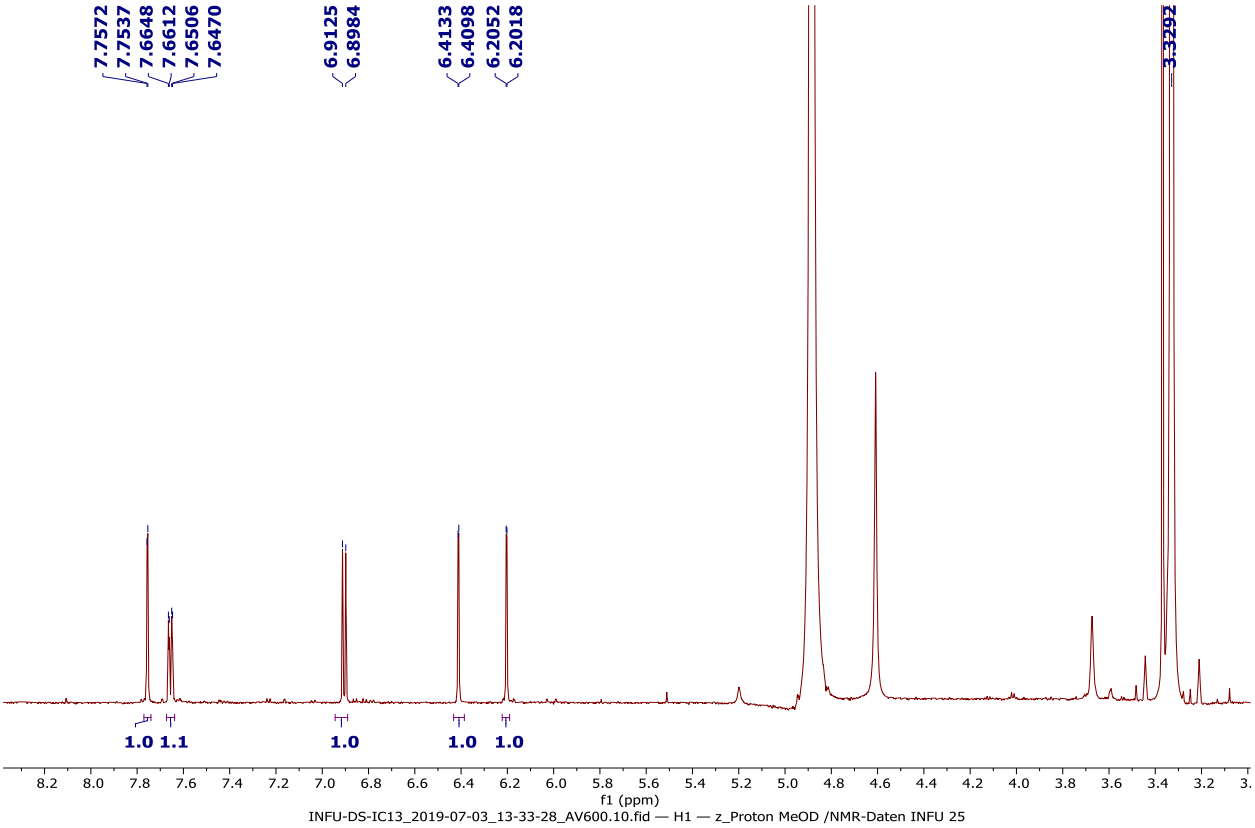

Appendix 28D: ^{13}C NMR spectrum (150 MHz, CD_3OD) of compound **201**

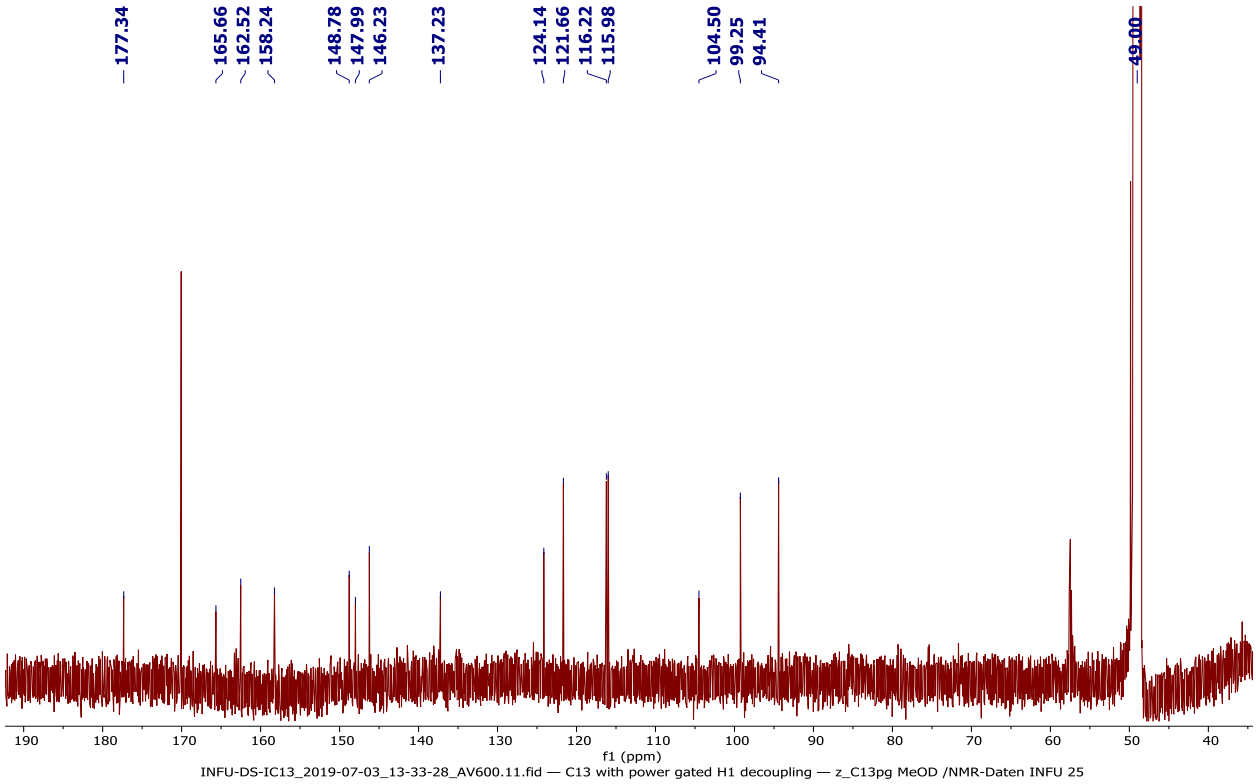

Appendix 28E: ^{1}H-^{1}H COSY spectrum (CD_3OD) of compound **201**

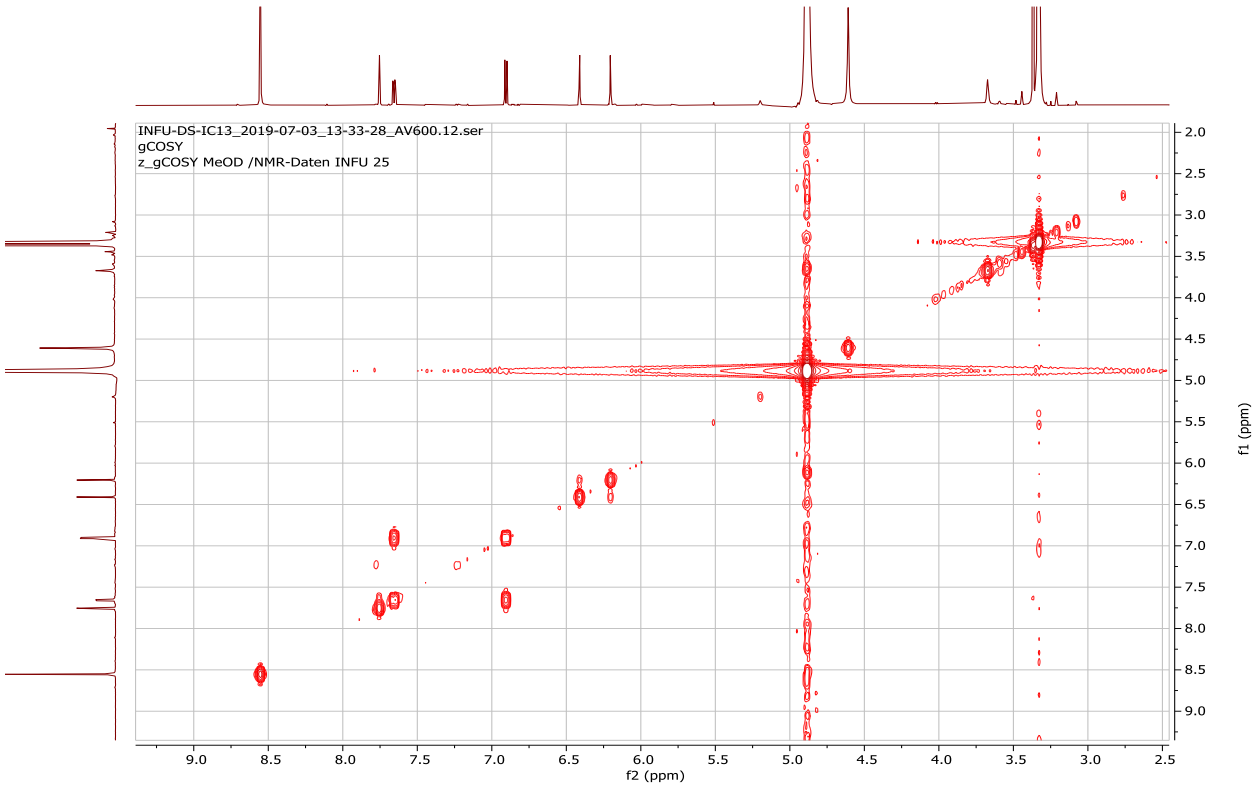

Appendix 28F: HSQC spectrum (CD_3OD) of compound **201**

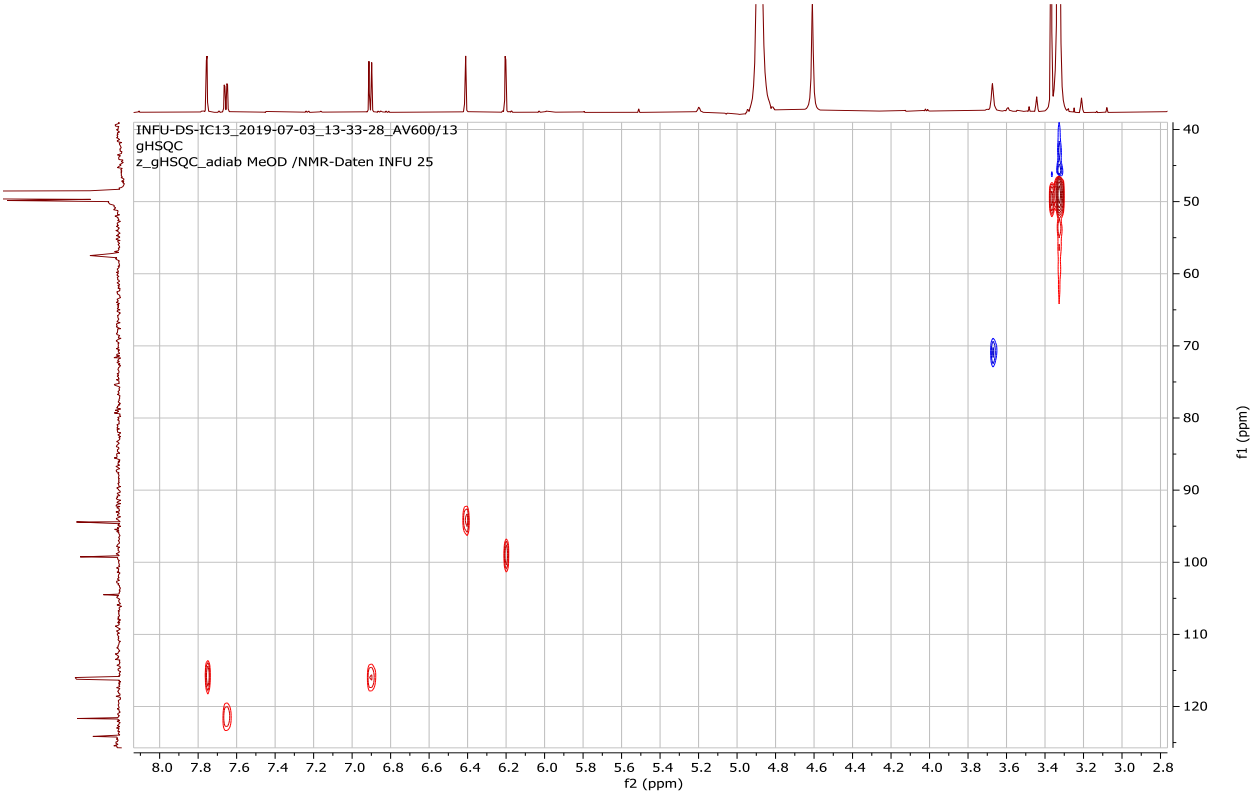

Appendix 28G: HMBC spectrum (CD_3OD) of compound **201**

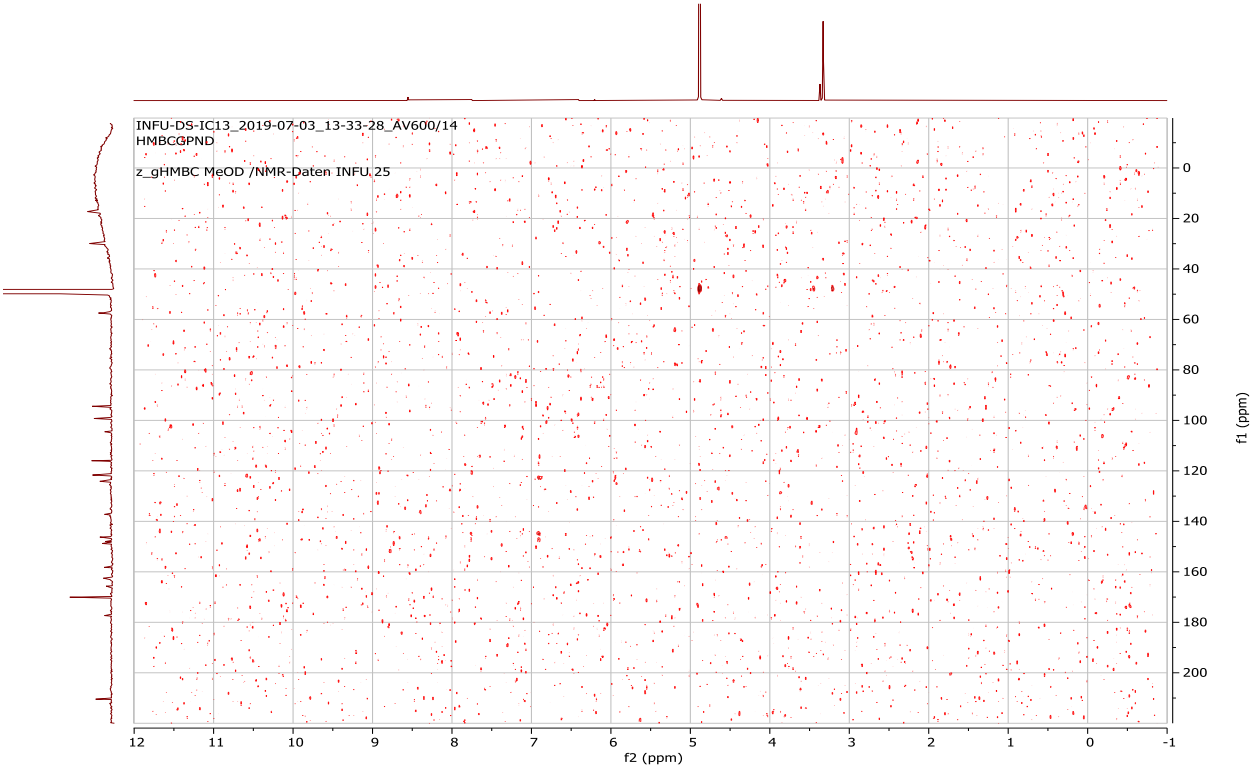

Appendix 29: NMR spectra for 4-(2′-formyl-1′-pyrrolyl)butanoic acid (**202**)

Appendix 29A: HRESIMS of compound **202**

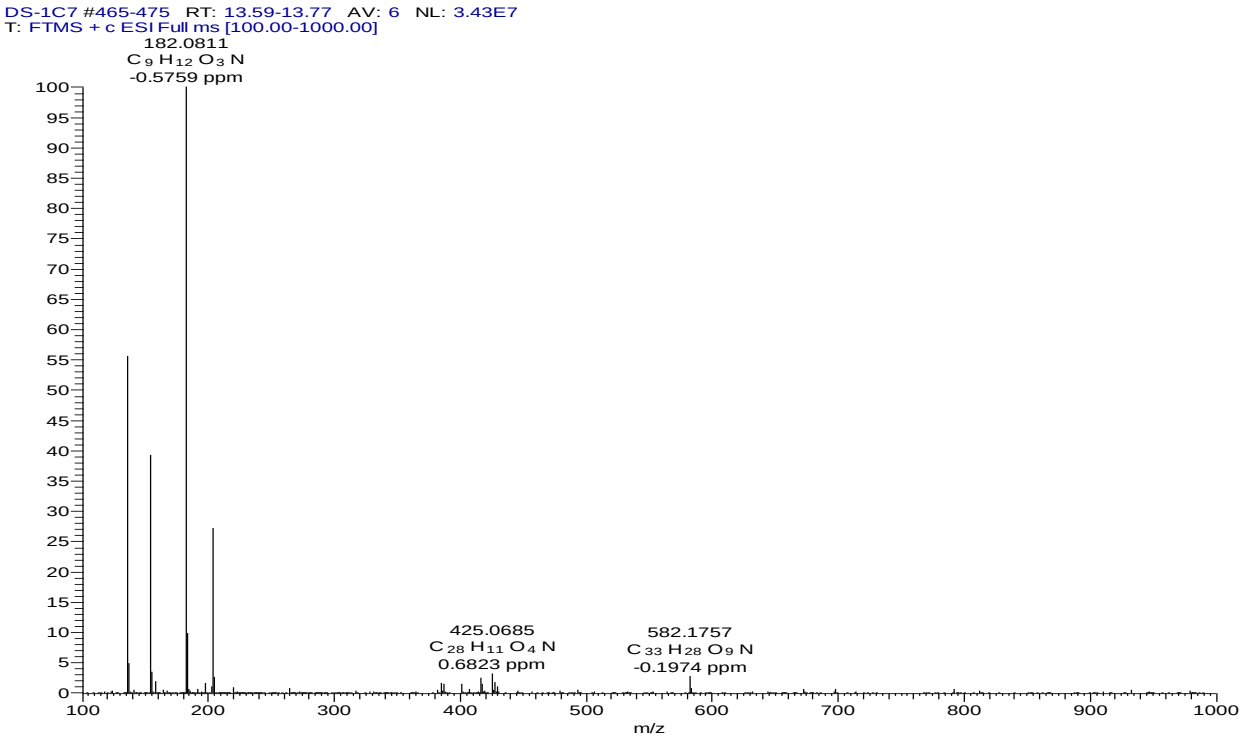

Appendix 29B: LC-UV spectrum of compound **202**

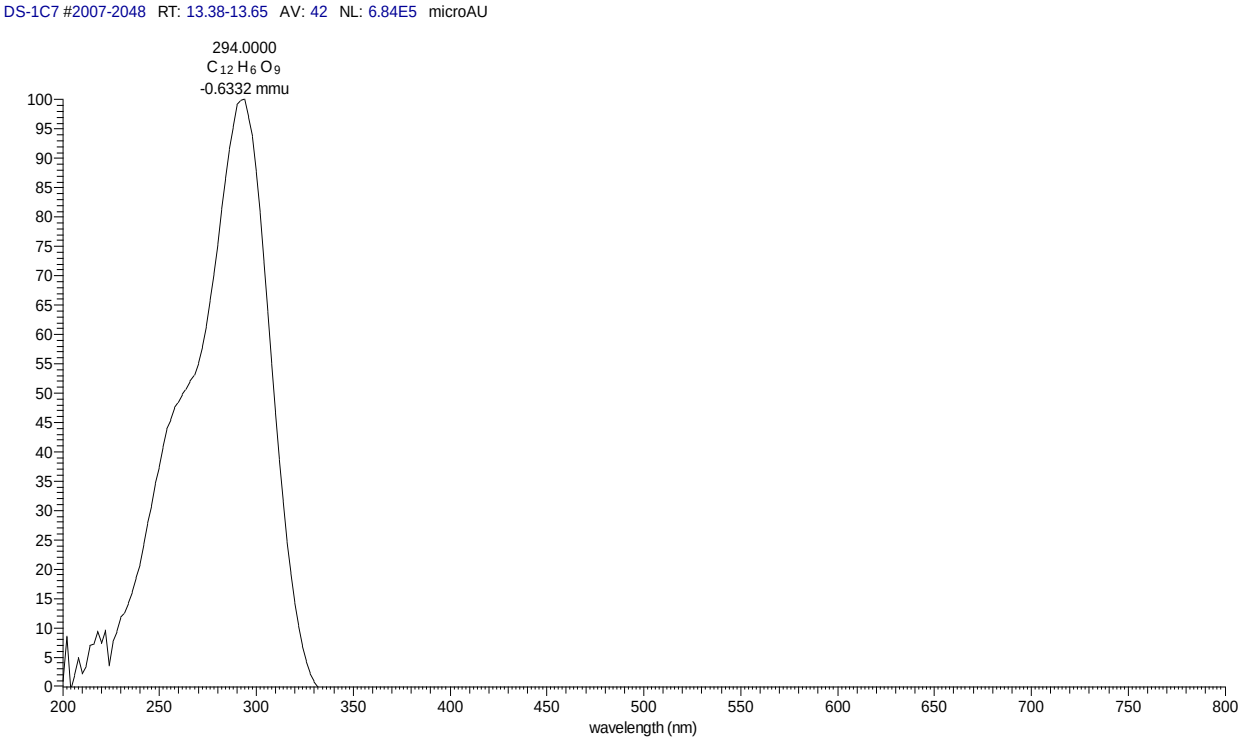

Appendix 29C: ^{1}H NMR spectrum (600 MHz, CD_3OD) of compound **202**

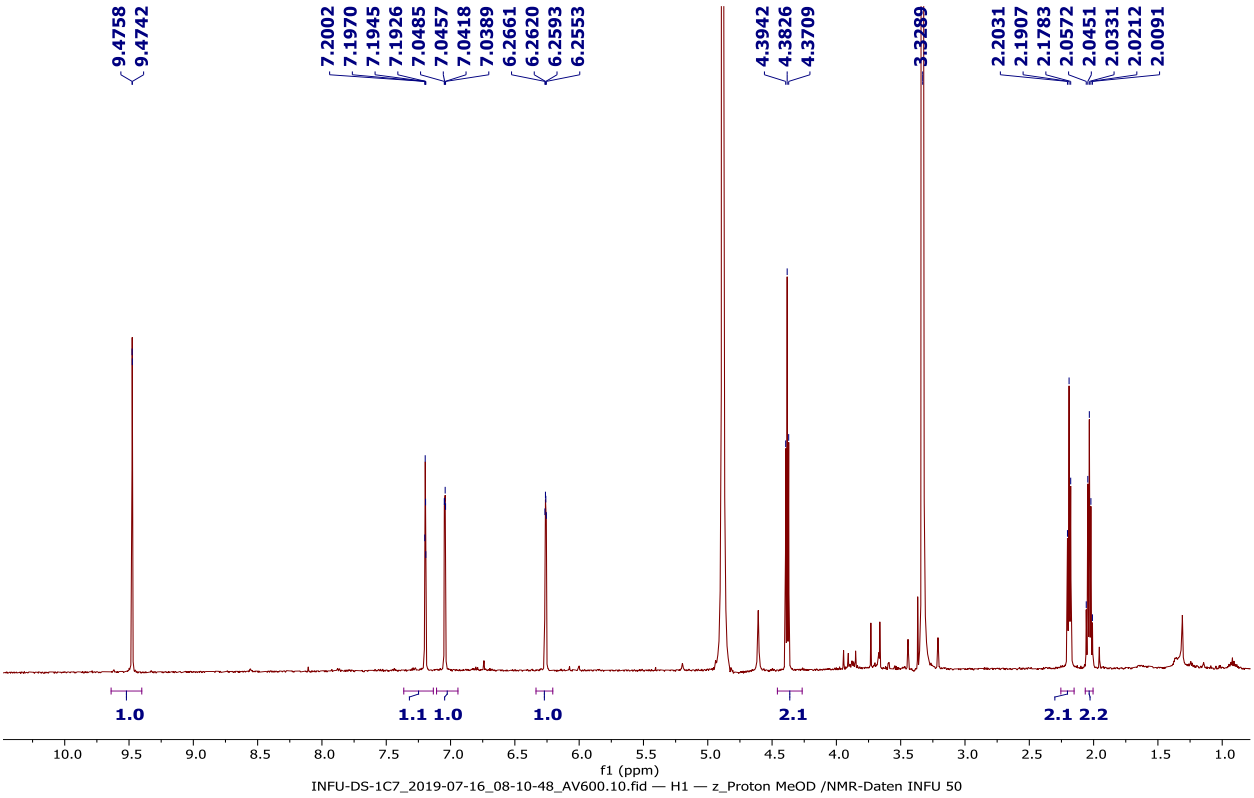

Appendix 29D: ^{13}C NMR spectrum (150 MHz, CD_3OD) of compound **202**

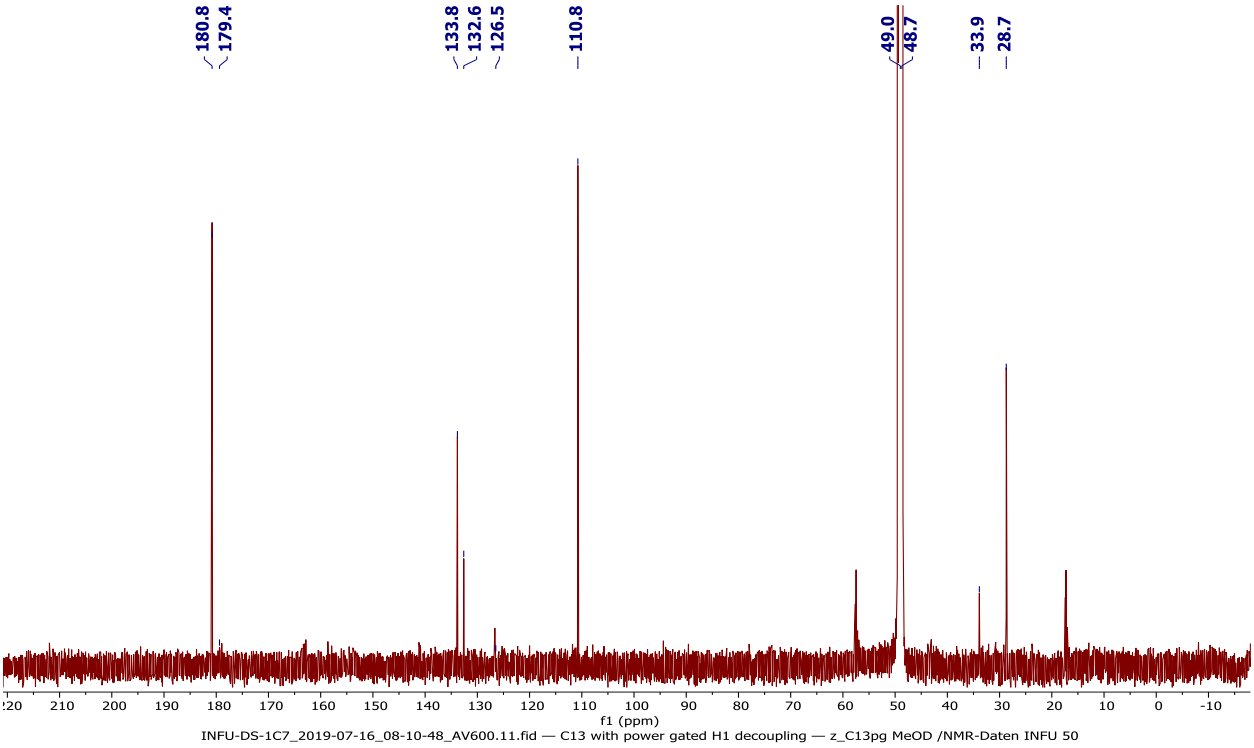

Appendix 29E: ^{1}H-^{1}H COSY spectrum (CD_3OD) of compound **202**

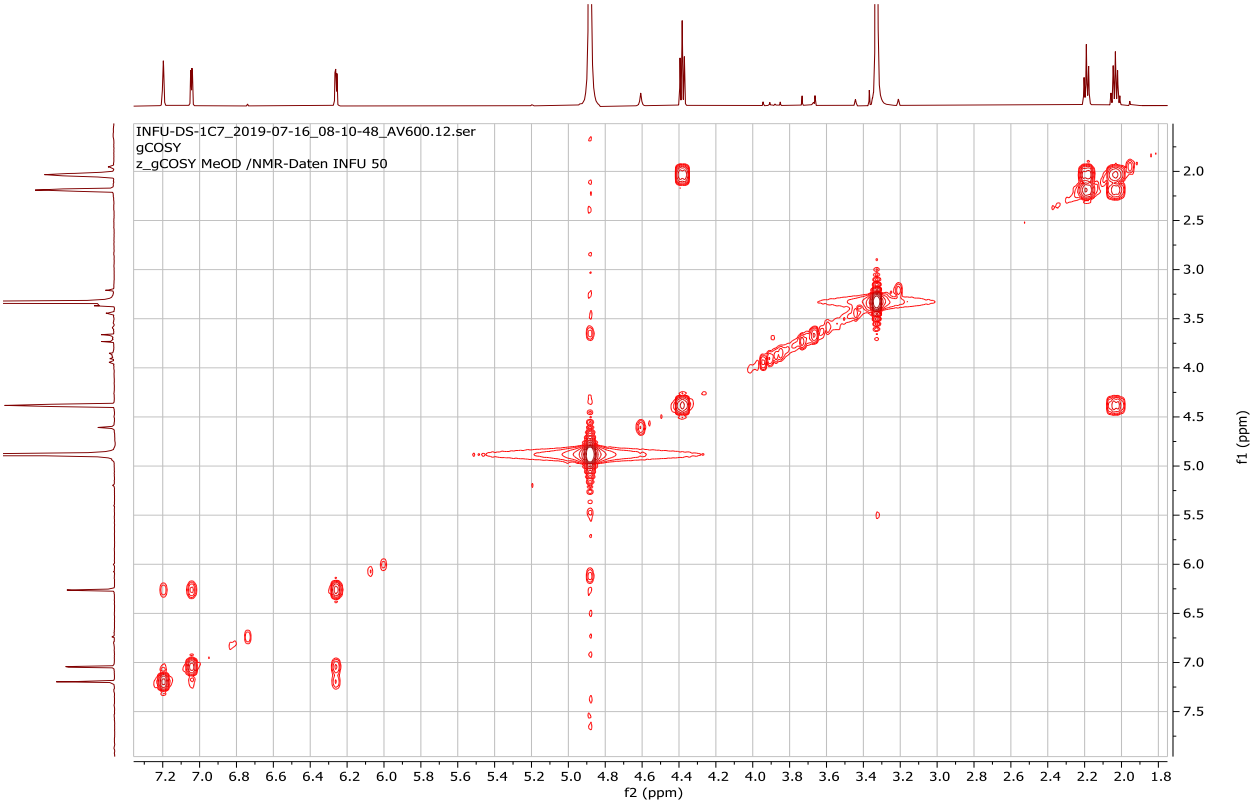

Appendix 29F: HSQC spectrum (CD_3OD) of compound **202**

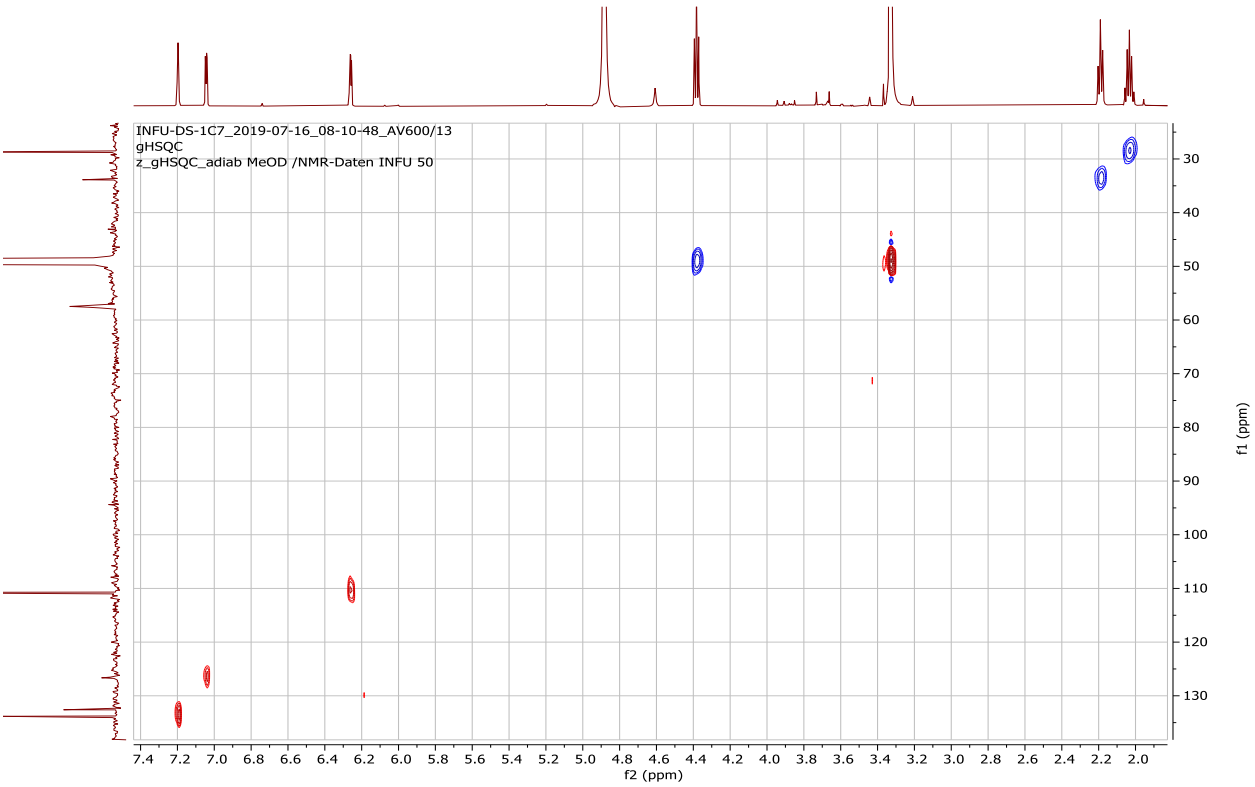

Appendix 29G: HMBC spectrum (CD_3OD) of compound **202**

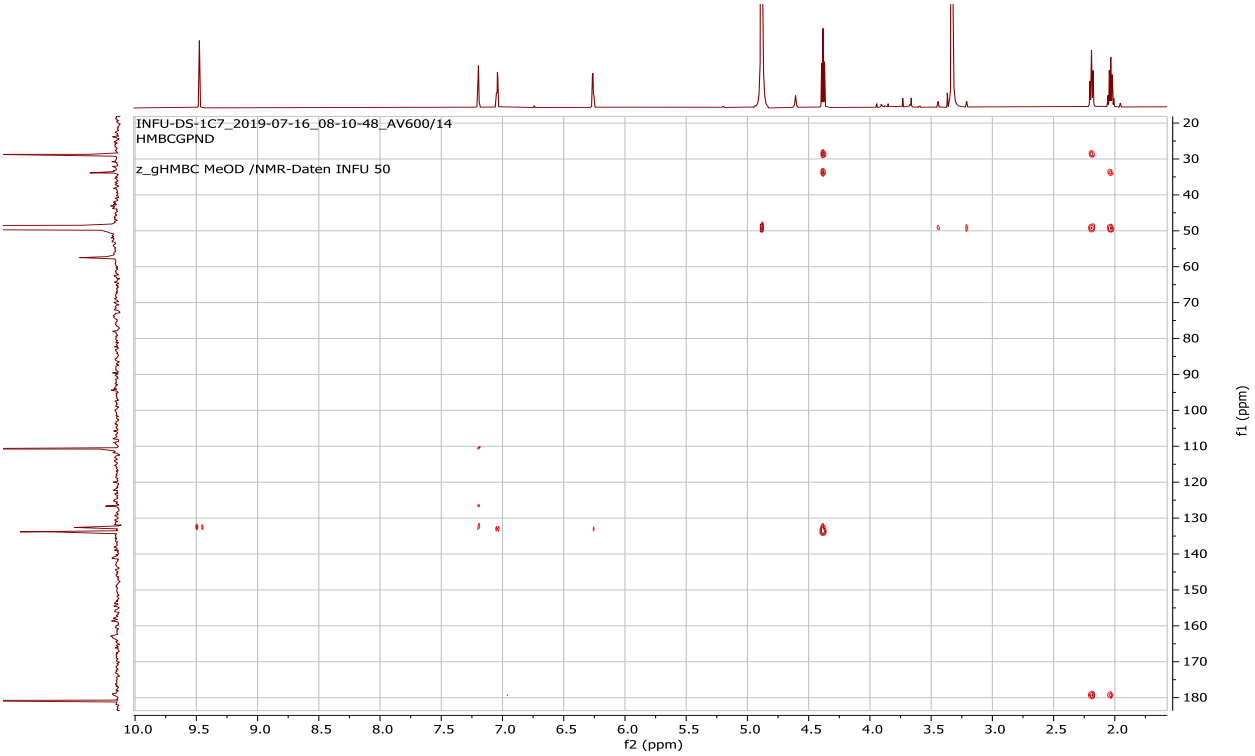

Appendix 30: NMR spectra for 3,5,7-trihydroxy-6-methyl-3′,4′-methylenedioxyflavone (**203**)

Appendix 30A: HRESIMS of compound **203**

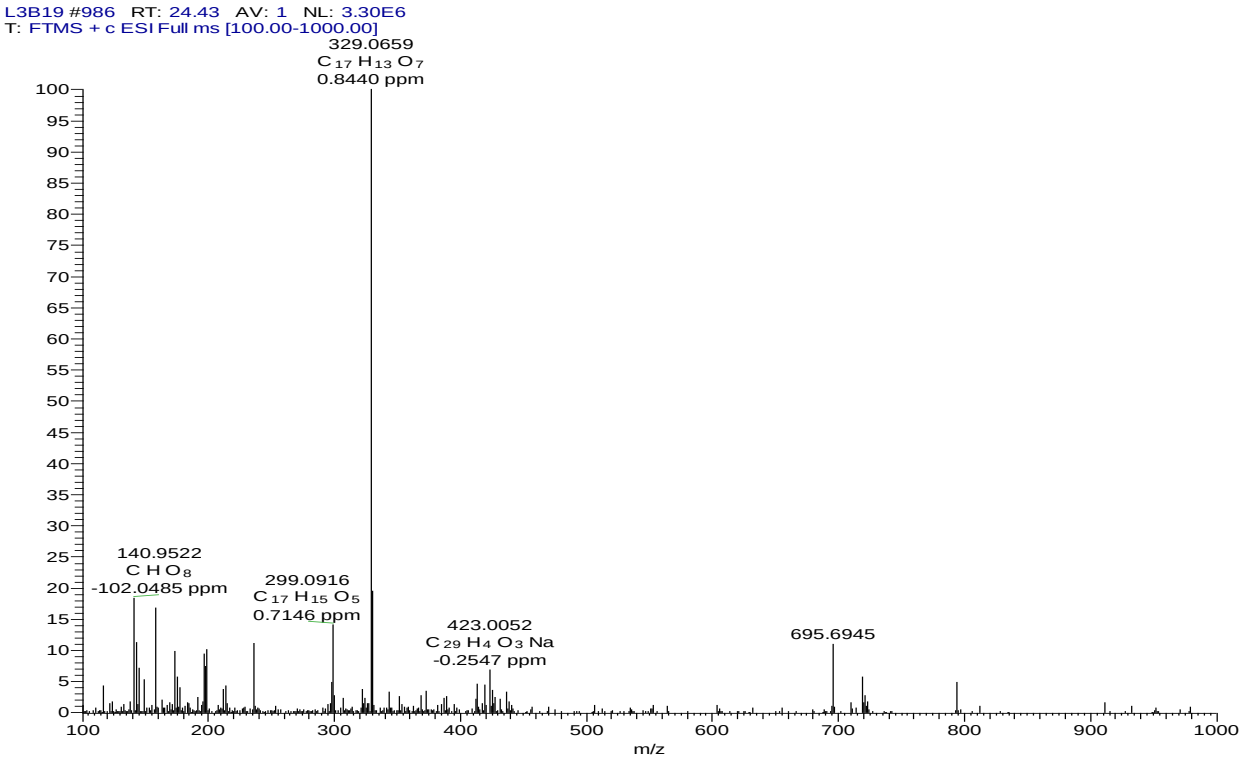

Appendix 30B: HRESIMS/MS of compound **203**

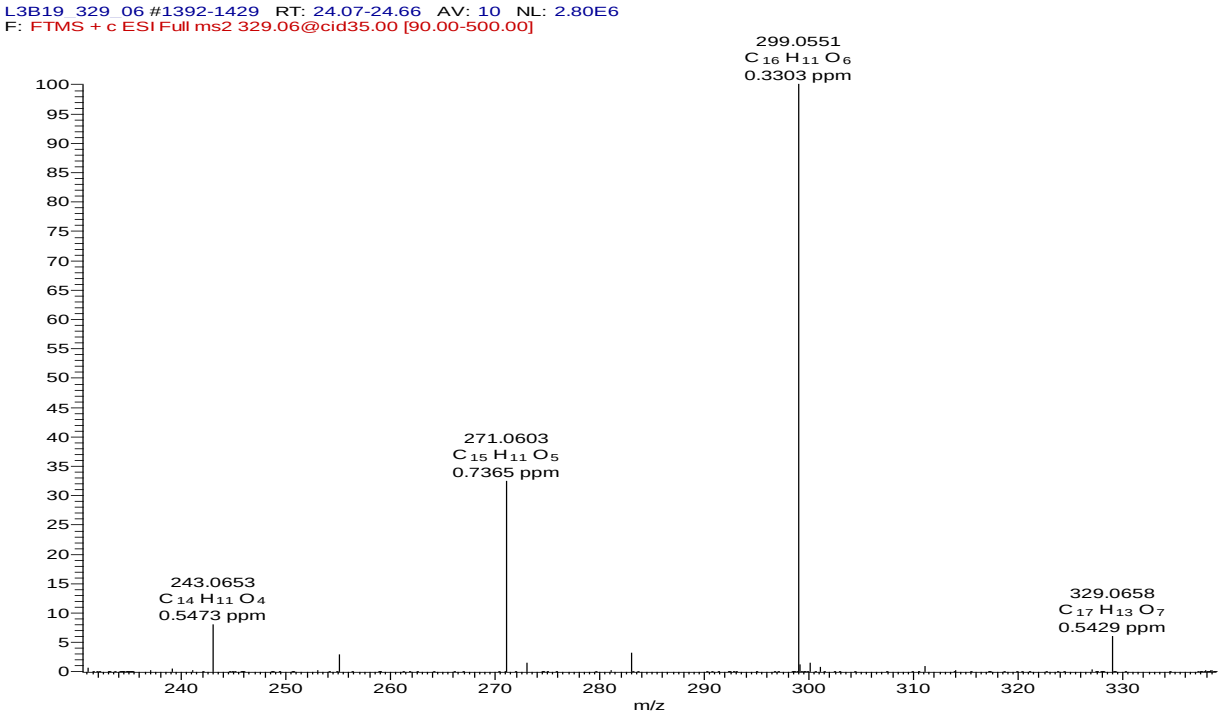

Appendix 30C: LC-UV spectrum of compound **203**

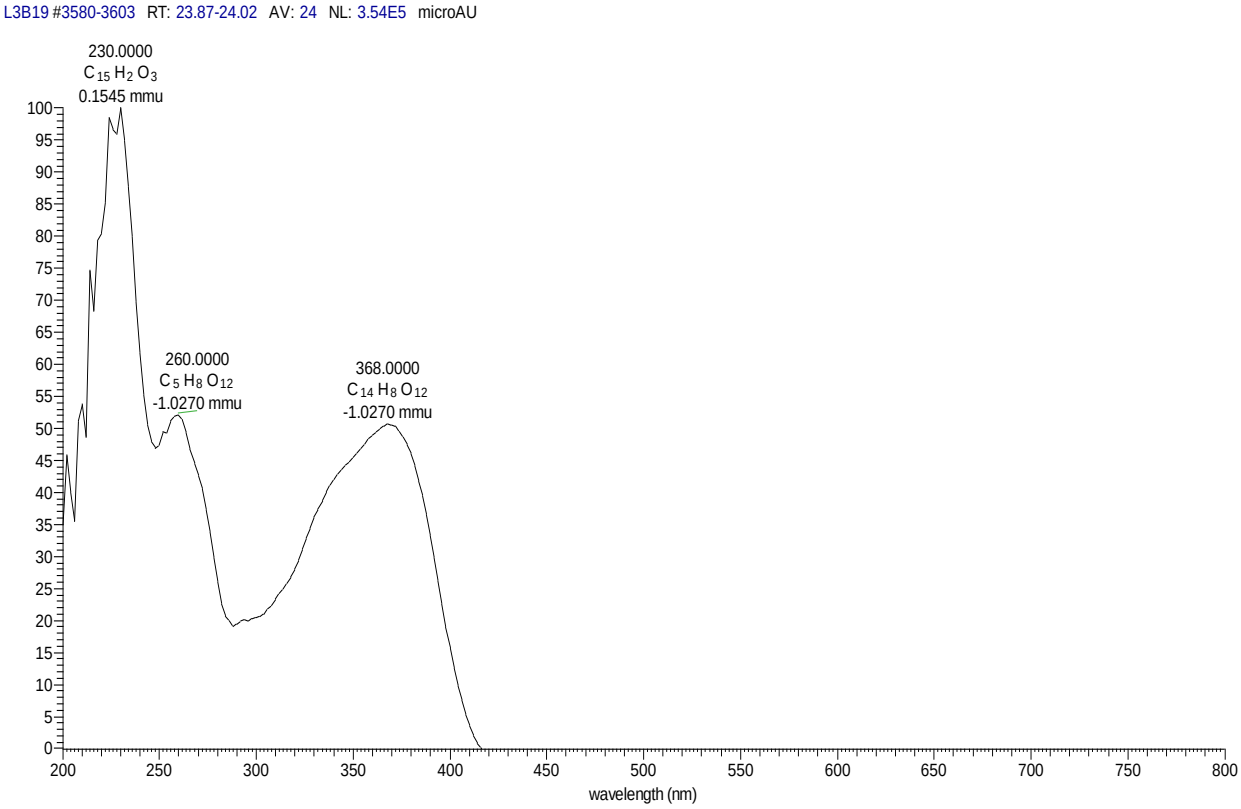

Appendix 30D: FT-IR spectrum of compound **203**

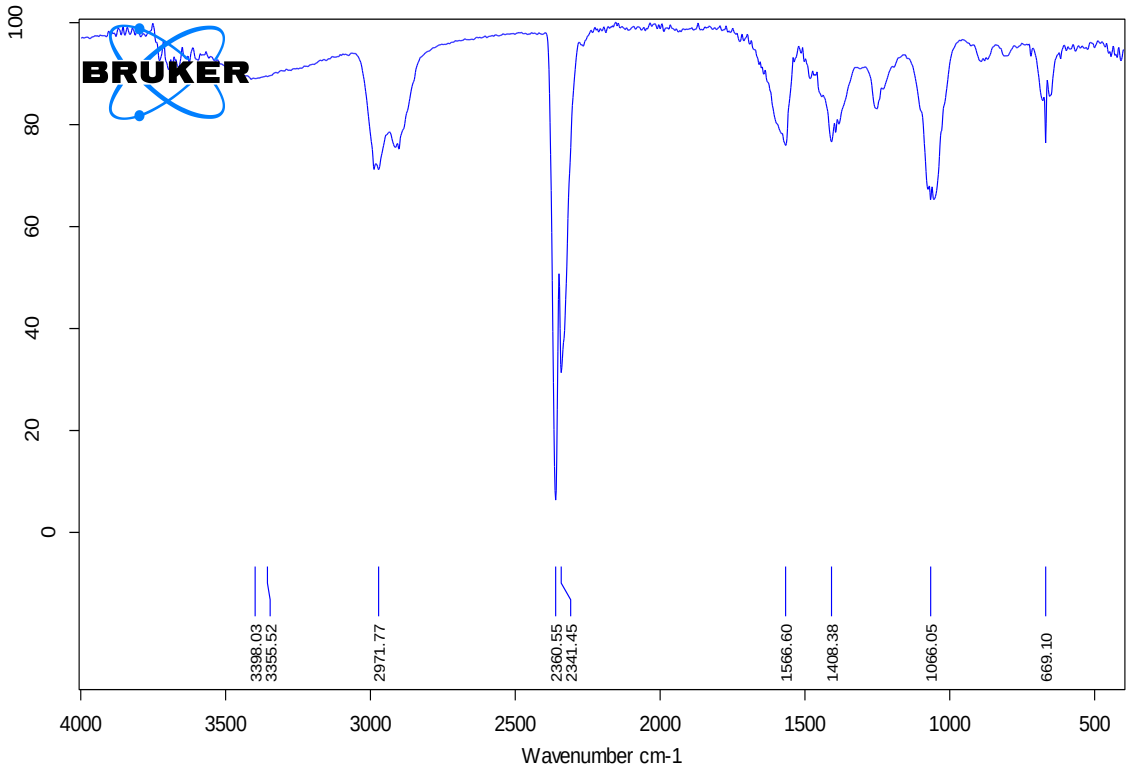

Appendix 30E: ^{1}H NMR spectrum (600 MHz, CD_3OD) of compound **203**

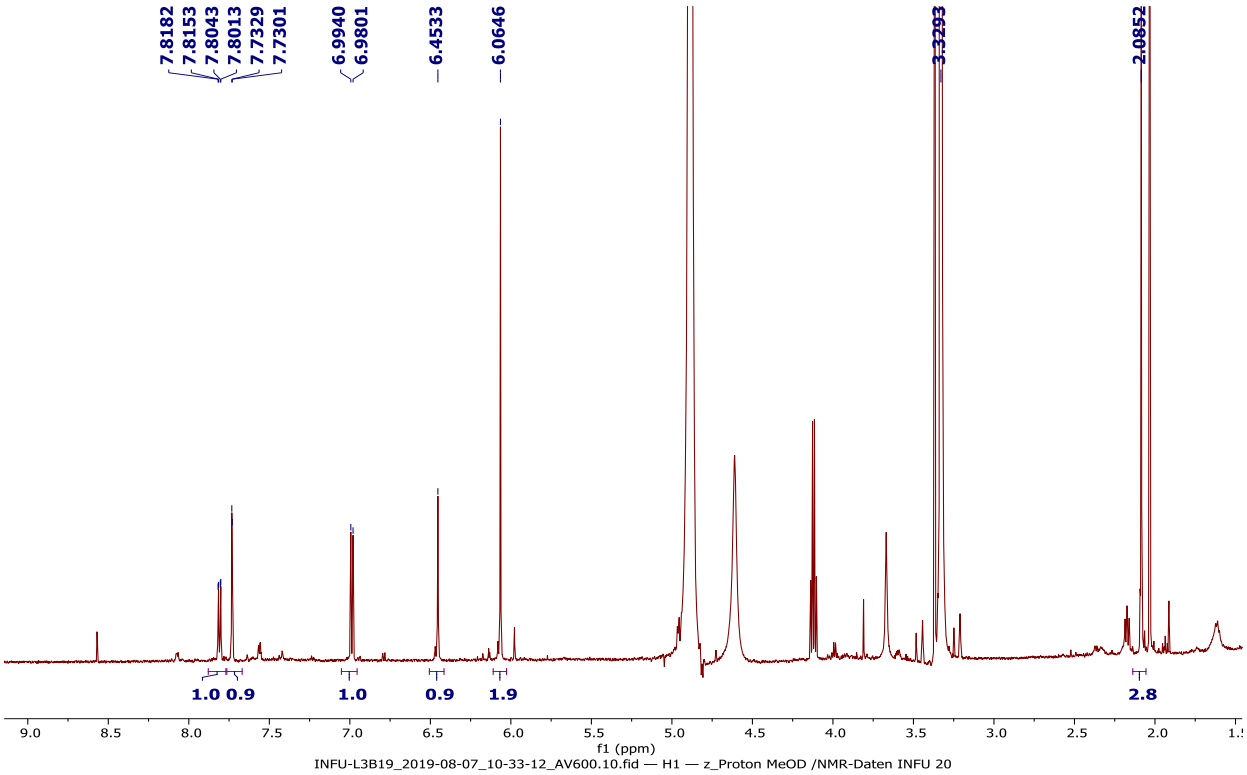

Appendix 30F: ^{13}C NMR spectrum (150 MHz, CD_3OD) of compound **203**

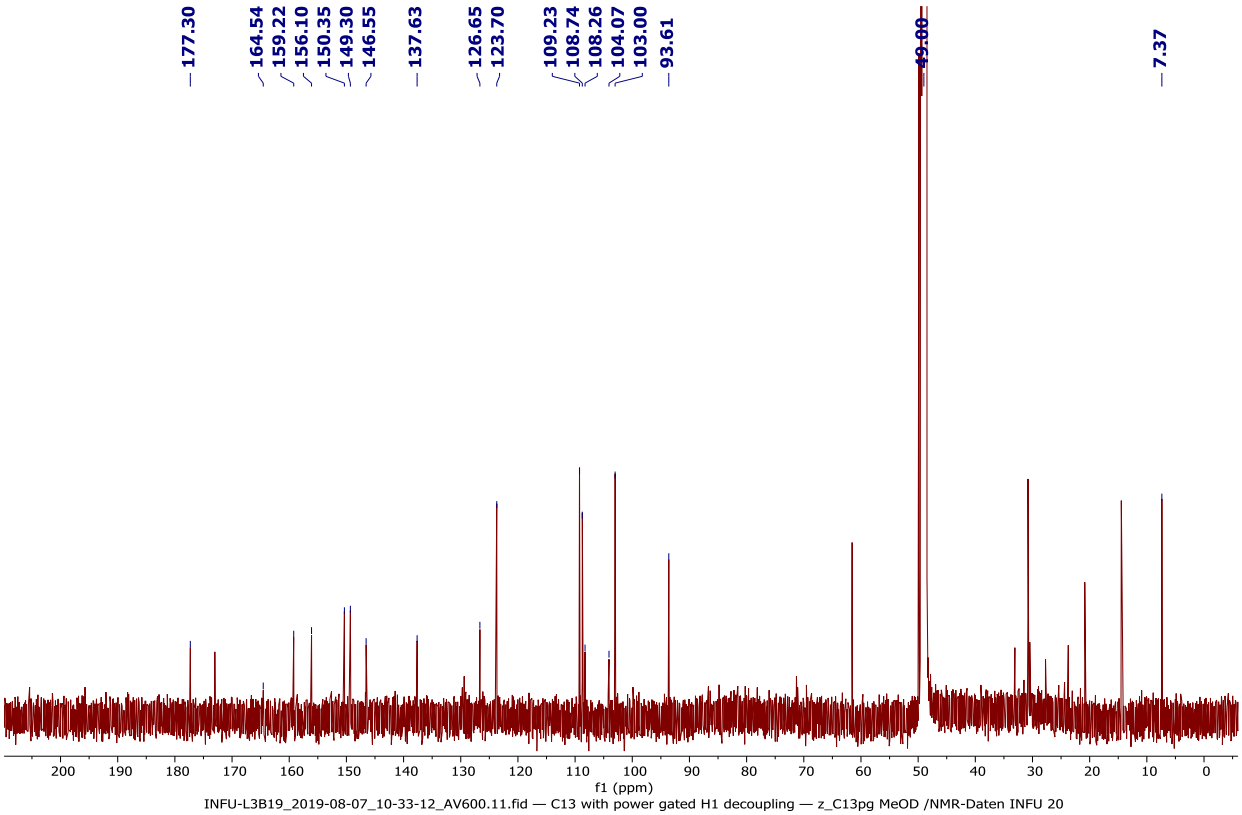

Appendix 30G: ^{1}H-^{1}H COSY spectrum (CD_3OD) of compound **203**

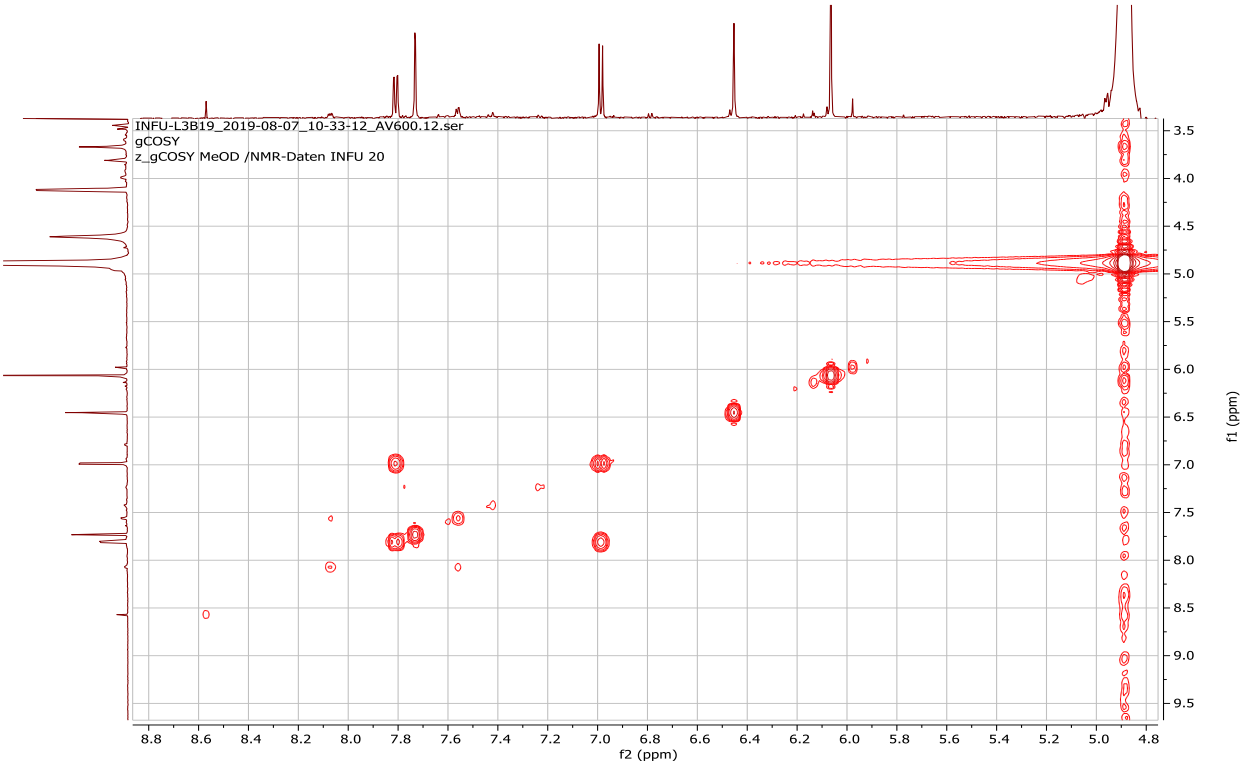

Appendix 30H: HSQC spectrum (CD_3OD) of compound **203**

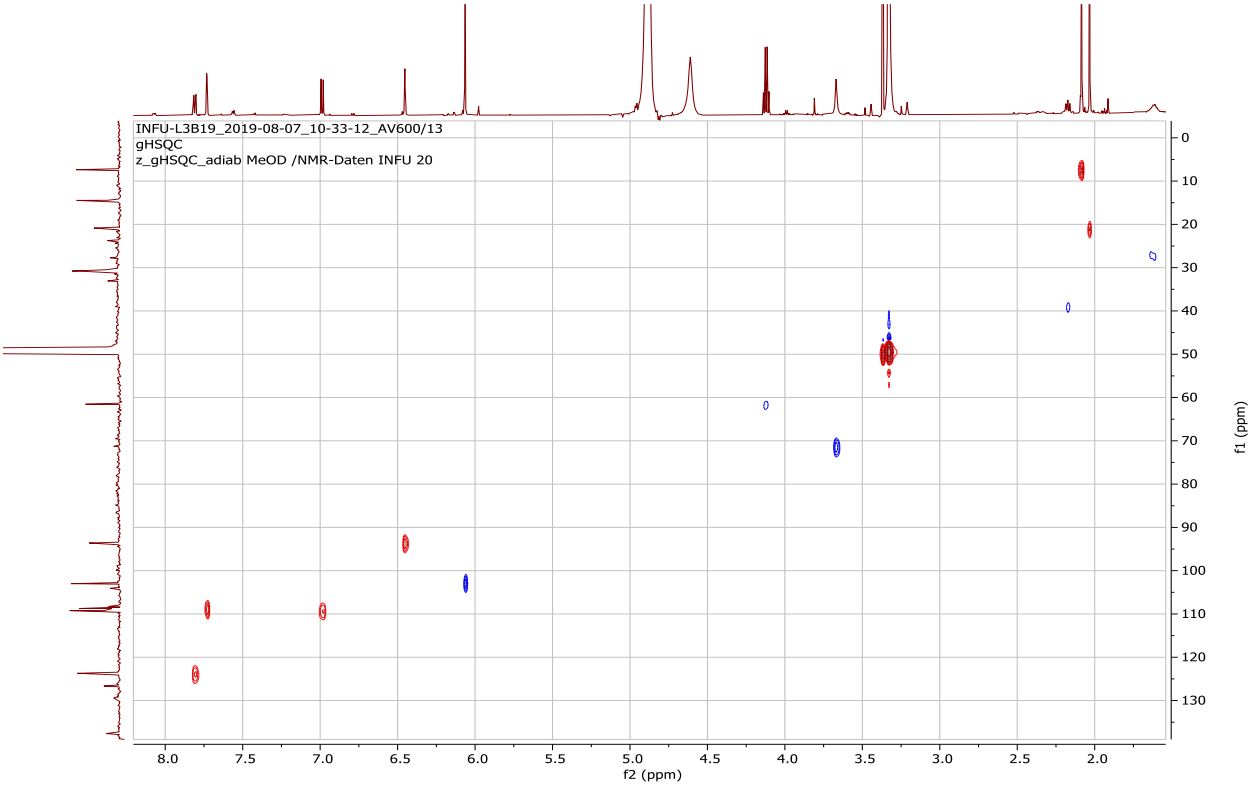

Appendix 30I: HMBC spectrum (CD_3OD) of compound **203**

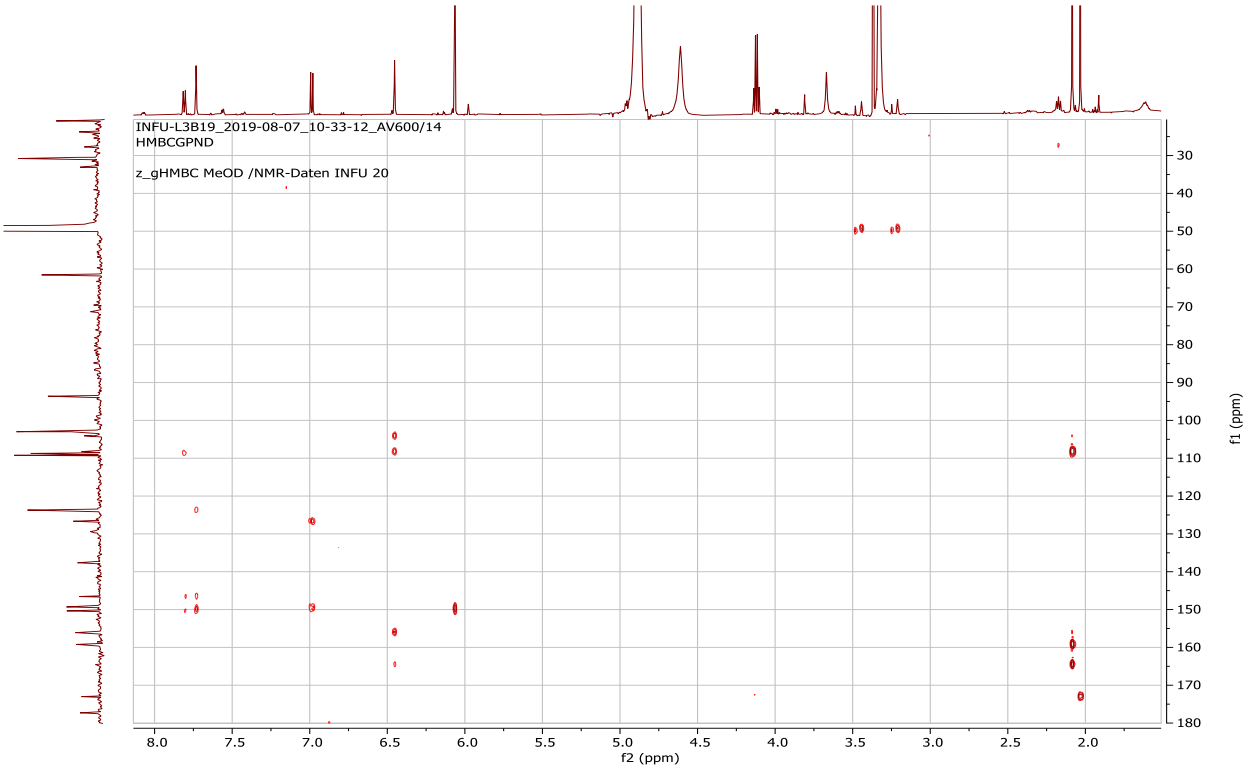

Appendix 31: NMR spectra for 5,7-dihydroxy-3-methoxy-6-methyl-3′,4′-methylenedioxyflavone (**204**)

Appendix 31A: HRESIMS of compound **204**

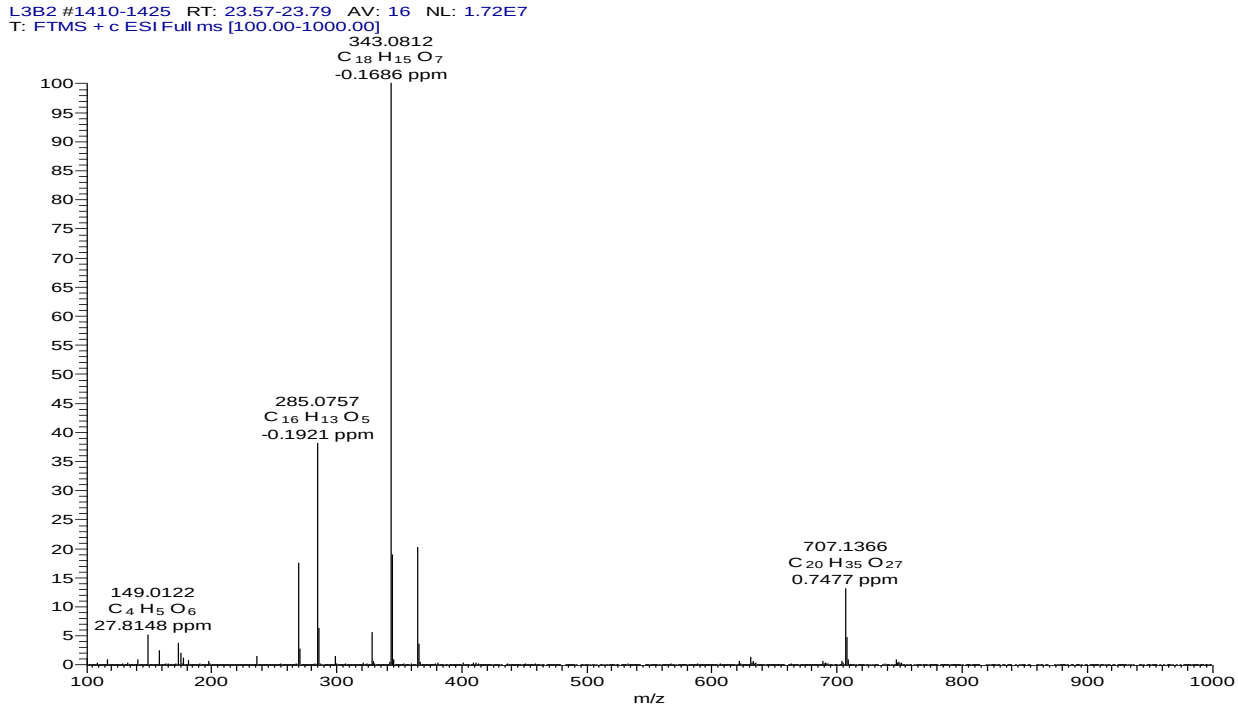

Appendix 31B: HRESIMS/MS of compound **204**

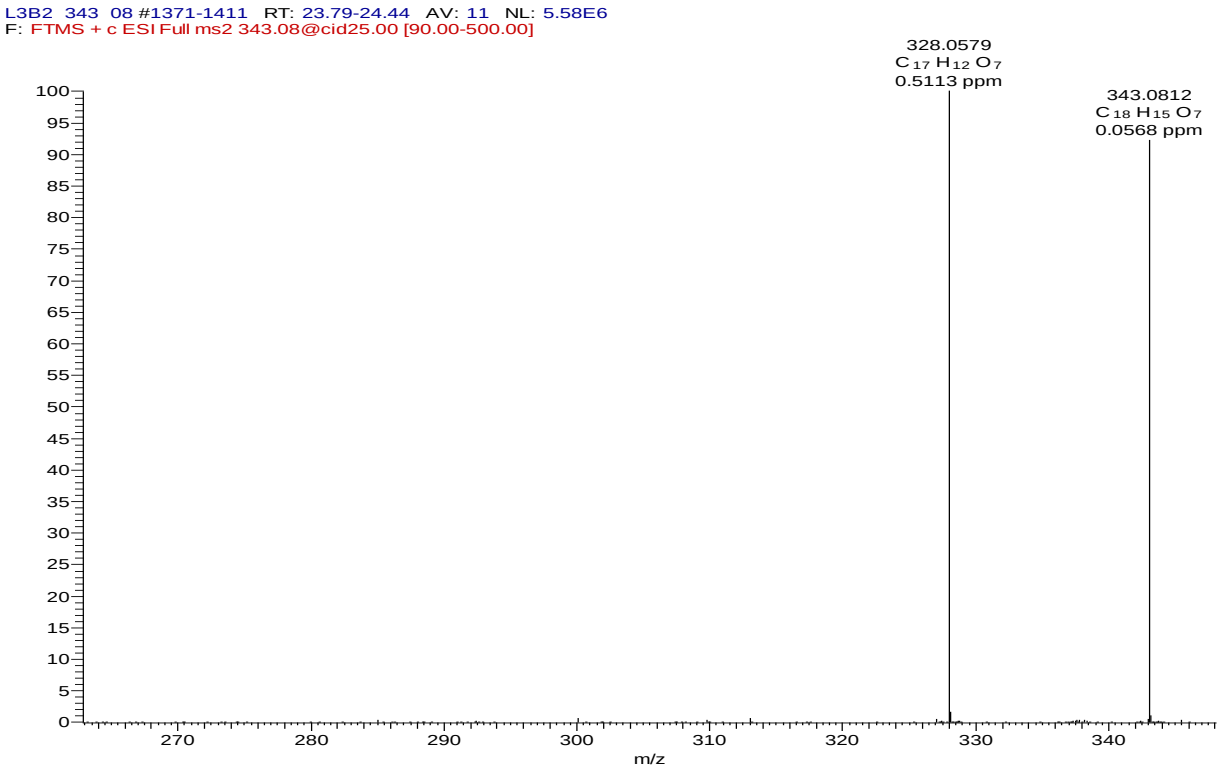

Appendix 31C: LC-UV spectrum of compound **204**

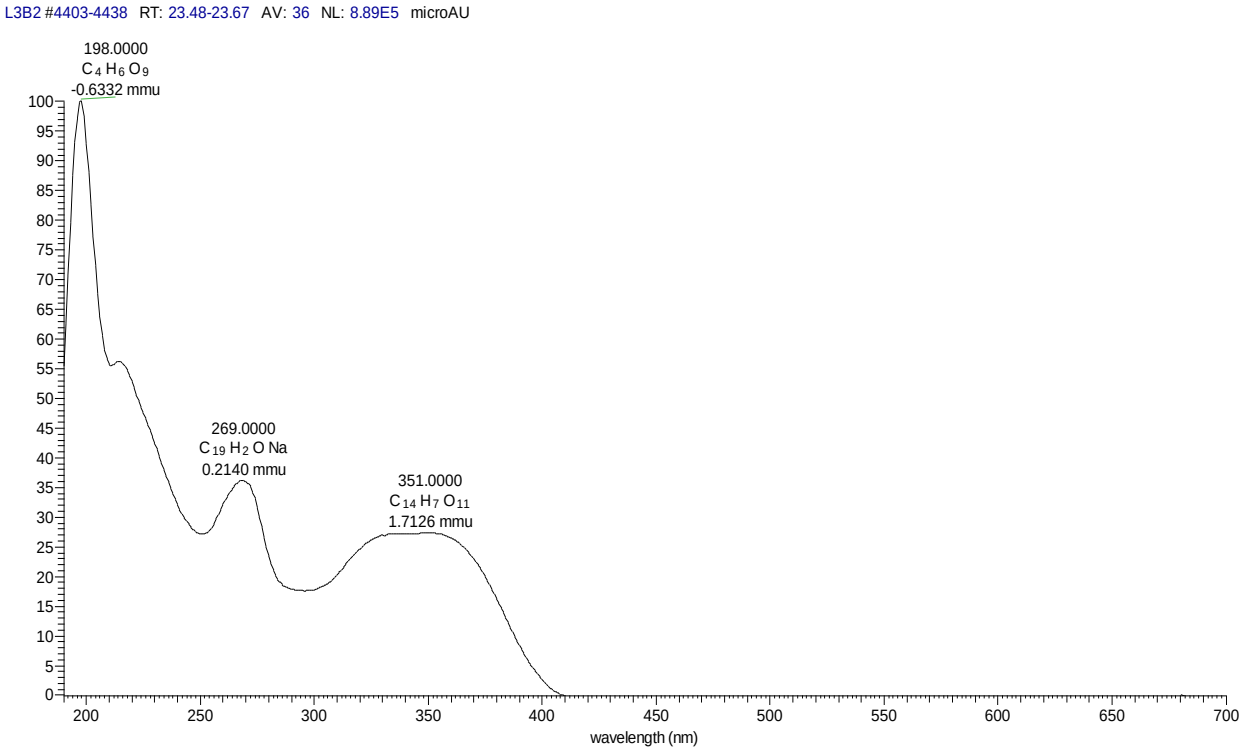

Appendix 31D: FT-IR spectrum of compound **204**

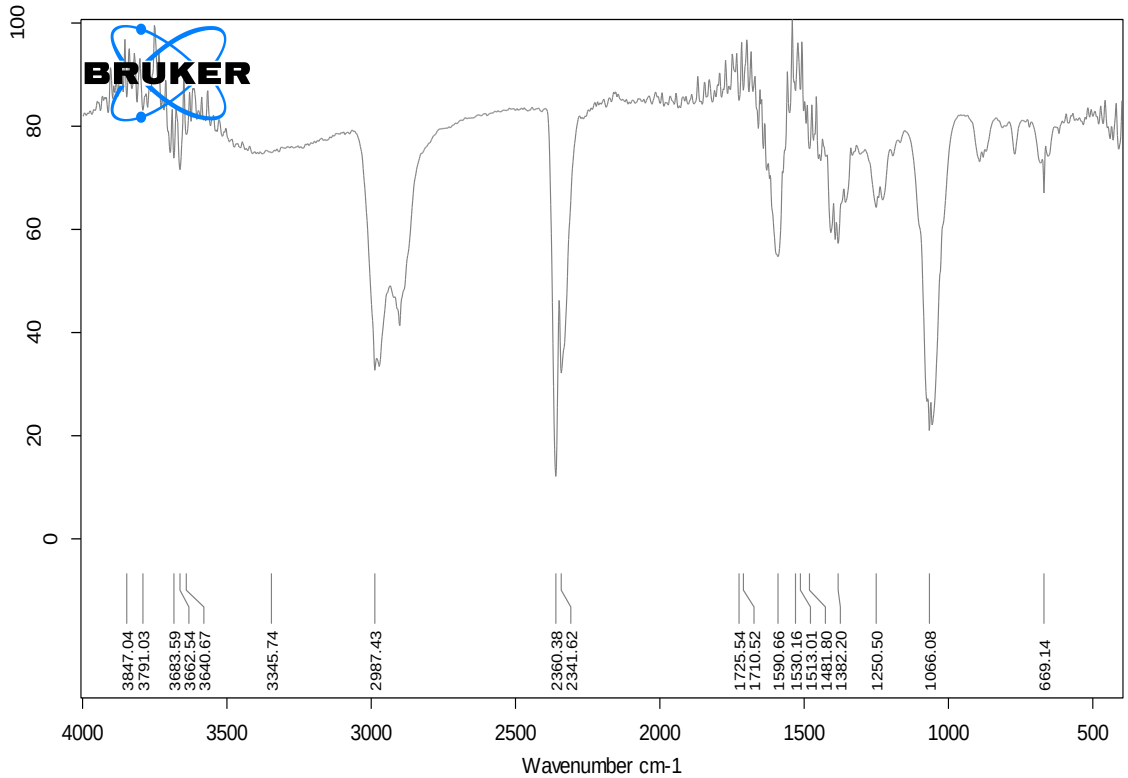

Appendix 31E: ^{1}H NMR spectrum (700 MHz, DMSO-d_6) of compound **204**

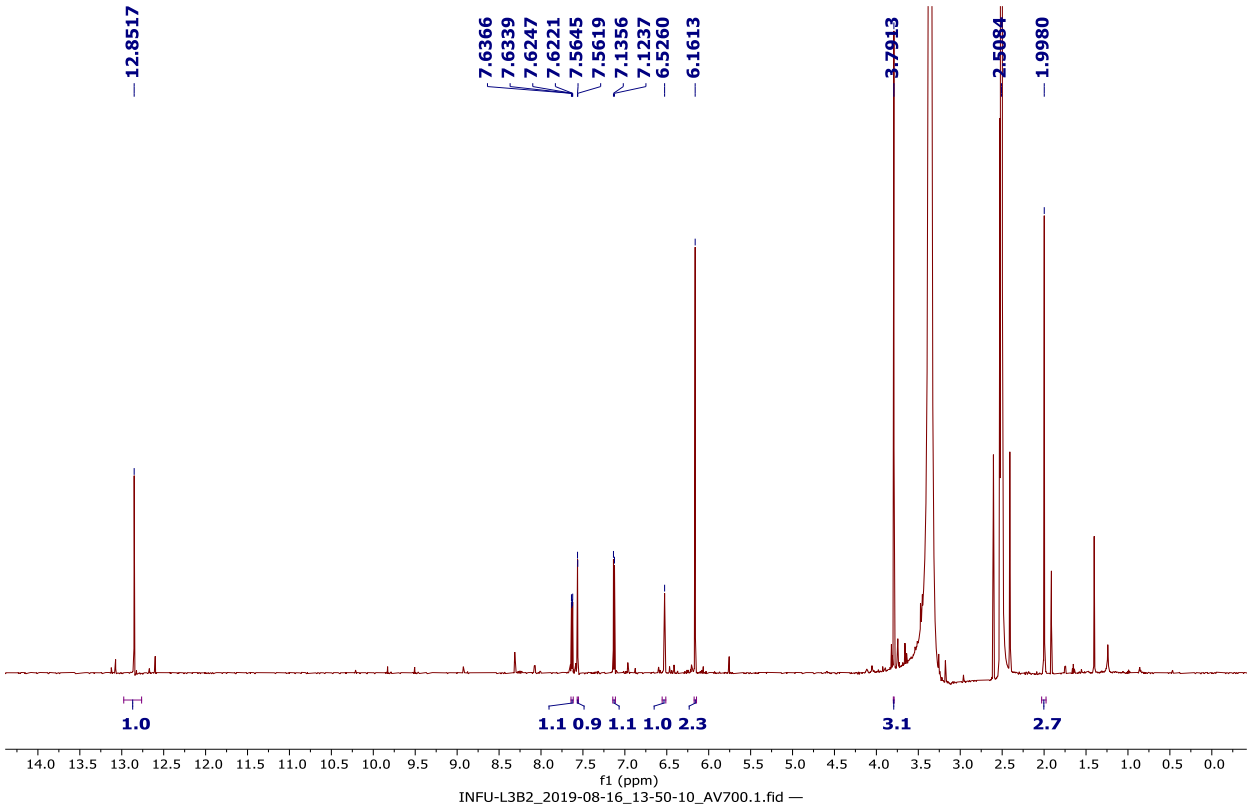

Appendix 31F: ^{13}C NMR spectrum (175 MHz, DMSO-d_6) of compound **204**

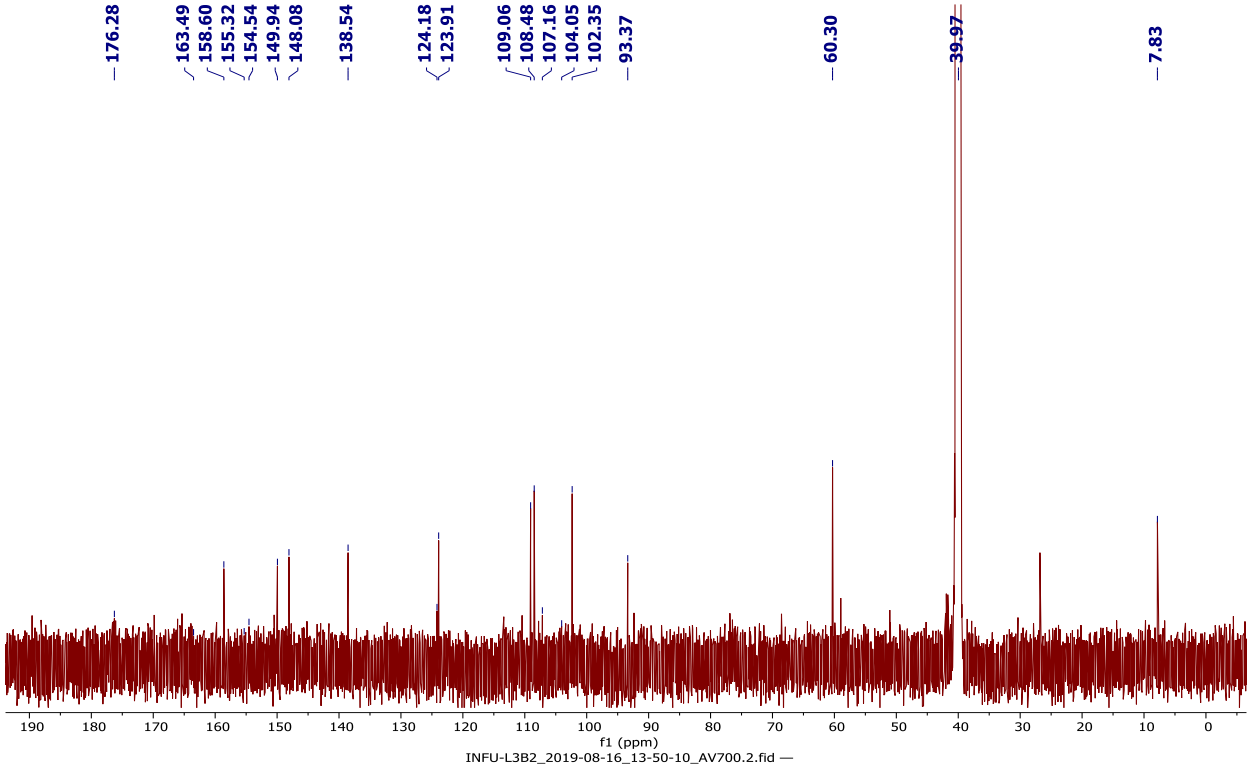

Appendix 31G: ^{1}H-^{1}H COSY spectrum (DMSO-d_6) of compound **204**

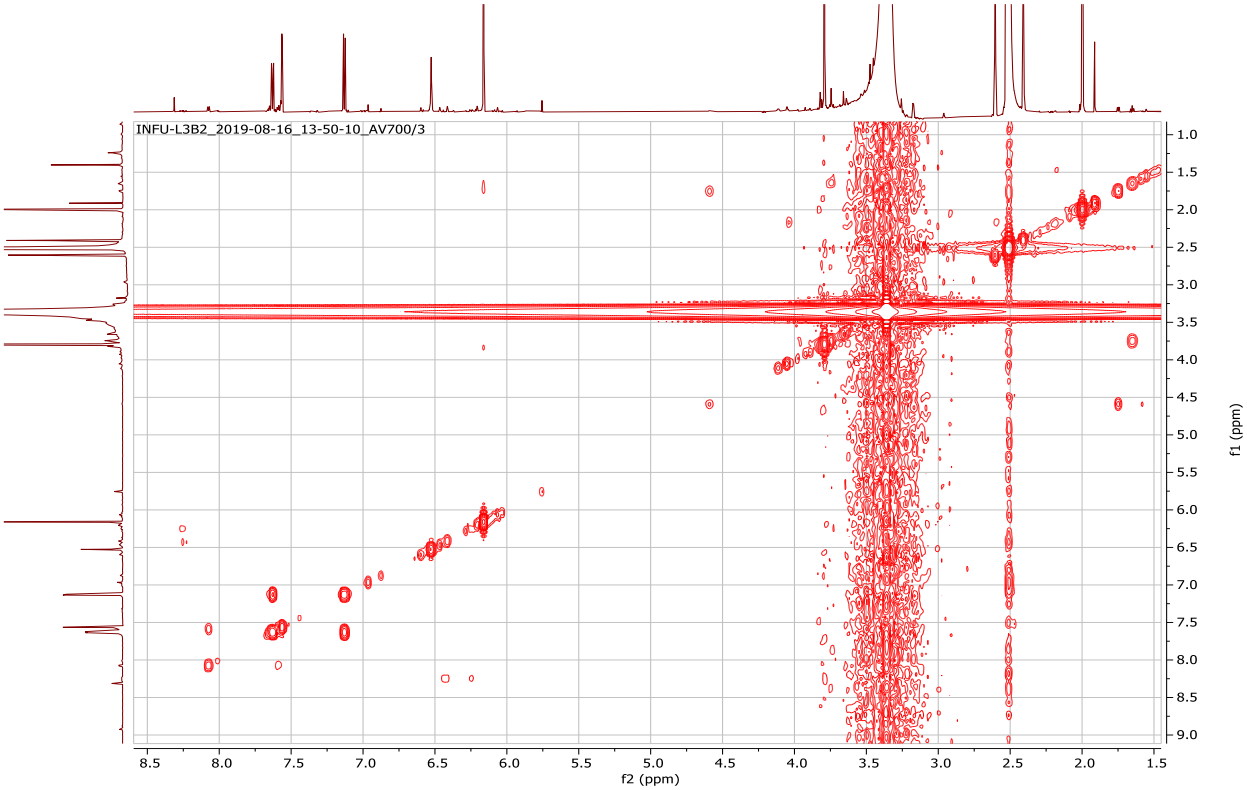

Appendix 31H: HSQC spectrum (DMSO-d_6) of compound **204**

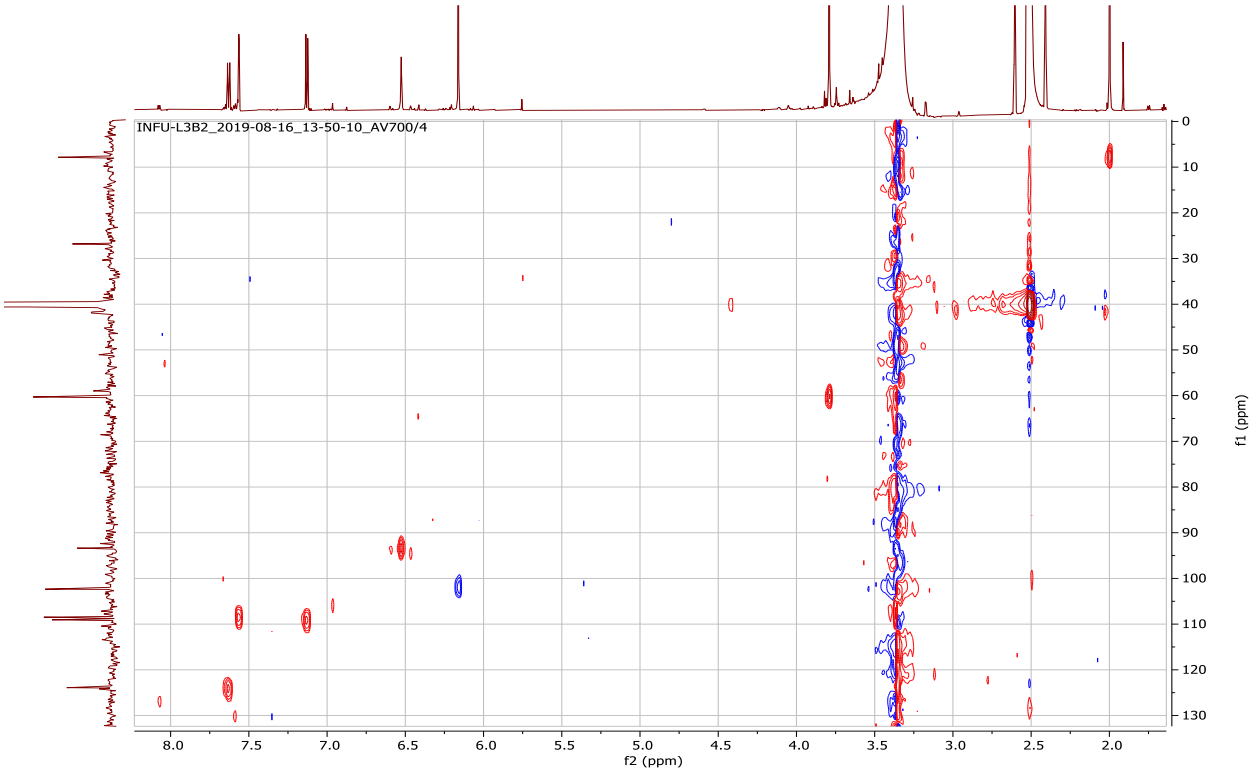

Appendix 31I: HMBC spectrum (DMSO-d_6) of compound **204**

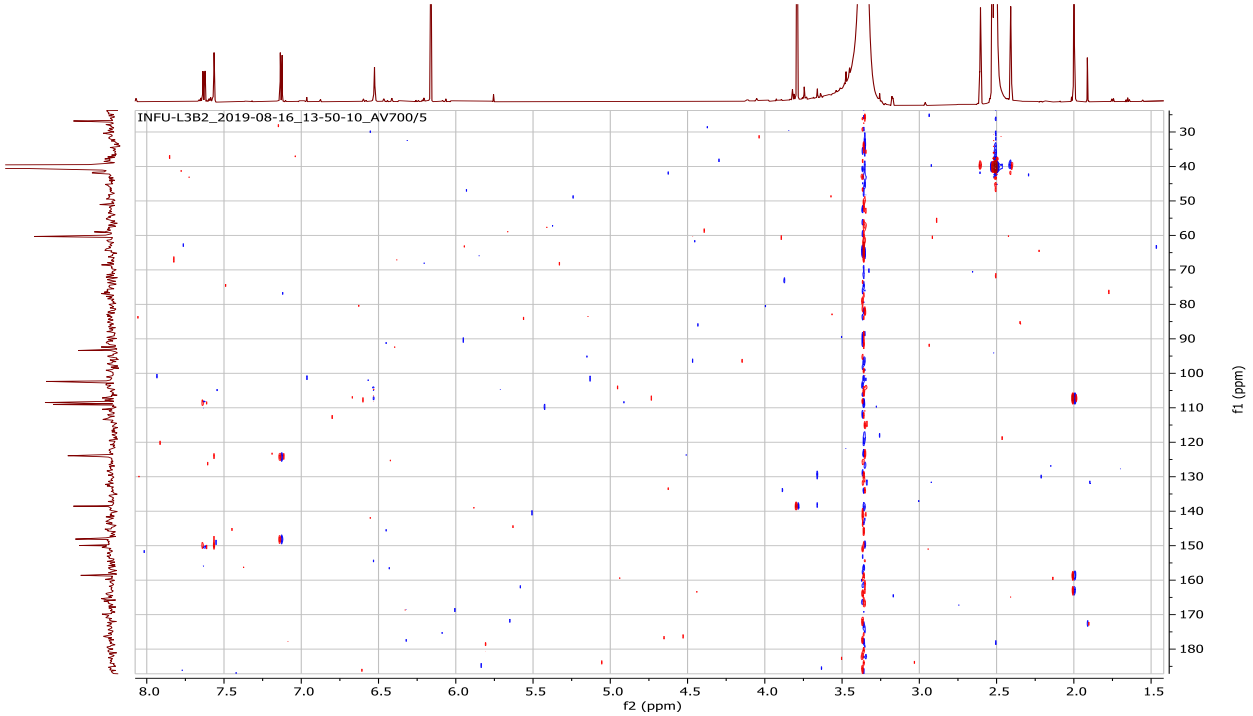

Appendix 32: NMR spectra for 3,5,7-trihydroxy-6-methoxy-3′,4′-methylenedioxyflavone (**205**)

Appendix 32A: HRESIMS of compound **205**

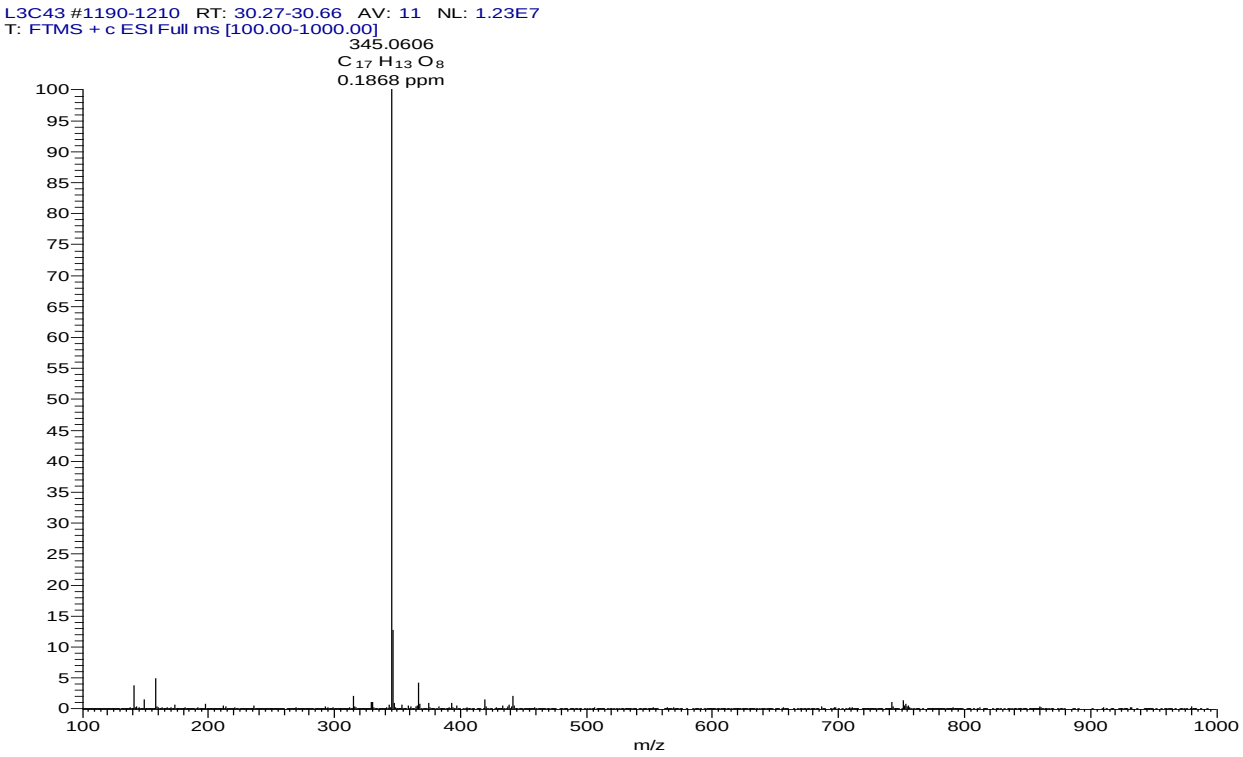

Appendix 32B: HRESIMS/MS of compound **205**

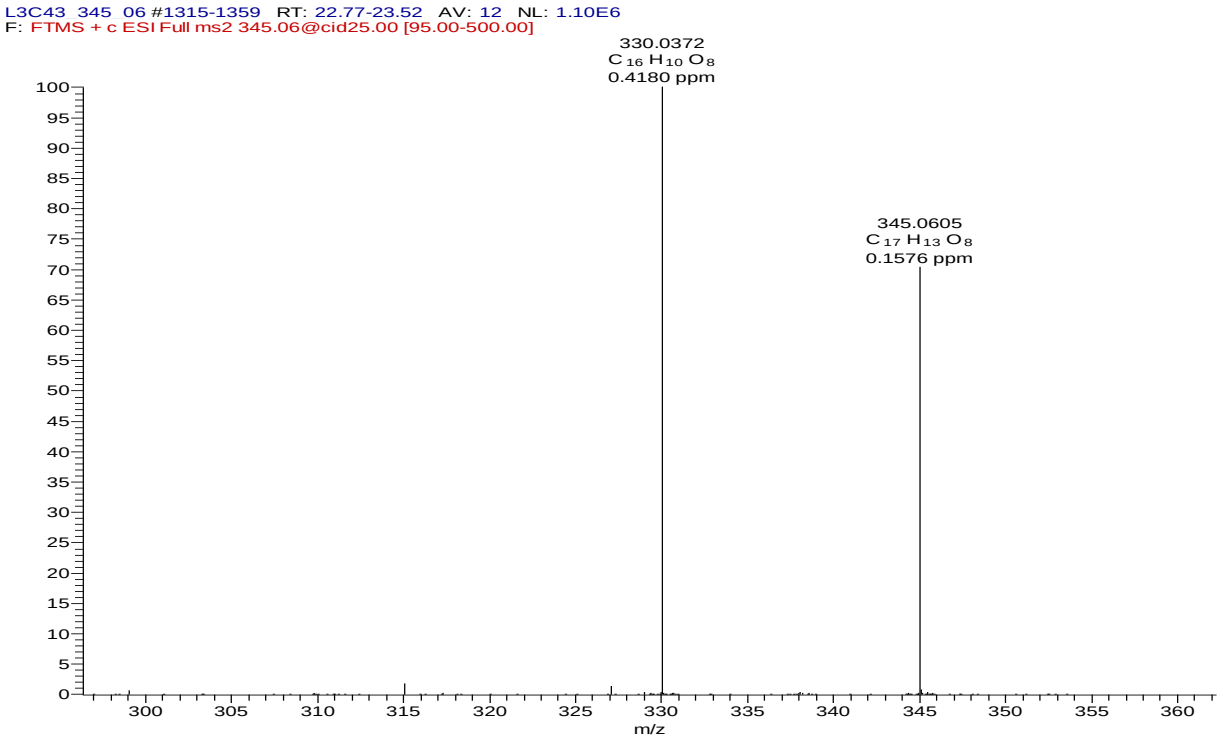

Appendix 32C: LC-UV spectrum of compound **205**

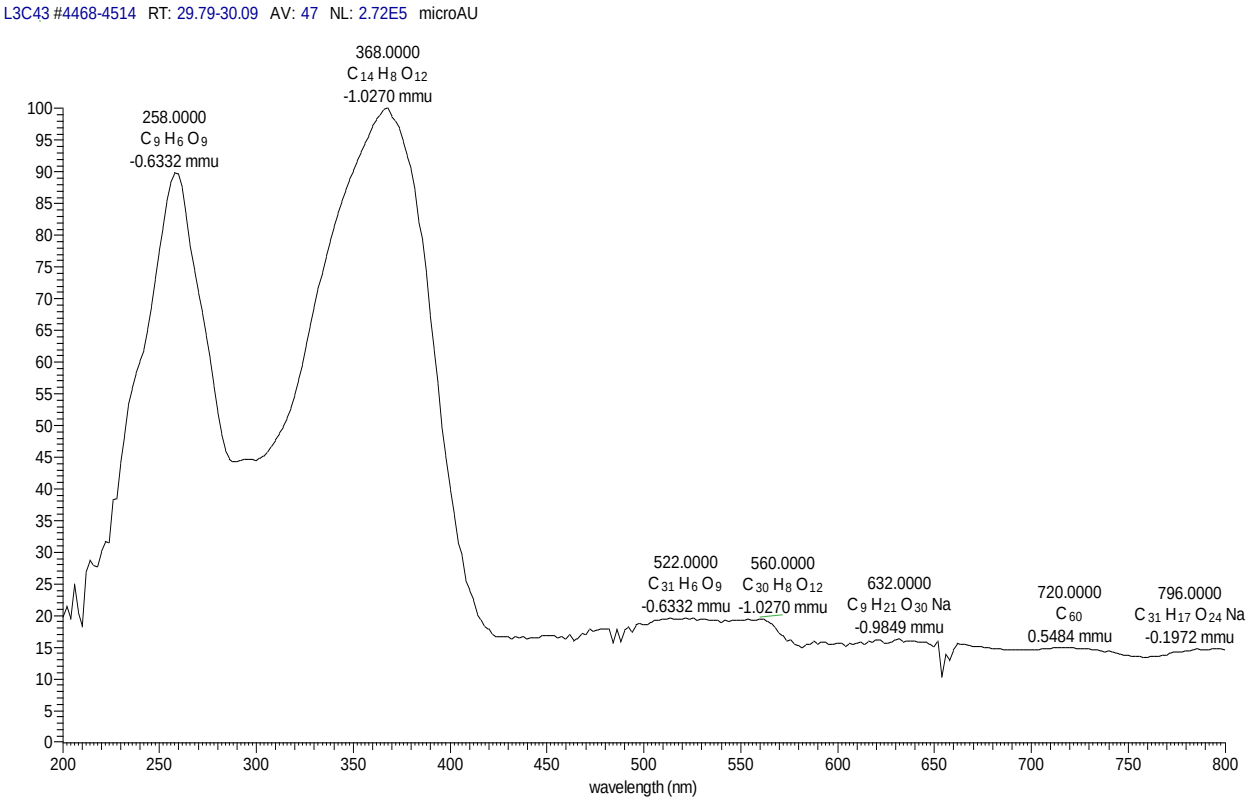

Appendix 32D: FT-IR spectrum of compound **205**

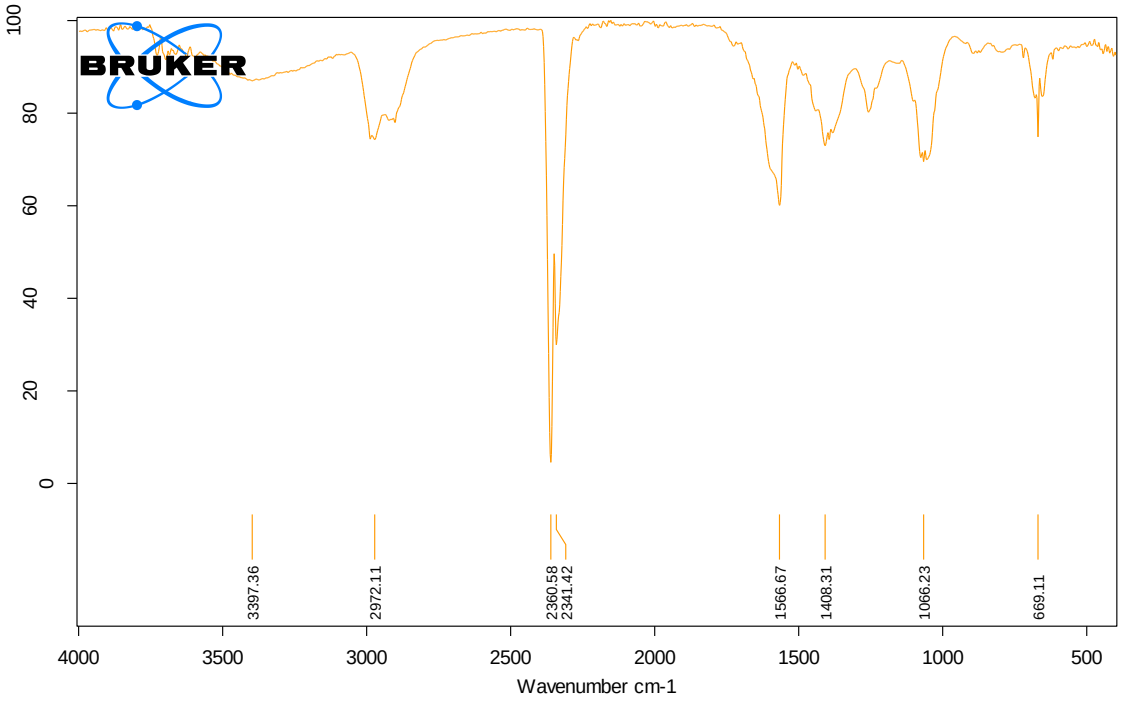

Appendix 32E: ^{1}H NMR spectrum (600 MHz, CD_3OD) of compound **205**

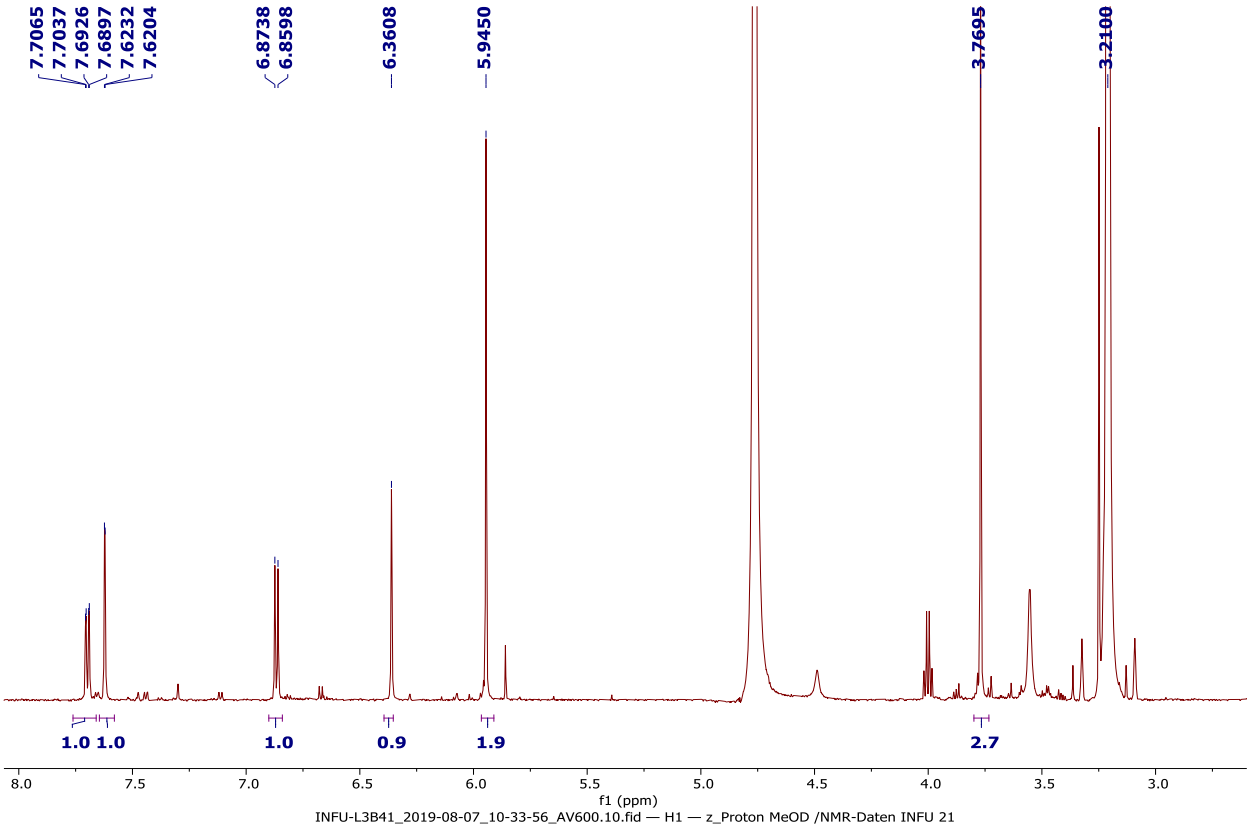

Appendix 32F: ^{13}C NMR spectrum (150 MHz, CD_3OD) of compound **205**

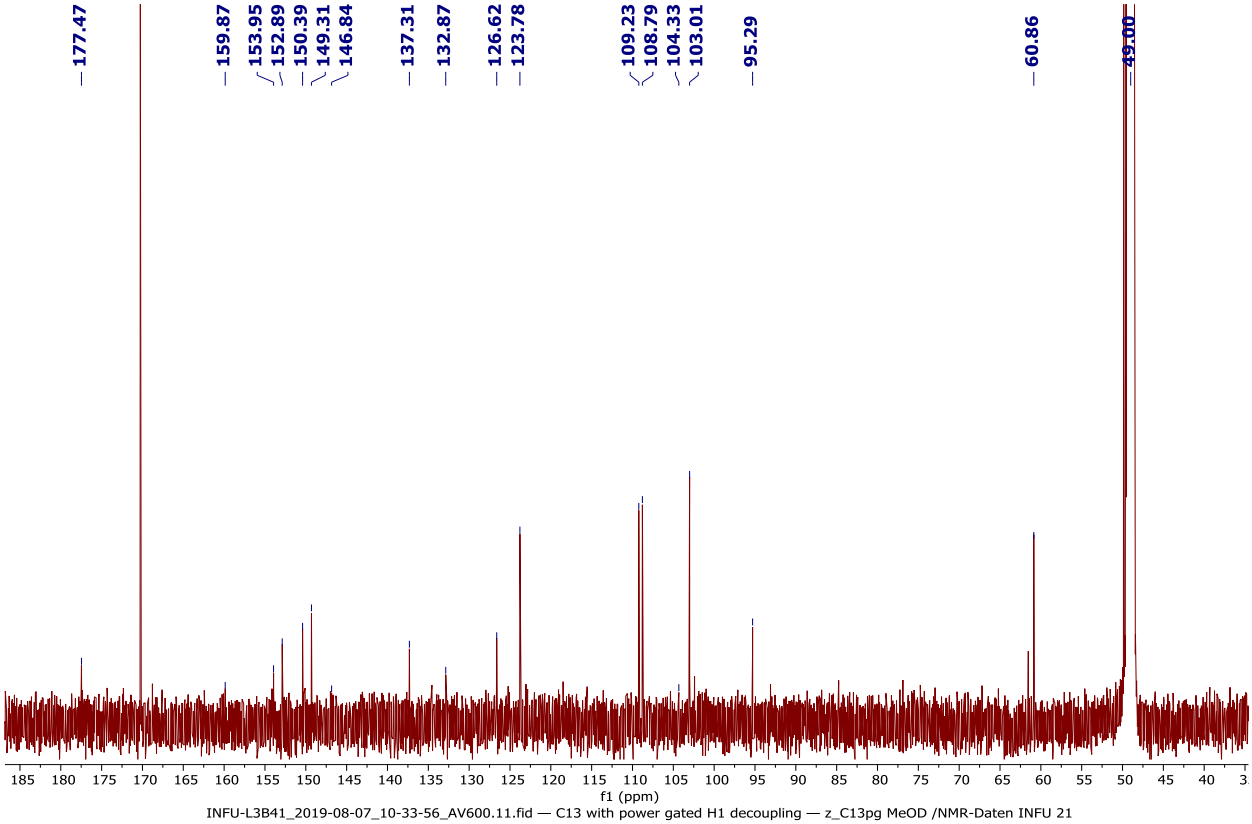

Appendix 32G: ^{1}H-^{1}H COSY spectrum (CD_3OD) of compound **205**

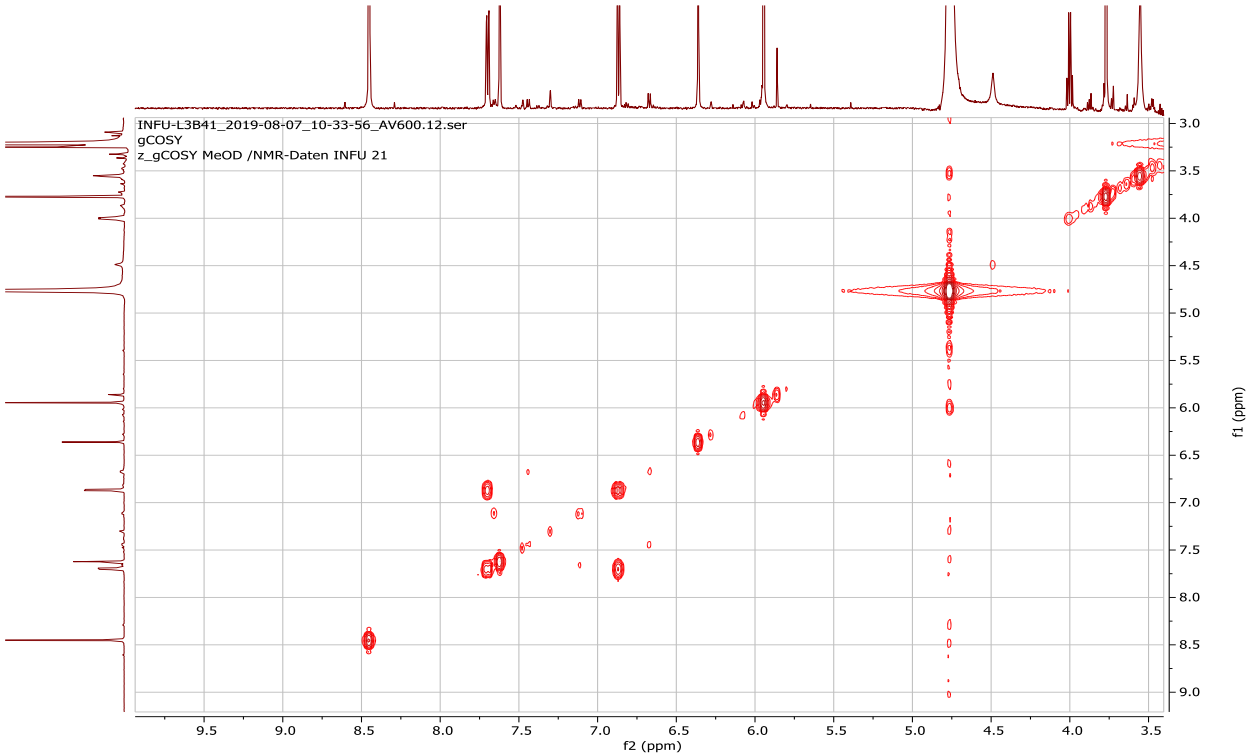

Appendix 32H: HSQC spectrum (CD_3OD) of compound **205**

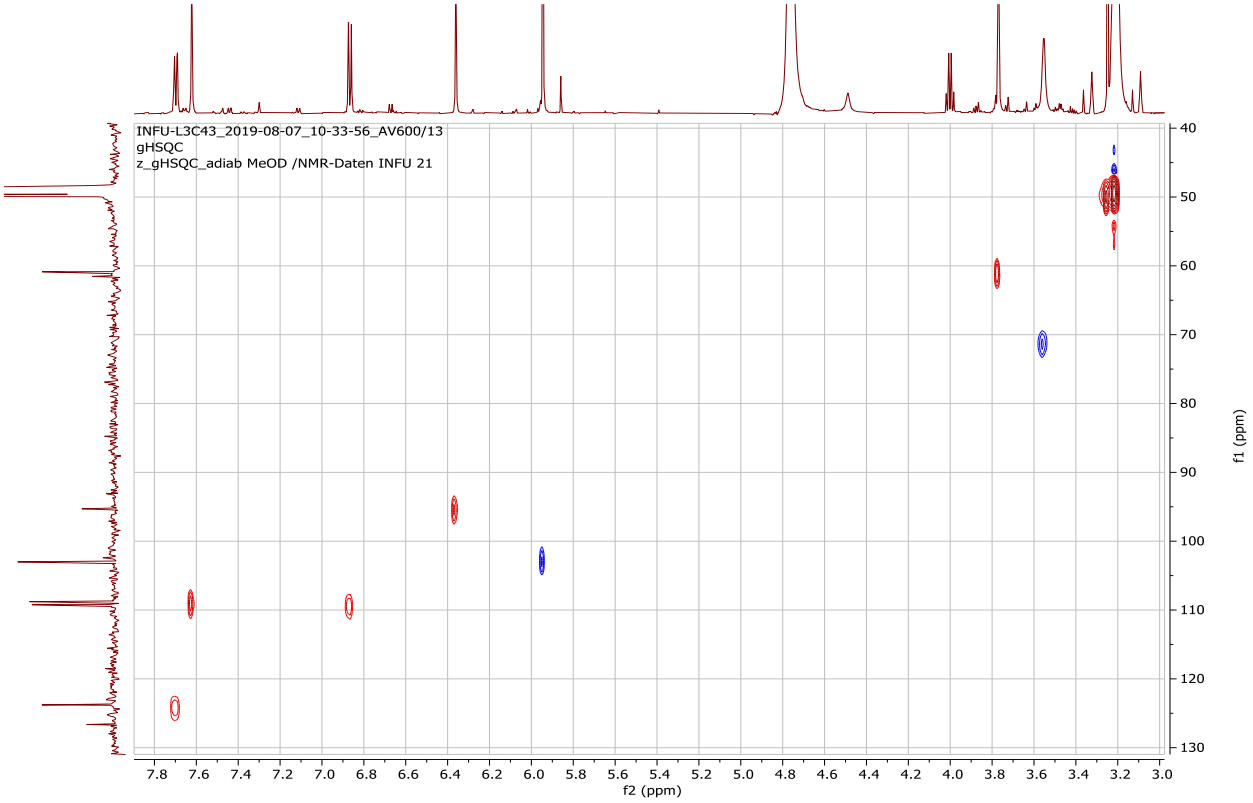

Appendix 32I: HMBC spectrum (CD_3OD) of compound **205**

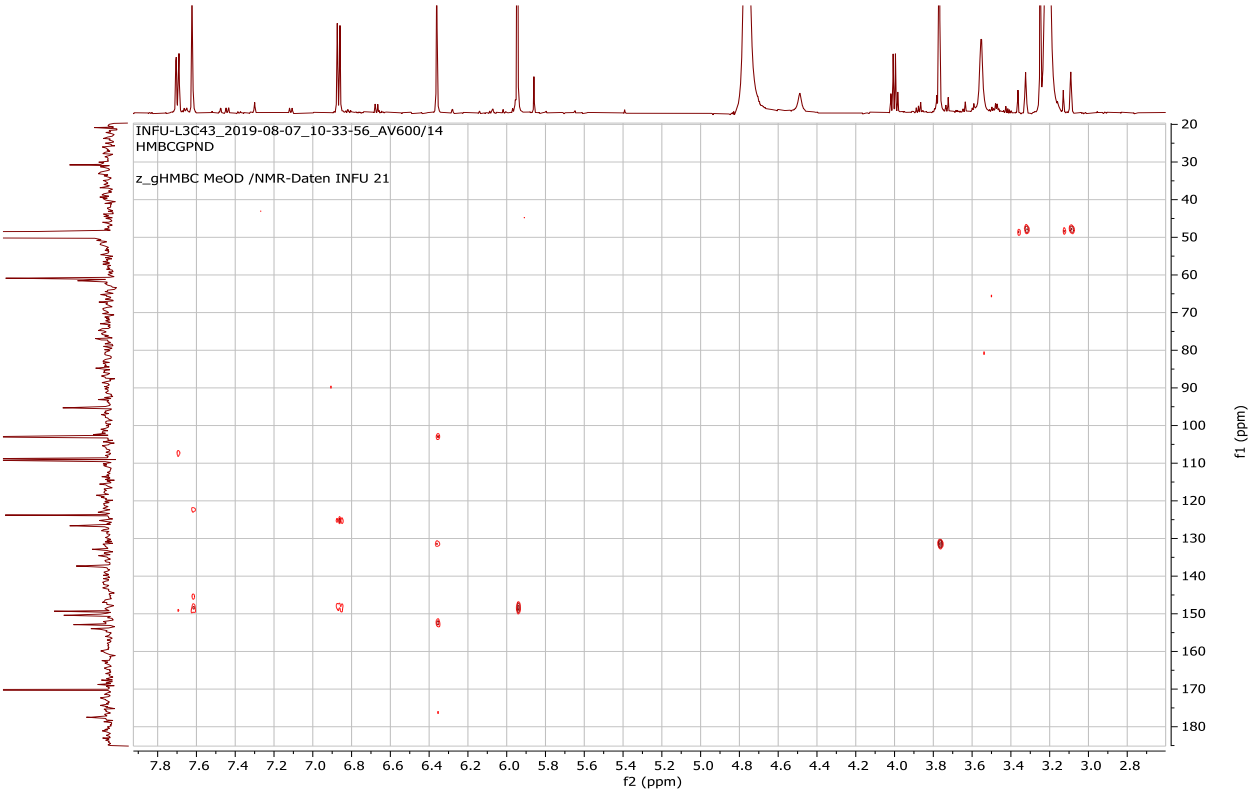

Appendix 33: NMR spectra for (2*S*,3*S*)-3,7-dihydroxy-6-methoxy-3′,4′-methylenedioxyflavanone (**206**)

Appendix 33A: HRESIMS of compound **206**

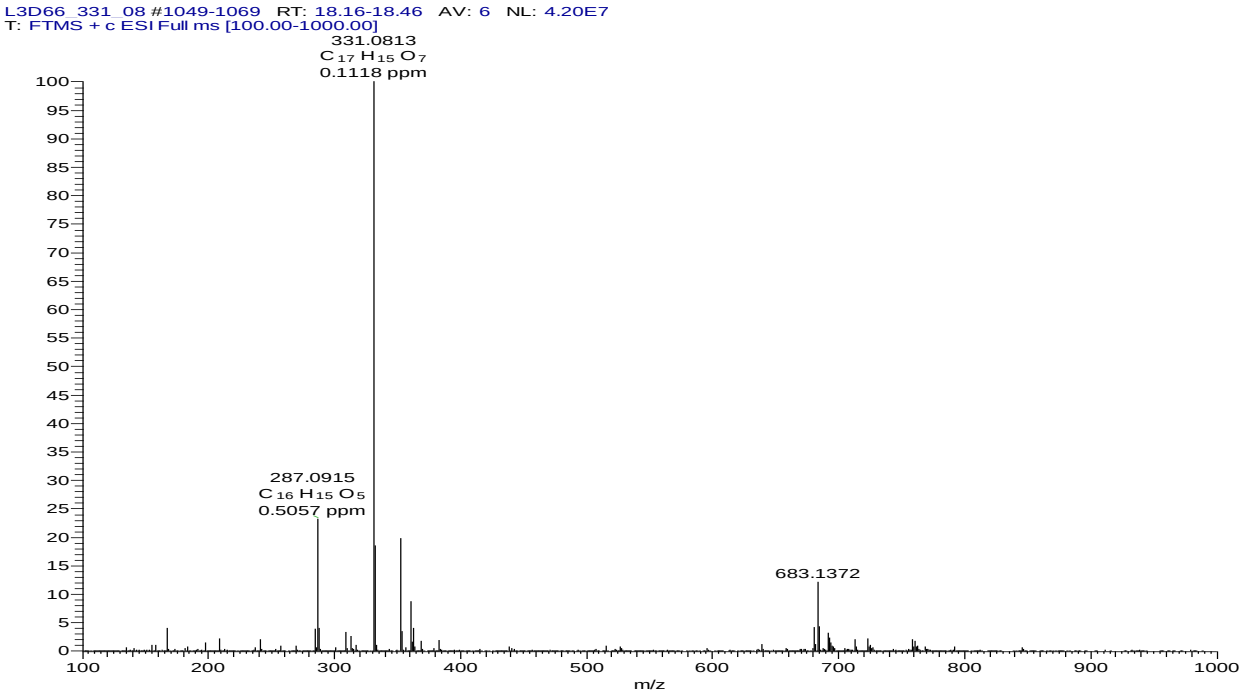

Appendix 33B: HRESIMS/MS of compound **206**

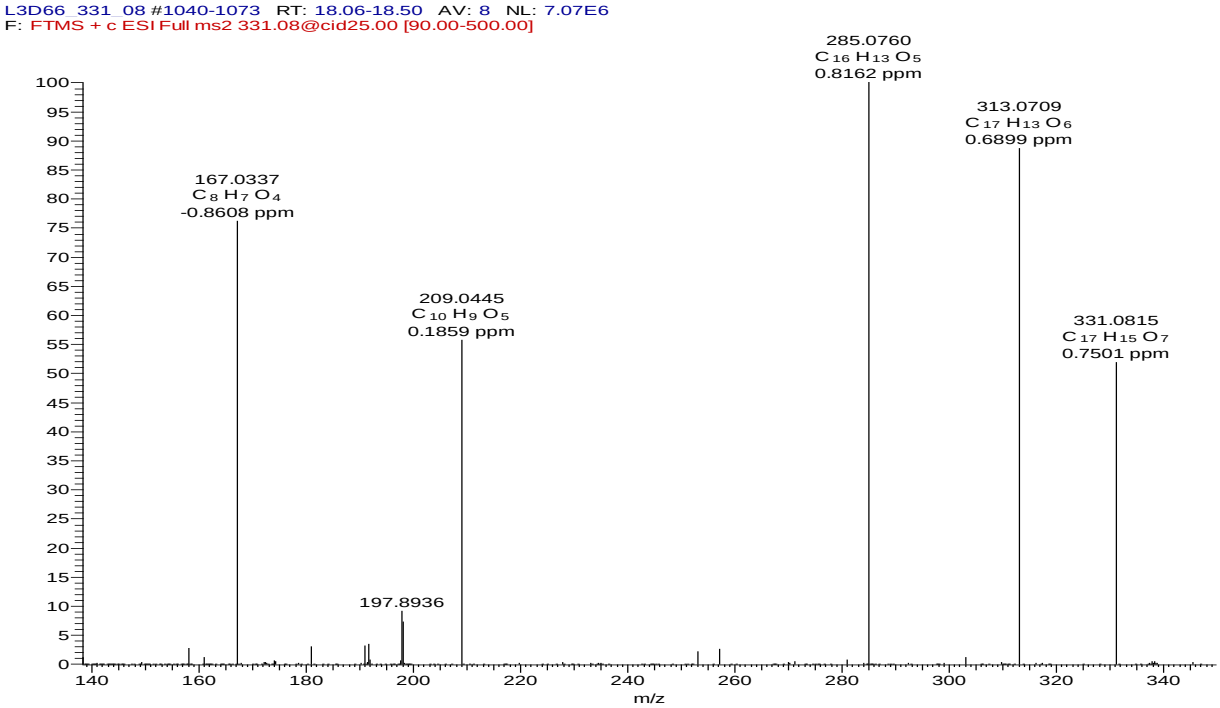

Appendix 33C: LC-UV spectrum of compound **206**

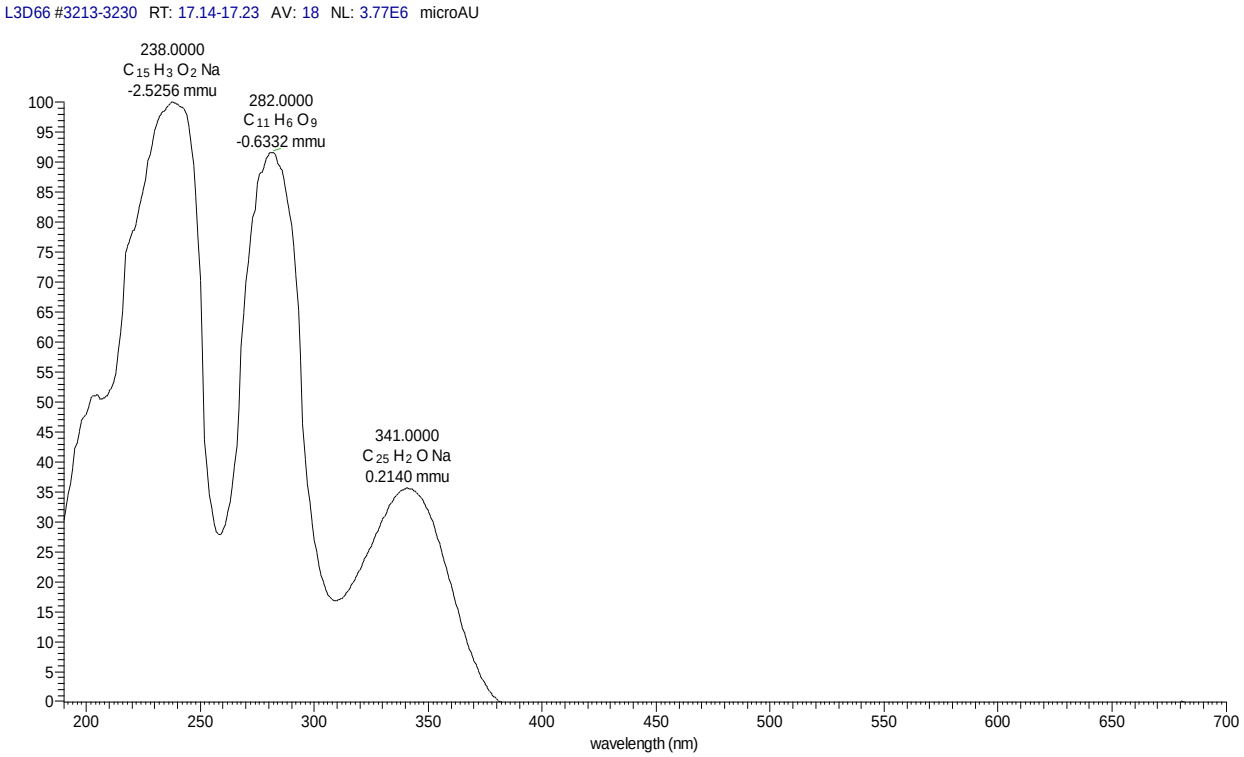

Appendix 33D: FT-IR spectrum of compound **206**

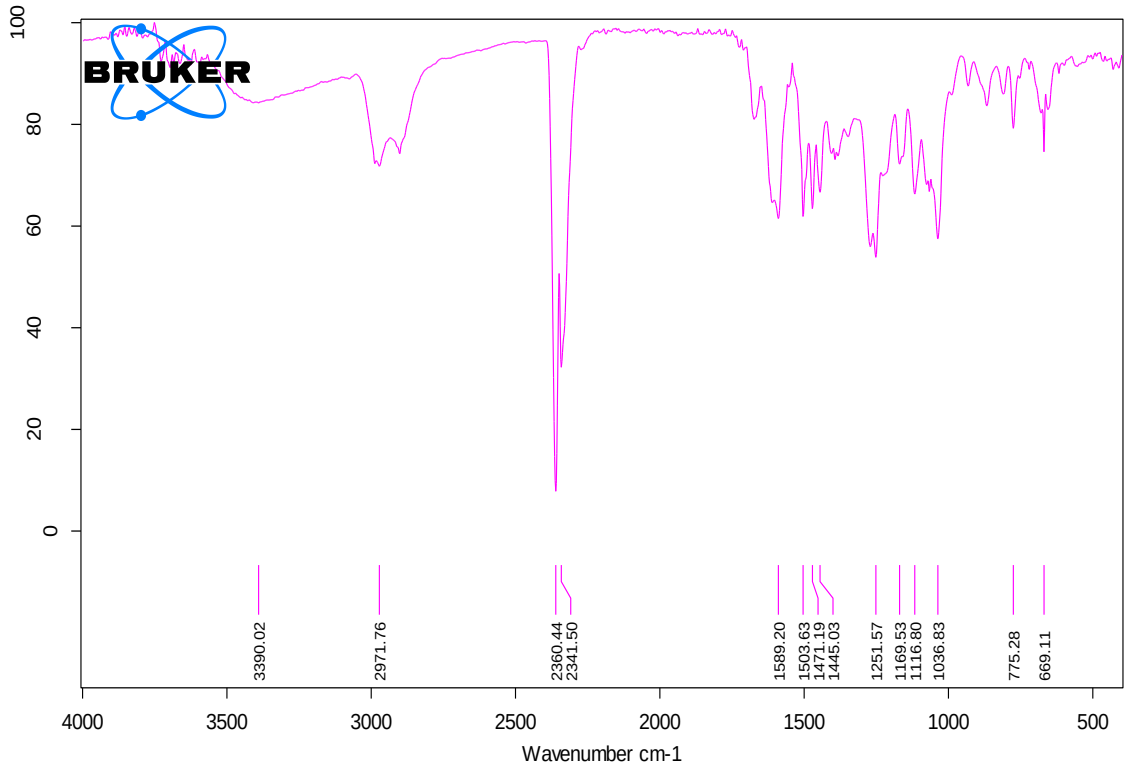

Appendix 33E: ^{1}H NMR spectrum (600 MHz, CD_3OD) of compound **206**

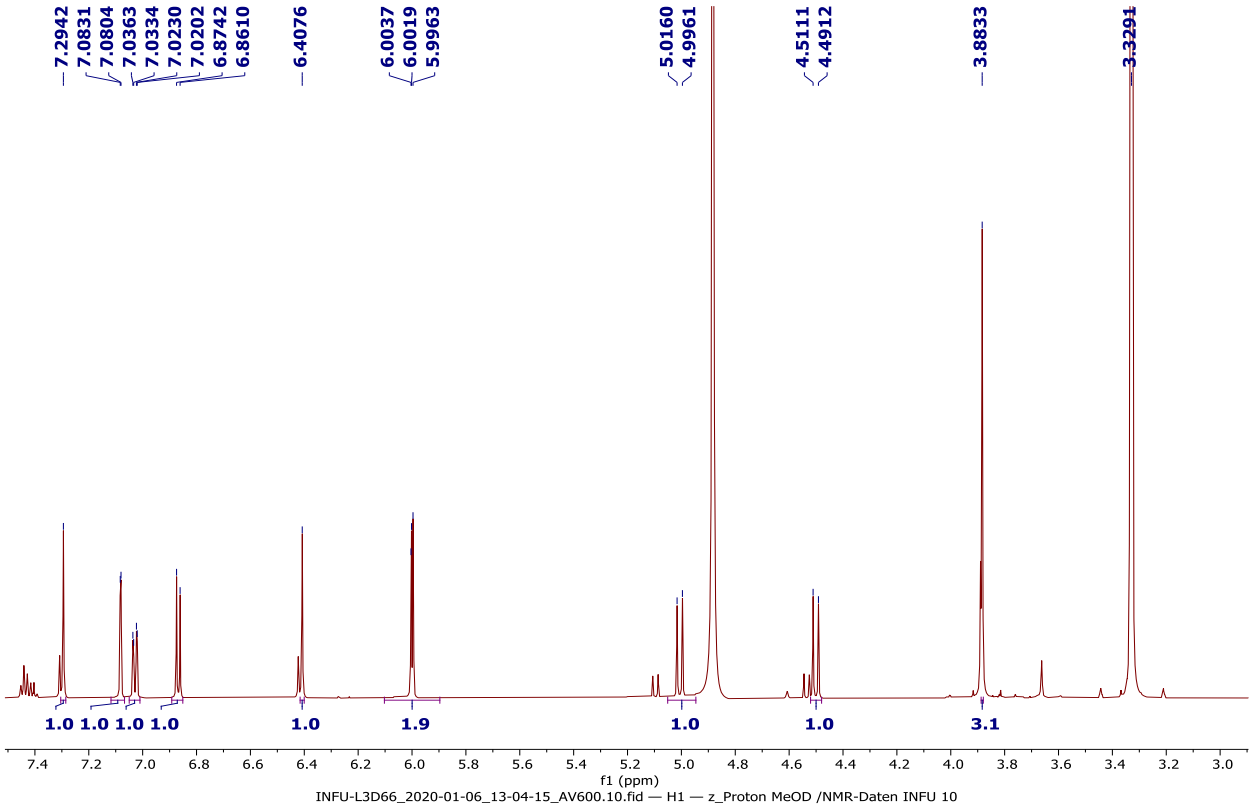

Appendix 33F: ^{13}C NMR spectrum (150 MHz, CD_3OD) of compound **206**

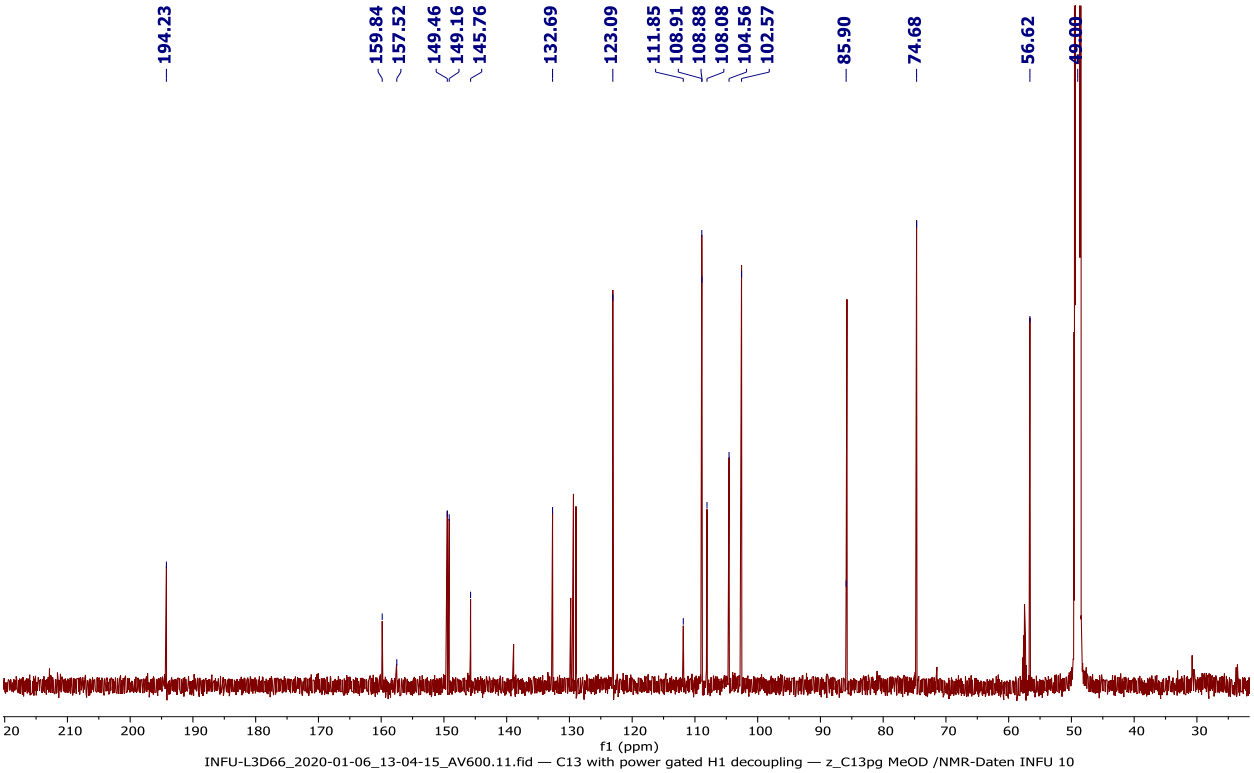

Appendix 33G: ^{1}H-^{1}H COSY spectrum (CD_3OD) of compound **206**

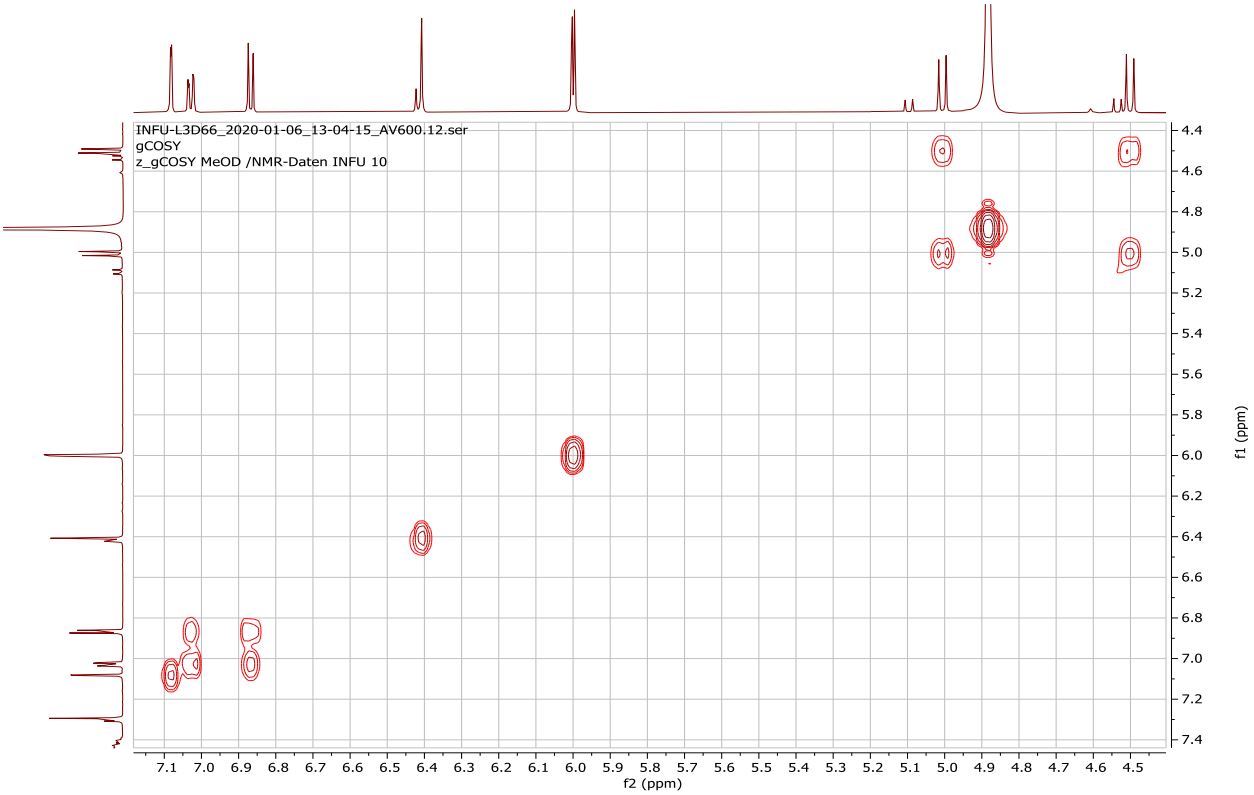

Appendix 33H: NOESY spectrum (CD_3OD) of compound **206**

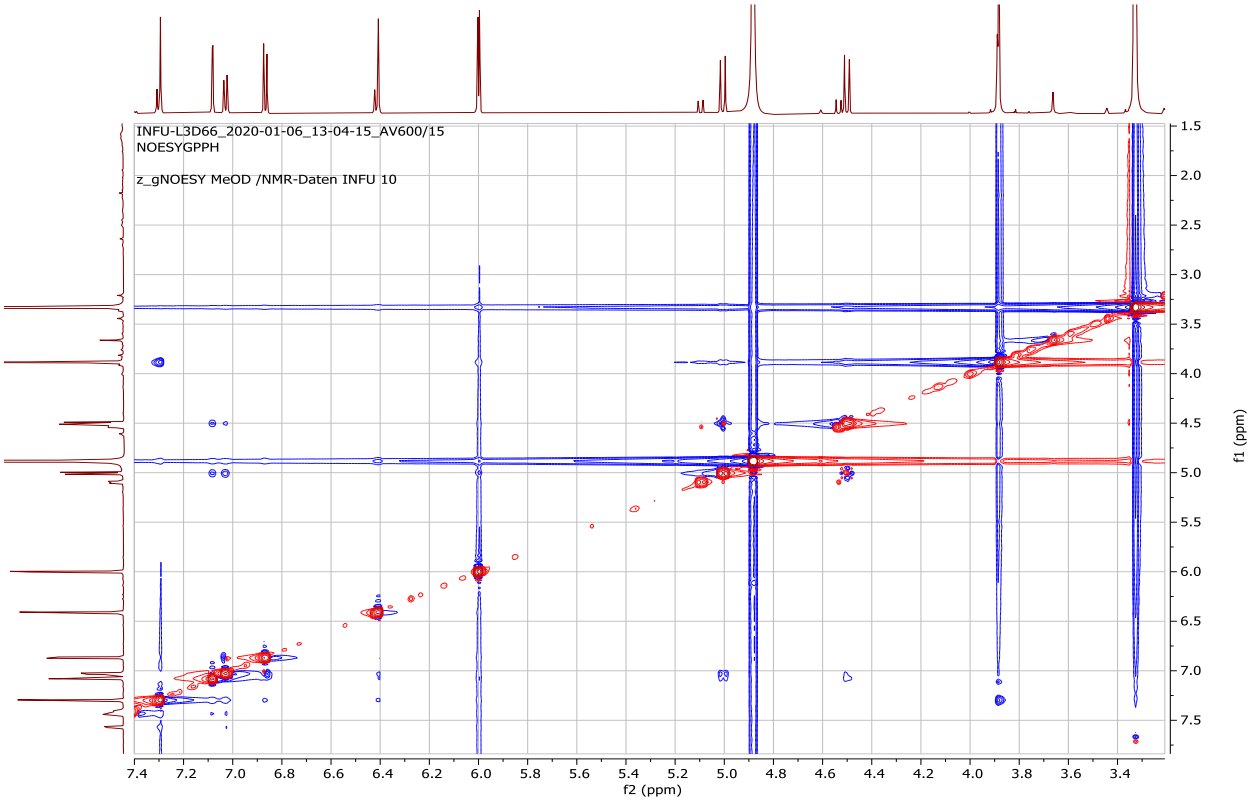

Appendix 33I: HSQC spectrum (CD_3OD) of compound **206**

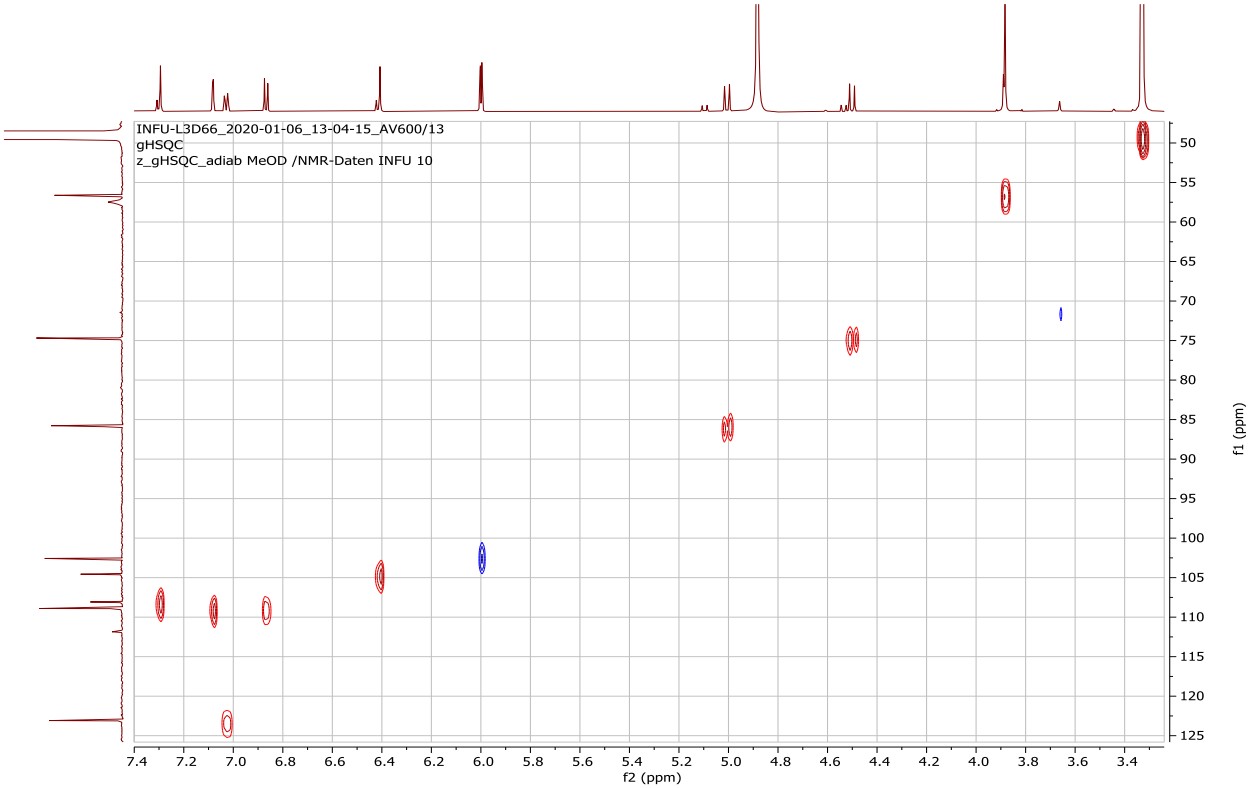

Appendix 33J: HMBC spectrum (CD_3OD) of compound **206**

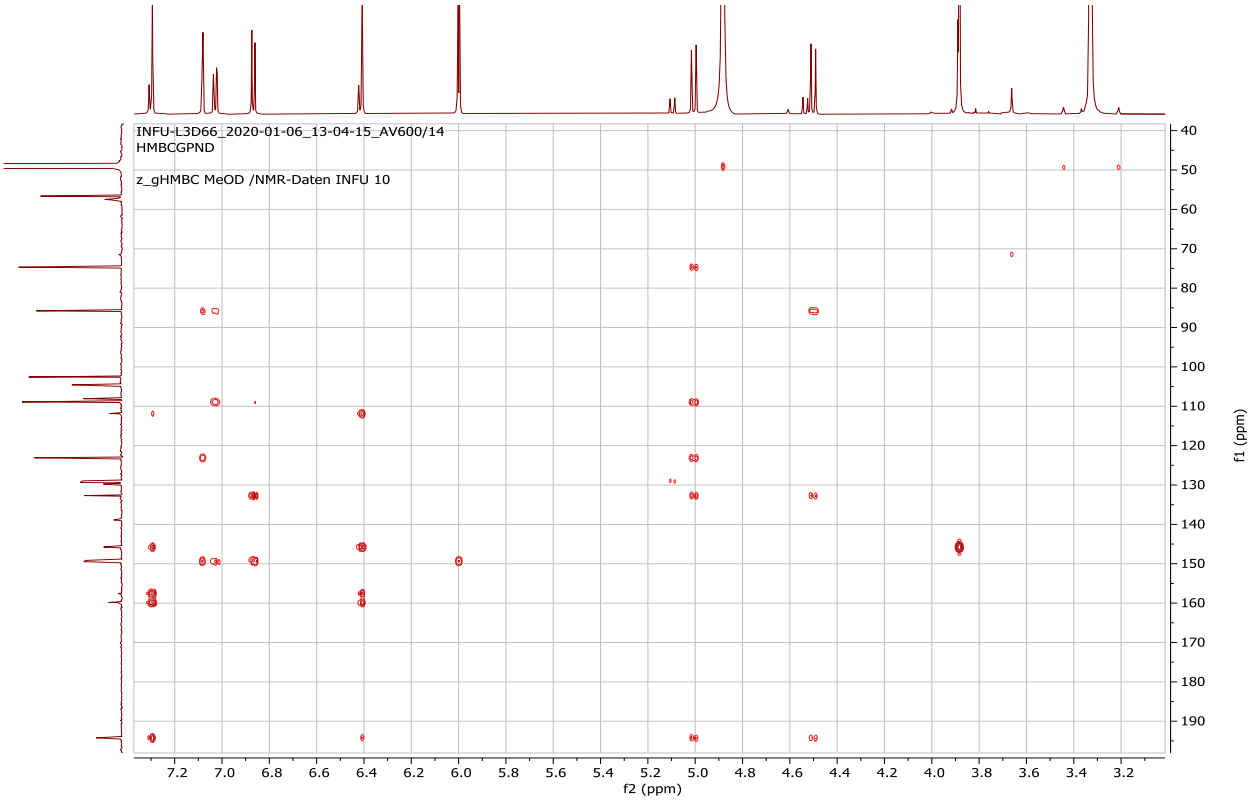

Appendix 34: NMR spectra for 4′,5,7-trihydroxy-3,3′,8-trimethoxy-6-methylflavone (**207**)

Appendix 34A: HRESIMS of compound **207**

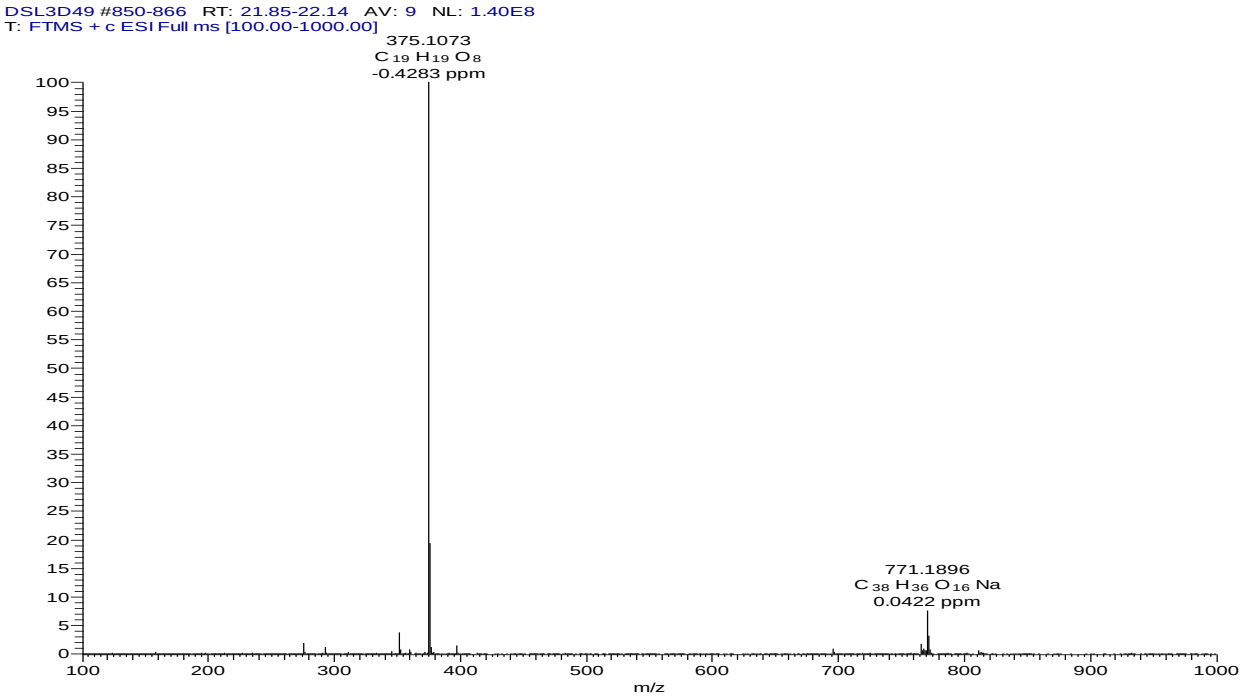

Appendix 34B: HRESIMS/MS of compound **207**

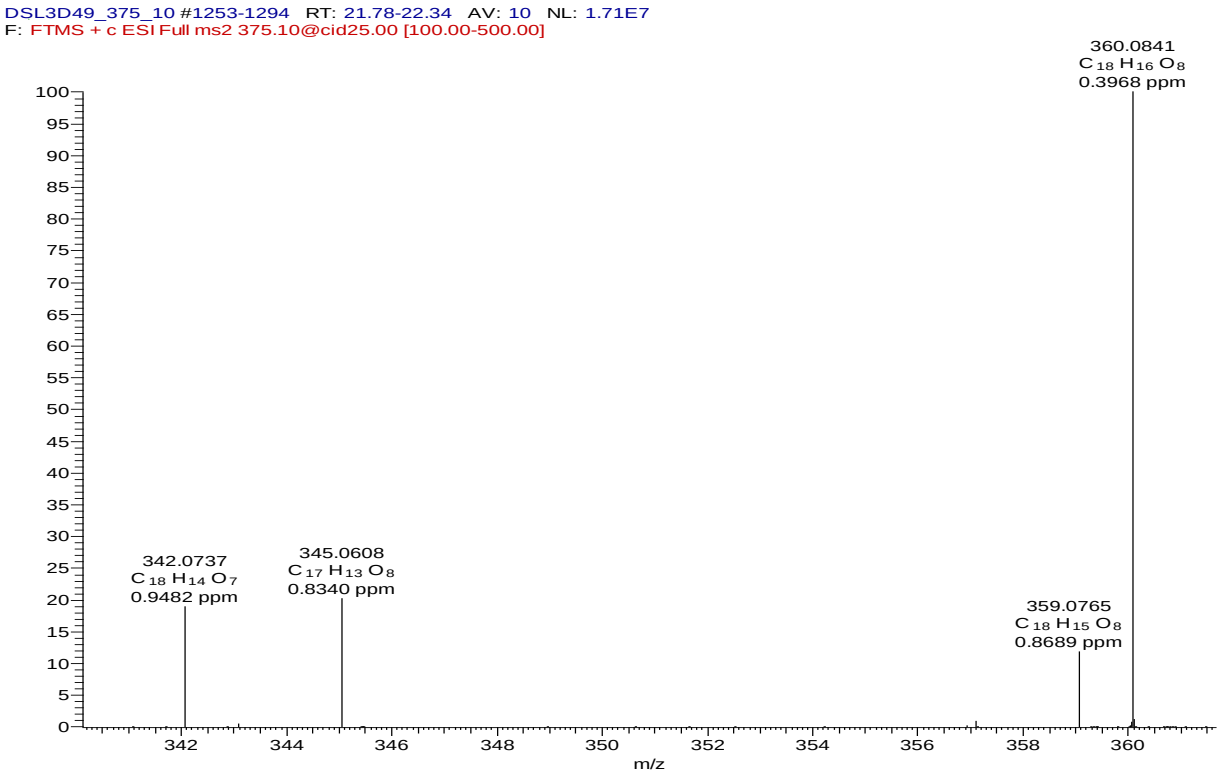

Appendix 34C: LC-UV spectrum of compound **207**

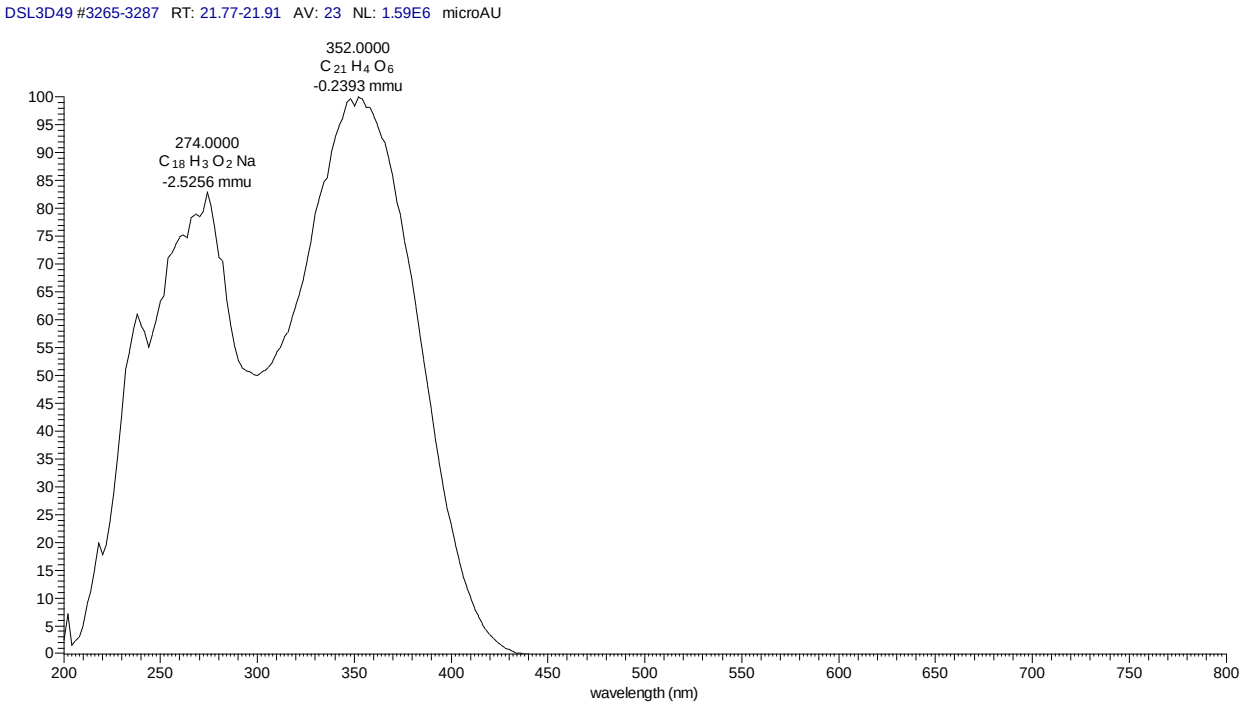

Appendix 34D: FT-IR spectrum of compound **207**

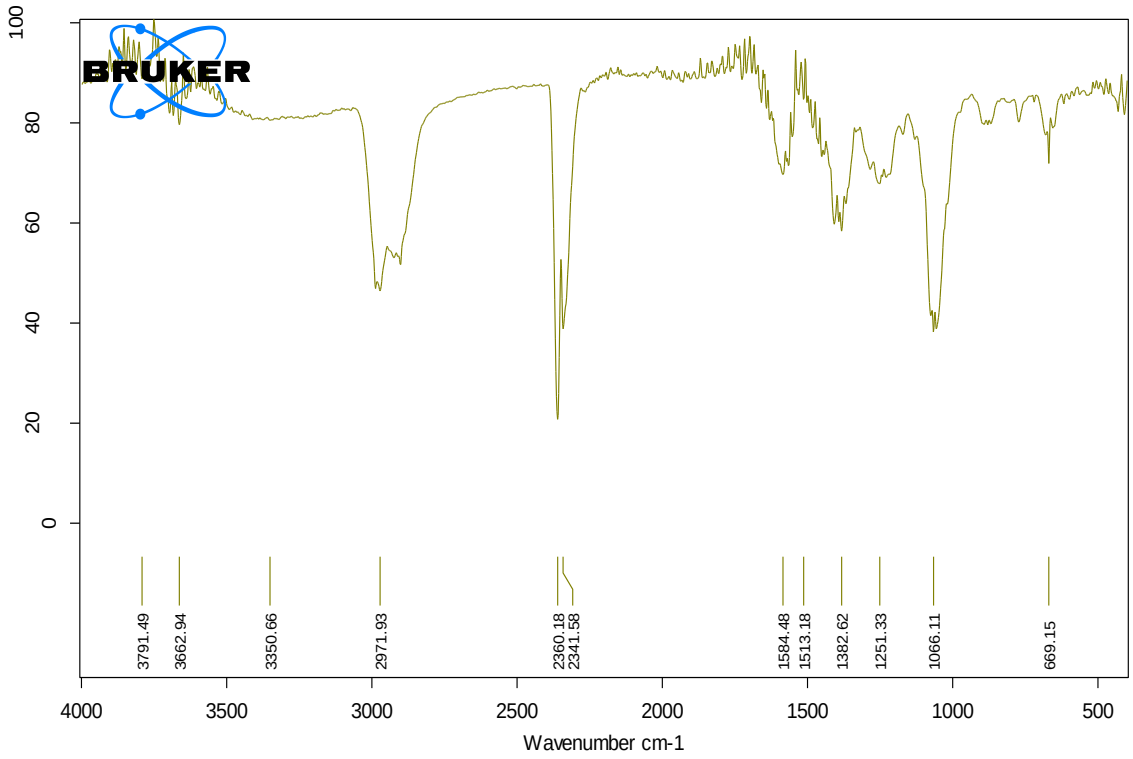

Appendix 34E: ^{1}H NMR spectrum (700 MHz, CD_3OD) of compound **207**

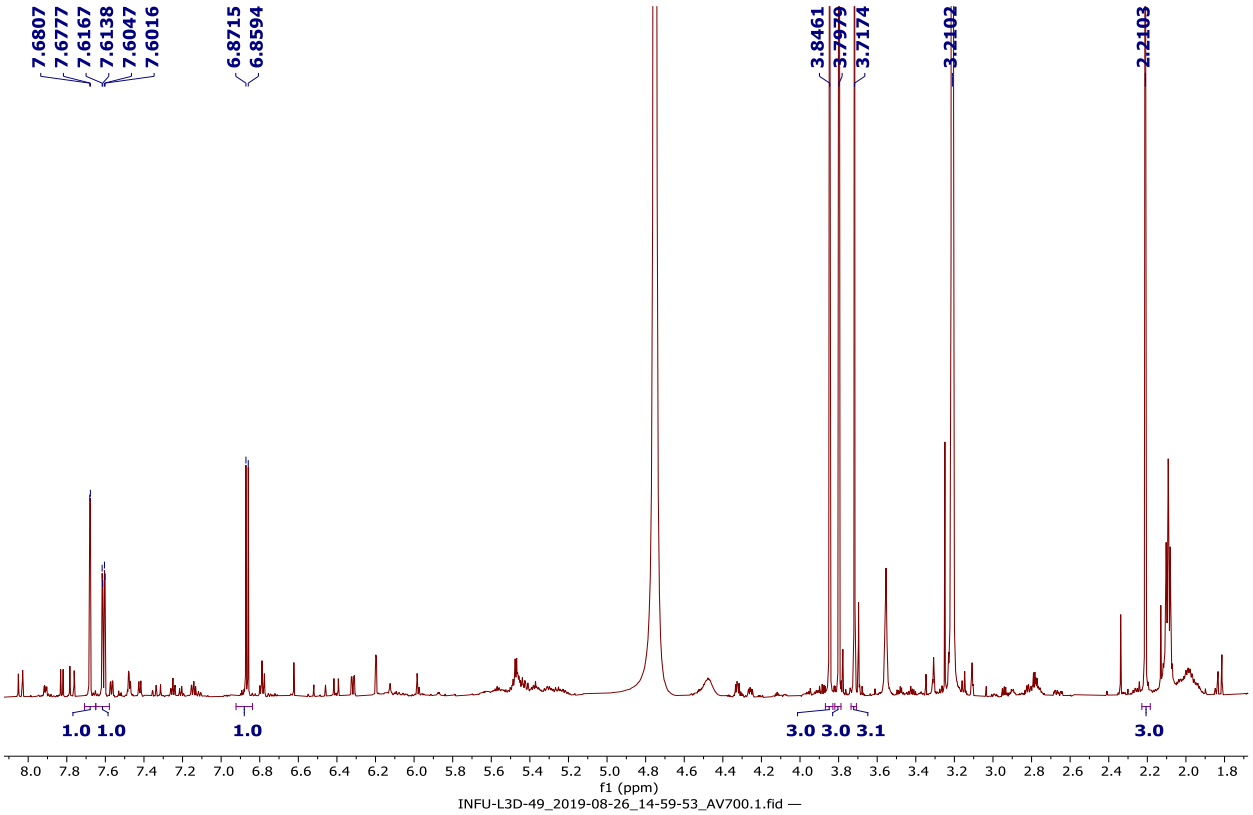

Appendix 34F: ^{13}C NMR spectrum (175 MHz, CD_3OD) of compound **207**

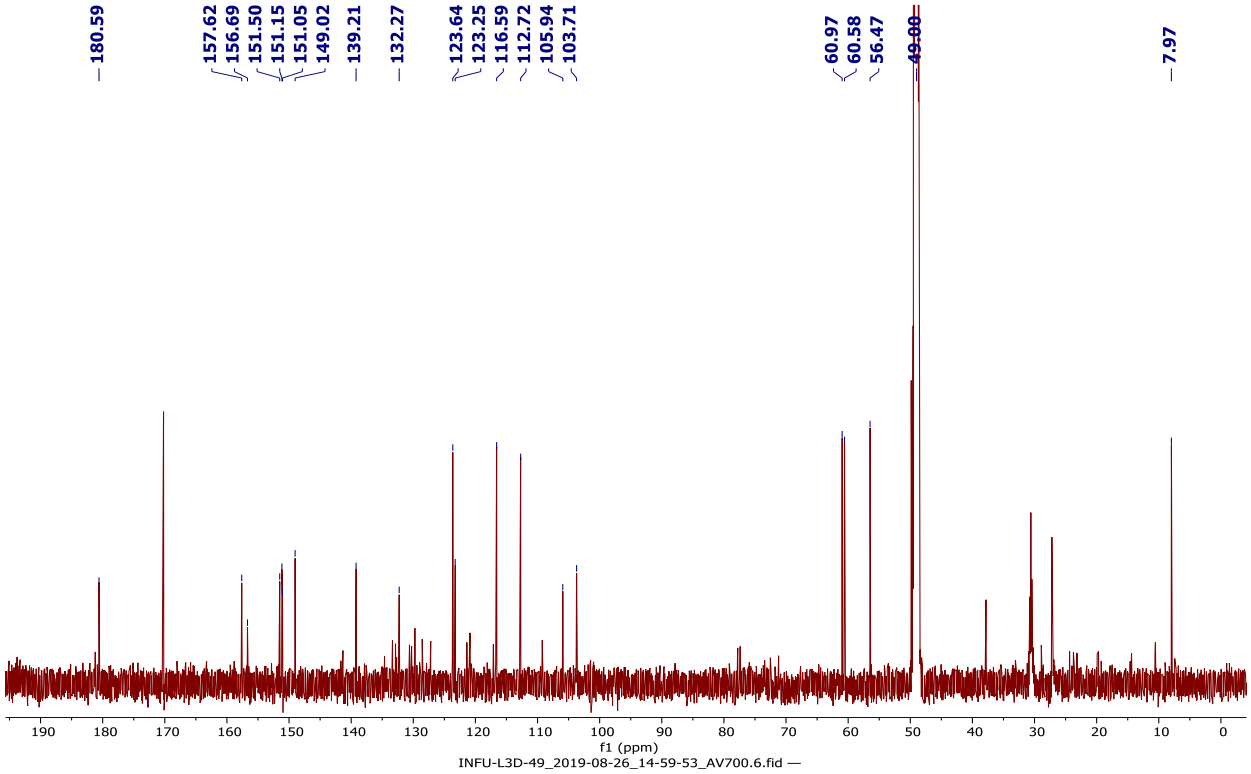

Appendix 34G: ^{1}H-^{1}H COSY spectrum (CD_3OD) of compound **207**

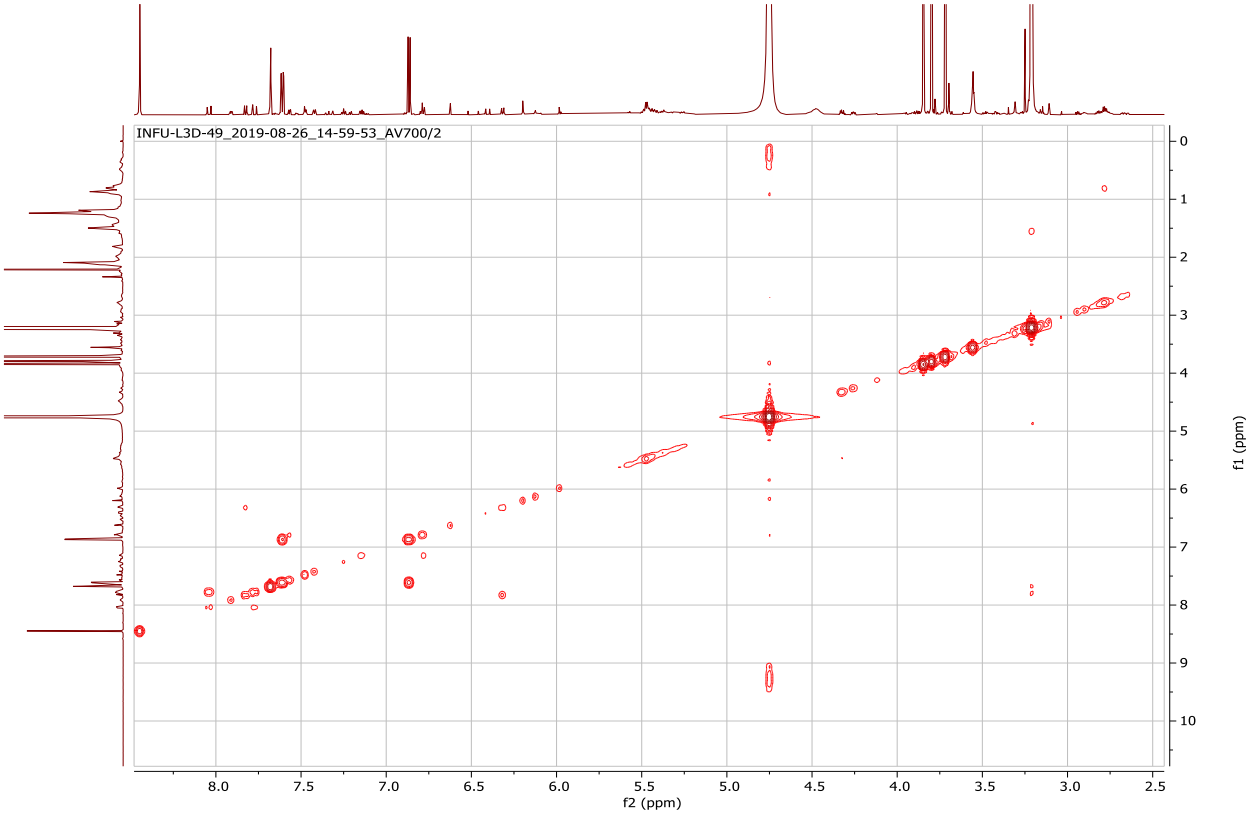

Appendix 34H: NOESY spectrum (CD_3OD) of compound **207**

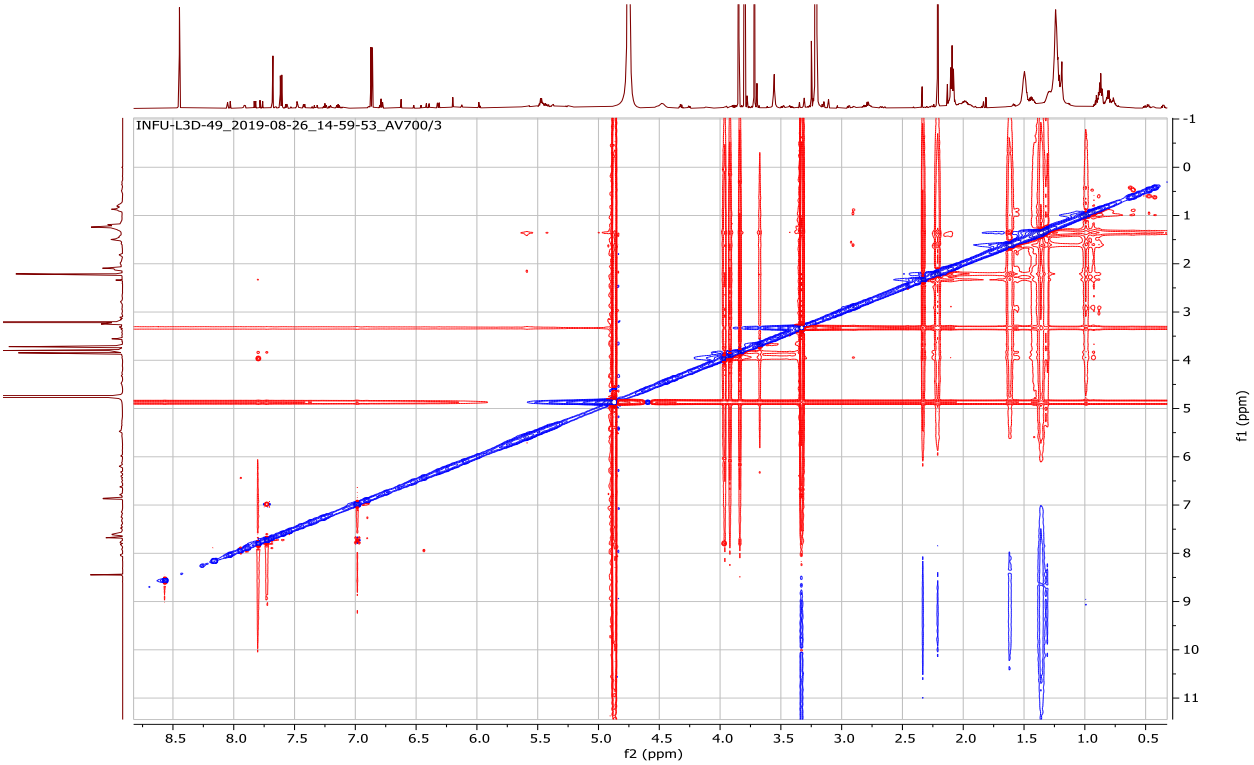

Appendix 34I: HSQC spectrum (CD_3OD) of compound **207**

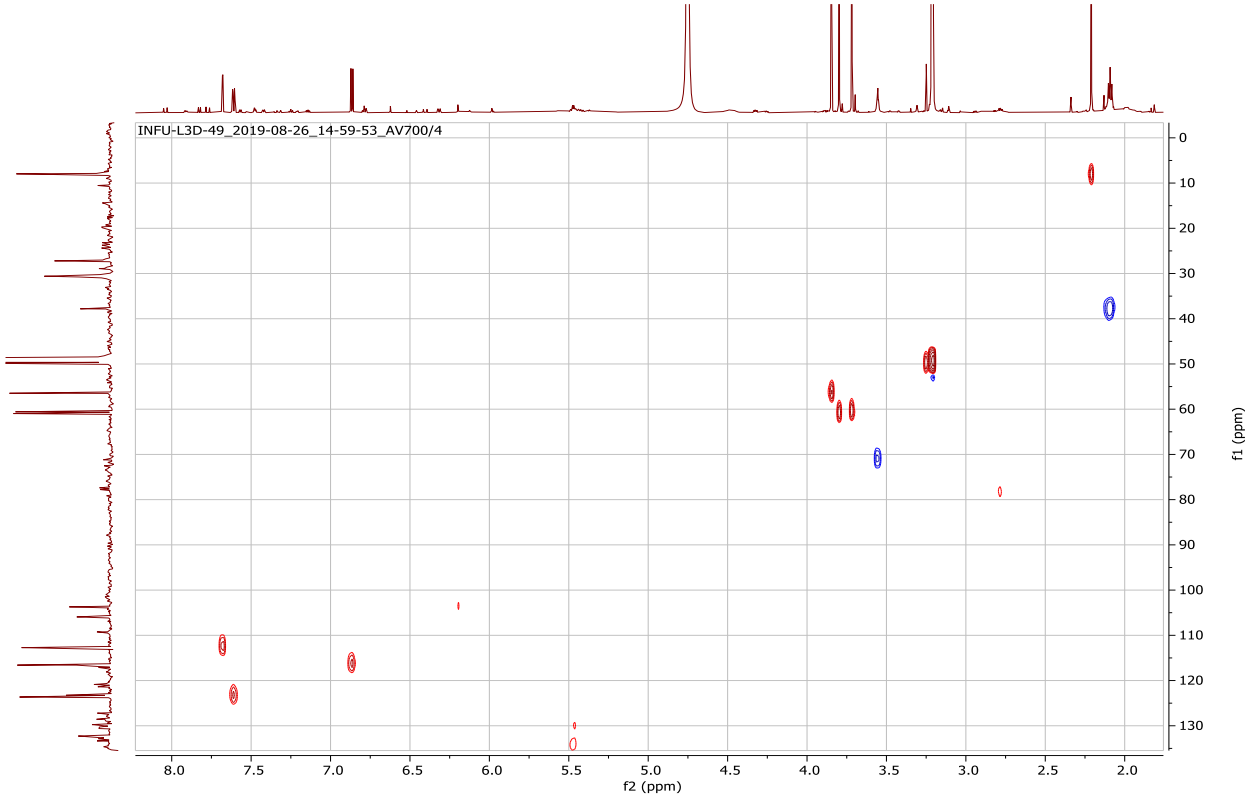

Appendix 34J: HMBC spectrum (CD_3OD) of compound **207**

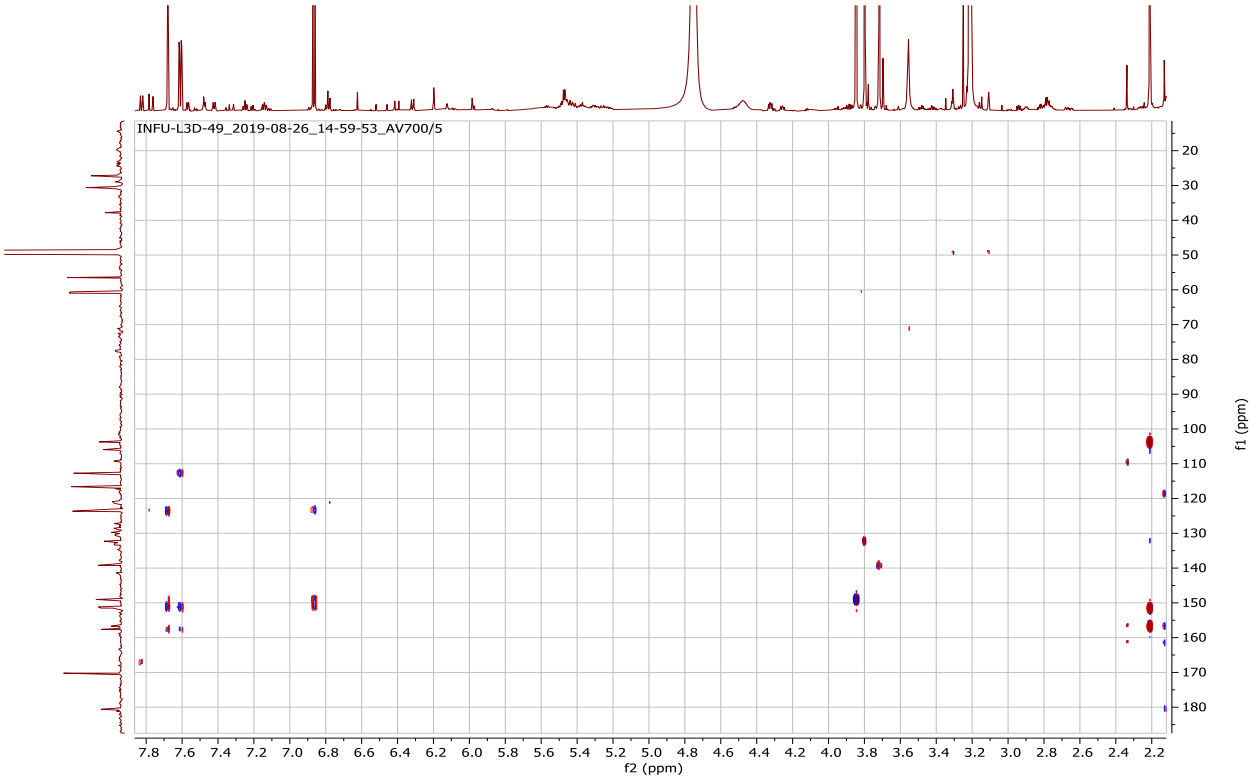

Appendix 35: NMR spectra for (2*R*) 7-hydroxy- 2′,8-dimethoxyflavanone (**208**)

Appendix 35A: HRESIMS of compound **208**

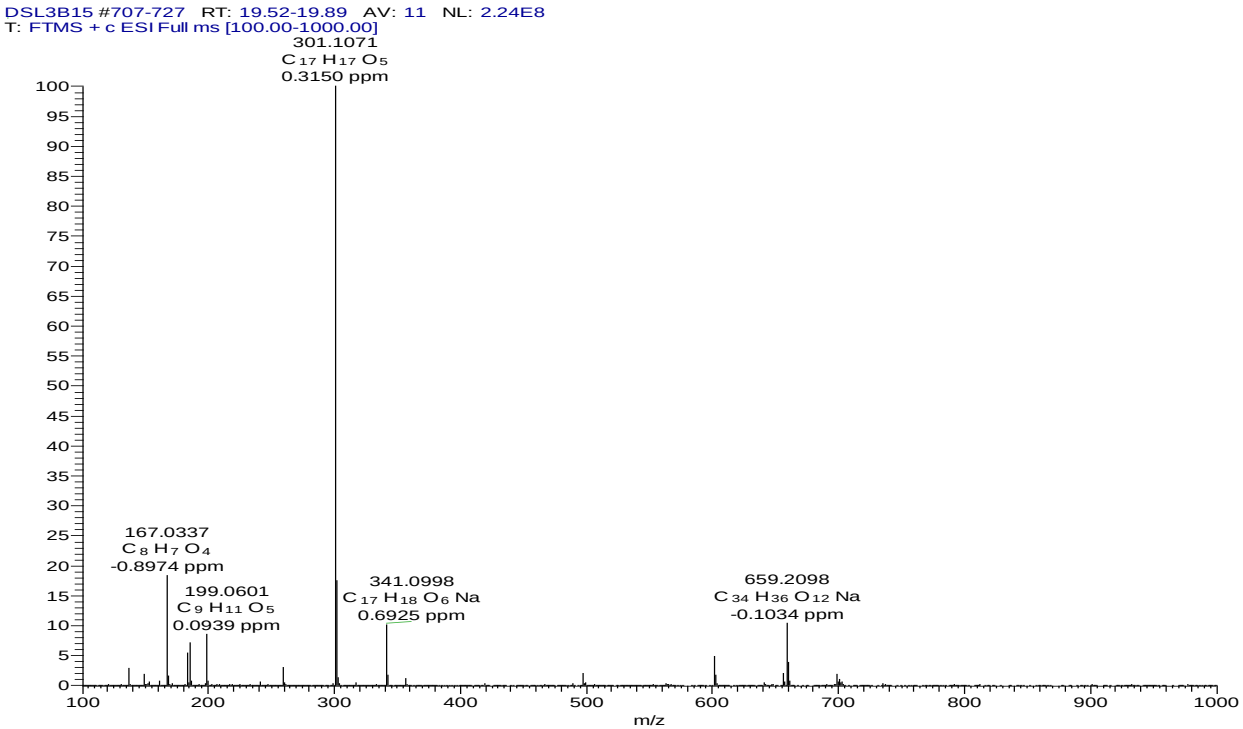

Appendix 35B: HRESIMS/MS of compound **208**

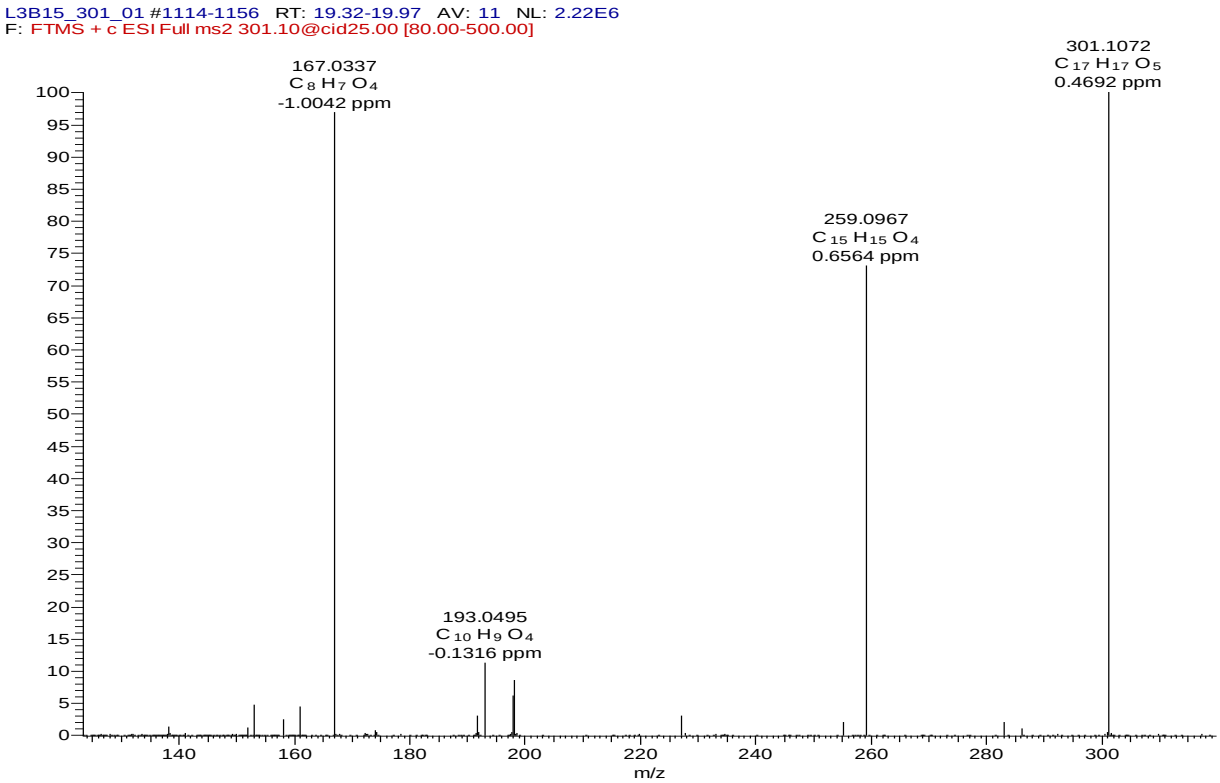

Appendix 35C: LC-UV spectrum of compound **208**

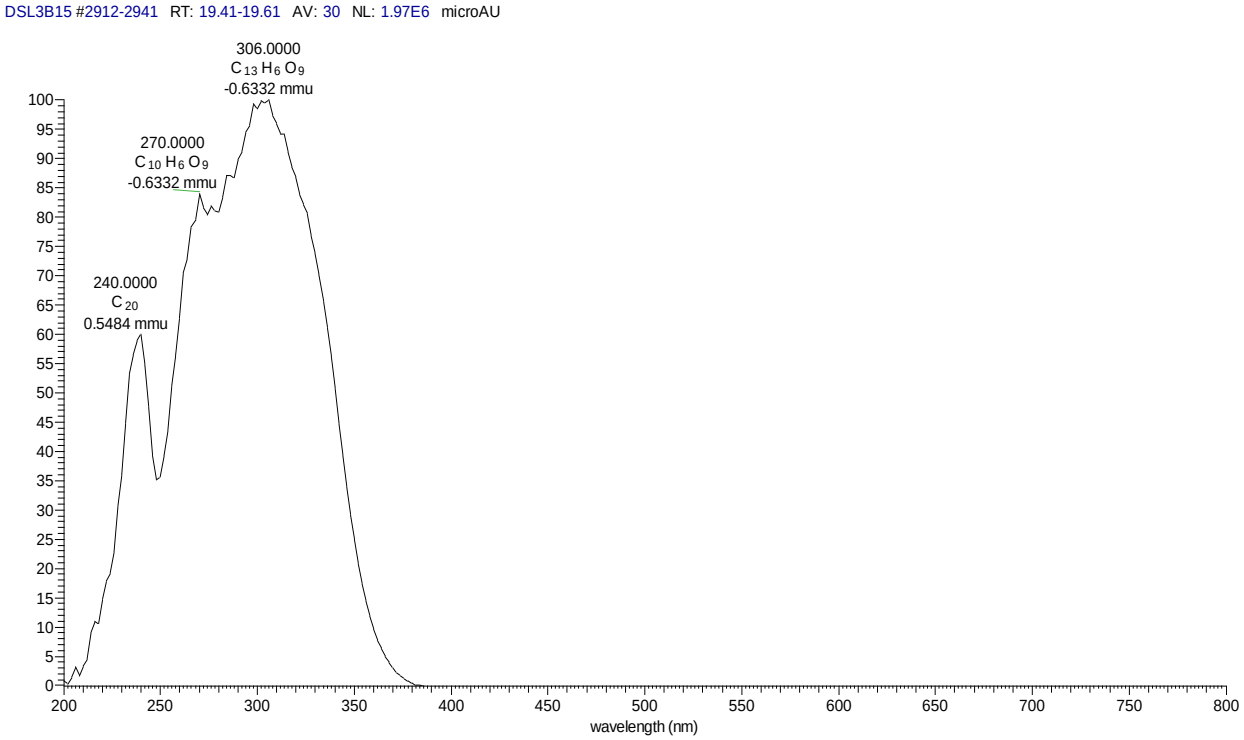

Appendix 35D: FT-IR spectrum of compound **208**

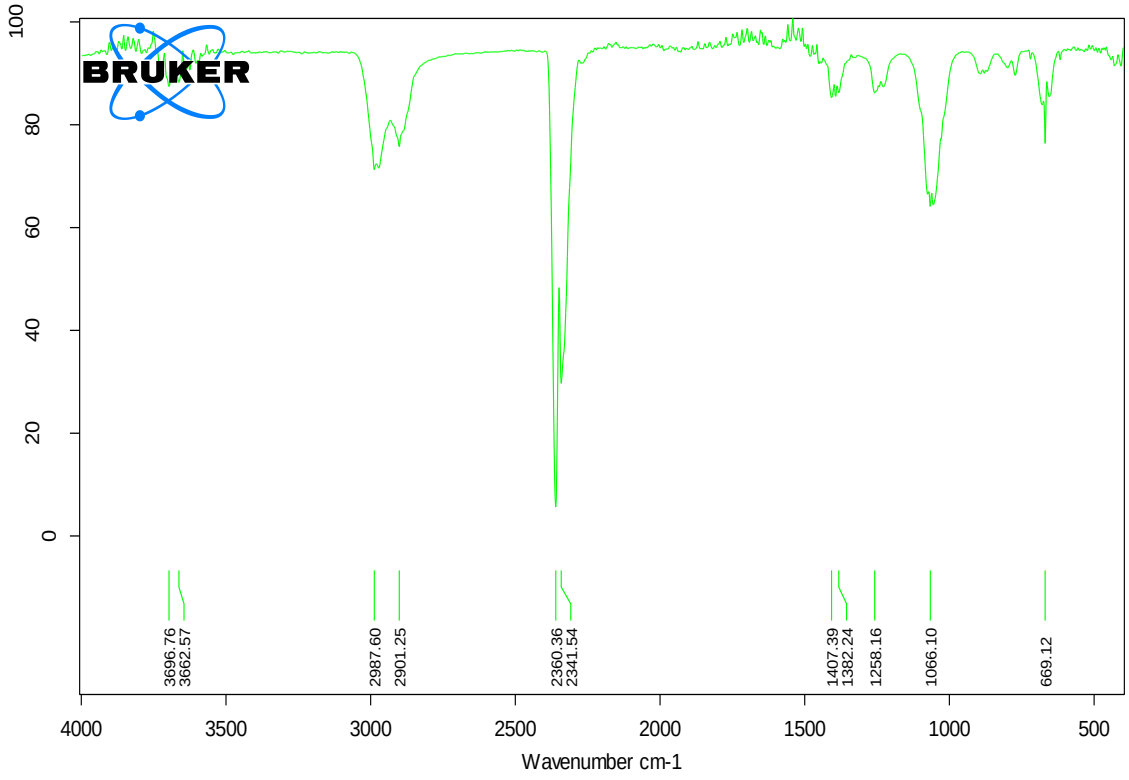

Appendix 35E: ^{1}H NMR spectrum (700 MHz, CD_3OD) of compound **208**

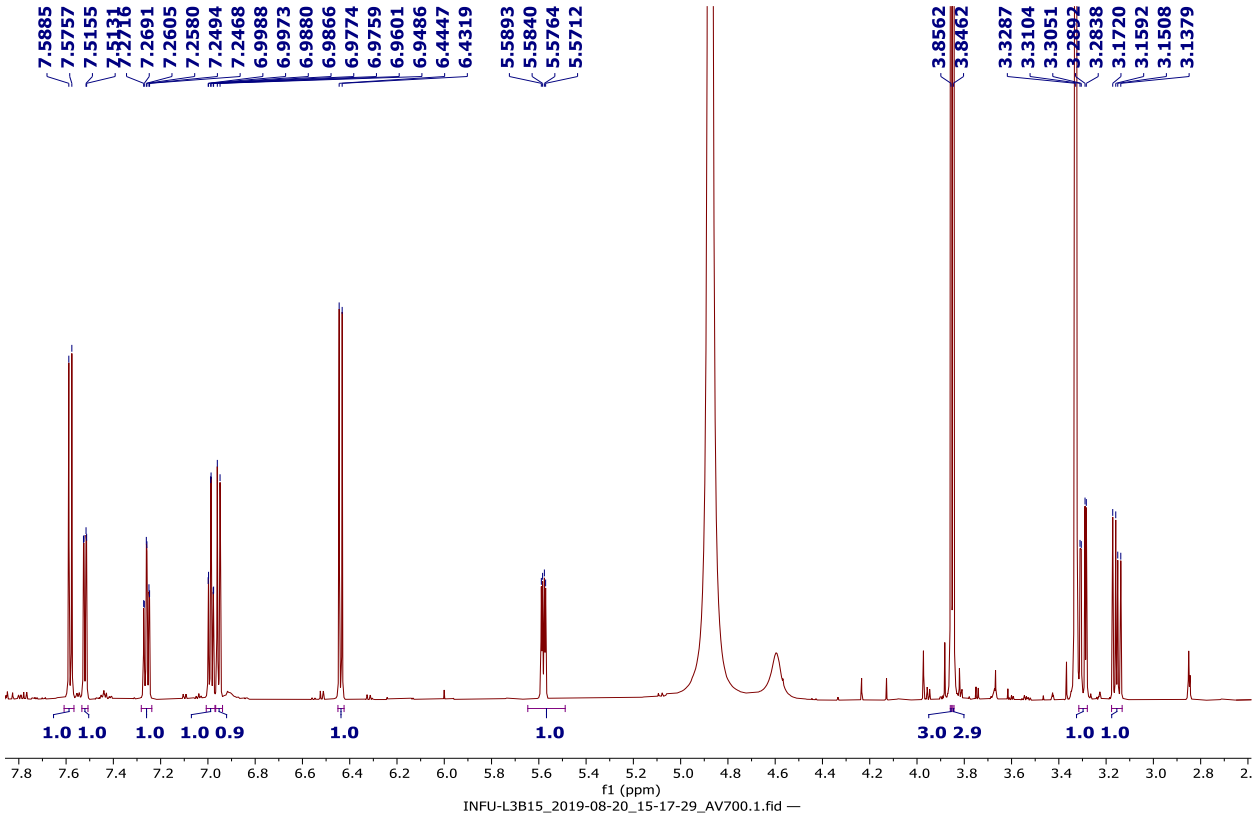

Appendix 35F: ^{13}C NMR spectrum (175 MHz, CD_3OD) of compound **208**

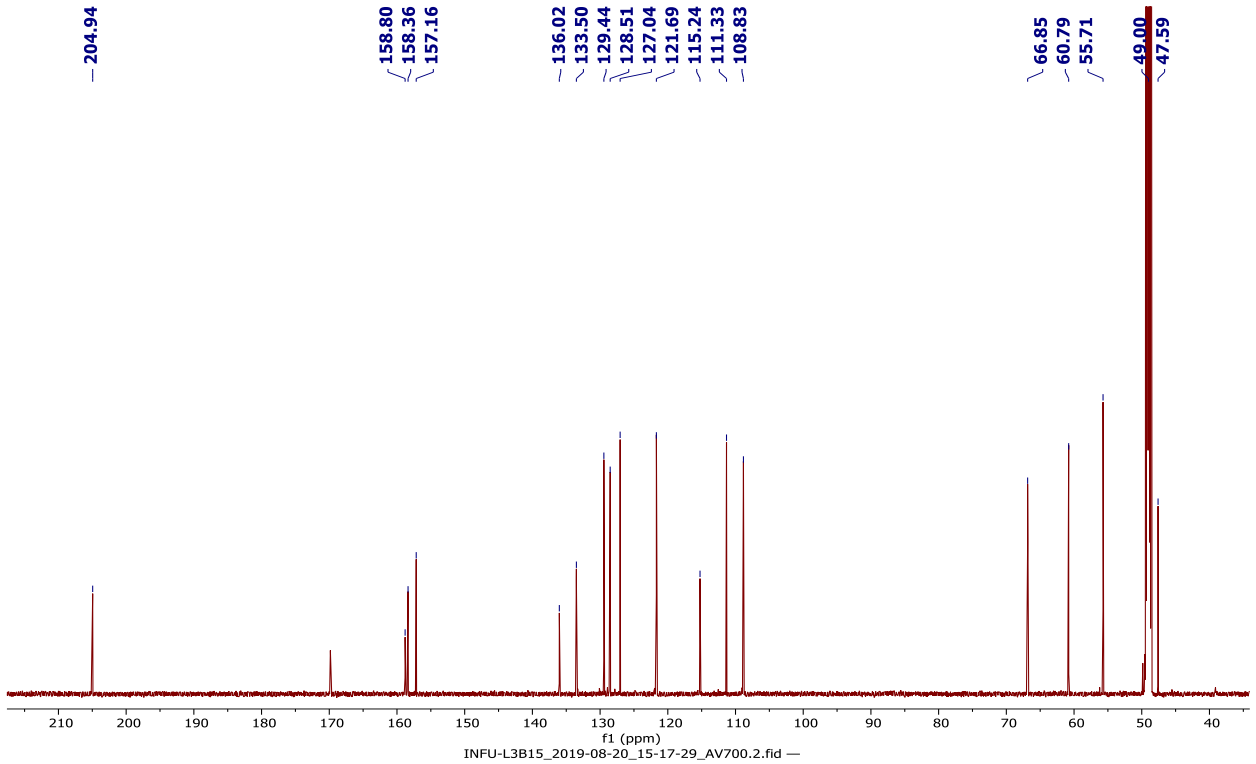

Appendix 35G: ^{1}H-^{1}H COSY spectrum (CD_3OD) of compound **208**

Appendix 35H: NOESY spectrum (CD_3OD) of compound **208**

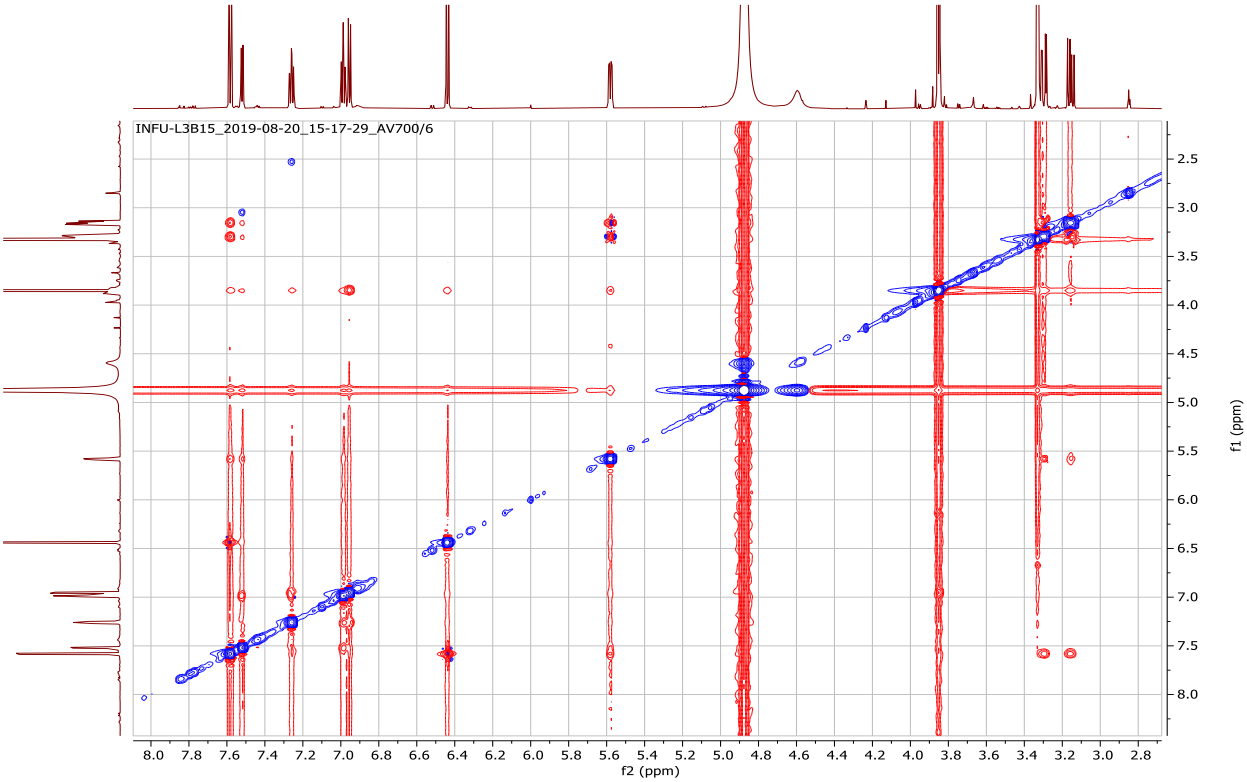

Appendix 35I: HSQC spectrum (CD_3OD) of compound **208**

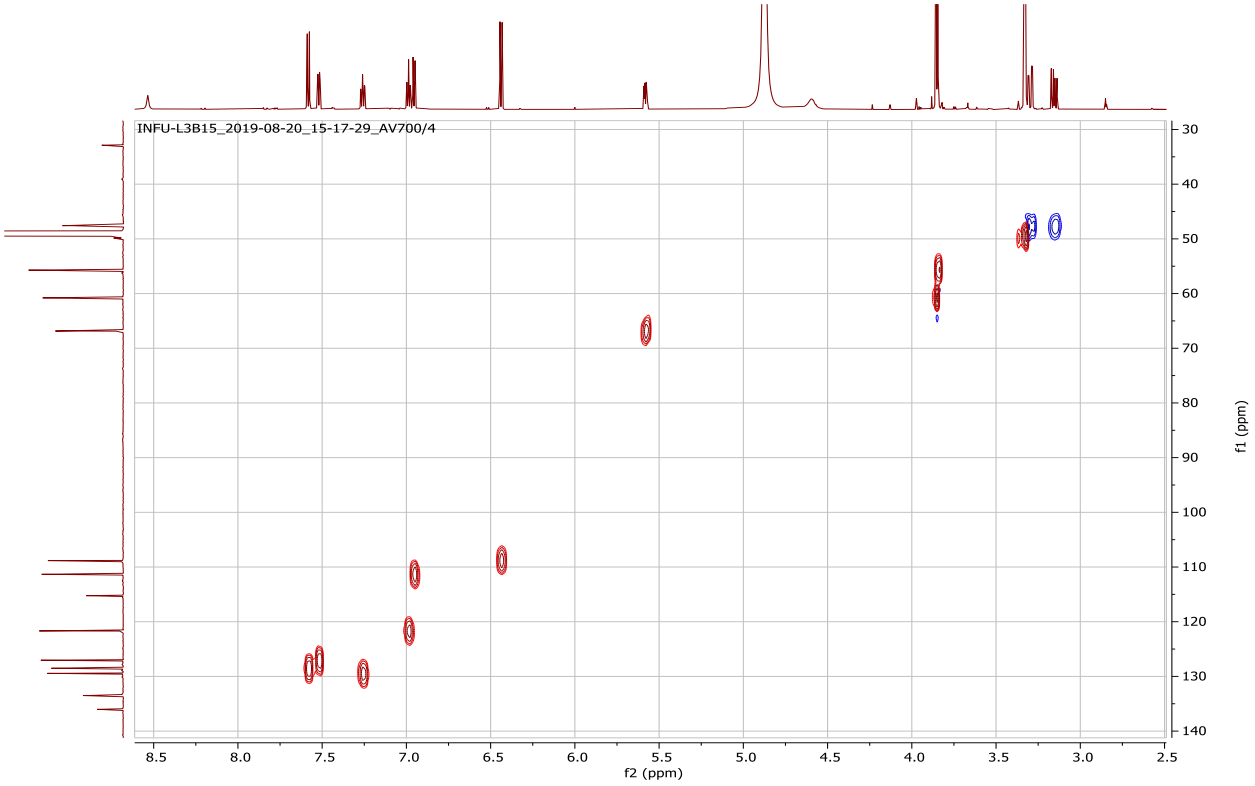

Appendix 35J: HMBC spectrum (CD_3OD) of compound **208**

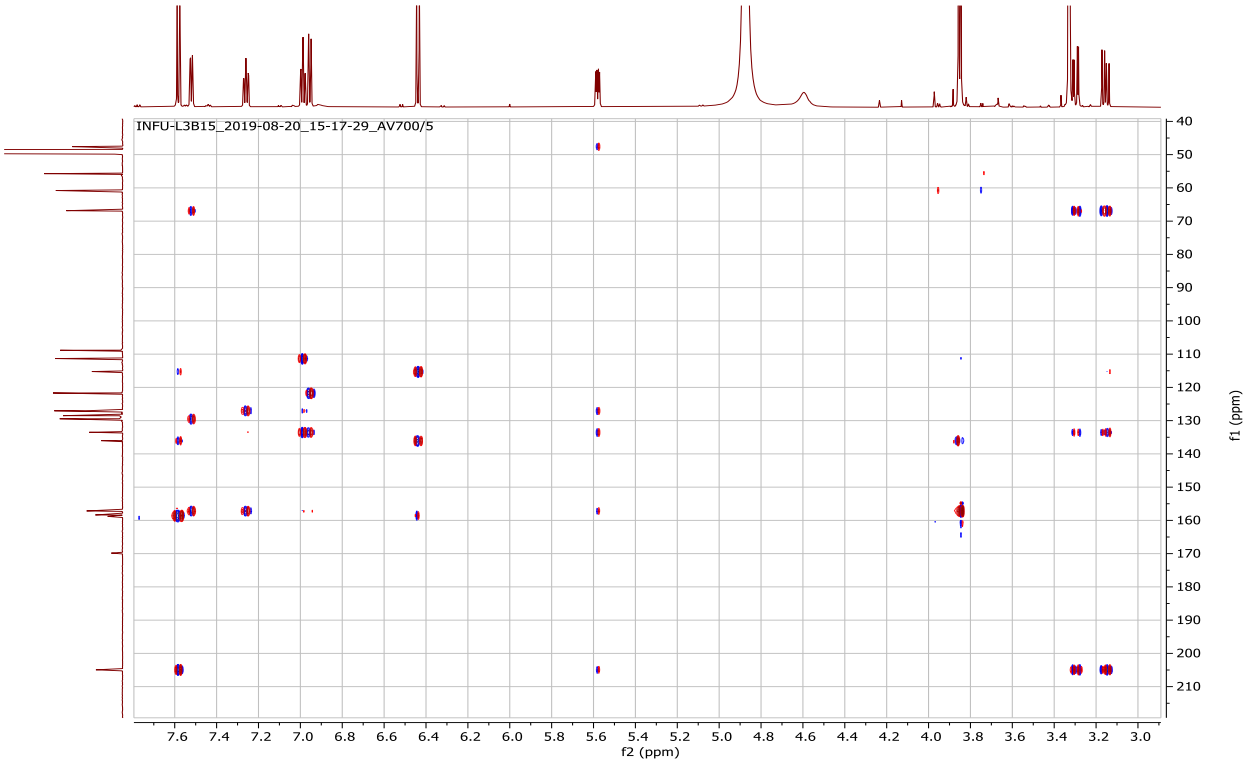

Appendix 36: NMR spectra for dihydrooroxylin A (**209**)

Appendix 36A: HRESIMS of compound **209**

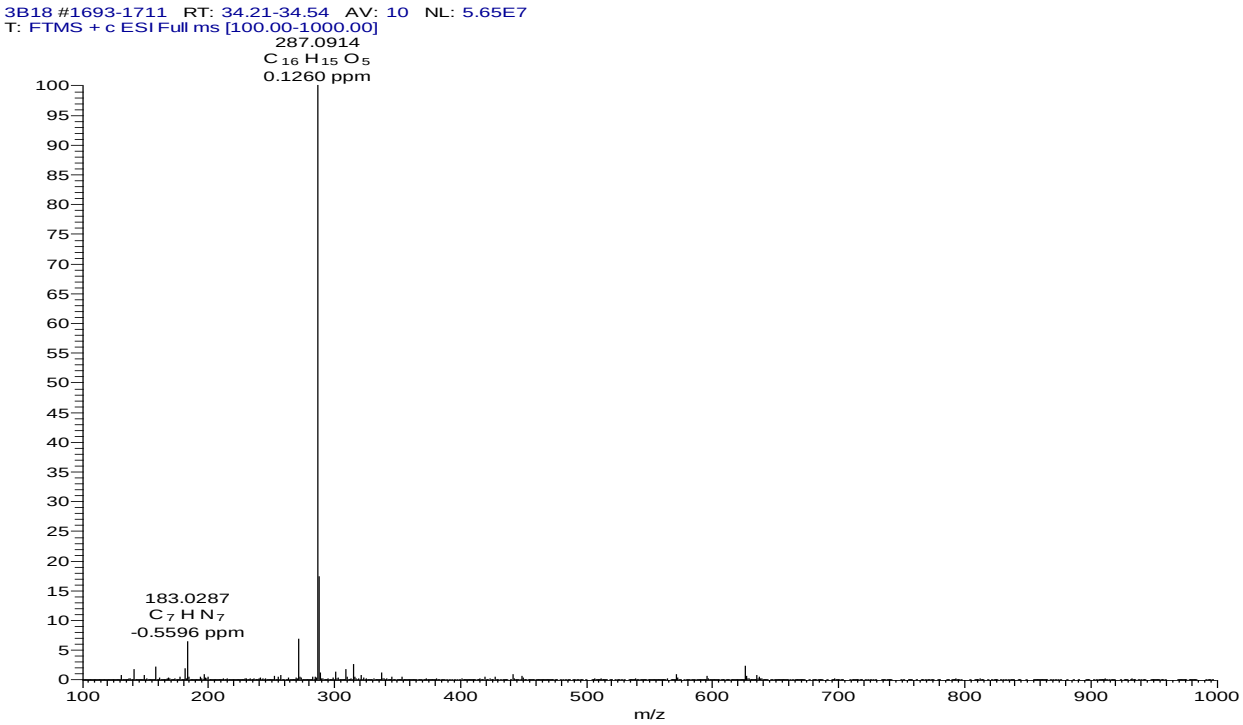

Appendix 36B: LC-UV spectrum of compound **209**

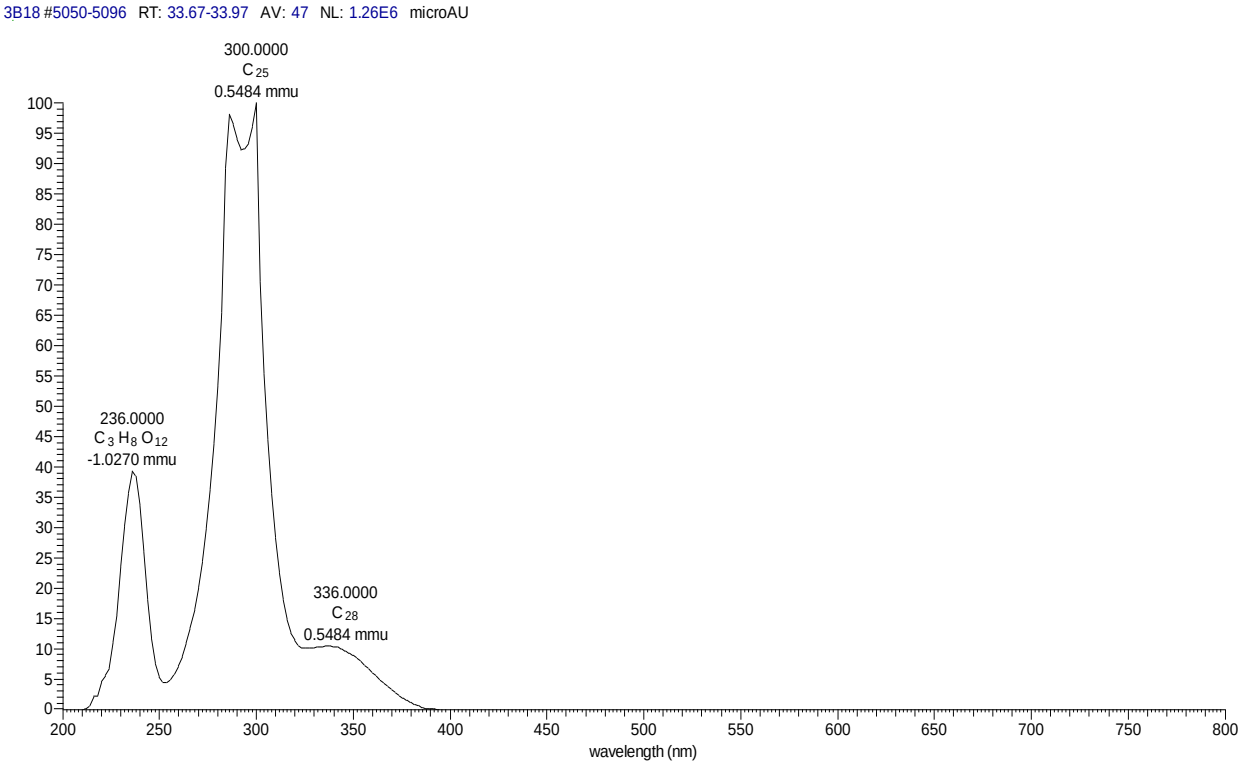

Appendix 36C: ^{1}H NMR spectrum (600 MHz, CD_3OD) of compound **209**

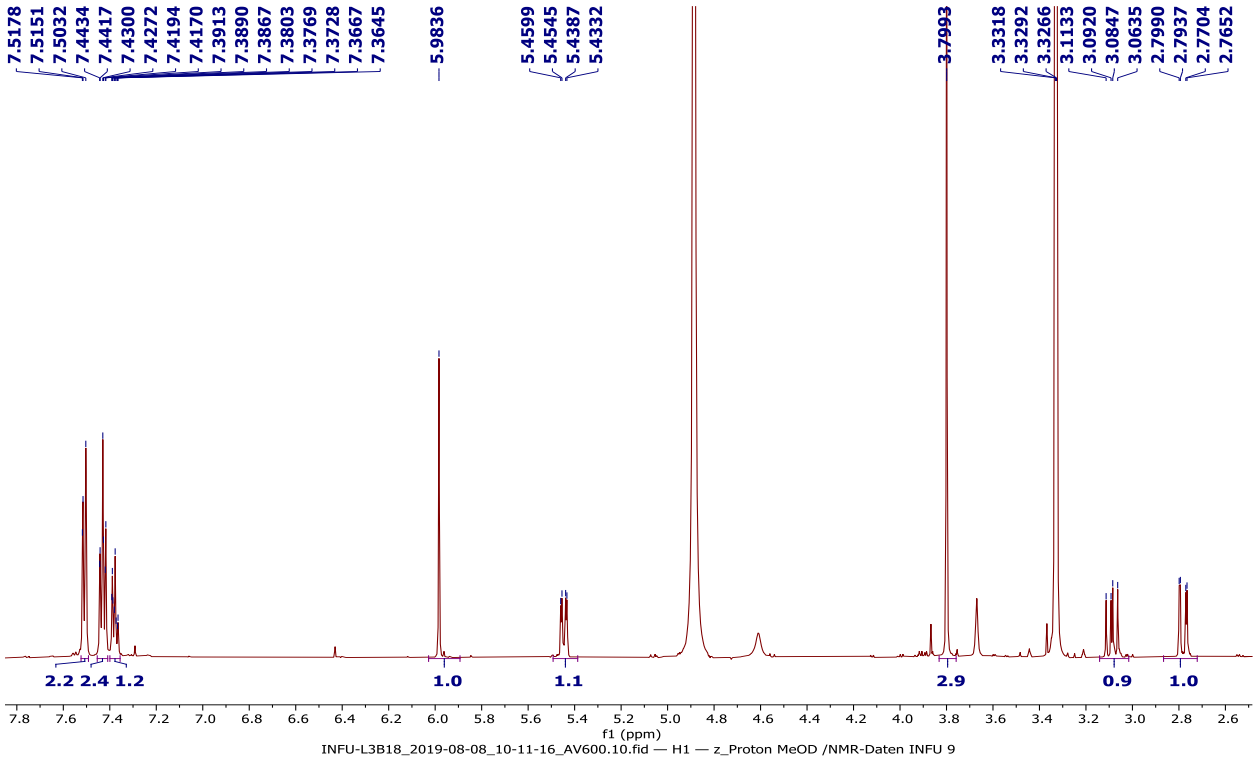

Appendix 36D: ^{13}C NMR spectrum (150 MHz, CD_3OD) of compound **209**

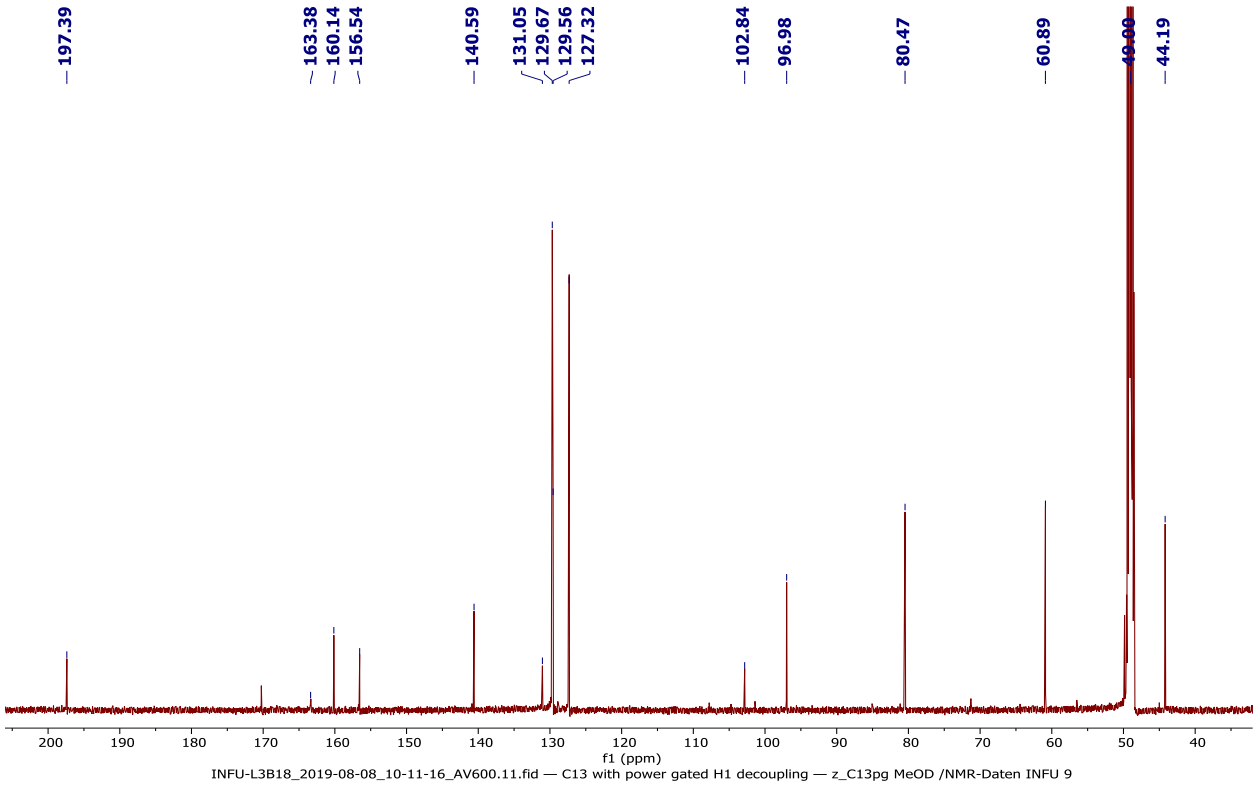

Appendix 36E: ^{1}H-^{1}H COSY spectrum (CD_3OD) of compound **209**

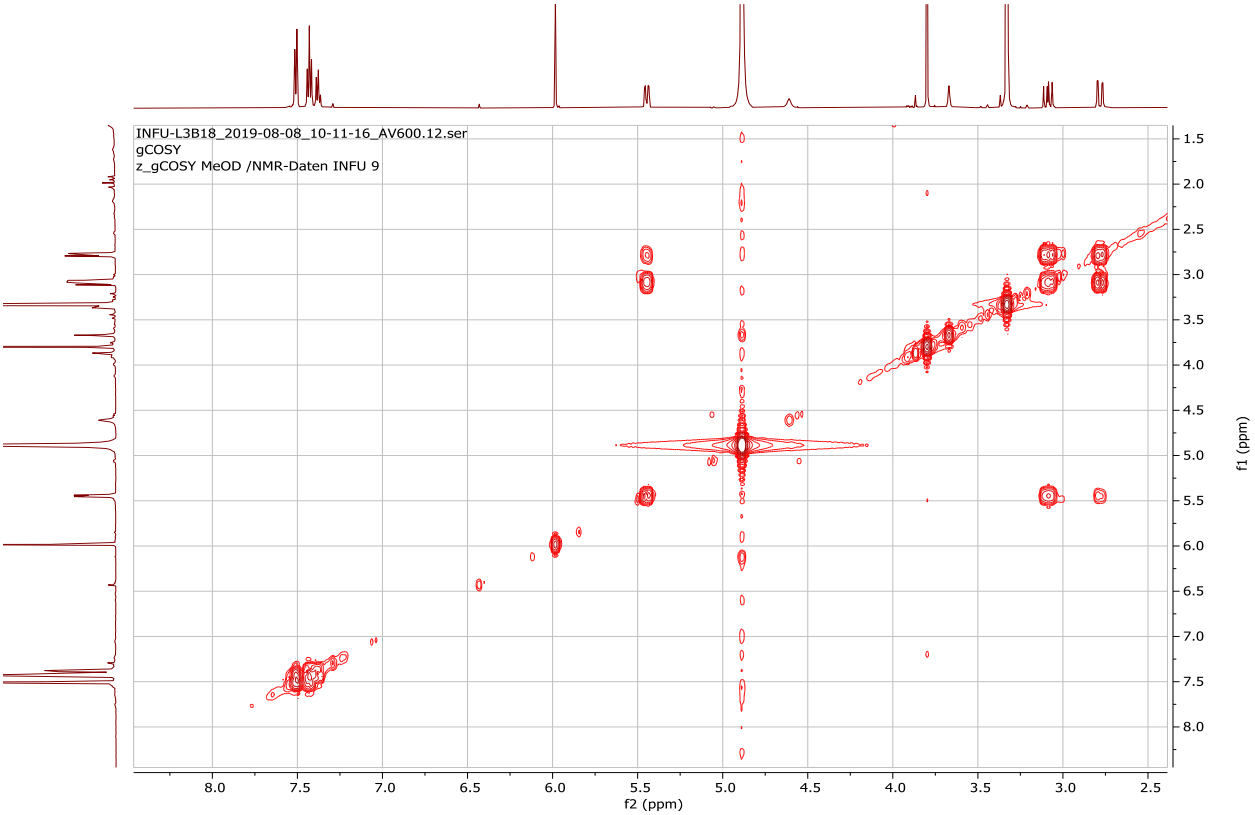

Appendix 36F: HSQC spectrum (CD_3OD) of compound **209**

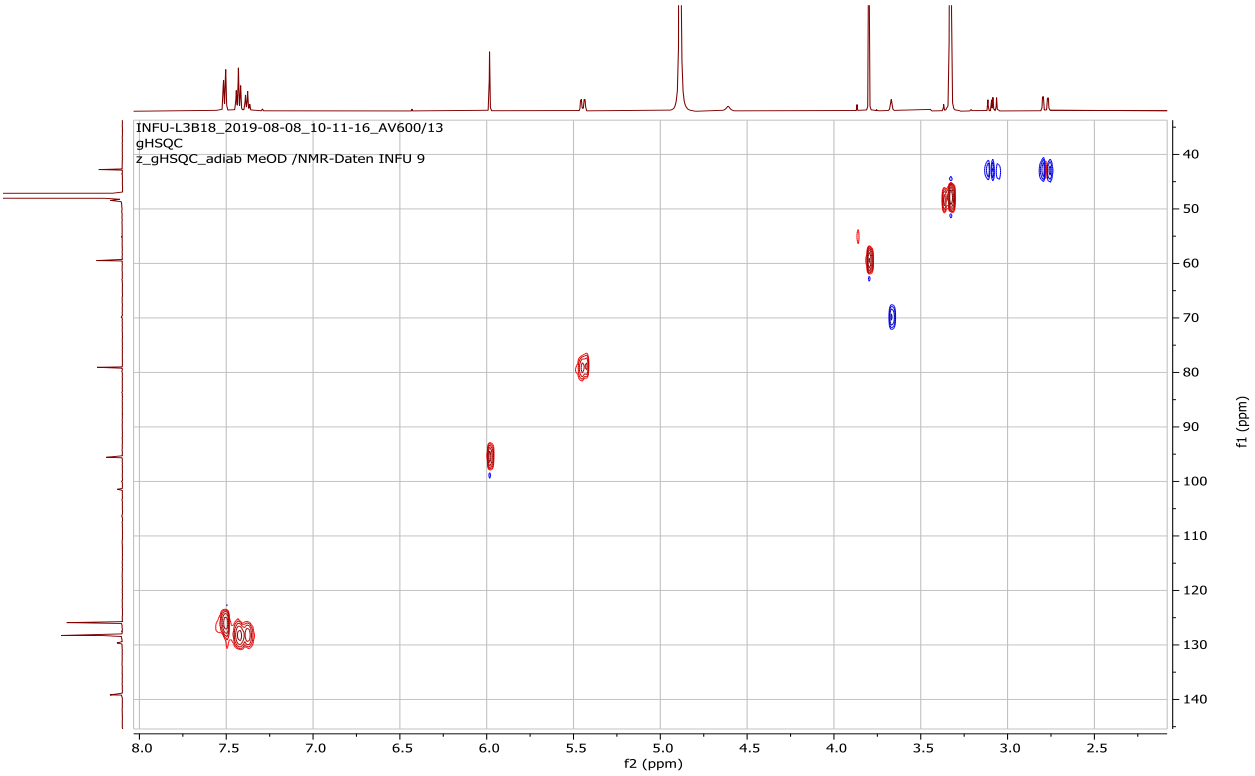

Appendix 36G: HMBC spectrum (CD_3OD) of compound **209**

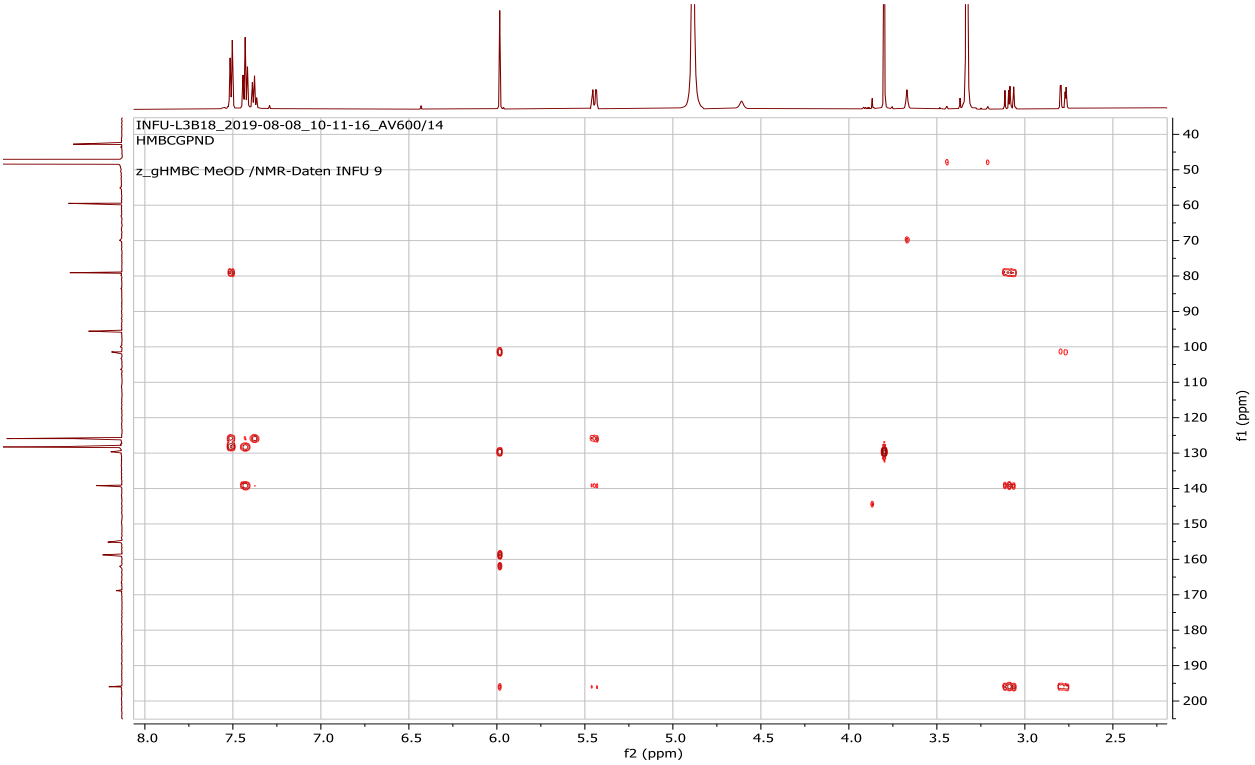

Appendix 37: NMR spectra for 7-hydroxy-6-methoxyflavanone (**210**)

Appendix 37A: HRESIMS of compound **210**

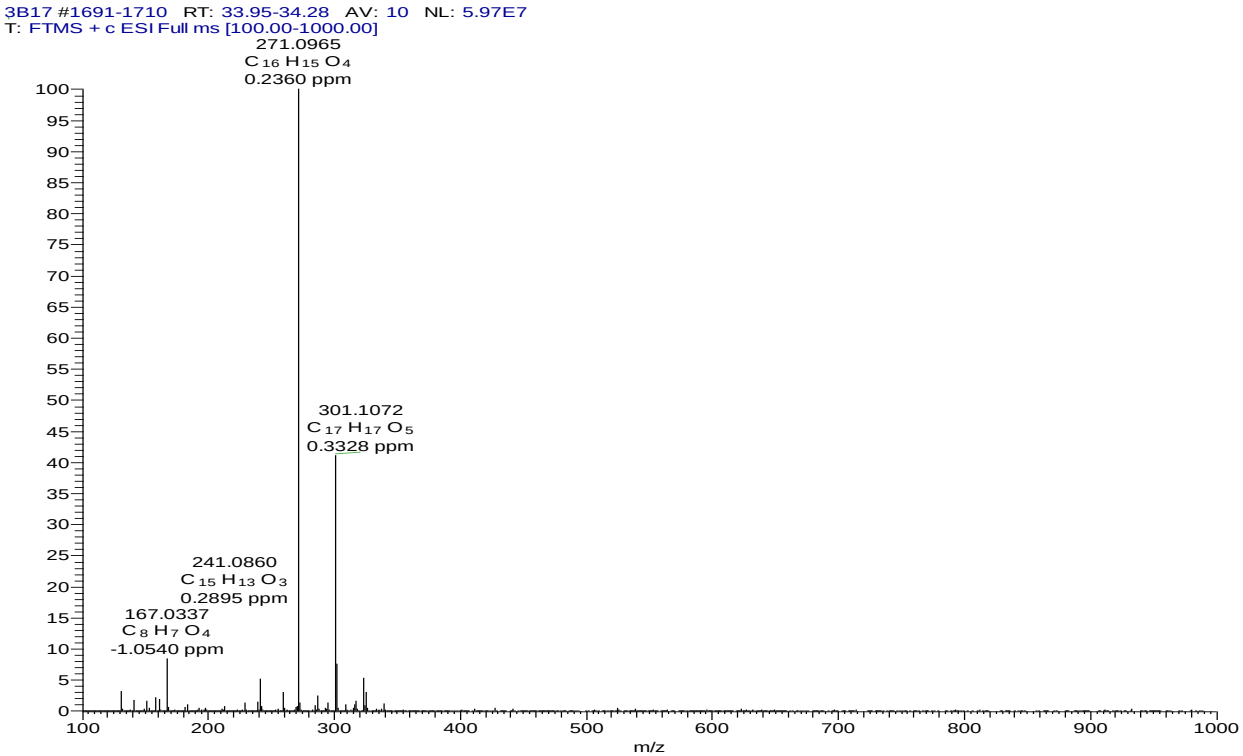

Appendix 37B: LC-UV spectrum of compound **210**

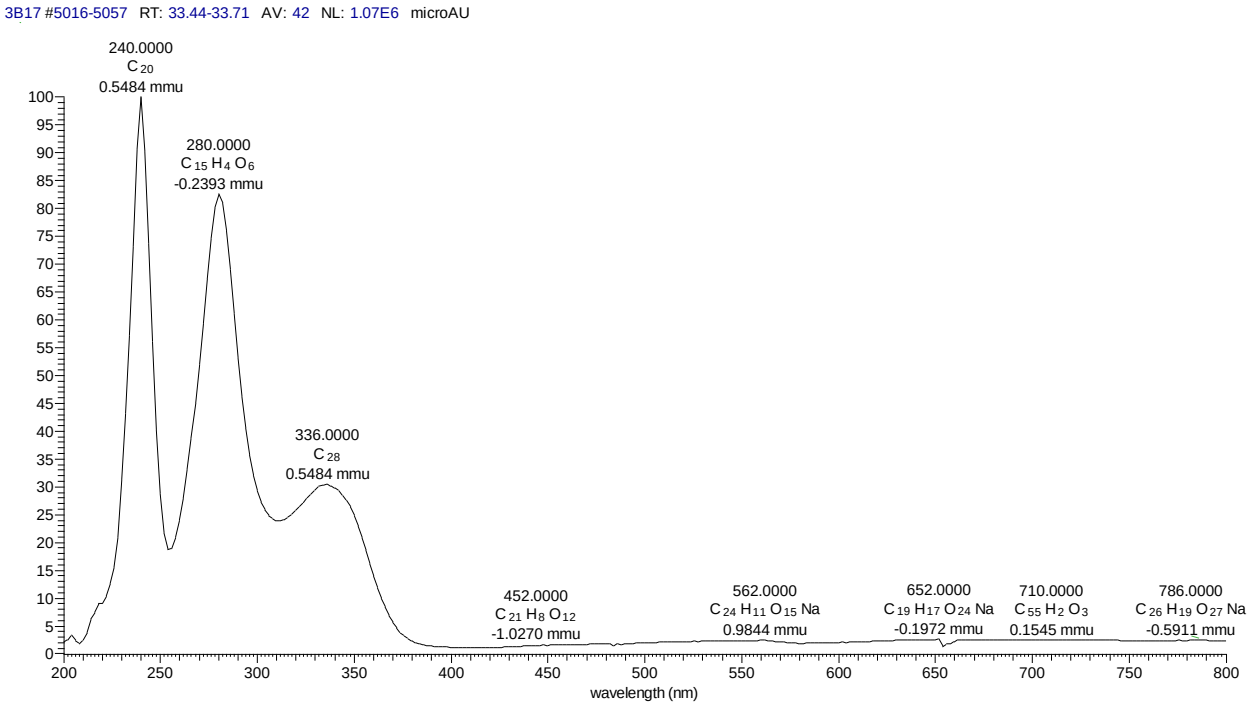

Appendix 37C: ^{1}H NMR spectrum (600 MHz, CD_3OD) of compound **210**

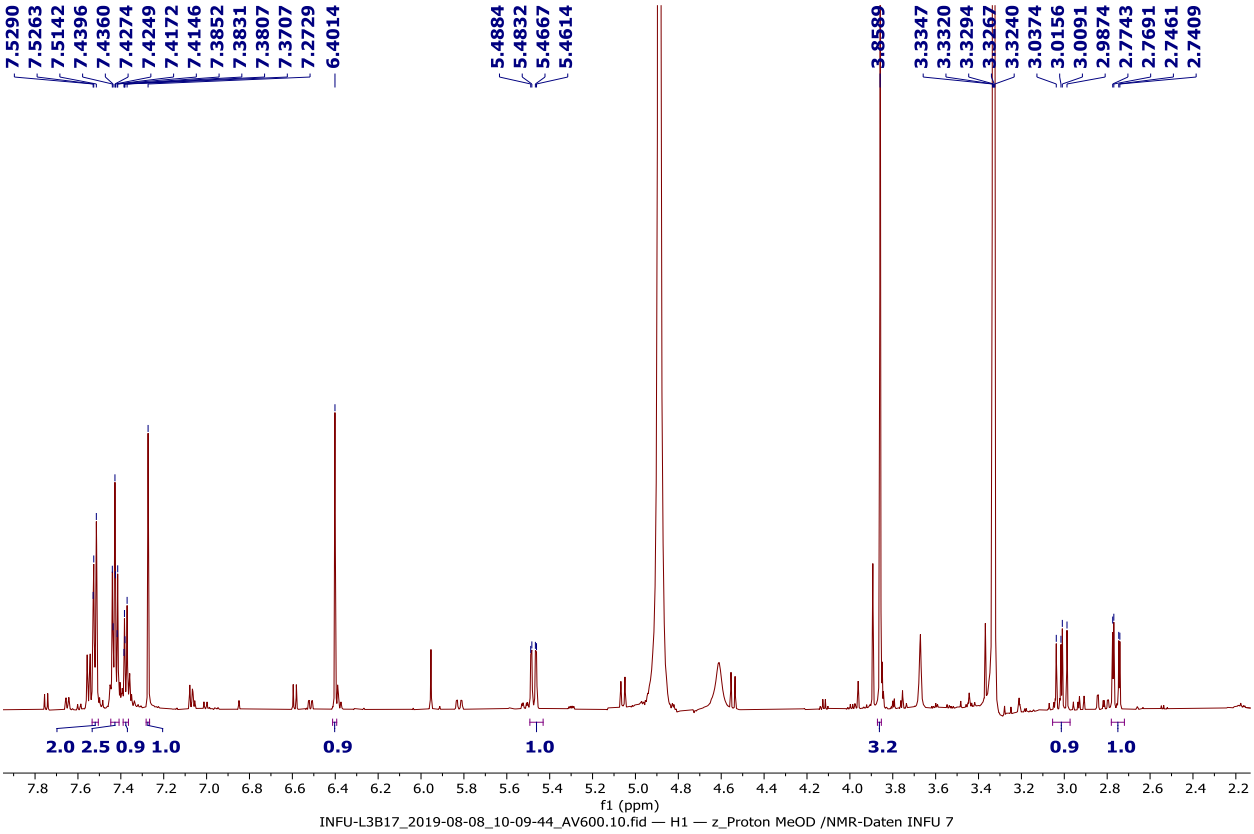

Appendix 37D: ^{13}C NMR spectrum (150 MHz, CD_3OD) of compound **210**

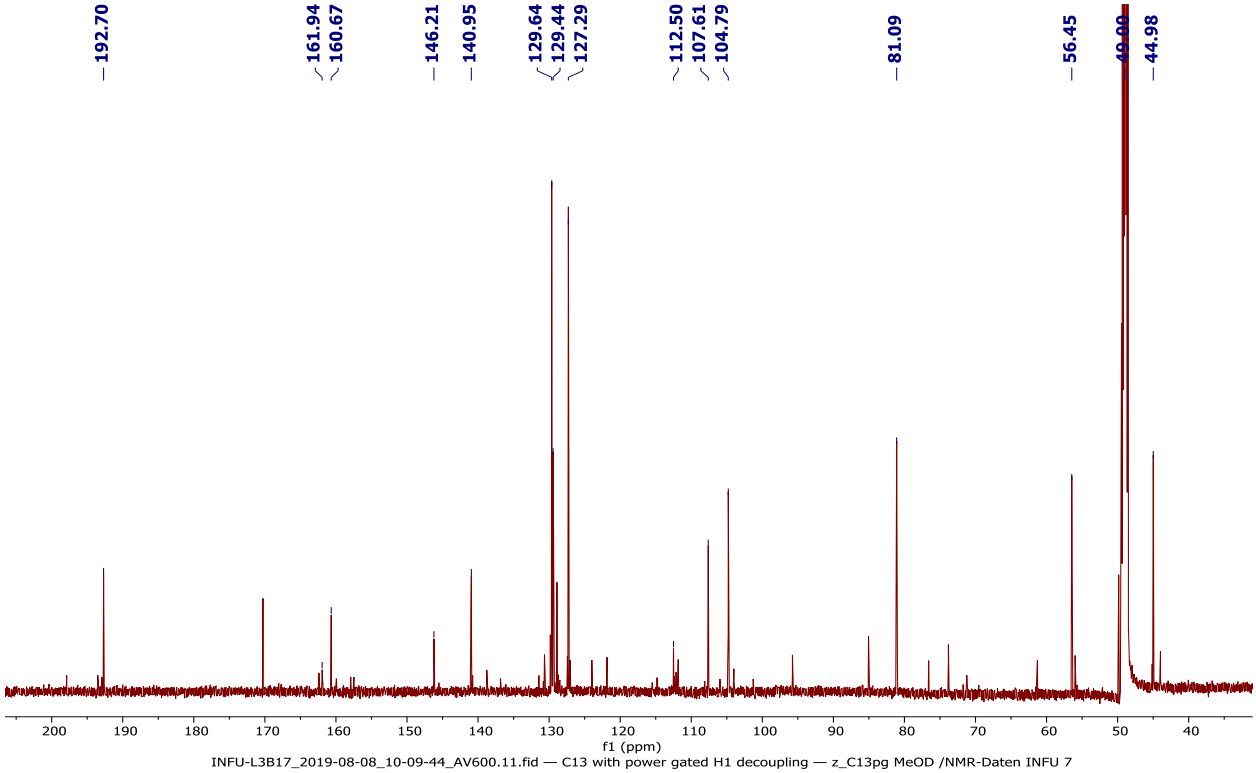

Appendix 37E: ^{1}H-^{1}H COSY spectrum (CD_3OD) of compound **210**

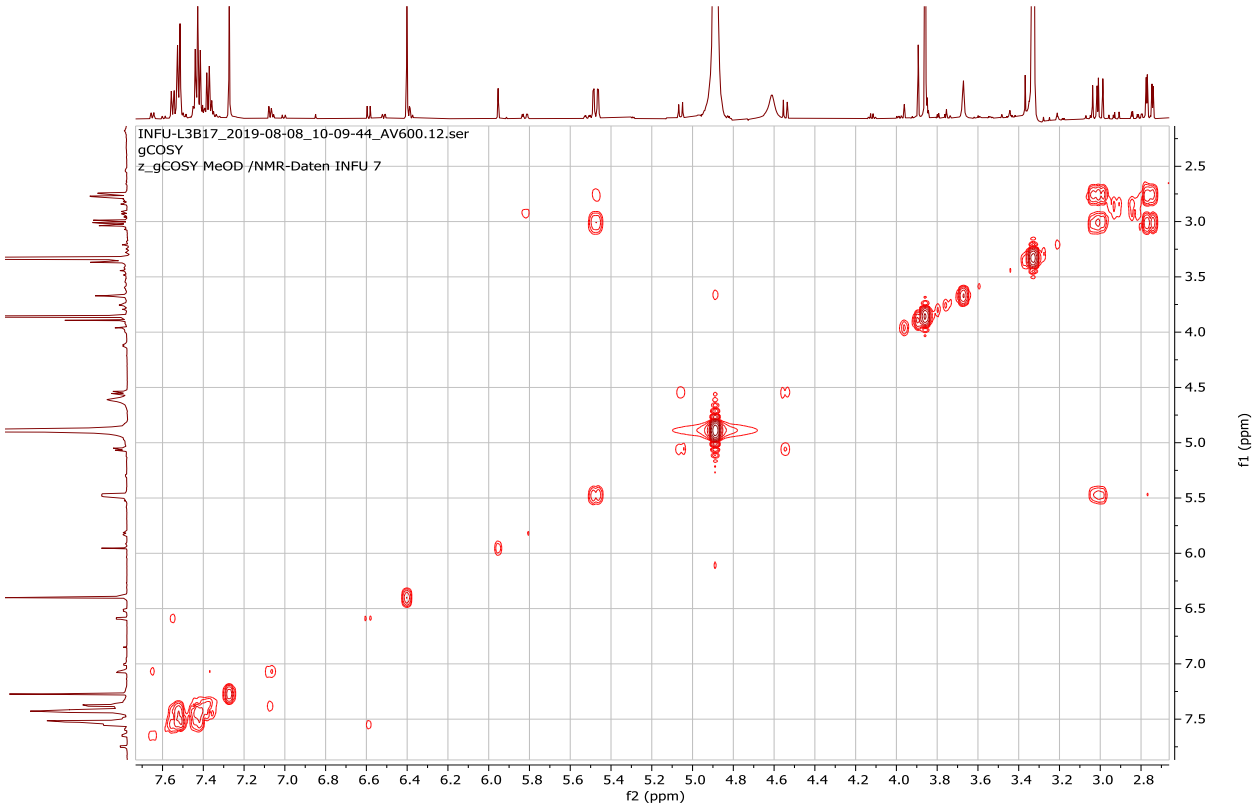

Appendix 37F: HSQC spectrum (CD_3OD) of compound **210**

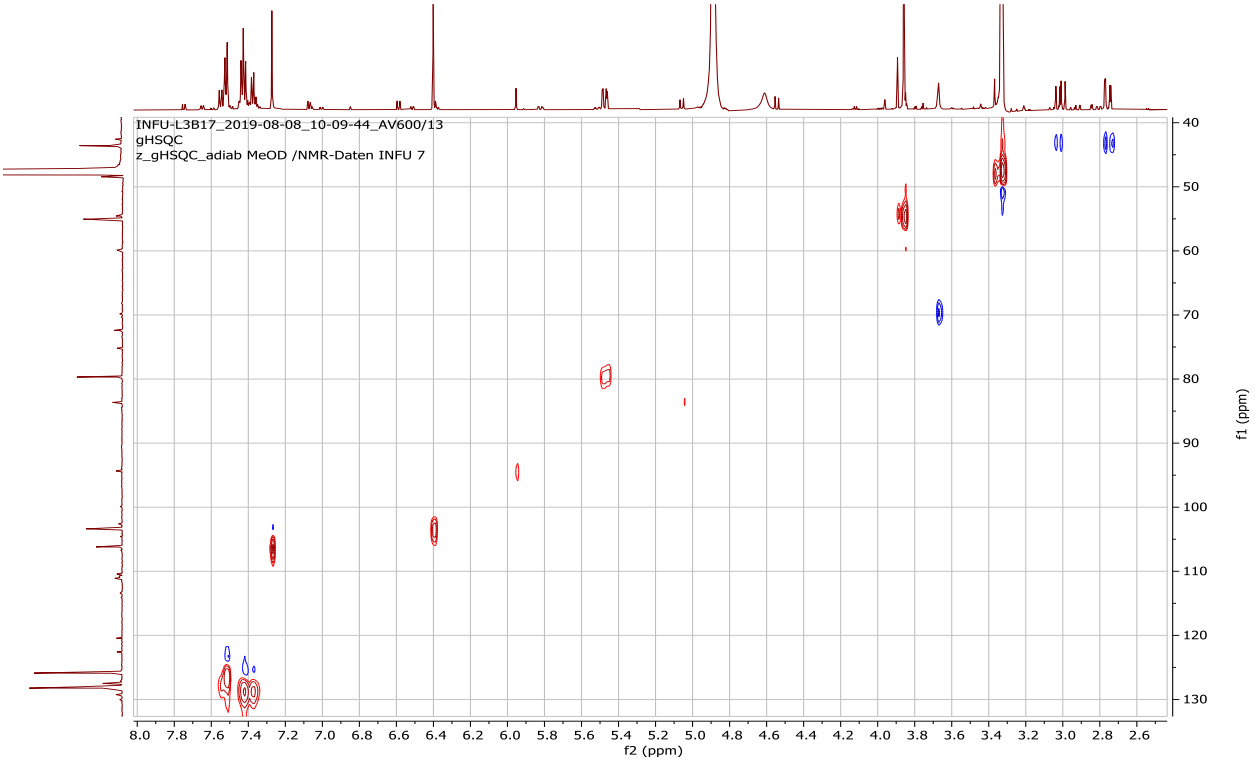

Appendix 37G: HMBC spectrum (CD_3OD) of compound **210**

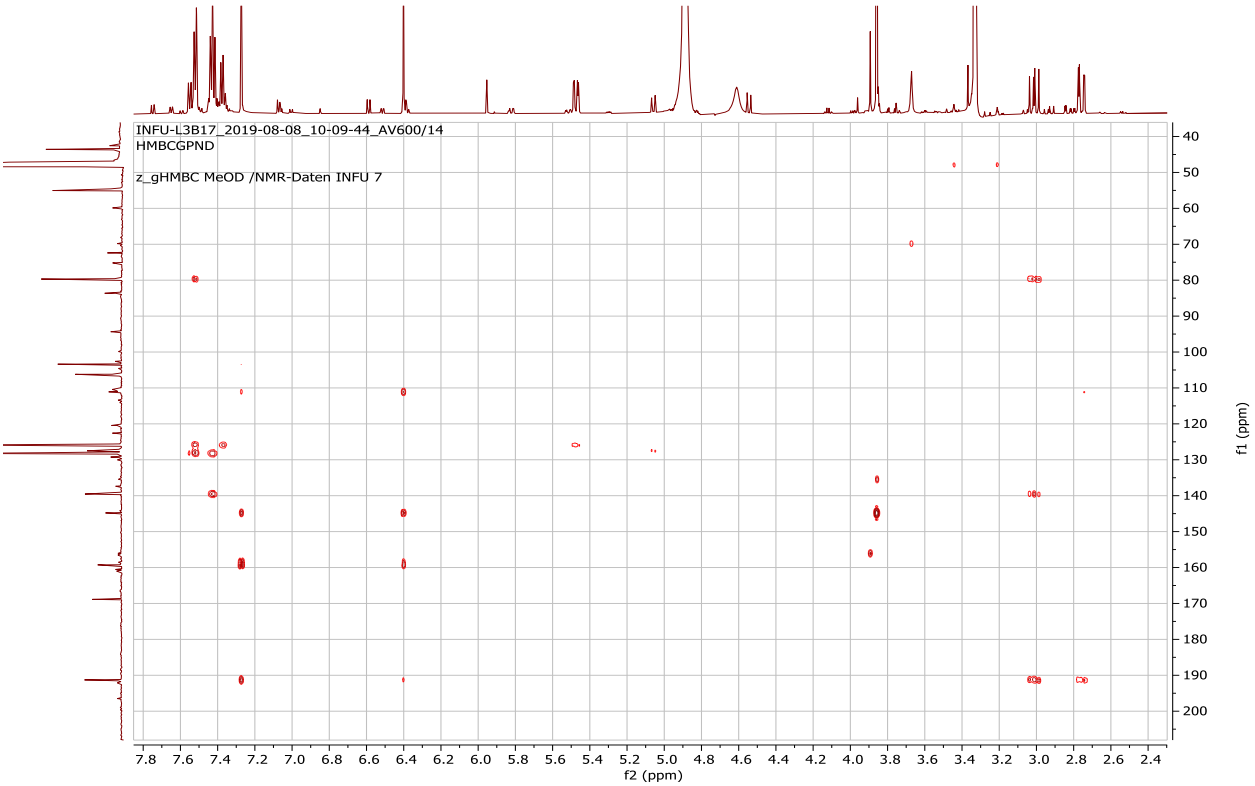

Appendix 38: NMR spectra for 4′,5,7-trihydroxy-6-methylflavanone (**211**)

Appendix 38A: HRESIMS of compound **211**

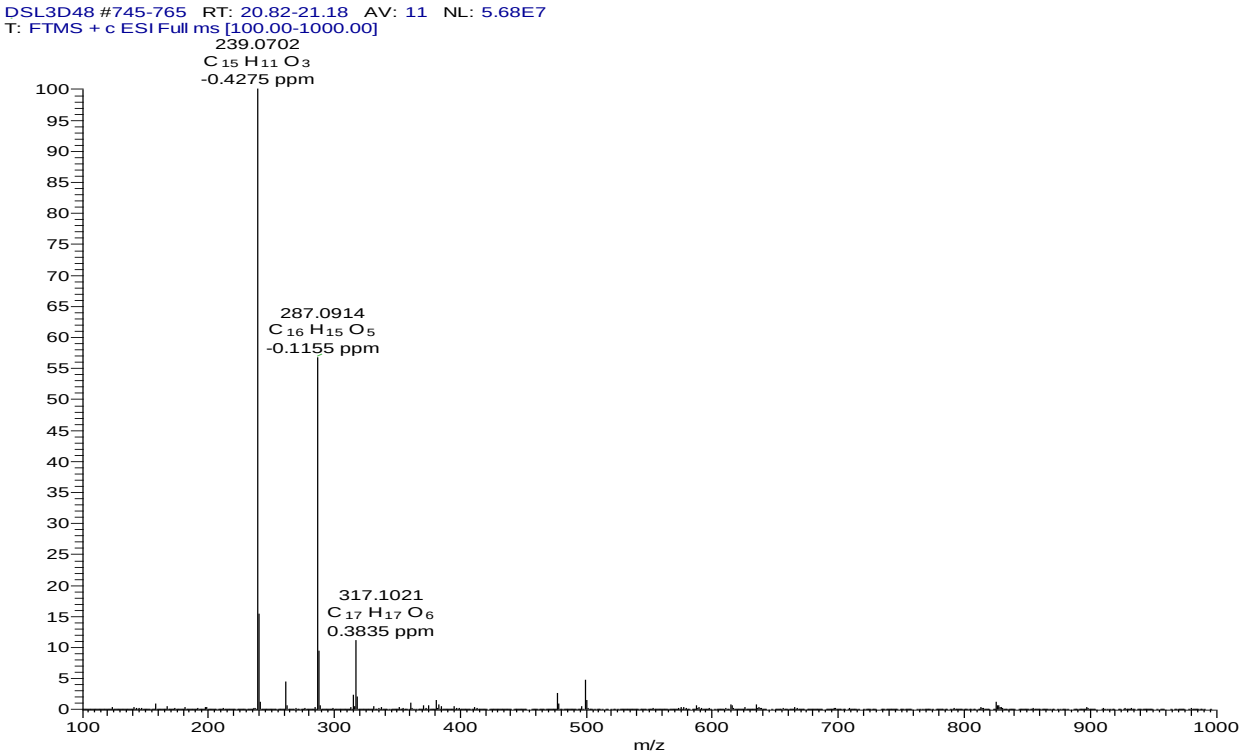

Appendix 38B: LC-UV spectrum of compound **211**

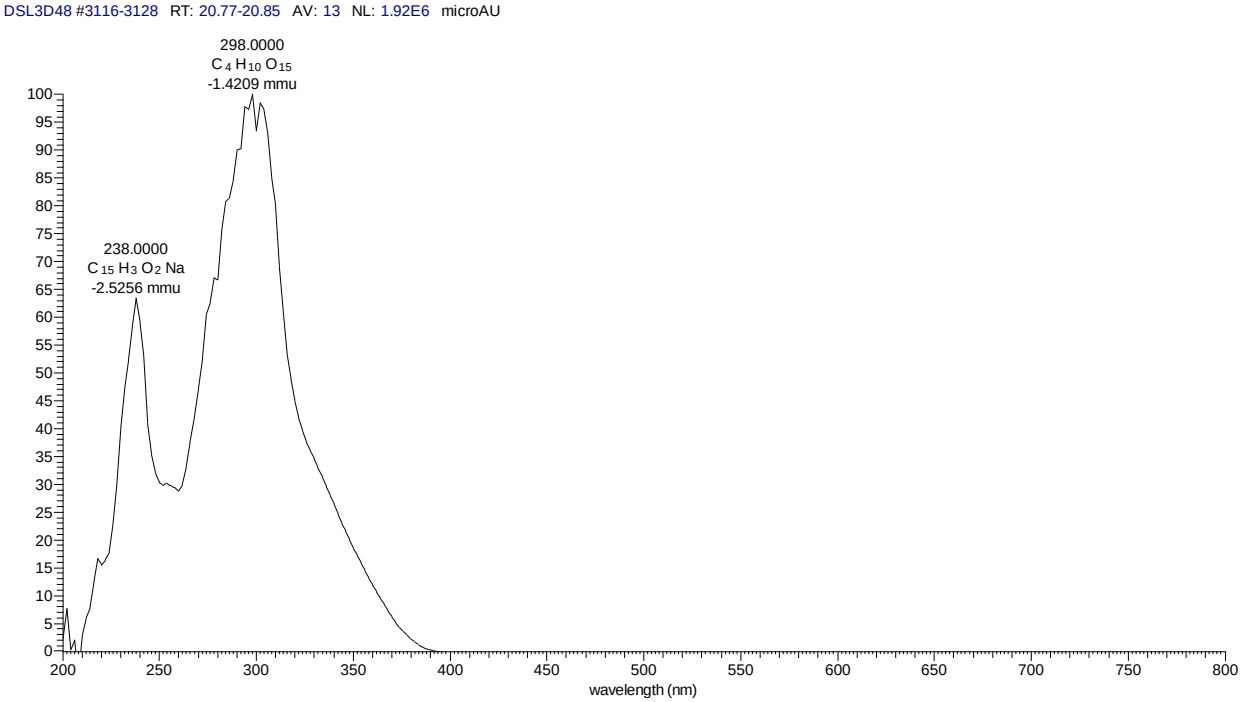

Appendix 38C: ^{1}H NMR spectrum (700 MHz, CD_3OD) of compound **211**

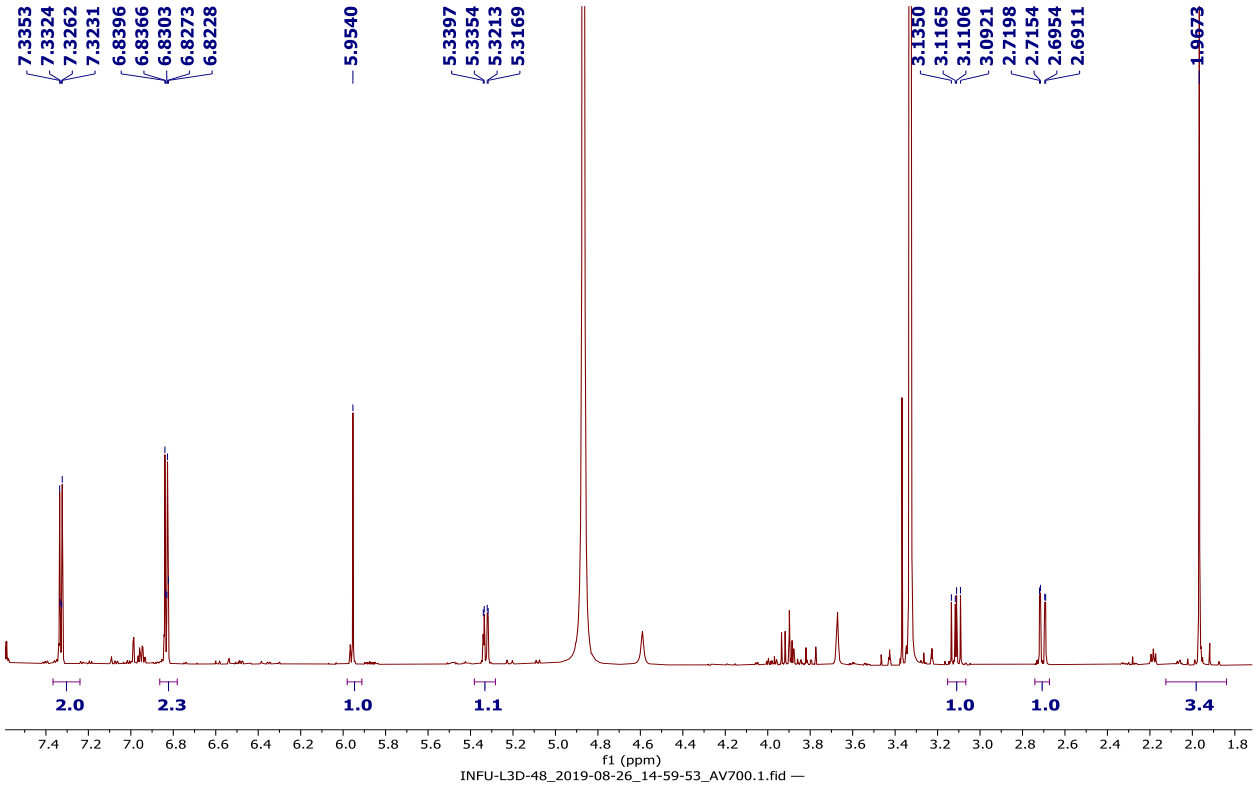

Appendix 38D: ^{13}C NMR spectrum (175 MHz, CD_3OD) of compound **211**

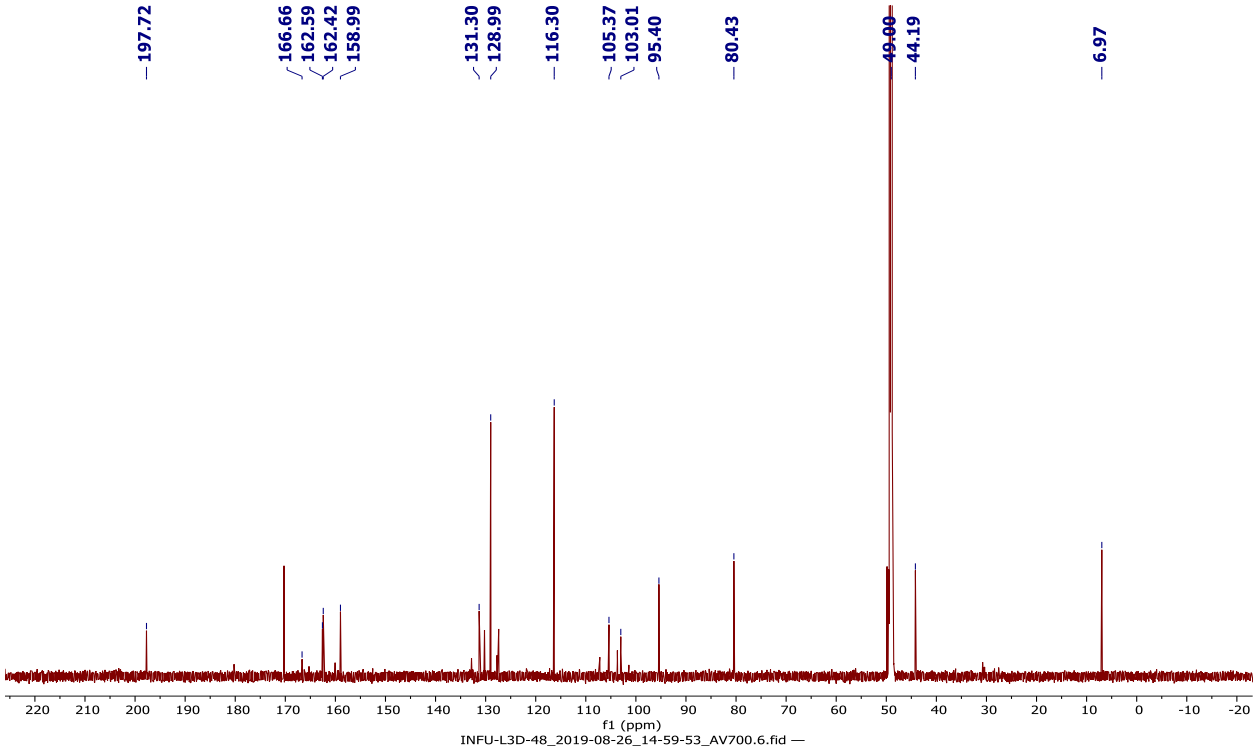

Appendix 38E: ^{1}H-^{1}H COSY spectrum (CD_3OD) of compound **211**

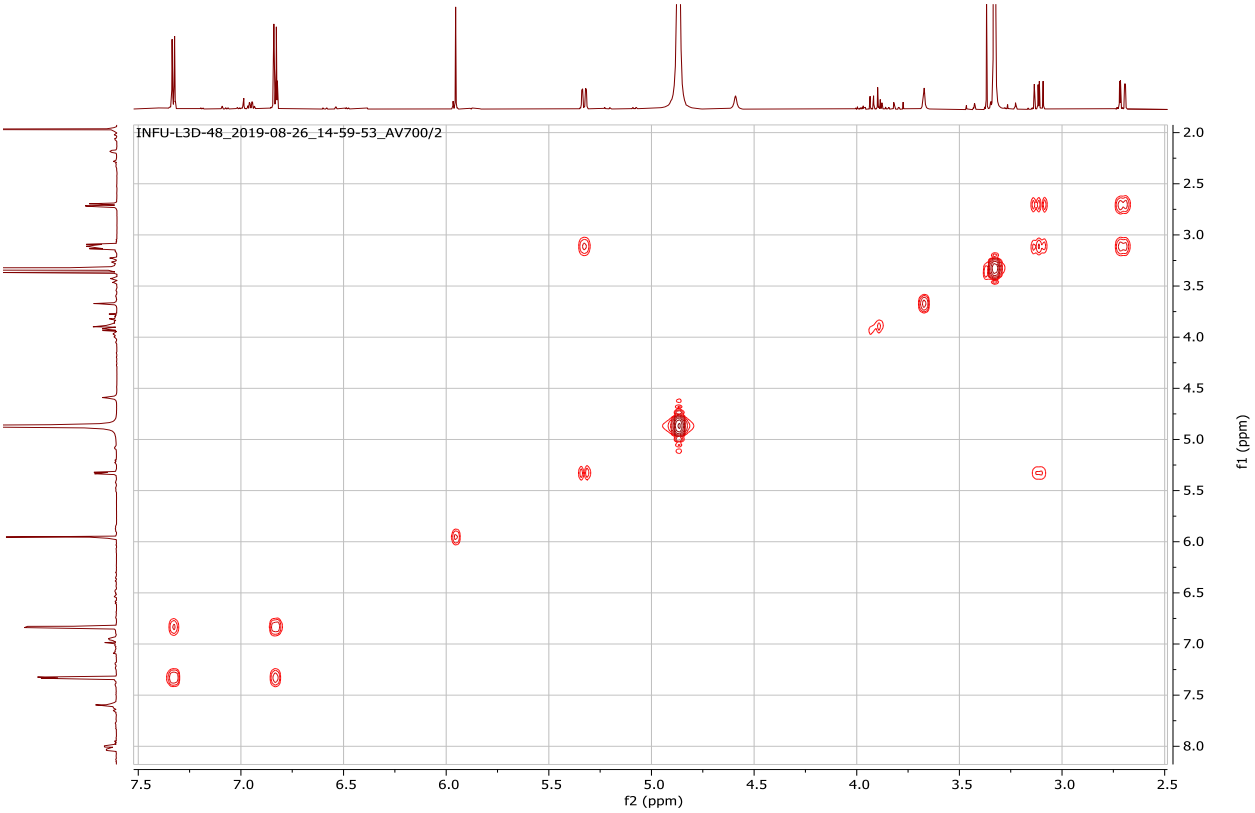

Appendix 38F: HSQC spectrum (CD_3OD) of compound **211**

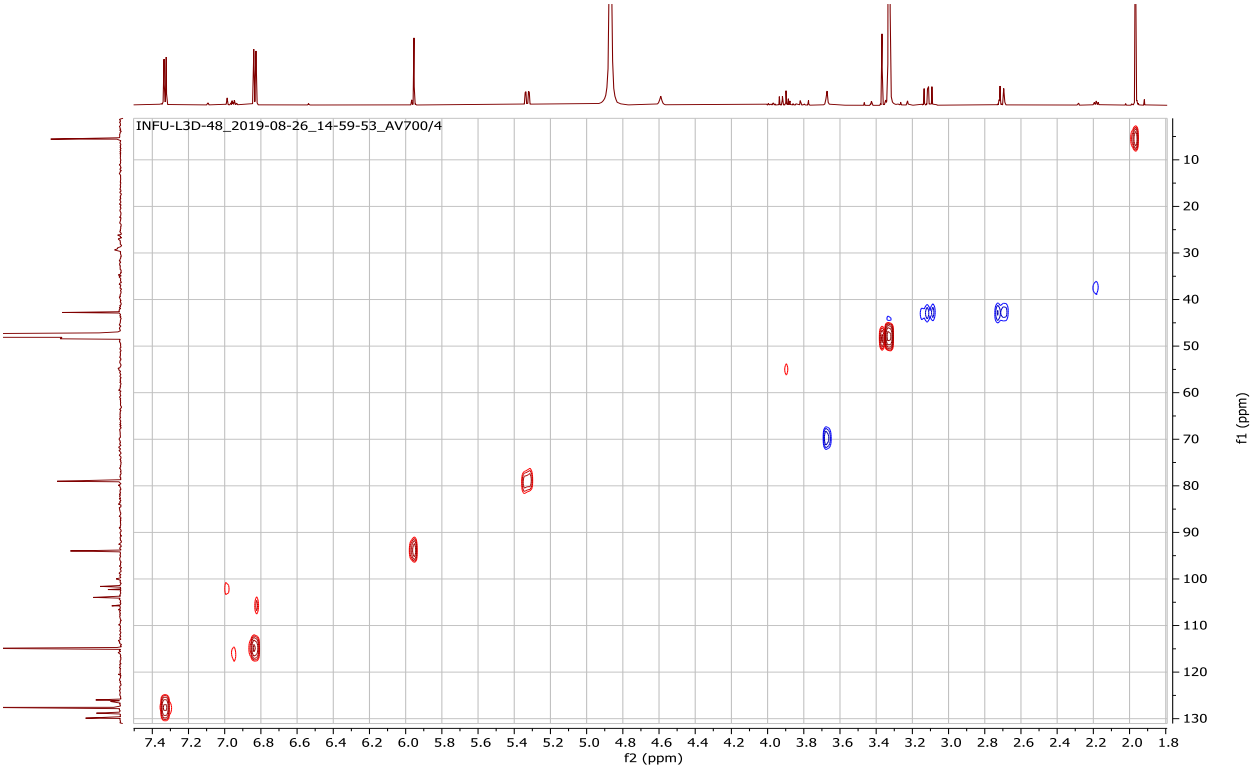

Appendix 38G: HMBC spectrum (CD_3OD) of compound **211**

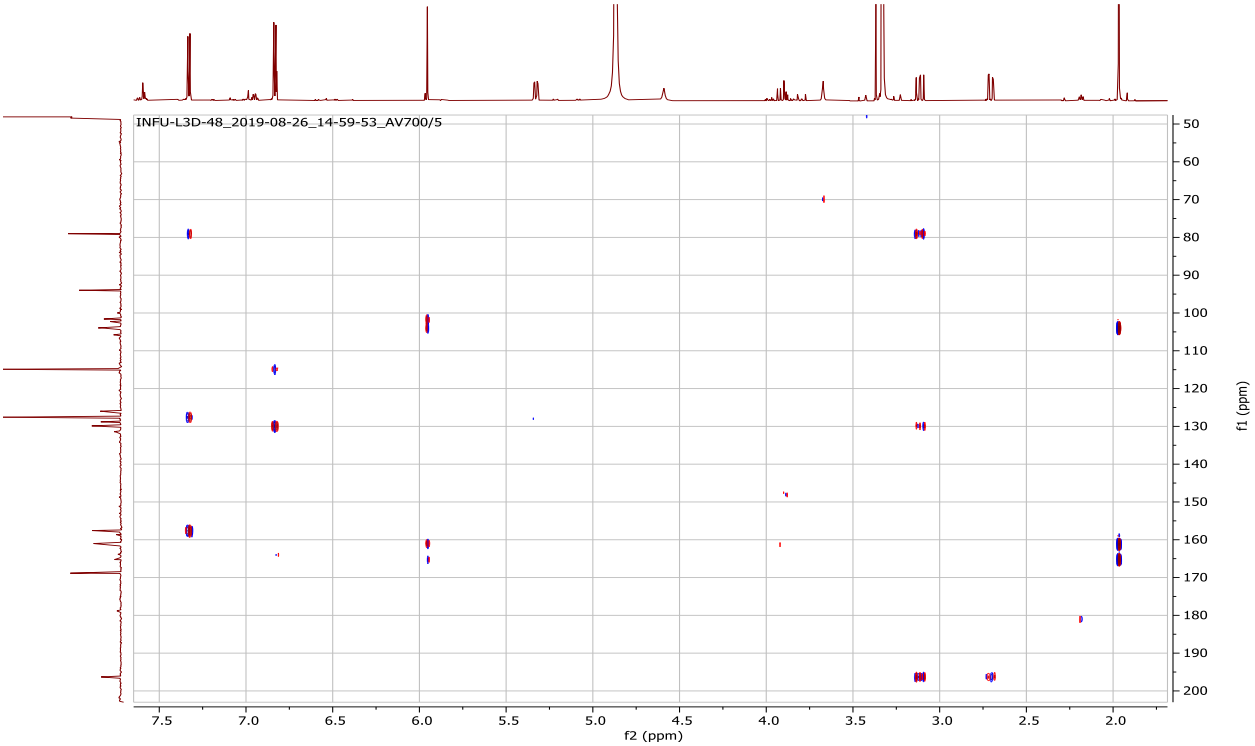

Appendix 39: NMR spectra for quercetin-4′-methyl ether (**212**)

Appendix 39A: HRESIMS of compound **212**

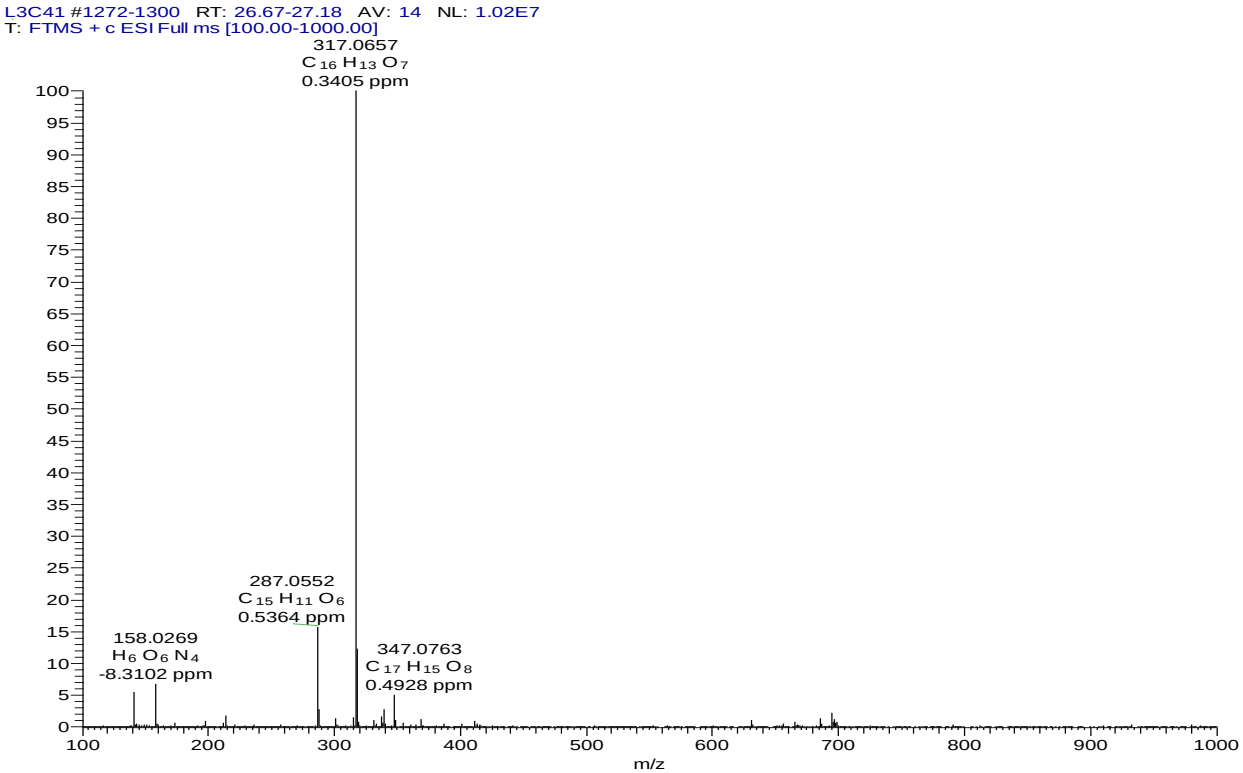

Appendix 39B: LC-UV spectrum of compound **212**

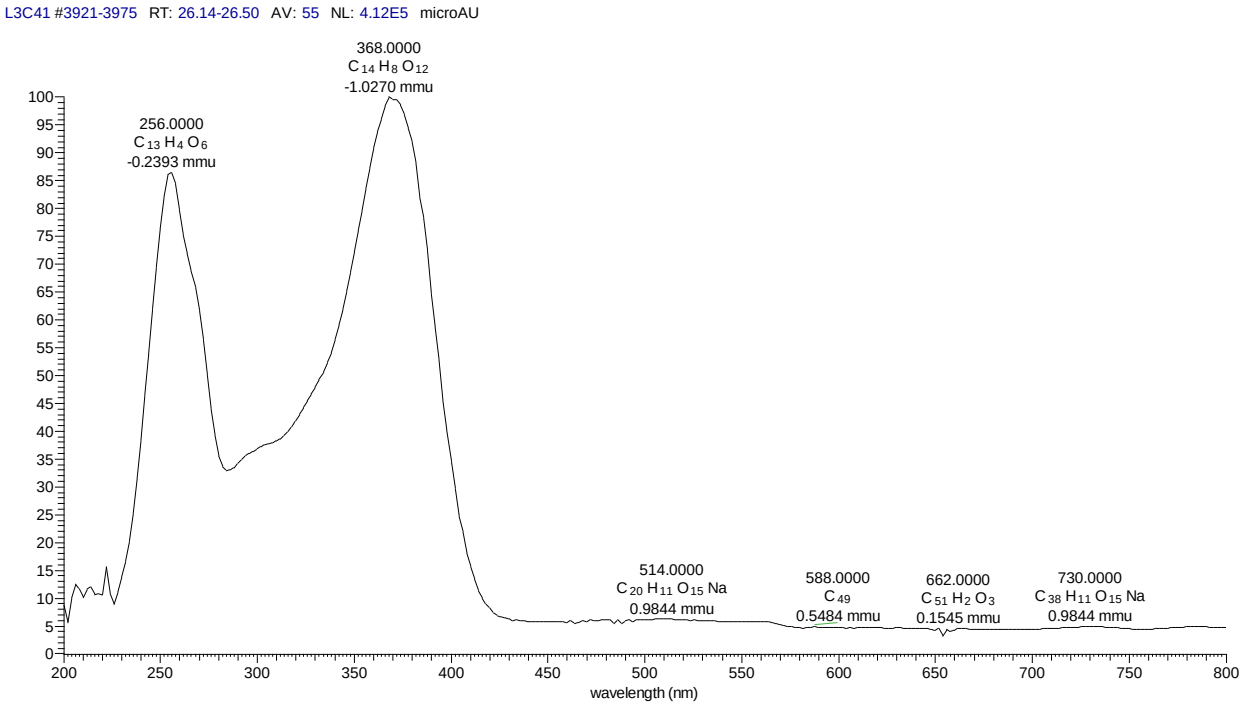

Appendix 39C: ^{1}H NMR spectrum (600 MHz, DMSO-d_6) of compound **212**

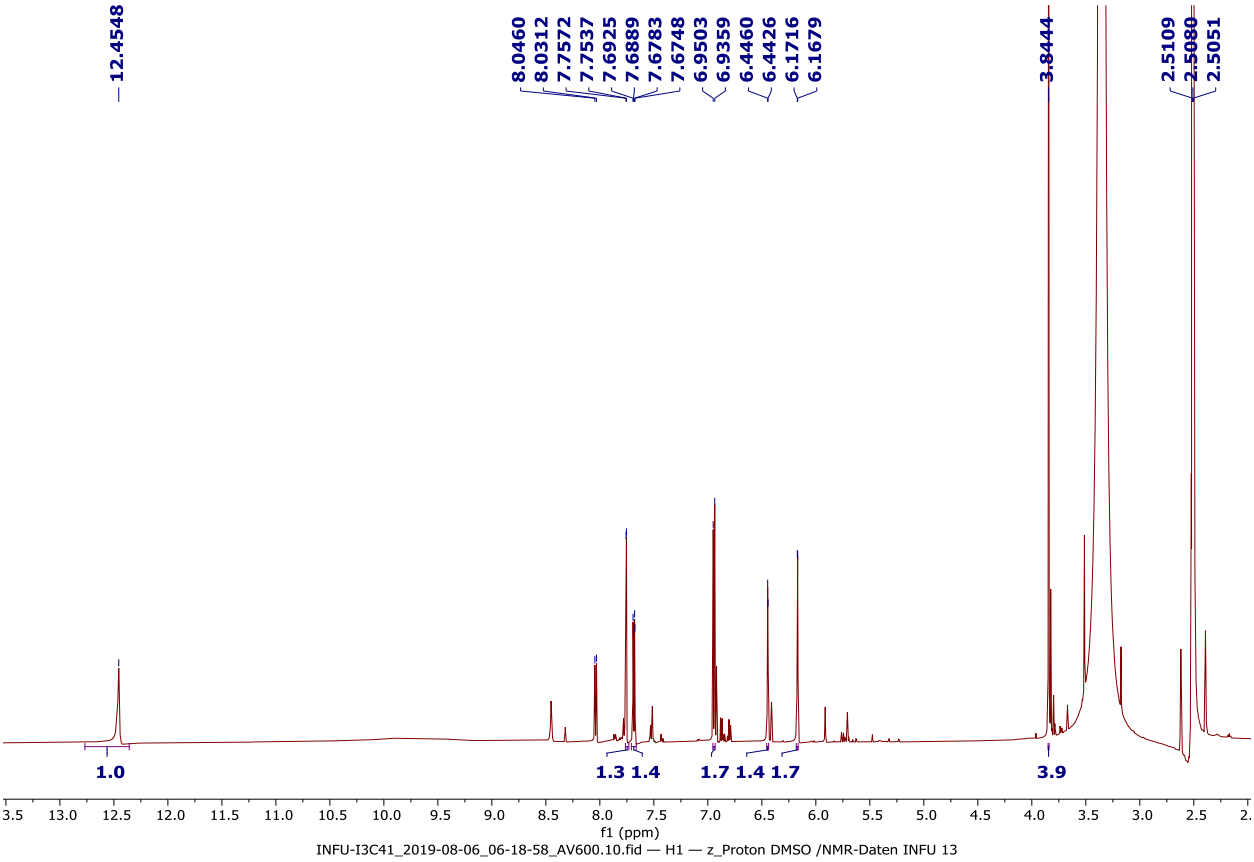

Appendix 39D: ^{13}C NMR spectrum (150 MHz, DMSO-d_6) of compound **212**

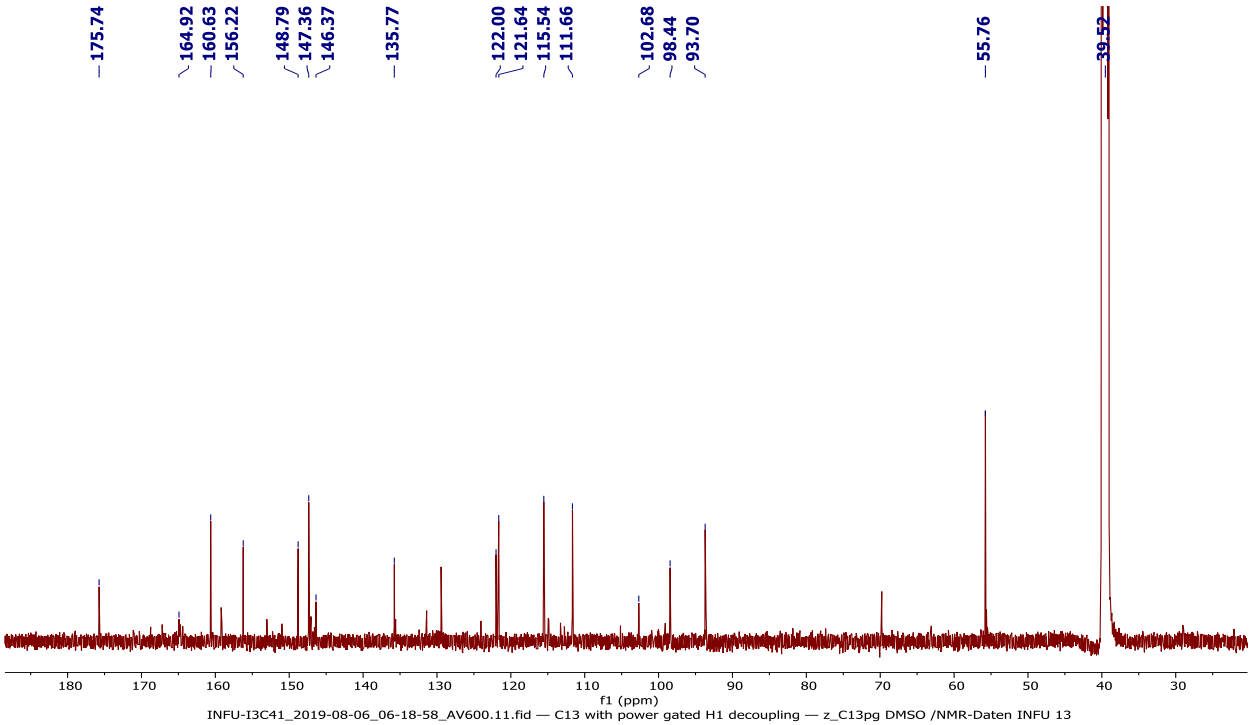

Appendix 39E: ^{1}H-^{1}H COSY spectrum (DMSO-d_6) of compound **212**

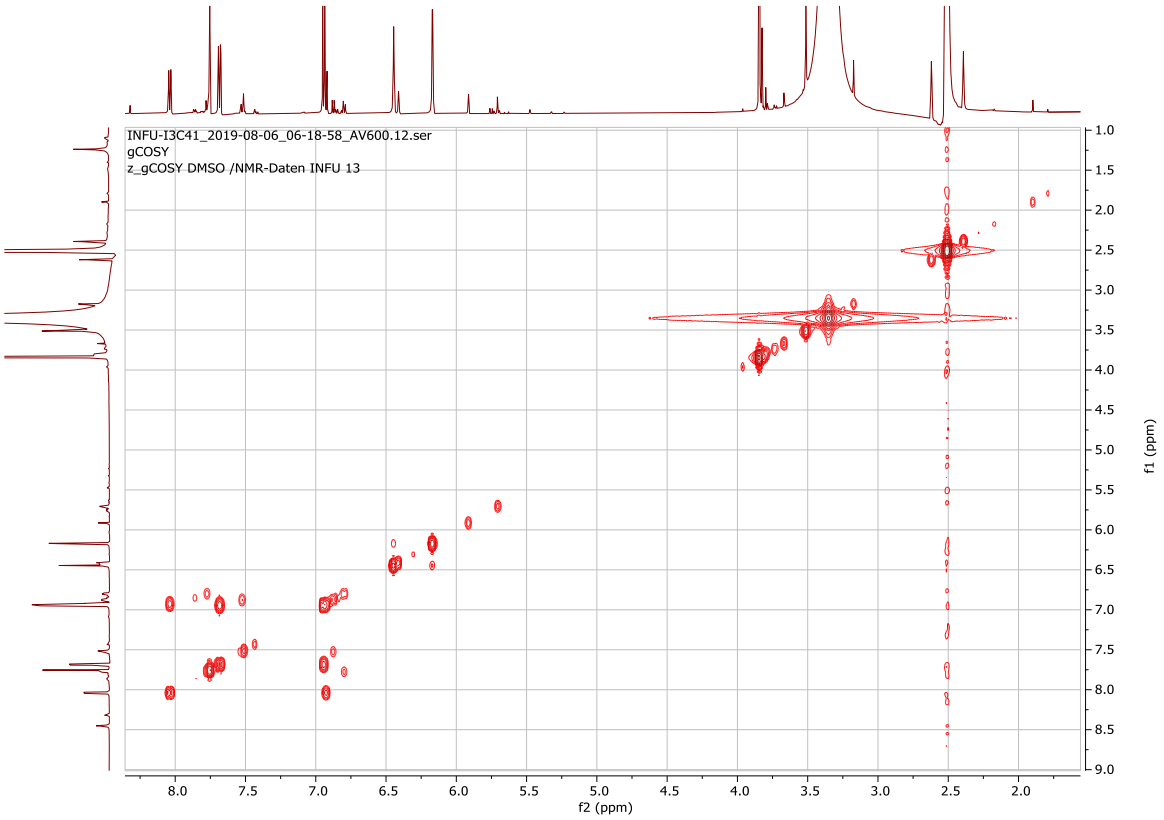

Appendix 39F: NOESY spectrum (DMSO-d_6) of compound **212**

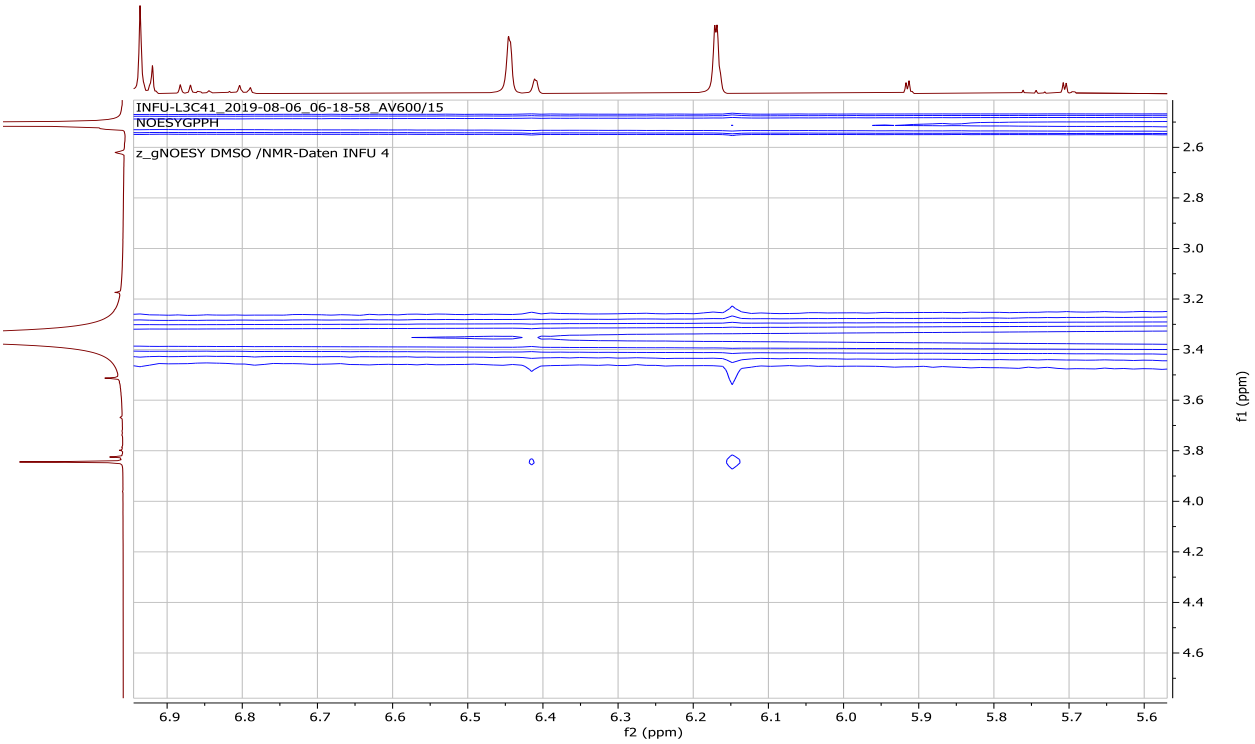

Appendix 39G: HSQC spectrum (DMSO-d_6) of compound **212**

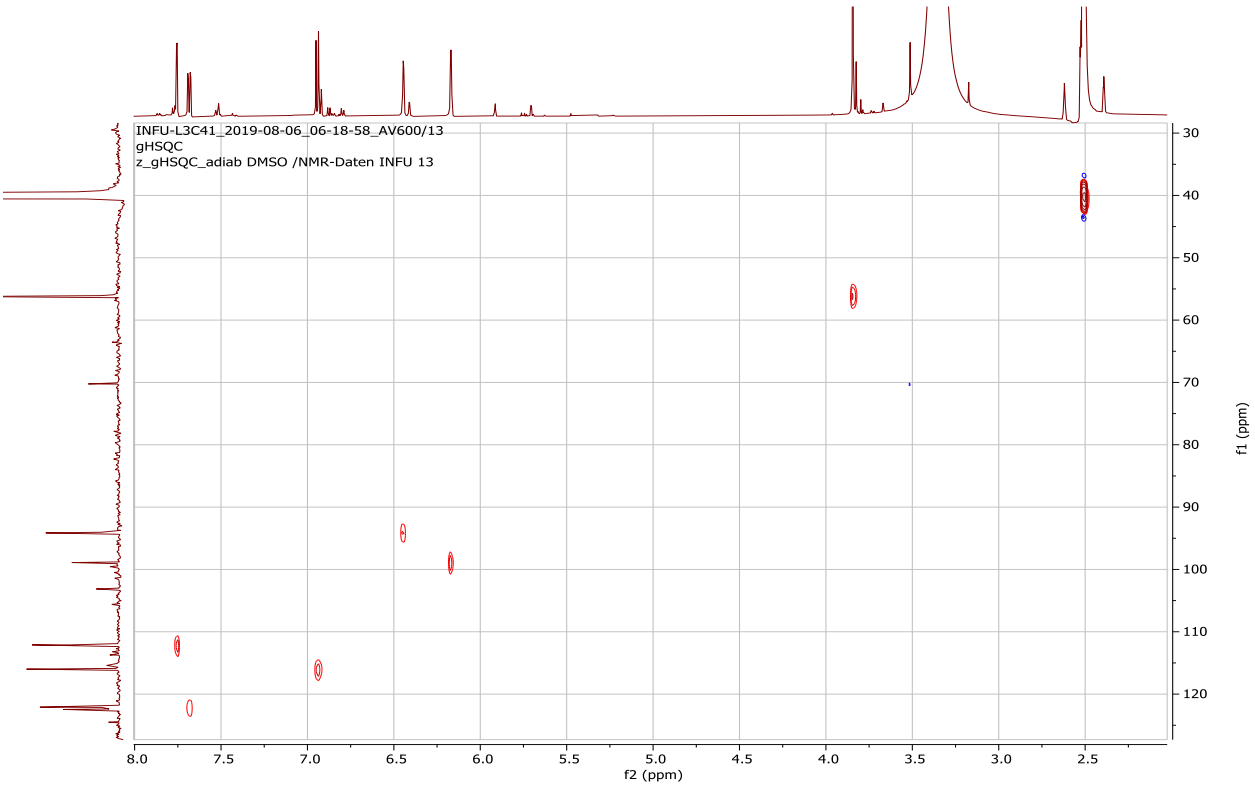

Appendix 39H: HMBC spectrum (DMSO-d_6) of compound **212**

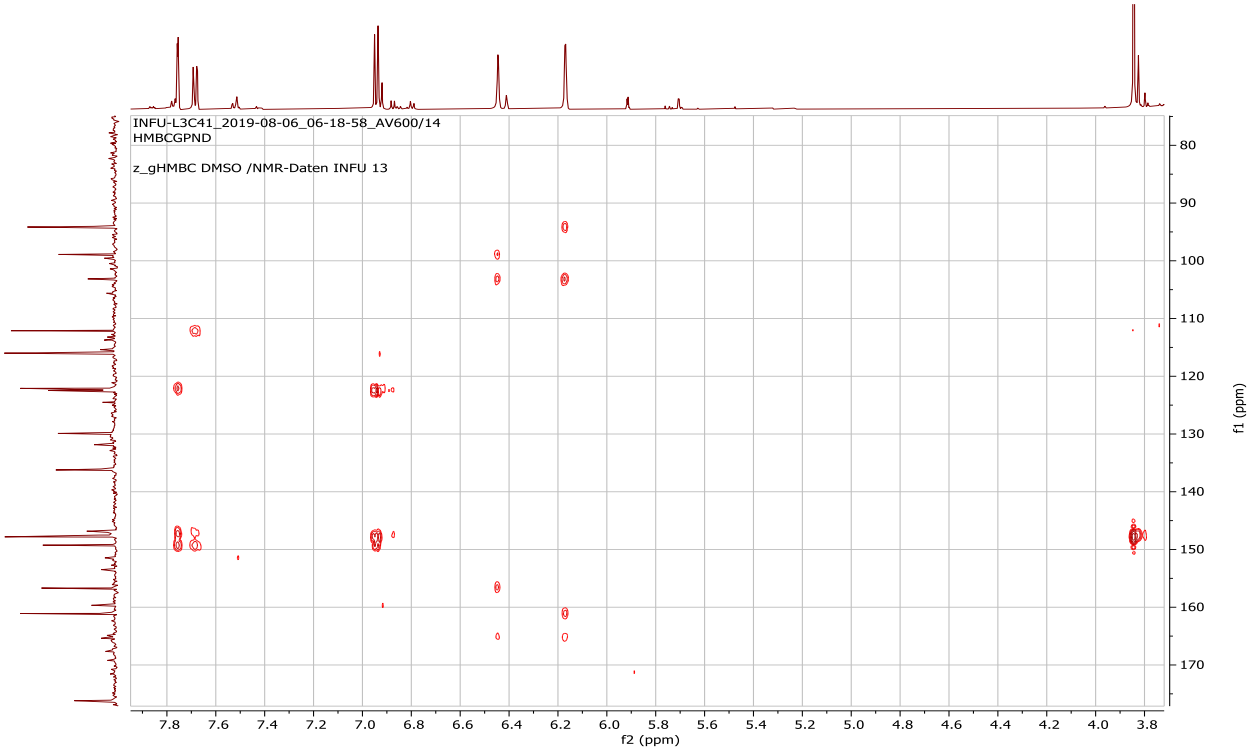

Appendix 40: NMR spectra for 3,3′-di-*O*-methylquercetin (**213**)

Appendix 40A: HRESIMS of compound **213**

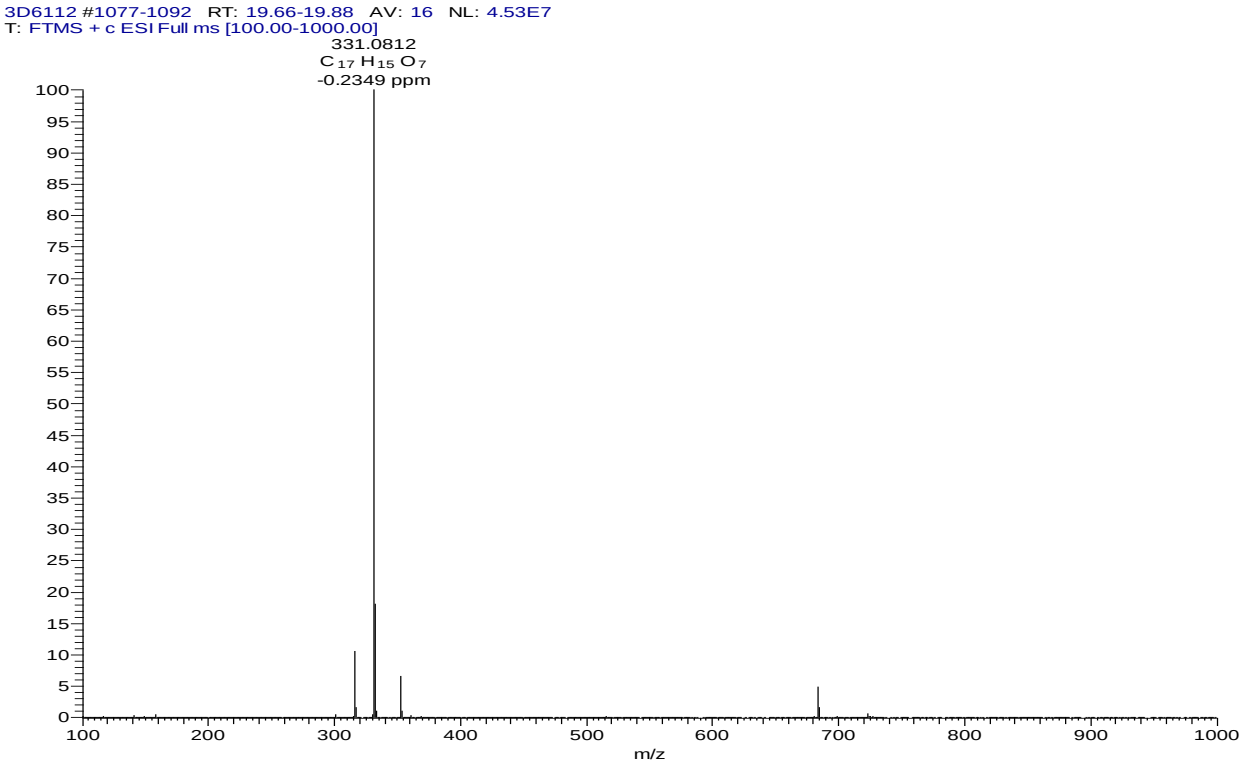

Appendix 40B: LC-UV spectrum of compound **213**

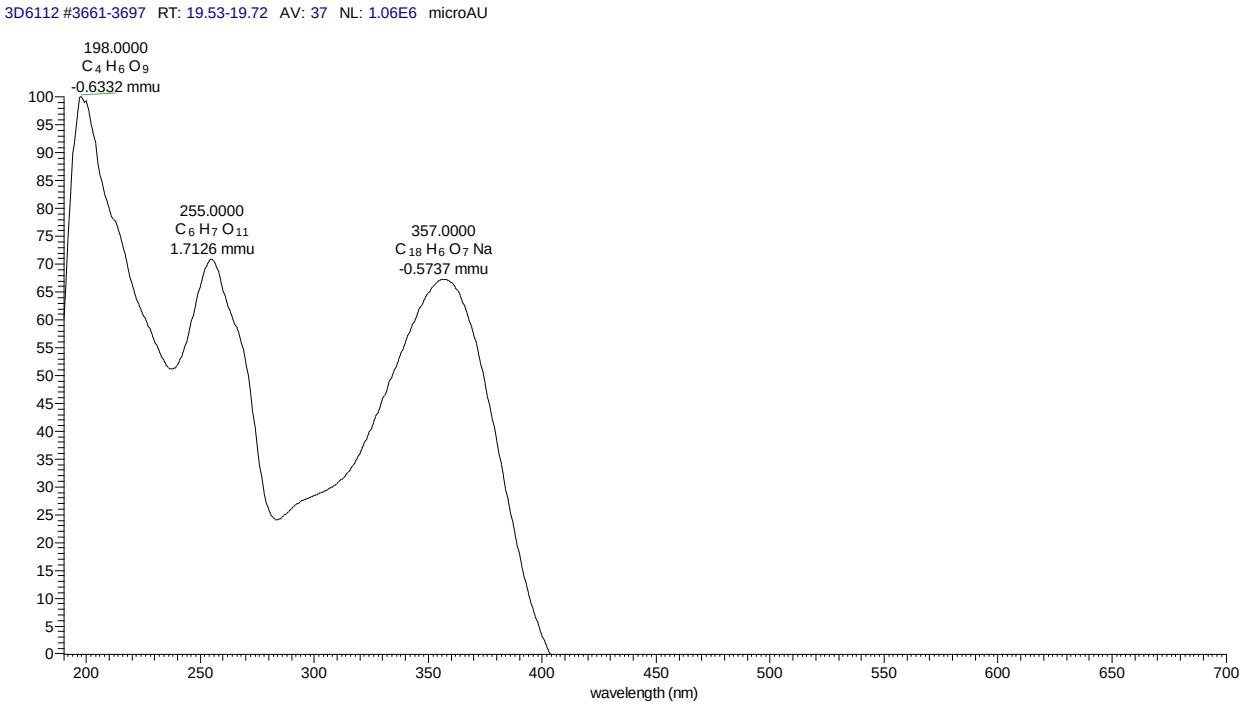

Appendix 40C: ^{1}H NMR spectrum (500 MHz, CD_3OD) of compound **213**

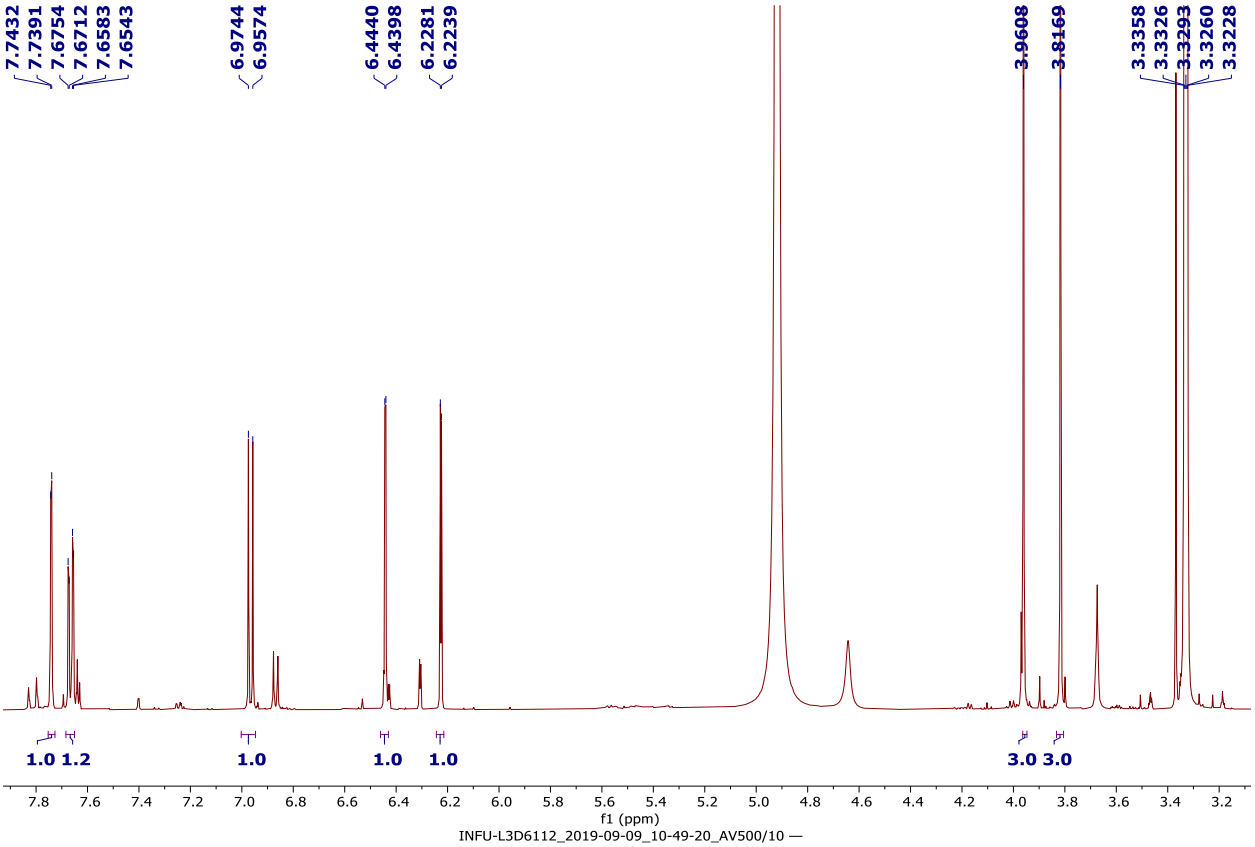

Appendix 40D: ^{13}C NMR spectrum (125 MHz, CD_3OD) of compound **213**

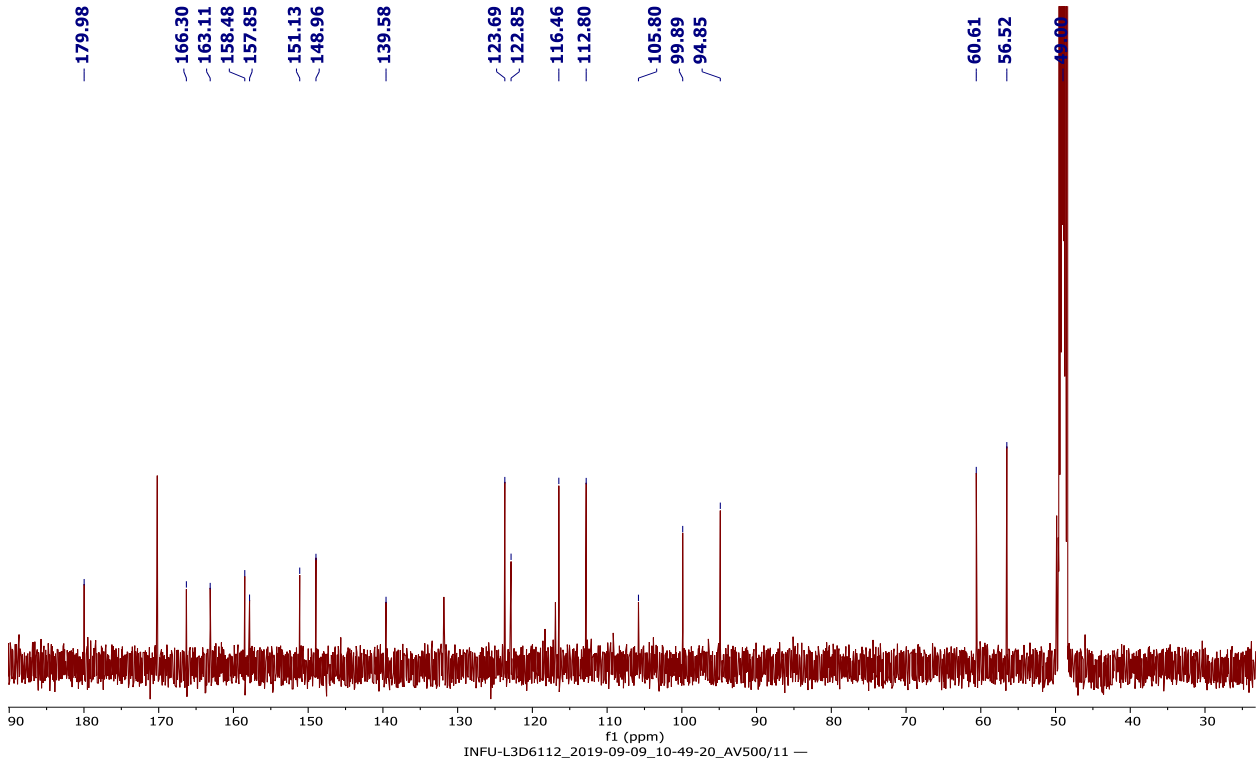

Appendix 40E: ^{1}H-^{1}H COSY spectrum (CD_3OD) of compound **213**

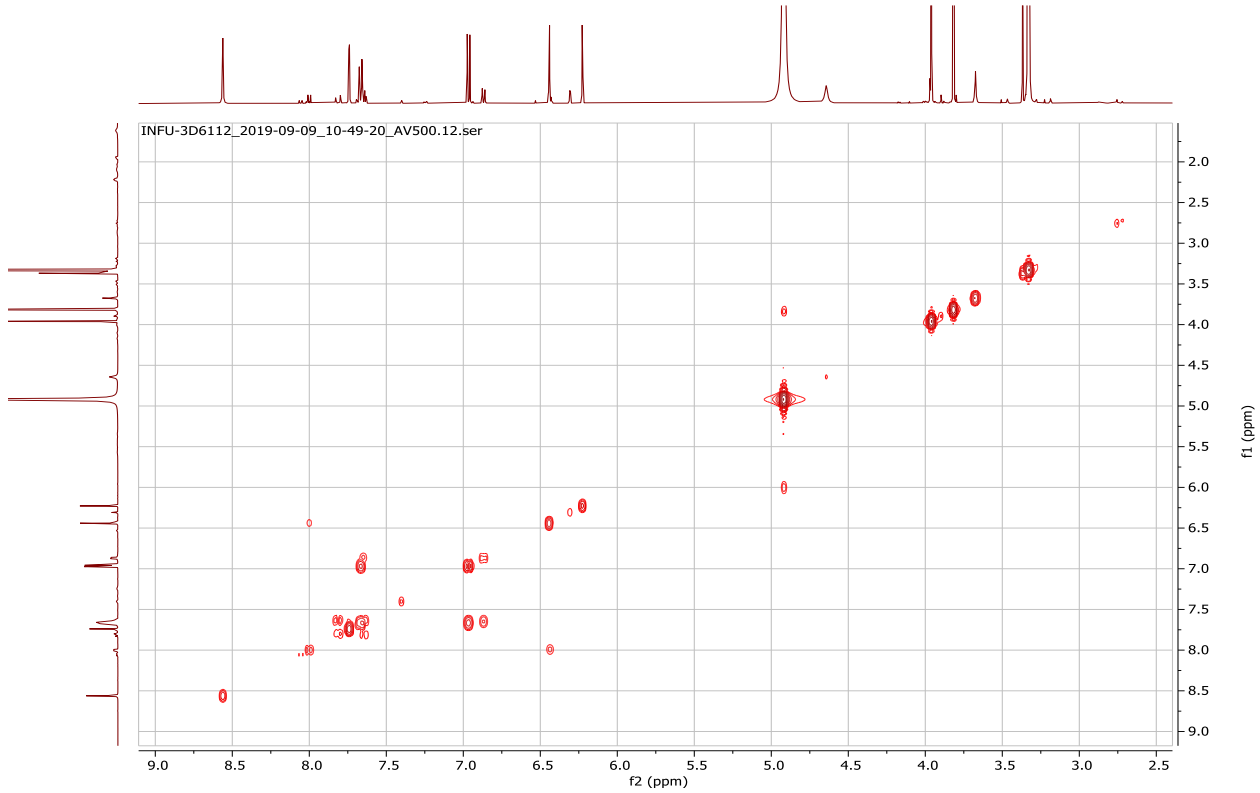

Appendix 40F: NOESY spectrum (CD_3OD) of compound **213**

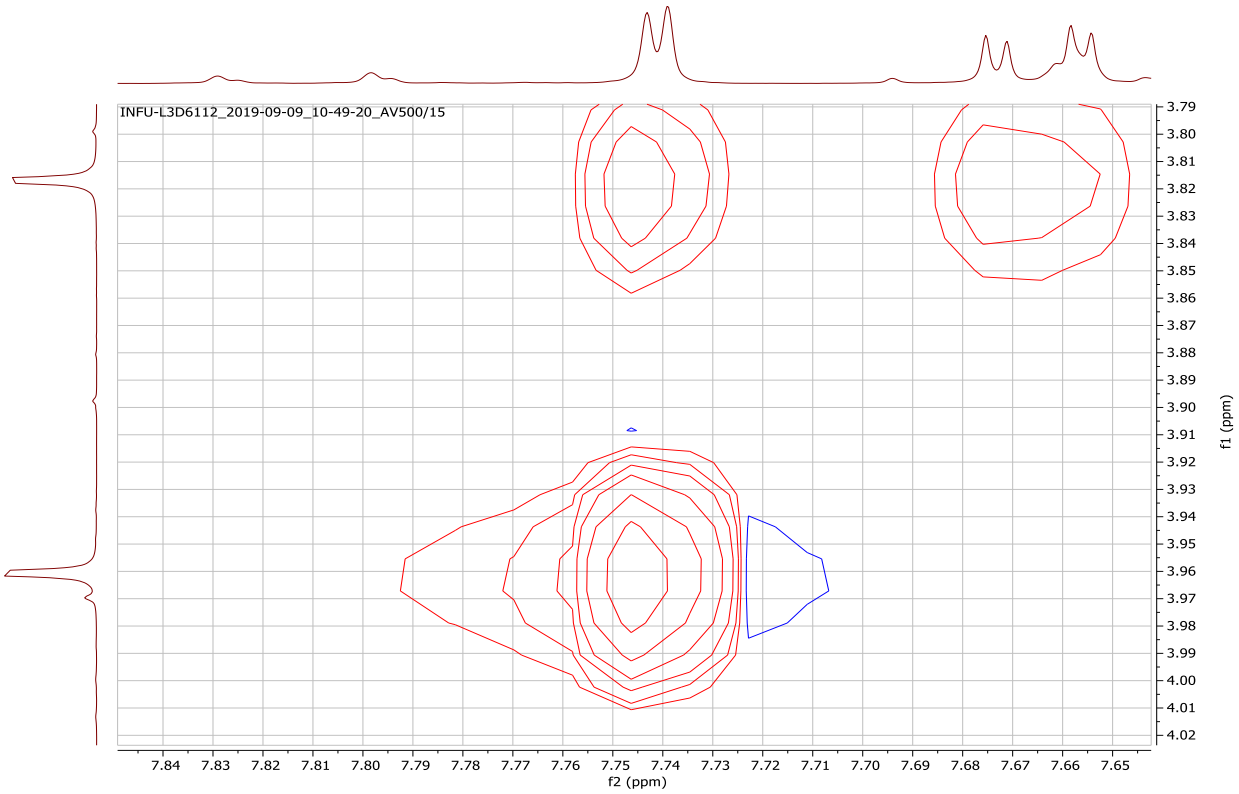

Appendix 40G: HMBC spectrum (CD_3OD) of compound **214**

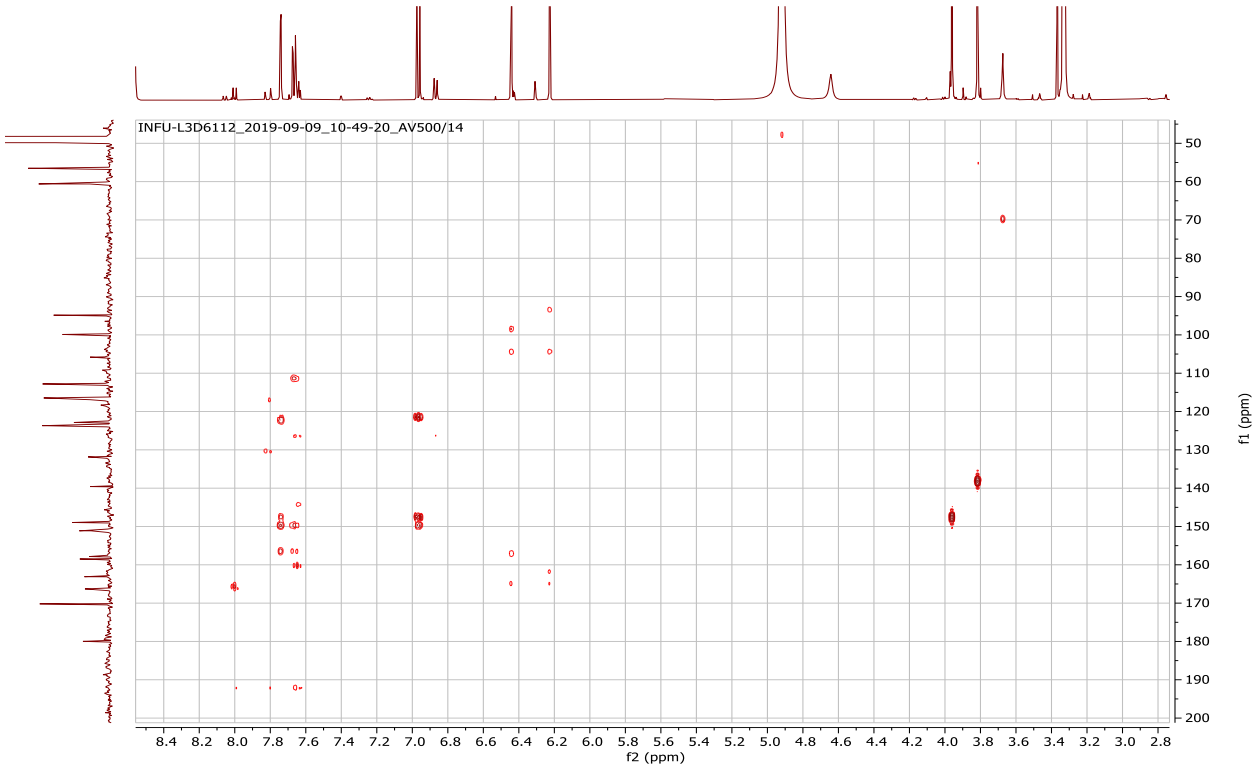

Appendix 41: NMR spectra for kaempferol 3-methyl ether (**214**)

Appendix 41A: HRESIMS of compound **214**

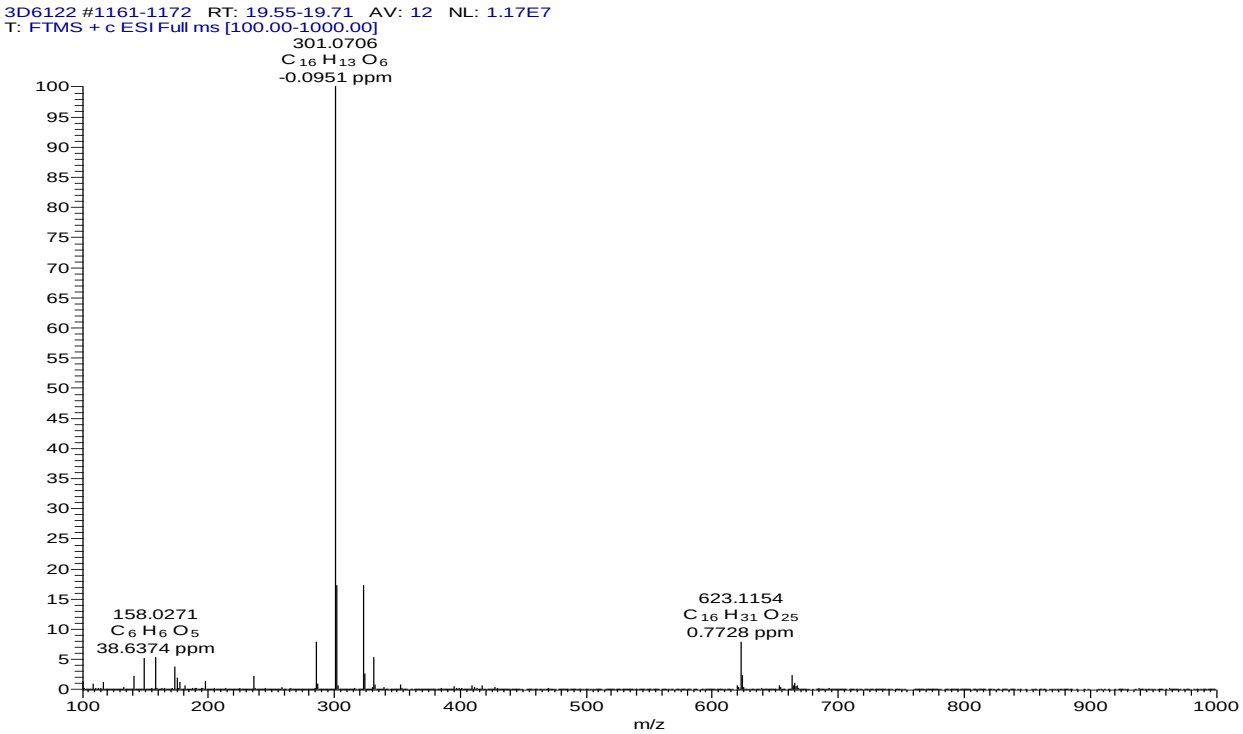

Appendix 41B: LC-UV spectrum of compound **214**

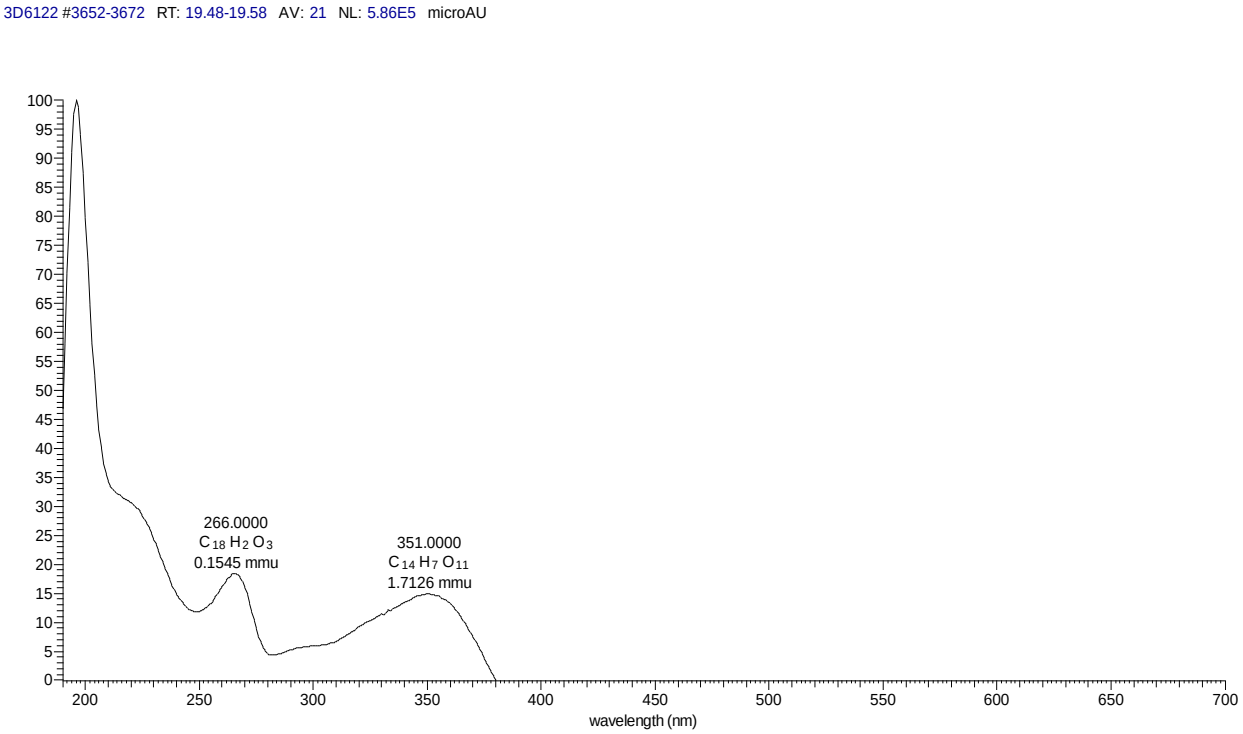

Appendix 41C: ^{1}H NMR spectrum (700 MHz, CD_3OD) of compound **214**

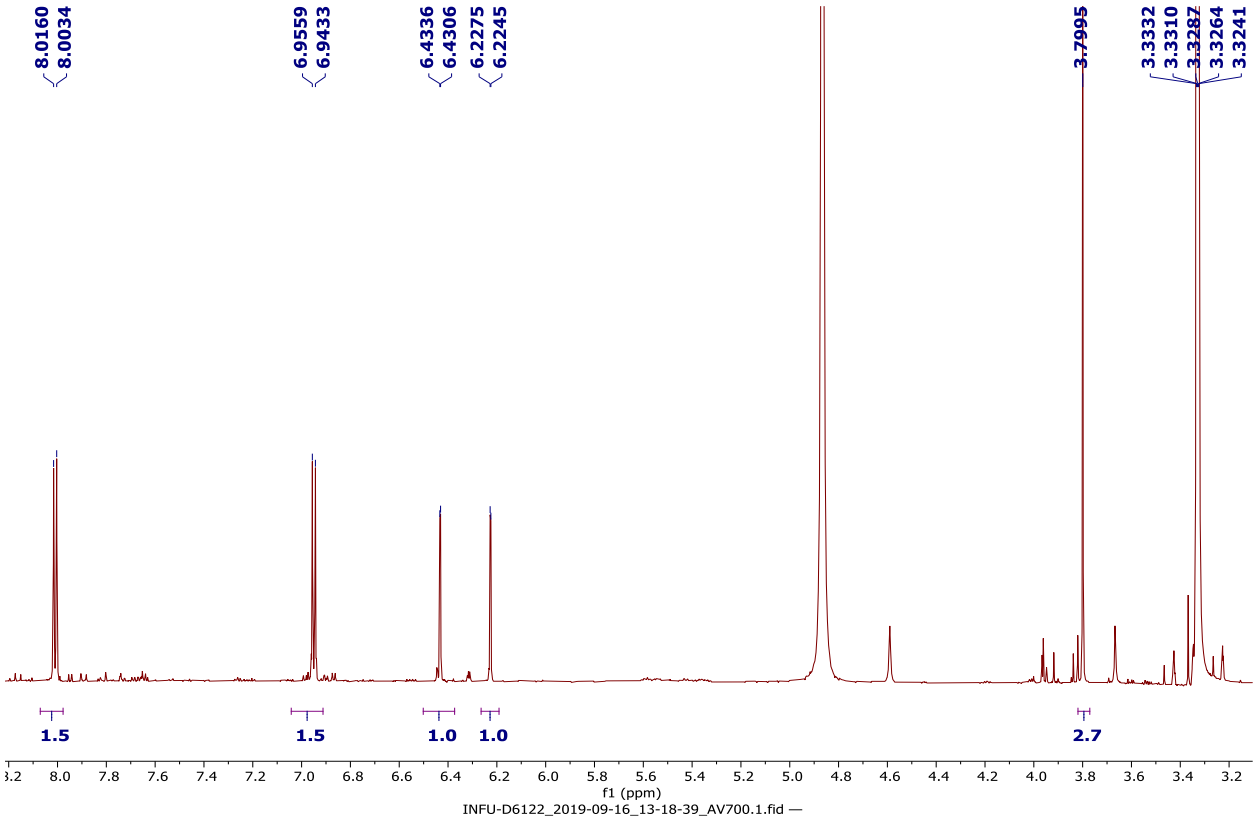

Appendix 41D: ^{13}C NMR spectrum (175 MHz, CD_3OD) of compound **214**

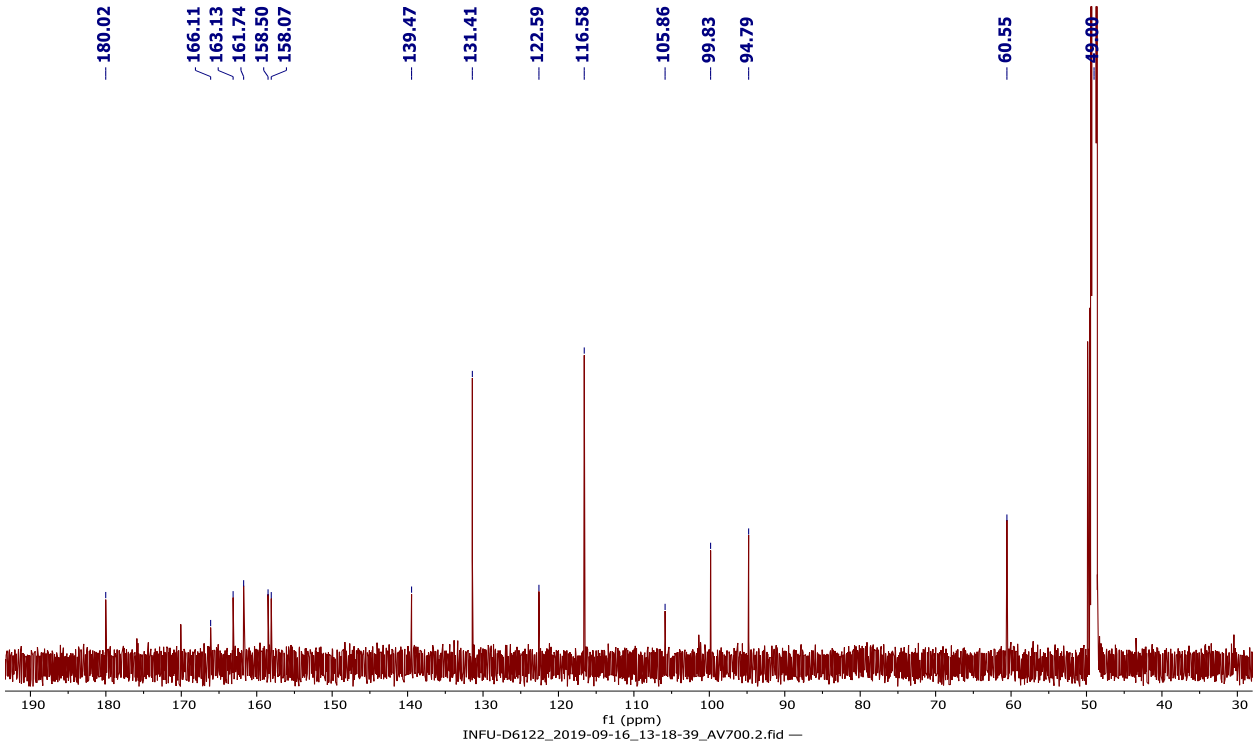

Appendix 41E: ^{1}H-^{1}H COSY spectrum (CD_3OD) of compound **214**

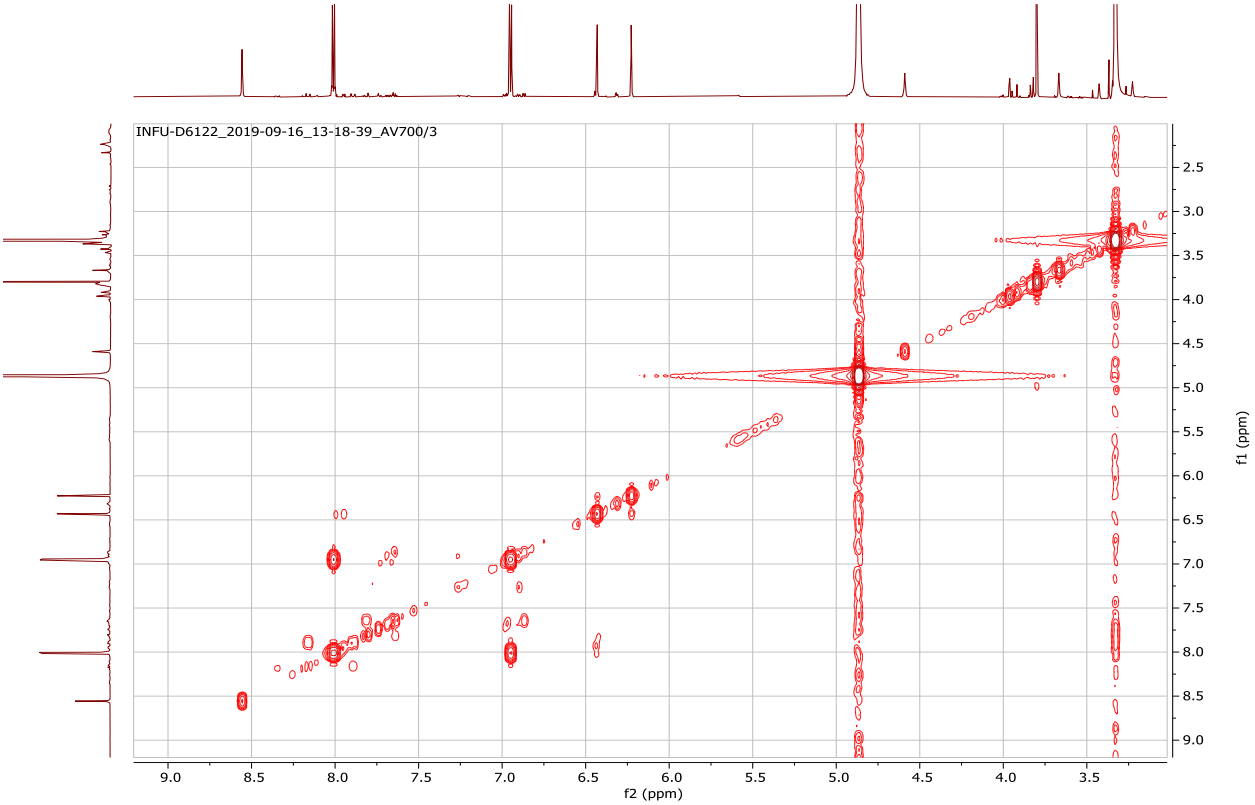

Appendix 41F: HSQC spectrum (CD_3OD) of compound **214**

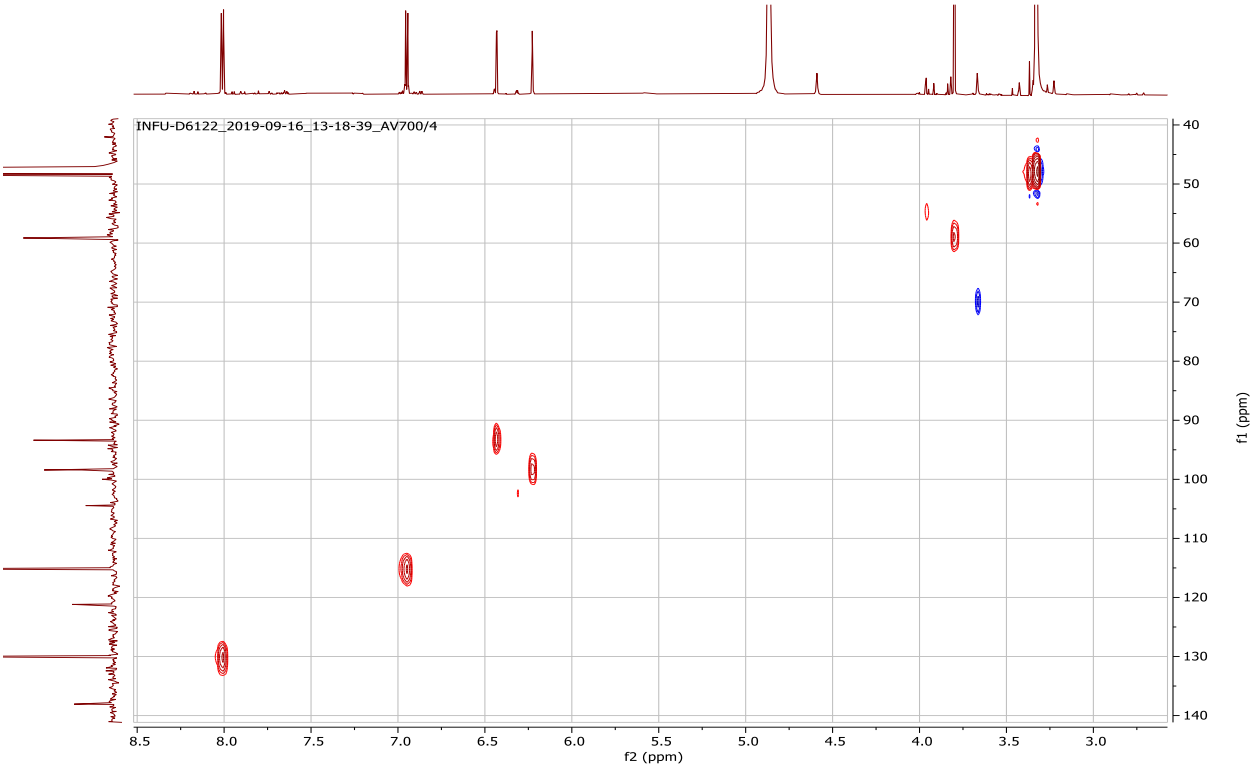

Appendix 41G: HMBC spectrum (CD_3OD) of compound **214**

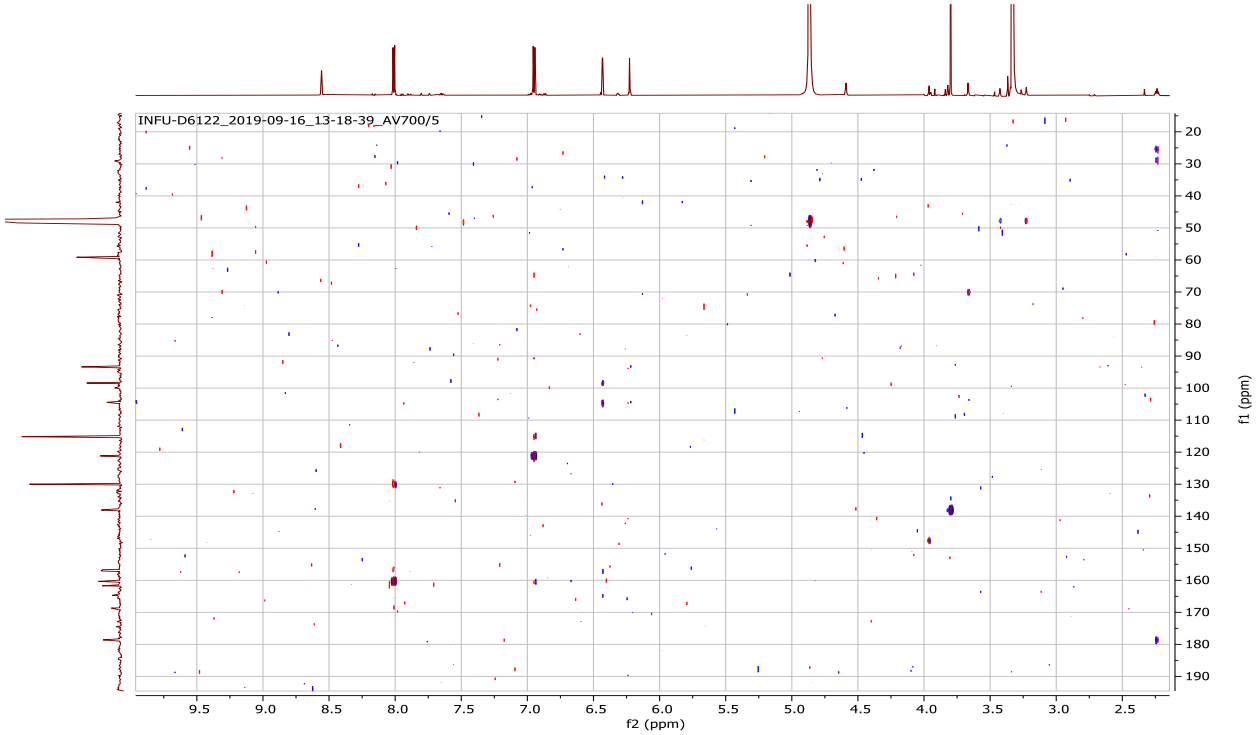

Appendix 42: NMR spectra for jaceidin (**215**)

Appendix 42A: HRESIMS of compound **215**

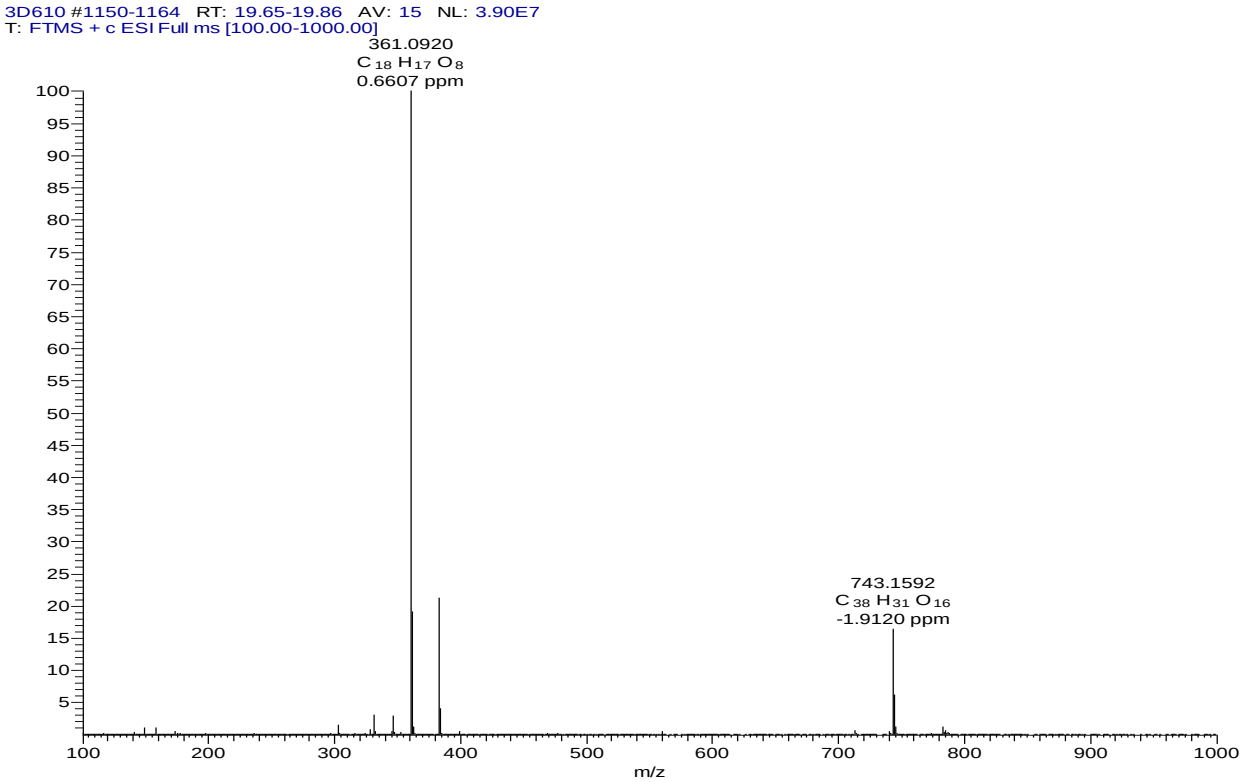

Appendix 42B: LC-UV spectrum of compound **215**

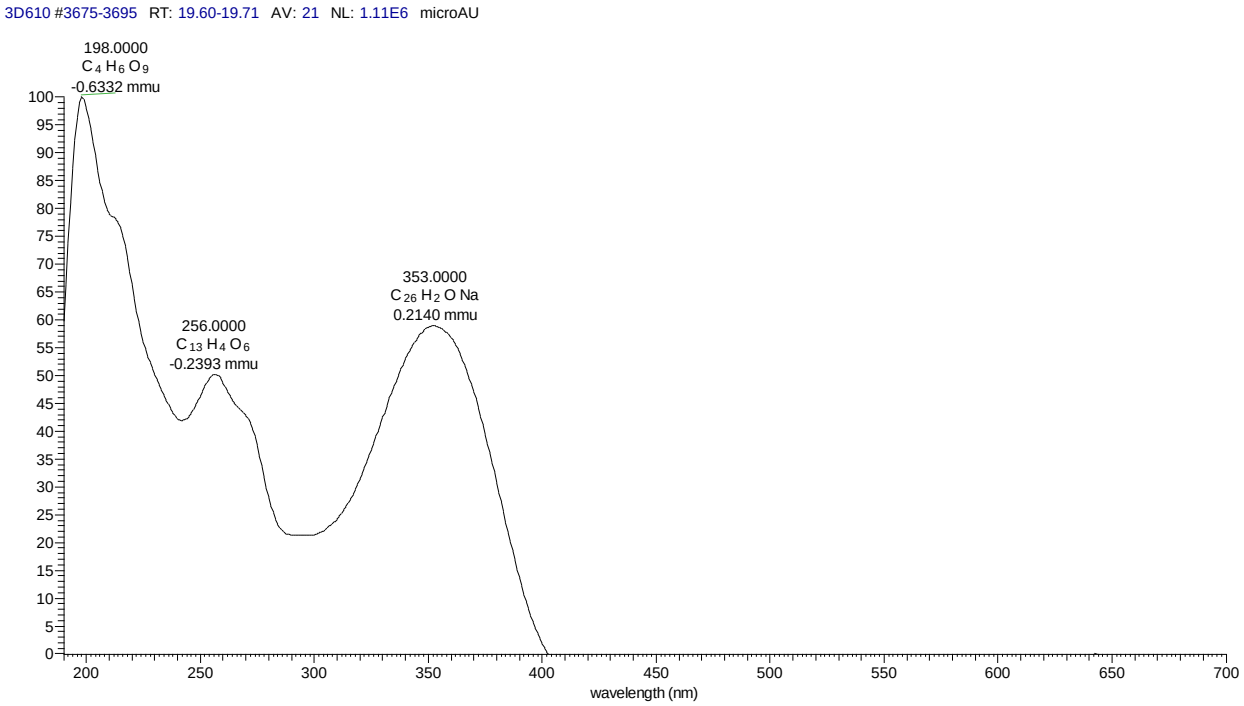

Appendix 42C: ^{1}H NMR spectrum (700 MHz, CD_3OD) of compound **215**

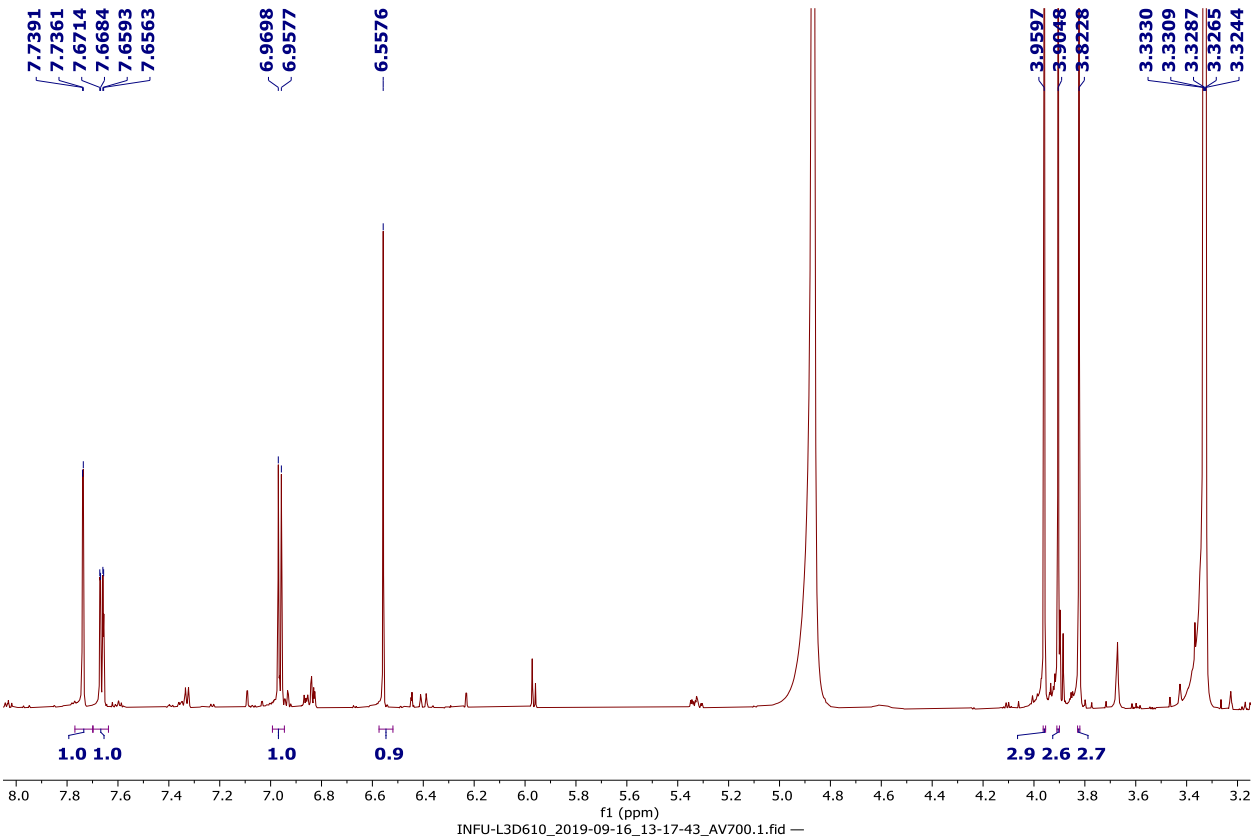

Appendix 42D: ^{13}C NMR spectrum (175 MHz, CD_3OD) of compound **215**

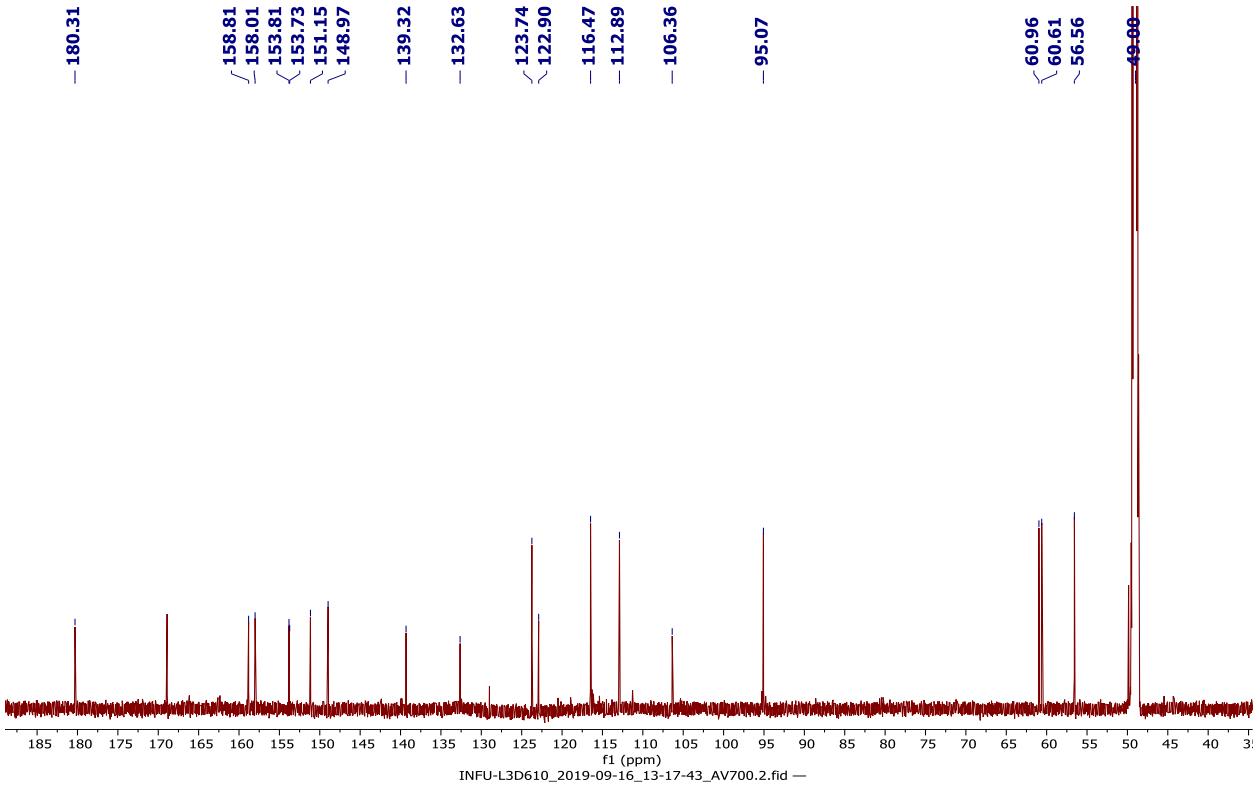

Appendix 42E: ^{1}H-^{1}H COSY spectrum (CD_3OD) of compound **215**

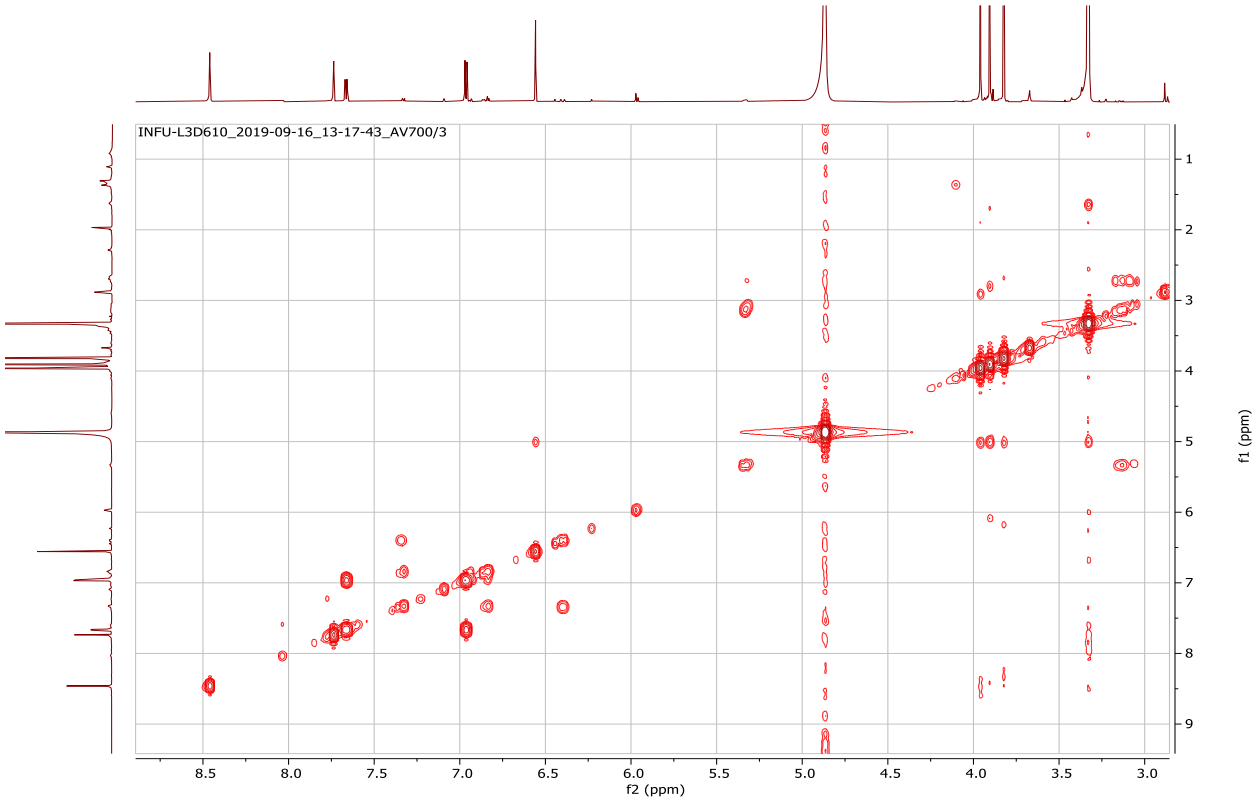

Appendix 42F: NOESY spectrum (CD_3OD) of compound **215**

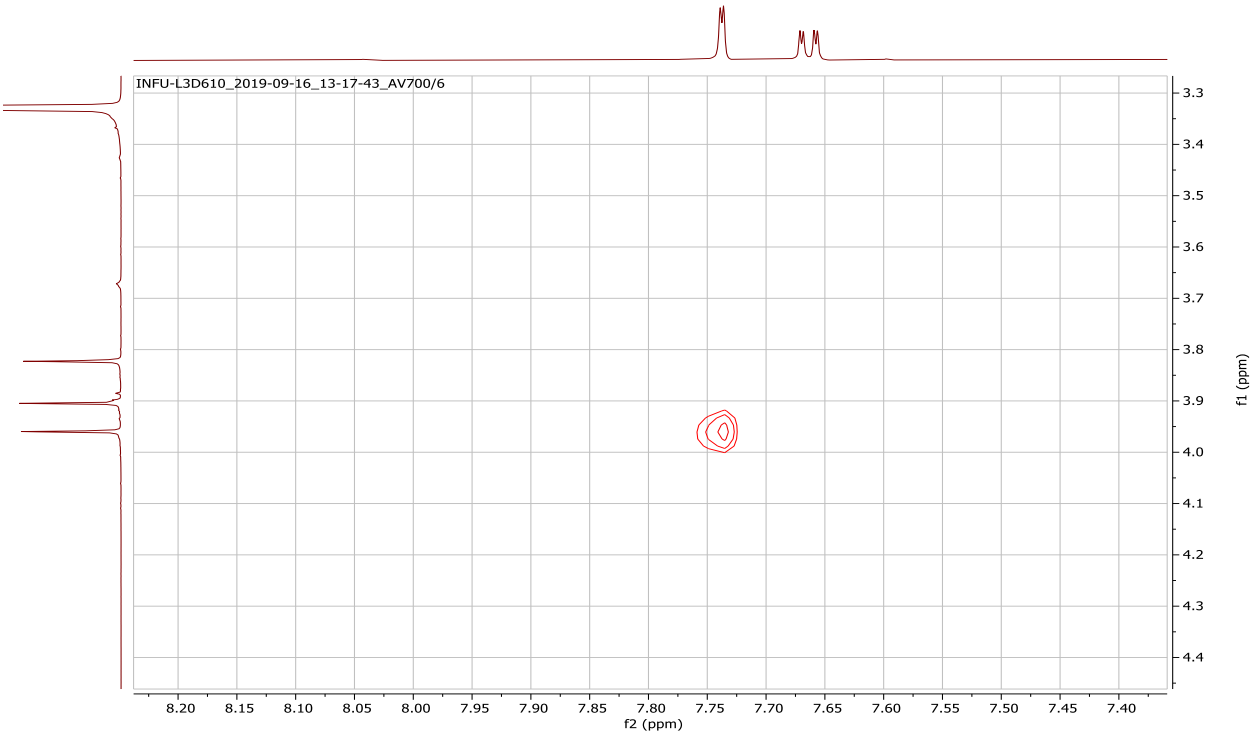

Appendix 42G: HSQC spectrum (CD_3OD) of compound **215**

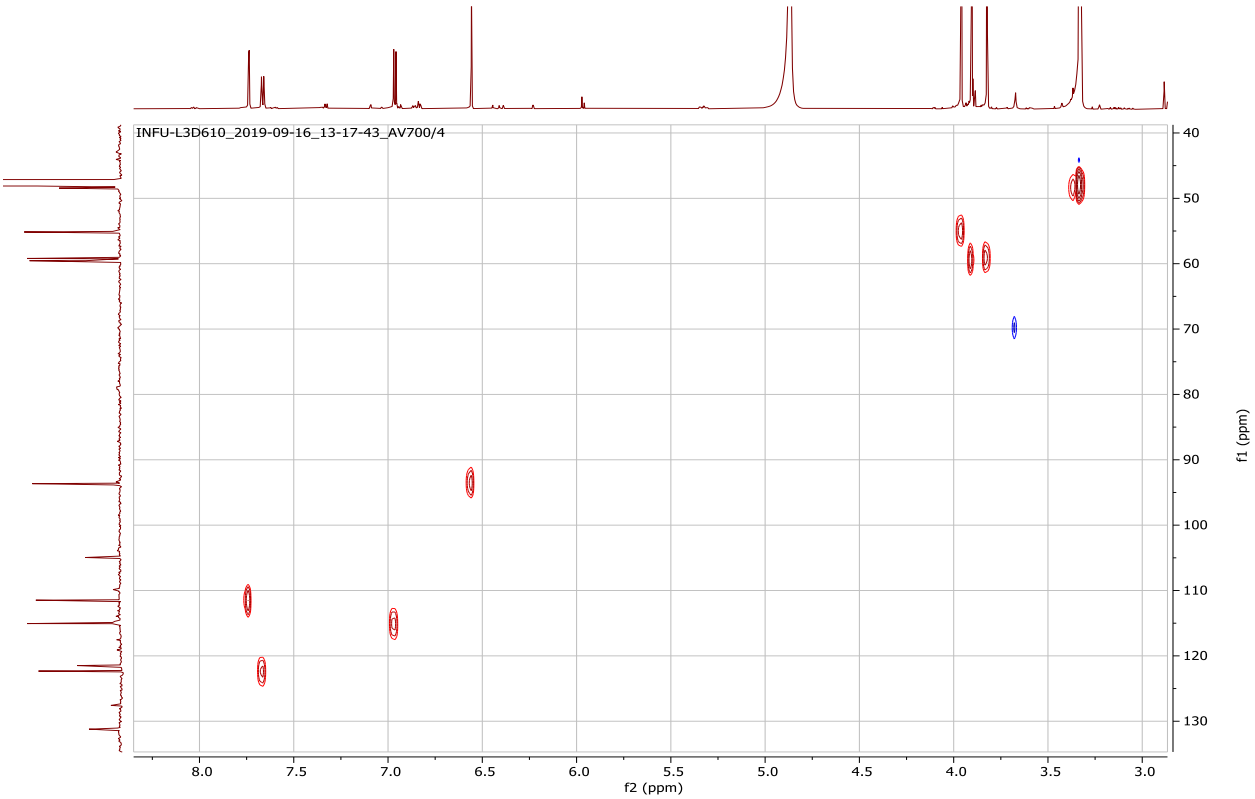

Appendix 42H: HMBC spectrum (CD_3OD) of compound **215**

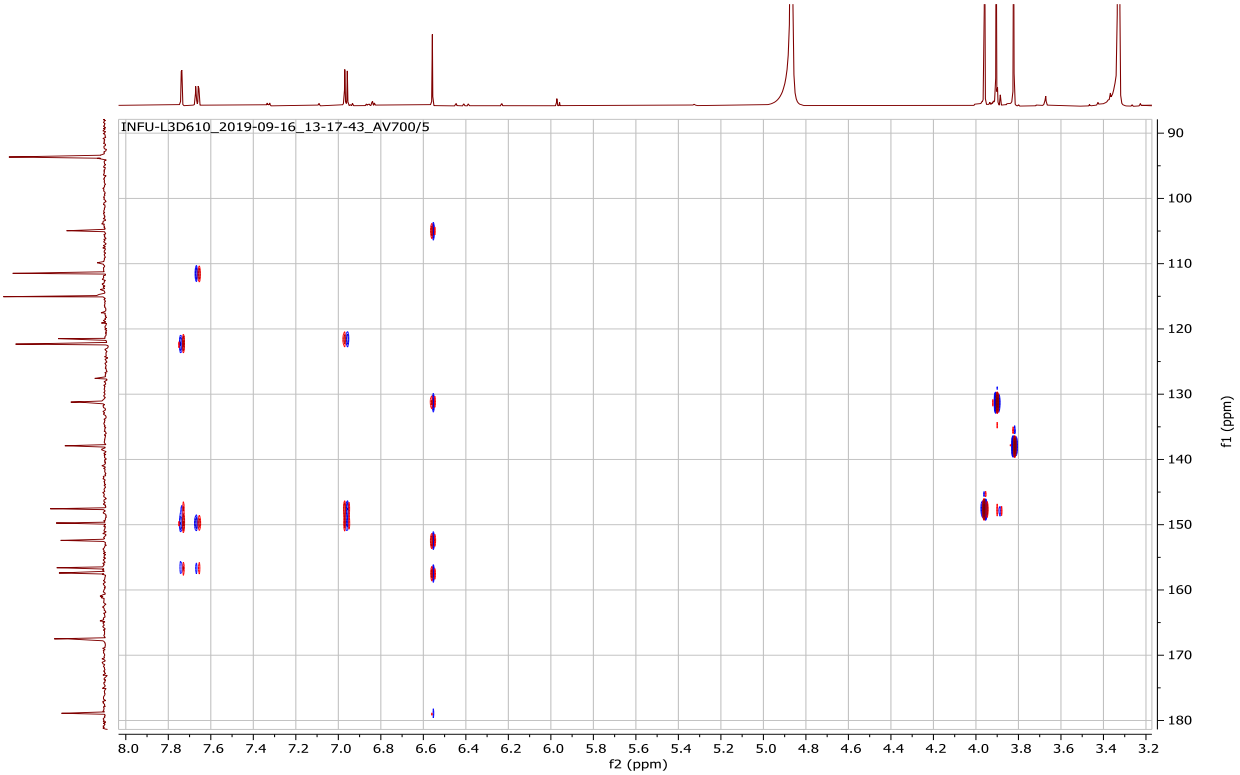

Appendix 43: NMR spectra for 7-hydroxy-6-methoxyflavone (**216**)

Appendix 43A: HRESIMS of compound **216**

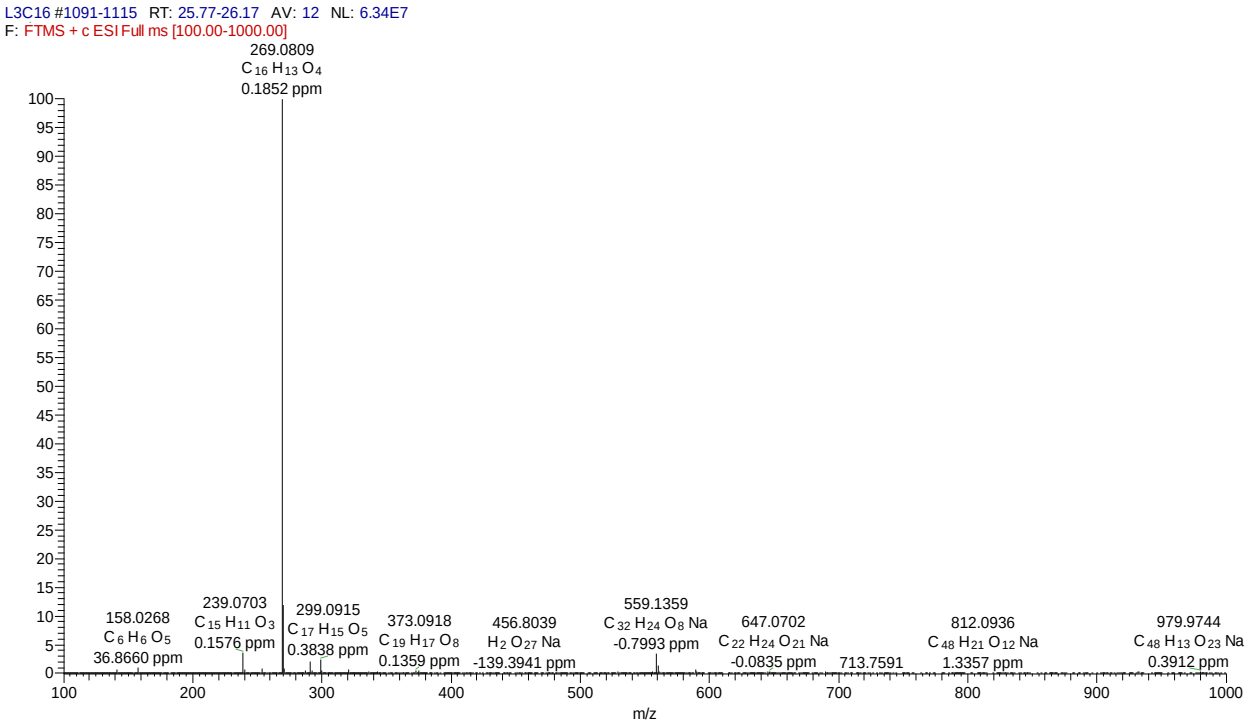

Appendix 43B: LC-UV spectrum of compound **216**

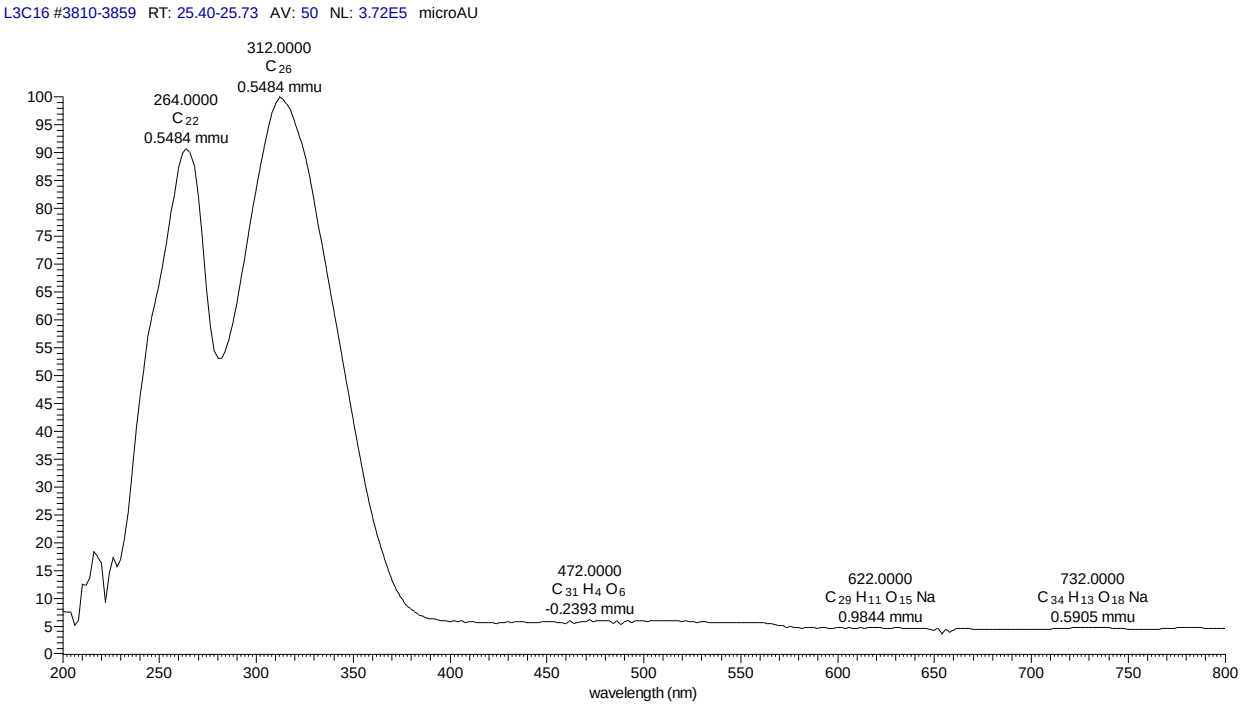

Appendix 43C: ^{1}H NMR spectrum (600 MHz, CD_3OD) of compound **216**

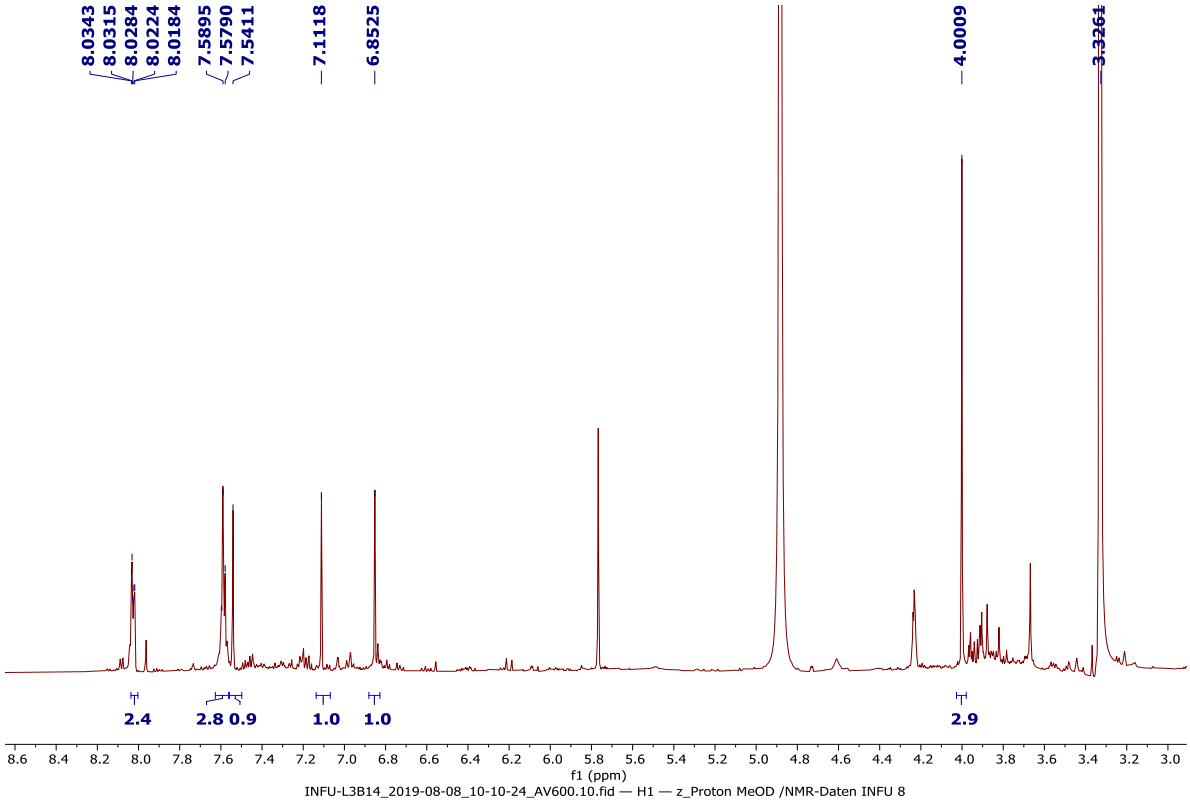

Appendix 43D: ^{13}C NMR spectrum (150 MHz, CD_3OD) of compound **216**

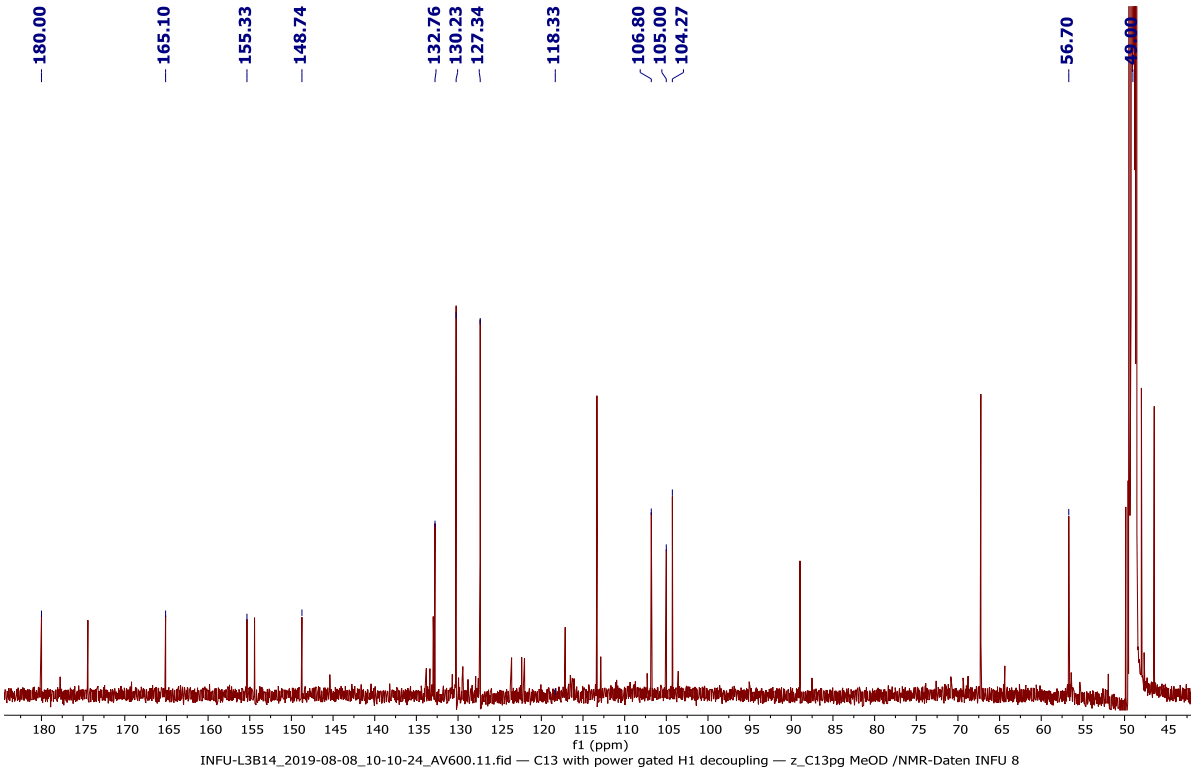

Appendix 43E: ^{1}H-^{1}H COSY spectrum (CD_3OD) of compound **216**

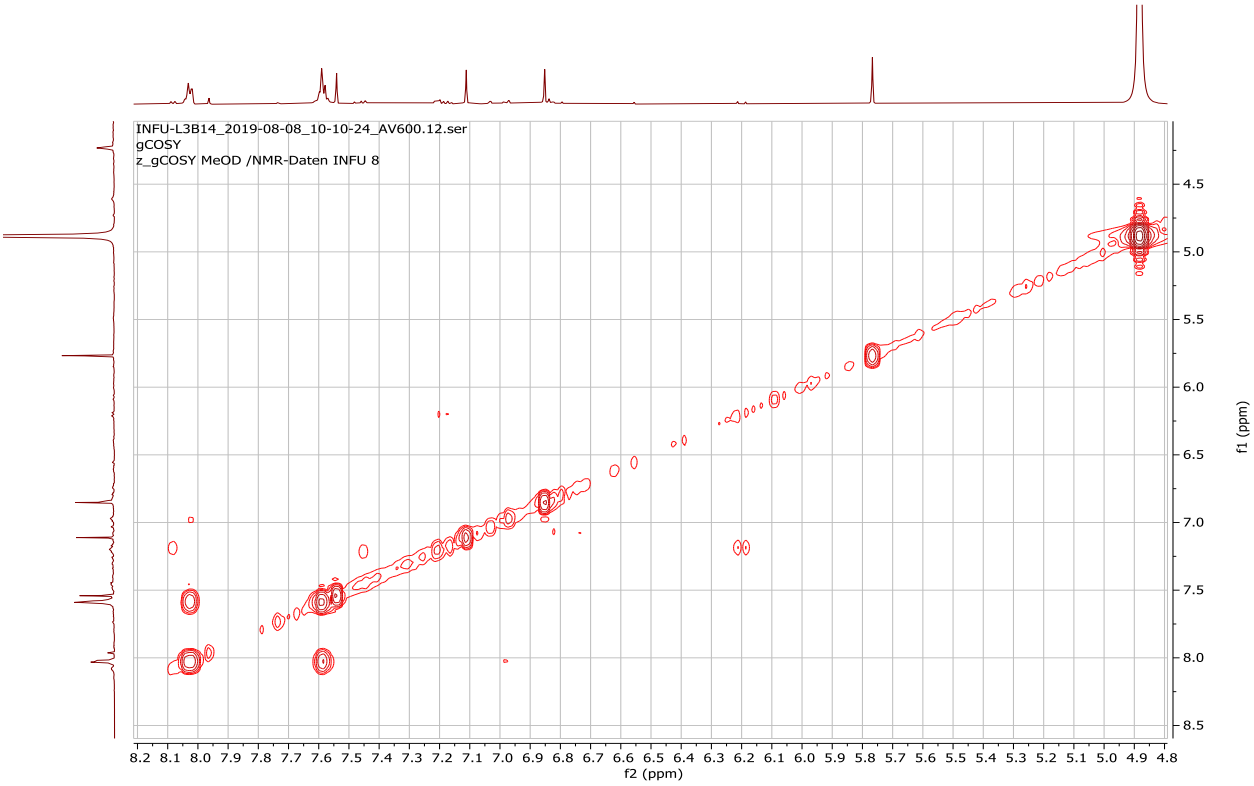

Appendix 43F: NOESY spectrum (CD_3OD) of compound **216**

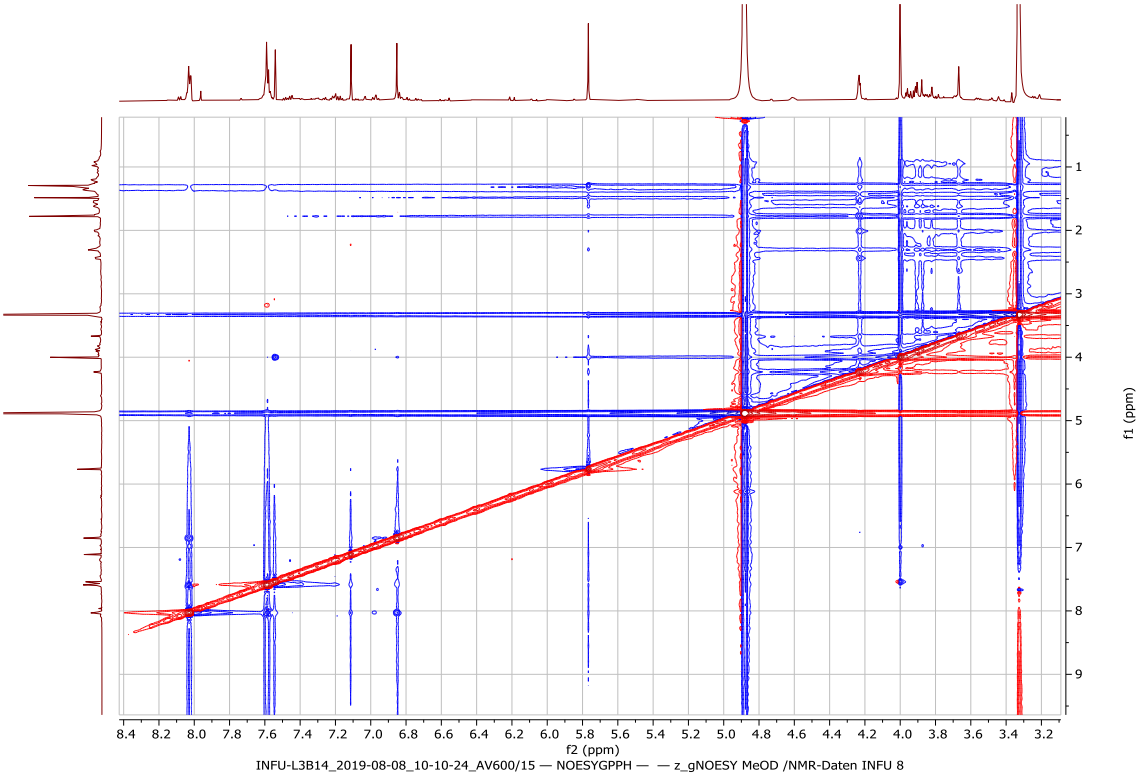

Appendix 43G: HSQC spectrum (CD_3OD) of compound **216**

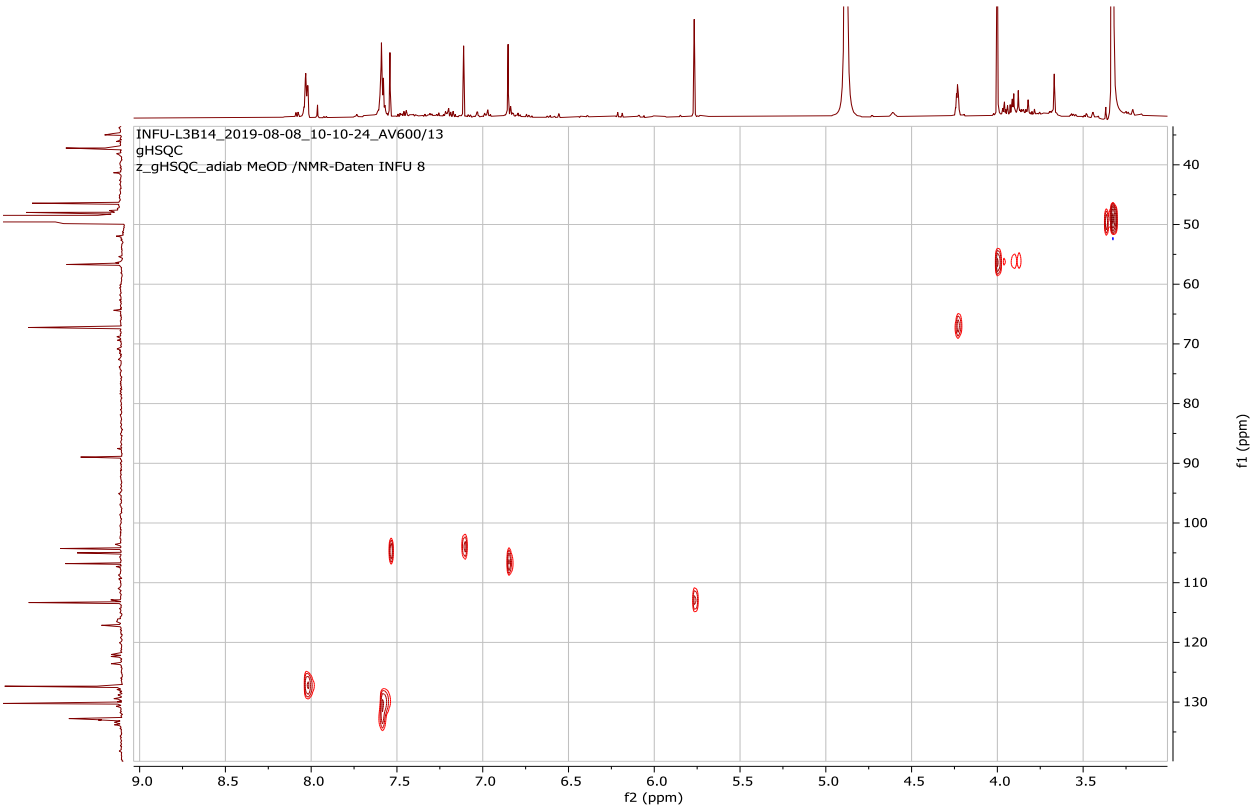

Appendix 43H: HMBC spectrum (CD_3OD) of compound **216**

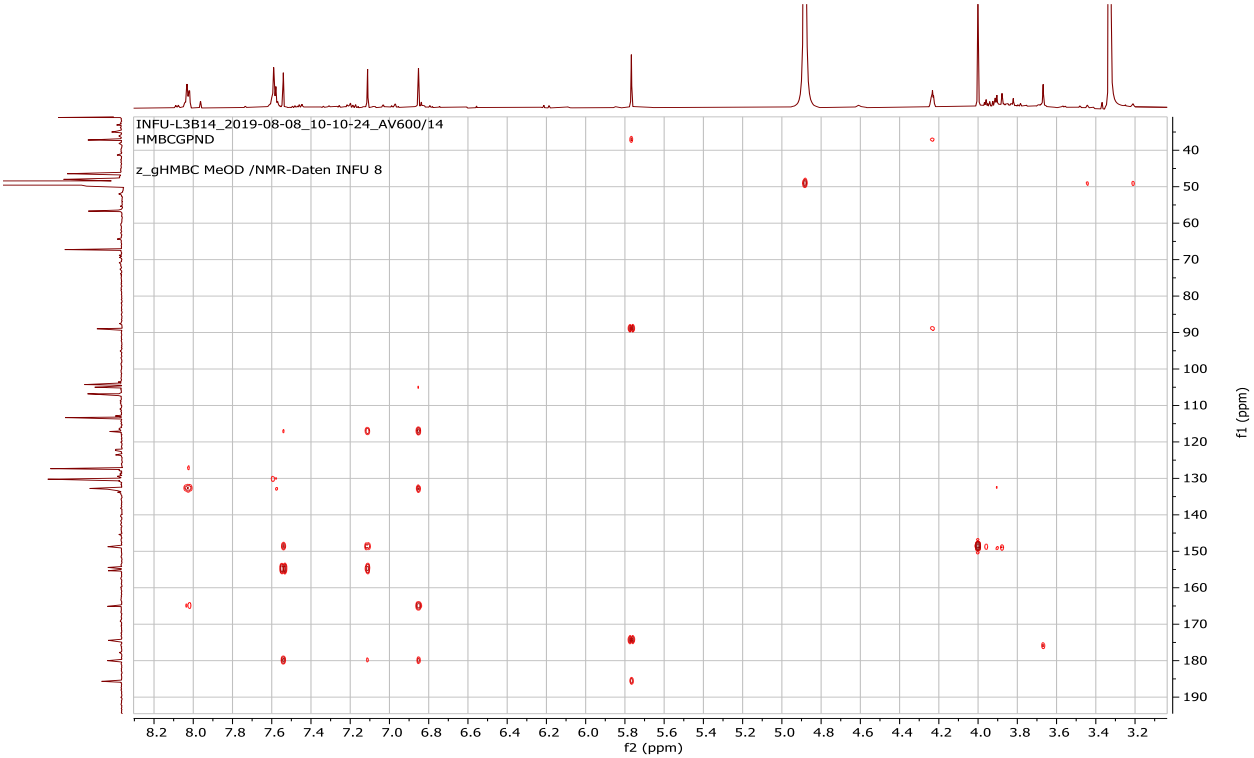

Appendix 44: NMR spectra for 6,8-dimethylchrysin (**217**)

Appendix 44A: HRESIMS of compound **217**

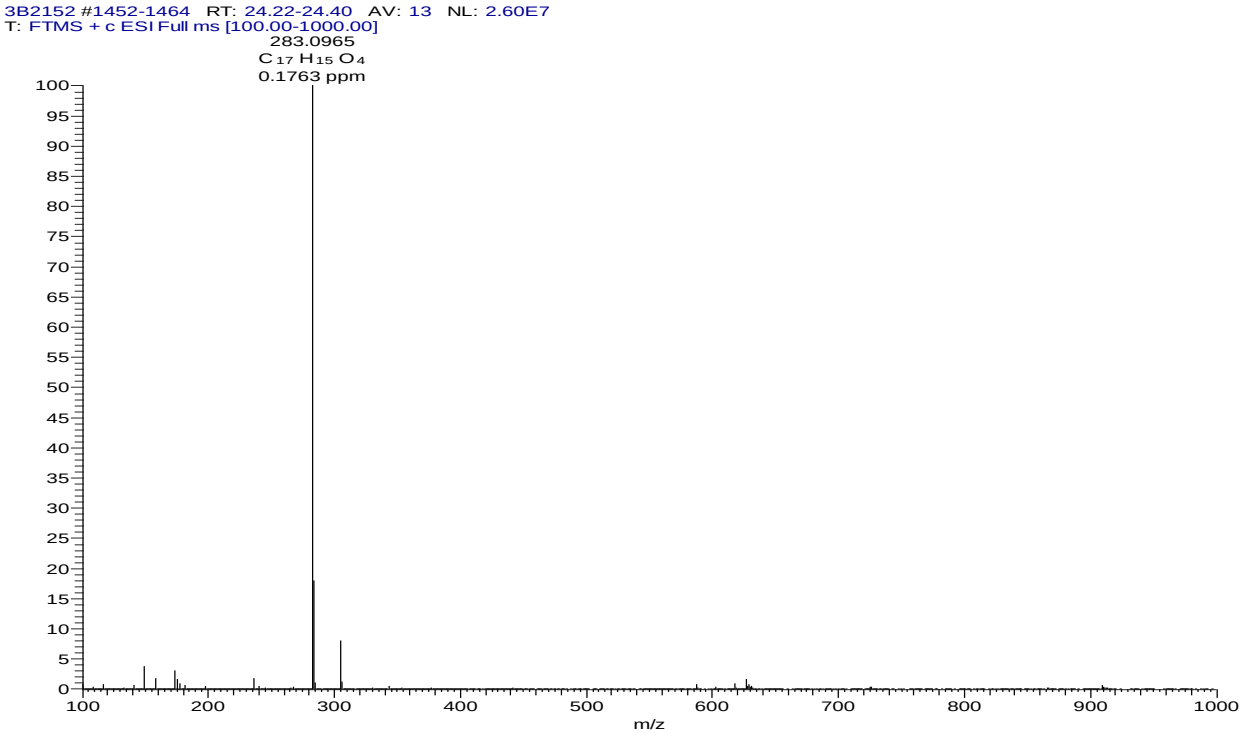

Appendix 44B: LC-UV spectrum of compound **217**

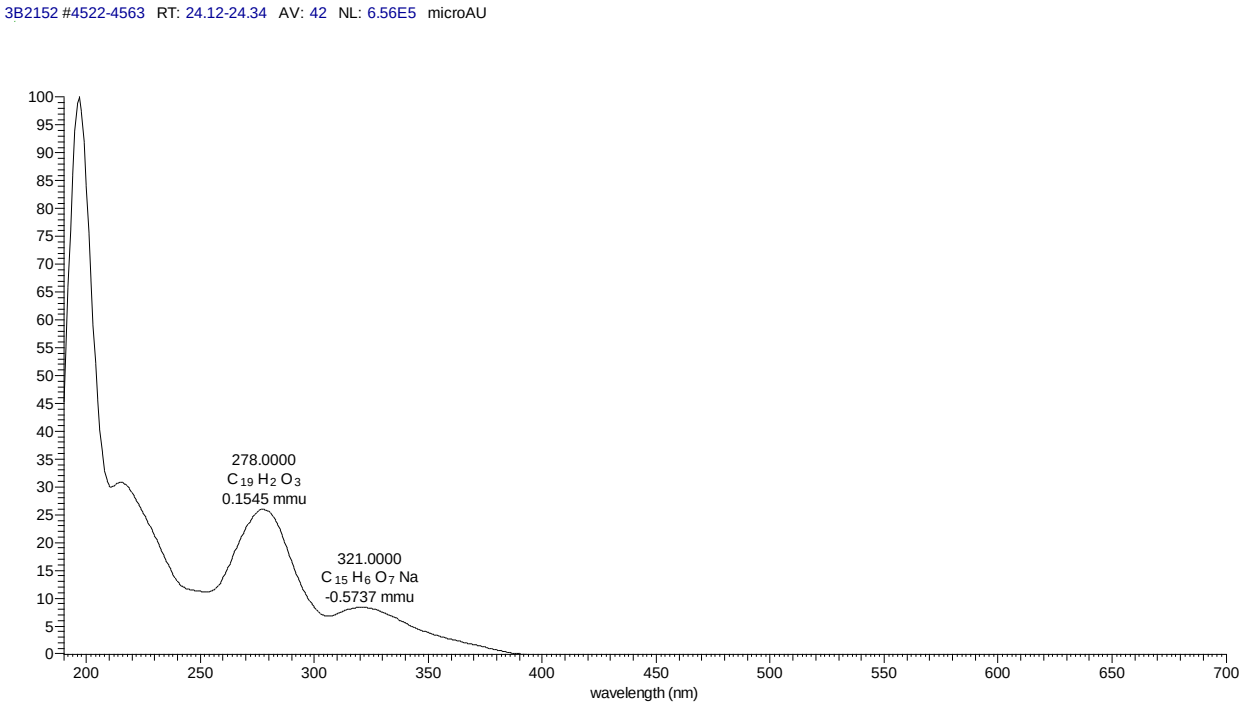

Appendix 44C: ^{1}H NMR spectrum (700 MHz, CD_3OD) of compound **217**

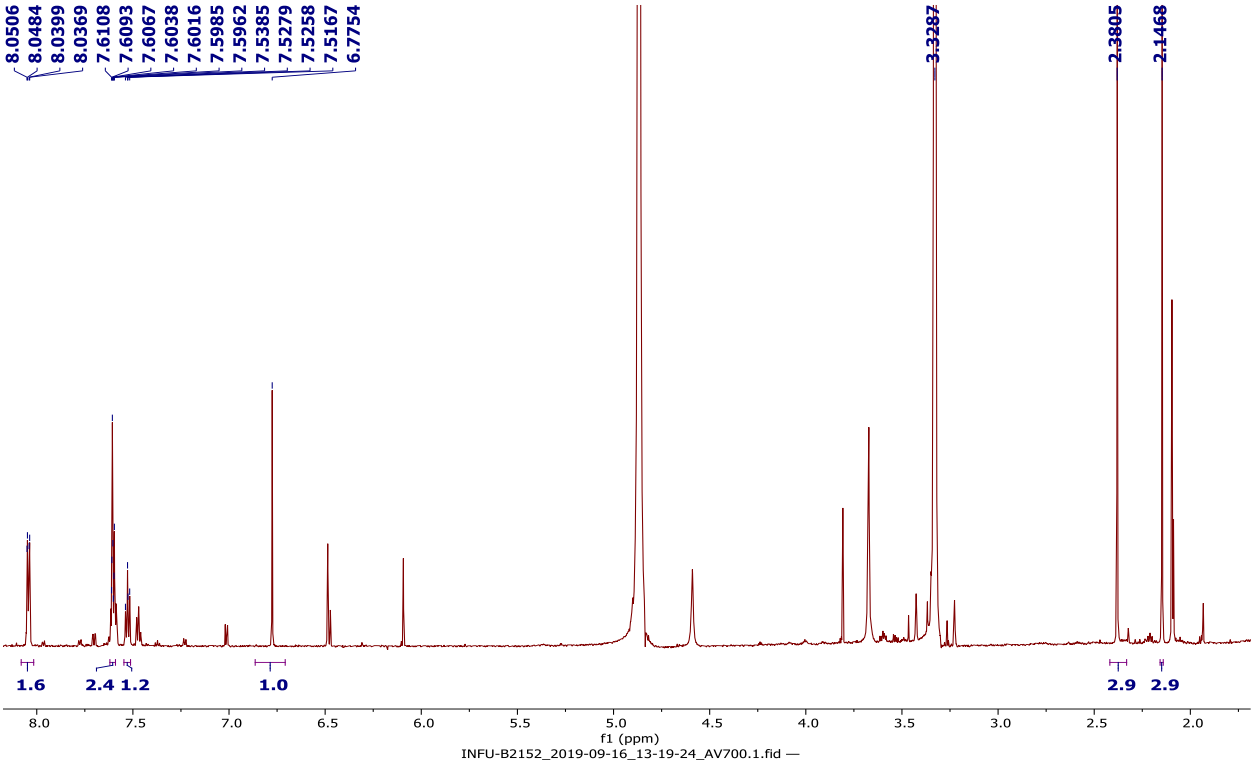

Appendix 44D: ^{13}C NMR spectrum (175 MHz, CD_3OD) of compound **217**

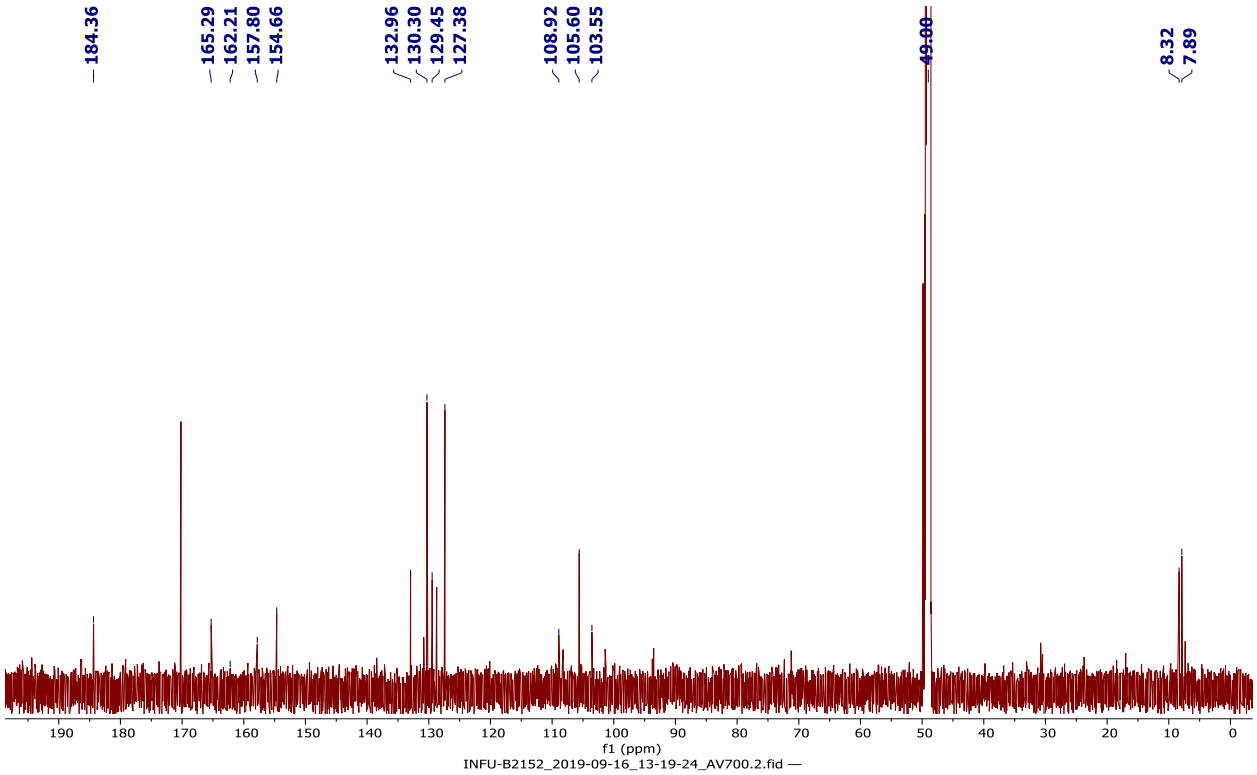

Appendix 44E: ^{1}H-^{1}H COSY spectrum (CD_3OD) of compound **217**

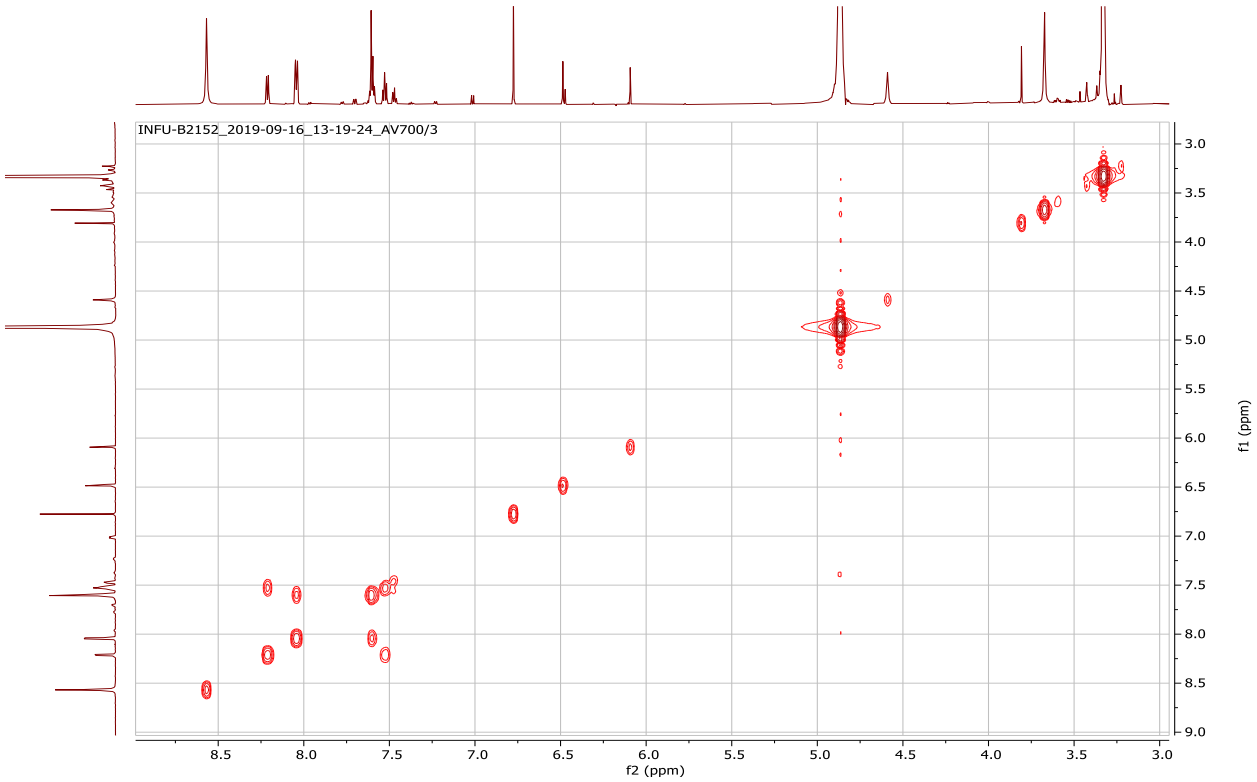

Appendix 44F: HSQC spectrum (CD_3OD) of compound **217**

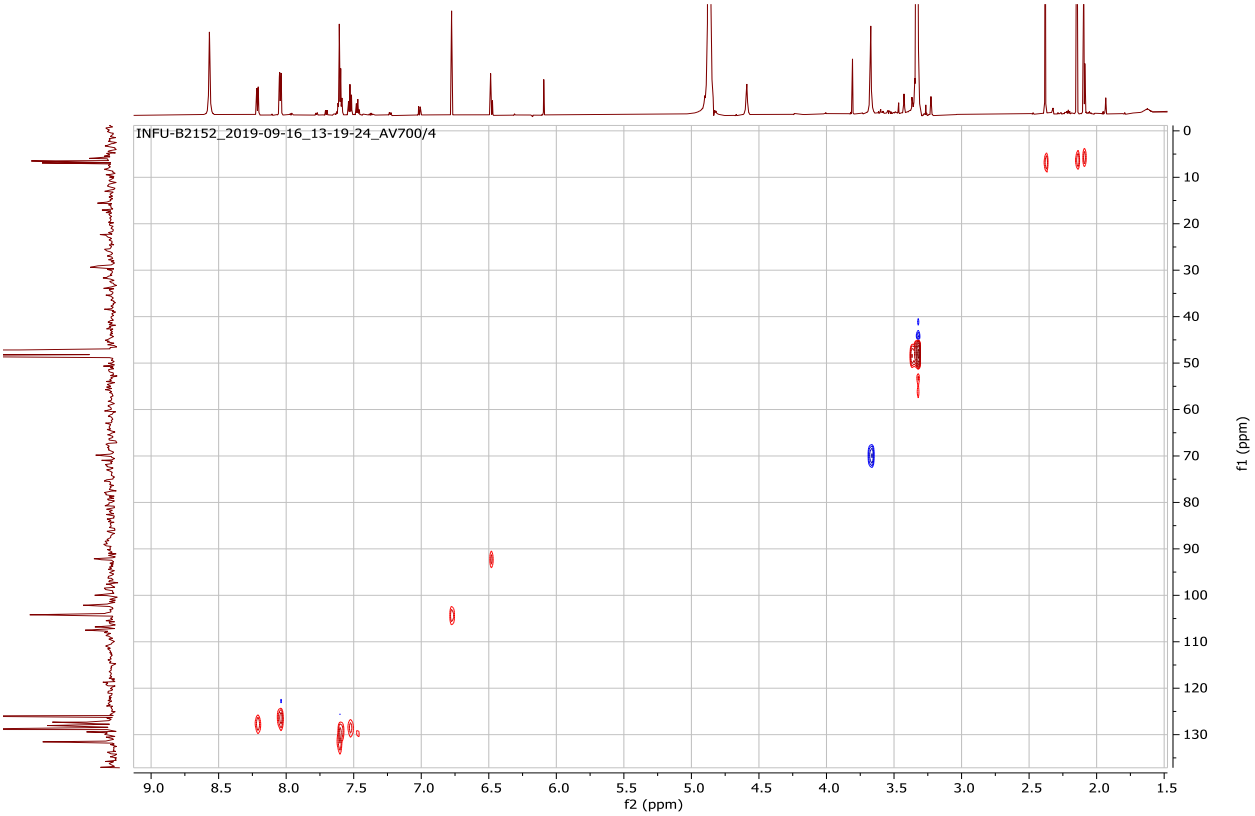

Appendix 44G: HMBC spectrum (CD_3OD) of compound **217**

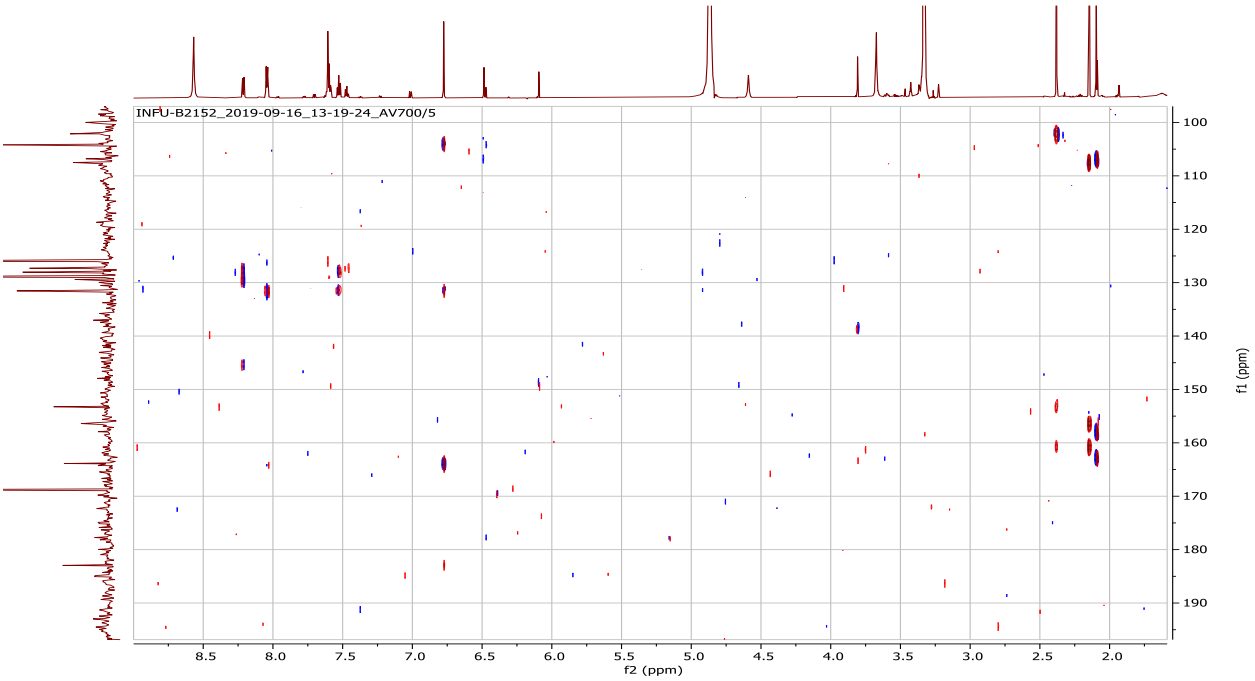

Appendix 45: NMR spectra for strobochrysin (**218**)

Appendix 45A: HRESIMS of compound **218**

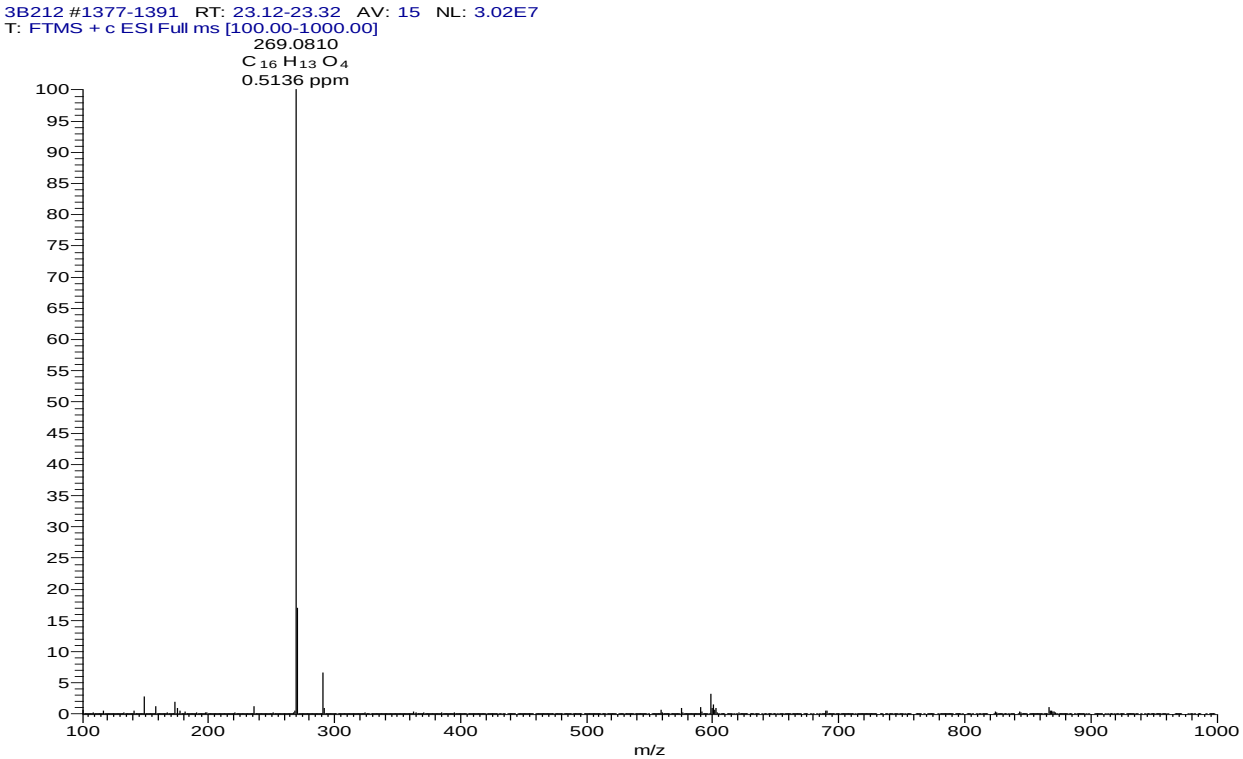

Appendix 45B: LC-UV spectrum of compound **218**

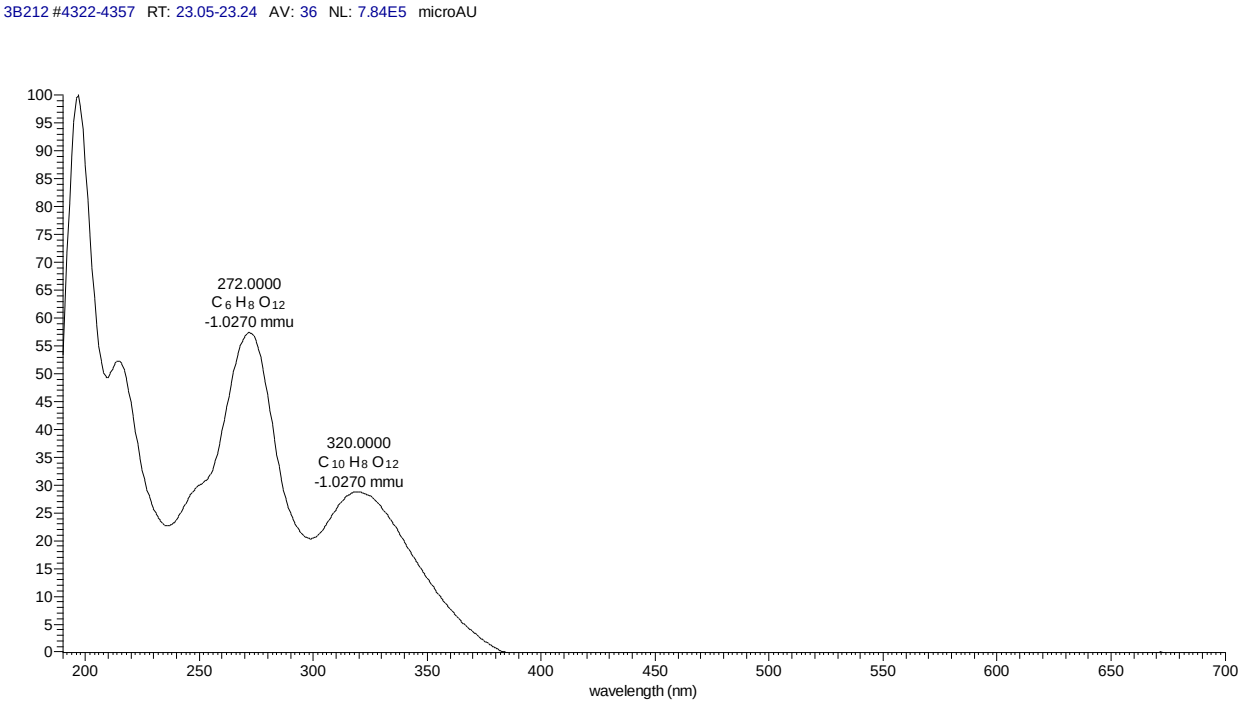

Appendix 45C: ^{1}H NMR spectrum (600 MHz, DMSO-d_6) of compound **218**

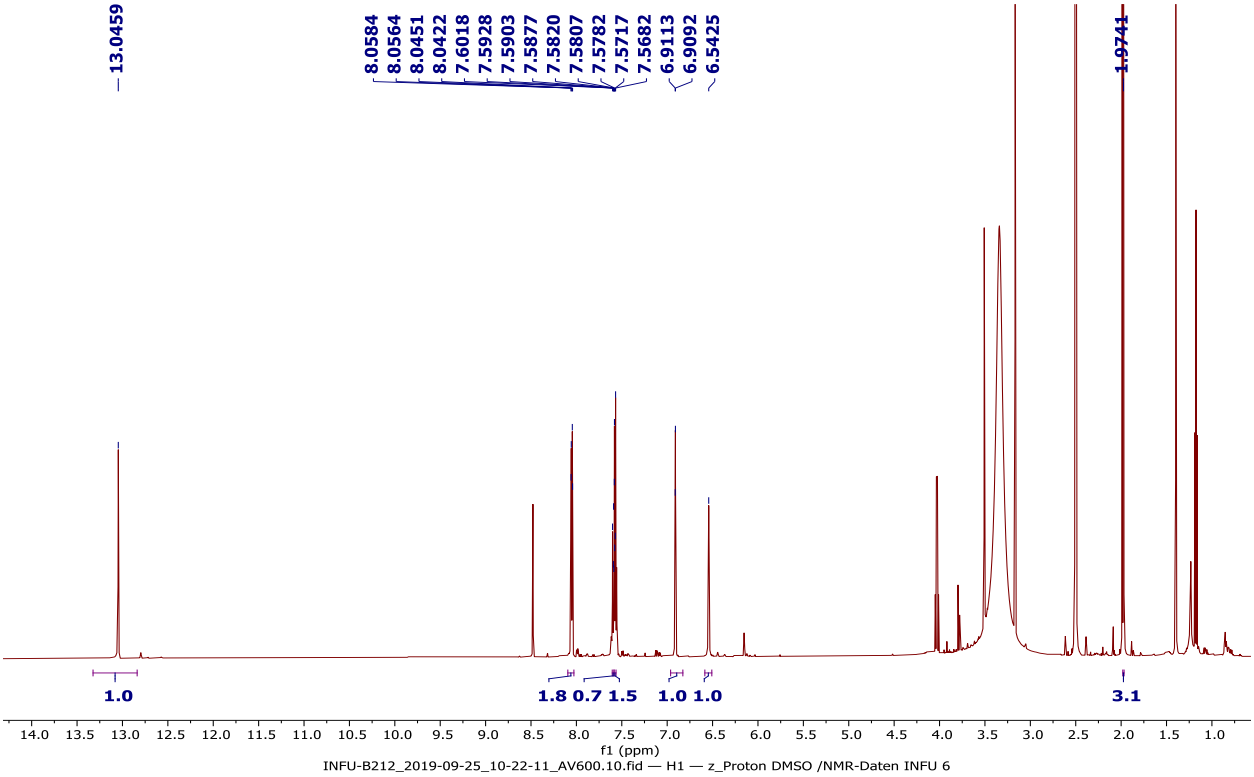

Appendix 45D: ^{13}C NMR spectrum (150 MHz, DMSO-d_6) of compound **218**

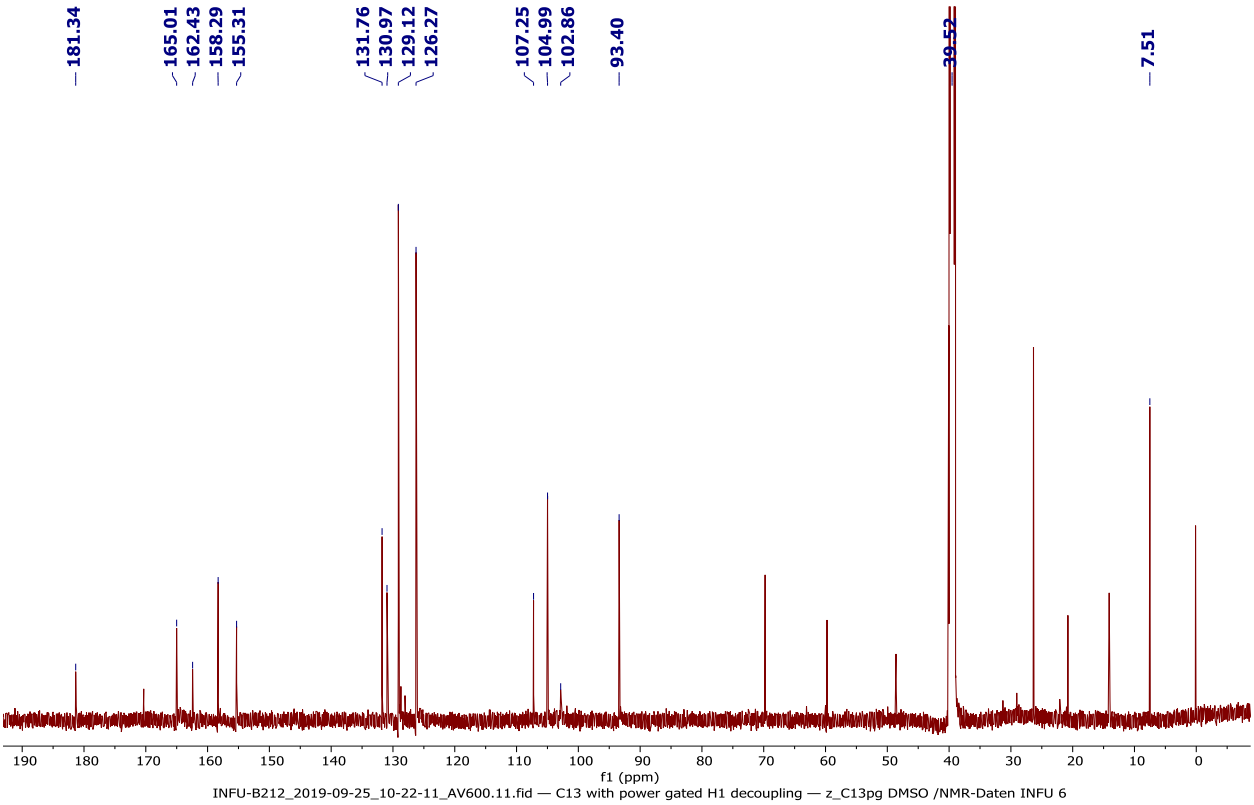

Appendix 45E: ^{1}H-^{1}H COSY spectrum (CD_3OD) of compound **218**

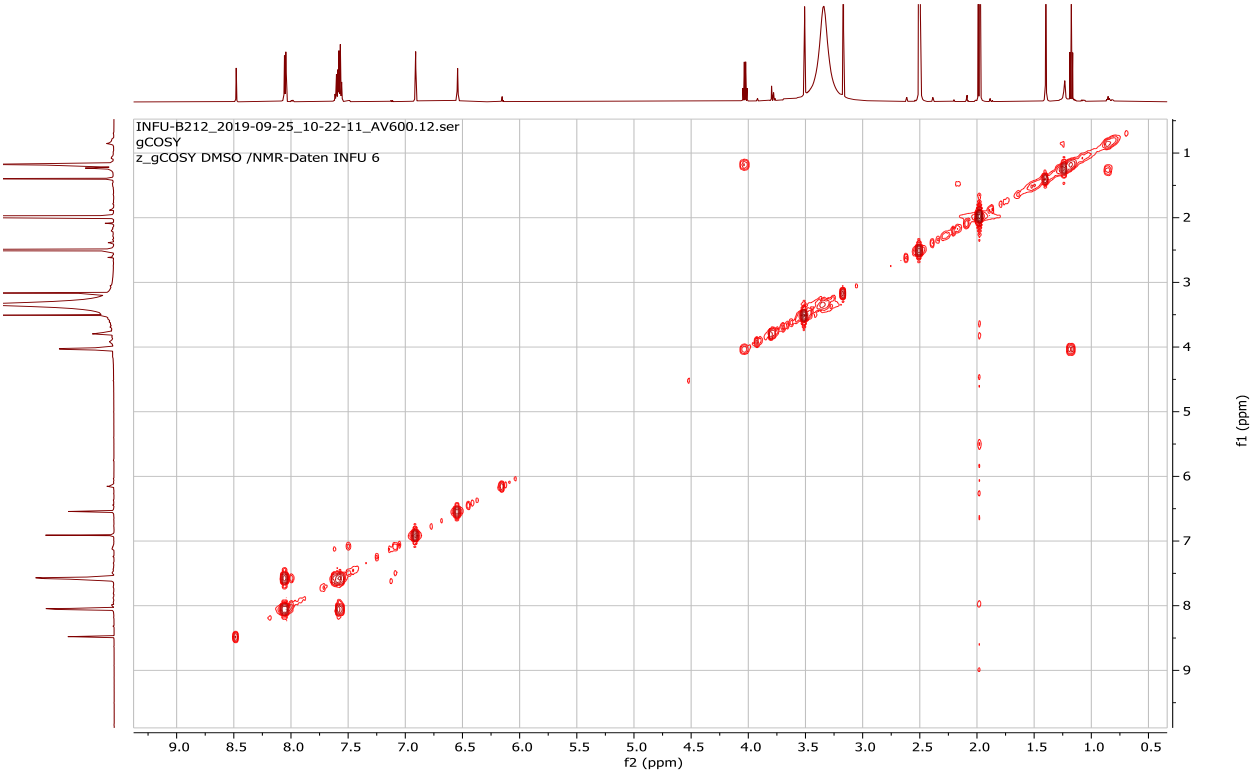

Appendix 45F: HSQC spectrum (CD_3OD) of compound **218**

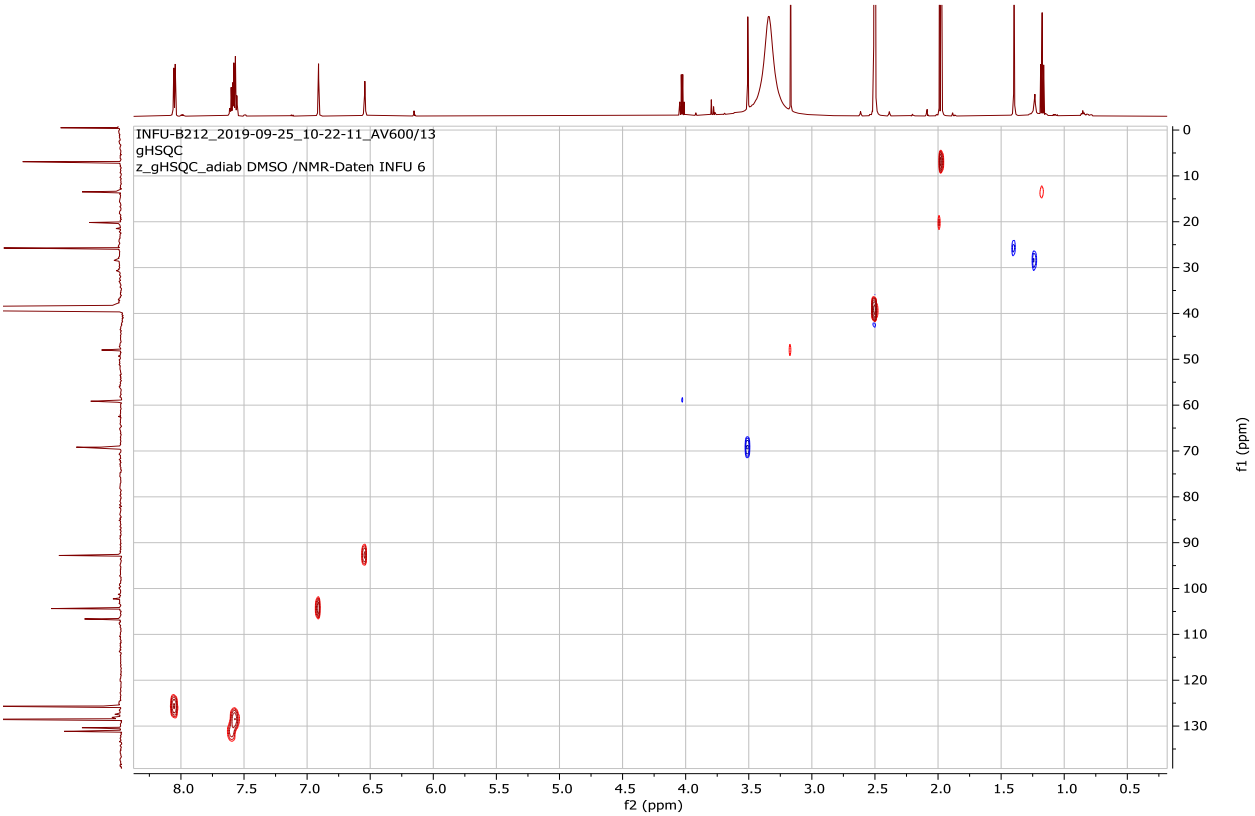

Appendix 45G: HMBC spectrum (CD_3OD) of compound **218**

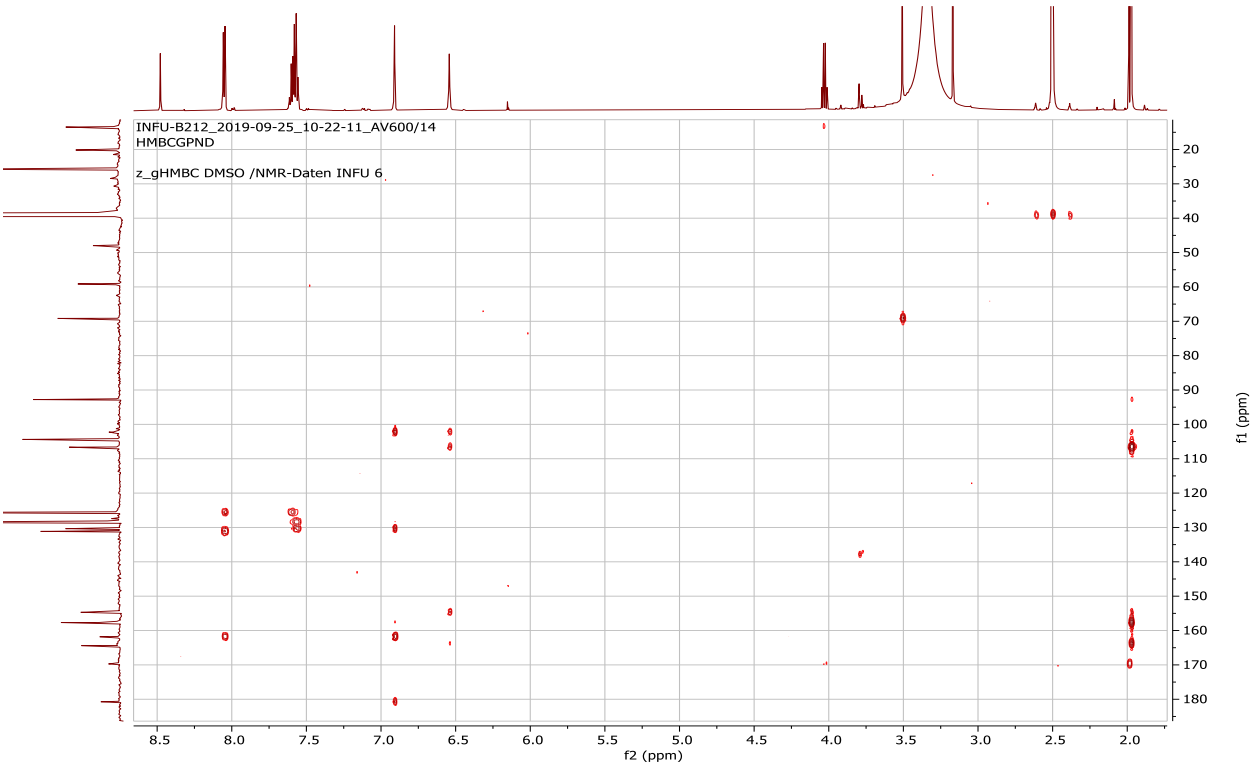

Appendix 46: NMR spectra for 3,5,7-trihydroxy-6-methylflavanone (**219**)

Appendix 46A: HRESIMS of compound **219**

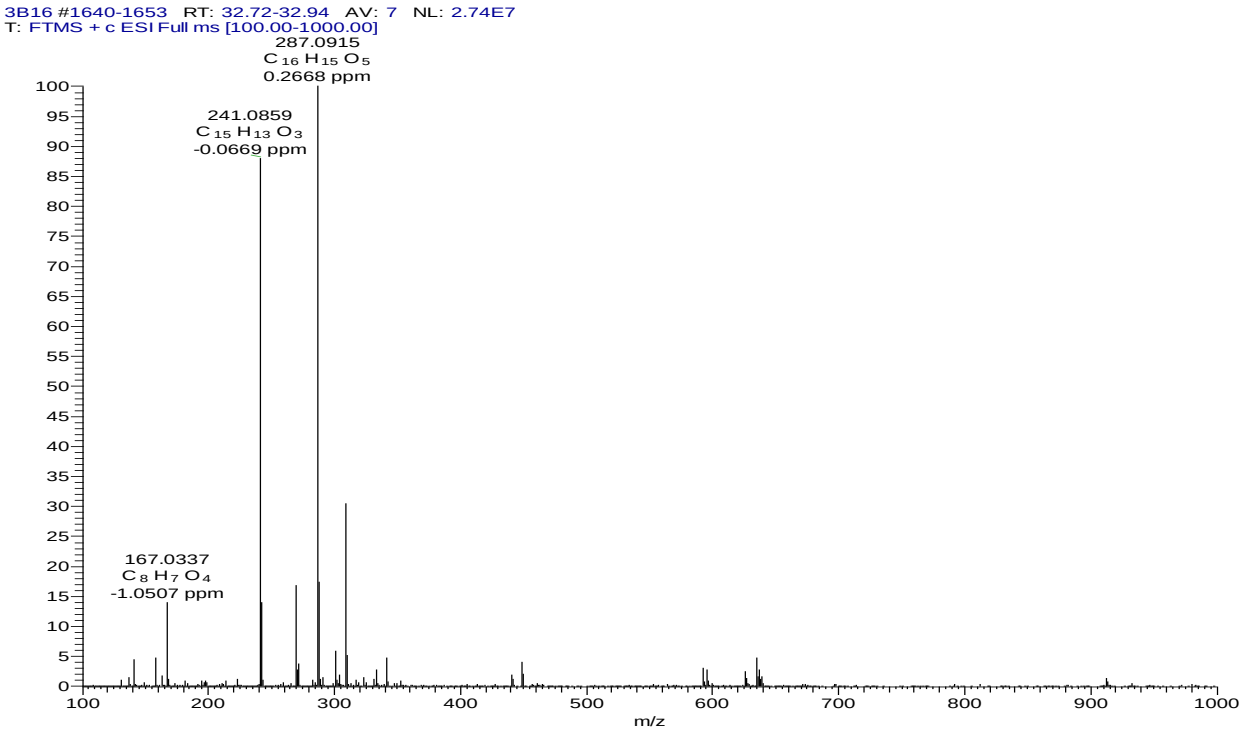

Appendix 46B: LC-UV spectrum of compound **219**

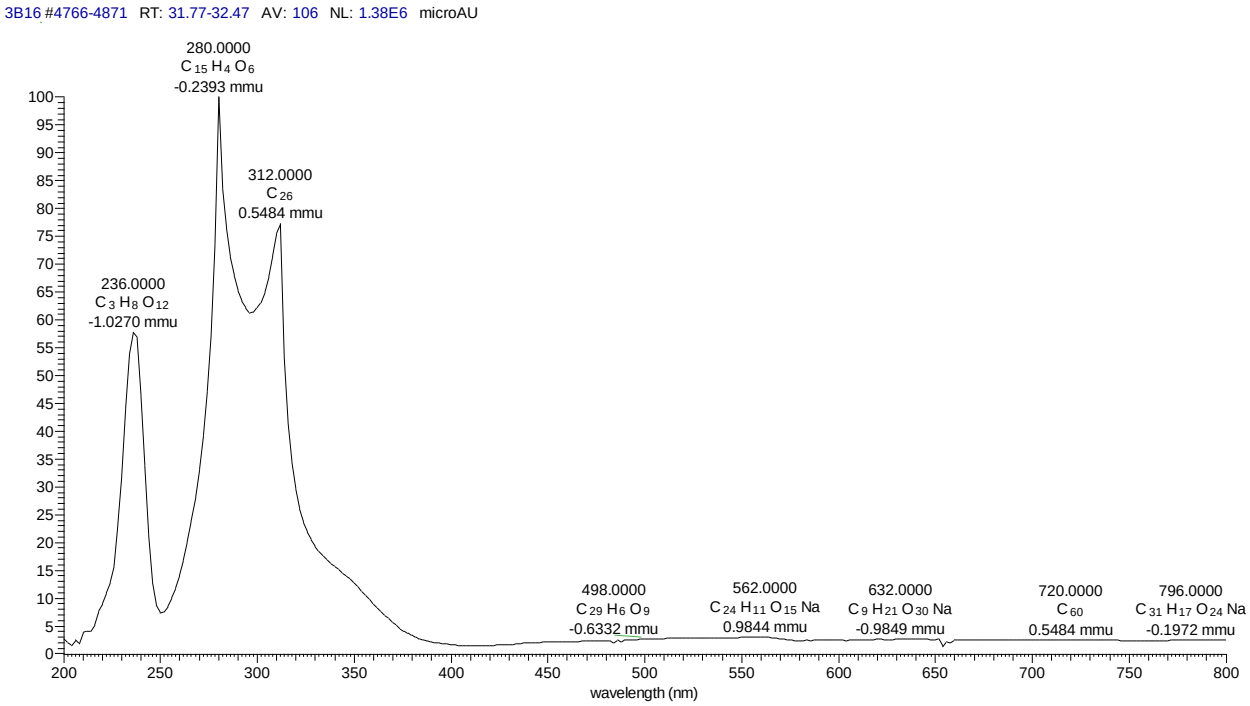

Appendix 46C: ^{1}H NMR spectrum (600 MHz, CD_3OD) of compound **219**

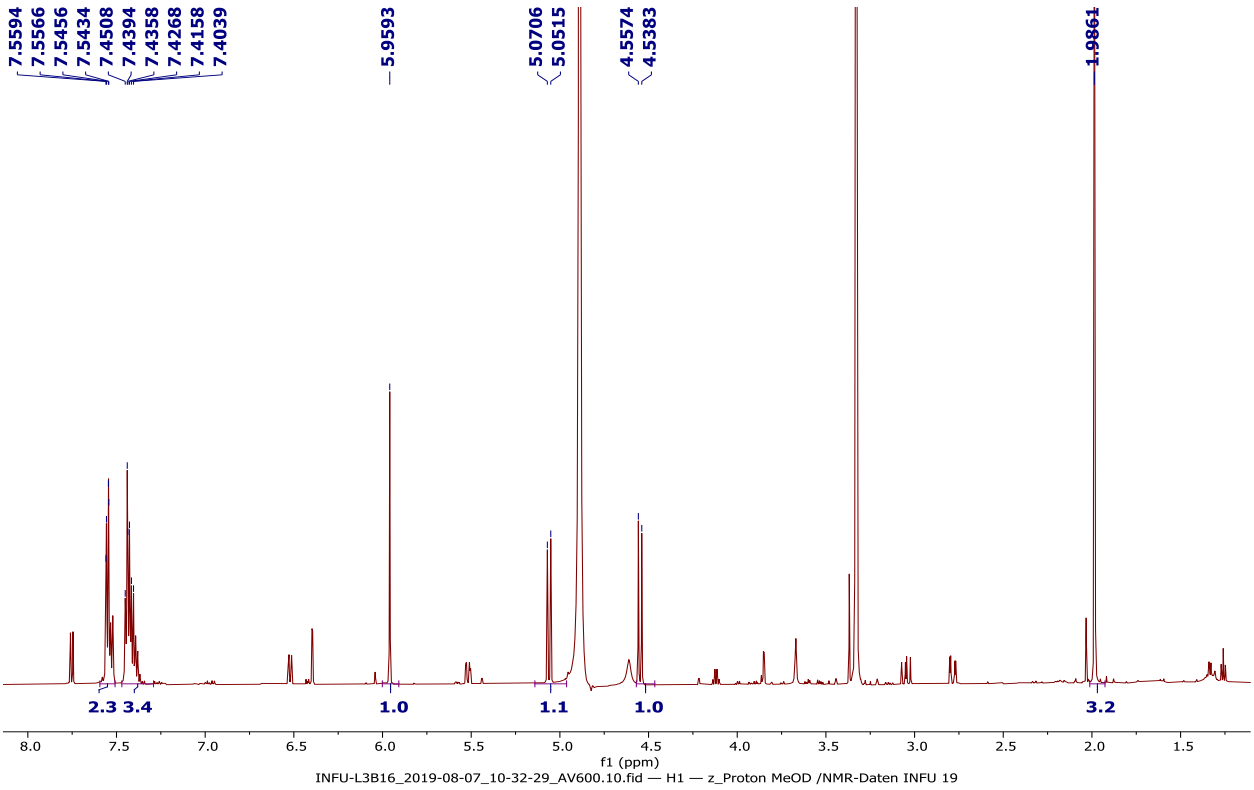

Appendix 46D: ^{13}C NMR spectrum (150 MHz, CD_3OD) of compound **219**

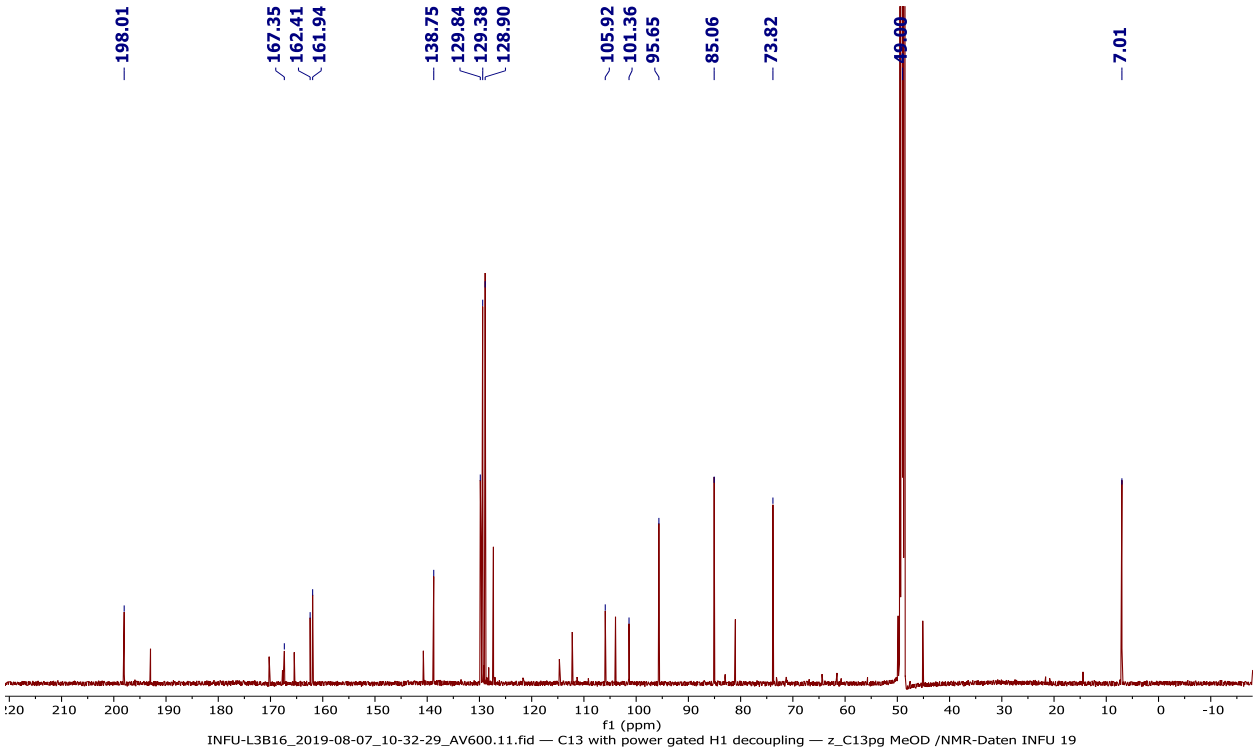

Appendix 46E: ^{1}H-^{1}H COSY spectrum (CD_3OD) of compound **219**

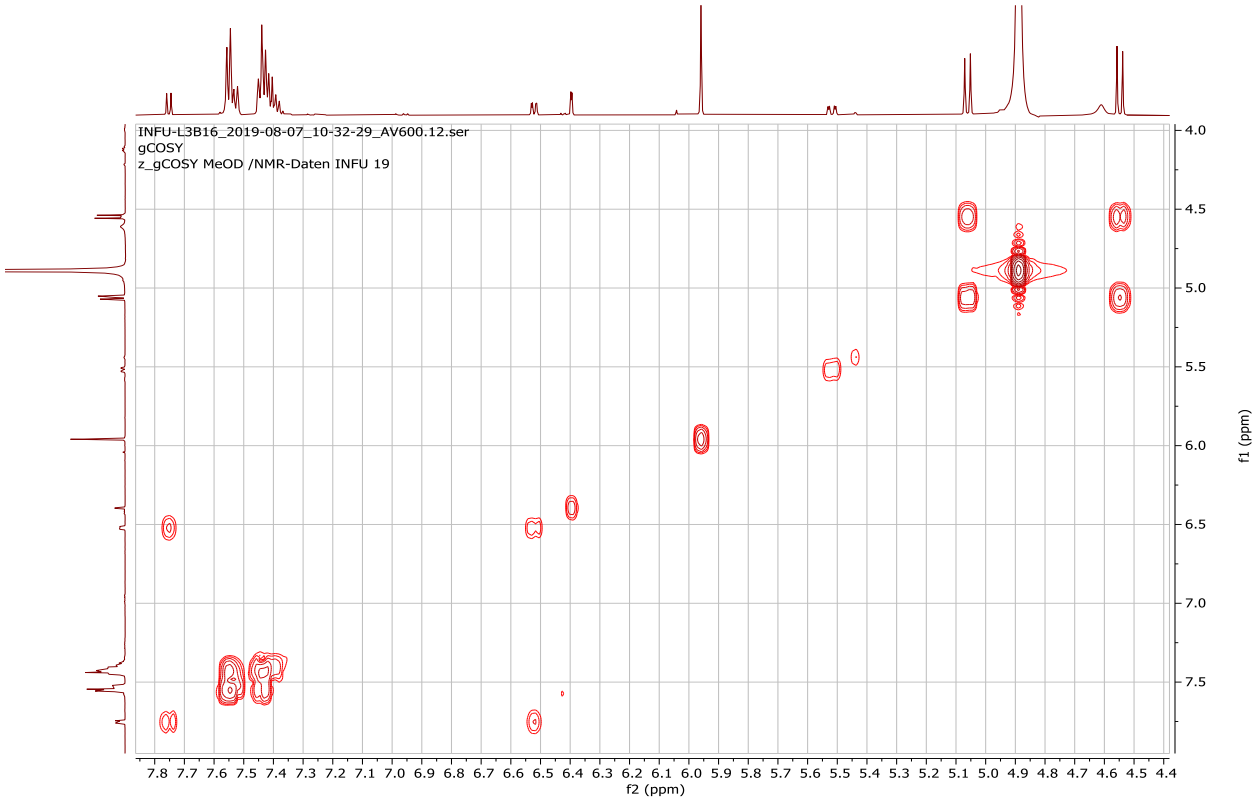

Appendix 46F: HSQC spectrum (CD_3OD) of compound **219**

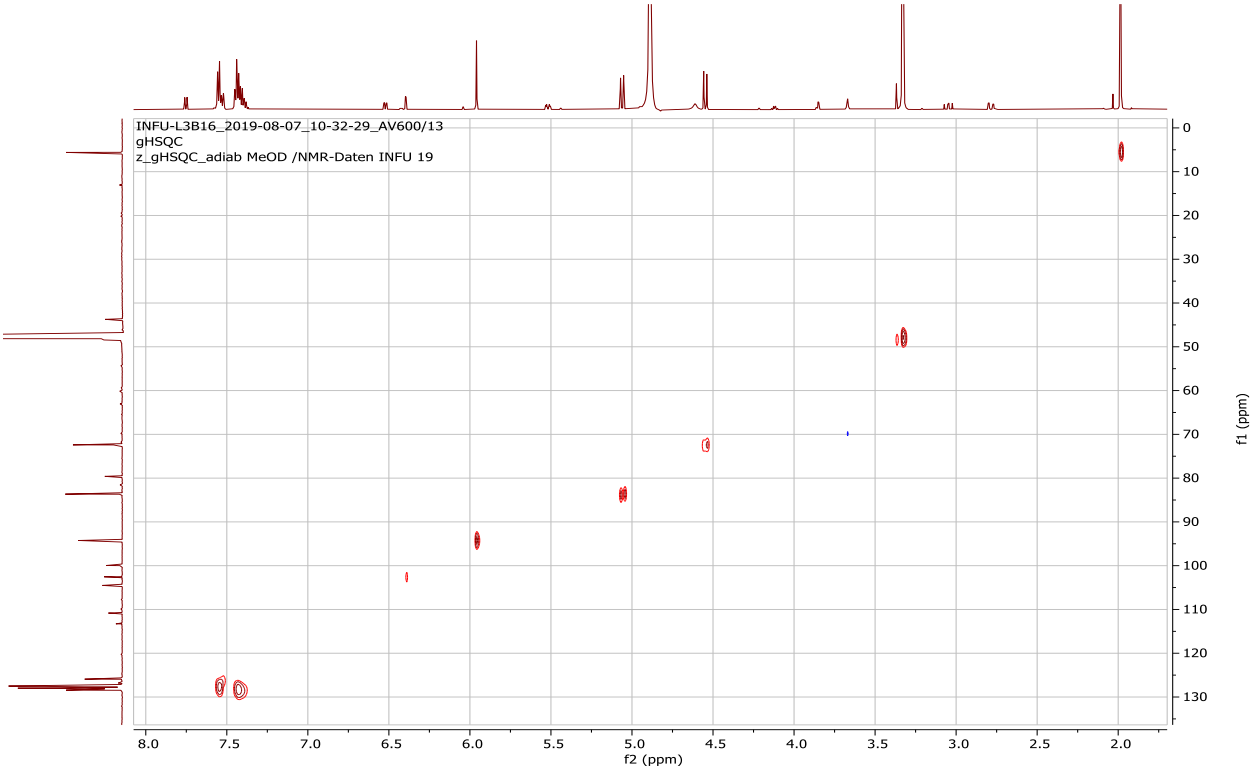

Appendix 46G: HMBC spectrum (CD_3OD) of compound **219**

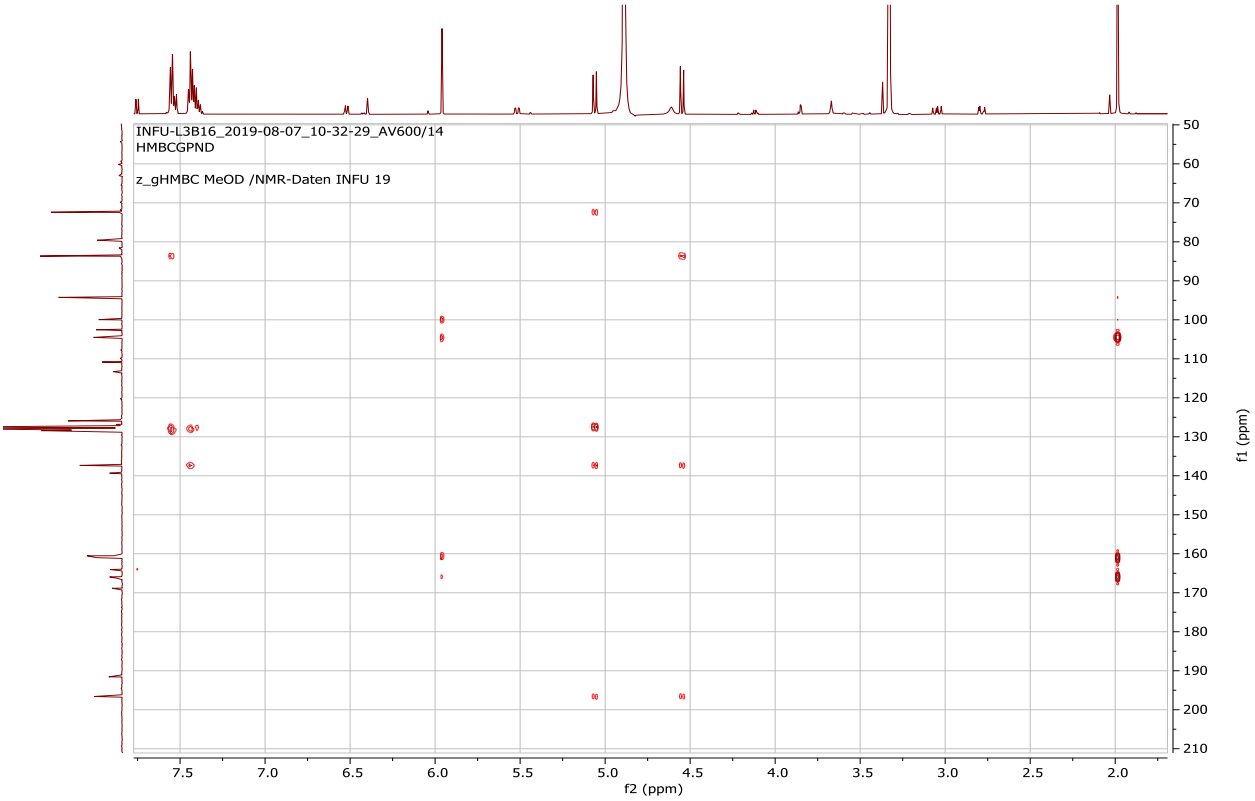

Appendix 47: NMR spectra for 3,5,7-trihydroxy-6-methoxyflavanone (**220**)

Appendix 47A: HRESIMS of compound **220**

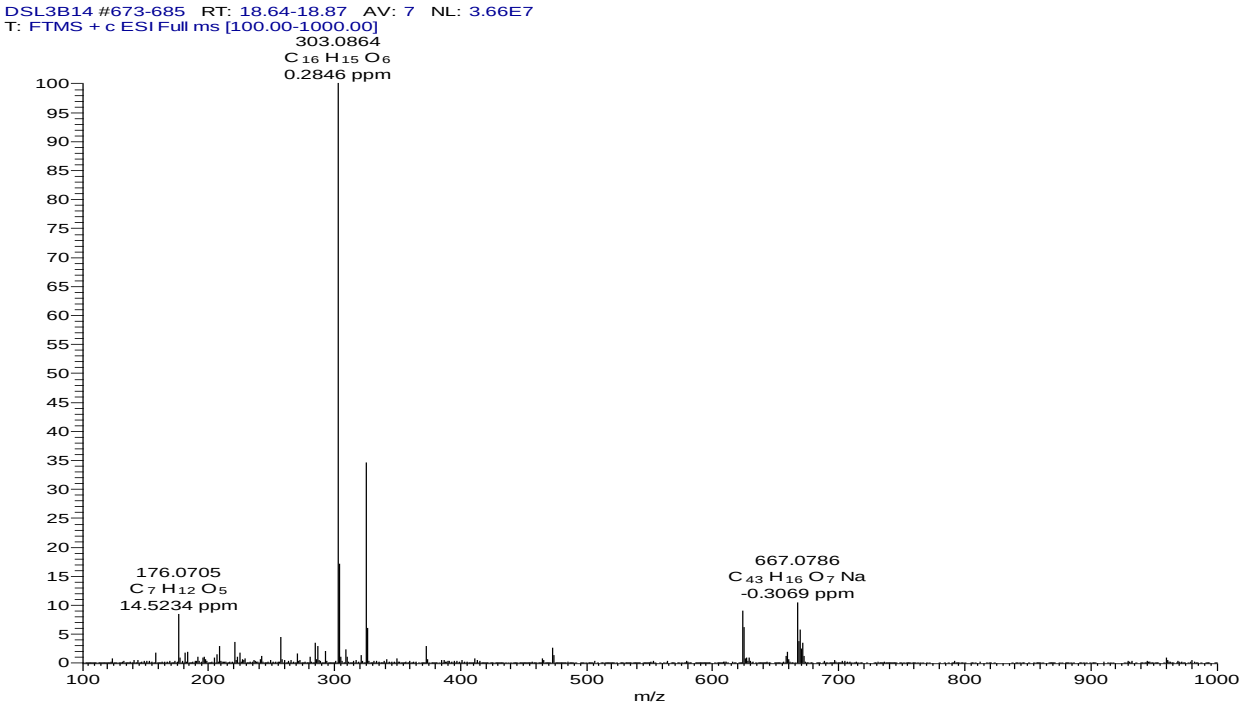

Appendix 47B: LC-UV spectrum of compound **220**

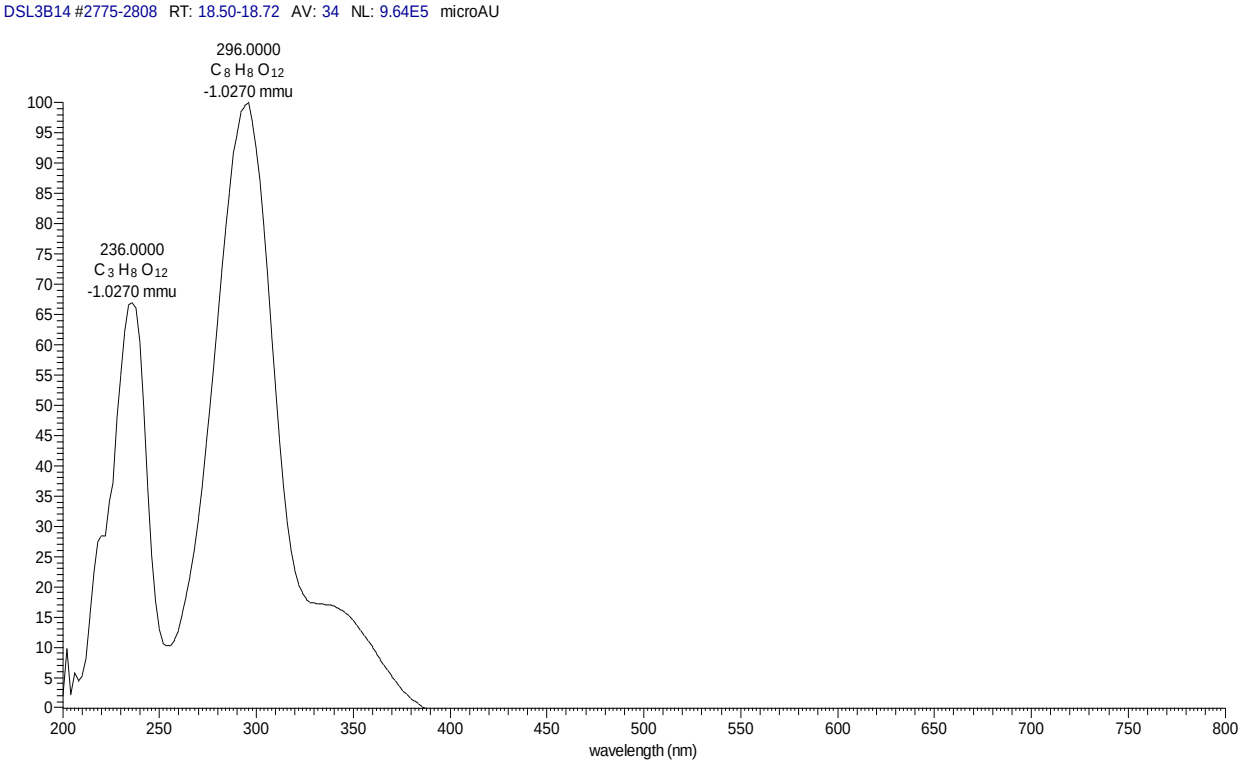

Appendix 47C: ^{1}H NMR spectrum (700 MHz, CD_3OD) of compound **220**

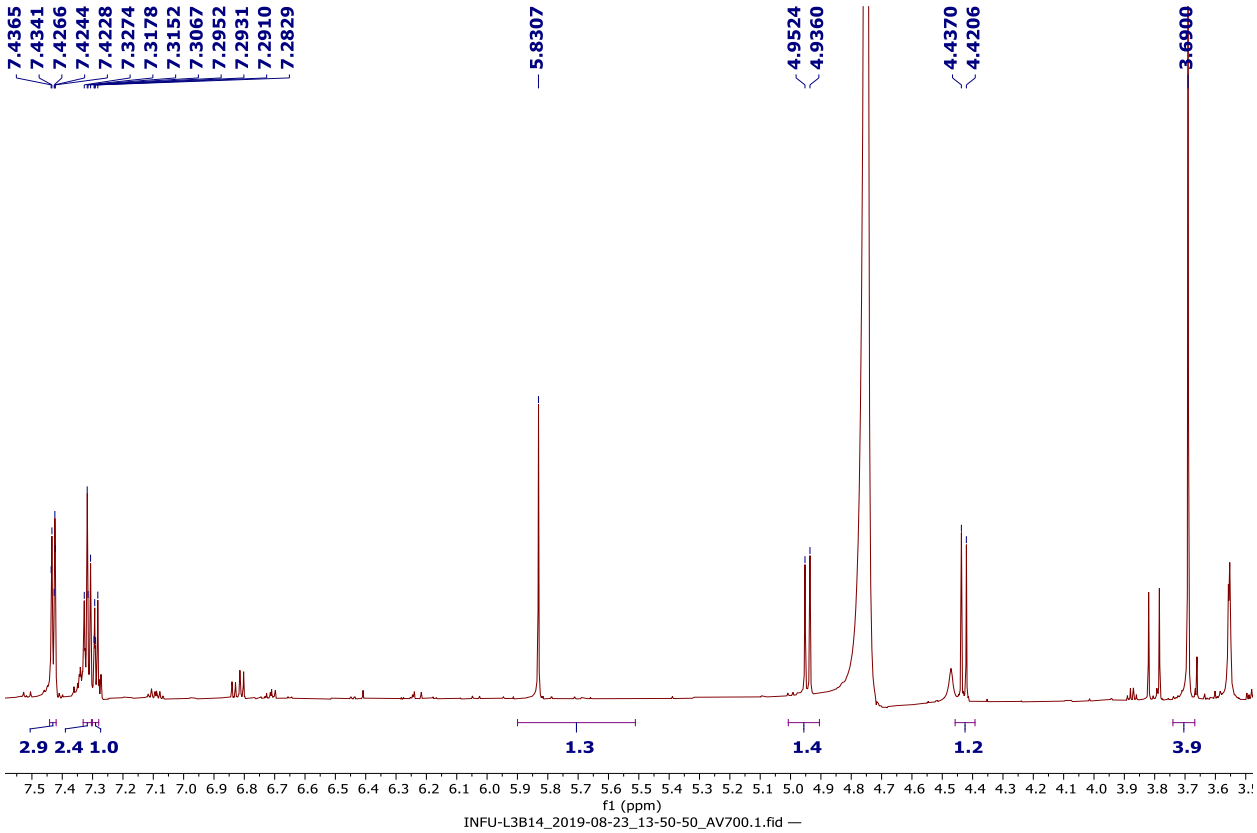

Appendix 47D: ^{13}C NMR spectrum (175 MHz, CD_3OD) of compound **220**

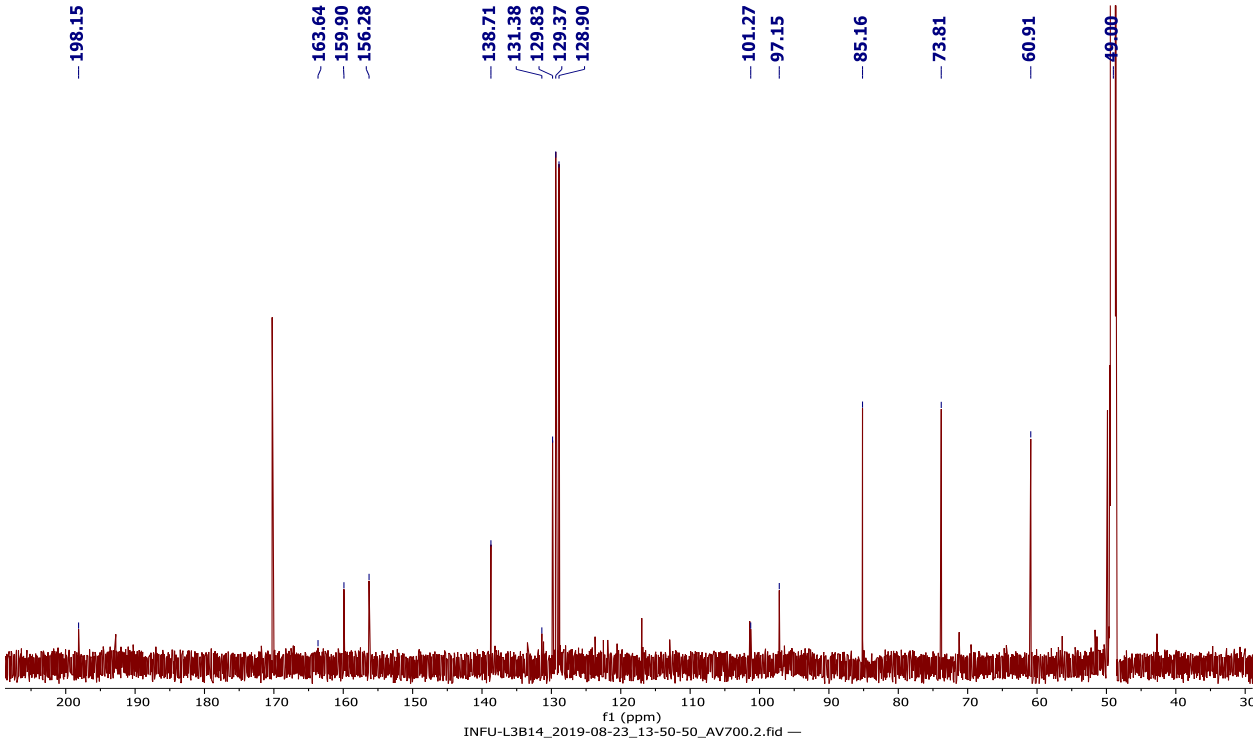

Appendix 47E: ^{1}H-^{1}H COSY spectrum (CD_3OD) of compound **220**

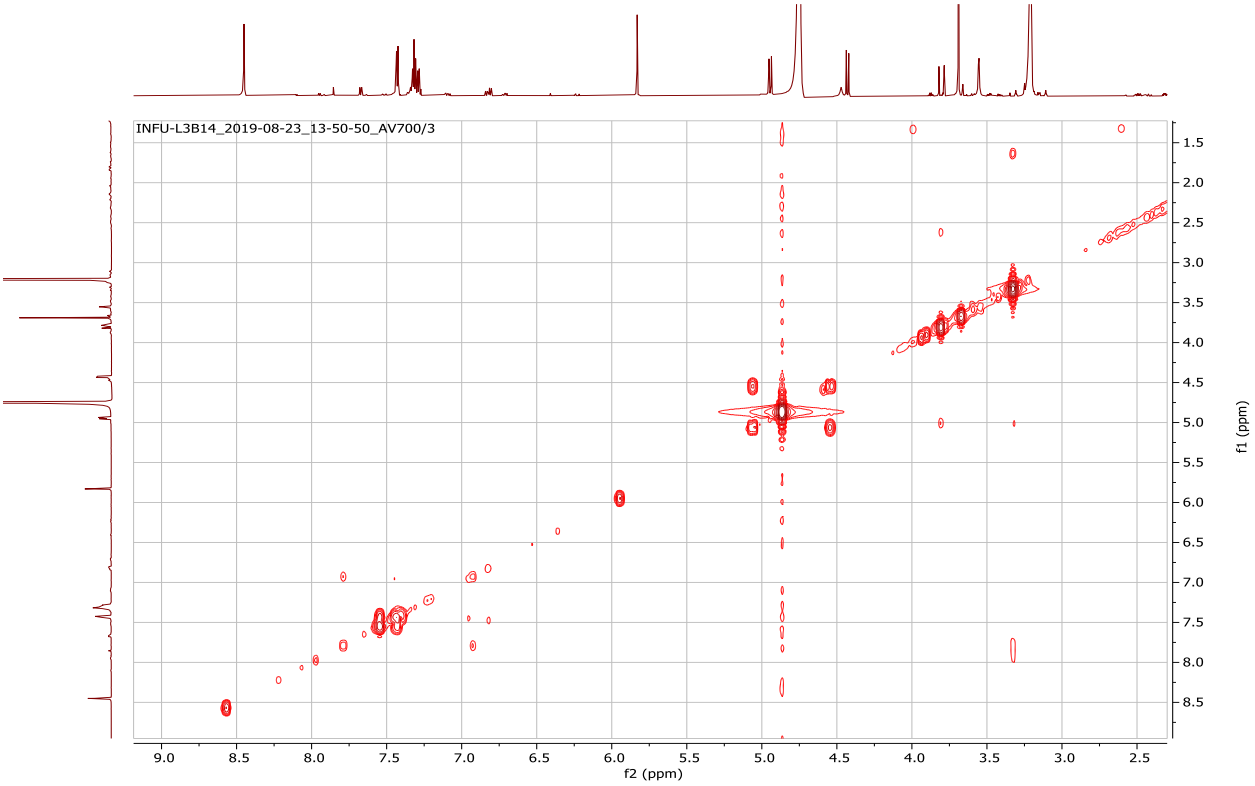

Appendix 47F: HSQC spectrum (CD_3OD) of compound **220**

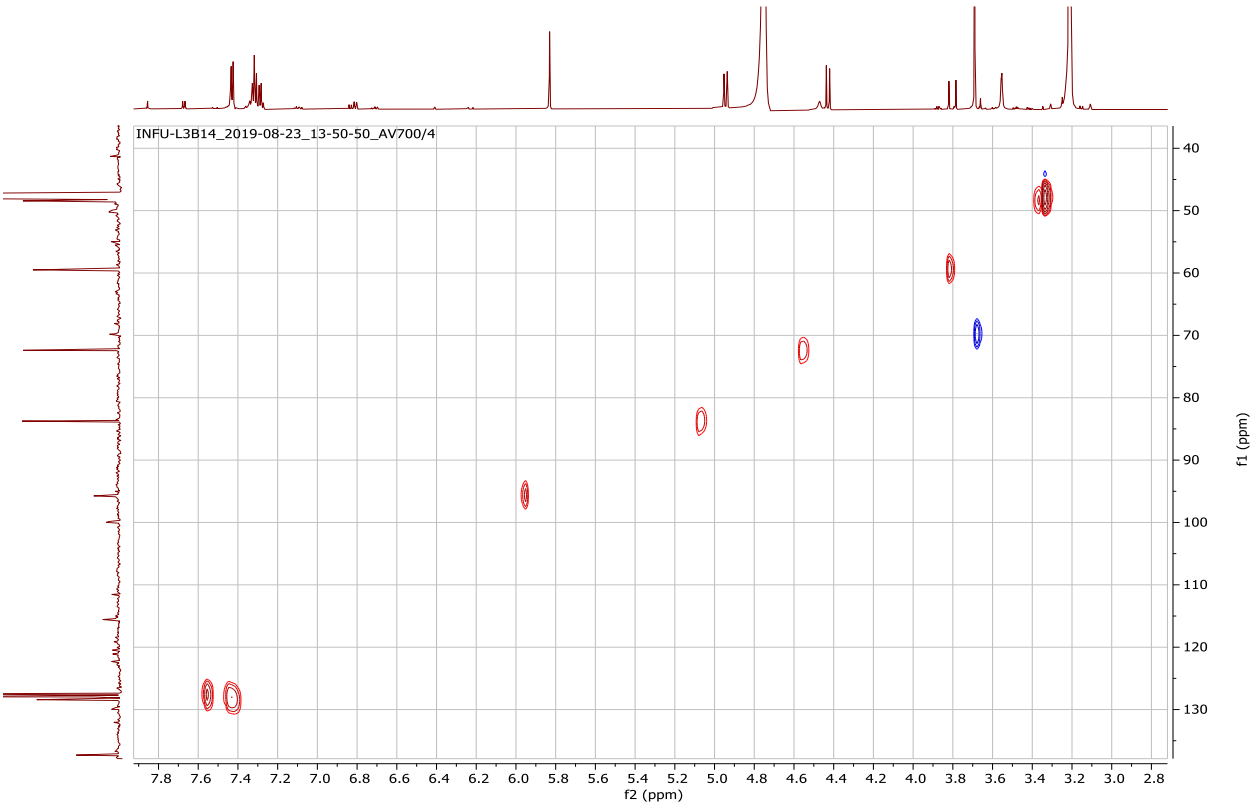

Appendix 47G: HMBC spectrum (CD_3OD) of compound **220**

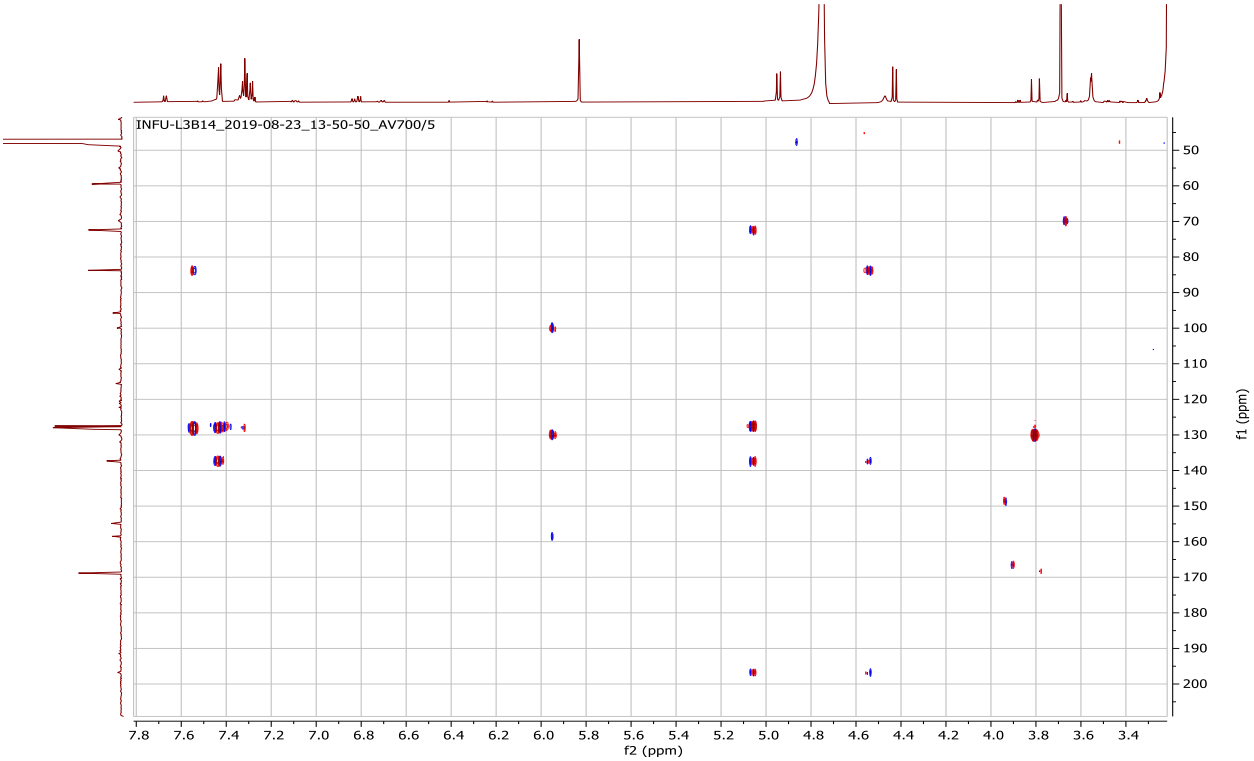

Appendix 48: NMR spectra for 3,7-dihydroxy-6-methoxyflavanone (**221**)

Appendix 48A: HRESIMS of compound **221**

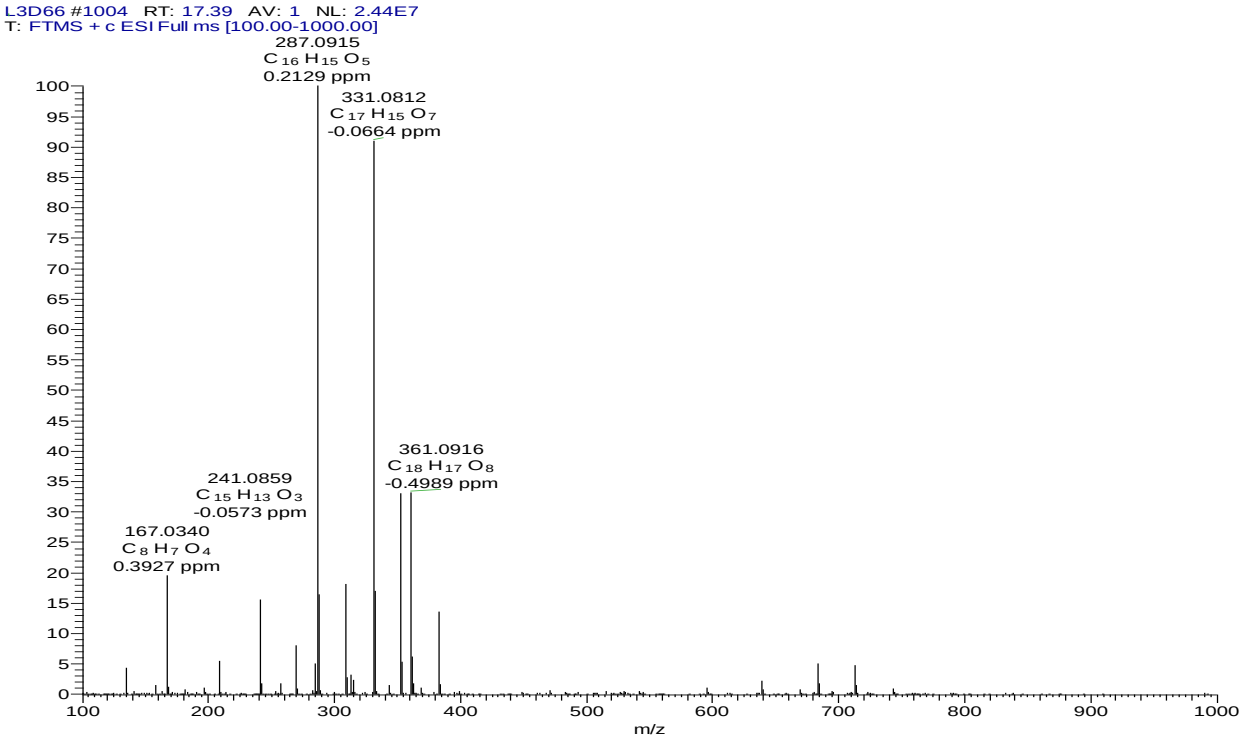

Appendix 48B: ^{1}H NMR spectrum (700 MHz, Acetone-d_6) of compound **221**

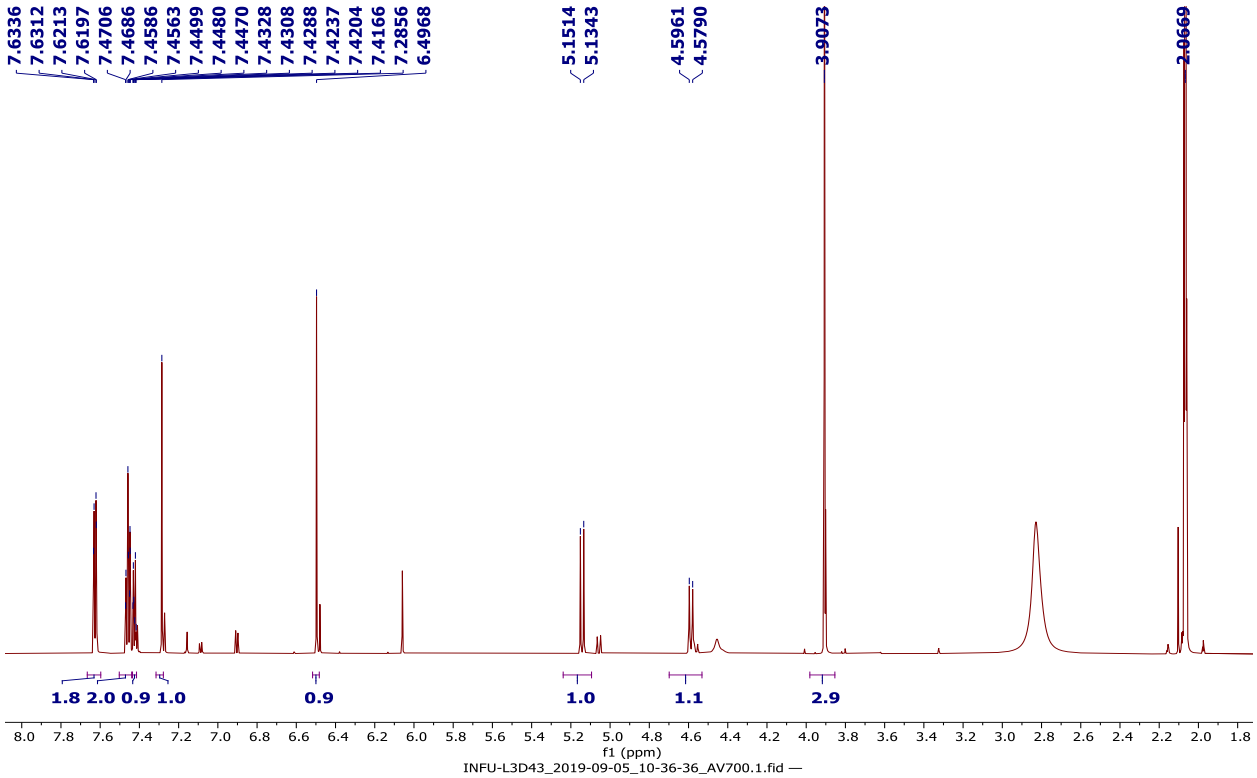

Appendix 48C: ^{13}C NMR spectrum (175 MHz, Acetone-d_6) of compound **221**

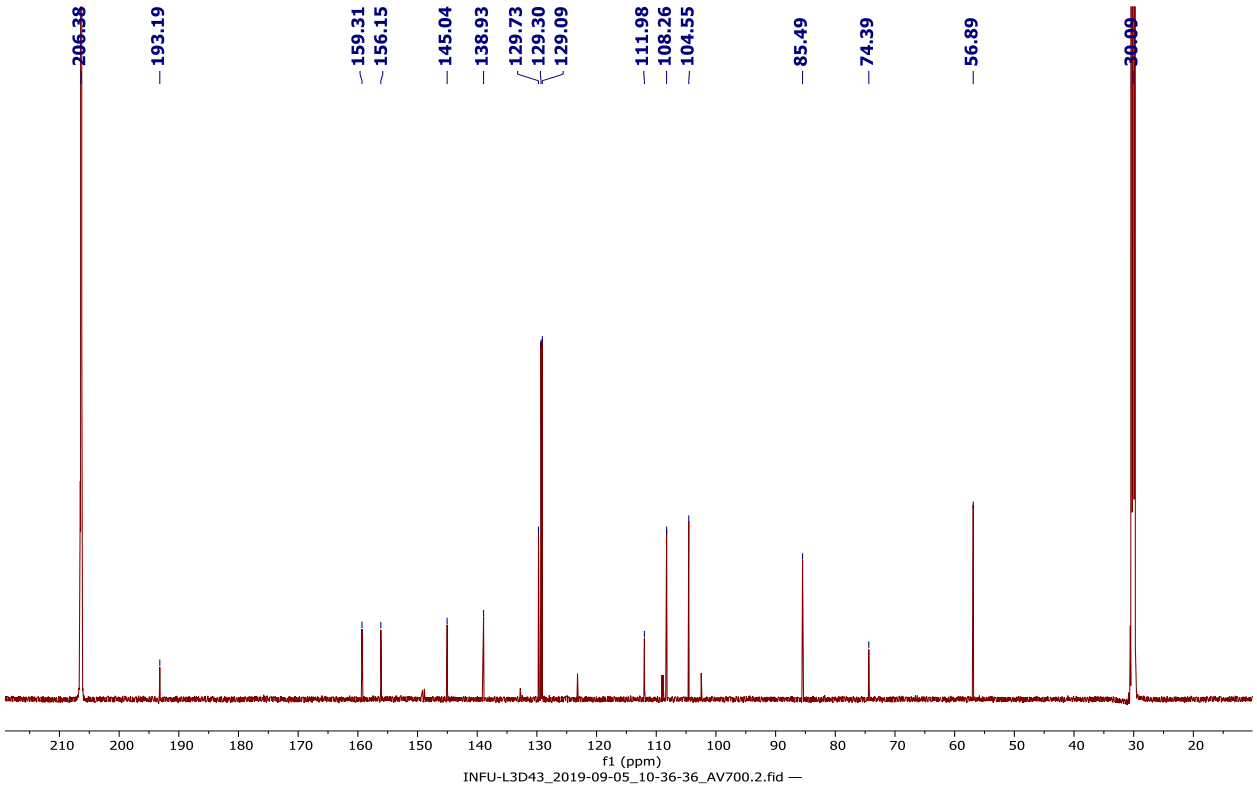

Appendix 48D: ^{1}H-^{1}H COSY spectrum (Acetone-d_6) of compound **221**

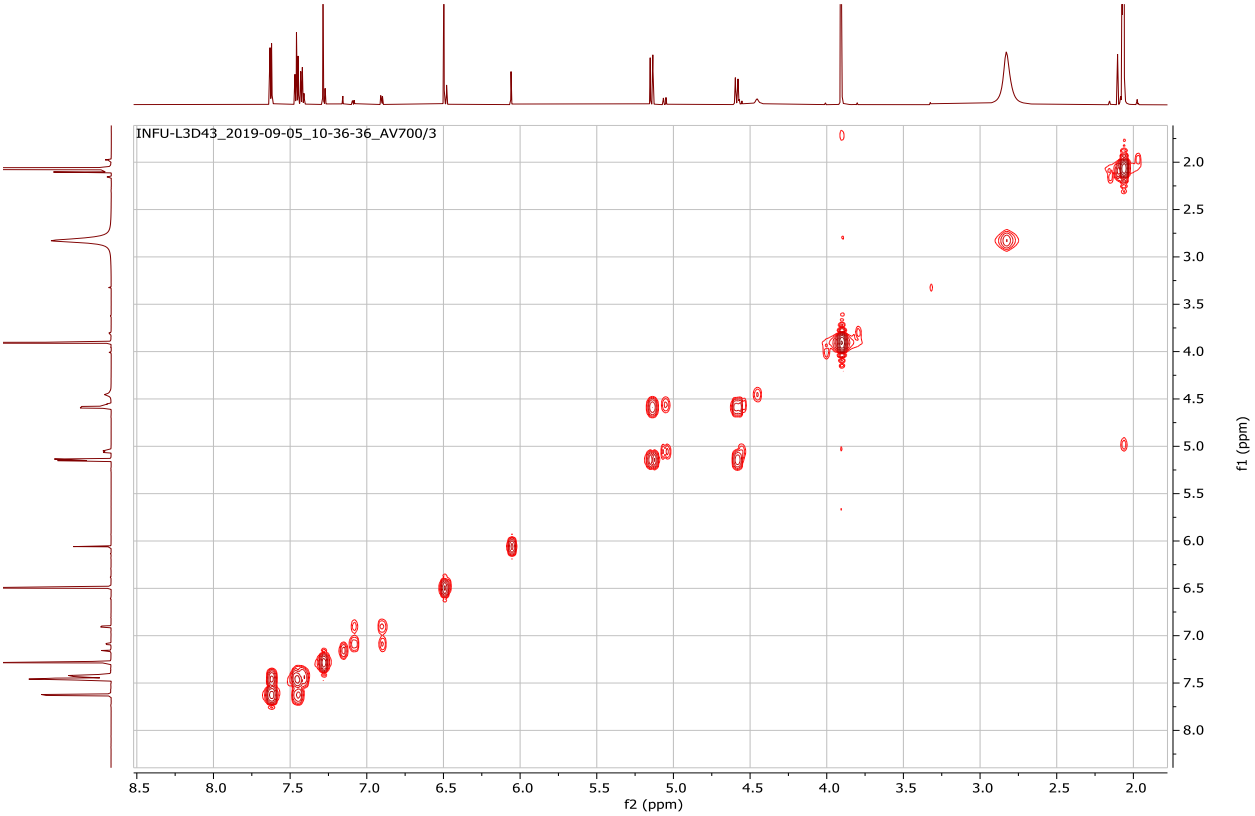

Appendix 48E: NOESY spectrum (Acetone-d_6) of compound **221**

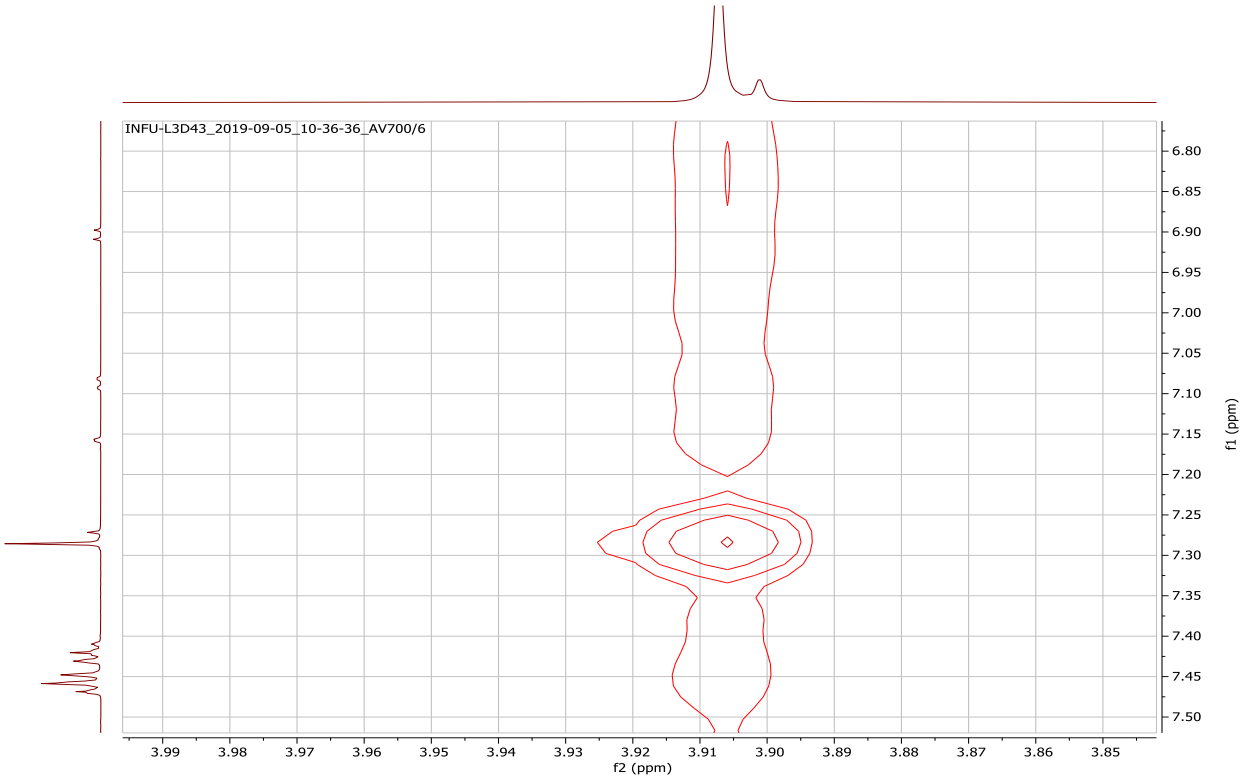

Appendix 48F: HSQC spectrum (Acetone-d_6) of compound **221**

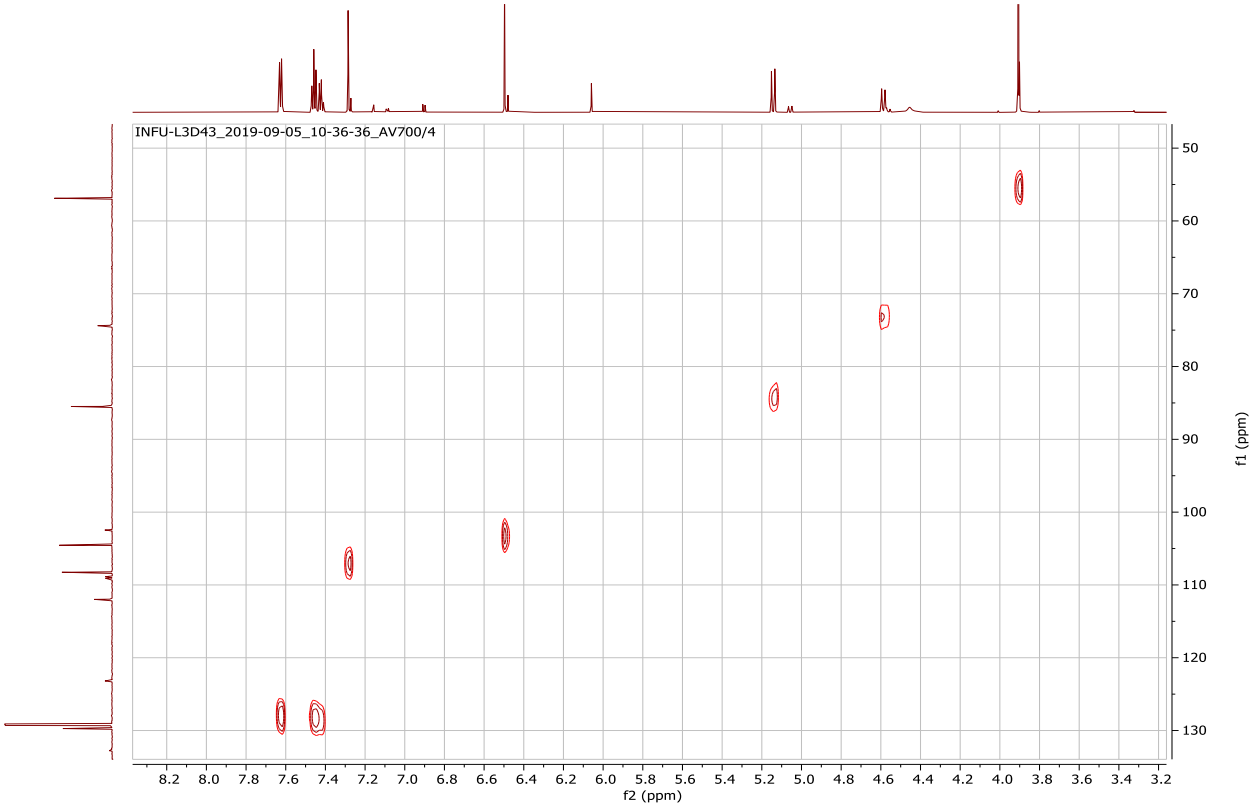

Appendix 48G: HMBC spectrum (Acetone-d_6) of compound **221**

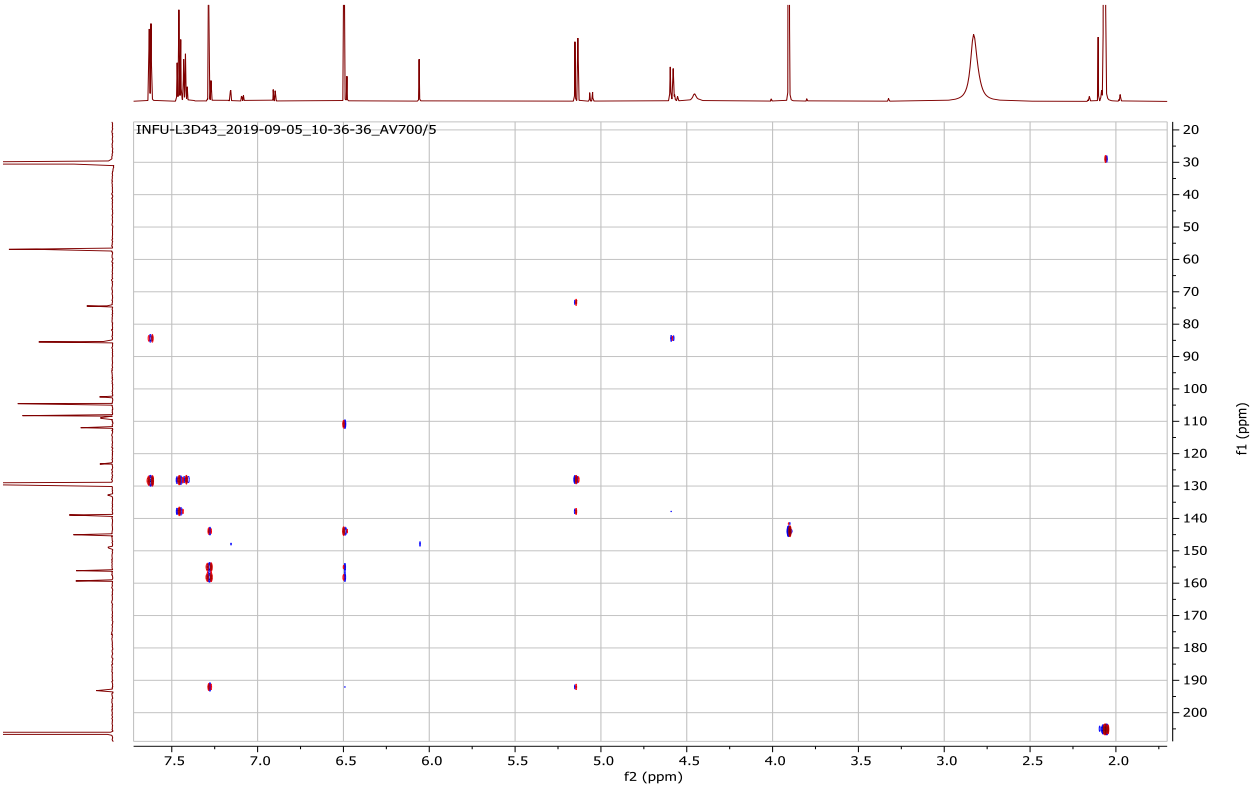

Appendix 49: NMR spectra for *para*-hydroxybenzoic acid (**222**)

Appendix 49A: HRESIMS of compound **222**

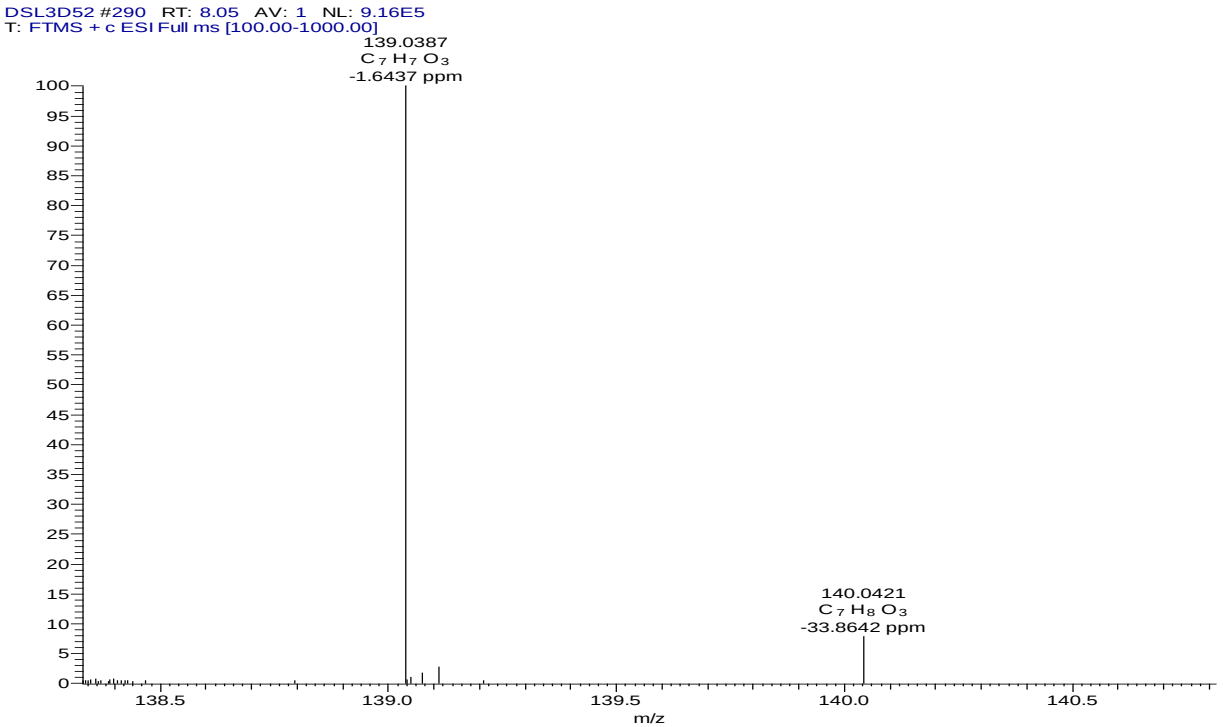

Appendix 49B: LC-UV spectrum of compound **222**

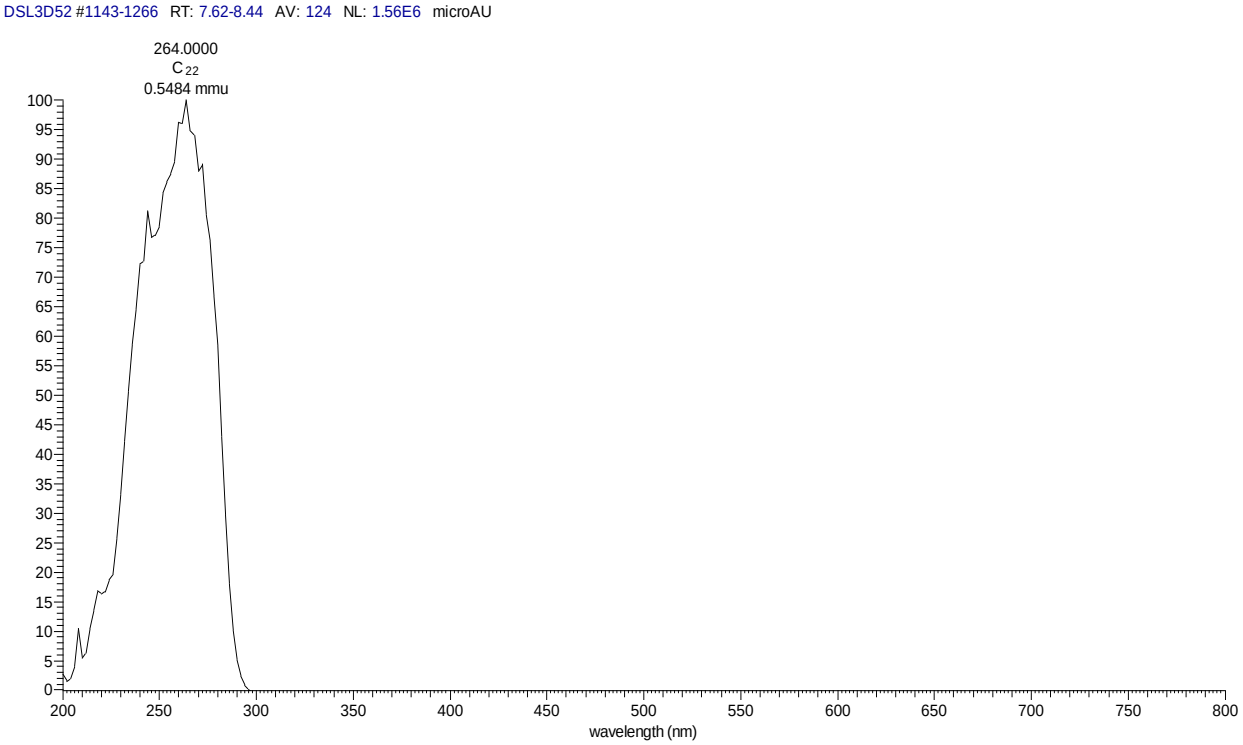

Appendix 49C: ^{1}H NMR spectrum (700 MHz, DMSO-d_6) of compound **222**

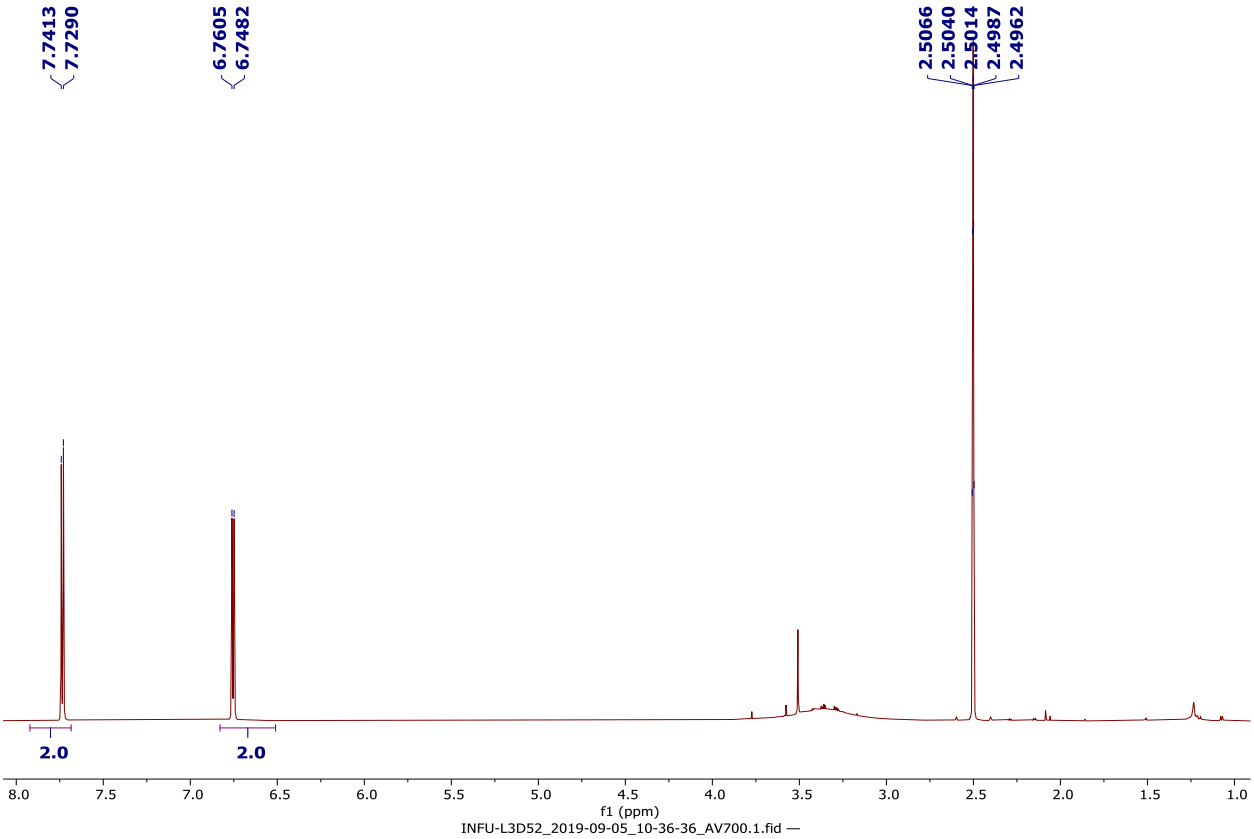

Appendix 49D: ^{13}C NMR spectrum (175 MHz, DMSO-d_6) of compound **222**

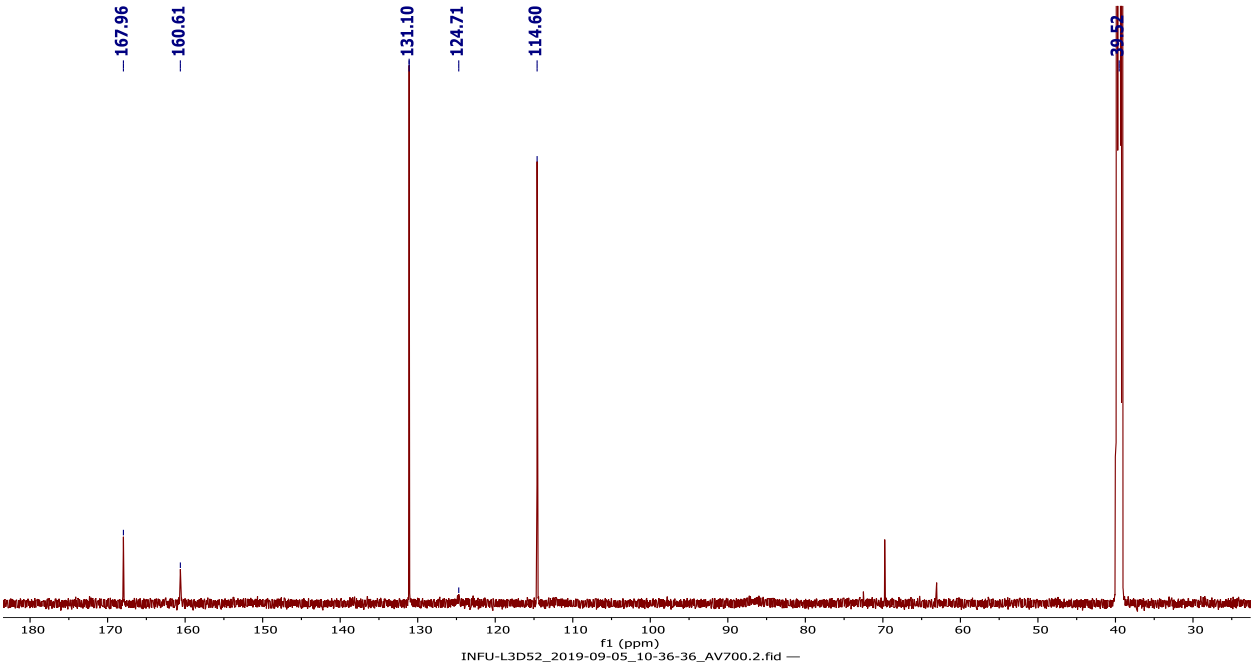

Appendix 49E: ^{1}H-^{1}H COSY spectrum (DMSO-d_6) of compound **222**

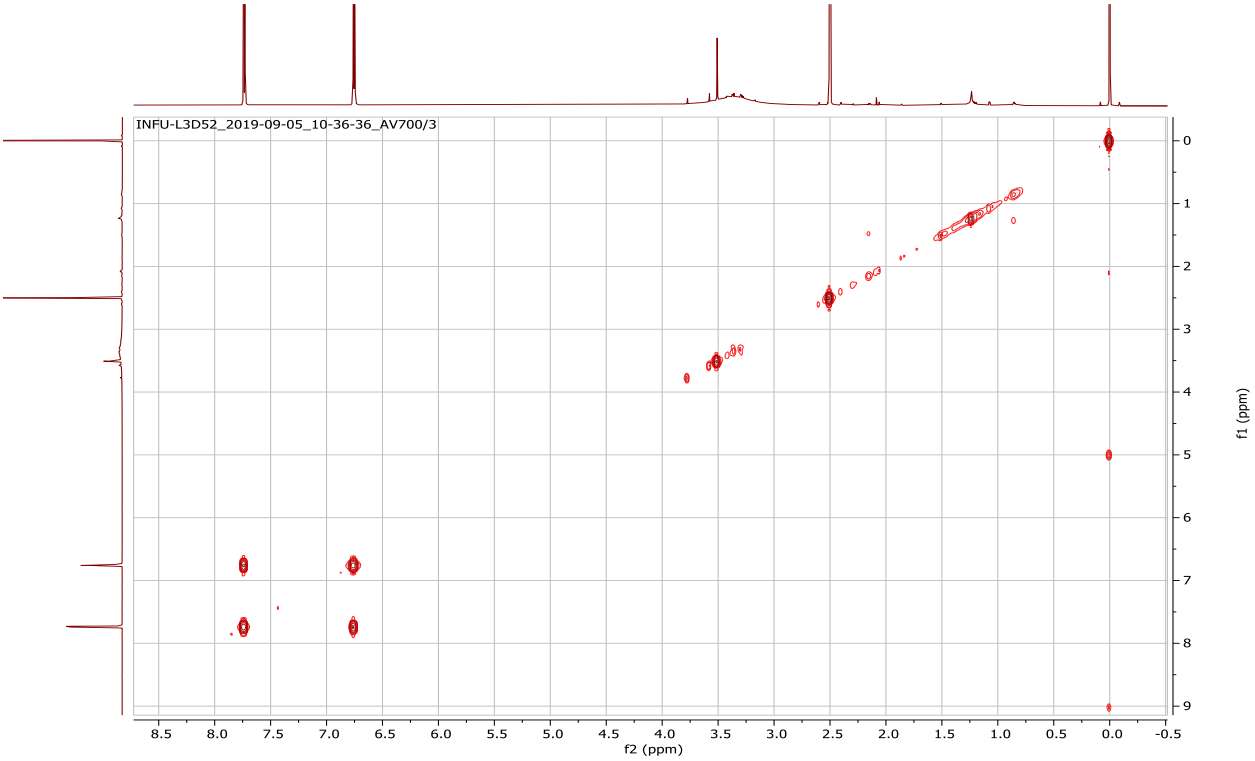

Appendix 49F: HSQC spectrum (DMSO-d_6) of compound **222**

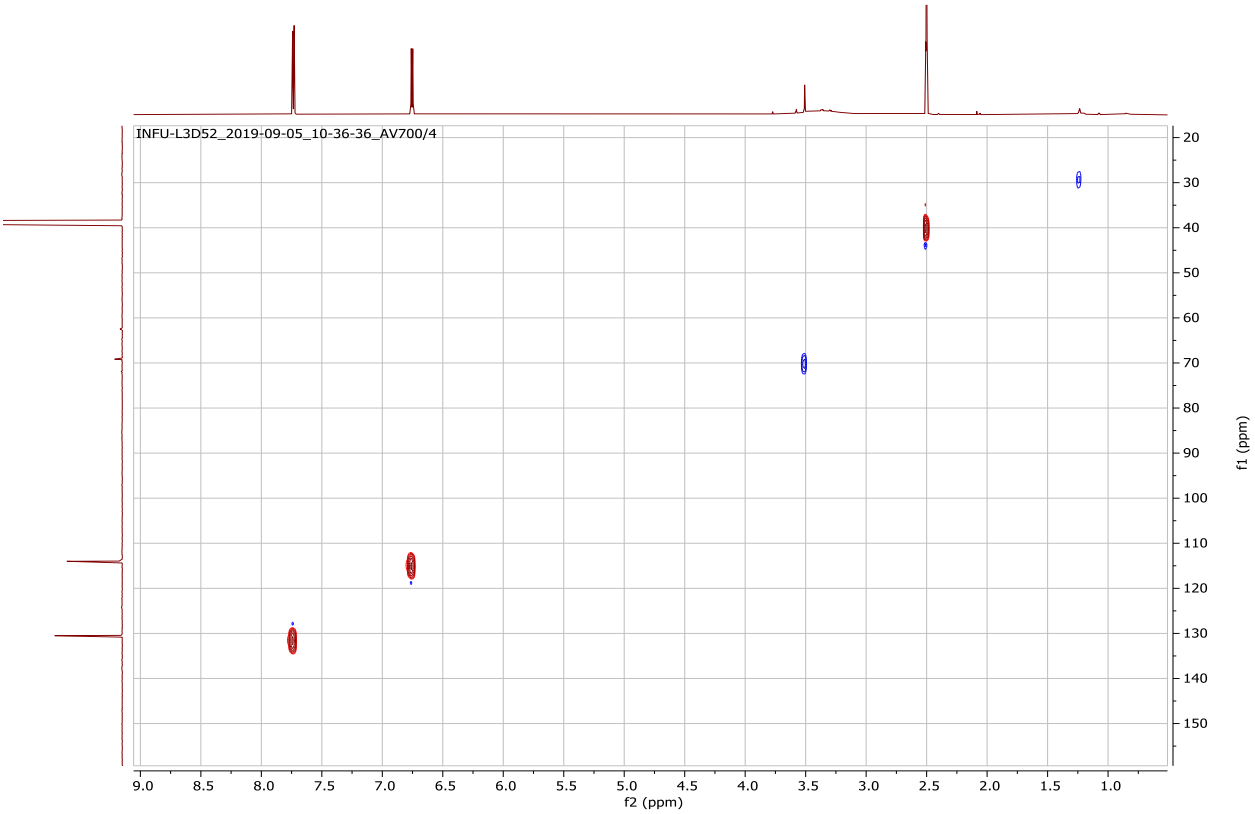

Appendix 49G: HMBC spectrum (DMSO-d_6) of compound **222**

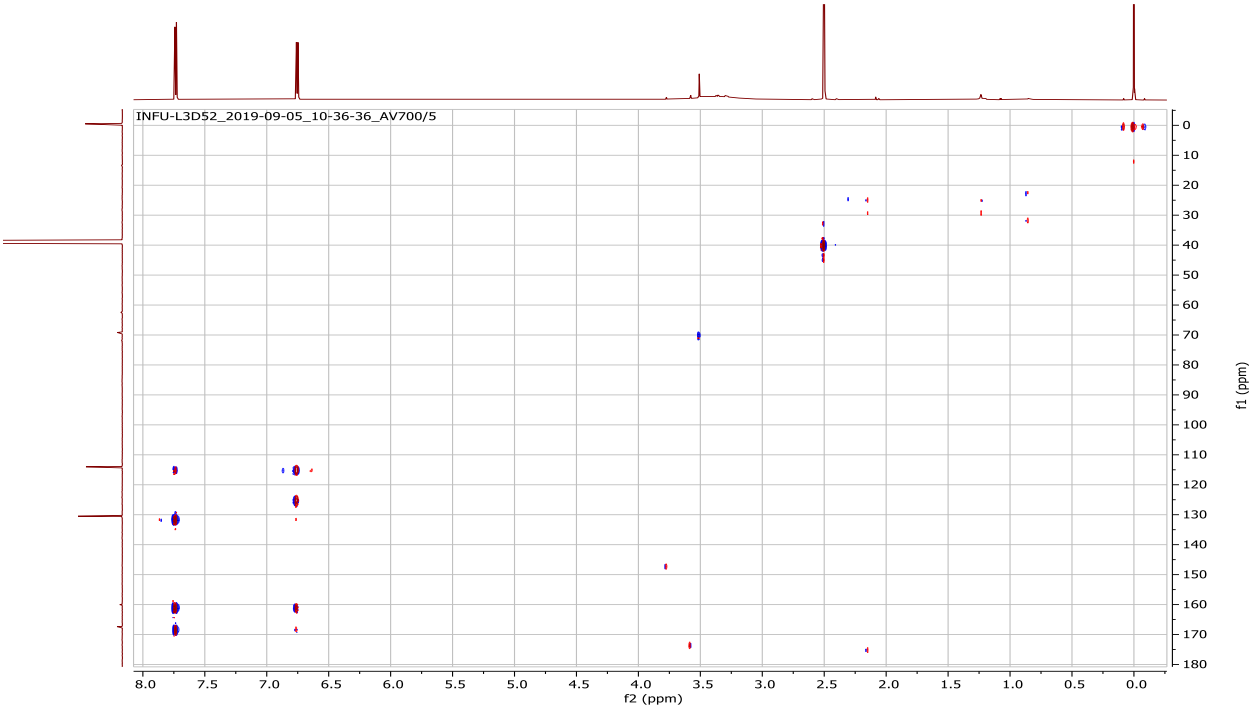

Appendix 50: NMR spectra for indole-3-carboxaldehyde (**223**)

Appendix 50A: HRESIMS of compound **223**

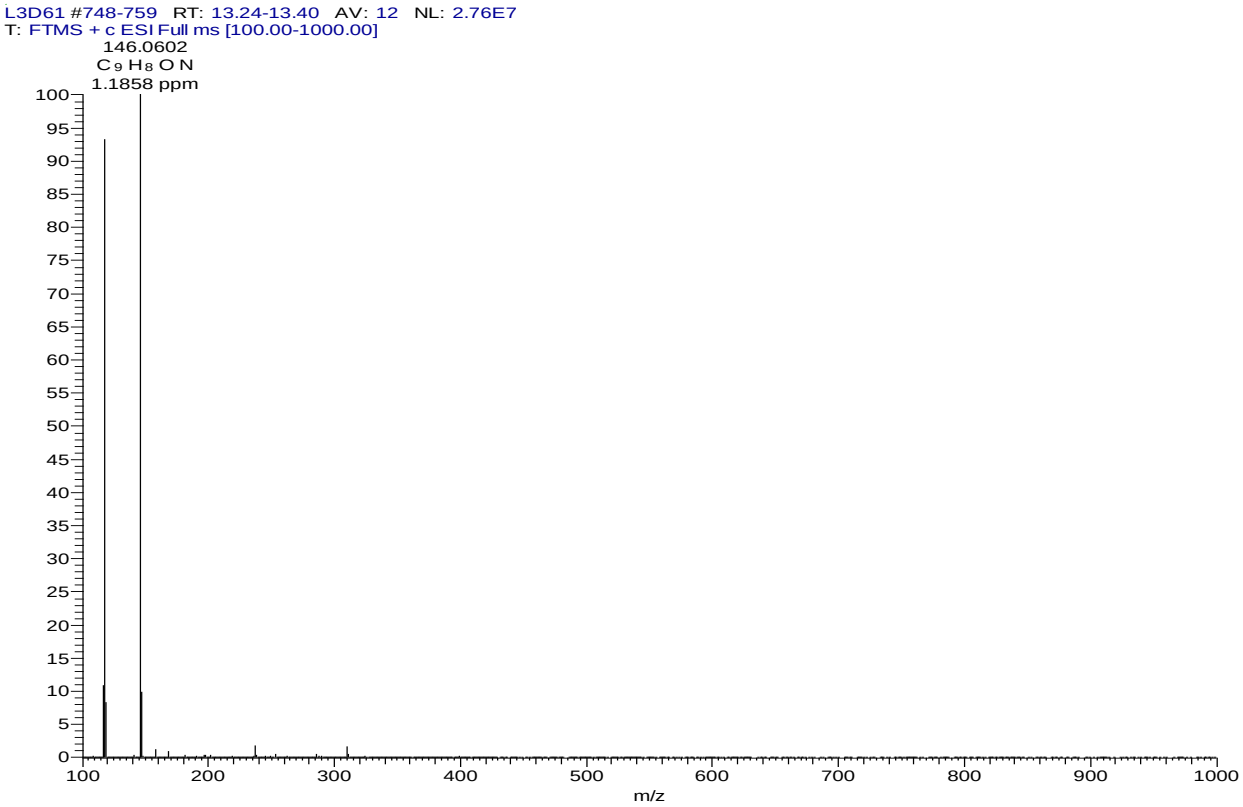

Appendix 50B: LC-UV spectrum of compound **223**

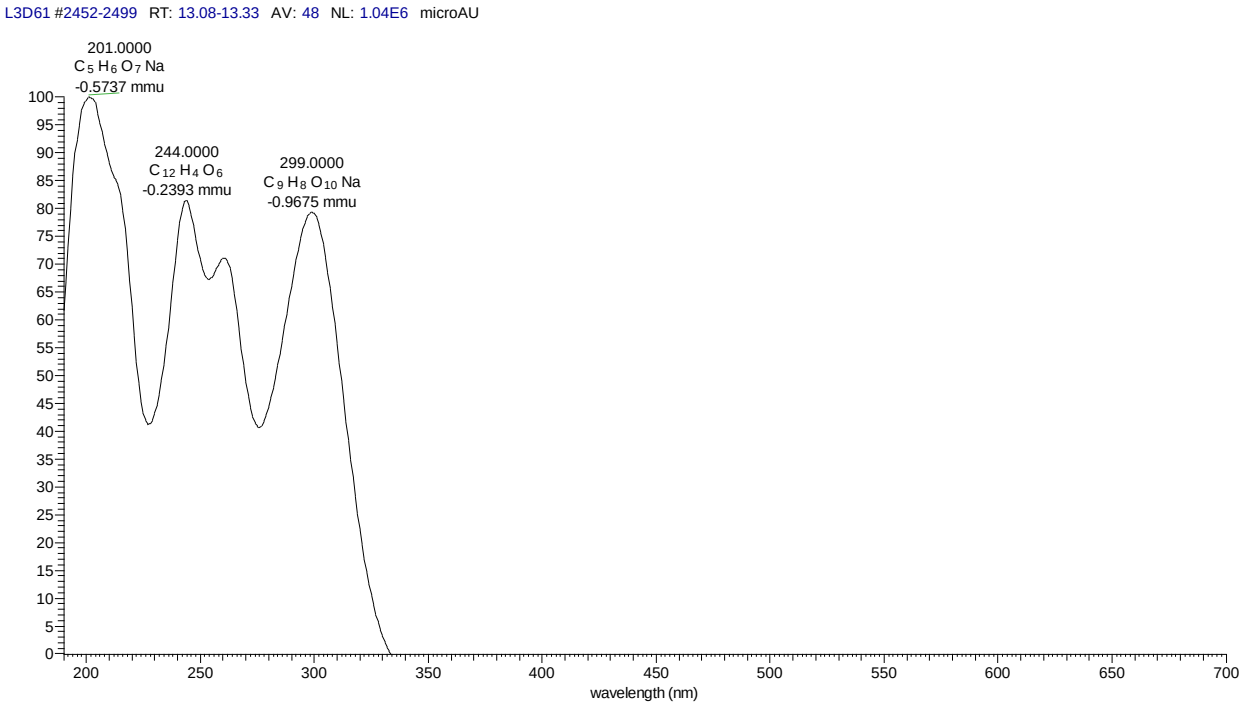

Appendix 50C: ^{1}H NMR spectrum (600 MHz, DMSO-d_6) of compound **223**

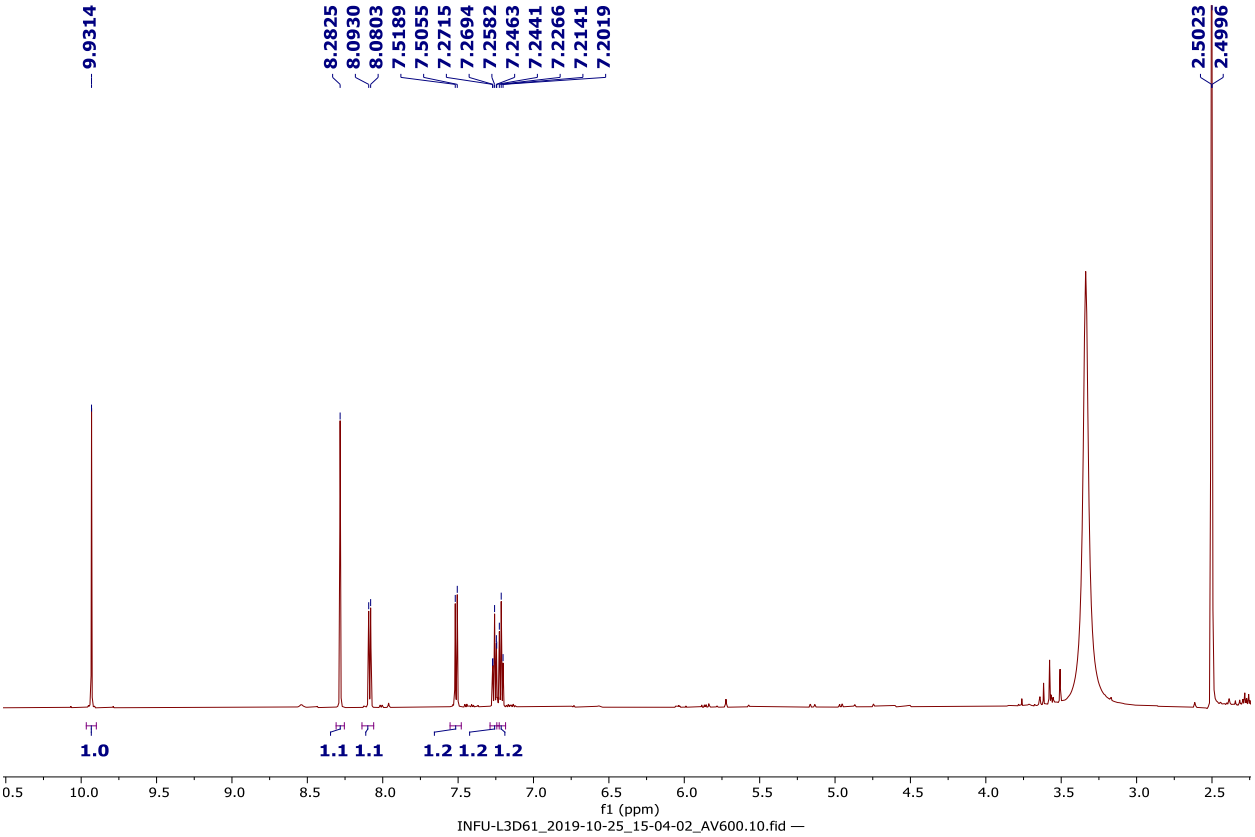

Appendix 50D: ^{13}C NMR spectrum (150 MHz, DMSO-d_6) of compound **223**

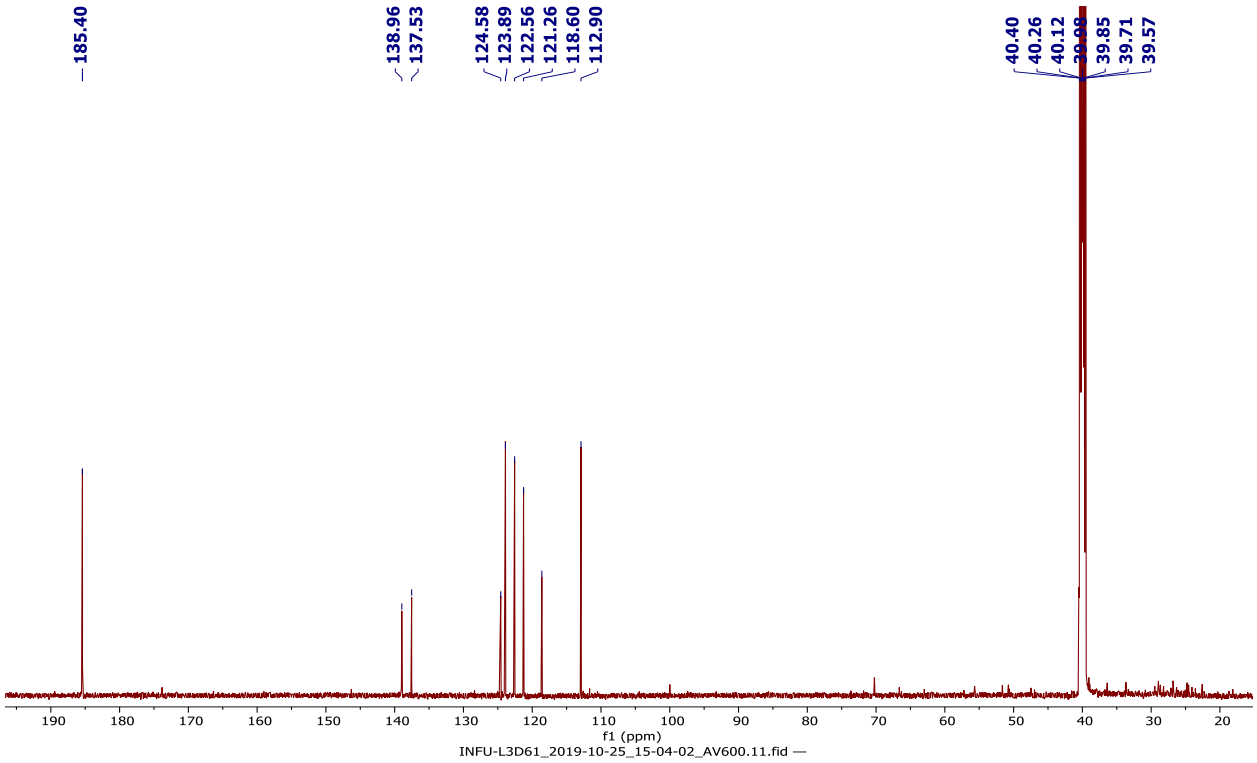

Appendix 50E: ^{1}H-^{1}H COSY spectrum (DMSO-d_6) of compound **223**

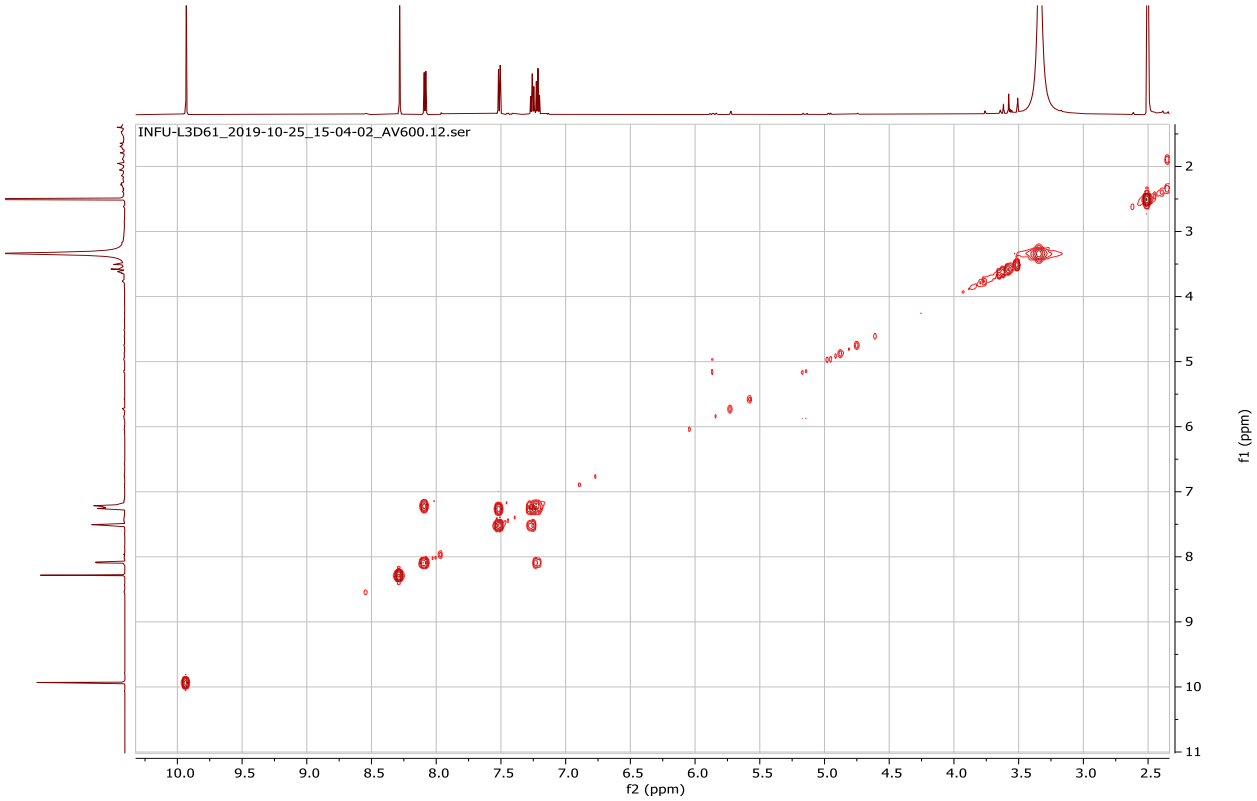

Appendix 50F: HSQC spectrum (DMSO-d_6) of compound **223**

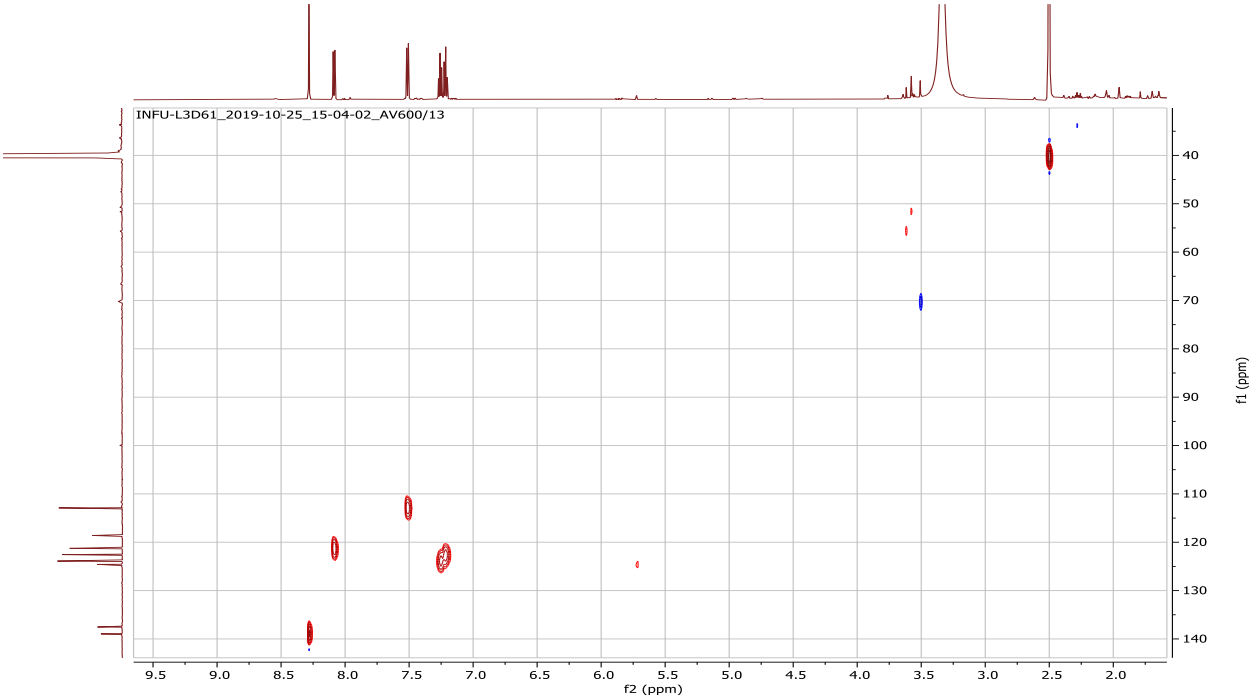

Appendix 50G: HMBC spectrum (DMSO-d_6) of compound **223**

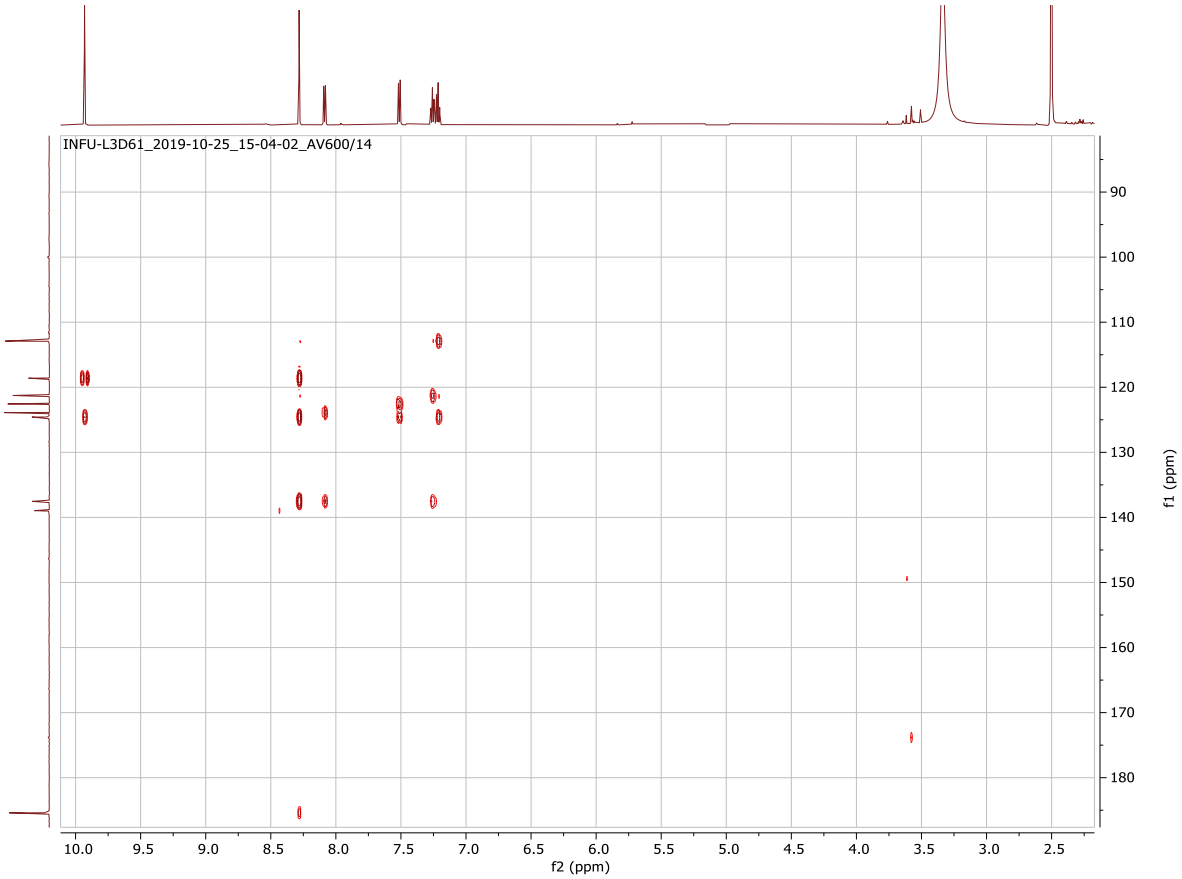

Table S1: Concentration of different cytokines (IL-1β, IL-2, GM-CSF and TNF-α) after incubation of PBMCs with lipopolysaccharide (LPS, 10 μg/mL) and co-incubation with LPS (10 μg/mL) and ibuprofen (100 μM), respectively, compared to the medium (mean ± SD, n = 3)

Controls		Inflammatory mediators release [pg/mL]			
		IL-1β	IL-2	GM-CSF	TNF-α
Medium	Mean	568.68	229.25	56.33	334.79
	SD	26.22	14.03	8.87	19.97
LPS	Mean	9080.11	70.45	108.06	1815.02
	SD	712.46	7.28	5.24	271.69
Ibuprofen	Mean	1995.27	70.45	54.25	1404.79
	SD	287.26	7.28	12.69	357.71
Ibuprofen	% of LPS control	21.97	100.00	50.21	77.40

Table S2: Concentration of different cytokines (IL-1β, IL-2, GM-CSF and TNF-α) after co-incubation of PBMCs with lipopolysaccharide (LPS, 10 μg/mL) and the test compounds or ibuprofen (100 μM), respectively, compared to the medium and to the medium incubated with LPS (10 μg/mL) only (mean ± SD, n = 2)

Compounds	Cytokine release [pg/mL]			
	IL-1β	IL-2	GM-CSF	TNF-α
176	10117.67 ± 1455.66	40.89 ± 14.53	67.93 ± 8.03	1315.91 ± 36.04
177	3200.12 ± 267.60	51.16 ± 0.00	55.91 ± 0.78	267.16 ± 15.24
178	9219.43 ± 466.83	72.56 ± 8.92	167.29 ± 11.21	984.23 ± 87.49
179	4838.02 ± 851.30	72.56 ± 8.92	138.42 ± 21.01	593.41 ± 33.48
180	318.31 ± 118.79	19.40 ± 15.87	1.74 ± 0.00	32.52 ± 5.95
190	3348.20 ± 372.61	40.89 ± 14.53	159.80 ± 23.87	598.42 ± 54.97
181	10137.78 ± 163.17	51.16 ± 0.00	6.61 ± 1.15	333.03 ± 17.48
182	1314.98 ± 151.59	40.89 ± 14.53	53.77 ± 7.43	556.07 ± 48.07
170	5362.04 ± 1596.78	66.25 ± 0.00	139.14 ± 54.45	1244.83 ± 239.83
194	4049.39 ± 417.99	66.25 ± 0.00	84.62 ± 7.18	576.37 ± 67.12
171	6250.45 ± 76.62	66.25 ± 0.00	77.24 ± 3.25	574.77 ± 40.76
183	2682.45 ± 324.10	58.70 ± 10.67	71.42 ± 2.15	205.50 ± 20.72
184	194.34 ± 58.71	8.18 ± 0.00	1.74 ± 0.00	1.13 ± 0.00

Table S3: Concentration of different cytokines (IL-1β, IL-2, GM-CSF and TNF-α) after co-incubation of PBMCs with lipopolysaccharide (LPS, 10 μg/mL) and the test compounds or ibuprofen (100 μM), respectively, compared to the medium and to the medium incubated with LPS (10 μg/mL) only (mean ± SD, n = 2)

Compounds	Cytokine release [pg/mL]			
	IL-1β	IL-2	GM-CSF	TNF-α
203	12730.05 ± 2686.78	58.70 ± 10.67	399.11 ± 82.73	733.63 ± 164.81
204	12187.72 ± 1292.67	89.46 ± 14.98	365.28 ± 104.57	1268.12 ± 323.15
205	11005.15 ± 874.06	66.25 ± 0.00	187.25 ± 0.00	1126.84 ± 59.26
206	8862.66 ± 1417.09	84.42 ± 7.86	191.07 ± 66.97	962.72 ± 327.70
207	1112.24 ± 235.85	58.70 ± 10.67	97.89 ± 19.59	179.54 ± 47.12
208	5615.06 ± 136.00	66.25 ± 0.00	189.30 ± 13.74	813.71 ± 88.76
209	5611.75 ± 772.87	65.01 ± 19.59	156.87 ± 28.69	787.21 ± 98.35
210	6070.05 ± 1583.37	78.87 ± 0.00	283.86 ± 49.23	657.33 ± 66.46
211	5061.73 ± 2029.16	58.70 ± 10.67	203.11 ± 60.09	633.28 ± 147.60
212	8952.95 ± 2810.49	65.01 ± 19.59	147.58 ± 44.24	799.43 ± 229.30
213	10693.95 ± 337.19	51.16 ± 0.00	42.52 ± 1.74	112.08 ± 5.42
214	7420.70 ± 558.93	58.70 ± 10.67	132.48 ± 17.72	324.17 ± 25.03
215	7986.71 ± 3038.74	51.16 ± 0.00	43.03 ± 12.11	123.47 ± 21.53
216	31.83 ± 5.75	19.40 ± 15.87	1.74 ± 0.00	49.08 ± 5.77
217	8493.58 ± 1478.25	66.25 ± 0.00	229.59 ± 9.70	833.65 ± 41.96
218	8759.66 ± 3240.72	66.25 ± 0.00	220.13 ± 38.47	1040.58 ± 190.34
219	4342.07 ± 266.84	58.70 ± 10.67	223.50 ± 30.03	503.25 ± 26.64
220	6577.39 ± 1452.01	58.70 ± 10.67	138.90 ± 54.11	745.14 ± 181.09
221	8720.10 ± 14.12	51.16 ± 0.00	102.40 ± 5.02	620.40 ± 42.91

Single-Crystal X-ray Diffraction Analysis

Compound **176** was crystallized from methanol-water (9:1). The crystals were analyzed on Bruker D8 VENTURE area detector diffractometer according to our method described earlier (Kamtcha *et al*., 2018). Crystal data of compound **176** has been deposited at the Cambridge Crystallographic Data Centre with deposition number CCDC 2001270. A copy of the data can be obtained free of charge from https://www.ccdc.cam.ac.uk/ after registration or by e-mailing to deposit@ccdc.cam.ac.uk.

Crystal Data for Dracaenogenin C (176)

Formula $C_{27}H_{38}O_4$ (M =426.57 g/mol): orthorhombic, space group $P2_12_12_1$ (no. 19), a = 12.2257(5) Å, b = 12.2902(5) Å, c = 15.6061(6) Å, V = 2344.91(16) Å^3, Z = 4, T = 100.0 K, μ(CuKα) = 0.626 mm^{-1}, $Dcalc$ = 1.208 g/cm^3, 34657 reflections measured (9.158° ≤ 2Θ ≤ 155.896°), 4976 unique (R_{int} = 0.0325, R_{sigma} = 0.0185) which were used in all calculations. The final R_1 was 0.0303 (I > 2σ(I)) and wR_2 was 0.0787 (all data).